U.S.NRC
United States Nuclear Regulatory Commission
Protecting People and the Environment

NUREG/CR-7110, Vol. 2

State-of-the-Art Reactor Consequence Analyses Project

Volume 2: Surry Integrated Analysis

Office of Nuclear Regulatory Research

AVAILABILITY OF REFERENCE MATERIALS IN NRC PUBLICATIONS

NRC Reference Material

As of November 1999, you may electronically access NUREG-series publications and other NRC records at NRC's Public Electronic Reading Room at http://www.nrc.gov/reading-rm.html.
Publicly released records include, to name a few, NUREG-series publications; *Federal Register* notices; applicant, licensee, and vendor documents and correspondence; NRC correspondence and internal memoranda; bulletins and information notices; inspection and investigative reports; licensee event reports; and Commission papers and their attachments.

NRC publications in the NUREG series, NRC regulations, and *Title 10, Energy*, in the Code of *Federal Regulations* may also be purchased from one of these two sources.

1. The Superintendent of Documents
   U.S. Government Printing Office
   Mail Stop SSOP
   Washington, DC 20402–0001
   Internet: bookstore.gpo.gov
   Telephone: 202-512-1800
   Fax: 202-512-2250
2. The National Technical Information Service
   Springfield, VA 22161–0002
   www.ntis.gov
   1–800–553–6847 or, locally, 703–605–6000

A single copy of each NRC draft report for comment is available free, to the extent of supply, upon written request as follows:

Address: U.S. Nuclear Regulatory Commission
Office of Administration
Publications Branch
Washington, DC 20555-0001
E-mail: DISTRIBUTION.SERVICES@NRC.GOV
Facsimile: 301–415–2289

Some publications in the NUREG series that are posted at NRC's Web site address http://www.nrc.gov/reading-rm/doc-collections/nuregs are updated periodically and may differ from the last printed version. Although references to material found on a Web site bear the date the material was accessed, the material available on the date cited may subsequently be removed from the site.

Non-NRC Reference Material

Documents available from public and special technical libraries include all open literature items, such as books, journal articles, and transactions, *Federal Register* notices, Federal and State legislation, and congressional reports. Such documents as theses, dissertations, foreign reports and translations, and non-NRC conference proceedings may be purchased from their sponsoring organization.

Copies of industry codes and standards used in a substantive manner in the NRC regulatory process are maintained at—

The NRC Technical Library
Two White Flint North
11545 Rockville Pike
Rockville, MD 20852–2738

These standards are available in the library for reference use by the public. Codes and standards are usually copyrighted and may be purchased from the originating organization or, if they are American National Standards, from—

American National Standards Institute
11 West 42nd Street
New York, NY 10036–8002
www.ansi.org
212–642–4900

Legally binding regulatory requirements are stated only in laws; NRC regulations; licenses, including technical specifications; or orders, not in NUREG-series publications. The views expressed in contractor-prepared publications in this series are not necessarily those of the NRC.

The NUREG series comprises (1) technical and administrative reports and books prepared by the staff (NUREG–XXXX) or agency contractors (NUREG/CR–XXXX), (2) proceedings of conferences (NUREG/CP–XXXX), (3) reports resulting from international agreements (NUREG/IA–XXXX), (4) brochures (NUREG/BR–XXXX), and (5) compilations of legal decisions and orders of the Commission and Atomic and Safety Licensing Boards and of Directors' decisions under Section 2.206 of NRC's regulations (NUREG–0750).

NUREG/CR-7110, Vol. 2

U.S.NRC
United States Nuclear Regulatory Commission
Protecting People and the Environment

State-of-the-Art Reactor Consequence Analyses Project

Volume 2: Surry Integrated Analysis

Manuscript Completed: January 2012
Date Published: January 2012

Prepared by:
Sandia National Laboratories
Albuquerque, New Mexico 87185
Operated for the U.S. Department of Energy

NRC Job Code N6306

Office of Nuclear Regulatory Research

Sandia National Laboratories is a multi-program laboratory managed and operated by Sandia Corporation, a wholly owned subsidiary of Lockheed Martin Corporation, for the U.S. Department of Energy's National Nuclear Security Administration under contract DE-AC04-94AL85000.

ABSTRACT

The evaluation of accident phenomena and the offsite consequences of severe reactor accidents has been the subject of considerable research by the U.S. Nuclear Regulatory Commission (NRC) over the last several decades. As a consequence of this research focus, analyses of severe accidents at nuclear power reactors are more detailed, integrated, and realistic than at any time in the past. A desire to leverage this capability to address conservative aspects of previous reactor accident analysis efforts was a major motivating factor in the genesis of the State-of-the-Art Reactor Consequence Analysis (SOARCA) project. By applying modern analysis tools and techniques, the SOARCA project developed a body of knowledge regarding the realistic outcomes of severe nuclear reactor accidents. To accomplish this objective, the SOARCA project used integrated modeling of accident progression and offsite consequences using both state-of-the-art computational analysis tools and best modeling practices drawn from the collective wisdom of the severe accident analysis community. This study has focused on providing a realistic evaluation of accident progression, source term, and offsite consequences for the Surry Nuclear Power Station. By using the most current emergency preparedness practices, plant capabilities, and best available modeling, these analyses are more detailed, integrated, and realistic than past analyses. These analyses also consider all mitigative measures, contributing to a more realistic evaluation.

PAPERWORK REDUCTION ACT STATEMENT

This NUREG contains and references information collection requirements that are subject to the Paperwork Reduction Act of 1995 (44 U.S.C. 3501 et seq.). These information collection requirements were approved by the Office of Management and Budget, approval number 3150-0011.

PUBLIC PROTECTION NOTIFICATION

The NRC may not conduct or sponsor, and a person is not required to respond to, a request for information or an information collection requirement unless the requesting document displays a currently valid OMB control number.

TABLE OF CONTENTS

LIST OF FIGURES

LIST OF TABLES

EXECUTIVE SUMMARY

The U.S. Nuclear Regulatory Commission (NRC), the nuclear power industry, and the international nuclear energy research community have devoted considerable research over the last several decades to examining severe reactor accident phenomena and offsite consequences. Following the terrorist attacks of 2001, an NRC initiative reassessed severe accident progression and offsite consequences in response to security-related events. These updated analyses incorporated the wealth of accumulated research and used more detailed, integrated, and best-estimate modeling than past analyses. An insight gained from these security assessments was that the NRC needed updated analyses of severe reactor accidents to reflect realistic estimates of the more likely outcomes, considering the current state of plant design and operation and the advances in understanding of severe accident behavior.

The NRC initiated the State-of-the-Art Reactor Consequence Analyses (SOARCA) project to develop best estimates of the offsite radiological health consequences for potential severe reactor accidents for two pilot plants: the Peach Bottom Atomic Power Station in Pennsylvania and the Surry Power Station in Virginia. Peach Bottom is generally representative of U.S. operating reactors using the General Electric boiling-water reactor (BWR) design with a Mark I containment. Surry is generally representative of U.S. operating reactors using the Westinghouse pressurized-water reactor (PWR) design with a large, dry (subatmospheric) containment. SOARCA results, while specific to Peach Bottom and Surry, may be generally applicable to plants with similar designs. Additional work would be needed to confirm this, however, since differences exist in plant-specific designs, procedures, and emergency response characteristics.

The SOARCA project evaluates plant improvements and changes not reflected in earlier NRC publications such as NUREG/CR-2239, "Technical Guidance for Siting Criteria Development," NUREG-1150, "Severe Accident Risks: An Assessment for Five U.S. Nuclear Power Plants," and WASH-1400, "Reactor Safety Study: An Assessment of Accident Risks in U.S. Commercial Nuclear Power Plants." SOARCA includes system improvements, improvements in training and emergency procedures, offsite emergency response, and security-related improvements, as well as plant changes such as power uprates and higher core burnup. To provide perspective between SOARCA results and more conservative offsite consequence estimates, SOARCA results are compared to NUREG/CR-2239, "Technical Guidance for Siting Criteria Development," issued in 1982 and referred to in this report as the Siting Study. Specifically, SOARCA results are compared to the Siting Study siting source term 1 (SST1). SST1 assumes severe core damage, loss of all safety systems, and loss of containment after 1.5 hours. The SOARCA report helps the NRC to communicate its current understanding of severe-accident-related aspects of nuclear safety to stakeholders, including Federal, State, and local authorities, licensees, and the general public.

The SOARCA project sought to focus its resources on the more important severe accident scenarios for Peach Bottom and Surry. The project narrowed its approach by using an accident sequence's possibility of damaging reactor fuel, or core damage frequency (CDF), as a surrogate for risk. The SOARCA scenarios were selected from the results of existing probabilistic risk assessments (PRAs). Core damage sequences from previous staff and licensee PRAs were

identified and binned into core damage groups. A core damage group consists of core damage sequences that have similar timing for important severe accident phenomena and similar containment or engineered safety feature operability. It is important to note that each core damage sequence that belongs to a given core damage group is initiated by a specific cause (for example, a seismic event, a fire, or a flood), and that the frequency of each core damage group was estimated by aggregating the CDFs of the individual sequences that belong to the group. This approach was taken to help ensure that the contributions from all core damage sequences were accounted for during the sequence selection process. During the consequence analysis, the core damage groups for station blackouts were analyzed as if they were initiated by a seismic event. This approach was taken because seismically induced equipment failures occur immediately following the seismic event, which produces the severe challenge to the plant. The groups were screened according to their approximate CDFs to identify the most risk significant groups. SOARCA analyzed scenarios with a CDF equal to or greater than 10^{-6} (1 in a million) per reactor-year. SOARCA also sought to analyze scenarios leading to an early failure or bypass of the containment with a CDF equal to or greater than 10^{-7} (1 in 10 million) per reactor-year, since these scenarios have a potential for higher consequences and risk. This approach allowed a more detailed analysis of accident consequences for the more likely, although still remote, accident scenarios.

The staff used updated and benchmarked standardized plant analysis risk (SPAR) models and available plant-specific external events information in the scenario-selection process and identified two major groups of accident scenarios for analysis. The first group common to both Peach Bottom and Surry includes short-term station blackout (STSBO) and long-term station blackout (LTSBO). Both types of SBOs involve a loss of all alternating current (ac) power. The STSBO also involves the loss of turbine-driven systems through loss of direct current (dc) control power or loss of the condensate storage tank and therefore proceeds to core damage more rapidly (hence "short term"). The STSBO has a lower CDF, since it requires a more severe initiating event and more extensive system failures. SBO scenarios can be initiated by external events such as a fire, flood, or earthquake. SOARCA assumes that an SBO is initiated by a seismic event since this is the most extreme case in terms of both the timing and amount of equipment that fails. Notwithstanding the SOARCA scenario screening process, SBO scenarios are commonly identified as important contributors in PRA because of the common cause of failure for both reactor safety systems and containment safety systems.

SOARCA's second severe accident scenario group, which was identified for Surry only, is the containment bypass scenario. For Surry, two containment bypass scenarios were identified and analyzed. The first bypass scenario is a variant of the STSBO scenario, involving a thermally-induced steam generator tube rupture (TISGTR). The second bypass scenario involves an interfacing systems loss-of-coolant accident (ISLOCA) caused by an unisolated rupture of low-head safety injection piping outside containment. The CDF for the ISLOCA, 3×10^{-8} (3 in 100 million) per reactor-year, falls below the SOARCA screening criterion for bypass events but it is analyzed for completeness because NUREG-1150 identified ISLOCA, in addition to SBO and SGTRs, as principal contributors to mean early and latent cancer fatality risks. This scenario-selection process captured the more important internally and externally initiated core damage scenarios.

SOARCA's analyses were performed with two computer codes, MELCOR for accident progression and the MELCOR Accident Consequence Code System, Version 2 (MACCS2) for offsite consequences. The NRC staff's preparations for the analyses included extensive cooperation from the licensees of Peach Bottom and Surry to develop high-fidelity plant systems models, define operator actions including the most recently developed mitigation actions, and develop models for simulation of site-specific and scenario-specific emergency planning and response. Moreover, in addition to input for model development, licensees provided information on accident scenarios from their PRAs. Through tabletop exercises of the selected scenarios with senior reactor operators, PRA analysts, and other licensee staff, licensees provided input on the timing and nature of the operator actions to mitigate the selected scenarios. The licensee input for each scenario was used to develop assumed timelines of operator actions and equipment configurations for implementing available mitigation measures which include mitigation measures beyond those routinely credited in current PRA models. A human reliability analysis, commonly included in PRAs to represent the reliability of operator actions, was not performed for SOARCA, but instead tabletop exercises, plant walkdowns, simulator runs and other inputs from licensee staff were employed to ensure that operator actions and their timings were correctly modeled.

SOARCA modeled several types of mitigation measures, including those specified in emergency operating procedures (EOPs), severe accident management guidelines (SAMGs), and Title 10 to the *Code of Federal Regulations* (10 CFR) 50.54(hh). The 10 CFR 50.54(hh) mitigation measures refer to additional equipment and strategies required by the NRC following the terrorist attacks of September 11, 2001, to further improve each plant's capability to mitigate events involving a loss of large areas of the plant caused by fire and explosions. To assess the benefits of mitigation measures and to provide a basis for comparison to the past analyses of unmitigated severe accident scenarios, the SOARCA project analyzes the selected scenarios twice: first assuming that the event proceeds unmitigated, and then assuming that mitigation is successful. SOARCA's unmitigated cases assumed neither 10 CFR 50.54(hh) equipment nor a subset of other key operator actions that would prevent core damage were implemented. The subset of operator actions not credited was specific to each individual scenario and included such actions as use of the residual heat removal system for the Surry ISLOCA.

For the LTSBO scenarios for both Peach Bottom and Surry (the most likely severe accident scenario for each plant considered in SOARCA) analyzed assuming no mitigation, core damage begins in 9 to 16 hours, and reactor vessel failure begins at about 20 hours. Offsite radiological release due to containment failure begins at about 20 hours for Peach Bottom (BWR) and at 45 hours for Surry (PWR). The SOARCA analyses therefore show that time may be available for operators to take corrective action and get additional assistance from plant technical support centers even if initial efforts are assumed unsuccessful. For the most rapid events (i.e., the unmitigated STSBO in which core damage may begin in 1 to 3 hours), reactor vessel failure begins at roughly 8 hours, possibly allowing time to restore core cooling and prevent vessel failure. In these cases, containment failure and radiological release begins at about 8 hours for Peach Bottom and at 25 hours for Surry. For the unmitigated Surry ISLOCA, the offsite radiological release begins at about 13 hours and in the other bypass event analyzed, the TISGTR, the radiological release begins at about 3.5 hours but is shown by analyses to be substantially smaller than the 1982 Siting Study SST1 release.

In addition to delayed radiological releases relative to the 1982 Siting Study SST1 case, the SOARCA study demonstrates that the amount of radioactive material released is much smaller as shown in Figures ES-1 (Iodine-131) and ES-2 (Cesium-137) below. The Surry ISLOCA iodine release is calculated to be 16 percent of the core inventory, but the results are more generally in the range of 0.5 to 2 percent for iodine and cesium for the other scenarios analyzed. By contrast, the 1982 Siting Study SST1 case calculated an iodine release of 45 percent and a cesium release of 67 percent of the core inventory.

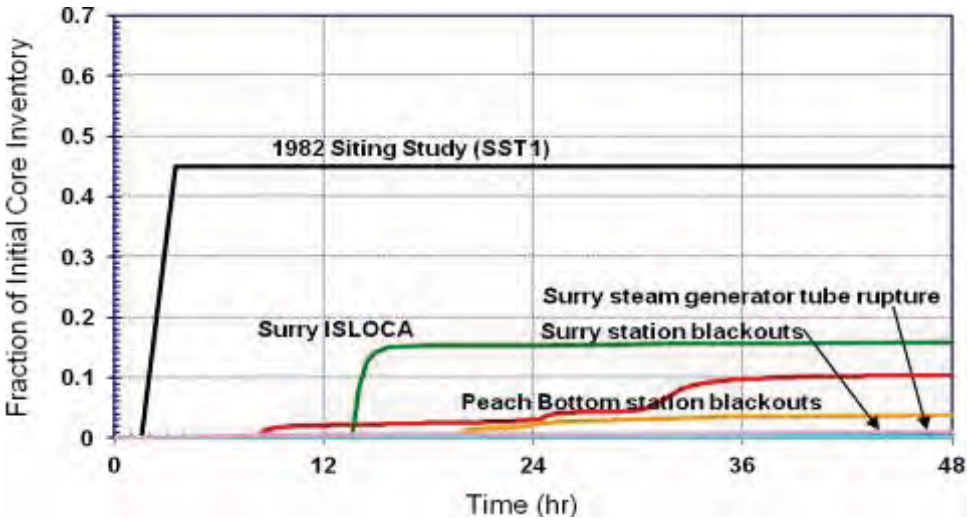

Figure ES-1 Iodine release to the environment for SOARCA unmitigated scenarios and the 1982 Siting Study SST1 case

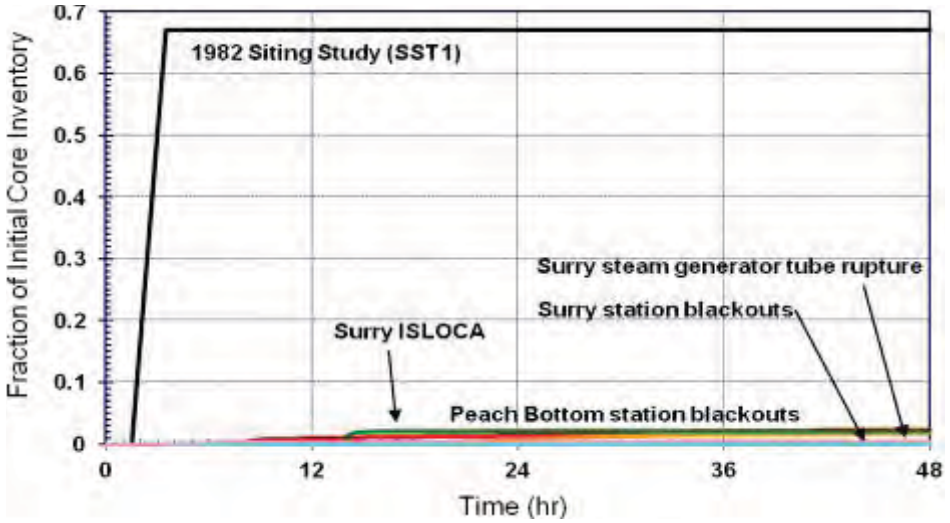

Figure ES-2 Cesium release to the environment for SOARCA unmitigated scenarios and the 1982 Siting Study SST1 case

Past PRAs and consequence studies showed that sequences involving large early releases were important risk contributors. For example, the PWR SBO with a TISGTR was historically believed to result in a large, relatively early release potentially leading to higher offsite consequences. However, MELCOR analysis of Surry performed for SOARCA shows that the release is small, because other reactor coolant system piping inside containment (i.e., hot leg nozzle) fails soon after the tube rupture and thereby retains the fission products within the containment. Additional work would be needed to determine if this result generally applies for all types of PWRs.

The SOARCA results demonstrate the potential benefits of employing 10 CFR 50.54(hh) mitigation enhancements for the scenarios analyzed. MELCOR analyses were used both to confirm the time available to implement mitigation measures and to confirm that those measures, once taken, are effective in preventing core damage or significantly reducing radiological releases. When successful mitigation is assumed, the MELCOR results indicate no core damage for all scenarios except the Surry STSBO and its TISGTR variant. The security-related mitigation measures that provide alternative ac power and portable diesel-driven pumps are especially helpful in counteracting SBO scenarios. For the Surry STSBO and its TISGTR variant, the mitigation is sufficient to flood the containment through the containment spray system to cover core debris resulting from vessel failure. For the ISLOCA scenario, installed equipment unrelated to 10 CFR 50.54(hh) is effective in preventing core damage owing to the time available for corrective action.

For scenarios that release radioactive material to the environment, MACCS2 uses site-specific weather data to predict the downwind concentration of material in the plume and the resulting population exposures and health effects. The analysis of offsite consequences in SOARCA incorporates the improved modeling capability reflected in the MELCOR and MACCS2 codes as well as detailed site-specific public evacuation models. These models were developed for each scenario based on site-specific emergency preparedness programs and State emergency response plans to reflect timing of onsite and offsite protective action decisions and the evacuation time estimates and road networks at Peach Bottom and Surry. Scenarios that are assumed to be initiated by a seismic event consider the earthquake's impact on implementing emergency plans from loss of infrastructure (i.e., long-span bridges, traffic signals, sirens).

The unmitigated versions of the scenarios analyzed in SOARCA have lower risk of early fatalities than calculated in the 1982 Siting Study SST1 case. SOARCA's analyses show essentially zero risk of early fatalities. Early fatality risk was calculated to be ~ 10^{-14} for the unmitigated Surry ISLOCA (for the area within 1 mile of Surry's exclusion area boundary) and zero for all other SOARCA scenarios. In comparison, 92 early fatalities for Peach Bottom and 45 early fatalities for Surry were calculated for the SST1 case in the 1982 Siting Study.

SOARCA results indicate that bypass events (e.g., Surry ISLOCA) do not pose a higher scenario-specific latent cancer fatality risk than non-bypass events (e.g., Surry SBO). While consequences are greater when the bypass scenario happens, this is offset by the scenario being less likely to happen. SOARCA reinforces the importance of external events relative to internal events and the need to continue ongoing work related to external events risk assessment.

Offsite radiological consequences were calculated for each scenario expressed as the average individual likelihood of an early fatality and latent cancer fatality. Tables ES-1 (Peach Bottom) and ES-2 (Surry) show, for both mitigated and unmitigated cases, conditional (on the occurrence of the core damage scenario) scenario-specific probabilities of a latent cancer fatality for an individual located within 10 miles of the plant. Tables ES-1 and ES-2 show the results using the linear no-threshold (LNT) dose-response model, which assumes that the health risk is directly proportional to the exposure and even the smallest radiation exposure carries some risk. The tables also provide the scenario-specific latent cancer fatality risk for an individual located within 10 miles of the plant, taking into account the scenario's core damage frequency.

Table ES-1 Offsite Consequence Results for Peach Bottom Scenarios Assuming Linear No-Threshold (LNT) Dose-Response Model

Scenario	Core damage frequency [CDF] (per reactor-year)	Mitigated		Unmitigated	
		Conditional scenario-specific probability of latent cancer fatality for an individual located within 10 miles	Scenario-specific risk [CDF x Conditional] of latent cancer fatality for an individual located within 10 miles (per reactor-year)	Conditional scenario-specific probability of latent cancer fatality for an individual located within 10 miles	Scenario-specific risk [CDF x Conditional] of latent cancer fatality for an individual located within 10 miles (per reactor-year)
Long-term SBO	3×10^{-6}	No Core Damage		9×10^{-5}	$\sim 3\times10^{-10}$ ***
Short-term SBO	3×10^{-7}	No Core Damage **		2×10^{-4}	$\sim 6\times10^{-11}$ ***
Short-term SBO with RCIC Blackstart*	3×10^{-7}			7×10^{-5}	$\sim 2\times10^{-11}$ ***

* Blackstart of the reactor core isolation cooling (RCIC) system refers to starting RCIC without any ac or dc control power. Blackrun of RCIC refers to the long-term operation of RCIC without electricity, once it has been started. This typically involves using a portable generator to supply power to indications such as reactor pressure vessel (RPV) level to allow the operator to manually adjust RCIC flow to prevent RPV overfill and flooding of the RCIC turbine.

** If the RCIC system is successfully controlled, i.e., successful blackstart and blackrun, then both mitigated Short-term SBO scenarios would be functionally similar to the mitigated Long-term SBO (i.e., no core damage). This was qualitatively determined based on the timing and equipment availabilities from the other SBO analyses.

*** Estimated risks below 1 x 10^{-7} per reactor year should be viewed with caution because of the potential impact of events not studied in the analyses and the inherent uncertainty in very small calculated numbers..

Table ES-2 Offsite Consequence Results for Surry Scenarios Assuming LNT Dose-Response Model

Scenario	Core damage frequency [CDF] (per reactor-year)	Mitigated		Unmitigated	
		Conditional scenario-specific probability of latent cancer fatality for an individual located within 10 miles	Scenario-specific risk [CDF x Conditional] of latent cancer fatality for an individual located within 10 miles (per reactor-year)	Conditional scenario-specific probability of latent cancer fatality for an individual located within 10 miles	Scenario-specific risk [CDF x Conditional] of latent cancer fatality for an individual located within 10 miles (per reactor-year)
Long-term SBO	2×10^{-5}	No Core Damage		5×10^{-5}	$\sim 7\times10^{-10}$ ***
Short-term SBO	2×10^{-6}	No Containment Failure *		9×10^{-5}	$\sim 1\times10^{-10}$ ***
Short-term SBO with TISGTR	4×10^{-7}	3×10^{-4} **	$\sim 1\times10^{-10}$ ***	3×10^{-4}	$\sim 1\times10^{-10}$ ***
Interfacing systems LOCA	3×10^{-8}	No Core Damage		3×10^{-4}	$\sim 9\times10^{-12}$ ***

* Accident progression calculations were run showing that source terms in the mitigated case are smaller than in the unmitigated case. Offsite consequence calculations were not run since the containment fails at about 66 hours. A review of available resources and emergency plans shows that adequate mitigation measures could be brought on site within 24 hours and connected and functioning within 48 hours. Therefore 66 hours would allow ample time for mitigation via measures brought to the site from offsite.

** Containment failure is delayed by about 46 hours in the mitigated case relative to the unmitigated case. Rounding to one significant figure shows conditional LCF probabilities of 3×10-4 for both mitigated and unmitigated cases, however the original values were 2.8×10-4 for the mitigated case and 3.2×10-4 for the unmitigated case.

*** Estimated risks below 1 x 10^{-7} per reactor year should be viewed with caution because of the potential impact of events not studied in the analyses and the inherent uncertainty in very small calculated numbers.

LCF risks using alternate dose-response models, as well as LCF risks for circular areas out to a radius of 50 miles, are also presented. Using a dose-response model that truncates annual doses below normal background levels (including medical exposures) results in a further reduction to the latent cancer fatality risks (by a factor of 100 for smaller releases and a factor of 3 for larger releases). Latent cancer fatality risk calculations are generally dominated by long-term exposure to small annual doses (~500 mrem per year corresponding to state return criteria) by evacuees returning to their homes after the accident and being exposed to residual radiation over a long period of time. SOARCA's calculated LCF risk results are smaller than extrapolations of 1982 Siting Study SST1 LCF risk results. However, the difference diminishes when considering larger areas, out to a distance of 50 miles from the plant.

Figure ES-3 compares SOARCA's scenario-specific latent cancer fatality risks for an individual within 10 miles of the plant to the NRC Safety Goal and to an extrapolation of the 1982 Siting Study SST1[1] results.

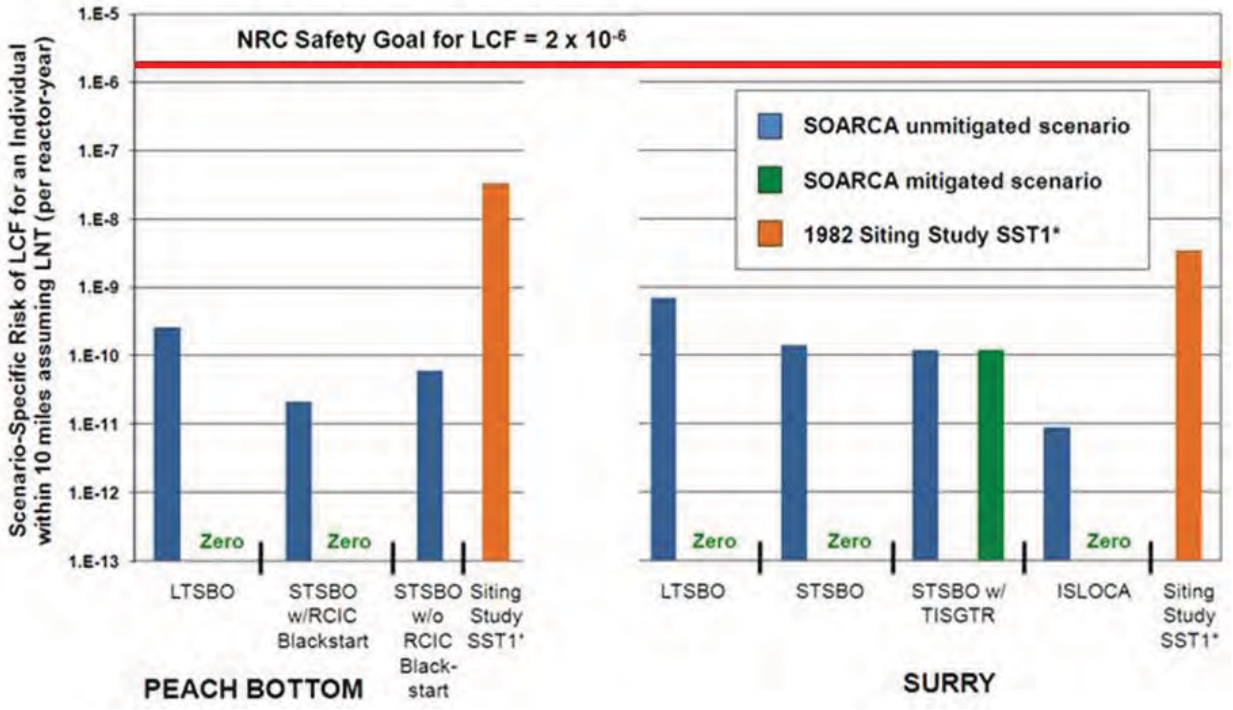

Figure ES-3 Comparison of individual LCF risk results for SOARCA mitigated and unmitigated scenarios to the NRC Safety Goal and to extrapolations of the 1982 Siting Study SST1 ***(plotted on logarithmic scale)***

The NRC Safety Goal for latent cancer fatality risk from nuclear power plant operation (i.e., $2x10^{-6}$ or two in one million) is set 1,000 times lower than the sum of cancer fatality risks resulting from all other causes (i.e., $2x10^{-3}$ or two in one thousand). The calculated cancer fatality risks from the selected, important scenarios analyzed in SOARCA are thousands of times lower than the NRC Safety Goal and millions of times lower than the general U.S. cancer fatality risk.

Comparisons of SOARCA's calculated LCF risks to the NRC Safety Goal and the average annual US cancer fatality risk from all causes are provided to give context that may help the reader to understand the contribution to cancer risks from these nuclear power plant accident scenarios. However, such comparisons have limitations for which the reader should be aware. Relative to the safety goal comparison, the safety goal is intended to encompass all accident scenarios. SOARCA does not examine all scenarios typically considered in a PRA, even though it includes the important scenarios. In fact, any analytical technique, including PRAs, will have

[1] The Siting Study did not calculate LCF risks. Therefore, to compare the Siting Study SST1 case to LCF results for SOARCA, the SST1 source term was put into the MACCS2 offsite consequence code files for the Peach Bottom and Surry unmitigated STSBO calculations.

inherent limitations of scope and method. As a result, comparison of SOARCA's scenario-specific calculated LCF risks to the NRC Safety Goal is necessarily incomplete. However, it is intended to show that adding multiple scenarios' low risk results in the ~ 10^{-10} range to approximate a summary risk from all scenarios, would yield a summary result that is also below the NRC Safety Goal of $2x10^{-6}$ or two in one million.

Relative to the U.S. average individual risk of a cancer fatality comparison, the sources of an individual's cancer risk include a complex combination of age, genetics, lifestyle choices, and other environmental factors whereas the consequences from a severe accident at a nuclear plant are involuntary and unlikely to be experienced by most individuals.

The SOARCA analyses show that emergency response programs, implemented as planned and practiced, reduce the scenario-specific risk of health consequences among the public during a severe reactor accident. Sensitivity analyses of seismic impacts on site-specific emergency response (e.g., loss of bridges, traffic signals, and delayed notification) at Peach Bottom and Surry do not significantly affect LCF risk.

In summary, the staff believes SOARCA has achieved its objective to develop a body of knowledge regarding detailed, integrated, state-of-the-art modeling of the most important severe accident scenarios for Peach Bottom and Surry. SOARCA analyses indicate that successful implementation of existing mitigation measures can prevent reactor core damage or delay or reduce offsite releases of radioactive material. All SOARCA scenarios, even when unmitigated, progress more slowly and release much less radioactive material than the 1982 Siting Study SST1 case. As a result, the calculated risks of public health consequences from severe accidents modeled in SOARCA are very small.

The SOARCA study was nearing completion when the Fukushima Daiichi accident occurred on March 11, 2011. The Fukushima accident has many similarities and differences with some of the Peach Bottom severe accident scenarios analyzed in SOARCA. While there are significant gaps in information and uncertainties regarding what occurred in the Fukushima reactors, an appendix to this report compares and contrasts the SOARCA study and the Fukushima accident based on currently available information for the following topics: (1) operation of the RCIC system, (2) hydrogen release and combustion, (3) 48-hour truncation of releases in SOARCA, (4) multiunit risk, and (5) spent fuel pool risk.

ACKNOWLEDGEMENTS

The contributions from the following individuals in preparing this document are gratefully acknowledged.

Terry Brock	Nuclear Regulatory Commission
Richard Chang	Nuclear Regulatory Commission
Ata Istar	Nuclear Regulatory Commission
Robert Prato	Nuclear Regulatory Commission
Mark Orr	Nuclear Regulatory Commission
Jason Schaperow	Nuclear Regulatory Commission
Abdul Sheikh	Nuclear Regulatory Commission
Randolph Sullivan	Nuclear Regulatory Commission
Charles G. Tinkler	Nuclear Regulatory Commission
Nathan E. Bixler	Sandia National Laboratories
Shawn P. Burns	Sandia National Laboratories
Randall O. Gauntt	Sandia National Laboratories
Joseph A. Jones	Sandia National Laboratories
Raymond J. Jun	Sandia National Laboratories
Douglas M. Osborn	Sandia National Laboratories
Jesse Phillips	Sandia National Laboratories
Kyle Ross	Sandia National Laboratories
Mark T. Leonard	dycoda, LLC
Kenneth C. Wagner	dycoda, LLC

ACRONYMS

AC	Alternating Current
AFW	Auxiliary Feedwater
ANS	American Nuclear Society
ASME	American Society of Mechanical Engineers
CCI	Core Concrete Interactions
CDF	Core Damage Frequency
CST	Condensate Storage Tank
DC	Direct Current
DOE	Department of Energy
EAL	Emergency Action Levels
EAS	Emergency Alert System
ECST	Emergency Condensate Storage Tank
EDG	Emergency Diesel Generator
EOF	Emergency Operations Facility
EOP	Emergency Operating Procedure
EP	Emergency Preparedness
EPA	Environmental Protection Agency
EPZ	Emergency Planning Zone
ERO	Emergency Response Organization
ETE	Evacuation Time Estimate
GE	General Emergency
HPS	Health Physics Society
IPE	Individual Plant Examination
IPEE	Individual Plant Examination of External Event
ISLOCA	Interfacing System Loss of Coolant Accident
LERF	Large Early Release Frequency
LLNL	Los Alamos National Lab
LHSI	Low Head Safety Injection
LNT	Linear, No-Threshold
LOCA	Loss Of Coolant Accident
LOSW	Loss Of Service Water
LTSBO	Long-Term Station Blackout
MACCS2	MELCOR Accident Consequence Code System, Version 2
MCCI	Molten Corium-Concrete Interactions
MSIV	Main Steam Isolation Valve
MSVH	Main Steam Valve House
NPP	Nuclear Power Plant
NRC	Nuclear Regulatory Commission
NRCS	Natural Resources Conservation Service
NRF	National Response Framework
OREMS	Oak Ridge Evacuation Modeling System
ORO	Offsite Response Organization

PRT	Pressurizer Relief Tank
RCP	Reactor Coolant Pump
RCS	Reactor Coolant System
RHR	Residual Heat Removal
RPV	Reactor Pressure Vessel
RVLIS	Reactor Vessel Level Indication System
RWST	Refueling Water Storage Tank
SAE	Site Area Emergency
SAMG	Severe Accident Management Guidelines
SBO	Station Blackout
SECPOP	SECtor POPulation and Economic Estimator
SG	Steam Generator
SGTR	Steam Generator Tube Rupture
SNL	Sandia National Laboratories
SOARCA	State-of-the-Art Reactor Consequence Analysis Project
SORV	Stuck Open Relief Valve
SPAR	Standardized Plant Analysis Risk
SPRA	Seismic Probabilistic Risk Assessment
SRV	Safety Relief Valve
STSBO	Short-Term Station Blackout
TAF	Top of Active Fuel
TDAFW	Turbine Driven Auxiliary Feedwater
TSC	Technical Support Center
UE	Unusual Event

1. INTRODUCTION

This document describes the detailed severe accident analyses (i.e., MELCOR and the MELCOR Accident Consequence Code System, Version 2 (MACCS2) code calculations) performed for the Surry Power Station as part of the NRC's State-of-the-Art Reactor Consequence Analyses (SOARCA) project. A separate volume of this report describes severe accident analyses for the Peach Bottom Atomic Power Station.

1.1 Background

The evaluation of accident phenomena and offsite consequences of severe reactor accidents has been the subject of considerable research by NRC, the nuclear power industry, and the international nuclear energy research community. Most recently, with Commission guidance and as part of plant security assessments, updated analyses of severe accident progression and offsite consequences were completed using the wealth of accumulated research. These analyses are more detailed in terms of the fidelity of the representation and resolution of facilities and emergency response, realistic in terms of the use of currently accepted phenomenological models and procedures, and integrated in terms of the intimate coupling between accident progression and offsite consequence models.

An insight gained from these security assessments was that updated analyses of severe reactor accidents were needed to reflect realistic estimates of the more likely outcomes considering the current state of plant design and operation and the advances in our understanding of severe accident behavior. The SOARCA project evaluates plant improvements and changes (either of which can alter safety margins) not reflected in earlier assessments. These include system improvements, improvements in training and emergency procedures, offsite emergency response, and security-related improvements, as well as plant changes such as power uprates and higher core burnup. SOARCA's more realistic modeling updates the more conservative quantifications of offsite consequences found in earlier NRC publications such as NUREG/CR-2239, "Technical Guidance for Siting Criteria Development" referred to in this report as the Siting Study.

In addition to the improvements in understanding and calculational capabilities that have resulted from these studies, numerous influential changes have occurred in the training of operating personnel and the increased use of plant-specific capabilities. These changes include:

- The transition from event-based to symptom-based Emergency Operating Procedures (EOPs) for the pressurized-water reactor designs.
- The performance and maintenance of plant-specific probabilistic risk assessments (PRAs) that cover the spectrum of accident scenarios.
- The implementation of plant-specific, full-scope control room simulators to train operators.
- An industry wide technical basis, owners group specific guidance and plant-specific implementation of the Severe Accident Management Guidelines (SAMGs).

- Use of additional safety enhancements, described in Title 10, Section 50.54(hh) of the *Code of Federal Regulations* (10CFR50.54(hh)). These enhancements are intended to be used to maintain or restore core cooling, containment, and spent fuel pool cooling capabilities under the circumstances associated with loss of large areas of the plant due to explosions or fire, to include strategies in the following areas:(i) Fire fighting;(ii) Operations to mitigate fuel damage; and (iii) Actions to minimize radiological release. For the SOARCA scenarios, successful implementation of this equipment and procedures would prevent core damage and/or delay or prevent the release.

- Improved phenomenological understanding of influential processes such as:

    - in-vessel steam explosions
    - dominant chemical forms for fission products
    - direct containment heating
    - hot leg creep rupture
    - reactor pressure vessel failure, and
    - molten core concrete interactions.

1.2 Objective

The overall objective of the SOARCA project is to develop a body of knowledge regarding the realistic outcomes of severe reactor accidents. Corresponding and supporting objectives are as follows:

- Incorporate the significant plant improvements and updates not reflected in earlier assessments including system improvements, training and emergency procedures, offsite emergency response, and recent security-related enhancements described in Title 10, Section 50.54(hh) of the *Code of Federal Regulations* (10 CFR 50.54(hh)) as well as plant updates in the form of power uprates and higher core burnup.

- Incorporate state-of-the-art integrated modeling of severe accident behavior that includes the insights of some 25 years of research into severe accident phenomenology and radiation health effects.

- Evaluate the potential benefits of recent security related mitigation improvements in preventing core damage and reducing or delaying an offsite release should one occur.

- Enable NRC to communicate severe accident related aspects of nuclear safety to stakeholders including Federal, State, and local authorities, licensees, and the public.

- Update quantification of offsite consequences found in earlier NRC publications such as NUREG/CR-2239, “Technical Guidance for Siting Criteria Development” [1].

1.3 Outline of the Report

Section 2 of this report briefly summarizes the method used to select the specific accident scenarios subjected to detailed computational analysis. Additional details of this method can be found in NUREG-1935. Section 3 describes the results of the accident scenario selection process when it was applied to Surry. Section 4 describes the key features of the MELCOR model of the Surry Power Station. Section 5 describes the results of MELCOR calculations for severe accident progression and radionuclide release to the environment from each accident scenario. Section 6 describes the process in which plant-specific emergency response actions were represented in the MELCOR Accident Consequence Code System, Version 2 (MACCS2) calculations of offsite consequences. Section 7 describes the MACCS2 code site-specific parameters and the calculations of offsite consequences for each accident scenario. References cited in this report are listed in Section 8.

2. ACCIDENT SCENARIO DEVELOPMENT

The SOARCA project considered accident sequences that have an estimated frequency greater than $1x10^{-6}$ per reactor-year (pry) operation as candidate sequences for further deterministic evaluation. It also considered sequences with frequency as low as $1x10^{-7}$ pry if they were judged to proceed rapidly enough to have the potential for generating significant early releases of radionuclides to the environment or involve a radiological transport pathway from the reactor to the environment that bypasses the containment pressure boundary (i.e., bypass sequences). Section 2.1 and Section 2.2 summarize the methods used to identify these sequences and the screening process for retaining candidate sequences.

Once candidate accident sequences were identified, the analysts evaluated realistic opportunities for plant personnel to respond to the observed failures of control and safety systems. The manner in which mitigation measures were evaluated for each accident sequence is described in Section 2.3.

The end result of this process was a list of accident scenarios (i.e., event sequence plus options for mitigation), which were subjected to detailed analysis of plant response including, as appropriate, radionuclide release to the environment described in Sections 4 and 5 and offsite radiological consequence (see Sections 6 and 7).

2.1 Sequences Initiated by Internal Events

The following scenario selection process was used to determine the scenarios for further analyses:

1. Identify candidate accident sequences were identified in analyses using plant-specific Standardized Plant Analysis Risk (SPAR) models (Version 3.31).
    a. Initial Screening – Core damage sequences with low frequencies (less than $1x10^{-8}$ pry) were eliminated from consideration. This step eliminated 4% of the overall core damage frequency (CDF) for Surry.
    b. Sequence Evaluation – Dominant cutsets for the remaining sequences were reviewed to characterize system and equipment availabilities and accident sequence timing
    c. Sequence Grouping – Sequences cutsets with similar equipment availabilities and estimated time for the onset of core damage were aggregated into a single ‘sequence group’ or ‘scenario.’

2. The availability of containment systems was evaluated using system dependency tables. These tables delineate the support systems required for containment systems to function. The status of containment systems was then appended to the accident sequence description.

3. Core damage sequences from the licensee’s PRA model were compared with the scenarios determined by using the SPAR models. Differences were resolved during meetings with licensee staff.

4. The screening criteria described above were applied to eliminate extremely low frequency sequences from further analyses.

This process identified no accident sequences that met the screening criterion of $1x10^{-6}$ pry. One sequence group, however, met the screening criterion of $1x10^{-7}$ pry for events that have the potential to result in significant early releases to the environment, the spontaneous steam generator tube rupture (SGTR) with a frequency of $5x10^{-7}$ pry.

An additional sequence was retained for analysis, namely, an interfacing systems loss-of-coolant accident (ISLOCA). The ISLOCA scenario analyzed in SOARCA is a catastrophic failure of both of the inboard isolation check valve disks within the low-head safety-injection (LHSI) piping together with failure to refill the RWST or to cross-connect to the unaffected unit's refueling water storage tank (RWST). For this ISLOCA scenario, the NRC's SPAR model calculated a CDF of $3x10^{-8}$ pry, and the NRC's initial understanding was that the licensee's PRA calculated a CDF of $7x10^{-7}$ pry. SOARCA analyses included this scenario because the licensee's PRA for Surry included an ISLOCA frequency of $7x10^{-7}$ pry and it has been commonly identified as an important contributor in PRA.

During Surry site visits on January 19, 2011, and October 26, 2011, NRC staff learned that the licensee's current PRA model has the following two ISLOCA scenarios:

- Scenario 1: Catastrophic failure of one check valve, leak-by of the second check valve, and the motor-operated isolation valve (MOV) not being able to close

- Scenario 2: Catastrophic failure of two check valves

Scenario 1 would result in a leak between 50 - 300 gallons per minute (gpm) from the RCS. Anything less than 50 gpm would be mitigated by a relief valve on the low-pressure side of the LHSI injection line; pipe rupture would not occur. The frequency of the catastrophic failure of one check valve and the leak-by of the second check valve is $1x10^{-6}$ pry. When compounded by all the potential failure modes (e.g., operator error and mechanical or electrical failures) of the MOV, that lowers the frequency of Scenario 1 to $7x10^{-7}$ pry. This frequency does not include any consideration of averting core damage by refilling or cross-connecting RWSTs. This is a significant conservatism.

Scenario 2 would result in a leak above 300 gpm from the reactor coolant system (RCS). The licensee's current PRA model assumes that the probability for the catastrophic failure of both isolation check valves is approximately $3x10^{-8}$ pry. As with Scenario 1, this frequency does not include consideration of averting core damage by refilling or cross-connecting RWSTs.

Scenario 2 does not meet the SOARCA screening criterion of $1x10^{-7}$ pry for a bypass event. However, we elected to retain it as part of SOARCA because it has been commonly identified as an important contributor in PRA.

This process provides the basic characteristics of each scenario. However, it is necessary when calculating a consistent intergrated response to have more detailed information about the scenario than is provided in a PRA model. To capture the additional sequence details, the SOARCA project conducted further analysis of system descriptions and a review of the normal and emergency operation procedures.

2.2 Sequences Initiated by External Events

External events include internal flooding and fire; seismic events; extreme wind, tornado, and hurricane related events; and other similar events that may be applicable to a specific site. The external event scenarios developed for SOARCA analysis were derived from a review of past studies such as NUREG-1150 [2], individual plant examination for external event (IPEEE) submittals, and other relevant generic information.

Seismic initiators are considered to be limiting for two principal reasons. First, seismic initiators are more likely to result in the near immediate failure of systems, whereas fire and flood would be expected to result in delayed failures. Secondly, a seismic event may be more likely to fail passive components such as water tanks where fire and flood are not. Finally, seismic initiators may be more likely to have site-wide impacts. As a result, plant and offsite response to external event sequences were assumed to be represented by an earthquake of sufficiently large magnitude to result in wide-spread damage to important plant support systems such as electric power sources.

The sequence selection process identified two sequence groups that met the screening criteria of $1x10^{-6}$ pry for containment failure events and one event that met the screening criteria of $1x10^{-7}$ pry for events that have the potential to result in significant early releases to the environment:

- long-term station blackout (LTSBO) – $1x10^{-5}$ to $2x10^{-5}$ pry
- short-term station blackout (STSBO) – $1x10^{-6}$ to $2x10^{-6}$ pry
- STSBO with thermally induced steam generator tube rupture – $1x10^{-7}$ to $8x10^{-7}$ pry. This is a bypass event, which has a screening criterion of $1x10^{-7}$ pry.

2.3 Mitigative Measures

The site-specific mitigation measures assessments were performed during visits to the Surry Power Station site in June 2007 and were supplemented by follow-up telephone conferences and correspondence with the licensee later in 2007. The licensee senior reactor operators, PRA analysts, and other licensee staff were provided the initial conditions and subsequent failures for each of the sequence groups being analyzed. The operator and plant response was subsequently evaluated to develop timelines for operator actions and equipment lineup or setup times for the implementation of the available mitigation measures. These timelines were developed assuming minimum staffing. A result of these assessment and reviews boundary conditions were used to develop the MELCOR boundary conditions that included operator actions and applicable mitigation measures.

Mitigation measures considered in the SOARCA analyses include the licensee's EOPs, SAMGs, and mitigation measures and strategies incorporated into plant capabilities in response to the terrorist events of September 11, 2001 and codified in 10 CFR 50.54(hh).

2.3.1 Mitigation of Sequences Initiated by Internal Events

The mitigation measures assessment for internal events also included mitigation measures codified in 10 CFR 50.54(hh), but these measures were subsequently shown to be redundant to the wide variety of equipment and indications available for mitigating them. The identified internal events involve few equipment failures and are controlled by postulated operator errors.

2.3.2 Mitigation of Sequences Initiated by External Events

It was noted earlier that the initiating events for external event sequences were assumed to be seismic events, because they are considered to be limiting. For these sequence groups, the seismic PRA provided information on the initial availability of installed systems. Next, judgments were made concerning the general state of the plant to assess the availability of the mitigation measures codified in 10 CFR 50.54(hh) and the additional time to implement mitigation measures and activate emergency response centers (e.g., Technical Support Center (TSC) and Emergency Operations Facility (EOF)).

The seismic events considered in SOARCA result in loss of offsite and onsite AC power (i.e., LTSBO) and, for the more severe seismic events, loss of DC power (i.e., STSBO). Under these conditions, the use of the turbine driven auxiliary feedwater (TDAFW) system is an important mitigation measure. Diverse procedures have been developed for PWRs, including a procedure to start and operate the TDAFW system without DC control power, which facilitates a managed response to station blackout (SBO) conditions. These procedures were discussed during site visits. This is known as TDAFW blackstart. Under 10 CFR 50.54(hh), mitigation measures also include the long-term operation of the TDAFW system without electricity (i.e., TDAFW blackrun), using a portable generator to supply indications such as steam generator level, to allow the operator to manually adjust TDAFW flow to prevent steam generator overfill and flooding of the TDAFW turbine. For a LTSBO, TDAFW can be used to cool the core until battery exhaustion. After battery exhaustion, TDAFW blackrun can be used to continue to cool the core.

The external events PRA does not describe general plant damage and accessibility following a seismic event. NUREG/CR-4334 was consulted to assess the potential viability of safety-related piping after a 1.0g peak ground acceleration (pga) event [47]. For the short-term station blackout (i.e., 0.5-1.0g pga) the damage was assumed to be sufficiently widespread such that accessibility would be difficult. The TDAFW system was judged not initially available and was judged not recovered under these circumstances prior to fuel damage (i.e., fuel damage in 3 hours) due to immediate gross rupture of the emergency condensate storage tank (ESCT). However, extrapolating results from NUREG/CR-4334, the low-head safety water injection and containment spray safety-related piping were judged to remain intact. Other studies, including a German study that physically simulated ground motion equal to 1.0g pga on an existing plant, also supported this evaluation.

In the less severe long-term station blackout (i.e., 0.3 – 0.5g pga), the TDAFW system was available initially and the low-head safety injection and safety-related containment spray piping were also judged to remain intact. The integrity of the safety-grade piping provided a connection point for a portable, diesel-driven pump to inject water into the RCS or into the containment spray systems.

The 10 CFR 50.54(hh) mitigation measures include the application of portable equipment such as portable power supplies for the instrumentation, portable diesel-driven pumps, and portable air bottles to open air-operated valves. Applicable procedures have been written to implement these mitigative measures under severe accident conditions. The portable injection equipment and the site fire truck were observed stored onsite in a structure away from the containment. A walk-down of the storage building and pathway to the plant suggested that the operators would be able to retrieve the equipment following a seismic event.

The time estimates to implement individual mitigation measures were provided by the licensee staff for each sequence group based on the sequence descriptions provided by the NRC. The time estimates take into account the plant conditions following the seismic event. The time estimates reflect exercises run by licensee staff that provided actual times to move and connect the portable, diesel-driven pump. The time estimates for staffing the TSC and the EOF also were provided by licensee staff and reflect the possible effects of the seismic event on roads and bridges.

The mitigation measures assessment noted the possibility of bringing in equipment from offsite (e.g., fire trucks, pumps and power supplies from sister plants or from contractors), but it did not quantify the types, amounts, and timing of this equipment arriving and being implemented.

3. ACCIDENT SCENARIO DEFINITIONS

Sections 3.1 and 3.2 describe the long-term and short-term station blackouts scenarios, respectively, which were initiated by a seismic event. The spontaneous SGTR and ISLOCA accident scenarios are described in Sections 3.3 and 3.4 respectively, which were internal events initiated by piping failures. Each Section describes the initiating event, the available systems, the pertinent mitigative actions, and the detailed initial and boundary conditions for the severe accident code calculations. Section 3.5 provides discussion on the Surry Seismic PRA Study and how it compares to the SOARCA project.

3.1 Long-Term Station Blackout

The LTSBO is initiated by an earthquake (i.e., 0.3–0.5g peak ground acceleration - pga). It has an estimated frequency of $1x10^{-5}$ to $2x10^{-5}$ pry, which meets the SOARCA screening criterion of $1x10^{-6}$ pry.

Section 3.1.1 describes the initial status of the plant following the seismic event. The key system availabilities normally accessible during the course of the accident are summarized in Section 3.1.2. The pertinent mitigative measures available to address the accident progression are described in Section 3.1.3. Section 3.1.4 describes two scenarios that differ in the assumed success (or failure) of the mitigative actions. Mitigated scenarios are defined as those in which the mitigative actions are successful. Unmitigated scenarios are defined in which certain key mitigative measures are not successfully implemented.

For station blackout scenarios, boiling in the reactor coolant pump (RCP) seal could cause the spring-loaded part of the seal to pop open and stay open. As such, MELCOR modeling for Surry includes seal failure when conditions in the seal approach saturation. The hole size for this failure mode is that which produces a 180 gpm per pump flow rate at normal RCS temperature and pressure. Also, it has been hypothesized that seal failure could occur as early as 13 minutes into a station blackout scenario due to the loss of seal cooling. Seal cooling requires AC power. The conditional probability of this early seal failure (i.e., as early as 13 minutes) has been estimated by the industry to be 0.2 [36]. Applying this 0.2 probability to the Surry LTSBO scenario frequency of $1x10^{-5}$ to $2x10^{-5}$ pry results in an event frequency of $2x10^{-6}$ to $4x10^{-6}$ pry, which meets the SOARCA screening criteria of $1x10^{-6}$ pry. While seal failure could occur as early as 13 minutes into the scenario and could include seal failures in as many as all 3 RCPs, such early and multiple seal failures are less likely than single seal failures and would have a lower probability. However, to examine the potential range of system response, the project staff analyzed with MELCOR, LTSBO mitigated and unmitigated sensitivity cases assuming that the seals of all 3 RCP seals failed 13 minutes into the scenario.

3.1.1 Initiating Event

The seismic event results in the loss of offsite power and failure of onsite emergency AC power resulting in an SBO event where neither onsite nor offsite AC power are recoverable. All systems dependent on AC power are unavailable, including the containment systems (i.e., containment spray and fan coolers). In the long term, the loss of the TDAFW pump may occur due to battery depletion, deletion of the water source and loss of DC power for sensing and

control or deletion of the water source (i.e., the ECST). Nominal RCP leakage occurs due to the loss of pump seal cooling (i.e., initially 21 gpm per pump at normal operating pressure and temperature). The unmitigated and mitigated base cases include the potential for a later thermal-mechanical RCP seal failure. In addition, unmitigated and mitigated sensitivity cases are performed that include an early RCP seal failure (i.e., at 13 minutes).

3.1.2 System Availabilities

The TDAFW pump is available until the ECST empties. The station batteries give instrumentation until they exhaust. Batteries typically last for approximately 2 to 8 hours under normal loading conditions depending on the life cycle of the batteries[2]. At the beginning of its life, the battery duration is 8 hours. At the end of its life, the battery duration is 2 hours. It was assumed that the battery life for a seismic-initiated LTSBO was 8 hours due to the minimum loading conditions caused by the initiating event and the minimum loading expected throughout the event due to the limited equipment available. The secondary system power operated relief valves (PORVs) are initially available for a manual 100°F/hr system cooldown. The secondary system PORVs are assumed to close following battery failure. No other systems are available.

3.1.3 Operator Actions and Mitigative Measures

The LTSBO event results in the loss of offsite and onsite AC power. Under these conditions, the TDAFW pump is an important mitigation measure. The TDAFW pump is used to cool the core until battery exhaustion. After battery exhaustion, blackrun of the TDAFW pump is used to remove heat from the primary system.

The external events PRA does not describe general plant damage and accessibility following a seismic event. The damage was assumed to be widespread and accessibility to be difficult, consistent with the unavailability of many plant systems. The ECST initially supplies the TDAFW pump but has finite resources (i.e., empty in 5 hours). However, assuming successful mitigation, it was assessed that the operators would have adequate time, access, and resources to make up water for injection.

The low-head safety injection and safety-related containment spray piping were judged not likely to fail for this scenario. The integrity of this piping provided a connection point for a portable, diesel driven pump to inject into the RCS. Licensee staff estimated that transporting the pump and connecting it to plant piping takes about two hours. Hence, the availability of the vessel injection was assessed to occur at 3.5 hours, or 2 hours after the action was recommended by the operators and support staff. Companion unmitigated analyses were also performed to quantify the response without successful mitigation by portable pumps.

In summary, the following actions are credited in the mitigated scenario calculations:

[2] The Surry DC station batteries are required to last for 2 hours. Initially, the licensee estimated a best-estimate life of 8 hours. Following completion of the analysis, 6 hours was thought to be more realistic. However, the ECST ran out of water at 5 hours and stopped the TDAFW pump. Consequently, the most significant benefit of the station batteries failed at 5 hours, which was less than the best-estimate battery life.

- Provide vessel injection using a portable, high-pressure, diesel driven (Kerr) pump through three drain lines on the low head safety injection (LHSI) piping

- Use portable air bottles to operate the steam generator power operated relief valves, which allows for depressurization and cooldown of the RCS

- A portable power supply is used to restore SG and RCS level indication

- Manual operation of the TDAFW pump without DC power is credited

- A portable, diesel driven, low-pressure (Godwin) pump is used to supply water to the fire header. The firewater can then be supplied via fire hose to the AFW pumps.

While not used in the mitigated scenario calculations, the following additional mitigative measures were identified as additional options for consideration.

- Use firewater or pumper truck for cooloing the charging pump oil cooler
- Use an alternative power source for high-head safety injection pump RCS makeup.

3.1.4 Scenario Boundary Conditions

Section 0 lists the sequence of events in the mitigated LTSBO calculation. Section 3.1.4.2 summarizes the sequence of events in the unmitigated LTSBO calculation. Mitigated and unmitigated sensitivity cases were also performed that include an early failure of the RCP seals.

3.1.4.1 Mitigated Cases

There is one mitigated base case and one mitigated sensitivity case. The mitigated sensitivity case includes an early failure of the RCP seal on all three pumps. The boundary conditions for the two cases are listed below.

Mitigated Case (using portable mitigation equipment)

Event Initiation

- Loss of offsite power followed by a station blackout

- The reactor trips and the MSIVs close

- The DC buses are available, at minimum loading, currently being used for instrumentation, PORV operation, and TDAFW operation

- The TDAFW system auto-initiates providing make-up to the steam generators

- The TDAFW system takes suction water from the ECST

- RCP seal leakage begins at 21 gpm per pump. The RCP seals may subsequently fail due to high temperatures causing a leak of 182 gpm per pump (see Section 4.1 for a description of the failure model).

- Emergency core cooling systems (ECCSs) are inoperable

- Containment cooling systems are inoperable

- Containment is isolated

- Recovery of offsite power is not expected during the mission time

15 minutes

- Initial Operations assessment of plant status complete, initiate the following actions:
    - Attempt manual start of EDGs
    - Operation of SG PORVs available for 30 minutes using a dedicated internal battery for RCS pressure control

- Station batteries are available

- Steam Generator (SG) level being maintained by AFW, RCS is cooling down, no RCS makeup currently available

1 hour

- Manual start of EDGs assumed to be unsuccessful due to initiating event

- The TSC is manned and operational. The primary function of the TSC would be to review initiating event, plant status, and operator action to provide guidance on alternative mitigation measures.

1.5 hours

- The offsite EOF is manned. The primary function of the EOF would be to review initiating event, plant status, and operator action to provide guidance on alternative mitigation measures. The TSC staff members are the primary users of SAMGs and mitigation measures codified in 10 CFR 50.54(hh). Shift supervisors and TSC supervisors are trained on these procedures.

- Operations initiate a controlled depressurization of the SGs to approximately 120 psi to achieve an RCS cooldown of $< 100^{o}$F per hour by manually opening the SG PORVs

- TSC and EOF review actions taken by Operations and determine the availability of the portable, diesel-driven pumps and the station pumper truck stored outside the protected area. Recommend the following actions:
    - Connect the portable, high-pressure, diesel-driven (Kerr) pump to three drain lines of the LHSI piping for RCS makeup and use portable air bottles for manual operation of primary system PORVs, as needed

- Hook up portable power supply to power instrumentation
- Use the 2 firewater storage tanks (250,000 gallons per tank), the portable, low-pressure, diesel-driven (Godwin) pump, and the fire pumper truck to supply water via the firewater system for AFW suction, if necessary
- Setup to provide the firewater system or a portable, low-pressure, diesel-driven (Godwin) pump to the containment spray header in preparation for containment cooling

1.75 hours

- Operations assesses and concurs with TSC and EOF recommendations. Operations prioritizes recommendation based on plant conditions and begins implementation.

3.5 hours

- The Kerr pump provides emergency 65 gpm makeup flow to the RCS[3,4]
- A portable power supply provides power to the instrumentation
- TDAFW pump maintaining SG level
- Pre-staging and lineups are ongoing for other mitigation measures:
  - Setup to provide the firewater system or a portable, low-pressure, diesel-driven (Godwin) pump to the firewater system in preparation for containment cooling
  - Use the 2 firewater storage tanks (250,000 gallons per tank), the portable, low-pressure, diesel-driven (Godwin) pump, and the fire pumper truck to supply water via the firewater system for AFW suction, if necessary

Mitigated Case (using portable mitigation equipment) + early RCP seal failure

Identical sequence of events as the unmitigated base case but includes an early RCP seal failure at 13 minutes.

13 minutes

- All three RCP seals fail and leak at a nominal rate of 182 gpm per pump

[3] An effective flowrate of 65 gpm at 500 rpm was determined using pump data provided by the Kerr Pump Corporation that includes 95% and 92% mechanical and volumetric efficiencies.

[4] Per SOARCA request in August 2010, Surry sent a timeline to connect the Kerr pump. The timeline showed 30 minutes to recognize the event and perform the initial damage assessment per procedures. At 30 minutes, Operations would begin deploying the Kerr pump and be ready for injection at 150 minutes from the initiating event. It was recognized that post-seismic conditions could complicate the process. The start of injection at 3.5 hours versus 150 min includes a 1-hour conservatism.

3.1.4.2 Unmitigated Cases

There is one unmitigated base case and one unmitigated sensitivity case. The unmitigated sensitivity case includes early failures of the RCP seals. The boundary conditions for the two cases are listed below.

Unmitigated Case (without portable mitigation equipment)

Event Initiation

- Loss of offsite power followed by a station blackout
- The reactor trips and the main steam isolation valves (MSIVs) close
- The DC buses are available, at minimum loading, currently being used for instrumentation, PORV operation, and TDAFW system operation
- The TDAFW system auto-initiates providing make-up to the SGs
- The TDAFW system takes suction water from the ECST
- RCP seal leakage begins at 21 gpm per pump. The RCP seals may subsequently fail due to high temperatures causing a leak of 182 gpm per pump (see Section 4.1 for a description of the failure model).
- ECCSs are inoperable
- Containment cooling systems are inoperable
- Containment is isolated
- Recovery of offsite power is not expected during the mission time

15 minutes

- Initial Operations assessment of plant status complete, initiate the following actions:
    - Attempt manual start of EDGs
    - Operation of SG PORVs available for 30 minutes using a dedicated internal battery for RCS pressure control
- Station batteries are available
- The SG level is being maintained by AFW, RCS is cooling down, no RCS makeup currently available

1 hour

- Manual start of EDGs assumed to be unsuccessful due to initiating event

- The TSC is manned and operational. The primary function of the TSC would be to review the initiating event, plant status, and operator action to provide guidance on alternative mitigation measures.

1.5 hours

- The EOF is manned. The primary function of the EOF would be to review initiating event, plant status, and operator action to provide guidance on alternative mitigation measures. The TSC staff members are the primary users of SAMGs and mitigation measures codified in 10 CFR 50.54(hh). Shift supervisors and TSC supervisors are trained on these procedures.

- Operations initiate a controlled depressurization of the SGs to approximately 120 psi to achieve an RCS cooldown of <100°F per hour by manually opening the SG PORVs

- The TSC and EOF review actions taken by Operations and determine the availability of the portable, diesel-driven pumps and the station pumper truck stored outside the protected area. Recommend the following actions:
    - Connect the portable, high-pressure, diesel-driven (Kerr) pump to three drain lines of the LHSI piping for RCS makeup and use portable air bottles for manual operation of primary system PORVs, as needed.
    - Hook up portable power supply to power instrumentation
    - Use the 2 firewater storage tanks (250,000 gallons per tank), the portable, low-pressure, diesel-driven (Godwin) pump, and the fire pumper truck to supply water via the firewater system for AFW suction, if necessary
    - Setup to provide the firewater system or a portable, low-pressure, diesel-driven (Godwin) pump to the containment spray header in preparation for containment cooling

1.75 hours

- Operations assesses and concurs with TSC and EOF recommendations. Operations prioritizes recommendations based on plant conditions.

>1.75 hours

- All mitigative actions are unsuccessful including connecting a portable, diesel-driven pump for vessel injection, refilling the water supply for the TDAFW (i.e., the ECST), and maintaining instrumentation using a portable power supply

8 hours

- DC station batteries are exhausted[5]
- SG PORVs reclose
- Loss of control and instrumentation for the TDAFW

[5] The Surry DC station batteries are required to last for 2 hours. Initially, the licensee estimated a best-estimate life of 8 hours. Following completion of the analysis, 6 hours was thought to be more realistic. However, the ECST ran out of water at 5 hours and stopped the TDAFW pump. Consequently, the most significant benefit of the station batteries failed at 5 hours, which was less than the best-estimate battery life.

Unmitigated Case (without portable mitigation equipment) + early RCP seal failure

Identical sequence of events as the unmitigated base case but includes an early RCP seal failure at 13 minutes.

13 minutes

- All three RCP seals fail and leak at a nominal rate of 182 gpm per pump

3.2 Short-Term Station Blackout

The STSBO is initiated by an earthquake (0.5–1.0g pga). It is more severe than the LTSBO and has an estimated frequency of $1x10^{-6}$ to $2x10^{-6}$ pry, which meets the SOARCA screening criterion of $1x10^{-6}$ pry.

Section 3.2.1 describes the initial status of the plant following the seismic event. The key system availabilities during the course of the accident are summarized in Section 3.2.2. The pertinent mitigative measures available to address the accident progression are described in Section 3.2.3. Section 3.2.4 describes two scenarios that differ in the assumed success (or failure) of the mitigative actions. Mitigated scenarios are defined as those in which mitigative actions are successful. Unmitigated scenarios are defined as those in which certain key mitigation measures are not successfully implemented. In addition, mitigated and unmitigated scenarios are defined that include a thermally-induced steam generator tube rupture (TI-SGTR).

3.2.1 Initiating Event

The seismic event results in a loss-of onsite power and failure of onsite emergency AC power resulting in a SBO event where neither onsite nor offsite AC power are recoverable. All systems dependent on AC power are unavailable, including all active ECCSs and the containment engineered safety systems (e.g., the containment sprays and fan coolers). The seismic event also causes a loss of DC power, which makes it impossible to remotely control the TDAFW pump. The RCS and containment are undamaged and the containment is isolated. No instrumentation is available. Significant structural damage is judged to have occurred, including structural failure of the turbine building and loss of access to the condenser blow down valves. Additionally, the seismic event has caused a failure of the ECST, the source of water for the TDAFW system. Auxiliary building accessibility is difficult, due to fallen piping and cabling, steam and water leaks, and damaged stairways. Following the loss of the seal cooling flow, the RCP seals will nominally leak at 21 gpm (i.e., at normal operating pressure and temperature). The RCP seals may fail later in the accident if the RCP seal region heats to saturated conditions.

Both unmitigated and mitigated sensitivity cases are performed that include a TI-SGTR(s). Thermally-induced steam generator tube ruptures are a known risk contributor and have been investigated by industry and the NRC. The SBO has an estimated frequency of $1x10^{-6}$ to $2x10^{-6}$ pry, and the conditional probability of tube rupture have been estimated by the NRC to be in the range of 0.1 to 0.4 [34]. Therefore, the overall frequency of this sequence group is $1x10^{-7}$ to $8x10^{-7}$ pry, which meets the SOARCA screening criterion of $1x10^{-7}$ pry for bypass events. In the context of the short-term station blackout sequence evaluations, sensitivity studies are performed to examine the response with a TI-SGTR.

3.2.2 System Availabilities

Systems available include the ECCS accumulators, portable power supplies, portable air bottles, and portable high-pressure (Kerr) and low-pressure (Godwin) diesel driven pumps. Containment spray and firewater piping is assumed to remain intact.

3.2.3 Mitigative Actions

The TDAFW system was assumed not to be available initially and was judged not recovered under these circumstances prior to fuel damage (i.e., fuel damage in 3 hours) due to immediate gross rupture of the ECST and lack of alternative suction sources that could be aligned within 3 hours. However, there was significant time, access, and resources to establish containment sprays with the portable emergency pump by 8 hours. This action both mitigates the release and delays containment failure.

NUREG/CR-4334 was consulted to assess the potential viability of safety-related piping after a 1.0g pga event [47]. Extrapolating results from NUREG/CR-4334, the low-head safety water injection and safety-related containment spray piping were judged to remain intact. Other studies, including a German study that physically simulated ground motion equal to 1.0g pga on an existing plant, also supported this evaluation. The integrity of the safety-grade piping provided a connection point for a portable, diesel-driven pump to inject water into the RCS or into the containment spray systems. The licensee staff estimated that transporting the pump and connecting it to plant piping takes about two hours. Because of difficult accessibility, the set-up of the containment spray system following a large seismic event was assumed to require 8 hours. Hence, water provided to the diesel-driven portable emergency pump was assumed to be available only after vessel failure (i.e., the MELCOR results indicate 3 hours to core damage and 7 hours to lower head failure). Thus, it was provided only to the containment sprays. Additional unmitigated analyses were performed to quantify the response without successful mitigation by a portable pump.

3.2.4 Scenario Boundary Conditions

Section 3.2.4.1 lists the sequence of events in the unmitigated STSBO calculation.
Section 3.2.4.2 summarizes the sequence of events in the mitigated STSBO calculation that credits one additional manual action. Sensitivity cases for the mitigated and unmitigated TI-SGTRs are also described.

3.2.4.1 Unmitigated Cases

There is one unmitigated base case and two unmitigated sensitivity cases. The unmitigated sensitivity cases include thermally induced steam generator tube ruptures prior to creep rupture in any other RCS location. Since the sensitivity cases include a stuck open secondary system relief valve, there is an open containment bypass pathway to release radionuclides to the environment. In the base case, the secondary system relief valve closes when the pressure falls below the closing setpoint. Additionally, operators are assumed to not connect the portable, diesel driven (Godwin) pump in all three cases.

Unmitigated base case

Event Initiation

- Loss of offsite power followed by the failure of all diesel generators and a station blackout
- Successful reactor trip and Main Steam isolation Valves (MSIVs) close
- RCS and containment are undamaged and the containment isolates
- Failure of TDAFW system due to failure of the ECST
- An early RCP seal failure during subcooled conditions is not included in this scenario, but late RCP seal failures may occur (see Section 4.1 for a discussion on RCP seal failure)
- Active ECCS equipment is inoperable due to electrical and system damage
- Containment cooling systems are inoperable due to electrical and system damage
- Recovery of offsite and onsite power is not expected during the mission time

30 minutes

- Initial Operations assessment of plant status complete; Operations initiates the following action:
  - Attempt manual start of the EDGs and SBO diesel generator
- RCS pressure being maintained by code safety valves, PORVs not currently available because of loss of instrument air and backup air

1 hour

- Manual start of EDGs and SBO diesel generator assumed to be unsuccessful due to initiating event
- Offsite EOF is manned. The primary function of the EOF is review of initiating event, plant status, and operator action to provide guidance on alternative mitigation measures. The TSC staff members are the primary users of SAMGs and mitigation measures codified in 10 CFR 50.54(hh). Shift supervisors and TSC supervisors are trained on these procedures.

1.5 hours

- Offsite EOF reviews actions taken by operations. Recommend the following actions:
  - Connect portable power supply for instrumentation
  - Connect the portable, high-pressure, diesel-driven (Kerr) pump to three drain lines of the LHSI piping for RCS makeup and use portable bottles for manual operation of SG PORVs, as needed
  - Connect the portable, diesel-driven (Godwin) pump for containment spray or containment flooding

1.75 hours

- Operations assesses and concurs with offsite EOF recommendations. Operations prioritizes recommendations based on plant conditions and begins implementation.

2 hours

- The TSC is manned and operational. Because of the magnitude of the seismic event, a one-hour delay in reporting of TSC members was assumed. The primary function of the TSC would be to review the initiating event, plant status, and operator action to provide guidance on alternative mitigation measures.

- EOF is manned and operational

3.5 hours

- Determine the availability of the portable, diesel-driven (Godwin) pump, portable air bottles, and portable power supply

- Portable air bottles connected to the steam generator PORVs are available for depressurizing RCS

- The portable diesel-driven pumps are being positioned and the connections are being assessed

>6.5 hours

- Unable to connect portable injection systems
- No other mitigation attempts are successful

Unmitigated sensitivity cases with TI-SGTRs

The unmitigated sensitivity cases have an identical sequence of events as the unmitigated base case but include a stuck open relief valve on the secondary side that leads to a TI-SGTR.

3 hours

- The lowest-pressure safety relief valve sticks open on the steam generator with the tube rupture

At a time calculated by MELCOR to be 3 hr 33 min

- A TI-SGTR is assumed to occur when the hot leg C cumulative creep damage index exceeds 5%. A hot leg creep rupture index of 100% is used to predict hot leg failure. Consequently, the TI-SGTR is specified to occur prior to hot leg creep rupture failure.
    - Sensitivity Case 1 – rupture area is the equivalent of 100% of the tube flow area
    - Sensitivity Case 2 – rupture area is the equivalent of 200% of the tube flow area

3.2.4.2 Mitigated Cases

There is a mitigated base case and a mitigated sensitivity case, both involving the use of a diesel driven (Godwin) pump for containment sprays. The mitigated sensitivity case includes a thermally induced steam generator tube rupture prior to any other RCS creep rupture failure. Since the sensitivity case includes a stuck open secondary system relief valve, there is an open containment bypass pathway to release radionuclides to the environment. In the base case, the secondary system relief valve closes when the pressure falls below the closing setpoint.

Mitigated base case

Event Initiation

- Loss of offsite power followed by a station blackout
- Successful reactor trip and MSIVs close
- RCS and containment undamaged and the containment isolated
- Failure of TDAFW pump due to failure of the ECST
- An early RCP seal failure during subcooled conditions is not included in this scenario, but late RCP seal failures may occur (see Section 4.1 for a discussion on RCP seal failure)
- ECCSs are inoperable due to electrical and system damage
- Containment cooling systems are inoperable due to electrical and system damage
- Recovery of offsite power is not expected during the mission time

30 minutes

- Initial Operations assessment of plant status complete; Operations initiates the following action:
    - Attempt manual start of EDGs and SBO diesel generator
- The RCS pressure is maintained by code safety valves. The pressurizer PORVs are not currently available because of loss of instrument air and backup air.

1 hour

- Use portable power supply to restore minimum instrumentation (e.g., RCS level, RCS pressure, SG level)

- Manual start of EDGs and SBO diesel generator assumed to be unsuccessful due to initiating event

- The EOF is manned. The primary function of the EOF would be to review initiating event, plant status, and operator action to provide guidance on alternative mitigation measures. The TSC staff members are the primary users of SAMGs and mitigation measures codified in 10 CFR 50.54(hh). Shift supervisors and TSC supervisors are trained on these procedures.

1.5 hours

- Offsite EOF reviews actions taken by operations. Recommend the following actions:
  - Maintain portable power supply for instrumentation
  - Connect the portable, high-pressure, diesel-driven (Kerr) pump to three drain lines of the LHSI piping and use portable bottles for manual operation of SG PORVs, as needed
  - Connect the portable, diesel-driven (Godwin) pump for containment spray or containment flooding

1.75 hours

- Operations assesses and concurs with offsite EOF recommendations. Operations prioritizes recommendations based on plant conditions and begins implementation.

2 hours

- The TSC is manned and operational. Because of the magnitude of the seismic event, a one-hour delay in reporting of TSC members was assumed. The primary function of the TSC would be to review the initiating event, plant status, and operator action to provide guidance on alternative mitigation measures.

- EOF is manned and operational

3.5 hours

- Determined the availability of the remotely located portable, diesel-driven (Godwin) pump, portable air bottles, and portable power supply

- Portable air bottles to the steam generator PORVs are available for depressurizing RCS

- The portable diesel-driven pumps are being positioned and the connections are being assessed.

8 hours

- The portable, diesel-driven (Godwin) pump is staged at the discharge canal and pumps water through the established piping and into the fire protection system. Fire hose would take the water from the hydrants to the special fitting on the containment spray pumps.[6]

Mitigated case with TI-SGTR

The mitigated sensitivity case has an identical sequence of events as the mitigated base case but includes a stuck open relief valve on the secondary side that leads to a TI-SGTR.

3 hours

- The lowest-pressure safety relief valve sticks open on the steam generator with the tube rupture.

At a time to be calculated by MELCOR (which was 3 hr 33 min)

- A TI-SGTR is assumed to occur when the hot leg C cumulative creep damage index exceeds 5%. A hot leg creep rupture index of 100% is used to predict hot leg failure. Consequently, the TI-SGTR is specified to occur prior to hot leg creep rupture failure.

- The steam generator tube rupture area is the equivalent of 100% of the tube flow area

3.3 Spontaneous SGTR

Section 3.3.1 describes the initial status of the plant following the tube rupture. The key system availabilities during the course of the accident are summarized in Section 3.3.2. The pertinent mitigative measures available to address the accident progression are described in Section 3.3.3. Section 3.3.4 delineates various scenarios based on the success of the mitigative actions. In particular, a mitigated scenario is defined where the mitigative actions are successful. Two unmitigated scenarios are also defined where certain key operator actions are not successfully performed.

3.3.1 Initiating Event

This sequence group consists of a spontaneous rupture of a steam generator tube equivalent to 100% of the tube flow area, 0.47 in^2. The leak is assumed to occur near the steam generator inlet-side tube sheet.

3.3.2 System Availabilities

The full complement of systems is considered functional in this scenario including all systems associated with engineered safeguards and instrumentation and control as well as all auxiliary

[6] Per SOARCA request in August 2010, Surry sent a timeline to connect the Godwin pump. The timeline showed 30 minutes to recognize the event and perform the initial damage assessment per procedures. At 30 minutes, operations would begin deploying the Godwin pump and be ready for injection at 120 minutes from the initiating event. It was recognized that post-seismic conditions could complicate the process. The start of injection at 8 hours versus 2 hours includes a 6-hour conservatism.

and emergency systems. The operators fail to 1) isolate the faulted SG, 2) depressurize and cooldown the RCS, and 3) refill the RWST or cross-connect to the unaffected unit's RWST.

3.3.3 Mitigative Actions

The SPAR model and the licensee's PRA concluded that the spontaneous SGTR event proceeds to core damage because of the above errors. However, the PRA models do not appear to have credited the significant time available for the operators to correct their mistakes. They also do not appear to credit technical assistance from the TSC and the EOF. The subsequent accident simulation showed that 27 to 46 hours are available for mitigative actions before the core damage begins (see Section 5.4). Therefore, the licensee provided realistic estimates of the times by which the operators would respond to the event. These time estimates included consideration of indications that the operators would have of the bypass accident, operator training on plant procedures for dealing with bypass accidents and related drills, and assistance from the TSC and EOF, which were estimated to be manned and operational by 1 to 1.5 hours into the event.

Operator actions in this scenario are essentially those expected per training and procedure. Specifically, the operators are trained to perform the following actions to mitigate the sequence:

- Secure AFW delivery to the steam generator with the broken tube (the faulted steam generator)
- Secure 1 of the 3 total high head safety injection (HHSI) pumps
- Isolate the faulted steam generator, i.e., close the MSIVs serving the faulted steam generator
- Secure the remaining HHSI pumps once the faulted generator is isolated, which will end the RCS leakage
- Perform a 100°F/hr cool-down of the RCS
- Establish long-term cooling with residual heat removal

The following other mitigation measures were identified but not used.

- Use the pressurizer PORVs to depressurize the RCS to get an accumulator injection at low pressure
- Cross-connect to the unaffected unit's RWST
- Use firewater makeup to RWST from the firewater header at ~300 gpm from the two 300,000 gallons firewater storage tanks, then the James River
- The portable, low-pressure, diesel-driven (Godwin) pump is available to makeup to the RWST and the CST at ~2000 gpm at 120 psi

- ~190,000 gallons available from the spent fuel pool for rapid RWST makeup

- Procedures exist to align firewater to the suction of the AFW pump via installed piping and valves from firewater storage tanks and the James River

- Two portable, high-pressure, diesel-driven (Kerr) pumps are available to inject into RCS using water from the RWST at 2.5 hours (i.e., assumes guidance from TSC and EOF at 1.5 hours and an hour to implement)

3.3.4 Boundary Conditions

Section 3.3.4.2 lists the sequence of events to be prescribed in the mitigated spontaneous steam generator tube rupture where the operator successfully performs the actions described in Section 3.3.3. Section 3.4.4.1 summarizes the sequence of events in two unmitigated scenarios where the operator does not successfully perform the actions described in Section 3.3.3. The second unmitigated scenario uses the same failed operator actions but also includes the failure of the steam generator secondary system relief valve to create a sustained containment bypass pathway for fission products.

3.3.4.1 Unmitigated Cases

There are two unmitigated cases. No other successful operator actions are credited after 2.5 hours.

Unmitigated Case 1

2.5 hours

- Fail to isolate the faulted steam generator

- Fail to depressurize and cool down the RCS

- Fail to extend the available duration of ECCS injection by refilling the RWST or cross connecting to the other unit's RWST

Unmitigated Case 2

Exactly the same boundary conditions as Unmitigated Case One but include an additional equipment failure.

At a time to be calculated by the severe accident analysis code which was 44 minutes

- Fail the secondary system relief valve open when water first reaches the valve. The stuck-open valve creates an open bypass containment pathway to the environment (see *Note* below).

2.5 hours

- Fail to isolate the faulted steam generator

- Fail to depressurize and cool down the RCS

- Fail to extend the available duration of ECCS injection by refilling the RWST or cross connecting to the other unit's RWST

Note: There was some uncertainty whether water could reach the secondary system relief valve. The utility stated that the secondary system would not fill up completely due to the large volume of piping and 12 steam traps (i.e., eight 1.5" lines and four 1" lines) open to the main condenser. The MELCOR model did not represent the steam traps or steam dump valves to the condenser. The calculation conservatively neglected any leakage pathways for water from the steam line except for the cycling relief valve.

3.3.4.2 Mitigated Case

There is one mitigated base case. Although the operator initially fails to implement the correct procedures, the errors are eventually identified by the technical support groups and the correct procedures are followed. The boundary conditions are listed below.

Event Initiation

- Spontaneous tube rupture equivalent to 100% of the tube flow area (i.e., 0.47 in^2)

- The reactor trips

- The turbine stop valves automatically close

- The 8 steam dump valves automatically go to the full open position and then throttle open and close to maintain RCS T_{ave} at 547 °F

- Containment Phase 1 isolation auto-initiates

- The HHSI auto-initiates and all three pumps start and operate as designed. The operator secures one charging pump early in the event as required by procedure. The water source is the RWST (380,000 gallons).

- The one turbine-driven and two motor-driven auxiliary feedwater pumps automatically start on a low-level actuation signal. The initial water source is the ECST (110,000 gallons) but can be refilled from the CST, which has 300,000 gallons.

- Reactor coolant pumps continue to run

- Operators fail to: 1) isolate the faulted SG, 2) depressurize and cooldown the RCS, and 3) refill the RWST or cross-tie to the unaffected unit's RWST.

10 minutes

- Initial Operations assessment of plant status complete

15 minutes

- RCS level being maintained by HHSI, operator secures one of the three HHSI pumps per procedure

- Operator takes control of AFW to maintain level in the SGs

- When level in the faulted SG reaches the top of fill range, AFW flow will be stopped to that SG

30 minutes

- Damaged SG continues to fill, overflowing into the TDAFW pump turbine causing it to shut down

- The two MDAFW pumps provide makeup to non-faulted SGs

1 hour

- The TSC is manned and operational. The primary function of the TSC would be to review initiating event, plant status, and operator action to provide guidance on alternative mitigation measures.

1.5 hours

- RCS and SG levels being maintained by HHSI and AFW, respectively

- Offsite EOF is manned. The primary function of the EOF would be to review initiating event, plant status, and operator action to provide guidance on alternative mitigation measures. The TSC staff members are the primary users of SAMGs and mitigation measures codified in 10 CFR 50.54(hh). Shift supervisors and TSC supervisors are trained on these procedures.

- The TSC and EOF recognize that the damaged SG is not isolated, the operators are not implementing procedure E-3, "Steam Generator Tube Rupture" and the RCS is not being cooled down and depressurized. Recommends to the operators that they implement the following actions:
  - Implement procedure E-3
  - Isolate the damaged S/G
  - Cooldown and depressurize the RCS

1.75 hours

- Operations assesses TSC and EOF diagnoses, concurs with their determination, and implements procedure E-3,

2.5 hours

- Within 45 minutes the damaged SG is isolated, HHSI is secured, and the RCS is undergoing a normal cooldown

Event Termination

- Establish long-term cooling using the residual heat removal (RHR) system (i.e., closed-circuit cooling system)
  - RCS at 400-450 psi and ~350 ˚F for RHR entry conditions
  - Operators verify RCS is 30 ˚F sub-cooled, pressure stabilized, pressurizer level in normal band and stabilized, and non-affected SG levels in normal band and stabilized

3.4 Interfacing Systems LOCA

This sequence group is initiated by a common mode failure of both low-head safety injection (LHSI) inboard isolation check valve disks. The open pathway pressurizes and ruptures the low-pressure piping outside the containment, which opens a containment bypass LOCA. This sequence group consists of the bypass LOCA followed by operator failure to refill the RWST, or cross-connect to the unaffected unit's RWST.

Section 3.4.1 describes the initial status of the plant following the pipe rupture. The key system availabilities during the course of the accident are summarized in Section 3.4.2. The pertinent mitigative measures available to address the accident progression are described in Section 3.4.3. Section 3.4.4 describes two scenarios that differ in the assumed success (or failure) of the mitigative actions. Mitigated scenarios are defined as those in which mitigative actions are successful. Unmitigated scenarios are defined as those in which certain key mitigation measures are not successfully implemented.

3.4.1 Initiating Event

The ISLOCA initiates with failure of both of the inboard isolation check valve disks resulting in over-pressurization and failure of the LHSI discharge side piping outside of containment in the Safeguards Building. The resulting double-ended guillotine pipe break permits back-flow of the high-pressure RCS water into the Safeguards Building.[7] Water will also spill into the Safeguards Building via forward flow through the LHSI pumps to the pipe break. The broken LHSI line has a number of flow restrictions, including a 2.57" venturi between the RCS and the break that will limit the break flow.

3.4.2 System Availabilities

The full complement of systems is considered functional in this scenario including all systems associated with engineered safeguards and instrumentation and control as well as all auxiliary and emergency systems.

3.4.3 Mitigative Actions

The SPAR model and the licensee's PRA concluded that the ISLOCA proceeds to core damage. However, the PRA models do not appear to have credited the significant time available for the

[7] A double-ended break was specified in the scenario description. A detailed separate effects model of the LHSI piping was developed that included flow restrictions, bends, elevation changes and other losses. The break in the low-pressure piping was expected to occur between the end of the high-pressure piping and a third check valve. If the break was under water, it could offer some fission product scrubbing benefit. The results of the break location analyses are reported in Section 4.12.

operators to respond adequately. The PRA model also does not appear to credit technical assistance from the TSC and EOF. The more realistic analysis of thermal hydraulics in Section 5.5.3 subsequently estimated 6 hours until the RWST is empty and 13 hours until the fission product releases begin, providing considerable time for the operators to respond. The ISLOCA time estimates are based on a double-ended pipe rupture, which drains the RWST at the maximum rate.

Operator actions in this scenario are essentially those expected per training and procedure. Specifically, the operators are trained to perform the following actions to mitigate the sequence:

1. Per the Surry EOPs, only two HHSI pumps are required. All HHSI pumps will start but one is secured. Per results of the table-top scenario development with Surry operations using the emergency operating procedures, the redundant HHSI pump would be isolated in 15 minutes.

2. Per the Surry EOPs, a LOCA outside the containment would be identified and the LHSI pumps would be isolated.[8]

3. Per the Surry EOPs, the operators would isolate the leakage from the RWST side of the break into the Safeguards Building (i.e., by closing the LHSI pump suction valves). [9]

4. Per results of the table-top scenario development with Surry operations using the EOPs, the operators will take control of the AFW pumps to maintain normal level in the steam generators after 15 minutes.

5. Per results of the table-top scenario development with Surry operations, the operators will shift HHSI injection from the cold leg to the hot leg to minimize backflow leakage to the Safeguards Building by 1 hour and 45 minutes. An additional HHSI pump can be secured if an adequate water level can be maintained to minimize the spill rate into the Safeguard Building.

6. Per results of the table-top scenario development with Surry operations, the operators will start a cooldown at 1 hour. In order to minimize break flow, the operators would completely depressurize the steam generators.

The following other mitigation measures were identified but not used in the unmitigated ISLOCA calculations.

- Per the Surry EOPs, Operations would establish residual heat removal (RHR) cooling of the RCS once entry conditions are established.

[8] Per best-estimate timing for the ISLOCA in the Surry full-scope training simulator following EOPs, LHSI Pump A would be isolated in 6 minutes and 17 seconds and the LHSI Pump B would be isolated at 15 minutes and 44 seconds. Surry Operations obtained these timings from a training exercise that simulated the initial portion of the subject ISLOCA.

[9] Per best-estimate timing for the ISLOCA in the Surry full-scope training simulator following EOPs, the LHSI pump suction would be isolated in 16 minutes and 18 seconds. Surry Operations obtained these timings from a training exercise that simulated the initial portion of the subject ISLOCA.

- The RWST can be refilled using firewater makeup from the firewater header at ~300 gpm from two 250,000 gallon firewater storage tanks, then from the James River.

- The portable, low-pressure, diesel-driven (Godwin) pump is available to makeup to the RWST and the CST at ~1200 gpm

- 190,000 gallons available from the spent fuel pool are available for rapid RWST makeup

- Operations could align the unaffected unit's HHSI pumps and RWST to the affected unit through a series of operator actions.[10]

3.4.4 Boundary Conditions

Section 3.4.4.1 lists the sequence of events to be prescribed in the unmitigated ISLOCA, which credits all operator actions identified in Section 3.3.3, but does not credit any of the additional mitigative actions identified at the end of the section (e.g., RHR). Section 3.4.4.2 summarizes the sequence of events in the mitigated ISLOCA, which credits additional operator actions.

3.4.4.1 Unmitigated Interfacing Systems LOCA

Event Initiation

- The LHSI inboard isolation check valves fail causing a pipe break in the low pressure piping in the Safeguards Building

- The reactor trips on low pressure

- Containment Phase-1 isolation auto-initiates

- All three HHSI pumps auto-initiate on the ECCS injection signal.

- LHSI initiates on the ECCS injection signal, which pumps water into the Safeguards Building through the pipe break until the LHSI pump motors become submerged or are isolated

- The MSIVs close

- The RCPs trip or are shutdown once two-phase conditions develop at the pump

- The one turbine-driven and two motor-driven auxiliary feedwater pumps automatically start on a low-level actuation signal. The initial water source is the ECST (110,000 gallons) but can be refilled from the CST, which has 300,000 gallons.

[10] The shift to the unaffected unit's HHSI and RWST is not in the normal emergency procedures but is well known to the operators and is a redundant design feature of the Surry ECCS. Since it would temporarily affect the other unit's resources, it is a 10CFR50.54 decision (i.e., a directive that the operators can go outside of their procedures if necessary to ensure the safety of the plant).

3 minutes

- The LHSI outboard isolation valve (i.e., Valve 1890C) is flooded and becomes inaccessible. This flooding is shown in the MELCOR results in Section 5.5. Therefore, the ISLOCA cannot be isolated from the RCS.

5 minutes

- Initial Operations assessment of plant status is complete. A LOCA outside the containment identified.

6 minutes 18 sec

- LHSI Pump A is isolated

15 minutes

- 3 HHSI pumps confirmed as running, one pump is isolated

15 minutes and 44 seconds

- LHSI Pump B is isolated

16 minutes and 18 seconds

- Operations isolate the LHSI pump suctions. The action ends the RWST spillage to Safeguards Building.

45 minutes

- Operations transfers HHSI injection to the RCS hot legs

50 minutes

- The TSC is manned. Primary function would be to review initiating event, the plant status, and the operator action to provide guidance on alternative mitigation measures. The TSC staff is the primary users of SAMGs and extreme damage mitigation guidelines (EDMGs). Shift supervisors and TSC supervisors are trained on SAMGs and EDMGs.

- The EOF is manned. Primary function would be to review the initiating event, the plant status, and the operator action to provide guidance on alternative mitigation measures.

1 hour

- Operators begin RCS cooldown

1.25 hours

- The TSC is operational

1.5 hours

- The EOF is operational

- The TSC and EOF review and concur with actions taken by operations. They recommend:

- Using RHR to terminate the accident
- Refilling the RWST
- Reducing the RWST draindown by terminating another HHSI if level can be maintained above the top of active fuel
- Shifting to the unaffected unit's RWST, if necessary, to maintain injection.

1.75 hours

- Secure second HHSI pump

>1.75 hours

- Operations do not successfully implement any further mitigative actions. All injection will terminate when the RWST empties.

3.4.4.2 Mitigated Interfacing Systems LOCA

The mitigated case has an identical sequence of events until 1.75 hours, the time assessed to implement the TSC and EOF recommendations. The operator successfully initiates the following actions, starting at 1.75 hours.

1.75 hours

- Operations assesses TSC and EOF recommendation to lineup the unaffected unit's RWST to provide makeup to the RWST while continuing to provide RCS makeup with the same RWST.

- Operations reviews and prepares to swap HHSI flow to unaffected unit's RWST, if necessary. At 1.75 hours, approximately 160,000 gallons are still available.

  Note: The HHSI pumps could trip off line if the Auxiliary Building is allowed to flood to approximately 5 feet above the Auxiliary Building basement floor without mitigation measures. The volume of the Auxiliary Building basement that will result in flooding of the HHSI pumps is 530,000 gallons. Another mitigation option is to use portable submersible pumps to pump out the Auxiliary Building basement to preclude flooding of the HHSI pumps. This option is recognized by the licensee but is not included in plant procedures.

- Operations recommends establishing long-term cooling using the RHR system per emergency operating procedures (i.e., closed-circuit cooling system)

- Secure 3rd HHSI when level is stable and RHR cooling is established

3.5 Surry Seismic PRA Study

Late in the SOARCA project, well after the process of scenario selection and accident analysis was completed, the team became aware of a new relevant seismic PRA (SPRA) study that was conducted for the Surry plant. This study, entitled *Surry SPRA Pilot Plant Review*, was sponsored by the Electric Power Research Institute (EPRI), Simpson Gumpertz and Heger (SGH) and Dominion Resources. The objectives of the study were:

- To evaluate the process and requirements involved in updating a seismic PRA originally developed for the IPEEE program in order to meet the intent of the new ASME/ANS Level 1 Seismic PRA Standard for Capability Category II [75], and

- To review the requirements of the seismic PRA standard for clarity and reasonableness given the current state of the art in performing seismic PRAs.

The Surry SPRA study started with the Surry seismic assessment developed for the IPEEE and updated various elements of that seismic assessment in order to meet the author's interpretation of the requirements in the new ASME/ANS Seismic PRA Standard. While the Surry SPRA study represents an updated examination of the Surry plant, including a new seismic hazard and calculation of the site response to the new hazard, the primary purpose of the Surry SPRA study was to examine issues attendant to implementation of the new ASME/ANS Standard. Surry served as a representative plant for the SPRA study. In some instances not essential to the objective of the Surry SPRA study, the evaluation relied upon generic or expected fragility parameters that may be different from the Surry-specific values. Thus, the CDF and the large early release frequency (LERF) results presented in the Surry SPRA study may not be reflective of the Surry plant. Nevertheless, certain results and assumptions in this SPRA study may have a bearing on the SOARCA project.

The Surry SPRA study produced a total CDF, which is comparable to the CDF of the SOARCA external events on the order of $2x10^{-5}$/yr, and the risk profile peaks at a seismic interval corresponding to approximately 0.4g pga. However, the dominant scenario, comprising 50% of the total CDF, was identified as a loss of service water (LOSW). Such an event was not analyzed in SOARCA and thus some discussion of its significance relative to SOARCA events is needed.

The LOSW event in the Surry SPRA study occurs as a result of failure of the turbine building's steel superstructure that is assumed to damage the cables that power the circulating water isolation valves leaving the valves in the open position. With the valves in the open position, the intake canal, the source of service water, gravity drains because the seismic event causing a loss of offsite power which causes failure of the circulating water pumps which supply the intake canal. The intake canal is estimated to drain in a time interval ranging from 45 minutes to 6 hours, depending on the number of circulating water isolation valves assumed to fail open. The intake canal is the ultimate heat sink for the plant. Thus, its loss results in a loss of the component cooling water system, which cools high-pressure injection pumps and reactor coolant pump seals. The timing of core damage is not specified in the Surry SPRA study other than to note that recovery of offsite power is not expected within the 24-hour mission time. In addition, the Surry SPRA study assumes the ECST and the fire protection water tanks are not available due to their low capability to withstand seismic loading. If indeed these tanks are assumed to fail catastrophically this would result in immediate loss of auxiliary feedwater (AFW) unless other sources of water for the AFW system can be aligned.

In terms of frequency, the LOSW described in the Surry SPRA study most closely matches the SOARCA scenario described as a long-term SBO (i.e., $2x10^{-5}$/yr). In certain respects, the

LTSBO scenario may qualitatively serve as a surrogate for the LOSW event. In both instances, the plant is undergoing a loss of heat removal transient with potential reactor coolant pump seal leakage. If the intake canal does not drain for several hours then the availability of service water together with injection capability (e.g., feed and bleed) may delay core damage in much the same way that AFW delays core damage in the LTSBO scenario. In the Surry SPRA study, the EDGs would be expected to be functional for some time for the less severe seismic events. Thus, core cooling could be achieved by primary system depressurization via relief valves coupled with low-pressure injection, which does not require component cooling water since it has its own radiator cooling. The RWST is available for some of the dominant (i.e., 0.4g pga) seismic events. Further, if the ECST and fire protection water tanks do not fail catastrophically, AFW may be available for some period as is the case in the LTSBO scenario. In addition, an alternative water source exists in the emergency condensate makeup tank together with AC powered emergency condensate booster pumps. Further, the emergency condensate makeup tank NPSH without the booster pumps may provide some capability. Finally, the B.5.b Godwin pump may be used to provide feedwater to the steam generators via the firewater/feedwater connection using the discharge canal as the water source. Thus, for some number of the LOSW permutations the timing of core damage would be comparable to or longer than that of the LTSBO scenario. It is clear that the worst-case LOSW scenario as identified in the Surry SPRA study combined with the loss of the ECST would still be bounded by the unmitigated short-term SBO scenario consequences, since that scenario credits no primary side injection or auxiliary feedwater.

4. MELCOR MODEL OF THE SURRY PLANT

The Surry MELCOR model applied in this report was originally generated at Idaho National Engineering Laboratories (INEL) in 1988 [10]. The model was updated by Sandia National Laboratories (1990 to present) for the purposes of testing new models, advancing the state-of-the-art in modeling of PWR accident progression, and providing support to decision-makers at the NRC for analyses of various issues that may affect operational safety. Significant changes were made during the last twenty years in the approach to modeling core behavior and core melt progression, as well as the nodalization and treatment of coolant flow within the RCS and reactor vessel. Detailed reports have been prepared to discuss this model evolution as part of the MELCOR code development program [13], and these discussions will not be repeated here. It is simply noted that the model described herein is a culmination of these efforts and represents the state-of-the-art in modeling of potential PWR severe accidents.

In preparation for the SOARCA analyses described in this report, the model was further refined and expanded in two areas. The first area is an upgrade to MELCOR Version 1.8.6 core modeling. These enhancements include:

- A hemispherical lower head model that replaces the flat bottom-cylindrical lower head model,
- New models for the core former and shroud structures that are fully integrated into the material degradation modeling, including separate modeling of debris in the bypass region between the core barrel and the core shroud,
- Models for simulating the formation of molten pools both in the lower plenum and the core region, crust formation, convection in molten pools, stratification of molten pools into metallic and oxide layers, and partitioning of radionuclides between stratified molten pools,
- A reflood quench model that separately tracks the component quench front, quench temperature, and unquenched temperatures,
- A control rod silver aerosol release model, and
- An application of the CORSOR-Booth release model for modern high-burn-up fuel.

The second area focused on the addition of user-specified models to represent a wide spectrum of plant design features and safety systems to broaden the capabilities of MELCOR to a wider range of severe accident sequences. These enhancements included:

- Update of the containment leakage/failure model (see Section 4.7),
- Update of core degradation modeling practices,

- Modeling of individual primary and secondary system relief valves with failure logic for rated and degraded conditions,

- Update of the containment flooding characteristics,

- Heat loss from the reactor to the containment,

- Separate motor and turbine-driven auxiliary feedwater models with control logic for plant automatic and operator cooldown responses,

- New turbine-driven auxiliary feedwater models for steam flow, flooding failure, and performance degradation at low pressure,

- Nitrogen discharge model for accumulators,

- Update of the fission product inventory, the axial and radial peaking factors, and an extensive fission product tracking control system, and

- Improvements to the natural circulation in the hot leg and steam generator and the potential for creep rupture (see Section 4.4).

Table 4-1 provides a brief summary of plant design parameters that are helpful in comparing the configuration of Surry to other reactors of interest.

The model description is subdivided into description of the vessel and reactor coolant system (Section 4.1), primary and secondary system relief valve modeling (Section 4.2), the decay heat power modeling (Section 4.3), the natural circulation modeling (Section 4.4), the core degradation modeling (Section 4.5), the containment model (Section 4.6), the containment leakage model (Section 4.7), and the auxiliary building model (Section 4.8). Section 4.9 summarizes the best modeling practices applied to accident progression analyses conducted under the SOARCA project. The best practices include discussions of the base case approach to modeling key phenomena that have significant importance to the progression of the accident and uncertainty in their response. The Safeguards Area, Contaiment Spray Pump Area, and Main Steam Valve House are described in Section 4.10. The Safeguards ventilation system is described in Section 4.11, and the low head safety injection piping is described in Section 4.12. Section 4.13 describes the radionuclide deposition model for the low head safety injection piping, and Section 4.14 describes the methodology used for the two MELCOR models involving the low head safey injection piping.

Table 4-1 Important Design Parameters for Surry

Parameter	Value (SI units)	Value (British units)
Rated Core Power [MW_{th}]	2,546	
Number of Fuel Assemblies in Core	157	
Rod Array	15 x 15	
Fuel Rods per Assembly	204	
Fuel (UO_2) Mass [kg / lb]	79,650	175,600
Zircaloy Mass in Fuel Cladding [kg / lb]	16,465	36,300
RPV Inner Diameter [m / ft]	1.994	6.542
RPV Height and Closure [m / ft]	12.319	40.417
Pressurizer Relief Valves [kg/s / lbm/hr]	2 x 26.46	2 x 210,000
Pressurizer Safety Valves [kg/s / lbm/hr]	3 x 36.96	3 x 293,330
Pressurizer Relief Tank Volume [m^3 / ft^3]	36.8	1300
Pressurizer Relief Tank Liquid Volume [m^3 / ft^3]	25.5	900
Pressurizer Relief Tank Design Pressure [bar / psig]	6.89	100
Reactor Inlet / Outlet Temperature [ºC/ºF]	282 / 319	540 / 606
RCS Coolant Flow [kg/s / lbm/hr]	12,738	$101.1x10^6$
Nominal RCS Pressure [MPa /psia]	15.5	2,250
Number of Steam Generators	3	
Steam Generator Recirculation Rate	3.4	
Steam Generator Heat Transfer Area [m^2 / ft^2]	4,785	51,500
Secondary Pressure [MPa /psia]	15.5	2,250
Secondary Side Water Mass [kg / lbm]	41,640	91,800
Secondary Side Volume [m^3 / ft^3]	166	5,868
Emergency Condensate Storage Tank Water Volume (ISLOCA / Other Scenarios) [L / gal]	416,395 / 363,400	110,000* / 96,000**
Refueling Water Storage Tank Water Volume [L / gal]	1,511,893	399,400
Turbine-driven Aux. Feedwater Pump [m^3/s / gpm]	1 x 0.442 @ 832 m	1 x 700 @ 2,730 ft
Motor-driven Aux. Feedwater Pump [m^3/s / gpm]	2 x 0.221 @ 832 m	2 x 350 @ 2,730 ft
Containment Design Pressure [MPa / psig]	0.31	45
Containment Volume [m^3 / ft^3]	50,970	1,800,000
Containment Operating Pressure [bar, psia]	0.62 to 0.71	9 to 10.3
Containment Operating Temperature [ºC/ºF]	24 to 52	75 to 125
Accumulator Water Volume [m^3/ft^3]	3 x 27.6	3 x 975
Accumulator Pressure [bar / psig]	4.14 to 4.59	600 to 665
High Head Safety Injection [m^3/s / gpm]	3 x 0.0095 @ 1,768 m	3 x 150 @ 5,800 ft
Low Head Safety Injection [m^3/s / gpm]	2 x 0.189 @ 69 m	2 x 3,000 @ 225 ft

* best estimate for ISLOCA scenario

** minimum amount required by technical specifications

4.1 Vessel and Reactor Coolant System

Figure 4-1 illustrates the configuration of the hydrodynamic model for the Surry RCS. The model includes explicit representation of the entire reactor coolant system including each of the three reactor coolant loops¸ steam generators, and reactor coolant pumps, the steam lines out to the isolation valves and associated safety and power-operated relief valves. On Loop C, the pressurizer and associated safety and power-operated relief valves, and the pressurizer relief tank are modeled. Boundary conditions are used to represent the turbine pressure and feedwater flow to allow direct calculation of the nominal, full-power steady state operating conditions.

Logic models with mass and energy sources and sinks model the accumulators, the ECCSs, the main feedwater, and the motor and turbine-driven auxiliary feedwater. Separate logic models are used to represent the plant control systems such as the reactor scram logic, the emergency core cooling signal, the main feedwater control and trip logic, the turbine control valve isolation logic, reactor trip logic, reactor pump trip and failure logic, the containment spray actuation, the containment recirculation spray and the residual heat removal, the containment fan cooler actuation, and the plant station batteries.

Following a loss of seal cooling, water will leak through the pump seals. Under high temperature and two-phase degraded accident conditions, the pumps seals could fail and create a large leak. For each pump, three flow paths model the pump seal leakage. These leak paths describe chronic leaks from the RCS pump seals that are estimated to leak at 21 gpm at full reactor pressure [22]. The leakage model is also set up to mimic the seal failures in the pump using guidance from the utility's probabilistic pump seal leakage model [23]. For example, the failure of the second stage seals was modeled to occur coincidently with loss of liquid subcooling in the RCP pump (i.e., voiding of the RCP). The model is set up to include the following leak rates for each of the three loops:

- 21 gpm nominal leakage at 15.5 MPa with failure of the seal cooling system (i.e., no AC power)
- 182 gpm at 15.5 MPa (failure of the #1 and #2 seal following change to saturated conditions in pump)[11]
- 480 gpm at 15.5 MPa (i.e., blowout of the seal internals with flow being controlled by the Labyrinth seal upstream of the seal package)

MELCOR's choked flow model will predict the change in seal leakage flowrate as a function of pressure, quality, and liquid and gas temperature.

[11] Upon failure of the #1 seal, the #2 seal is also expected to immediately fail [Dominion, ET-CME-05-0020].

Figure 4-2 shows a detailed illustration of the reactor vessel hydrodynamic nodalization and the corresponding spatial divisions of the core. The core is represented by five concentric rings of hydrodynamic control volumes and core structures (i.e., fuel assemblies, control rods, and the supporting steel internal structures). Each ring is divided into five vertically stacked hydrodynamic control volumes. The axial length of the fuel in each ring is represented by ten axial cells in each ring. The outer ring (i.e., Ring 5) in the active fuel region is further subdivided into two regions. The inside region of Ring 5 models the peripheral assemblies of the core. The outer region of Ring 5 models the bypass region between the core shroud around the fuel and the core barrel. The detailed nodalization was required to simulate evolving, two-dimensional natural circulation flow as the core level dropped and a more accurate and continuous representation of the fuel power profile and subsequent degradation.

As shown on the left-hand side of Figure 4-2 a 6-ring by 7-axial level nodalization is used in the lower plenum, offering a detailed radial spatial representation of the bottom of the vessel and associated structures. Ring 6, which is not included in the active fuel region, represents the outer radial region beneath the vessel downcomer. Separate axial levels represent the core plate, the flow mixer, and the lower core plate. Between the core supporting structures are the support columns, which transmit the load within the core to the lower support plate. The vessel lower head is subdivided into 10-radial by 6-azimuthal segments for a two-dimensional conduction solution. The lower head failure is evaluated using a one-dimensional mechanical response model that determines the stresses and strains in the lower head to predict creep-rupture failure. The lower head structural creep (i.e., plastic strain) failure is calculated using the default Larson-Miller lifetime damage model.

A matrix of axial and radial flow paths simulates two-dimensional flow patterns in the core region. Each flow path in the core and lower plenum nodalization simulates the effects of flow blockages and changes in resistance during core degradation. Ring 5 also uses special flow paths to represent the hydraulic openings following the failure of the core shroud if such failure is predicted.

The five ring radial hydrodynamic nodalization from the core extends upward into the upper plenum of the vessel. The upper plenum is divided into two axial levels with radial flow between each ring. Each ring also includes a representation of the guide tubes. Gas or water can flow through the control rod guide tubes between the upper plenum and the upper head. In the outer radial ring, there are three axial levels to separate the natural circulation flow outward to the hot legs (CV-154) versus the returning flow (CV-153). The leakage pathways between the downcomer and the upper plenum and from the downcomer to the upper head are also represented. The upper plenum to downcomer leakage path is an important fission product gas pathway in the ISLOCA when the reactor coolant system loop seals are filled and residual vessel water blocks reverse gas flow from the core to the downcomer.

As indicated by the different colored regions in Figure 4-3, the core was subdivided into five regions. Each core region or “ring” (i.e., the terminology used in MELCOR) models the response of the included fuel assemblies. Figure 4-3 also shows the relative power of the fuel assemblies in each ring. The radial power profile in the center of the core is relatively flat.

However, the peripheral region has a sharp decrease in the assembly powers. The inner four rings were defined to provide some resolution in the power profiles and are similarly sized to the outer ring (i.e., important for the thermal response). The 5-ring nodalization balances the objectives of representing of the radial power variations in the core versus excessive complexity for computational efficiency. Once core degradation begins, the 5-ring nodalization provides a good representation of the regional fuel collapses and flow blockages.

The steam generator nodalizations are shown in Figure 4-4 and Figure 4-5. The red flowpaths are only active in natural circulation conditions. Both the hot legs and the steam generator tubes are split into two halves to permit counter-current natural circulation flows (see Section 4.4). The steam generator includes explicit modeling of the primary-side tubes, the steam generator inlet and outlet plenums, the secondary side of the steam generator, the steam lines, and the safety and power-operated relief valves. The hot leg and steam generator nodalization is somewhat complicated because it must simulate conditions ranging from (a) normal operating conditions, (b) single-phase liquid and two-phase accident conditions, and (c) single-phase gas natural circulation conditions. As will be discussed in Section 4.4, special flow paths are activated to simulate some of the natural circulation phenomena.

The model includes the heat loss from the reactor system to the containment. Each external structure of the vessel, the recirculation looping, the steam generators, and the steam lines transfer heat to the containment. These heat structures are coupled to the appropriate control volumes representing different regions of containment. The total heat loss to the containment at rated conditions is 0.08% (1.97 MW), (see Table 5.3-2 in reference [54]).

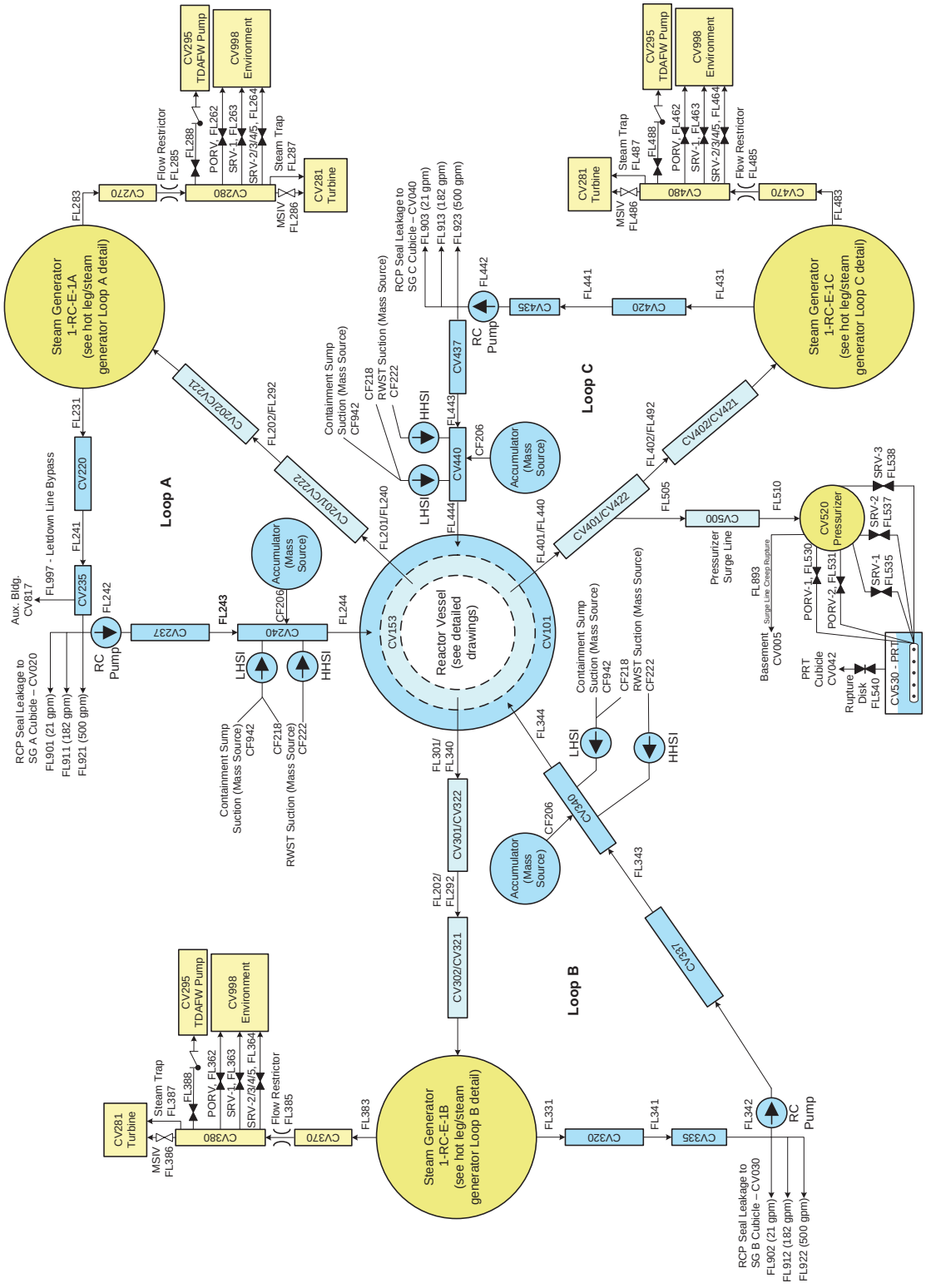

Figure 4-1 Surry Reactor Coolant System Hydrodynamic Nodalization

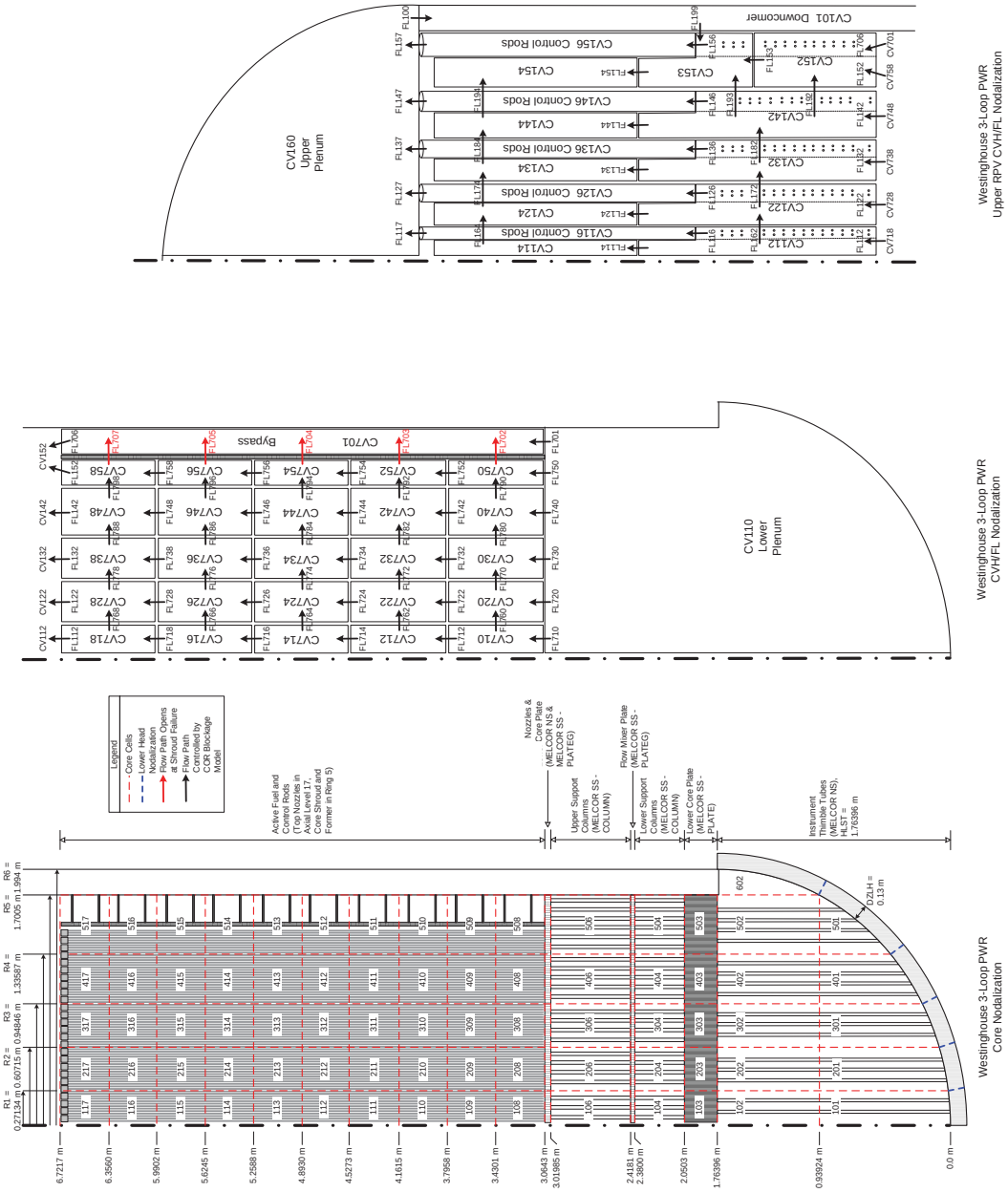

Figure 4-2 Surry Reactor Vessel Core, Lower Plenum, and Upper Plenum and Steam Dome Hydrodynamic and COR Structure Nodalization

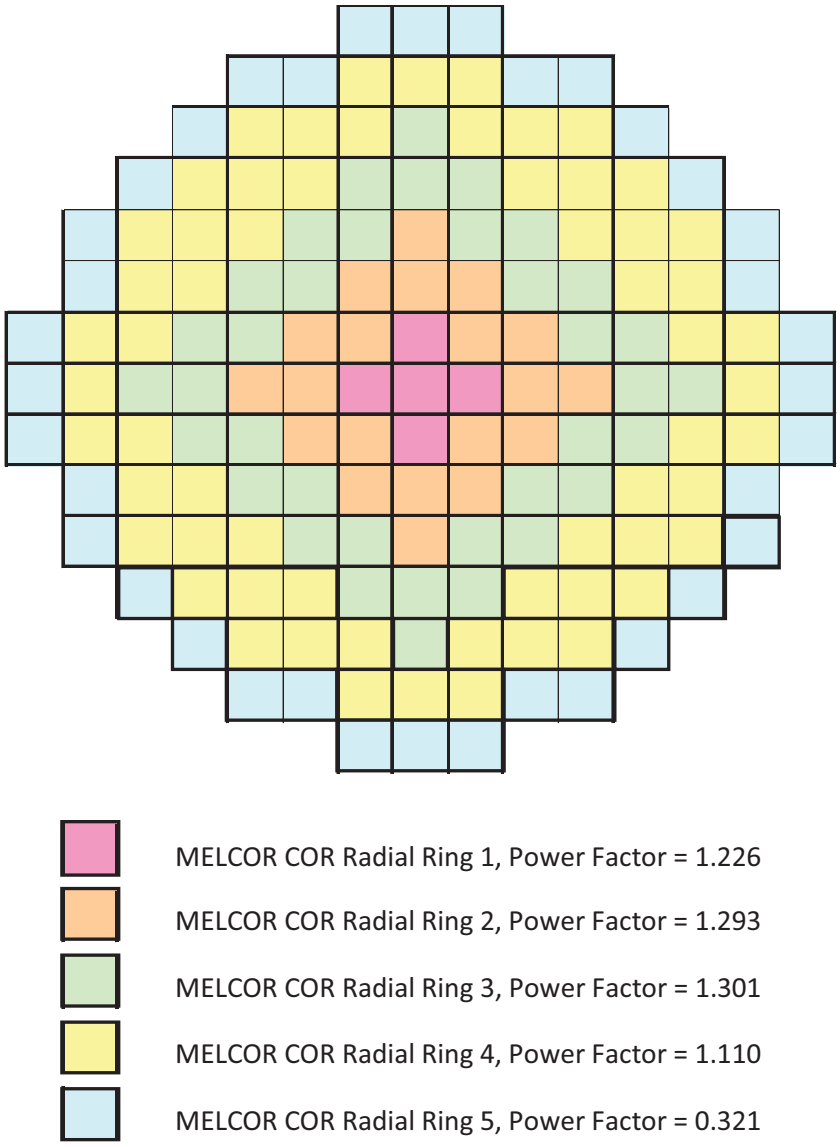

Figure 4-3 Surry Reactor Core Radial Power Profile and Nodalization

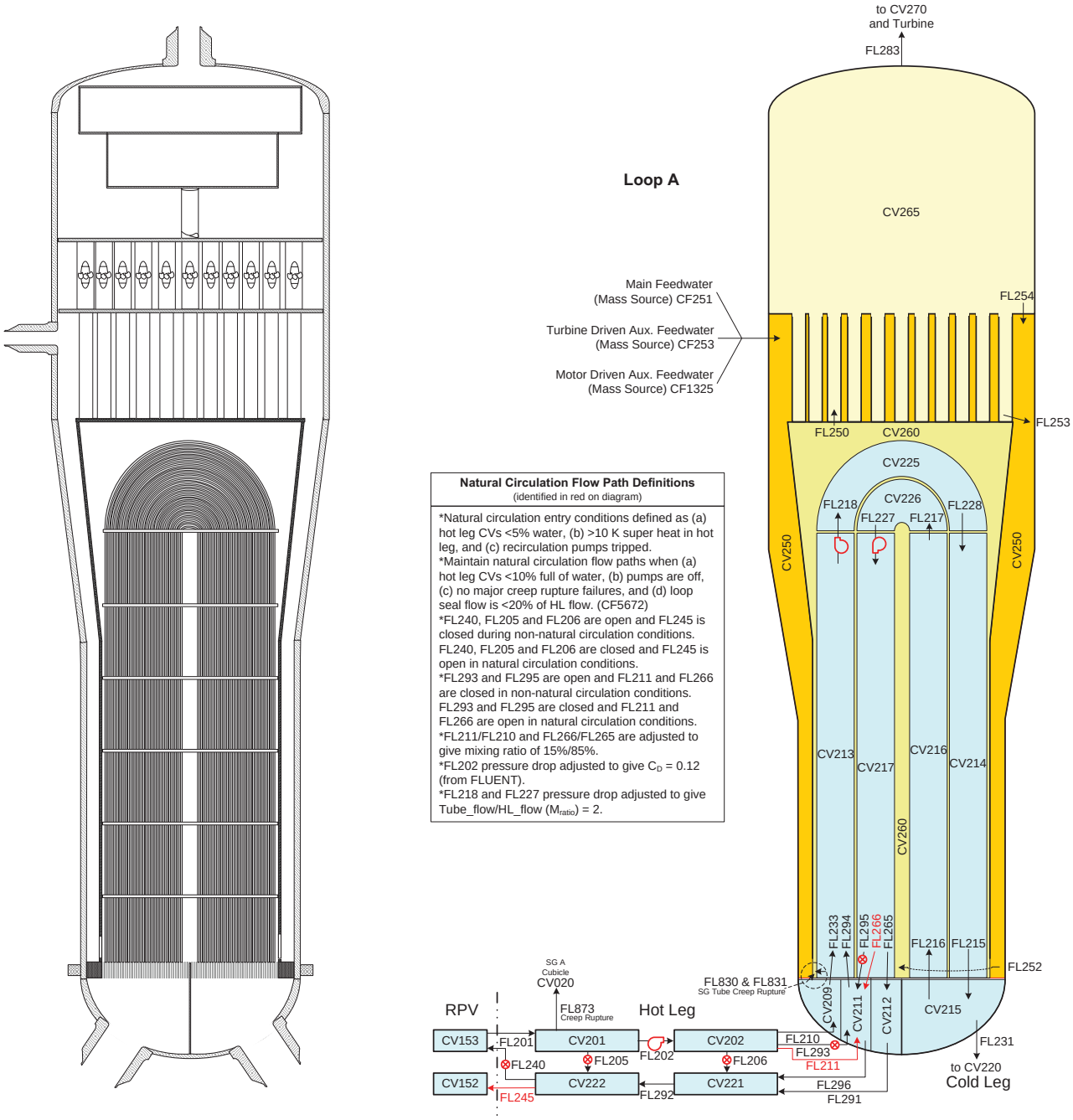

Figure 4-4 Surry Steam Generator A Hydrodynamic Nodalization

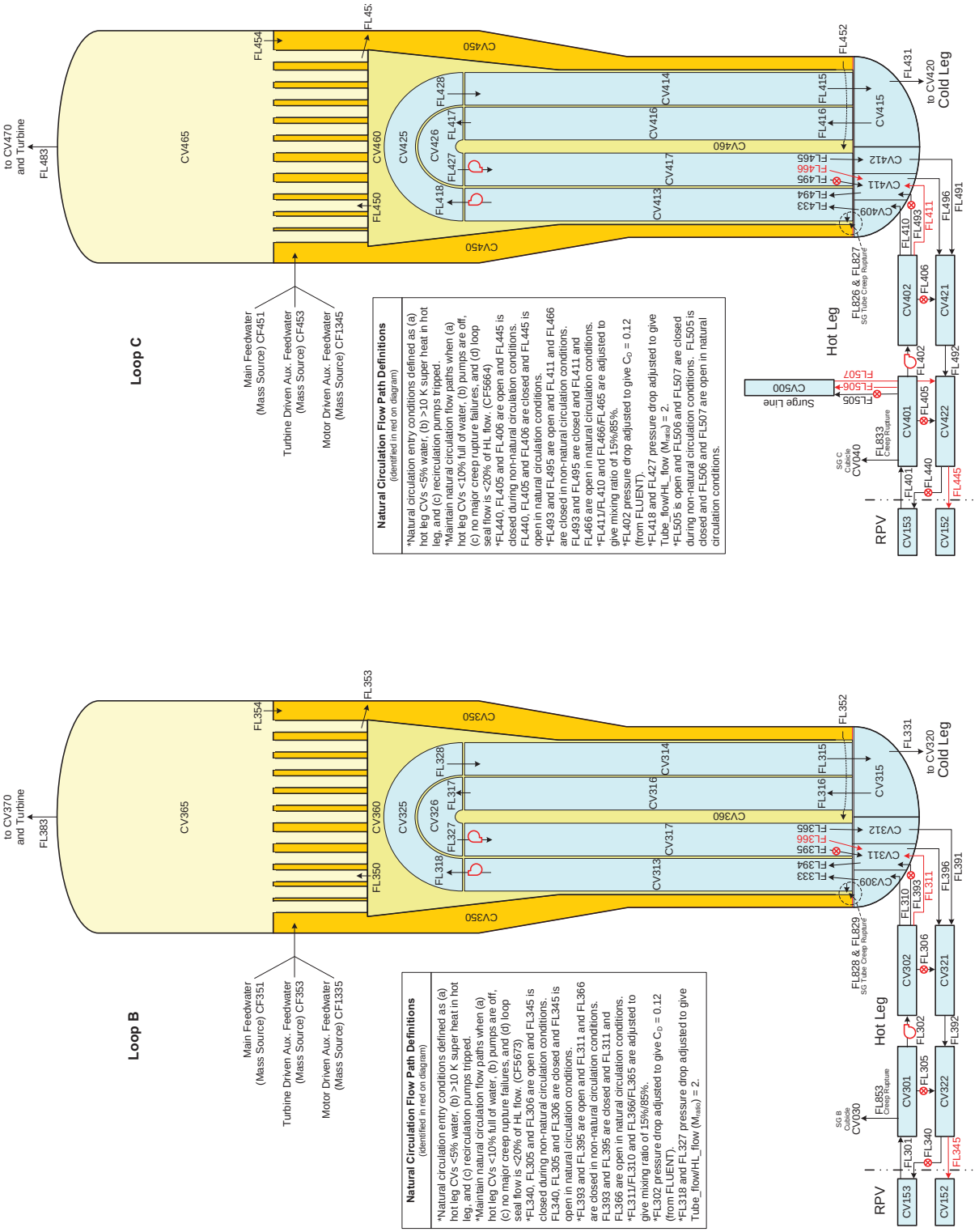

Figure 4-5 Surry Steam Generator B and C Hydrodynamic Nodalization

4.2 Primary and Secondary System Relief Valve Modeling

Special models were included to simulate the failure of the primary and secondary system relief valves. Each valve was individually modeled to accurately characterize its operational characteristics. The potential for failure under normal operating conditions and failure at high temperature, severe accident conditions was considered. Section 4.2.1 summarizes the primary system valve modeling on the pressurizer and Section 4.2.2 discusses the secondary system modeling. A peer review committee member noted there was a difference in the PWR versus BWR valve failure modeling under rated conditions. The explanation for the differences is discussed in Section 4.2.3.

4.2.1 Primary System Relief Valves

Each of the three safety relief valves (SRVs) on the pressurizer is represented separately in the MELCOR model. The valves are individually sized to flow 293,330 lb/hr (steam) at 2,485 psig [15]. Their opening pressures are staggered by 14.50 psi with the lowest opening pressure set to 2,485 psig. The valves close when pressure drops below 96% of their opening pressure [16]. The SRV with the lowest opening pressure is configured to fail open using the following criteria.

- A per demand failure probability of 0.0027 [16] and failure at a cumulative distribution function value of 0.5 (i.e., failure after 256 cycles by the relation: $P(n) = 1-(1-Pd)^n$ where $P(n)$ is the cumulative distribution function value, Pd is the per-demand failure probability, and n is the number of cycles), or

- 10 cycles above 1,000 K

Each valve is represented separately.

Each of the two PORVs on the pressurizer is also represented separately in the MELCOR model. The valves are individually sized to flow 210,000 lb/hr at 2,335 psig [15]. Their opening pressures are staggered by 14.50 psi with the lowest opening pressure set to 2,335 psig. The valves are defined to close when pressure drops below 96% of their opening pressure. The PORV with the lowest opening pressure is configured to fail open using the following criteria.

- A per demand failure probability of 0.0028 [16] and failure at a cumulative distribution function value of 0.5 (i.e., failure after 247 cycles), or

- 10 cycles above 1,000 K

The PORVs and SRVs empty into the Pressurizer Relief Tank (PRT), which is modeled as a separate control volume within the PRT cubicle in the containment. The PRT is 1300 ft^3 (36.8 m^3) and has a water volume of 900 ft^3 (24.4813 m^3). Included in the PRT are "rupture disks" that fail at a pressure of 100 psig and have a capacity of 900,000 lb/hr (113.4 kg/s) [15].

4.2.2 Secondary System Relief Valves

The PORVs on the main steam lines (i.e., one PORV on each of the three lines) are represented separately in the MELCOR model. The valves are sized to flow 373,000 lb/hr at 1,035 psig [15].

The valves are set to open at 1,035 psig, set to close at 96% of their opening pressure, and are configured to fail open using the following criteria.

- A per demand failure probability of 0.0058 [16] and failure at a cumulative distribution function value of 0.5 (i.e., failure after 119 cycles), or

- 10 cycles above 1,000 K

The three smaller SRVs (i.e., one per main steam line) of the 15 total SRVs in the main steam system (i.e., five SRVs per main steam line) are modeled individually in the MELCOR model. The smaller valves are sized to flow 361,750 lb/hr at 1,085 psig [16]. The valves are set to open at 1,085 psig, set to close at 96% of their opening pressure, and are configured to fail open using the following criteria.

- A per demand failure probability of 0.0027 [16] and failure at a cumulative distribution function value of 0.5 (i.e., failure after 256 cycles), or

- 10 cycles above 1,000 K

The SRVs other than the smaller ones are modeled jointly in the case of each steam line, i.e., in the case of each steam line, the four SRVs other than the one smaller SRV are represented jointly. The joint representation is based on the information shown in Table 4-2 regarding opening pressure and flow capacity [16].

Table 4-2 Safety Relief Valve Opening Pressure and Flow Capacity

Opening pressure (psig)	**Capacity at opening pressure (lb/hr)**
1,095	826,060
1,110	837,235
1,120	844,680
1,135	855,850

Accordingly, the SRVs in the MELCOR model jointly representing the four larger SRVs on a main steam line are sized to flow 3,423,400 lb/hr (i.e., 4 x 855,850 lb/hr) at 1,135 psig and are set to open at 1,115 psig. The valves are defined to close at 96% of their opening pressure. There are three of these valves in the MELCOR model, one for each main steam line.

4.2.3 PWR versus BWR Valve Failure Modeling

The PWR analysis selected a median or 50% failure probability for rated conditions at the beginning of the SOARCA. A 90% failure probability was used in the initial BWR calculations to represent a ‘high confidence’ level for an event that was perceived to be a ‘benevolent failure.’ These different modeling approaches were developed independently of each other, and the inconsistency was recognized later as a consequence of questions raised by the Peer Review panel. When the SOARCA analysis was revised to address these and other Peer Review

comments, the differences in failure criteria narrowed, but were also found to be unimportant to results, as explained below.

The approach used to model stochastic failure of an SRV to reclose in the BWR analysis was replaced by a more 'best estimate' approach based on early Peer Review comments. The revised criterion for stochastic SRV failure was defined based on the 'expected value' for the number of cycles a valve would experience at the time of failure. The 'expected value' is calculated as 1/Failure-Rate. If one translates this approach to a cumulative probability at the time of failure, the value corresponds to a 63% confidence level for BWRs, which is closer to, but still different from, the assumed 50% probability used in the PWR analysis. The calculated number of cycles experienced by primary and secondary coolant system relief and safety valves in the PWR is much less than the number corresponding to the median (i.e., 50%) failure probability.[12] Therefore, stochastic failure never occurs in the PWR calculations. Confidence in this observation would only increase if the failure condition were shifted from the median failure probability to the probability corresponding to the 'expected value' (i.e., 63%).

Due to the low sensitivity of the valve failure characteristics to the SOARCA sequences, new PWR calculations were not performed to explore valve failure characteristics on the progression of events (i.e., except as noted in footnote 12 for the SGTR). Future PWR calculations will adopt the 'expected value' as the recommended base case value. In contrast, the BWR results were sensitive to the valve failure characteristics and the impact of failure variations are examined in NUREG/CR 7110, Volume 1.

4.3 Decay Heat Power Modeling

Full-power steady state reactor power is 2546 MWth. The decay heat data for Surry was from a recent NRC project analyzing accident source terms for on high burnup (HBU) cores [70]. The core power profile was based on plant-specific, cycle-specific nuclear design reports obtained from the licensees. Three different recent cycles were examined to ensure that significant cycle-to-cycle variations were not observed. The Surry decay power was based on information for Unit 2 cycles 16 through 18 [71][72][73]. The core decay heat and fission product inventories were calculated using results from a SCALE/ORIGEN decay heat of the Surry core [74]. In the SCALE/ORIGEN analysis, the plant specific data from the recent cycles was extrapolated slightly to a burnup of 59 GWd/t for the lead assembly. The resultant HBU decay heat and fission product decay heat were slightly conservative relative to best-estimate values and significantly larger than low burnup values [70]. The decay heats, masses, and specific activities as a function of time were processed and applied as input data to MELCOR to define decay heat and the radionuclide inventory. Values used in the MELCOR calculations corresponded to those generated for equilibrium conditions, in the middle of an operating cycle. A summary of the total core-wide decay power generated by this process is listed in Table 4-3.

[12] The reactor coolant pump seal leakage in the station blackout sequences created a depressurization mechanism that reduced the requirement for relief valve flow. The ISLOCA depressurized due to the break and did not require primary system or secondary system relief, except in a controlled manner for the cooldown. The SGTR sequence did include considerable primary and secondary system cycling. An additional failure mechanism due to damage following solid liquid flow was examined as a sensitivity calculation. None of the PWR sequences resulted in any challenges to the high temperature, severe accident failure criteria (i.e., 10 cycles at >1000 K).

Table 4-3 Decay Power in Surry MELCOR Model

Time	Decay Power (MW)
0.0 sec	179.3
1.0 sec	165.8
3.0 sec	151.3
7.0 sec	136.5
13.0 sec	125.0
27.0 sec	111.7
54.0 sec	99.5
1.8 min	87.4
3.7 min	76.8
7.4 min	67.4
14.8 min	57.9
29.8 min	47.8
60.0 min	38.3
2.0 hr	30.9
12.0 hr	19.5
24.0 hr	16.1
48.0 hr	13.0

4.4 Natural Circulation Modeling

Three natural circulation flow patterns can be expected during a severe accident; (1) in-vessel circulation, (2) countercurrent hot leg flow, and (3) loop natural circulation (see Figure 4-6 [7]). Natural circulation is important in severe accident sequences because circulating steam from the core to upper reactor internals, the hot leg, and the SGs; (1) transfers heat away from the core, (2) changes the core melt progression, and (3) changes in-vessel fission product distribution. More importantly, the resultant heating of the external piping could progress to a thermal stress (i.e., creep rupture) failure of the primary pressure boundary and a resulting depressurization prior to lower head failure. For example, a high-pressure station blackout accident is not expected to result in full loop natural circulation flow (i.e., natural circulation pattern 3 shown on the left-hand side of Figure 4-6) at the start of the core degradation phase of the accident because the loop seal is not cleared. Consequently, the prediction of the first two natural circulation flow patterns is most critical [7]. The first two natural circulation flow patterns have been studied experimentally in the $1/7^{th}$ scale natural circulation test program by Westinghouse Corporation for the Electric Power Research Institute (EPRI) [17] [18], computationally using the FLUENT computational fluid dynamics computer program [8] [9], and with plant application analyses using SCDAP/RELAP5 [11]. Subsequently, MELCOR was used to model the $1/7^{th}$-scale natural circulation tests [21]. The reader is referred to References [2] through [4] for detailed discussions of natural circulation behavior.

More recently, NRC has continued improving natural circulation modeling as part of the steam generator tube integrity program [19] [20]. The natural circulation modeling techniques used in MELCOR plant models were based on work performed as part of the code assessment of the $1/7^{th}$ scale tests [21], which closely followed the previous work performed by Bayless [7]. The

natural circulation MELCOR modeling approach in the Surry model was updated for the SOARCA project to incorporate some of the recent modeling advances used by Fletcher with the SCDAP/RELAP5 severe accident analysis code [19].

The key features of the updated MELCOR natural circulation models are the following:

- 5 radial rings in the vessel and upper plenum for natural circulation
  - Separate axial and radial flow paths throughout the core and upper plenum
  - Radial and axial blockage models in the core during degradation

- Modeling important modes of heat transfer in the internal vessel,
  - Convective heat transfer
  - Gas-structure radiation in the upper plenum
  - Structure to structure thermal radiation within the core
  - Variable Zircaloy emissivity as a function oxide layer thickness
  - Variable steel emissivities in the core as a function temperature

- Hot leg counter-current natural circulation tuned to a Froude Number correlation using results from a NRC FLUENT CFD analysis [8] [9],

$$Q = C_D [\, g\, (\Delta\rho / \rho)\, D^5 \,]^{1/2}$$

  where: g is the acceleration due to gravity.
  Q is the volumetric flow rate in a horizontal duct
  ρ is the average fluid density (ρ)
  $\Delta\rho$ is the density difference between the two fluids
  C_D is the hot leg discharge coefficient
  D is the pipe hydraulic diameter

  - Hot leg split into upper and lower halves
  - C_D from FLUENT = 0.12

- Steam generator mixing fractions based on FLUENT CFD analysis [8] [9]
  - Inlet plenum subdivided into 3 regions for hot, mixed, and cold regions from plume analyses
  - Flow ratio from the inlet SG plenum into the hot SG tubes is 15% from the hot, unmixed plume and 85% from the mixed region
  - Flow ratio into the lower (and cooler) portion of the hot leg piping from the inlet SG plenum is 15% from the cold SG tubes and 85% from the mixed region
  - The SG is nodalized to have 50% of the SG tubes in upflow and 50% in downflow[13]

- Modeling important modes of heat transfer in the hot leg and steam generator

[13] Boyd, et al., and Fletcher and Beaton [9][19] used a 41%/59% flow split of hot tubes to cold tubes in the steam generator for natural circulation conditions. For simplicity, in non-natural circulation conditions, a 50/50 split was used in the MELCOR model.

    - Convective heat transfer

- Augmented in hot leg based on FLUENT turbulence evaluations
    - Gas to structure radiative exchange in the hot leg and steam generator tubes
    - Heat loss through the piping and insulation

- Steam generator tube to hot leg flow ratio tuned to results from the FLUENT CFD analysis [8] [9]
    - The ratio of the upward SG flow rate in the tubes to the horizontal flow rate from the reactor vessel into the hot leg piping was set to a value of 2 as in the FLUENT CFD analysis

- The pressurizer and steam generator PORV and safety valves were modeled individually to accurately represent the flow disruption to the natural circulation flow when individual valves opened

- Creep rupture modeling
    - Hot leg nozzle carbon safe zone
    - Hot leg piping
    - Surge line
    - Steam generator inlet tubes

The complexities of time-varying buoyant flows are impossible to resolve using MELCOR. Consequently, special flow paths are introduced to simulate natural circulation conditions measured in experiments and calculated using computational fluid dynamics codes. The red flow paths in Figure 4-4 and Figure 4-5 show the special flow paths in the hot legs and steam generators. As indicated in the legend, special flow paths are activated during natural circulation conditions to achieve the desired flow patterns. In particular, valves and additional head/drag terms are applied to match the desired phenomena. During natural circulation conditions (i.e., single-phase gas flow into the hot leg and steam generator), the red flow paths are activated. The result is a counter-current circulation flow pattern in the hot leg that matches the Froude Number correlation, a counter-current tube flow rate that is twice the hot leg flow, and 85% to 15% flow mixing between the mixture and hot and cold streams entering and leaving the steam generator inlet plenum. However, if conditions change that would preclude the natural circulation flow pattern (e.g., flooding by the accumulators or an injection system, a creep rupture piping failure, operation of multiple relief valves, etc.), the control logic reactivates MELCOR's normal two-phase thermal-hydraulic model with the base nodalization (i.e., the 'black' flow paths in Figure 4-4 and Figure 4-5).

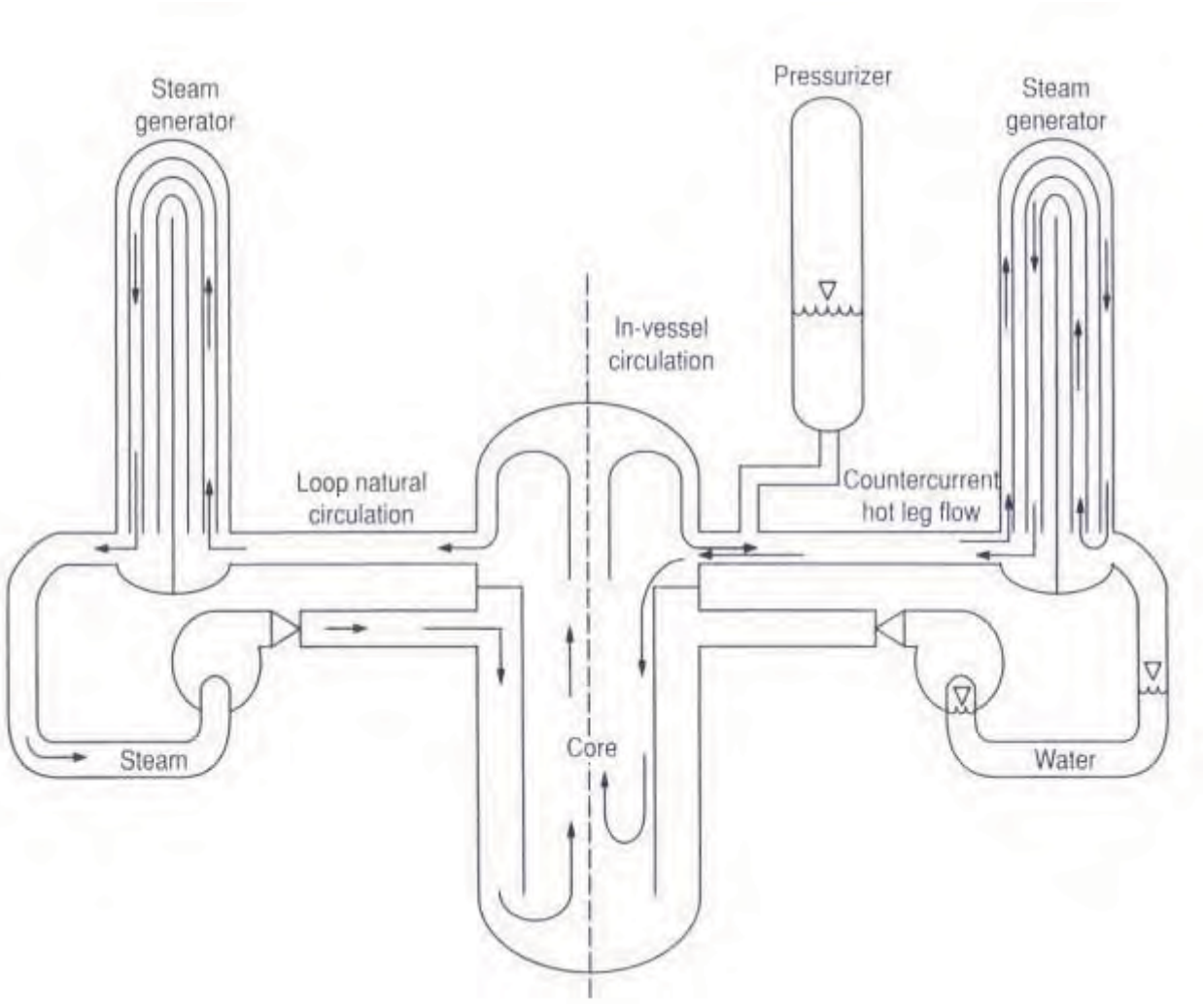

Figure 4-6 Natural Circulation Flow Patterns in a PWR

4.5 Core Degradation Modeling

The core support plate of the Surry reactor is column supported with the assemblies loading the plate between the columns. The lower core support structures are modeled using the plate and column structures. The core support plate is modeled as a grid supported support structure. The core support plate failure can fail due to stress, failure of the supporting columns, or can fail over time by creep at stresses below the yield stress, which is represented using a Larson-Miller creep-rupture model. Similarly, the support columns can fail by yielding and the failure of columns by buckling. The lower support plate is modeled as an edge supported plate, which can fail due to stress or can fail over time by creep at stresses below the yield stress. Non-supporting structures are used to represent the control rod tubes within the core in axial levels six through fifteen. These structures fail locally based on the thickness of the steel in the component.

The core melt progression modeling options have been set to be consistent with current best-practices guidelines, which are generally default models (i.e., see reference [13]). The fuel rod cladding ruptures at relatively low temperature (i.e., modeled at 800°C in MELCOR) and

releases fission gases from the fuel-cladding gap. As the fuel temperature increases, an oxide shell forms on the outer surface of the fuel cladding. Since the oxide shell has a higher melting temperature than the unoxidized Zircaloy inside of the fuel rod, the Zircaloy on the interior of the cladding will become molten once the temperature rises above the melting temperature (see Figure 4-7). Based on observations from Phebus tests, MELCOR includes a molten Zircaloy breakout model as the oxidized Zircaloy losses structural integrity. The molten Zircaloy flows through cracks in the cladding and relocates downward, which leaves a thin Zircaloy oxide shell holding the fuel pellets. Following the relocation of the molten Zircaloy, the local power due to Zircaloy oxidation ceases. The subsequent local thermal response is governed by decay heat and any relocation of molten material from above. The calculated failure rod collapse mechanisms include (a) failure collapse due to melting the oxidized shell or (b) failure collapse of the supporting structure, and (c), a time-at-temperature model that calculates the failure collapse of the oxidized Zircaloy shell holding the fuel rods. The time-at-temperature model acknowledges a thermal-mechanical weakening of the oxide shell as a function of temperature. As the temperature rises above Zircaloy melting temperature (i.e., represented as 2098 K in MELCOR) towards 2500 K, a thermal lifetime function linearly accrues increasing damage from 10 hours to 1 hour until a predicted local thermal-mechanical failure, respectively (see Table 4-4).

Table 4-4 Time versus Temperature Relationship for Fuel Rod Collapse

Temperature	**Time to Failure**
2000 K	Infinite
2090 K	10 days
2100 K	10 hr
2500 K	1 hr
2600 K	5 min
2700 K	30 sec

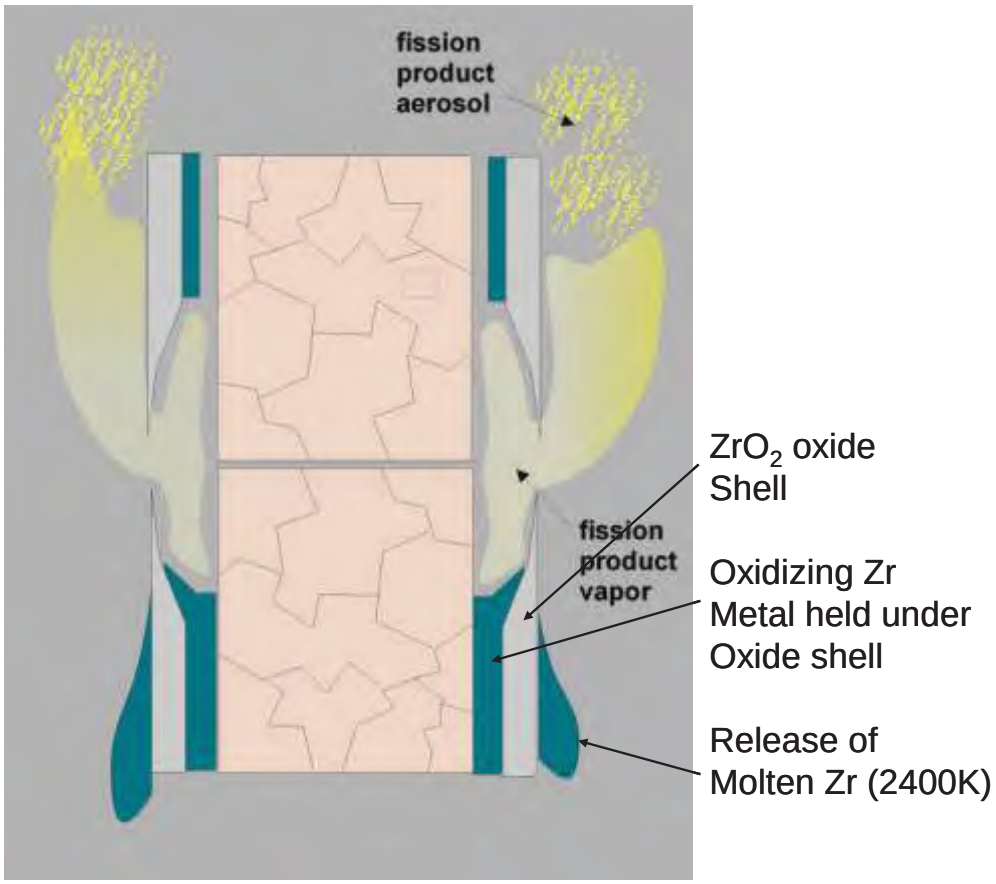

Figure 4-7 Depiction of the Fuel Rod Degradation

4.6 Containment

The containment is divided into a total of nine control volumes and seventeen flow paths. Figure 4-8 and Figure 4-9 show the hydrodynamic nodalization of the containment. The control volumes represent the basement, the cavity under the reactor, the three separate steam generator cubicles, the pressurizer cubicle, the pressurizer relief tank (PRT) cubicle, the lower dome, and the upper dome. The basement region includes the bottom part of the containment as well as the surrounding cavity that lies between the outer wall and internal crane wall.

The walls, floors, ceilings, and equipment in the containment are modeled as heat conducting structures. The structures will absorb and release heat during the course of an accident simulation. Fission products can deposit on any structure, however, gravitational settling only occurs on horizontal structures. The major walls include the outer walls of the containment that are shared with the environment (1.37 m thick), the wall separating the reactor cavity and basement (1.37 m thick), the wall separating the pressurizer cubicle and the outer cavity (0.61 m thick), and the PRT cubicle floor (0.3 m thick). Additional major walls include the outer wall separating the upper dome from the environment (1.37 m thick) and the wall separating the lower dome from the upper dome (0.76 m thick). Figure 4-8 shows these two wall sections have different thickness. The containment dome has a hemispherical geometry and is approximately 0.762 m thick.

The reactor cavity is represented using special physics models for core concrete interactions (CCI). The concrete floor is a combination of limestone aggregate and common sand concrete and has a 0.135 mass fraction of iron rebar. This concrete has an ablation temperature of 1650 K and an initial temperature of 311 K. The reactor cavity is represented with a flat-bottom cylindrical cavity that has an inner radius of 4.28 m and an outer radius of 5.58 m. The thickness of the concrete below the bottom of the cavity is 3.04 m.

The reactor cavity connects to the basement through a 12" diameter hole bored through the shield wall at elevation -25'-0" (centerline).[14] The centerline of this hole is located 2'-7" above the containment floor. Water in the basement or the cavity will flow through this hole when it is greater than 2'-7" deep. This has significance in the long-term boil-off of water when debris is located in the reactor cavity.

[14] The containment model is based on Unit 1. *Note:* Unit 2 does not have this hole.

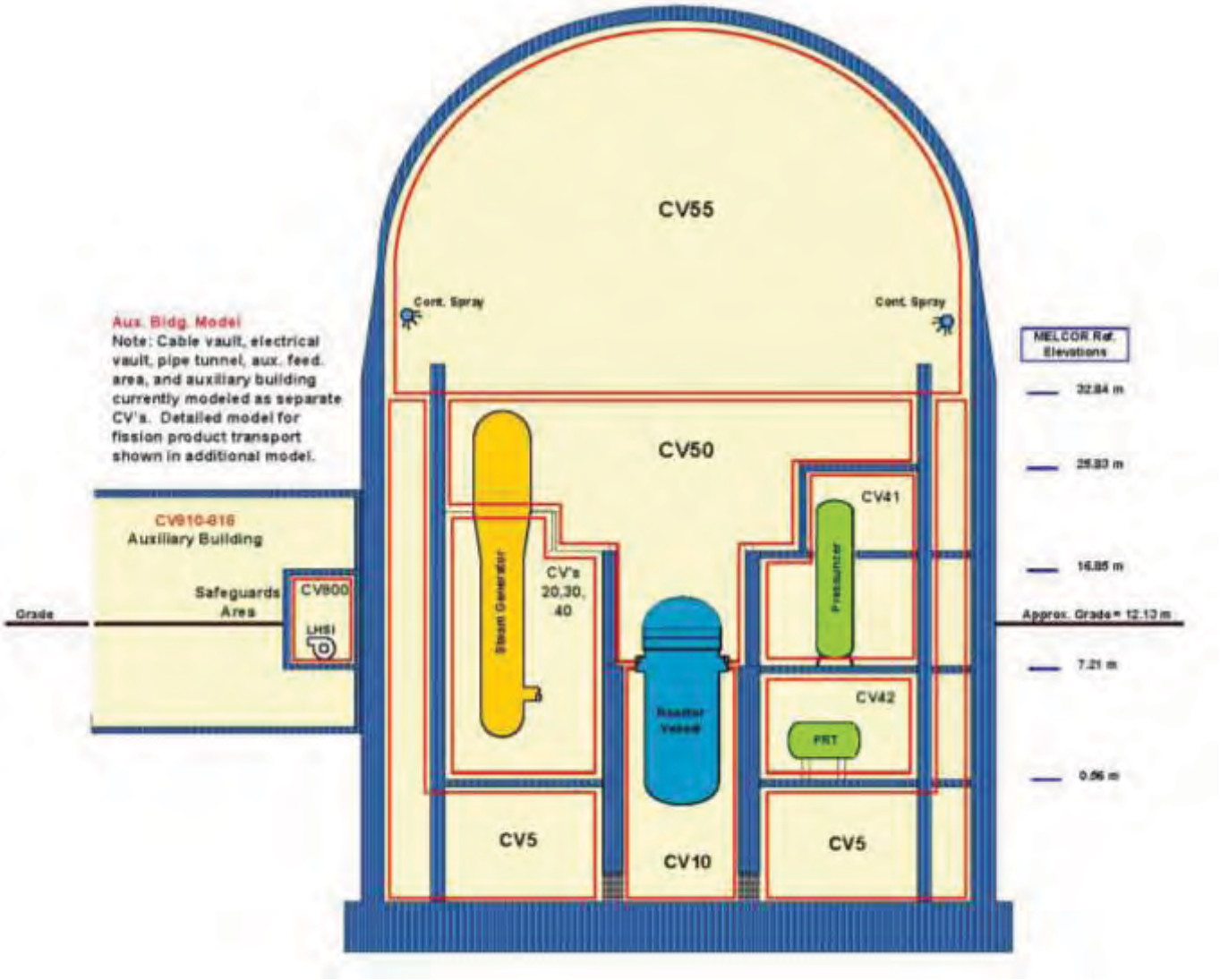

Figure 4-8 Containment Hydrodynamic Nodalization

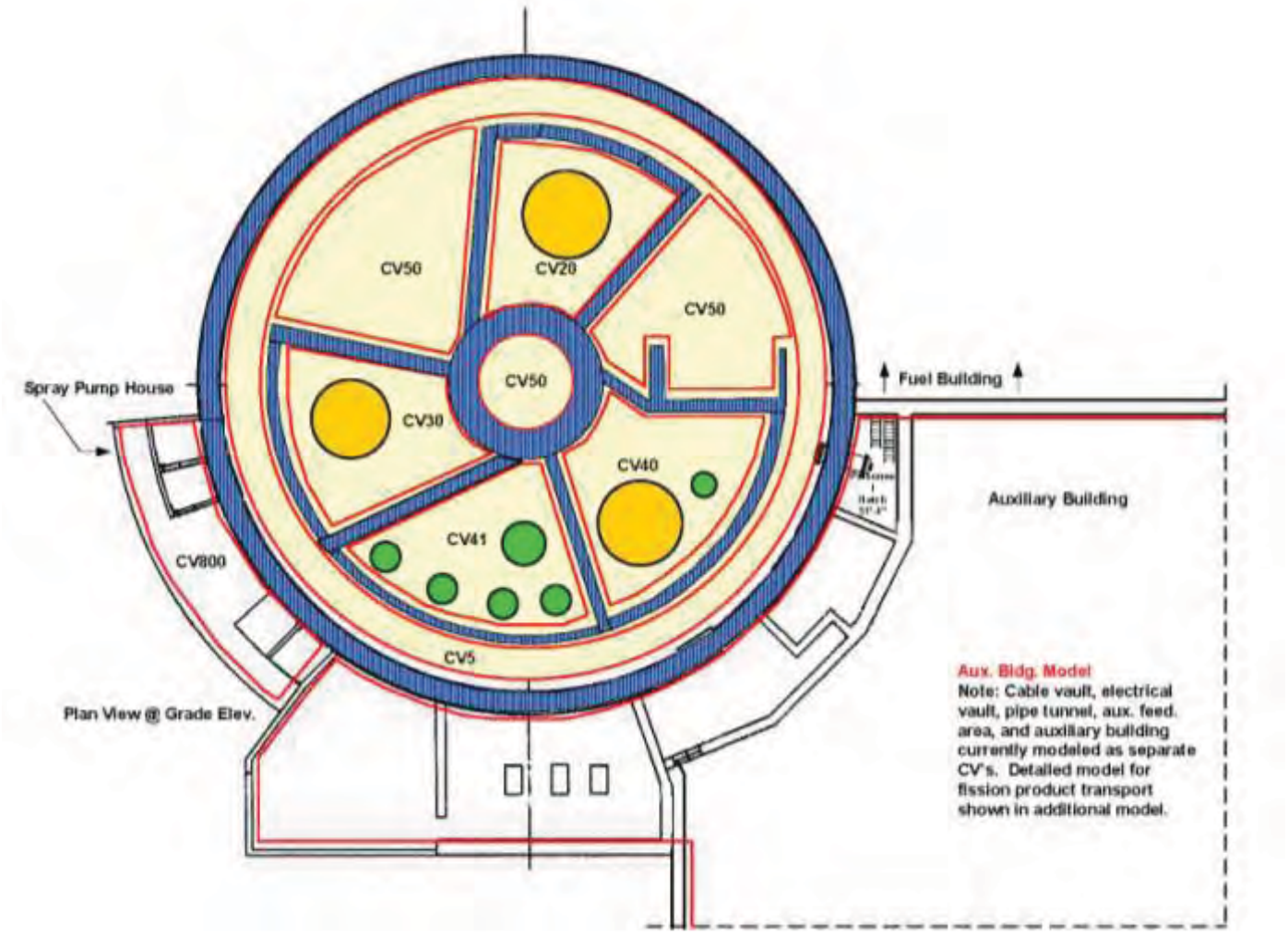

Figure 4-9 Containment Hydrodynamic Nodalization, Plan View

4.7 Containment Leakage Model

Extensive research and scale model testing of reinforced and pre-stressed concrete containments to determine behavior at beyond design basis accident pressure has been performed in the last 25 years at SNL [43] and the Central Electricity Generating Board (CEGB) [44]. Testing has shown that concrete containments start to leak at leak rates much higher than design leakage and well before a large rupture or gross failure would occur. This leakage could preclude the large rupture or failure. The relationship between containment leakage and internal pressures for reinforced concrete and pre-stressed concrete containment model tests is described in References 4 and 5. The details of the containment performance model developed by the NRC staff for use in this analysis are described in detail in Appendix A. The concrete containments start to leak appreciably once the liner plate yields and tears. The rate of leakage when the liner plate yields and tears is about 10 times more than normal leakage of 0.10 percent of containment air mass per day at the containment design pressure. The leakage rate increases appreciably with further

increases in test pressure. Once the rebar yields, the leakage rate is about 10-15 percent per day. Thereafter, the leakage rate continues to increase and reaches to about 60-65 percent per day when the strain in the rebar is about 1-2 percent. The containment pressure does not increase significantly after leakage rate exceeds 60-65 percent per day. The liner welds and concrete crack after the rebar and liner plate yields to create a path for leakage. The leakage occurs in areas such as equipment hatch, personnel airlocks, and penetrations where local strains are substantially higher than the global strains. All leakage was assumed to occur through the equipment hatch (i.e., the largest penetration into the containment), which conservatively releases all fission products to the environment. Leakage through most of the other penetrations would allow some fission product deposition in the connected buildings (e.g., the auxiliary and safeguards buildings).

The results in [45] and [46] are for scale model tests of two concrete containments. Rebar and concrete crack spacing, and aggregate size can affect the leakage rates in full size containments. However, based on the results of testing and analyses presented above, it is reasonable to conclude that all concrete containments start to leak once the rebar and liner plate yield. In addition, leakage becomes excessive once the strains in the reinforced and pre-stressed concrete containments reach about 2 and 1 percent, respectively. Based on information from the containment model test and analyses, it is reasonable to assume that containment leakage is about one percent of the containment mass per day when the liner plate yields. This increases to 13 percent of containment mass per day when rebar yield. Similarly, a leakage rate of 62 percent can be used in severe accident analysis when the containment global strains are 1-2 percent. The uncertainty in the leakage rate can be accounted for by conservatively reducing the yield and failure pressure calculated by simplified analysis to 85 percent of the calculated value.

The location of the leakage can have a significant effect on the results of the severe accident analysis and dose rates. For instance, if the containment leakage occurs through penetrations that are located inside adjoining plant buildings, the fission product release into atmosphere would be significantly less as compared to direct leakage to the environment. Previously, some of the severe accident analyses were based on the assumption that the leakage takes place at the top of the containment dome. A more realistic approach is to consider leakage to occur at the equipment hatch, which was done in SOARCA. Leakage through the equipment hatch discharges into the environment from the side of the containment dome.

The implementation into the Surry MELCOR model uses two containment failure mechanisms.

1. Nominal leakage per design specifications - 0.1% volume/day at P_{Design}, see Figure 4-10.
2. Containment overpressure leakage as described above - see Figure 4-11.

The nominal leakage is always active but very small. The containment overpressure failure occurs at 2.17 times the design pressure, or 0.775 MPa (112.4 psia). This estimate of 2.17 times the design pressure is derived from a curve fit of the three data points shown in Figure 4-11. The leakage starts very small but grows as the pressure increases. If the containment pressure subsequently decreases, the leakage area will not decrease from the maximum value.

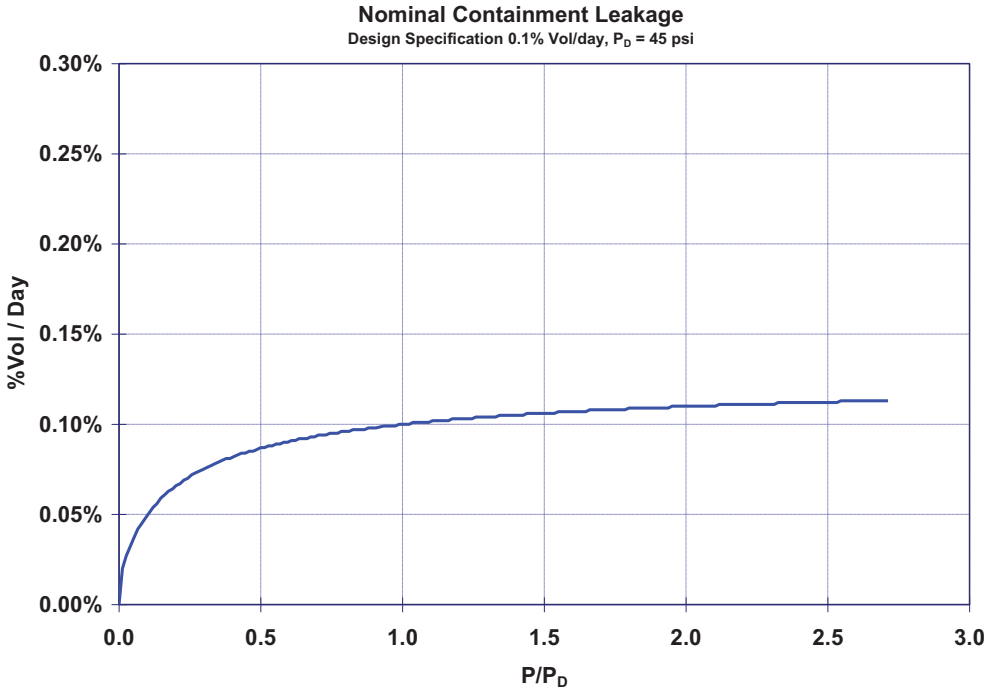

Figure 4-10 Nominal Containment Leakage Model

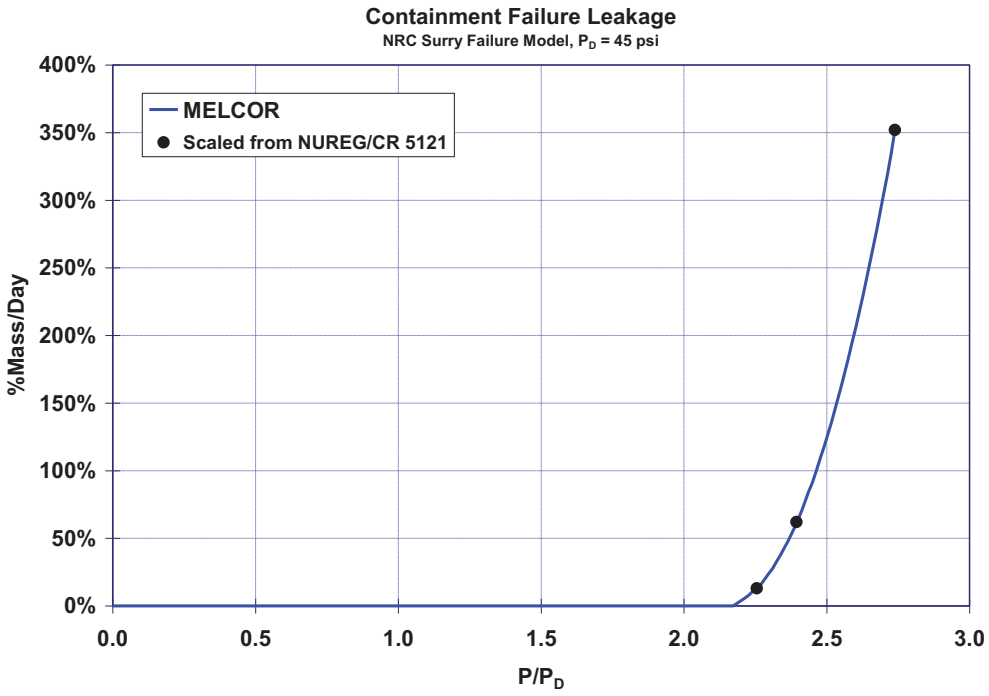

Figure 4-11 Containment Failure Leakage Model

4.8 Auxiliary Building

A total of 9 control volumes and 17 flow paths represent the Auxiliary Building (see Figure 4-12). The auxiliary building is modeled on a floor-by-floor basis beginning with the basement floor and rising up through the main floors up to the fourth floor. The first floor, at a 2'0" elevation, is broken up into four control volumes. The first floor is subdivided to represent major rooms at that elevation. The HHSI pumps and motors are located at this elevation. The second floor, at 13' elevation, is divided into 3 control volumes. A large room in the middle of the second floor contains boric acid transfer pumps as well as part of the boric acid tanks. The other two rooms contain the cable vault, electrical tunnel, and electrical vault. The middle room is connected to the side rooms by doorways. This floor also connects with the first floor by three separate stairwells. The third floor, at a 27'-6" elevation, is represented by a single control volume. The third floor contains the volume control tanks and part of the boric acid tanks. The third floor connects with the second floor by the stairwell located next to the elevator. The fourth floor, at a 45'-10" elevation is also represented by a single control volume. The fourth floor is where the personnel hatches are located along with the heating and ventilation equipment. There are many potential leakage locations to the environment on the fourth floor through ventilation ducting and the blowout panels. The leakage is represented as a 0.65 m^2 (7 ft^2) flow path to the environment.

Representations have been included in the Surry MELCOR model of the Safeguards Area, Containment Spray Pump Area, and Main Steam Valve House, as described in Section 4.10. Details of the Safeguards ventilation system and low head safety injection piping are described in Sections 4.11 and 4.12, respectively. Other buildings that are directly connected or could be involved as a fission product pathway (i.e., the turbine building) were not represented because they were not relevant fission product pathways for the sequences analyzed.

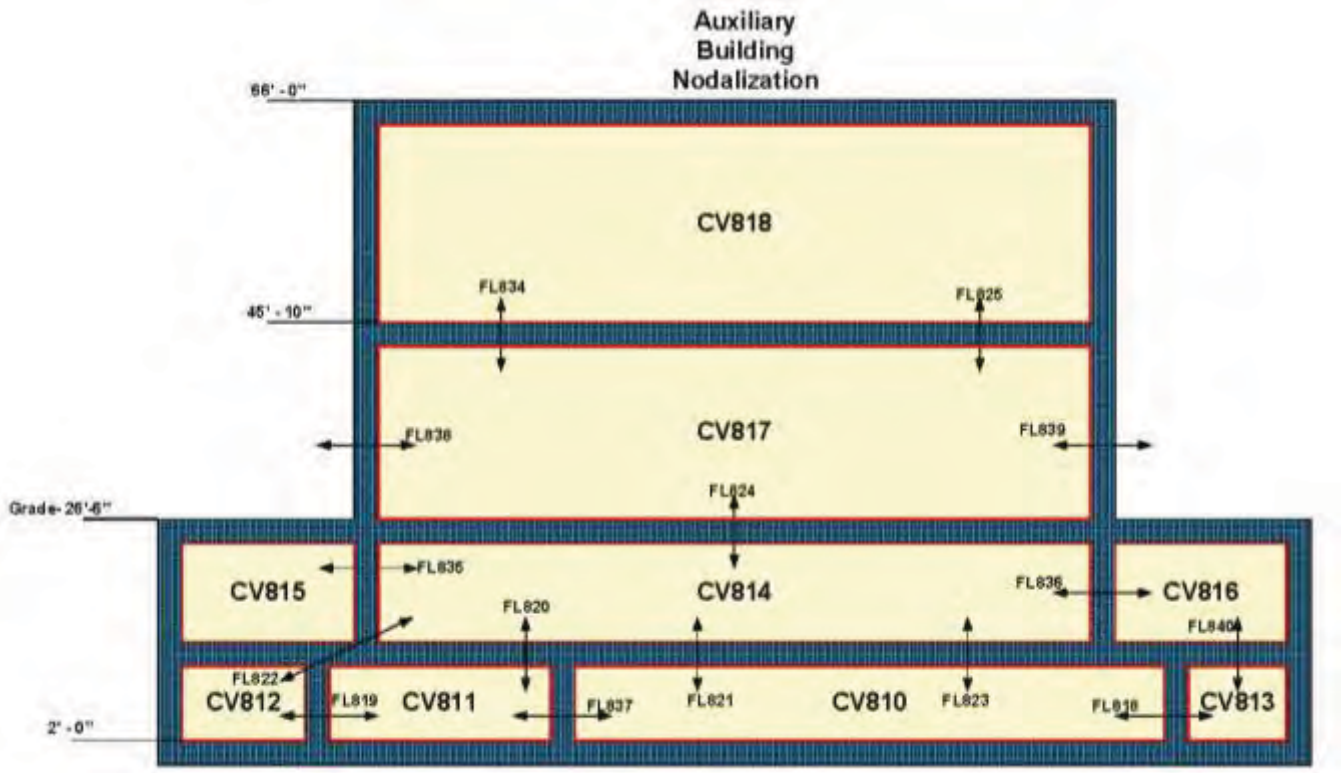

Figure 4-12 Auxiliary Building Hydrodynamic Nodalization

4.9 Best Modeling Practices

The SOARCA project is intended to provide a body of knowledge regarding the realistic outcomes of severe reactor accidents. To accomplish this objective, the SOARCA project used integrated modeling of accident progression and offsite consequences using both state-of-the-art computational analysis tools and best modeling practices drawn from the collective wisdom of the severe accident analysis community.

The MELCOR 1.8.6 computer code [13] embodies much of this knowledge and was used for the accident and source-term analysis. MELCOR includes capabilities to model the two-phase thermal-hydraulics, core degradation, fission product release, transport, deposition, and containment response. The SOARCA analyses include operator actions and equipment performance issues as prescribed by the sequence definition and mitigative actions. The MELCOR models are constructed using plant data and the operator actions were developed based on discussions with operators during site visits. The code models and user-specified modeling practices represent the current best practices.

Uncertainties remain in our understanding of the phenomena that govern severe accident progression and radionuclide transport. Consistent with the best-estimate approach in SOARCA, all phenomena were modeled using best-estimate characterization of uncertain phenomena and events. Important severe accident phenomena and the proposed approach to modeling them in the SOARCA calculations were presented to an external expert panel during a public meeting

sponsored by the NRC on August 21 and 22, 2006 in Albuquerque, New Mexico. A summary of this approach is described in Section 4.9.1. These phenomena are singled out because they are important contributors to calculated results and have uncertainty. Section 4.9.2 briefly describes the two other topics, steam explosions, and direct containment heating that had been previously included in lists of uncertain phenomena. Finally, a systematic evaluation of phenomenological uncertainties for a particular sequence is a separate task and not discussed in this report. That task will evaluate the importance and impact of alternative settings or approaches for key uncertainties.

4.9.1 Approach to Modeling Important Phenomena

A review of severe accident progression modeling for the SOARCA project was conducted at a public meeting in Albuquerque, New Mexico on August 21-22, 2006 [14]. This review focused primarily on best modeling practices for the application of the severe nuclear reactor accident analysis code MELCOR for realistic evaluation of accident progression, source term, and offsite consequences. The scope of the meeting also included consideration of potential enhancements to the MELCOR code as well as consideration of the SOARCA project in general.

The review was conducted by five panelists with demonstrated expertise in the analysis of severe accidents at commercial nuclear power plants. The panelists were drawn from private industry, the Department of Energy national laboratory complex, and a company working on behalf of German Ministries. The review was coordinated by Sandia National Laboratories and Nuclear Regulatory Commission staff.

The following important uncertain modeling practices were presented to the peer review panel. The review panel provided written comments and suggestions, which were incorporated into the subsequent analyses. Base case approaches were identified for these uncertain and typically important parameters.

- **Safety relief valve cycling and failure**
  Mean opening and reclosing failure probabilities for the pressurizer and steam generator power operated relief (PORV) and safety valves (SV) were applied in the calculations. A high temperature thermal failure model was also applied. This is discussed in further detail in Section 4.2.

- **Pump seal leakage and blowout**
  The base case pump seal leakage model described in Section 4.1 was identified as the base case modeling approach. In addition, early seal failure sensitivity calculations were performed for the LTSBO.

- **Loop seal clearing and effects on the accident progression**
  The most important impact from this event is an increased vulnerability of the steam generator tubes for failure due to a full loop circulation of hot gases from the core during core degradation. MELCOR has basic thermal-hydraulic modeling for calculating loop seal clearing. However, it is recognized that loop seal clearing is related to other complex and uncertain events, such sensitive system hydrodynamic pressure balances during core degradation events and pump seal leakage. NRC has a separate research program examining thermally-induced steam generator tube failure. Due to the potential importance of steam generator tube failure (i.e., the most important consequence of loop seal clearing), calculations were performed that included steam generator tube failure.

- **Fuel degradation and relocation treatment**
  An additional model has been added to characterize the structural integrity of the fuel rods under highly degraded conditions. The new failure model acknowledges a thermal-mechanical weakening of the oxide shell as a function of time and temperature. As the local cladding oxide temperature increases from the Zircaloy melting temperature (i.e., represented as 2098 K in MELCOR) towards 2500 K, a thermal lifetime function accrues increasing damage from 10 hours to 1 hour until a local failure of the oxide shell.

- **Lower plenum debris/coolant heat transfer**
  Following the fuel-debris slump into the lower plenum, there may be fuel-coolant interactions. The lower plenum heat transfer settings were updated to reflect the end-state thermal condition of the debris in the deep pool FARO tests (i.e., significant thermal interaction with the water). The resultant behavior resulted in debris cooling if there was a pool in the lower plenum. The subsequent heat up of the vessel lower head was delayed heat until the overlying water evaporated.

- **Core plate failure**
  The timing of core plate failure affects the relocation of the degraded core materials from the core region into the lower plenum. The local thermal-mechanical failure of the lower core plate, the flow mixer plate, and the lower support forging are calculated within MELCOR using the Roark engineering stress formulae. The yield stress is calculated based on the loading and local temperature.

- **Fission product release, speciation, and volatility**
  First, the CORSOR-Booth diffusion model was used to calculate the release of radionuclides from fuel.

  Second, the predominant speciation of cesium was changed based on detailed analysis of the deposition and transport of the volatile fission products in the Phebus facility tests. The analysis revealed molybdenum combined with cesium and formed cesium molybdate. Previously, the default predominant chemical form cesium was cesium hydroxide. As consistent with past studies, all the released iodine combines with the cesium. Applications of this information to the MELCOR models used in the SOARCA calculations are described in SAND2010-1633, “Synthesis of VERCORS and Phebus Data in Severe Accident Codes and Applications.”

- **RCS natural circulation treatment**
  The base case RCS natural circulation models described in Section 4.4 were identified as the base case modeling approach.

- **Vessel lower head failure and debris ejection**
  The base case approach of modeling the vessel lower head failure and debris ejection included some modifications in MELCOR. First, all the solid debris in the lower plenum is in contact with water, if present. Previously, a restrictive one-dimensional counter-current flooding limitation criterion prevented penetration of water into the debris bed. Second, the vessel lower head fails using a creep rupture model. A Larson-Miller failure criterion is calculated based on the one-dimensional conduction and stress profile through the lower head. The failure of a lower head penetration prior to gross head failure was judged unlikely based on observations from experimental studies at Sandia National Laboratories lower head failure (LHF) tests.

- **Ex-vessel phenomena - CCI**
  The default model's ex-vessel debris surface heat flux to an overlying pool of water was enhanced to replicate the magnitude observed the MACE tests. The default model did not include multi-dimensional effects of fissures, other surface non-uniformities, and side heat fluxes.

- **Ex-vessel phenomena - Hydrogen combustion**
  The default MELCOR ex-vessel combustion model was used with the modeling options to include horizontal and vertical propagation of burns and the time delay for the flame front to span the width of the control volume.

4.9.2 Early Containment Failure Phenomena

Two phenomenological issues not included in the best-estimate approach used in SOARCA include: (1) alpha-mode containment failure and (2) direct containment heating leading to containment failure. These severe phenomena leading to an early failure of the containment were included in some of the first studies to quantify the risks from nuclear reactors. However, they are not included in the SOARCA analyses because they are either extremely low likelihood or are physically unfeasible as described below.

The alpha-mode event is characterized by the supposition that an in-vessel steam explosion might be initiated during core meltdown by molten core material falling into the water-filled lower plenum of the reactor vessel. The concern was that the resulting steam explosion could impart sufficient energy to separate the upper vessel head from the vessel itself and form a missile with sufficient energy to penetrate the reactor containment. This would produce an early failure of the containment building at a time when the largest mass of fission products is released from the reactor fuel. In the following years, significant research was focused on characterizing and quantifying this hypothesized response in order to attempt to reduce the significant uncertainty. A group of experts ultimately concluded in a position paper published by the Nuclear Energy Agency's Committee on the Safety of Nuclear Installations that the alpha-mode

failure issue for Western-style reactor containment buildings can be considered resolved from a risk perspective, posing little or no significance to the overall risk from a nuclear power plant.

Similarly, direct containment heating (DCH) was another important event identified to cause early containment failure. NUREG-1150 [2] was an important risk study that included DCH as an early containment failure phenomenon. Extensive research was performed with the goal of characterizing DCH. Additionally, research was performed concerning other phenomena that can preclude an early, energetic failure of the containment (e.g., natural circulation leading to creep rupture of the RCS boundary, see Section 4.4). First, the extensive natural circulation research shows that RCS failure prior to vessel failure due to RCS creep rupture is most likely. In the unlikely event there is a high-pressure vessel failure (i.e., not within SOARCA's objectives for best-estimate evaluations), the resolution of the DCH issue found early containment failure to be very unlikely [25]. The issue resolution utilized a probabilistic framework that decomposes the DCH problem into three probability density functions that reflect the most uncertain initial conditions (i.e., UO_2 mass, zirconium oxidation fraction, and steel mass). Uncertainties in the initial conditions are significant, but the quantification approach established reasonable bounds that are not unnecessarily conservative. The phenomenological models in the probabilistic model were compared with an extensive database including recent integral simulations at two different physical scales (1:10-scale in the Surtsey facility at Sandia National Laboratories and 1:40-scale in the COREXIT facility at Argonne National Laboratory). The loads predicted by these models were significantly lower than those from previous parametric calculations. The containment load distributions do not intersect the containment strength (fragility) curve in any significant way, resulting in containment failure probabilities less than 10^{-3} for all scenarios considered. Sensitivity analyses did not show any areas of large sensitivity. Consequently, DCH is not a likely accident progression event and therefore not within SOARCA's best-estimate approach guidelines.

4.10 Safeguards Area, Containment Spray Pump Area, and Main Steam Valve House

Specifically for importance in the ISLOCA accident scenario, representations have been included in the Surry MELCOR model of the Safeguards Area, Containment Spray Pump Area, and Main Steam Valve House. These interconnected buildings, referred to collectively in this document as Safeguards or Safeguards buildings, are located outside and adjacent to each unit's reactor containment building. In the ISLOCA scenario postulated for Surry, the RCS blows down into the Safeguards Area and fission products are released to the environment through the Safeguards buildings.

Figure 4-13 illustrates the MELCOR nodalization constructed to represent the Safeguards buildings. The Safeguards Area and Containment Spray Pump Area are served by a safety-related filtered ventilation system. This system is represented in the MELCOR modeling of Safeguards. The nodalization employed for it is shown in Figure 4-14.

Access to the Safeguards Area is from the yard at approximately grade elevation. The building houses two of its reactor unit's four containment recirculation spray pumps and both of its unit's low-head safety injection pumps. The building has three levels. Ladders lead down from grade elevation to the spray pumps and safety injection pumps, each pump residing in a separate cubicle.

Adjacent to the Safeguards Area is the Containment Spray Pump Area. A unit's two containment spray pumps are located in its Containment Spray Pump Area. A unit's instrument air compressors are located in the basement of its Containment Spray Pump Area.

Adjacent to the Containment Spray Pump Area is the Main Steam Valve House. A unit's two electric-motor-driven auxiliary feedwater pumps and one steam-turbine-driven auxiliary feedwater pump are located in its Main Steam Valve House. Grating floors above the auxiliary feedwater pumps provides access to the main steam safety valves, steam generator power operated relief valves, and main steam trip valves.

A basement area common between the Containment Spray Pump Area and the Main Steam Valve House contains the auxiliary feedwater booster pumps and service water piping.

A noteworthy aspect of the construction of the Safeguards buildings is that these buildings do not have an integral back wall. The buildings back up to Containment and the Containment cylinder serves as a back wall to the buildings. Where the walls and roofs of the Safeguards buildings approach the Containment cylinder, there are 3" gaps (shaker spaces) covered with flashing or angle iron.

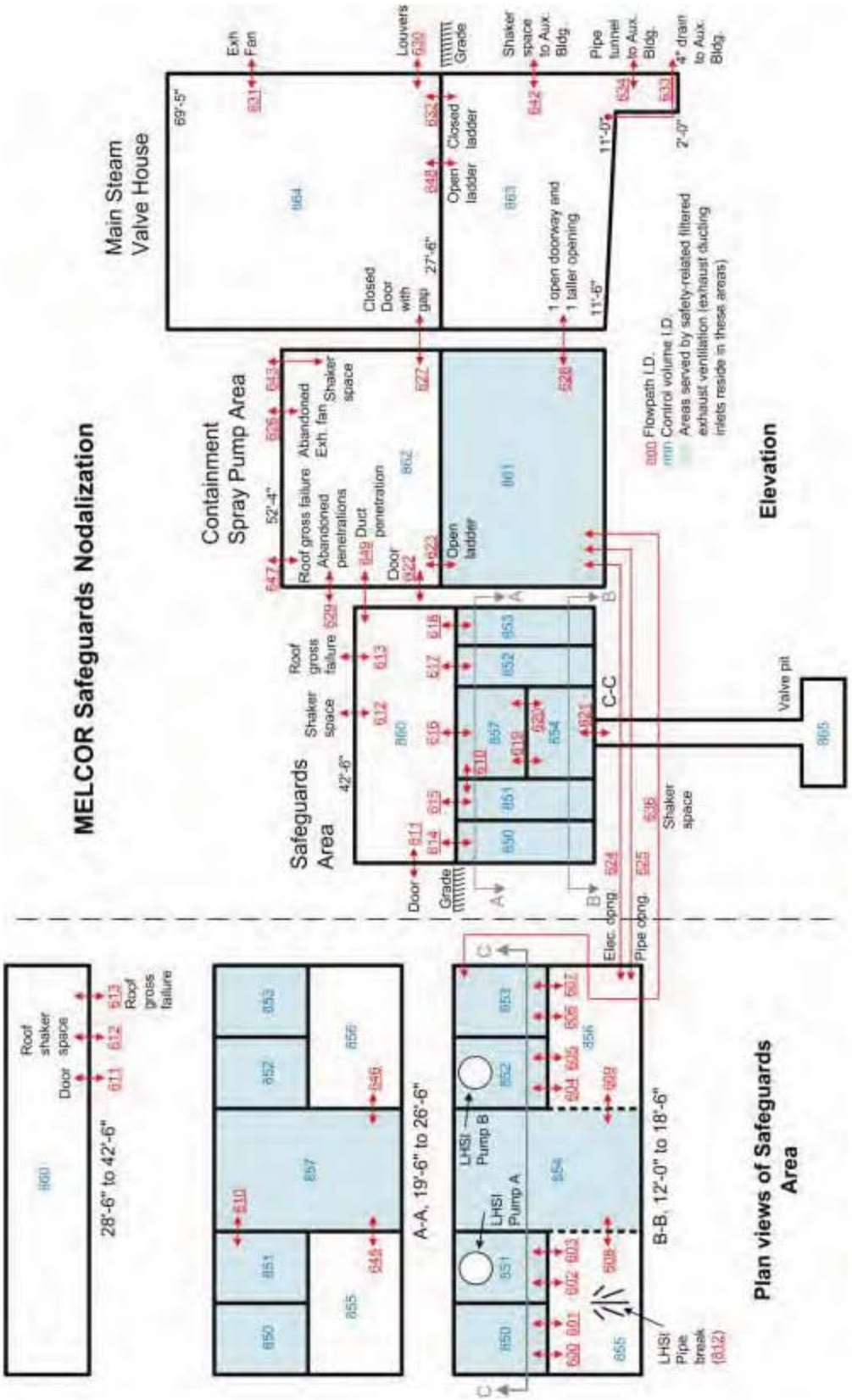

Figure 4-13 Safeguards Buildings MELCOR Nodalization

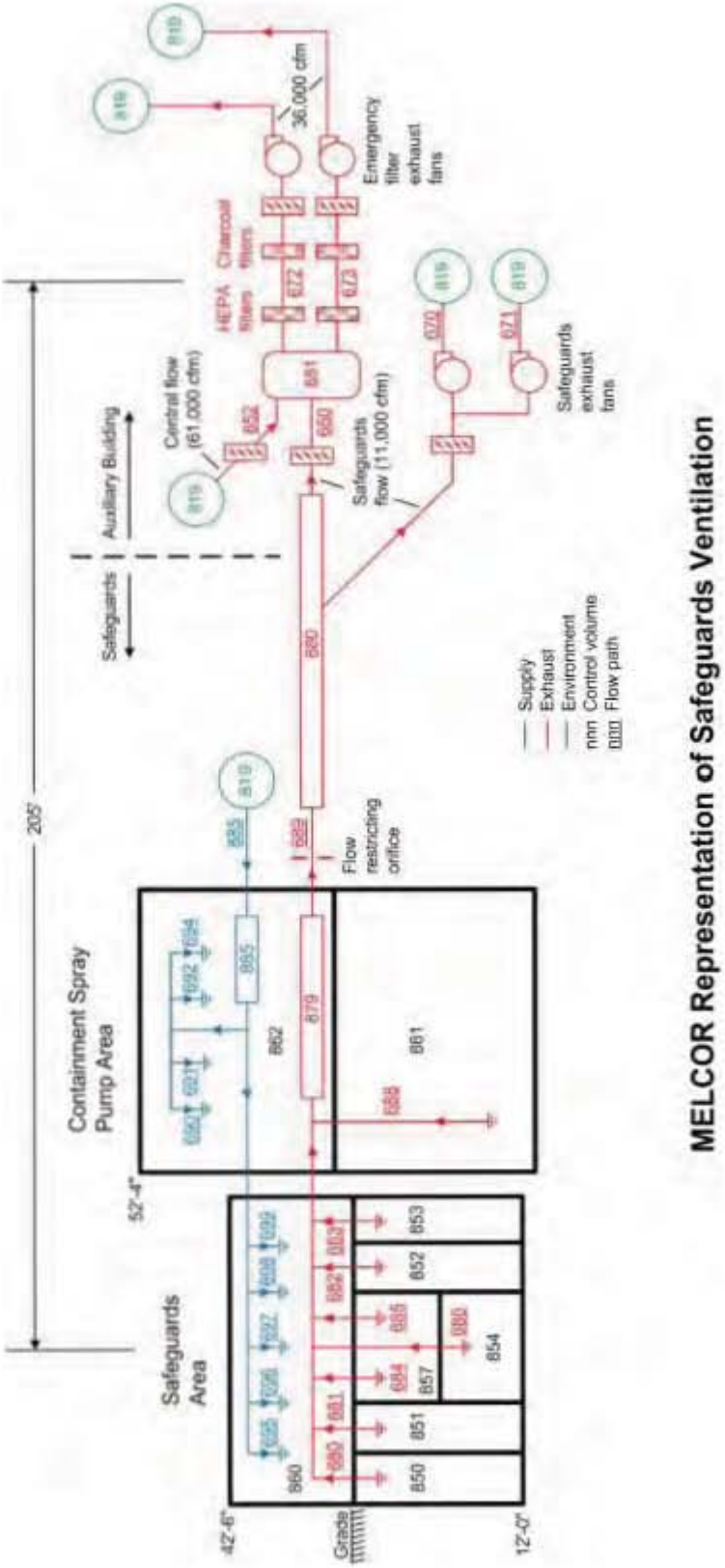

Figure 4-14 Safeguards Buildings Ventilation MELCOR Nodalization

4.10.1 Building Interconnectivity

A detailed accounting of the interconnectivity between the Safeguards buildings is presented in Appendix D. Key penetrations, doorways, etc., and their influences are described below.

Pipe penetration between Safeguards Area and Containment Spray Pump Area:
There is a rectangular opening in the wall between the Safeguards Area and the Containment Spray Pump Area that would limit the depth of the pool that could develop on the Safeguards Area floor given an ISLOCA. The depth of the pool would be important because the ISLOCA pipe break could potentially be submerged such that fission products emanating from the break could be captured (i.e., scrubbed) by the pool. A pool in the Safeguards Area would overflow to the Containment Spray Pump Area through the subject opening. The opening is 21" tall and 5' long. The base of the opening is 4'-9" off the Safeguards Area floor. The opening looks to be ~50% full of piping. It is represented by Flow Path 625.

The flooding in the Safeguards Area would submerge the non-submersible motor of isolation valve MOV 1890C making the ISLOCA unisolable. The flooding would not be sufficiently high to wet the LHSI pump motors. As the LHSI pumps are largely sheltered from the most likely pipe break and as the electrical wiring to their motors drops down from above, the LHSI pumps are judged unsusceptible to flooding from an ISLOCA.

Water level in the building would remain at the 4'-9" mark until water (liquid) stopped spilling from the break. From then on, level would slowly fall as the pool in the Safeguards Area leaked to the Containment Spray Pump Area past the flashing covering the shaker space between the two buildings. The ISLOCA pipe break, assumed centered 1'-9" off the floor, would potentially be submerged during core degradation. Submergence would support scrubbing of fission product aerosols and vapors by the pool. MELCOR addresses this phenomenon.

Shaker space between Safeguards Area and Containment Spray Pump Area:
As described earlier, the Safeguards buildings do not have integral back walls. The buildings back up to Containment and the Containment cylinder serves as a back wall to the buildings. Where the wall between the Safeguards Area and the Containment Spray Pump Area approaches the Containment cylinder, there is a 3" shaker space. The shaker space is covered by flexible metallic flashing on both sides of the wall. The flashing is close fitting but may not be watertight. Consequently, a pool in the Safeguards Area would leak past the flashing into the Containment Spray Pump Area and the depth of the pool would be influenced by the leakage as time progressed. As described previously, the depth of the pool would be important because the ISLOCA pipe break could potentially be submerged such that fission products emanating from the break could be scrubbed by the pool.

Appendix D includes a cross sectional drawing of the flashing. The flashing is represented by Flow Path 636. The flashing was assumed to have an effective 1/32"-wide leakage gap along its length. The flow-path distance through the gap (from the Safeguards area to the Containment Spray Pump Area) was assumed to be 6" based on the cross-section dimension of the angle iron. Flow Path 636, therefore, was defined with the flow area of a 1/32" gap, a length of 6", and a hydraulic diameter of 1/32". Entry and exit form losses of 0.5 and 1.0 were assumed on both sides of the wall for a combined form loss of 3.0. Uncertainty exists in the assumed 1/32"

effective leakage gap of the flashing given that that the walls of Safeguards Area are not especially flat and that the angle iron mating the flashing to the walls is rigid.

Open doorway and taller opening joining the basements of the Containment Spray Pump Area and the Main Steam Valve House:
The basements of the Containment Spray Pump Area and the Main Steam Valve House are largely open to each other via a doorway and a taller and wider opening. Water and air could flow freely between the basements. Flow Path 628 accomplishes this interconnectivity.

Water overflowing the Safeguards Area to the Containment Spray Pump Area would move readily across the largely open floor to the adjoining floor of the Main Steam Valve House and quickly fill a 9' pit there. A pipe tunnel leads from the pit to the Auxiliary Building. The tunnel is filled with fire-resistant penetration sealant. Water would pool on the Main Steam Valve House and Containment Spray Pump Area floors high enough for hydrostatic pressure to dislodge this sealant opening the tunnel. Water issuing from the ISLOCA pipe break and through the tunnel would ultimately flood the basement of the Auxiliary Building.

Pipe tunnel between Main Steam Valve House and Auxiliary Building:
As noted above, there is a pipe tunnel between the Main Steam Valve House and Auxiliary Building. The tunnel opens on the Main Steam Valve House side to a pit in the floor. The tunnel cross section is 18" (high) x 7'-7". The tunnel is not long, traversing only the thickness of the wall between the Main Steam Valve House and Auxiliary Building. The tunnel is crisscrossed with occasional rebar and filled with a sprayed penetration sealant. The sealant is thought to have little capacity to tolerate a pressure differential and so is assumed to dislodge in the ISLOCA scenario when the pit in the Main Steam Valve House floods. Water level would be 1'-3" above the top of the tunnel at this point. The question arises as to whether the sealant might survive 1'-3" of water. The question becomes mute however realizing that if the tunnel were blocked to flow, water level (in an ISLOCA) would rise to many feet in the Main Steam Valve House. It is not credible that the sealant could withstand many feet of water. The subject tunnel is represented by Flow Path 634.

4.10.2 Existing Potential Fission Product Release Pathways

Several potential pathways exist for the release of fission products from the Safeguards buildings given an ISLOCA resulting in core damage. These pathways are identified below.

Safeguards exhaust ventilation system:
The filtered exhaust ventilation system serving Safeguards would be a pathway for fission product release should the filters fail. The system and the modeling of it are described in Section 4.11. The filters could fail from exposure to excessive temperatures or excessive differential pressure. Excessive temperatures (> 250 ^{o}F) could arise from hot gasses passing through the filters or from the heat produced by the decay of fission products captured by the filter media. Excessive differential pressure (> 25 in H_2O) could develop across the filters as they load with aerosol and impede flow.

Safeguards supply ventilation system:
The supply ventilation system serving Safeguards would be a release pathway should Safeguards pressure become greater than ambient pressure. The system is fitted with continuous roll filters and steam heating coils for cold-weather space heating. The roll filters are not high efficiency aerosol filters. The system has a 16,000 cfm fan, but to ensure inward leakage to Safeguards, the fan is not operated. Section 4.11 describes the system and how it is modeled in MELCOR.

Safeguards Area personnel door:
The lone personnel door for accessing the Safeguards Area is centrally located in the top floor of the building at ground level. The door opens outward and is equipped with a closer. The door opens to a modest push by hand. It has no latch. Flow Path 611 shown in Figure 4-13 represents this door in the MELCOR model. Given a meaningful elevation of Safeguards Area pressure (i.e., 1 in H_2O gauge), this flow path is opened to the environment. The flow path is reclosed upon loss of the elevated pressure.

Abandoned penetrations in the Containment Spray Pump Area:
Two abandoned penetrations exist in the exterior wall of the upper level of the Containment Spray Pump Area. The penetrations lead directly to the environment. They are approximately 1' in diameter and 12' off the floor. Flow Path 629 shown in Figure 4-13 represents these penetrations.

Abandoned exhaust fan in the Containment Spray Pump Area:
An abandoned exhaust fan resides in the roof of the Containment Spray Pump Area. The opening in the roof associated with the fan was estimated to be 2' x 2'. Flow Path 626 shown in Figure 4-13 represents this opening.

Main Steam Valve House exhaust fan:
The upper level of the Main Steam Valve House has a wall-mounted exhaust fan that runs continuously. The fan flows 13,500 cfm. There is no filtering of the air exhausted by this fan, as the Main Steam Valve House is not considered a potentially contaminated area. Flow Path 631 shown in Figure 4-13 represents this fan.

Main Steam Valve House ventilation intake:
An air intake exists in the exterior wall of the upper level of the Main Steam Valve House. The intake is near the floor. It is 8' wide x 4'-6" wide and louvered. Flow Path 630 shown in Figure 4-13 represents this intake.

4.10.3 Potential Building Boundary Over-Pressure Failures

An ISLOCA at Surry and consequential RCS blowdown into the Safeguards Area would pressurize the Safeguards buildings. The buildings are reinforced concrete structures largely below grade with corrugated steel roofs. The construct of the buildings has been scrutinized and likely building boundary failures have been identified. The likely failures and the modeling of them are described below. Subsequent hydrogen burns in the Safeguards Area could be expected to further damage the building's structural boundary.

Tearing of Safeguards Area and/or Containment Spray Pump Area roof flashing:
The Safeguards buildings do not have integral back walls. The buildings back up to containment and the containment cylinder serves as a back wall to the buildings. The steel roofing on the buildings extends to within a few inches of the containment wall leaving a gap that is closed with flashing. This flashing has been judged as a weak point in the pressure boundaries of the Safeguards buildings. The flashing has been specified to tear given a pressure differential across it of 37.5 psf. The basis for this criterion is presented in Appendix D. The flashing is represented with Flow Paths 612 and 643 shown in Figure 4-13 for the Safeguards Area and the Containment Spray Pump Area, respectively. Flow Path 612 reflects a gap 3" wide by 60'-4" long while Flow Path 643 reflects a gap 3" wide by 22'-9" long.

Gross failure of Safeguards Area and/or Containment Spray Pump Area roofs:
The tearing of roof flashing described above would significantly vent the Safeguards buildings given an ISLOCA and consequential RCS blowdown into them. The venting, however, might not be sufficient to curtail further damage to the boundaries of the buildings from the blowdown or from subsequent hydrogen burns occurring within the buildings.

The Safeguards buildings are reinforced concrete structures largely below grade with corrugated steel roofs. From considerations presented in Appendix D, the roofs are identified as the weakest boundaries of the buildings and are taken to fail given a pressure differential of 75 psf across them. The failure is considered gross in that a large opening in the roof results. Flow Paths 613 and 647 shown in Figure 4-13 represent gross roof failures in the Safeguards Area and the Containment Spray Pump Area, respectively. These flow paths have an area of 10 m^2 each.

4.11 Safeguards Ventilation System

The Safeguards Area and the Containment Spray Pump Area are normally exhausted unfiltered by dual 6,000 cfm fans. As these buildings have recognized contamination potential, they are instead exhausted by a filtered safety-related ventilation system given a LOCA. On a safety injection signal, the normal exhaust fans are automatically isolated and the safety-related exhaust system is automatically started. The safety-related exhaust has particulate and iodine filtration and dual parallel redundant fans. The fans and filters serving the Safeguards Area and Containment Spray Pump Area reside in the Auxiliary Building. The fans exhaust through a stack above the roof of the Auxiliary Building. Figure 4-14 illustrates the configuration of the Surry Safeguards Ventilation System and the MELCOR representation of it. Fresh air to the Safeguards Area and Containment Spray Pump Area is supplied by ducting routed from a common intake point in the exterior wall of the Containment Spray Pump Area. As originally constructed, an intake fan forced fresh air through the ducting. To ensure negative pressures within the Safeguards buildings, this fan is no longer operated. Air is instead drawn though the intake ducting in response to the negative pressures developed in the Safeguards buildings by the exhaust ventilation system. Intake air is continually cleaned by roll filters and heated by steam coils in the winter. The roll filters are not high efficiency.

The safety-related exhaust fans and filters serving the Safeguards areas are not dedicated to these areas. Instead, the fans and filters serve many areas at Surry having recognized contamination potential. Of the combined 72,000 cfm drawn by the fans through the filters, 11,000 cfm would be drawn from Unit 1 or Unit 2 Safeguards following the generation of a safety injection signal

in whichever unit. A flow-restricting orifice in the exhaust ducting leading from each unit's Safeguards area limits flow.

Pressure switches installed in the inlets of the safety-related exhaust fans trip the fans should inlet pressure reduce to less than 21 inches H_2O gauge. Excessive aerosol loading on the filters could cause this condition. This functionality is captured in the MELCOR modeling. Heavy loading on the filters is not expected to result in tearing of the filters as the filter vendor has stated that the filters could easily withstand the maximum pressure head the fans can develop.

The particulate filters in the safety-related exhaust system are high-efficiency particulate air (HEPA) filters. Two banks of filters are installed, one associated with each fan. Each filter bank is constructed of 30 individual filter cells.

The filter units in the safety-related exhaust system, one filter unit for each fan, are constructed from individual filter cells. Each filter cell comprises a pre-filter, backed by a HEPA filter, backed by two parallel charcoal filters. The frontal area of a filter cell is 2' x 2'. The HEPA filters are 1' thick. Each filter unit is 10 filter cells wide by 3 filter cells high. The MELCOR modeling of the filter units represents:

- A 99.5% aerosol capture efficiency by the HEPA filters
- The clean flow resistance of the HEPA filters
- The added flow resistance of the HEPA filters due to aerosol loading within them
- Tearing of the HEPA filters from excessive pressure difference across them
- A 99.0% iodine and cesium iodide vapor capture efficiency by the charcoal filters
- The clean flow resistance of the charcoal filters

The pre-filters are not represented in the MELCOR modeling. The temperatures to which the HEPA filters are exposed are monitored in the ISLOCA calculations (i.e., relative to the 250 ^{o}F maximum continuous temperature rating for the filters) but no over temperature failure criterion is implemented in the modeling. While tearing of the HEPA filters on excessive differential pressure is implemented, the filters are not expected to tear given that the filter vendor concluded they could easily withstand the maximum pressure the fans could develop.

Substantial amounts of fission product aerosols could be expected to lodge in the HEPA filters of the safety-related exhaust system serving Safeguards given an ISLOCA at Surry. The potential exists for loading on the filters to be excessive in that the fans of the system shut down. A shutdown of the fans would leave the fission products lodged in the filters without a cooling flow of air. Decay heat generated by the fission products could be an issue with respect to overheating of the filters, the filter plenum, etc. The MELCOR modeling of the phenomena that could lead to filter loading shutting down the fans is complete and so the MELCOR calculations should indicate well a loss-of-cooling threat to the filters.

Appendix D describes the Surry Safeguards Ventilation System and the MELCOR modeling of it in detail.

4.12 Low Head Safety Injection Piping

The LHSI piping that would be subjected to RCS pressure, should the two serial check valves in any one of the three cold leg injection lines fail, extends backwards from the check valves into the Safeguards Area and then through the Containment Spray Pump Area and Main Steam Valve House well into the Auxiliary Building. Two MELCOR representations of LHSI piping were used in the ISLOCA analysis – a simple representation where the fluid volume and metal mass of the piping was unaccounted for and a detailed representation where these parameters were taken into account. In the simple representation, frictional losses, form losses, and critical flow areas were represented in a single flow path. No control volumes or heat structures were included in the simple representation. In the detailed representation, flow losses and critical flow areas were portioned among several flow paths and several control volumes and heat structures were included to account for the fluid volume and metal mass of the piping. The simple representation was used in the MELCOR full-plant ISLOCA calculation. The detailed representation was used in a MELCOR separate-effects calculation to estimate decontamination factors (DFs) associated with aerosol deposition for use in the full-plant calculation. Figure 4-15 illustrates the detailed MELCOR model of the LHSI piping and roughly identifies the attributes of the physical piping.

The location of the LHSI piping rupture could be in the Safeguards Area, the Containment Spray Pump Area, the Main Steam Valve House, or even in the Auxiliary Building. The break could be above the flood level or below it. If the break were in the Safeguards Area, some of the LHSI piping would be submerged throughout core degradation. If the break were elsewhere, none of the LHSI would be submerged. A submerged break location would support scrubbing of fission product aerosols and vapors by the pool. Submerged piping would stay relatively cold promoting fission product deposition in the piping.

From the check valves to isolation motor operated valve (MOV) 1890C, the 6” and 10” piping is Schedule 160 with 0.718” and 1.125” wall thicknesses, respectively, and a pressure rating higher than RCS operating pressure. From MOV 1890C back, none of the piping is rated strong enough to withstand RCS operating pressure. Between MOV 1890C and Flow Element (FE) 1945 for LHSI Train A and FE 1946 for LHSI Train B, the piping (10”) is Schedule 40 having a 0.365” wall thickness. The 8” piping in the Safeguards buildings and all of the way back to isolation points within the Auxiliary Building is Schedule 40 having a wall thickness of 0.322”. Between FEs 1945 and 1946 and the LHSI pump discharge check valves, the piping (10”) is Schedule 10 with a 0.165” wall thickness. It is these relatively short sections of thin-walled 10” piping that are judged as most susceptible to rupture given the dual check valve failure of the postulated ISLOCA. This piping ranges in centerline elevation from 13’-9” to 15’-8” (i.e., 1’-9” to 3’-8” off the floor). Significantly more of this piping exists outside the pump cubicles than inside them and slightly more of the piping is at the 13’-9” elevation than at the 15’-8” elevation. Figure 4-16 shows the location of the different LHSI pipe sections in the Safeguards Area.

The ISLOCA break is assumed to occur centered 1’-9” above the floor with an area equivalent to the orifice area of FE 1945 or FE 1946 each of which are of diameter 7.1469”. Only one of the thin-walled 10” piping sections is assumed to rupture not both. The break is assumed to happen outside of a LHSI pump cubicle.

Optional MELCOR pool scrubbing logic (SPARC) was enabled in the flow path representing the LHSI piping (Flow Path 812) in the simple representation. This logic removes radionuclide aerosols and vapors from a gas as it flows through a pool of water. The flow area of Flow Elements 1945/1946 (7.1469" diameter) was specified. A single vent hole with horizontal orientation was called out.

Long standing experiments presented in Section 4.13 suggest that much of the fission-product aerosol carried into the LHSI piping, as a consequence of an ISLOCA, would deposit in the piping. The deposition would be by means of turbulent deposition and impaction. As identified in Section 4.13, MELCOR has been modified as part of the ISLOCA analysis effort to account for these mechanisms. A consequence of large deposits of radioactive material in the LHSI piping is the associated decay heat. MELCOR appropriately associates decay heat by radionuclide class and local mass wherever material is carried throughout the construct of a model. As such, the heating of heat structures representing LHSI piping segments, and hence the heating of radionuclide deposits on them, is accounted for as the radionuclides decay. The result of this heating, as evidenced by MELCOR, is substantial revaporization of more volatile radionuclides (e.g., CsI) from deposits in the LHSI piping.

The energy emitted by fission product deposits in the LHSI piping would be in the form of beta particles and gamma radiation. The beta particles would be readily absorbed by the vapor in the pipe and by the steel pipe wall. The gamma radiation would be partially absorbed by the pipe wall. Trivial gamma radiation would be absorbed by the vapor. In modeling the LHSI piping, consistent with MELCOR's default assumption, it was assumed that half of the energy emitted by fission product deposits is associated with beta particles and half with gamma radiation. It was further assumed that half of the beta particles are absorbed by the vapor and half by the pipe wall. In evaluating the gamma absorption in the pipe wall, gamma ray attenuation was assumed given by [77]:

$$I = I_0 e^{-\mu x}$$

where,

I = attenuated radiation exposure rate
I_0 = original radiation exposure rate
μ = linear attenuation coefficient (cm^{-1})
x = absorber thickness (cm^{-1})

Given the half-value layer for steel associated with gamma radiation from cesium-137 equal to 1.6 cm [77], substituting into the equation above yields:

$$0.5 = e^{-\mu \times 1.6}$$

Solving this equation for μ:

$$\ln(0.5) = -\mu \times 1.6$$

$$\mu = 0.43322$$

For the steel pipe then:

$$\frac{I}{I_0} = e^{-0.43322x}$$

where x is the thickness of the pipe wall.

For the 6" Schedule 40 (0.719" wall) LHSI piping and the 10" Schedule 40 (0.365" wall) LHSI piping in Safeguards, I/I_o is equal to 0.453 and 0.669, respectively. These values relate to gamma absorption fractions of 0.547 and 0.331 for the 6" and 10" pipe, respectively. Considering these gamma absorption fractions, the equal partitioning of decay energy between beta particles and gamma radiation, and the equal partitioning of beta deposition between the vapor in the pipe and the pipe wall, the distribution of decay energy produced by fission product deposits in the LHSI piping was specified in the MELCOR modeling as:

- 25% to the vapor in the pipe, 52.3% to the pipe wall, and 22.7% to the environment in the case of 6" pipe

- 25% to the vapor in the pipe, 41.6% to the pipe wall, and 33.4% to the environment in the case of 10" pipe

Appendix D describes the Surry LHSI piping and the MELCOR modeling of it in further detail.

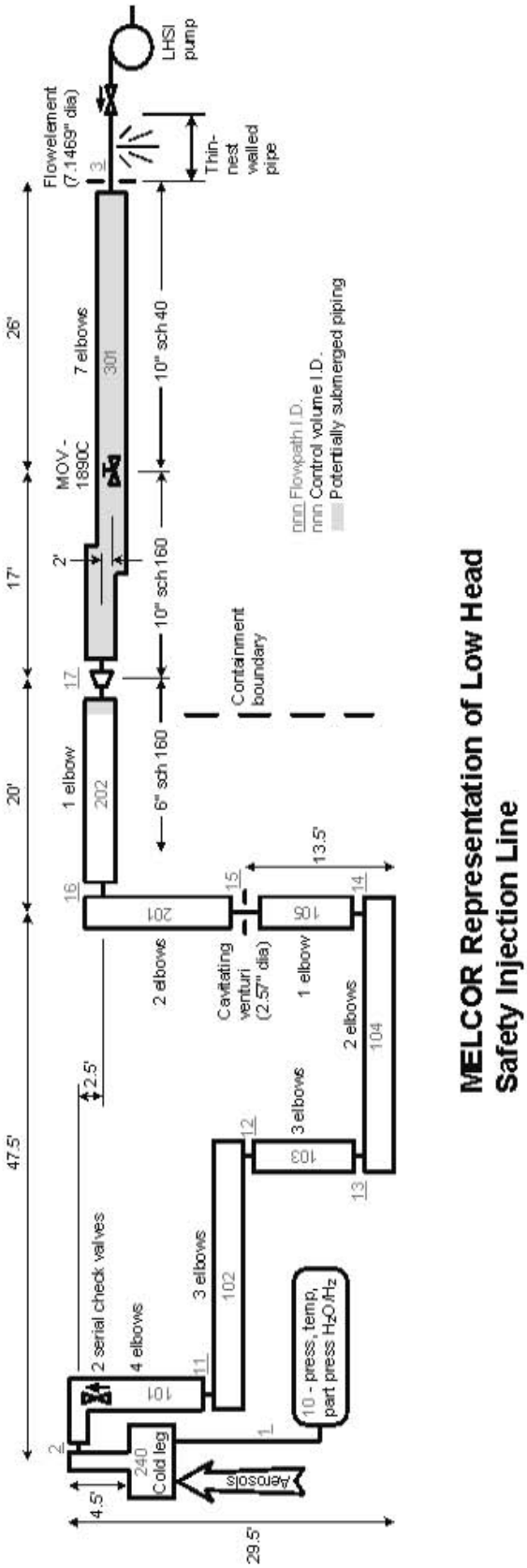

Figure 4-15 Low Head Safety Injection Piping MELCOR Nodalization

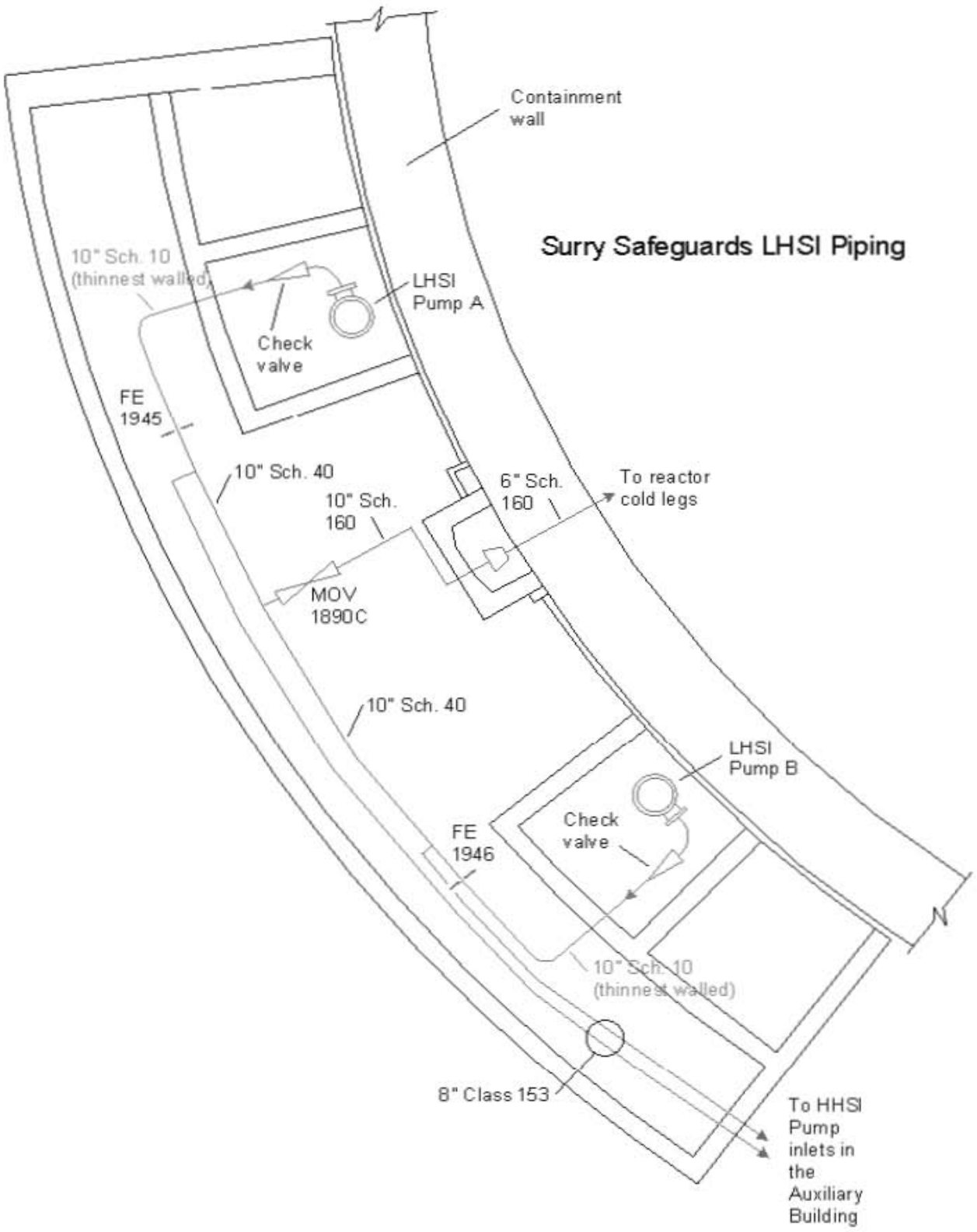

Figure 4-16 Low Head Safety Injection Pipe Sections in Safeguards Area

4.13 Radionuclide Deposition in LHSI Piping by Turbulent Deposition and Impaction Deposition in the LHSI Piping

During an ISLOCA, fission product aerosols and non-radioactive aerosols released from the core and core debris will transport and deposit along the following path:

- the reactor vessel and reactor coolant system,
- the low head safety injection (LHSI) piping, and
- the Safeguards Area.

From the Safeguards Area, the fission products can reach the environment through openings in the Safeguards Area or through the ESF ventilation system.

MELCOR calculates aerosol deposition using the following models: gravitational settling, thermophoresis, diffuseophoresis, and Brownian motion. This is sufficient for flow regimes typically encountered in severe accident analysis where the flow of steam and hydrogen is slow and wafting (e.g., 1 meter/second). However, a peer review committee member commented that, in an ISLOCA, flow rates in the LHSI piping which has an internal diameter of 5.2 inches can be high turbulent and turbulent aerosol deposition and inertial deposition from flow irregularities can be important.

Turbulent deposition results when particle trajectories depart from flow path-lines. This departure is caused by the mass of an aerosol particle, which causes it to accelerate or decelerate more slowly than a gas particle (molecule). Because of the chaotic motions of a highly turbulent flow, turbulent deposition can dominate over other deposition mechanisms.

Deposition induced by flow irregularities is generally by impaction of aerosol particles against surfaces in the vicinity of the geometrical irregularity. Deposition is caused by inertial effects; aerosol particles are unable to follow flow streamlines because the aerosol is denser than the surrounding fluid. Some of the aerosol particles thus collide with a surface and deposit. Generally, larger aerosol particles deposit preferentially over smaller ones, which are able to follow fluid streamlines more closely.

As a result of this peer review comment, new aerosol deposition models were added to MELCOR. Models for turbulent deposition in straight pipes and inertial deposition in elbows were taken from modeling developed by INEL [78] and from the VICTORIA code [79]. Adding models from these two sources enabled benchmarking of the two models against each other in addition to validating the results against experiments. Models for inertial deposition in a sudden contraction and a vena contracta (e.g., a venturi) were also added to MELCOR from the VICTORIA code.

The new MELCOR models for turbulent deposition in straight pipes and inertial deposition in elbows were validated against the results of the Light Water Reactor (LWR) Aerosol Containment Experiments (LACE) Project. The LACE project, organized by Electric Power Research Institute (EPRI), performed large-scale experiments to investigate aerosol behavior under simulated LWR accident conditions to provide a database for testing containment-aerosol and related thermal-hydraulic computer codes. The tests studied aerosol behavior under

postulated severe accidents conditions not adequately addressed by previous test programs. The studied conditions included total containment bypass (i.e., ISLOCA). Individual LACE tests that studied ISLOCA conditions were CB-1, CB-2, CB-3, LA1, LA3A, LA3B, and LA3C. LACE reports for these tests are the following:

- "Aerosol Behavior Under LWR Containment Bypass Conditions—Results of Tests CB-1, CB-2 and CB-3," LACE TR-001, November 1986

- "Aerosol Behavior in LWR Containment Bypass Piping—Results of LACE Test LA3," LACE TR-011, July 1987

- "Summary of Posttest Aerosol Code Comparisons for LWR Aerosol Containment Experiment (LACE) LA1," LACE TR-022, ORNL/M-365, October 1987

- "Summary of Posttest Aerosol Code-Comparisons Results for LWR Aerosol Containment Experiment (LACE) LA3," LACE TR-024, ORNL/M-492, June 1988

A summary of the LACE project is given in "The LWR Aerosol Containment Experiments (LACE) Project, Summary Report" [80]. Validation of the new MELCOR models against the LACE tests that studied ISLOCA conditions is documented in Appendix D.

The new MELCOR models were applied in a separate-effects calculation that used boundary conditions from the integral full-plant calculation to estimate aerosol retention in the LHSI piping. The estimated aerosol retention for each fission product class was in turn used to specify a DF for each MELCOR radionuclide class (see Appendix B, Table B-1) as input to the integral full-plant calculation which represented the LHSI piping as a single junction. The nodalization and the results of the separate-effects calculation are described in Section 4.14 and Section 5.5.2, respectively.

4.14 Analysis Methodology Involving Two MELCOR Models for LHSI Piping

Two MELCOR representations of the LHSI piping were utilized in the ISLOCA analysis:

1. A simple representation where the fluid volume and metal mass of the piping were unaccounted, and

2. A detailed representation where these parameters were taken into account.

The simple representation, which amounted to a single flow path, was defined as part of the overall MELCOR model representing the RCS, Containment, Safeguards Area, etc. The detailed representation consisting of several small control volumes, flow paths, and heat structures was defined as a much smaller standalone MELCOR problem (i.e., separate-effects problem) absent of an RCS, Containment, Safeguards Area, etc. The detailed representation was developed to best exercise the aerosol deposition (i.e., turbulent deposition and impaction) modeling newly incorporated into MELCOR as part of the ISLOCA analysis effort. It allowed sensitivity investigations into phenomena such as heat loss from the piping and gamma ray transmission through it to be accomplished efficiently. Boundary conditions were imposed on the separate-

effects problem reflective of the conditions in an initial overall ISLOCA calculation. Decontamination factors (DFs) determined from the separate-effects problem were then imposed on a final overall MELCOR calculation to account for the phenomena of turbulent deposition and impaction in the LHSI piping. The sequential steps taken to accomplish the ISLOCA calculation using the two MELCOR models were:

1. An initial overall ISLOCA calculation was carried out without particulate deposition accounted for in the LHSI piping. The calculation wrote files containing thermal hydraulic and aerosol transport information to be imposed on a separate-effects (deposition) calculation. The specific information written to the files consisted of:

    - Pressure in RCS Cold Leg A (CV 240)
    - Vapor temperature in Cold Leg A
    - Steam partial pressure in Cold Leg A
    - Mole fractions of oxygen, nitrogen, hydrogen, carbon monoxide, and methane in the noncondensable gas content of Cold Leg A
    - Pool level in the Safeguards Area
    - Pool temperature in the Safeguards Area
    - Integral masses of radionuclides by class and size bin transported into the LHSI piping
    - Mass transport rates of nonradioactive aerosols released from control rods (e.g., Ag, In, and Cd) and from zirconium cladding (i.e., Sn) into the LHSI piping. These rates were not written by size bin since the allocation of aerosols is not available (i.e., not reported by MELCOR) by size bin for nonradioactive aerosols.

2. A separate-effects calculation was carried out with the thermal hydraulic information identified above imposed as boundary conditions. The integral radioactive aerosol masses transported into the LHSI piping in the initial overall ISLOCA calculation were differentiated to form rates, and radioactive aerosols were sourced into the separate-effects calculation at these rates by class and size bin. Nonradioactive aerosols were sourced into the separate-effects calculation at the rates from the overall ISLOCA calculation assuming a lognormal size distribution with a 2-micron mass mean diameter and a geometric standard deviation of two. Figure 4-17 through Figure 4-19 illustrate the imposition of thermal hydraulic conditions. Figure 4-20 and Figure 4-21 show the sourcing of aerosols managed in the separate-effects calculation.

3. DFs were determined from the results of the separate-effects calculation reflecting the efficiency of aerosol deposition in the LHSI piping by radionuclide class. The DFs were

determined as the ratio of aerosol mass entering the piping to the difference between aerosol mass entering the piping and aerosol mass retained in the piping.

4. The DFs determined from the results of the separate-effects calculation by radionuclide class were imposed in a final overall ISLOCA calculation on the flow path representing the LHSI piping.

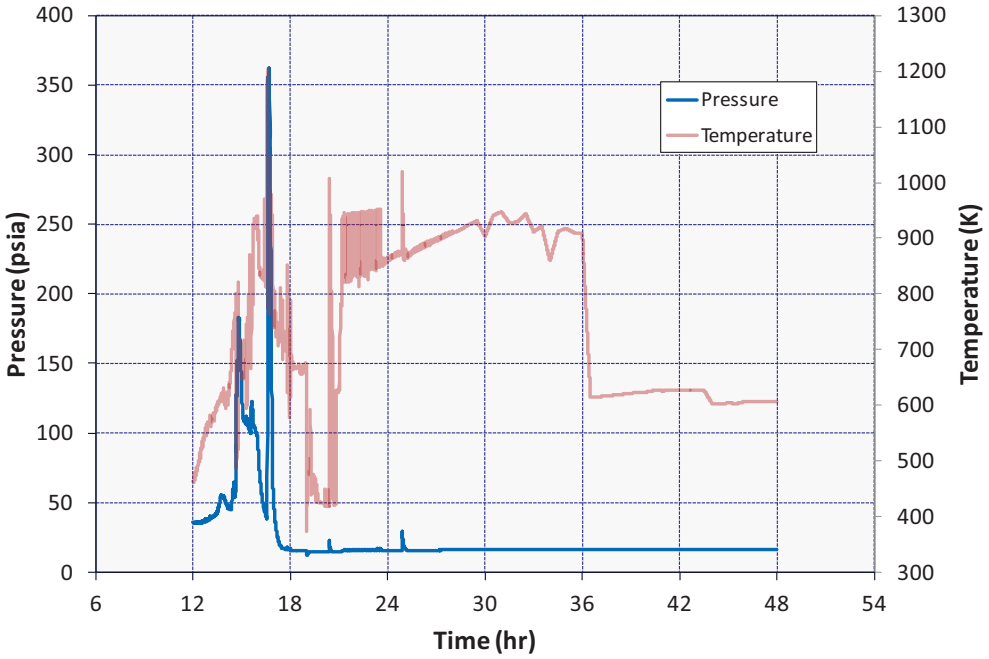

Figure 4-17 Cold Leg Pressure and Temperature Imposed on ISLOCA Deposition Calculation

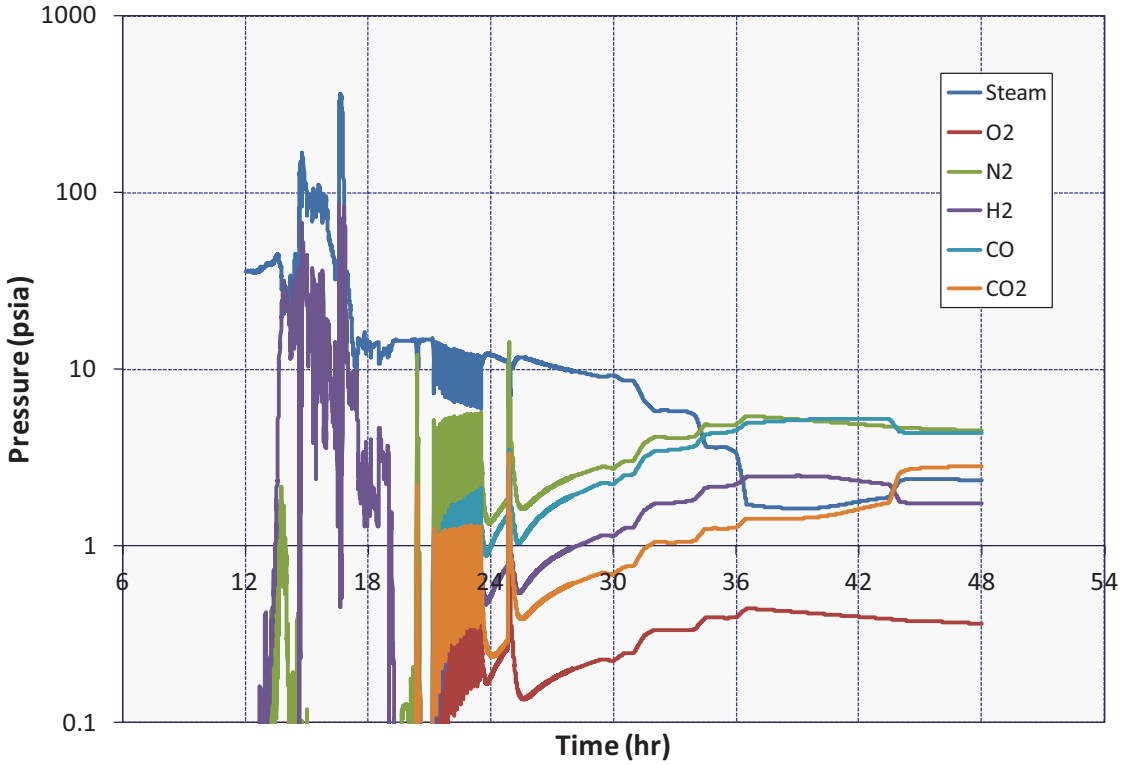

Figure 4-18 Cold Leg Partial Pressure Imposed on ISLOCA Deposition Calculation

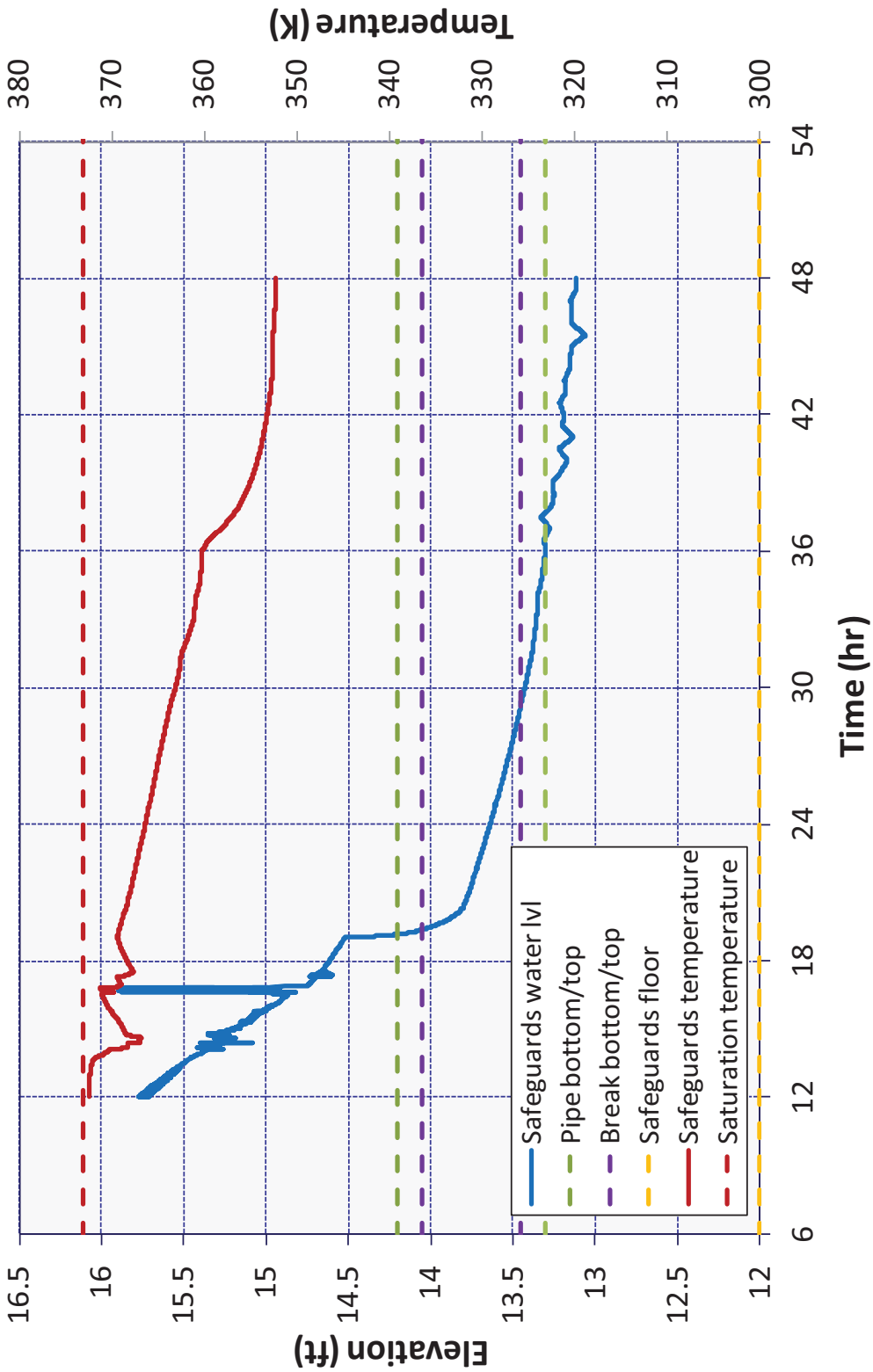

Figure 4-19 Safeguards Area Pool Level and Temperature Imposed on ISLOCA Deposition Calculation

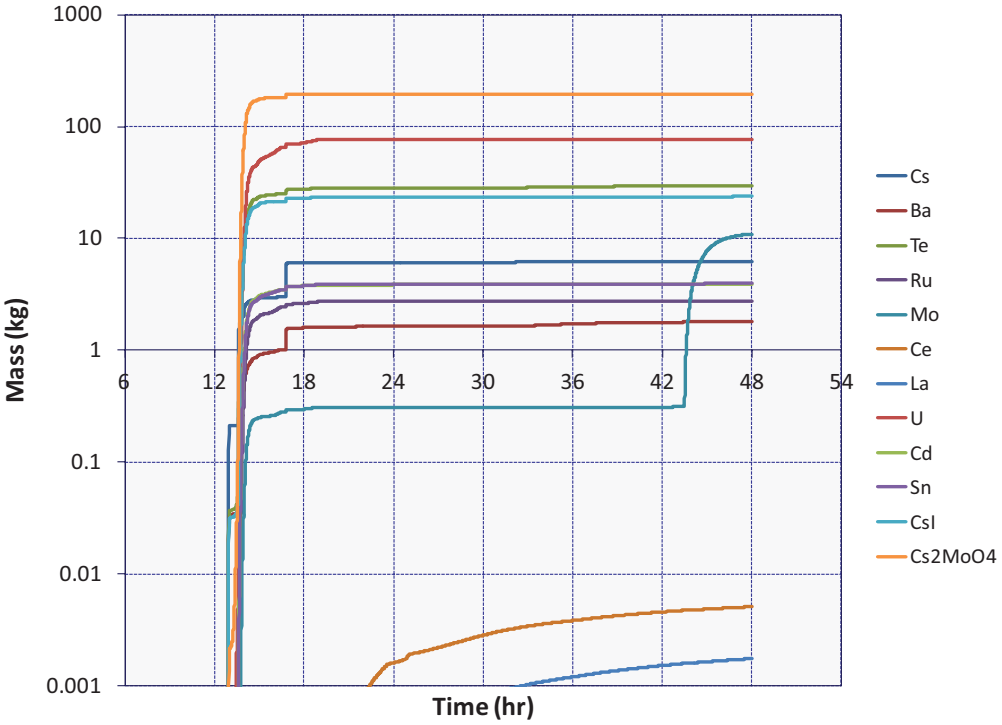

Figure 4-20 Radioactive Aerosol Sourcing into ISLOCA Deposition Calculation

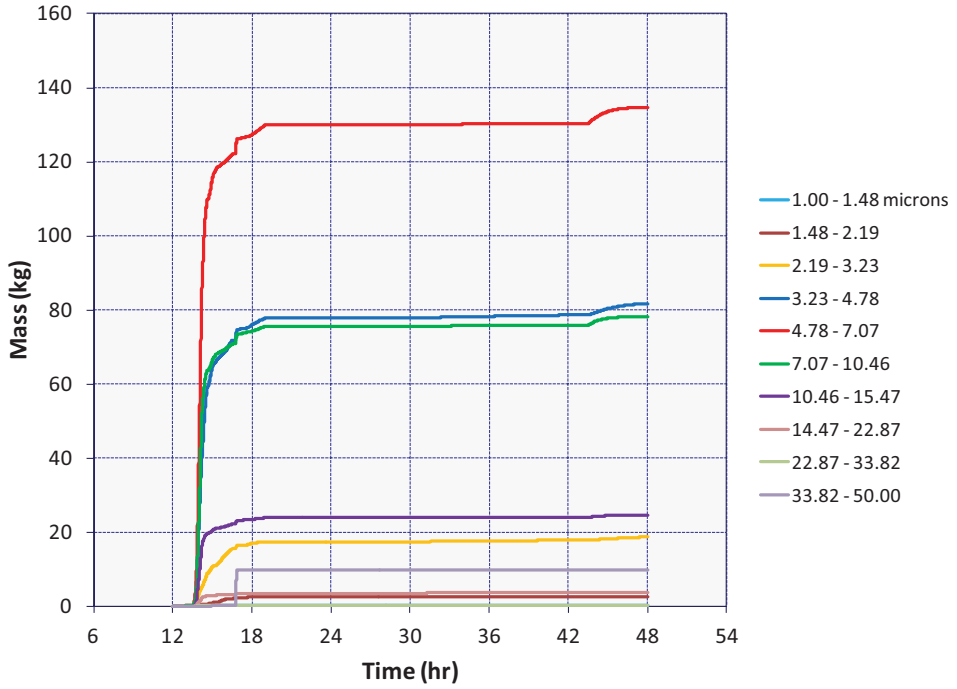

Figure 4-21 Masses of Radionuclides Sourced into the ISLOCA Deposition Calculation by Size

5. INTEGRATED THERMAL HYDRAULICS, ACCIDENT PROGRESSION, AND RADIOLOGICAL RELEASE ANALYSIS

This Section describes the integrated self-consistent analysis of each scenario using the MELCOR code. The analysis includes calculations to confirm the table top exercise results to ensure that the timing and capacity of mitigation measures are capable of preventing core damage or delaying or reducing fission product releases. This analysis also includes sensitivity calculations without B.5.b mitigation measures. Version 1.8.6YR of the MELCOR severe accident analysis code was used for the Surry analysis [8].

5.1 Long-Term Station Blackout

The long-term station blackout is assumed to be initiated by a seismic event. Section 5.1.1 presents the results of an unmitigated scenario with initially successful operator actions to depressurize the RCS and maintain TD-AFW flow.[15] However, once the DC station batteries fail at 8 hours, no more operator actions are successful. For the mitigated scenario in Section 5.1.2, a portable emergency pump is connected to the RCS at 3.5 hours and a continuous supply of water is maintained.

The Surry SPAR model assessed an early RCP seal failure with the credited operator actions as less likely than a late failure (i.e., 20% versus 80% likely). Sections 5.1.3 and 5.1.4 present the results of unmitigated and mitigated sensitivity calculations that assess the impact of an early RCP seal failure.

5.1.1 Unmitigated Long-Term Station Blackout

Table 5-1 summarizes the timing of the key events in the unmitigated LTSBO. As described in Section 3.1, the accident scenario initiates with a complete loss of all onsite and offsite AC power but the DC station batteries are available. The reactor successfully scrams and the containment isolates but all powered safety systems are unavailable except the TD-AFW. The timings of the key events are discussed further in Sections 5.1.1.1 and 5.1.1.2. However, it is worth noting that the fission product releases from the fuel do not begin until 16 hr and significant fission product releases to the environment do not begin until after 45 hr.

[15] Some successful operator actions were credited but actions to successfully connect the emergency diesel pumps for vessel injection were not. Hence, unmitigated refers to failure of specific critical actions that increased the severity of the sequence.

Table 5-1 Timing of key events for unmitigated LTSBO

Event Description	Time (hh:mm)
Initiating event Station blackout – loss of all onsite and offsite AC power	00:00
MSIVs close Reactor trip RCP seals initially leak at 21 gpm/pump	00:00
TD-AFW auto initiates at full flow	00:01
First SG SRV opening	00:03
Operators control TD-AFW to maintain level	00:15
Operators initiate controlled cooldown of secondary at ~100°F/hr	01:30
Upper plenum water level starts to decrease	01:57
Accumulators begin injecting	02:25
Vessel water level begins to increase	02:30
SG cooldown stopped at 120 psig to maintain TD-AFW flow	03:35
Emergency CST empty	05:08
DC Batteries Exhausted	08:00
S/G PORVs reclose	08:00
Pressurizer SRV opens	13:06
PRT failure	13:40
Start of fuel heatup	14:16
RCP seal failures (calculated)	14:46
First fission product gap releases	16:04
Creep rupture failure of the C loop hot leg nozzle	17:06
Accumulator empty	17:06
Vessel lower head failure by creep rupture	21:08
Debris discharge to reactor cavity	21:08
Cavity dryout	21:16
Containment at design pressure (45 psig)	28:00
Start of increased leakage of containment ($P/P_{design} = 2.18$)	45:32

5.1.1.1 Thermal-hydraulic Response

The responses of the primary and secondary pressures are shown in Figure 5-1. At the start of the accident sequence, the reactor successfully scrams in response to the loss of power. The main steam line and containment isolation valves close in response to the loss of power. The reactor coolant and main feedwater pumps also trip due to the loss of power. In response to the loss of the main feedwater, the turbine-driven auxiliary feedwater automatically starts. The TD-AFW initiates at full flow but is subsequently controlled by the operator after 15 min to maintain level. The TD-AFW restores the steam generator liquid levels by about 30 min and is throttled thereafter. After the closure of the main steam isolation valves, the secondary system quickly pressurizes to safety relief valve opening pressure, which causes the safety relief valves to open and then subsequently close when the closing pressure criterion is achieved. The relief flow through the SG SRVs is the principle primary system energy removal mechanism in the first 90 min.

The heat removal through the steam generator depressurizes the primary system to 10.3 MPa by 90 min. At 90 min, the operator starts a controlled (100^{o}F/hr) cooldown of the primary system by opening a steam generator power-operated relief valve (PORV). As the secondary pressure decreases, the saturation temperature of the water in the boiler section of the steam generator also decreases, which cools the primary system fluid. At about 3.5 hr, the steam generators reached 0.93 MPa (120 psig), where the secondary system pressure was stabilized. The TD-AFW can achieve full flow (700 gpm) at 600 psig, but degrades thereafter. It is described to work below 600 psig with an estimated lower limit of operability at 120 psig. Even with degraded performance at 120 psig, the TD-AFW adequately maintained the steam generator level until 5 hr 8 min when the ECST empties. In the unmitigated sequence, no operator actions were credited to replenish the ECST inventory. After 5 hr 8 min, the steam generator level starts to decrease and is empty by 12 hr 18 min.

By depressurizing the primary system to 120 psig via the secondary system cooldown, several beneficial results were achieved. First, the leakage through the RCP seals decreased from 21 gpm per pump at full operating pressure conditions to less than 7 gpm per pump. Furthermore, if a RCP seal should fail under these conditions, then the resulting leakage flow would be much lower than if the primary system pressure was not actively controlled to low pressure. Second, the accumulators begin injecting at 600 psig (4.1 MPa). The accumulators are a source of cold water to replace the losses due to RCP seal leakage and the volume shrinkage during the cooldown. By 8 hr, about 4500 gal had been discharged from each accumulator, or about two-thirds of the water inventory. Consequently, as shown in Figure 5-2, the inventory loss was minor during the first 8 hr.

At 8 hr, the station batteries were estimated to fail. At the same time, the steam generator relief valves closed and were no longer actively controlled. In response to the steam generator valve closure, both the primary and secondary systems rapidly pressurized to the secondary safety relief valve opening pressure. The primary system remained just above this pressure until about 12 hr 18 min, when the steam generators boiled dry. Subsequently, the primary system pressurized to the pressurizer safety relief valve opening set point and began to relieve steam and water. The fluid in the vessel heated to saturation conditions and then swelled in response to the heatup. Once the pressurizer safety relief valves began cycling, a significant amount of fluid is

vented out of the RCS and the vessel level dropped quickly (see Figure 5-2). The top of the fuel was uncovered by 14.3 hr and the core heatups began (see Figure 5-3).

Shortly after the start of the core uncovery, the RCP seals failed when saturated water started flowing through the loop seals. The effective leak rate increased from 21 gpm at full operating pressure and temperature to 182 gpm at full operating pressure and temperature.[16] Once the two-phase water level drops below the core plate, the decrease in the vessel two-phase level slows because the water level is below the bottom of the fuel (see Figure 5-2).

Similar to the STSBO (see Section 5.2.1), an in-vessel natural circulation flow develops between the hot fuel in the core and the cooler structures in the upper plenum. Hot gases rise out of the center of the core rise into the upper plenum and return down the cooler peripheral sections of the core. Simultaneously, a natural circulation circuit develops between the vessel and the steam generator. Due to its close proximity to the hot gases exiting in the vessel, the hot leg nozzle at the carbon steel interface region to the stainless steel piping was first predicted to fail by creep rupture at 17 hr 6 min.[17]

Following the accumulator injection, the decay heat from the fuel boiled away the injected water. By 18.2 hr, a large debris bed had formed in the center of the core. The debris bed continued to expand until 18.9 hr when all the fuel had collapsed and was resting on the core plate. The hot debris failed the lower core plate and fell onto the lower support plate, which failed at 19.9 hr. Following the lower support plate failure, the debris relocated onto the lower head. The small amount of remaining water in the lower head boiled away. As shown in Figure 5-4, the hot debris quickly heated the lower head to above the melting temperature of stainless steel (i.e., 1700 K) on the inside surface. As the heat transferred through the lower head, it eventually failed at 21 hr 8 min due to the creep rupture failure criterion (i.e., primarily due the thermal stress component due to the low differential pressure).

By 21.3 hr, nearly all the hot debris relocated from the vessel into the reactor cavity under the reactor vessel. The hot debris immediately boiled away the water in the reactor cavity and started to ablate the concrete. The ex-vessel core-concrete interactions (CCI) continued for the remainder of the calculation, which generated non-condensable gases. In addition, the hot gases exiting the reactor cavity and the radioactive heating from airborne and settled fission products steadily evaporated the water on the containment floor outside the reactor cavity from 21.1 hr to 67 hr. The resultant non-condensable and steam production pressurized the containment (see Figure 5-5). At 45.5 hr, the containment failed due to liner tearing near the containment equipment hatch at mid-height in the cylindrical region of the containment. The containment continues to pressurize until the leakage flow balanced the steam and

[16] The leak model is tuned to these values at normal operating conditions. In a transient calculation, the leakage flow rate changes as a function of subcooling, quality, and pressure.

[17] Alternate failure locations could include the pressurizer surge line and the steam generator tubes. In the MELCOR calculation, the RCP seals had failed so hot gases were no longer flowing out the pressurizer when the core exit temperatures were hottest. Due to the relatively high pressure in the steam generators' secondary side, the resultant thermal-mechanical stresses across the steam generator tubes were less severe than the hot leg nozzle. Consequently, the most vulnerable location was calculated to be the hot leg nozzle. The initial failure location for this scenario is also part of an on-going investigation of another research program in the NRC.

non-condensable gas generation. By 67 hr (2.8 days), all the water on the floor has evaporated. The containment depressurized thereafter due to only a smaller gas loading from the non-condensable gas generation. The conservatively assumed failure location was the around the equipment hatch, which is located on the side of the containment without a surrounding building (e.g., the auxiliary or safeguards buildings) other locations such as personnel airlocks and penetrations would result in lower releases due to a transport and deposition inside adjacent buildings. Consequently, any released fission products are released directly to the environment.

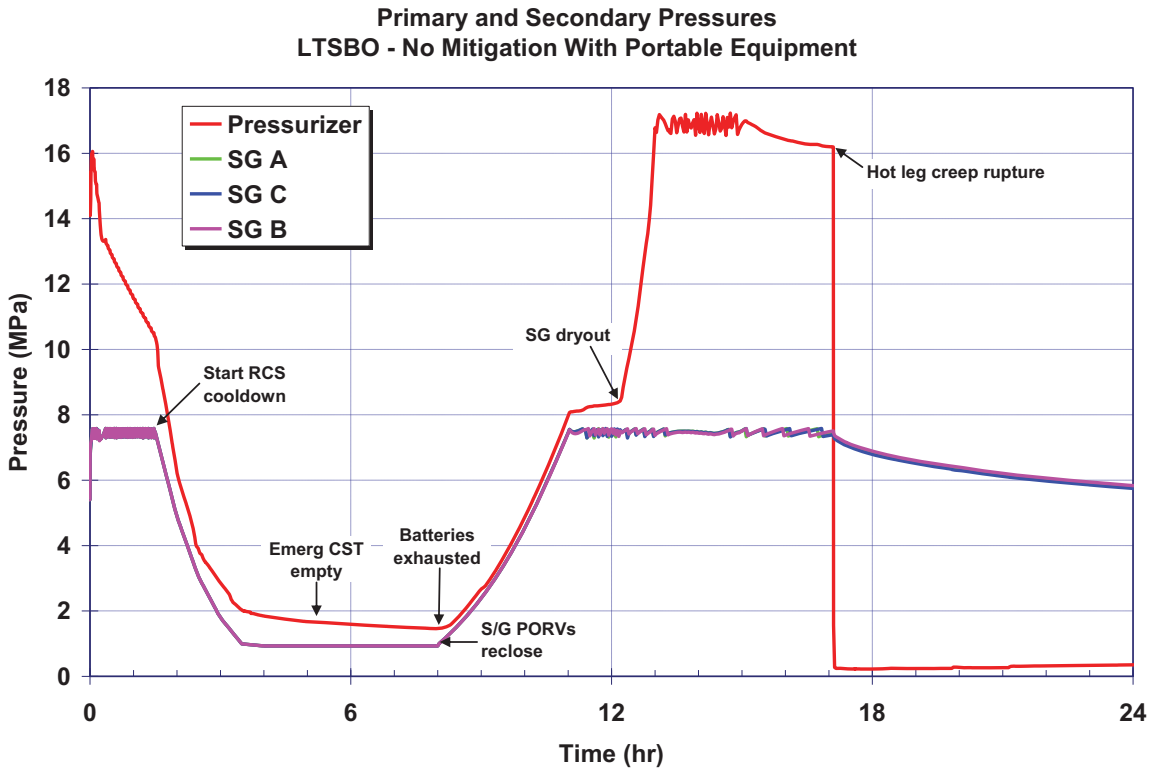

Figure 5-1 Unmitigated LTSBO primary and secondary pressure history

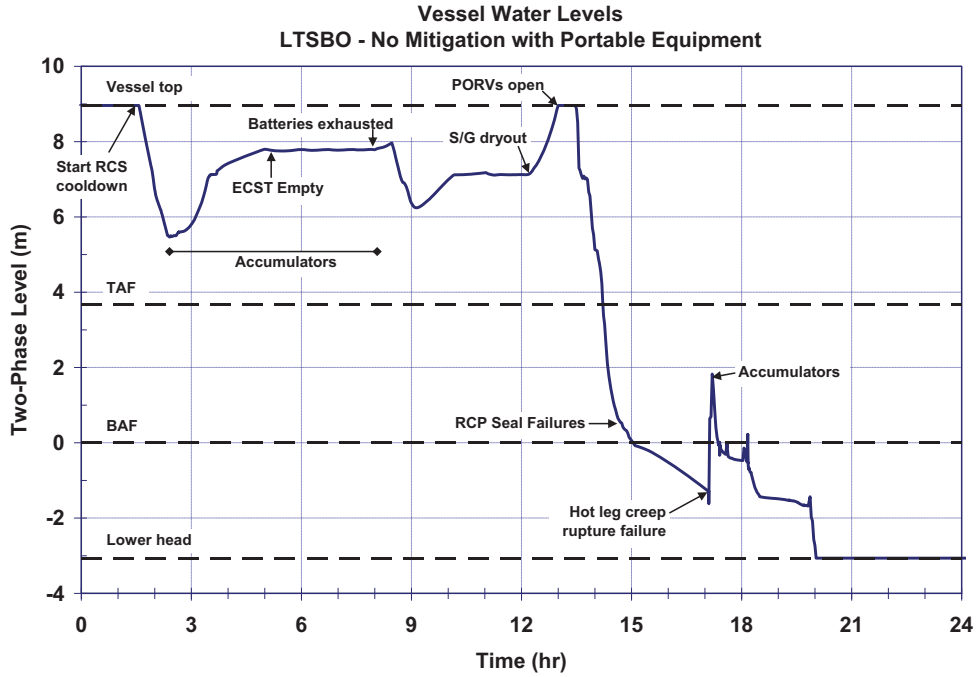

Figure 5-2 Unmitigated LTSBO vessel two-phase coolant level history

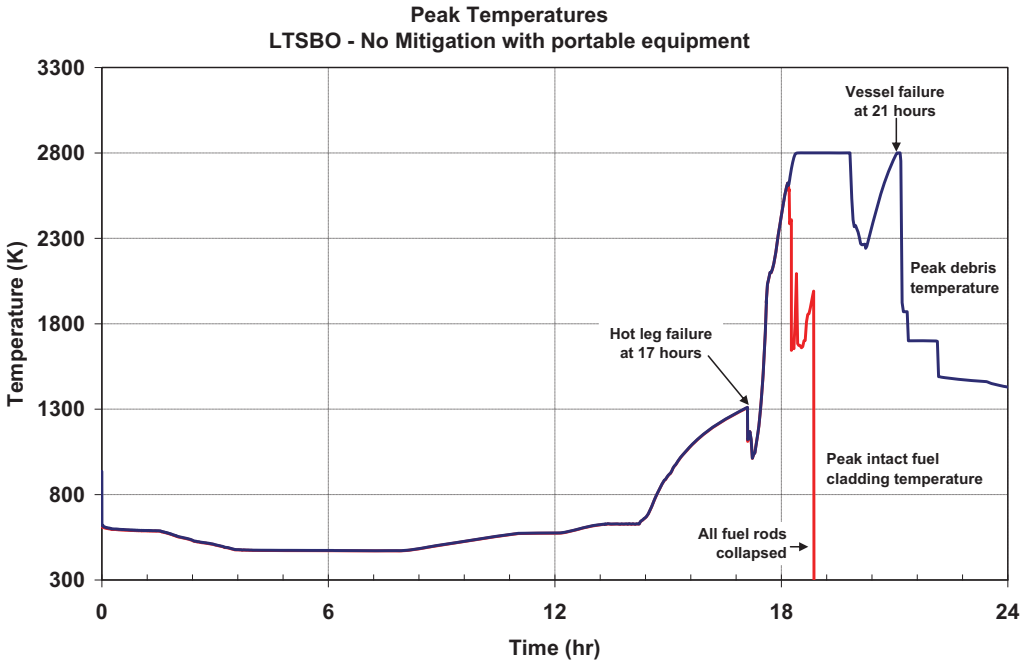

Figure 5-3 Unmitigated LTSBO core temperature history

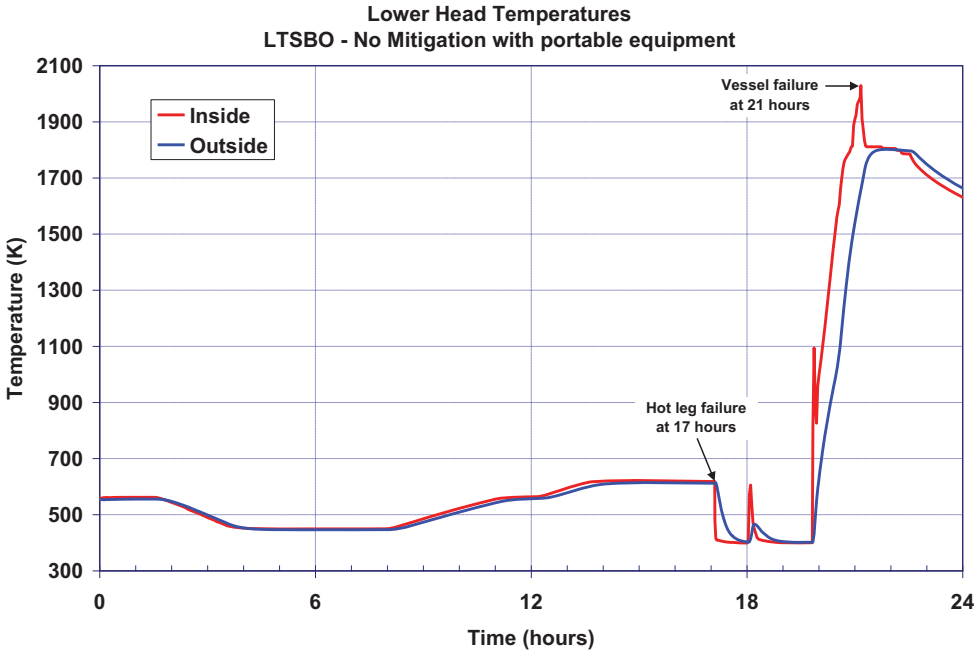

Figure 5-4 Unmitigated LTSBO lower head inner and outer temperature history

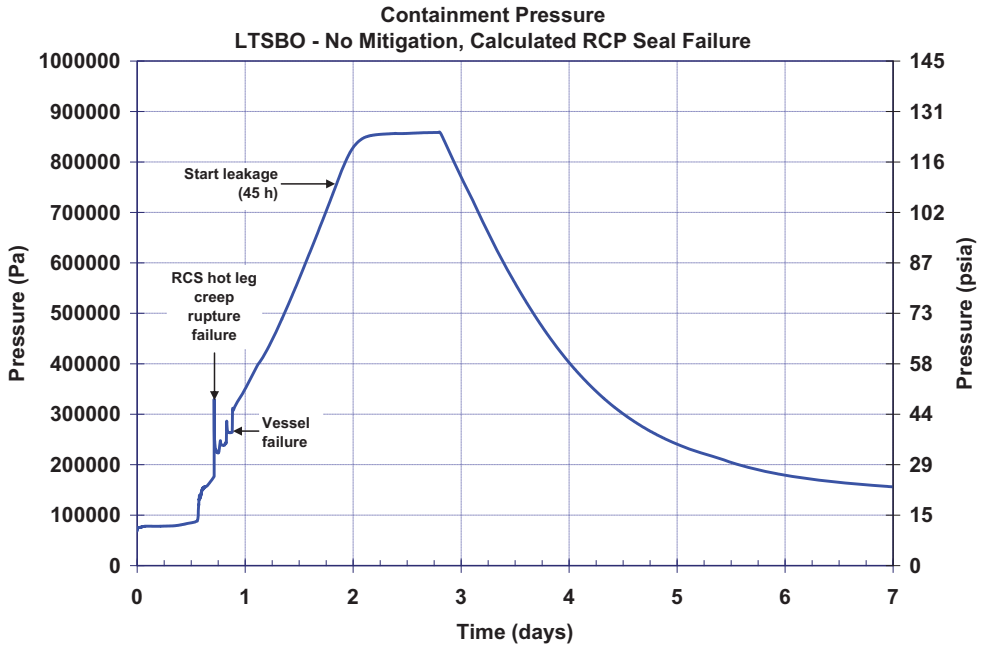

Figure 5-5 Unmitigated long-term station blackout containment pressure history

5.1.1.2 Radionuclide Release

The fission product releases from the fuel started following the first failures of the fuel cladding in the hottest rods at 16 hr 4 min, or about 1 hr 40 min after the uncovery of the top of the fuel rods. The in-vessel fission product release phase continued through vessel failure at 21.1 hr. Initially, the fission product releases from the fuel circulated through the primary system as well as being released to the containment through the pressurizer safety relief valves. The PRT rupture disk opened about 30 min before the start of the fission product releases. Subsequently, the fission product releases exiting through the pressurizer relief valves were not well retained in the PRT because the pool was nearly saturated and the PRT rupture disk was open. Following vessel failure, the fission product releases continued from the ex-vessel fuel in the reactor cavity.

Figure 5-6 and Figure 5-7 show the fission product distributions of the iodine and cesium radionuclides that were released from the fuel, respectively. Approximately 99% of the iodine and cesium were released from the fuel prior to vessel failure while the remaining amount was released ex-vessel. At the time of the hot leg failure, only a small portion of the volatile radionuclides (4.3% of the noble gases and ~1% of the cesium and iodine) had been released from the fuel. The resultant blowdown of the vessel immediately discharged the majority of the release to the containment. Following the RCS blowdown after the hot leg nozzle failure, more radionuclides were released from the fuel as the core further degraded. At low pressure conditions, the fission products continued to circulate within the vessel and to the steam generators with a portion being deposited on the structural surfaces (i.e., 10% and 15% of the iodine and cesium are retained in the RCS). However, as shown in the figures, the majority of the released radionuclides went to the containment. Within 36 hr, most of the airborne fission products in the containment settled on surfaces. This was significant because the containment failure occurred at 45 hr 32 min. Consequently, there was little airborne mass that would be released to the environment.

The chemical form of the released iodine was cesium iodide, which was more volatile than the predominant form of the released cesium, which was cesium-molybdate (Cs_2MoO_4). As shown in the iodine distribution figure (see Figure 5-6), the in-vessel iodine mass was slightly decreasing following vessel failure through 4 days. The slight decrease of mass represents a revaporization process of previously deposited radionuclides. The late in-vessel revaporization continued after containment failure and had a contribution to the environmental release. The primary thermal mechanisms for the revaporization of the iodine came from a natural circulation flow of hot gas. Very hot gases (i.e., from 990 K to >1616 K) flowed from the reactor cavity through the failed vessel lower head, through the reactor vessel, and out the failed hot leg nozzle. The combination of the decay heat and hot gases heated the deposited cesium iodide, which led to vaporization of some of the deposited cesium iodide. In addition, the cesium iodide dissociates when the cesium reacts with stainless steel surfaces. The residual elemental iodine vaporizes and contributes to the release. The natural circulation flow pattern subsequently vented the vaporized iodine radionuclides from the RCS to the containment and led to a small increase in the environmental source term.

In contrast to the iodine response in Figure 5-6, the deposited cesium-molybdate was less volatile and remained deposited in the RCS. Except for inside the reactor cavity, the containment was

cooler than vessel and well below conditions that would vaporize settled radionuclides. Consequently, none of the deposited radionuclides in the containment vaporized.

Finally, Figure 5-8 summarizes the releases of the radionuclides to the environment. At 4 days, 80% of the noble gases, 2.3% of the tellurium, 0.6% of the iodine, 0.75% of the radioactive cadmium, 0.08% of the cesium, 0.08% of the barium, and 0.04% of the radioactive tin had been released to the environment. All other releases were less than 0.02% of the initial inventory. As shown in the figure, there were some environmental releases prior to the containment failure at 45.5 hr due to nominal leakages (i.e., design specification of 0.1% vol/day at the design pressure). After the failure of the containment, the releases to the environment increased sharply. Over the first day after containment failure, 50% of the airborne noble gases in the containment were released. Over the next day, only 30% more was released.

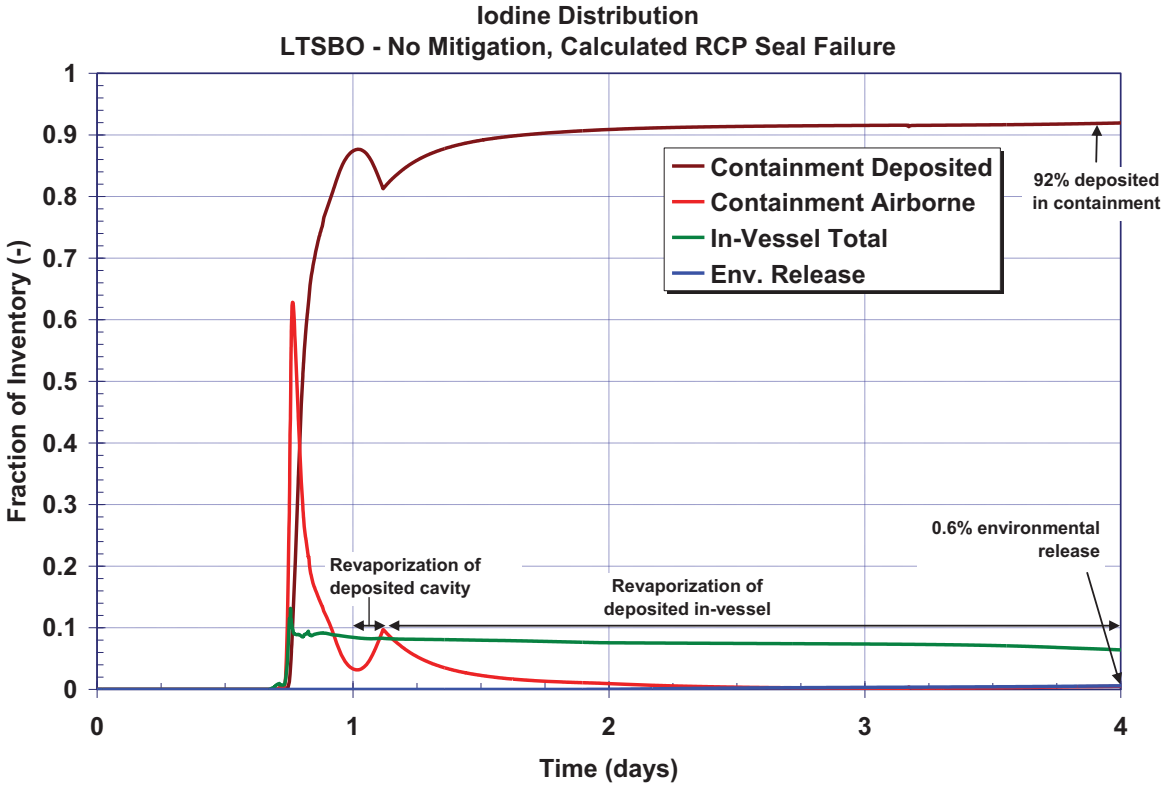

Figure 5-6 Unmitigated LTSBO iodine fission product distribution history

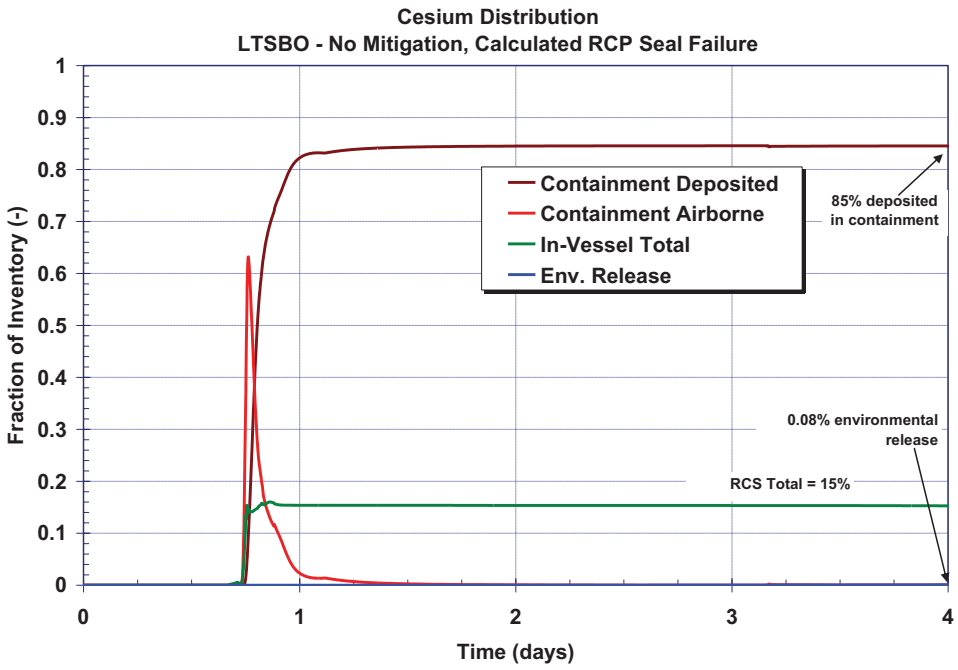

Figure 5-7 Unmitigated LTSBO cesium fission product distribution history

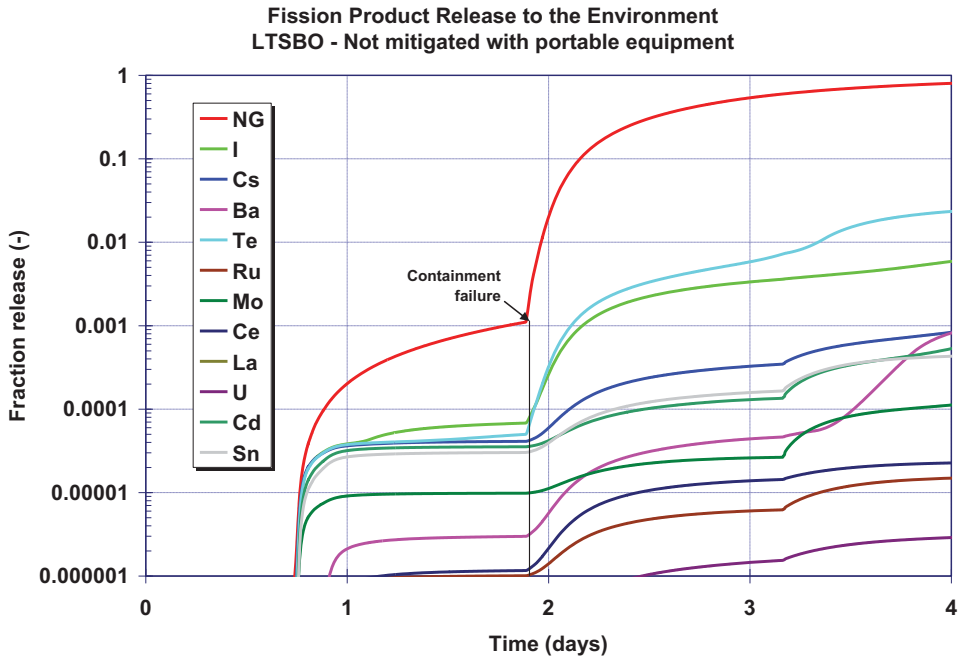

Figure 5-8 Unmitigated LTSBO environmental release history of all fission products

5.1.2 Mitigated Long-Term Station Blackout

Table 5-2 summarizes the timing of the key events in the mitigated LTSBO. As described in Section 3.1, the accident scenario initiates with a complete loss of all onsite and offsite power. The reactor successfully trips and the containment isolates but all powered safety systems are unavailable. The timings of the key events are discussed further in Section 5.1.2.1. Unlike the unmitigated LTSBO described in Section 5.1.1, the mitigated LTSBO credits the successful connection of the portable, diesel-driven (Kerr) pump to three drain lines of the LHSI piping to the RCS.[18] The Kerr pump is a positive displacement pump with a flow rate of 65 gpm at 500 rpm, which was determined with pump data obtained from the Kerr Pump Corporation.[19] The Kerr pump takes suction from the refueling water storage tank (RWST), which has a 387,000 gal capacity. The refueling water storage tank could be refilled as necessary. The sequence of events is identical to the unmitigated LTSBO until 3 hr 30 min when the Kerr pump starts operating. The Kerr pump operation starts prior to any core degradation. The emergency Kerr pump is effective at maintaining the vessel water level above the top of the fuel for the duration of the sequence. In fact, the pump was throttled to a small fraction of its rated flow.

[18] The utility has a 3-way connection from the Kerr pump to the three drain lines of the LHSI piping to the RCS.

[19] An effective flowrate of 65 gpm at 500 rpm was determined using pump data provided by the Kerr Pump Corporation that includes 95% and 92% mechanical and volumetric efficiencies.

Table 5-2 Timing of key events for mitigated LTSBO

Event Description	Time (hh:mm)
Initiating event Station blackout – loss of all onsite and offsite AC power	00:00
MSIVs close Reactor trip RCP seals initially leak at 21 gpm/pump	00:00
TD-AFW auto initiates at full flow	00:01
Operators control TD-AFW to maintain level	00:15
Vessel water level drains into upper plenum	00:30
Operators initiate controlled cooldown of secondary at ~100°F/hr	01:30
Upper plenum water level starts to decrease	01:57
Accumulators begin injecting	02:25
Vessel water level beings to increase	02:30
Start emergency diesel pump injection into RCS	03:30
SG cooldown stopped at 120 psig to maintain TD-AFW flow	03:35
DC station batteries fail but operator actions continue to control the secondary pressure at 120 psi and maintain TD-AFW flow	08:00
Level maintained at the cold leg elevation with emergency pump throttled to 5%	>03:30

5.1.2.1 Thermal-Hydraulic Response

The progression of events in the mitigated LTSBO is identical to the unmitigated LTSBO as described in Section 0 through the first 3 hr 30 min. In particular, the operators take actions to throttle the TD-AFW to maintain a normal level in the steam generators and perform a cool down of the RCS using the steam generator relief valves. Similar to the unmitigated case, the accumulators begin injecting at 2 hr 25 min in response to the decrease in the primary system pressure. It is estimated that the operators could begin RCS injection using the portable, diesel-driven Kerr pump by 3 hr 30 min.

At the time the emergency pump is ready for injection, the primary system pressure is 2.0 MPa (278 psig) or well within the pressure head capacity of the Kerr pump (see Figure 5-9). Similar to the unmitigated LTSBO, the secondary system is depressurized to 120 psi, or the lower limit of operability for the TD-AFW. Due to the RCP seal leakage and liquid volume shrinkage from the cool down, the vessel level initially decreased but started to recover after 2 hr 25 min following the start of the accumulator injection (see Figure 5-10). The peak fuel cladding temperature and vessel lower head followed the primary system liquid temperature, which was steadily cooled down by the steam generators (see Figure 5-11 and Figure 5-12, respectively).

At 3 hr 30 min, the emergency injection begins and supplements the RCS inventory make-up with the accumulators. For the purposes of the calculation, a simple control system was created to ramp the Kerr pump flow (i.e., maximum flow rate of 65 gpm at 500 rpm) based on the reactor vessel level indication system. The flow increases from 5% (3.2 gpm) to 65 gpm (100%) if the vessel water level drops below the hot leg elevation. Since the level remained above the bottom of the hot leg, the flow was throttled to 3.2 gpm for the entire transient (see Figure 5-14). Although there was a small mismatch between the leakage flow and the emergency injection flow, the swollen level in the vessel remained relatively constant (see Figure 5-10). Because of the relatively low level in the vessel, there was minimal excess spillage of the injected water into the cold leg, which would eventually be lost due to seal leakage.

Finally, since heat removal from the RCS was maintained for this sequence, there was not a significant challenge to the containment. As seen in Figure 5-13, the containment pressure only rose slightly due to heat losses from the RCS.

There were several lessons learned while investigating the mitigation of the LTSBO. First, the operator action to reduce the primary system pressure to the threshold of the TD-AFW operation allowed the maximum injection from the accumulators (i.e., two thirds of their liquid inventory). The accumulator flow was significant in the short-term restoration of the vessel liquid inventory. Hence, the depressurization to 120 psi maintained TD-AFW flow but allowed for significant accumulator flow. Second, the reduction of the primary system pressure reduced the RCP seal leakage flow from 21 gpm per pump to less than 3 gpm per pump. Furthermore, if a RCP seal should fail under these conditions, then the resulting leakage flow would be much lower than if the primary system pressure was not actively controlled to low pressure. Third, the emergency pumps have excess capacity to maintain long-term make-up. However, only a small fraction of the rated capacity is needed to maintain the level in the vessel at the hot leg elevation. Fourth, operator actions were required to replenish the water supply to the ECST for the TD-AFW (i.e., exhausted after 5.2 hours and required 545,000 gal for 4 days) but not the RWST for the emergency RCS injection (i.e., at 87% inventory after 4 days). Finally, if successful operation actions were taken to replenish the ECST water supply and maintain the steam generator pressure at 120 psi, then considerably more time is available to establish the RCS emergency injection.

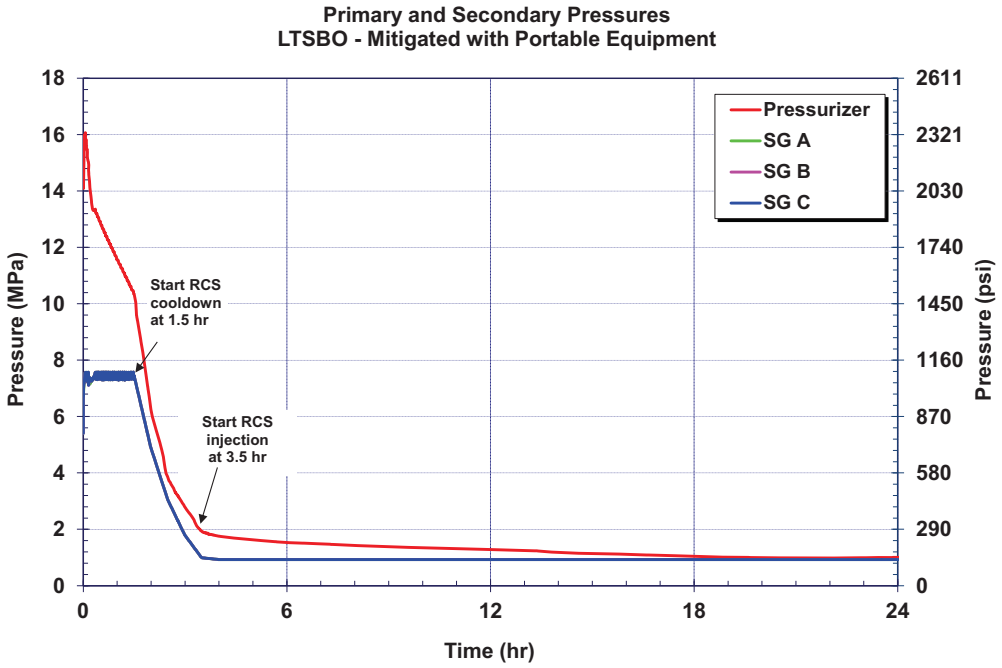

Figure 5-9 Mitigated long-term station blackout primary and secondary pressure history

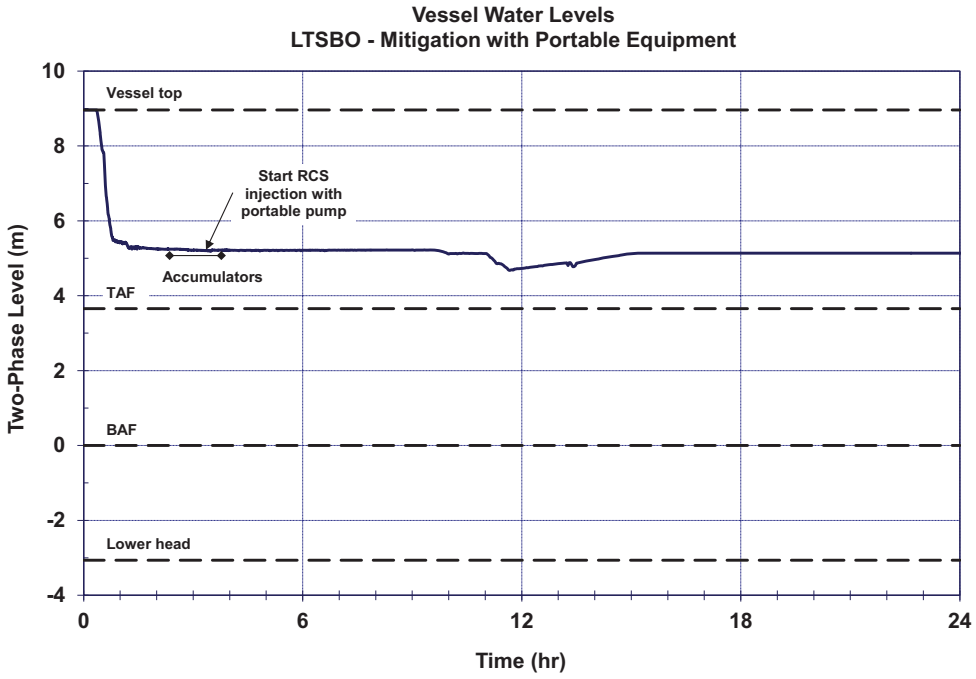

Figure 5-10 Mitigated long-term station blackout vessel two-phase coolant level

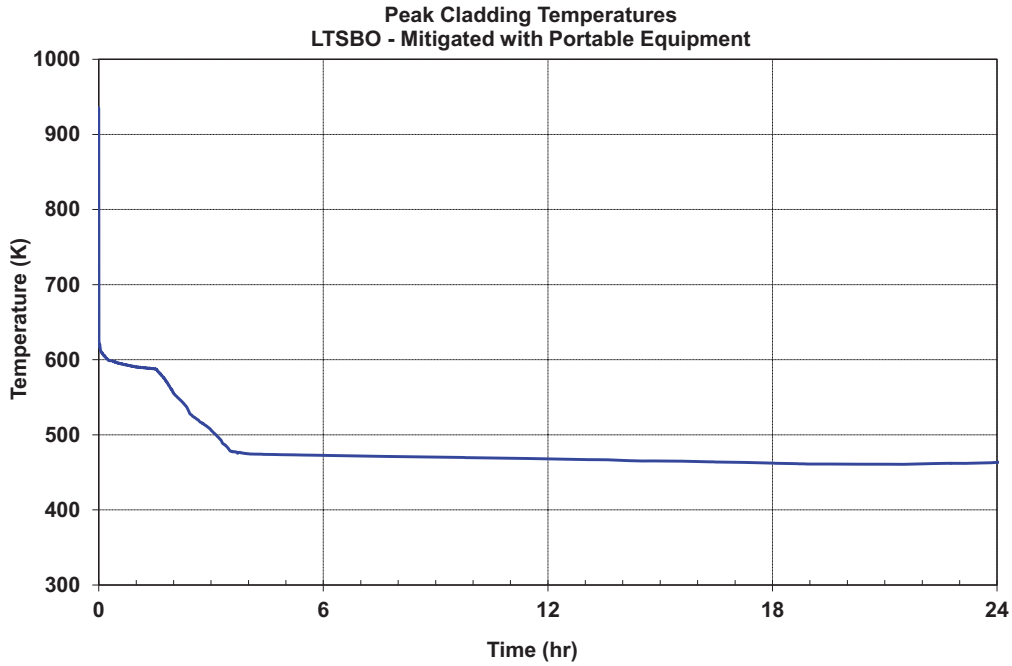

Figure 5-11 Mitigated long-term station blackout core temperature history

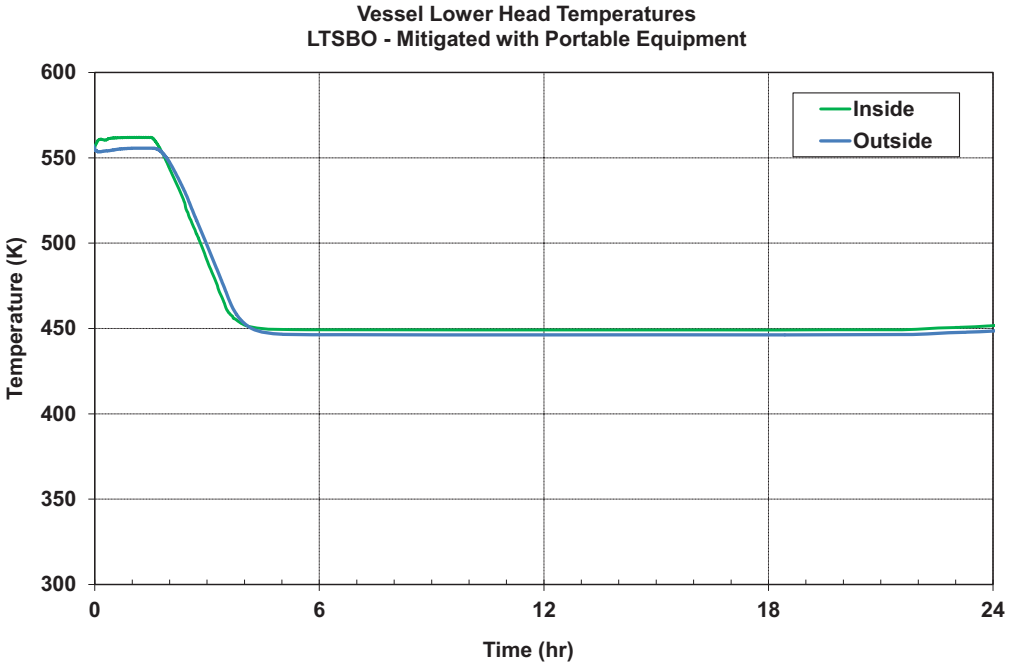

Figure 5-12 Mitigated long-term station blackout lower head inner and outer temperature history

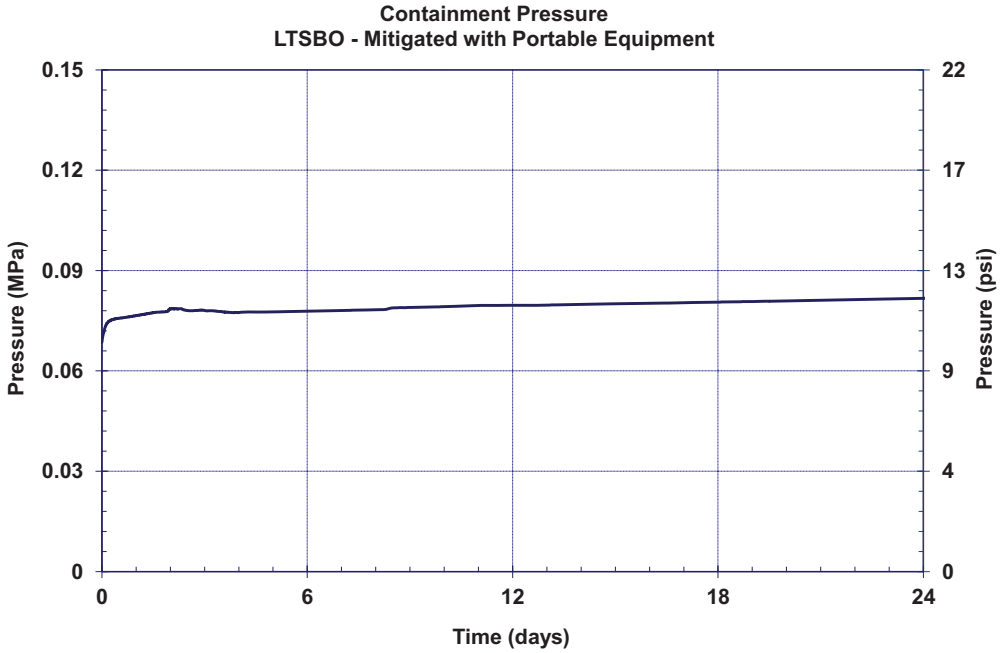

Figure 5-13 Mitigated long-term station blackout containment pressure history

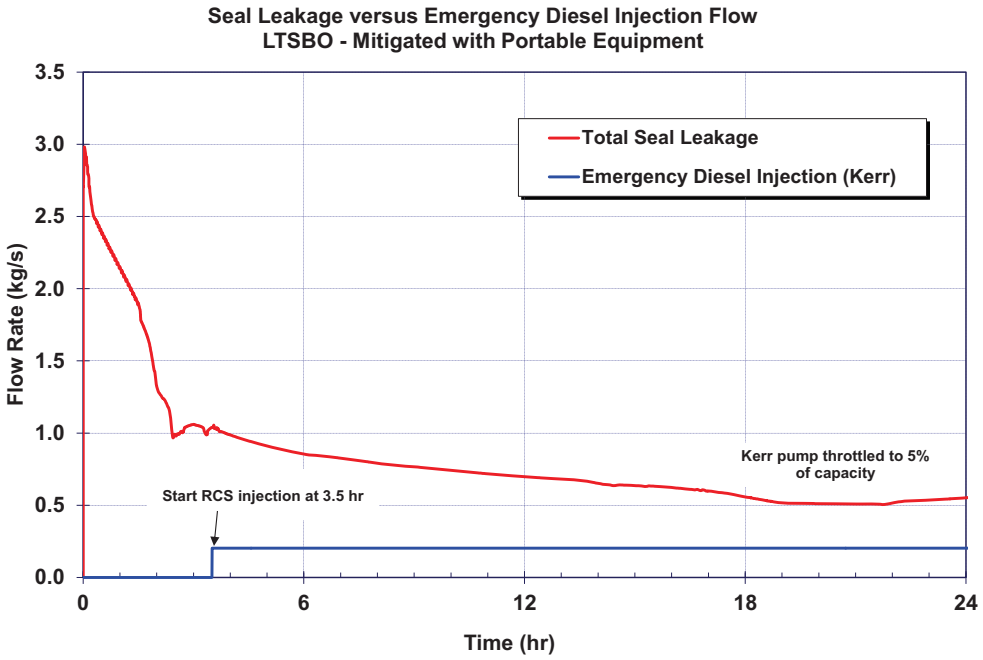

Figure 5-14 Mitigated LTSBO vessel emergency make up and pump seal leakage flows

5.1.2.2 Radionuclide Release

There was no fission product release for the mitigated LTSBO scenario.

5.1.3 Unmitigated Long-Term Station Blackout with Early RCP Seal Failure

Table 5-3 summarizes the timing of the key events in the unmitigated LTSBO with early and late RCP seal failure. As described in Section 3.1, the accident scenario initiates with a complete loss of all onsite and offsite AC power but the DC station batteries are available. The reactor successfully scrams and the containment isolates but all powered safety systems are unavailable except the TD-AFW.

Table 5-3 Comparison of the timings of key events for unmitigated LTSBO with and without early RCP seal failures

Event Description	Early Seal Failure Time (hh:mm)	Late Seal Failure Time (hh:mm)
Initiating event Station blackout – loss of all onsite and offsite AC power	00:00	00:00
MSIVs close Reactor trip RCP seals initially leak at 21 gpm/pump	00:00	00:00
TD-AFW auto initiates at full flow	00:01	00:01
First SG SRV opening	00:03	00:03
Assumed early RCP seal failures, 182 gpm/pump at full-pressure	00:13	n/a
Operators control TD-AFW to maintain level	00:15	00:15
Operators initiate controlled cooldown of secondary at ~100^{o}F/hr	01:30	01:30
Upper plenum water level starts to decrease	00:33	01:57
Accumulators begin injecting	02:13	02:25
Vessel water level begins to increase	n/a	02:30
SG cooldown stopped at 120 psig to maintain TD-AFW flow	03:35	03:35
Emergency CST empty	05:29	05:08
DC Batteries Exhausted	08:00	08:00
S/G PORVs reclose	08:00	08:00
Pressurizer SRV opens	n/a	13:06
PRT failure	n/a	13:40
Start of fuel heatup	09:38	14:16
RCP seal failures (calculated)	n/a	14:46
First fission product gap releases	11:03	16:04
Creep rupture failure of the C loop hot leg nozzle	12:29	17:06
Accumulator empty	12:29	17:06
Vessel lower head failure by creep rupture	14:26	21:08
Debris discharge to reactor cavity	14:26	21:08
Cavity dryout	14:36	21:16
Containment at design pressure (45 psig)	42:08	28:00
Start of increased leakage of containment (P/P_{design} = 2.18)	55:40	45:32

5.1.3.1 Thermal-hydraulic Response

The responses of the primary and secondary pressure systems are shown in Figure 5-15. The system pressure responses through the first 10 hours are very similar to the unmitigated case without an early RCP seal failure (see Figure 5-1). However, as will be discussed below, the early RCP seal failure had an important impact on primary system pressure response after 10 hours. As shown in Figure 5-16, the early RCP seal failures occur at 13 minutes versus 14 hours 46 minutes in the late failure case. Consequently, the early leakage flowrate is much higher than the late failure case. The high RCP seal leakage causes a faster decrease in the vessel water inventory (see Figure 5-17), earlier core degradation and start of fission product release, and earlier hot leg creep rupture failure and vessel failure (see Table 5-3).

The water level decreased more quickly in the early seal failure case but stabilized near 5.2 m after the accumulators discharged. At 5.2 m, the water level in the core is below the hot and cold leg elevations, so the seal leakage had a minor effect of the vessel water inventory. The discharge of the accumulator water partially subcooled the core. The fluid in the core began boiling again but reflux cooling in the SG kept the pressure and water level constant. Once the SG PORVs closed at 8 hours with the DC battery failure, the RCS pressurized; the inventory loss out the break increased; and the vessel water level began decreasing.

A comparison of the containment pressure responses for the cases with and without early RCP seal failures is shown in Figure 5-18. Although vessel failure occurs earlier in the case with early RCP leakage, the subsequent containment pressurization is slower. The long-term containment pressurization is due to two components: (1) non-condensable gas production from core-concrete interactions and (2) vaporization of water in the containment. The non-condensable gas production was similar in the two cases. However, the case with late failure of the RCP seals had more water available on the containment floor for vaporization. Since all the water on the containment floor eventually vaporized due to connectivity with the ex-vessel debris in the cavity, the total steam production was higher in the late RCP seal failure case.

Although the total amount of water discharged into the containment was approximately equal for both cases, the distribution of the water was different. In the early seal failure case, 217,000 kg of water was discharged through the RCP seals versus only 65,000 kg in the late seal failure case. Due to the interconnectivity of the containment compartments and the specific energy of the fluid being released, a significant portion of the water in the early seal failure case was held up in the pressurizer relief tank compartment, which did not directly communicate with the debris in the cavity (i.e., the location of the long-term, ex-vessel core debris heat source). In contrast, once the PRT rupture disk failed at 13.6 hr in the late RCP seal case, continued high energy steam from pressurizer safety valve cycling dumped 122,000 kg into the containment, which condensed on structures in the containment and mostly drained to the containment floor (i.e., rather than being retained in the pressurizer relief tank compartment). Therefore, more water was available in the late seal failure case for long-term boiling by the debris in cavity.

It is also interesting to look at similarities and differences in the events that affected the short-term containment pressurization. In the late RCP seal failure case, the containment pressurization had three events that caused step increases in the containment pressure. First, the

failure of the pressurizer relief tank caused the first significant pressurization of the containment at 13 hr 40 min (0.57 days). Some hydrogen burns also cause short-term pressurizations following this event. However, the containment pressure returned to the pre-burn pressure after the burn. The early RCP seal leakage case did not have this event (i.e., failure of the pressurizer relief tank). Second, the hot leg failed by creep rupture and suddenly increased the pressure in the containment in both cases (i.e., the net pressure increase following the coincidental hydrogen burn at hot leg failure). Since the hot leg failure in the late RCP seal failure case occurred from 16.2 MPa versus 6.4 MPa in the early RCP seal failure case, significantly more energy was released to the containment as evidenced by the rapid pressure response rise following hot leg creep rupture (see Figure 5-18). Finally, both cases had similar pressurizations following vessel failure when the core debris rapidly evaporated the water in the reactor cavity. In summary, the first rapid containment pressurization event only occurred in the late RCP failure case and the second event was more severe in the late RCP failure case (i.e., the net pressure increase after the hydrogen deflagration spike). The third event was longer duration in the late RCP failure case.

In an integral sense, a portion of the overall system energy generated in the late RCP seal failure case was released to the containment 4.5 hours after the early RCP failure case (i.e., the difference in the timings of the hot leg creep rupture failures, see Table 5-3)[20]. The additional energy storage in the primary system in the late seal failure case results in a higher pressure and temperature of the gas in the primary system at the time of the leg creep rupture. In contrast, a portion of the early RCP seal failure decay energy generated over the time period between hot leg creep ruptures in the two cases (i.e., 12 hr 29 min to 17 hr 6 min) is absorbed into the concrete by core-concrete interactions in the early RCP seal failure case (i.e., from 14 hr 26 min to 17 hr 6 min). The result was a higher heat load to the containment atmosphere in the early RCP seal failure case, which resulted in a faster evaporation rate of the water on the containment floor.

In addition to the faster rate of evaporation, more water was available to evaporate in the late RCP seal failure case (see Figure 5-19). Consequently, the resulting pressurization was faster and longer. The timings of the containment failure were 55.7 and 45.5 hours for the early and late RCP seal failure cases, respectively. Due to the additional water for vaporization in the late seal failure case, the resulting containment pressurization was not only faster but also resulted in a higher pressure (see Figure 5-18). The importance of the water vaporization is demonstrated by comparing Figure 5-18 and Figure 5-19. The containment depressurization does not begin until all the water is evaporated. Hence, the water vaporization was a significant component of the containment pressurization relative to the non-condensable CCI gas generation.

Finally, due to higher peak containment pressure in the late RCP seal failure case, the resultant containment leakage area was also slightly higher, 0.0053 m^2 (8.3 in^2) versus 0.0028 m^2 (4.4 in^2). Consequently, the long-term depressurization rate following the containment failure was faster in the late RCP seal failure case.

[20] The heat removal by the secondary system ended at approximately the same time in both cases. The energy released through the seal failure was lower in the late RCP seal failure until 14 hr 46 min, when the seal failed.

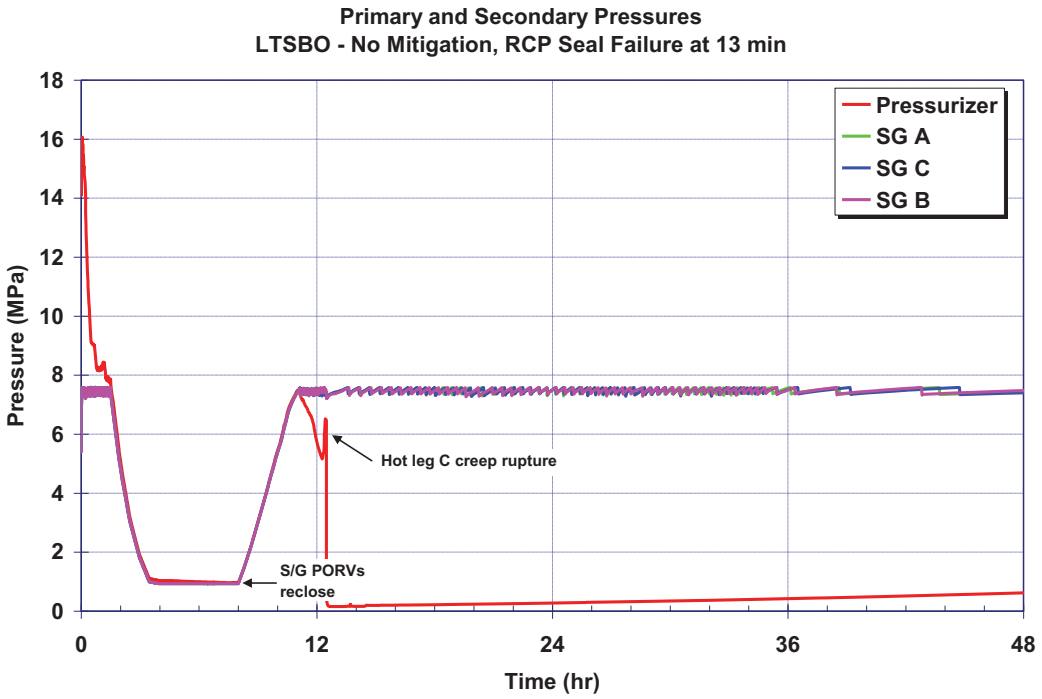

Figure 5-15 Unmitigated long-term station blackout primary and secondary pressure history

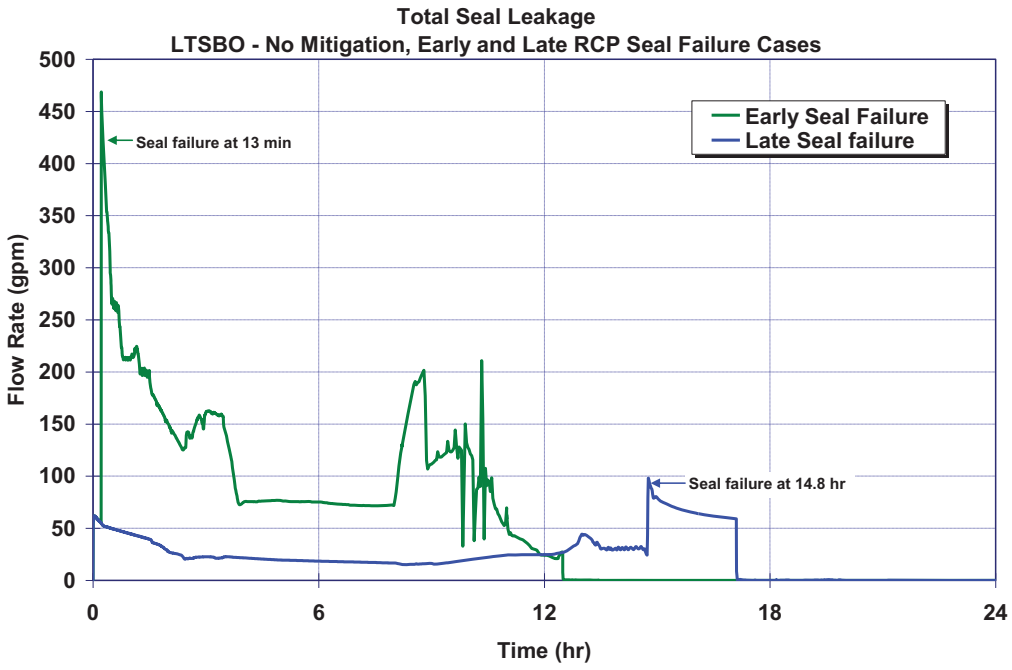

Figure 5-16 Comparison of the unmitigated long-term station blackout RCP seal leakages with and without early RCP seal failures

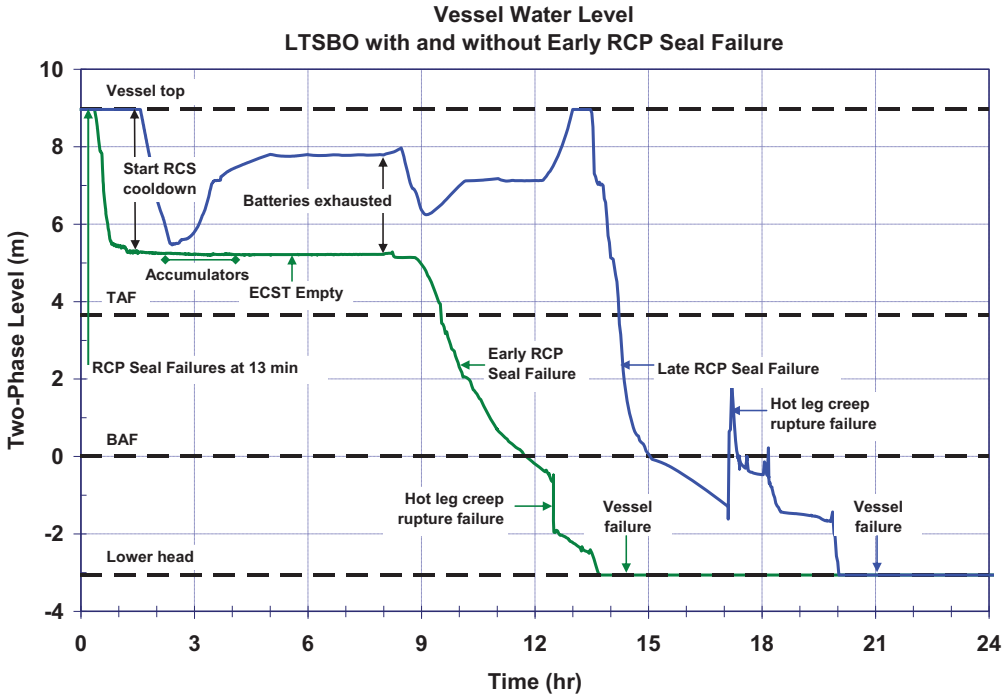

Figure 5-17 Comparison of the unmitigated long-term station blackout vessel level responses with and without early RCP seal failures

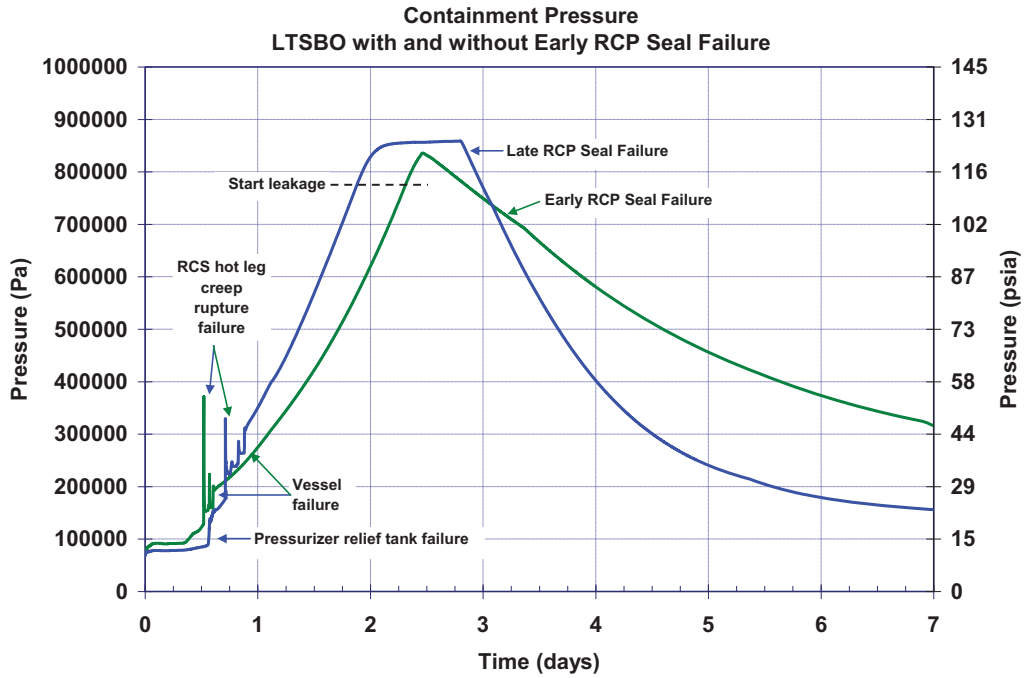

Figure 5-18 Comparison of the unmitigated long-term station blackout containment pressure responses with and without early RCP seal failures

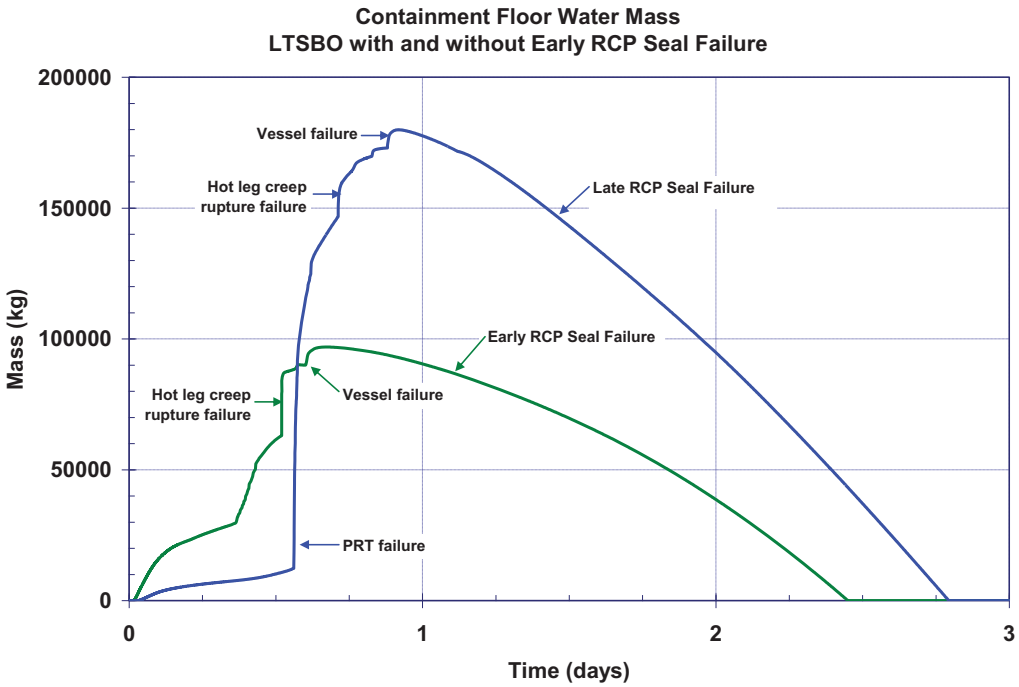

Figure 5-19 Comparison of the unmitigated long-term station blackout containment water pool masses with and without early RCP seal failures

5.1.3.2 Radionuclide Release

The environmental releases for the noble gases, iodine, and cesium for the two cases are shown in Figure 5-20 through Figure 5-22, respectively. The radionuclide behavior was similar to the late RCP seal failure responses described in Section 5.1.1. However, the magnitude and timing of the releases from the late RCP seal failure case bounded the response from the early RCP seal failure. The early RCP failure releases were smaller and delayed because: (a) the containment failure was later (2.3 days versus 1.9 days), (b) the containment failure area and associated depression rate were smaller (0.0028 m^2 versus 0.0053 m^2), and (c) the time for settling between hot leg failure and containment failure was longer (43 hours versus 28 hours). However, both cases had small environmental releases of iodine and cesium due to the late containment failure timing.

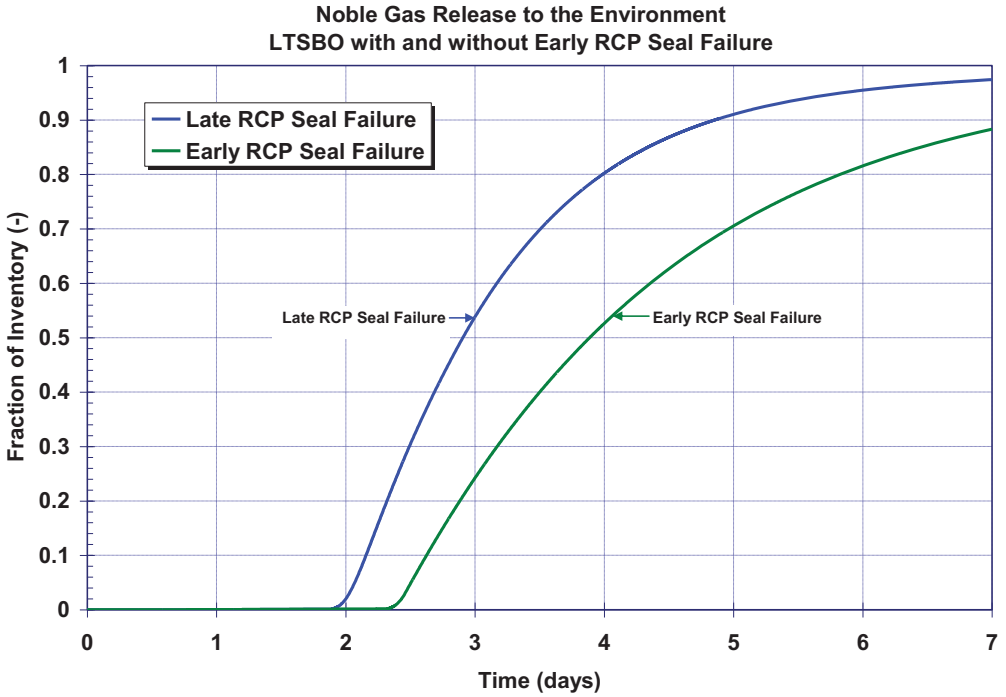

Figure 5-20 Comparison of the unmitigated long-term station blackout noble gas releases to the environment with and without early RCP seal failures

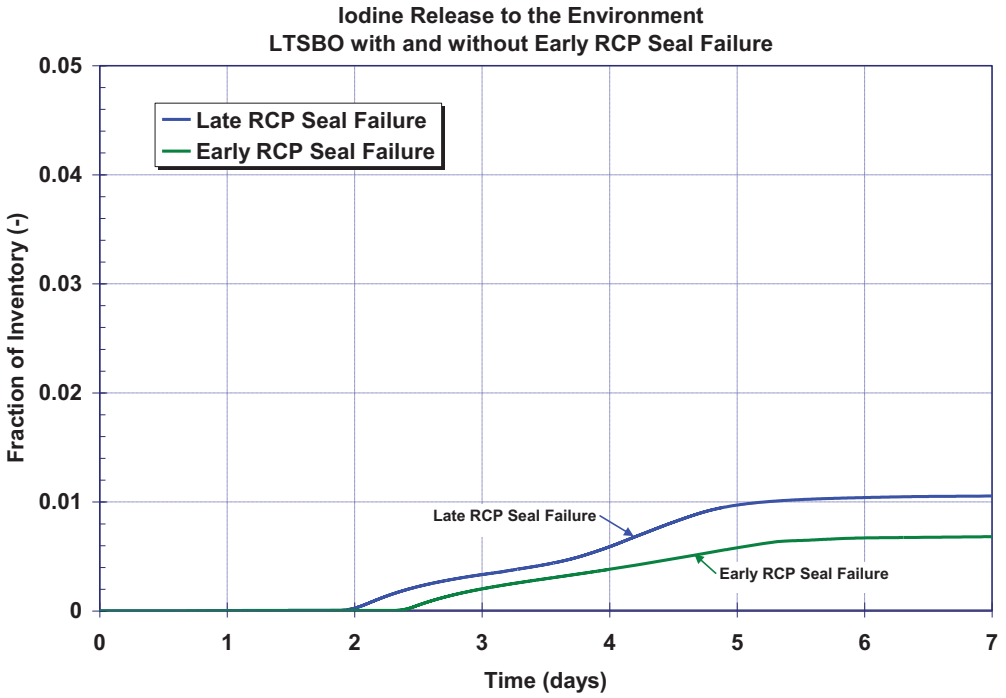

Figure 5-21 Comparison of the unmitigated long-term station blackout iodine releases to the environment with and without early RCP seal failures

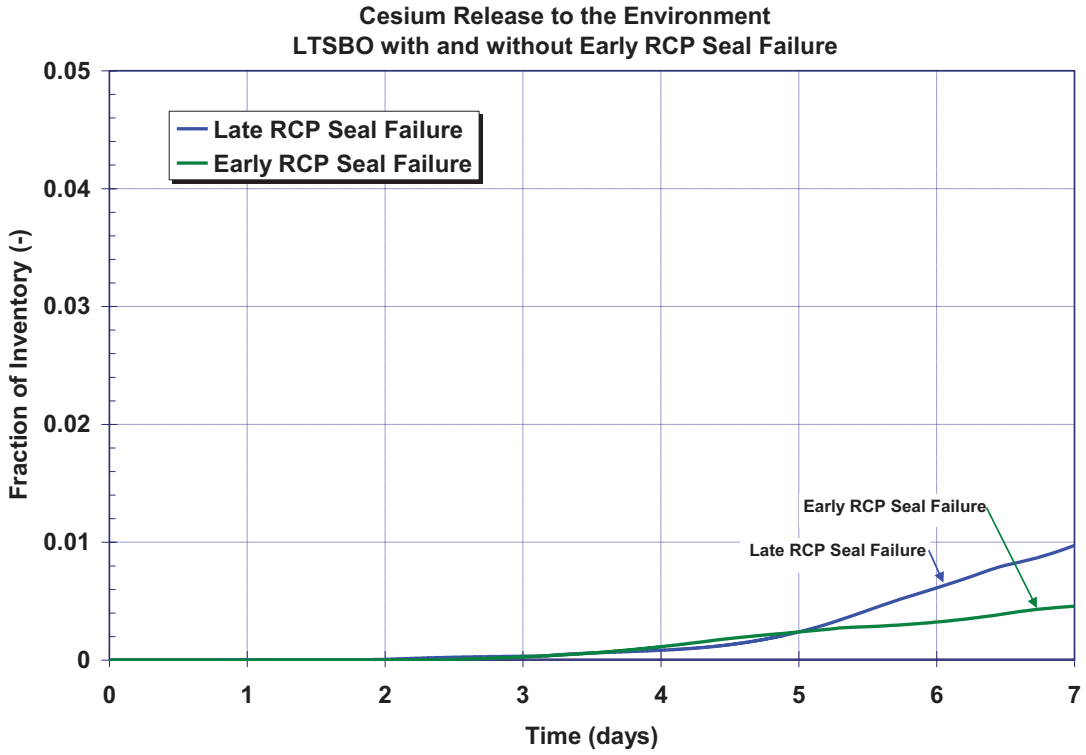

Figure 5-22 Comparison of the unmitigated long-term station blackout cesium releases to the environment with and without early RCP seal failures

5.1.4 Mitigated Long-Term Station Blackout with Early RCP Seal Failure

Table 5-4 summarizes the timing of the key events in the mitigated LTSBO. As described in Section 3.1, the accident scenario initiates with a complete loss of all onsite and offsite power. The reactor successfully trips and the containment isolates but all powered safety systems are unavailable. The loss of seal-cooling to the RCP causes relatively warm RCS fluid to flow into the RCP seal cavity. At 13 minutes, the RCP seal cavity fills with hot RCS water and the SPAR model assess a 20% probability of RCP seal failure, which is used in this case. Consequently, all three RCPs are specified to have seal failures that increases their leakage to a nominal value of 181 gpm/RCP-pump at full-power conditions. The mitigated LTSBO credits the successful connection of the portable, diesel-driven Kerr pump to three drain lines of the LHSI piping to the RCS. The Kerr pump is a positive displacement pump with a flow rate of 65 gpm at 500 rpm, which was determined with pump data obtained from the Kerr Pump Corporation.[21] The Kerr pump takes suction from the refueling water storage tank, which has a 387,000 gal capacity and could be refilled as necessary. In addition, a portable power supply was available to maintain the secondary cooldown after the DC batteries fail.

The sequence of events is similar to the unmitigated LTSBO with early RCP seal failure until 3 hr 30 min when the Kerr pump starts operating. The Kerr pump operation starts prior to any core degradation (see Table 5-4) and is effective at maintaining the vessel water level above the

[21] An effective flowrate of 65 gpm at 500 rpm was determined using pump data provided by the Kerr Pump Corporation that includes 95% and 92% mechanical and volumetric efficiencies.

top of the fuel for the duration of the sequence. Initially, the Kerr pump flow rate is 3.2 gpm. However, at 11.6 hr into the event sequence, the water level in the vessel falls below the bottom of the hot leg as observed on the reactor vessel level instrumentation system (RVLIS). Subsequently, the Kerr pump flow rate was increased up to 65 gpm and provided sufficient make-up to balance the loss of coolant through RCP seal leakage. The timings of the key events are discussed further in Section 5.1.2.

Table 5-4 Comparison of the timings of key events for mitigated LTSBO with and without early RCP seal failures

Event Description	Early Seal Failure Time (hh:mm)	Late Seal Failure Time (hh:mm)
Initiating event Station blackout – loss of all onsite and offsite AC power	00:00	00:00
MSIVs close Reactor trip RCP seals initially leak at 21 gpm/pump	00:00	00:00
TD-AFW auto initiates at full flow	00:01	00:01
RCP pump seals fail, 182 gpm/pump at full-pressure	00:13	n/a
Operators control TD-AFW to maintain level	00:15	00:15
Vessel water level drains into upper plenum	00:30	00:30
Operators initiate controlled cooldown of secondary at ~100^{o}F/hr	01:30	01:30
Upper plenum water level starts to decrease	01:13	01:57
Accumulators begin injecting	02:15	02:20
Vessel water level begins to increase	n/a*	02:25
Emergency diesel pump injection to RCS	03:30	03:30
SG cooldown stopped at 120 psig to maintain TD-AFW flow	03:35	03:35
DC station batteries fail but operator actions continue to control the secondary pressure at 120 psi and maintain TD-AFW flow	08:00	08:00
Water level falls below the bottom of the hot leg Emergency diesel pump injection to RCS increases to 65 gpm	11:36	n/a
Water level stabilizes at 8” above the bottom of the hot leg	14:00	n/a

* In the case early RCP seal leakage, the vessel water level stops decreasing following accumulator injection and remains relatively steady at ~1 m above the top of the fuel to the end of the calculation. The emergency pumps are adequate to maintain level at the bottom of the cold and hot legs. However, the RCS leakage through the three failed RCP seals is too high to raise the level above the hot and cold leg elevation.

5.1.4.1 Thermal-Hydraulic Response

The responses of the primary and secondary pressures are shown in Figure 5-23. The system pressure responses are very similar to the mitigated case without an early RCP seal failure (see Figure 5-9). The impact of the early RCP seal failure did not have a significant impact on pressure response. More important was the successful operator actions to depressurize the primary system using the secondary system PORVs. As shown in Figure 5-24, the early RCP seal failures occur at 13 minutes. However, the total RCP seal leakage was less than 70 gpm after 2 hours because of the successful RCS depressurization. The RCP seals were not predicted to fail in the mitigated case without early failure due to adequate subcooling.

As discussed in Section 5.1.2, the operators take actions to throttle the TD-AFW to maintain a normal level in the steam generators and perform a cooldown of the RCS using the steam generator relief valves. The accumulators begin injecting at 2 hr 15 min following the decrease in the primary system pressure below the pressure of the accumulators. The operators stage the portable, diesel-driven Kerr pump and begin injecting at 3 hr 30 min.

At the time the emergency pump is ready for injection, the primary system pressure is 2.0 MPa (278 psig) or well within the pressure head capacity of the Kerr pump (see Figure 5-23). The secondary system is depressurized to 120 psi, or the lower limit of operability for the TD-AFW. As shown in Figure 5-25, the vessel level decrease in the early RCP failure case was more severe than the late RCP seal failure case. However, accumulator injection maintained the vessel level in the upper plenum until the emergency portable in injection started. Consequently, there was no early fuel uncovery or fuel heatups.

At 3 hr 30 min, the emergency injection begins and supplements the RCS inventory make-up with the accumulators. For the purposes of the calculation, a simple control system was created to ramp the Kerr pump flow (maximum flow rate of 65 gpm at 500 rpm) based on the reactor vessel level indication system. The flow increases from 5% (3.2 gpm) to 65 gpm (100%) if the vessel water level drops below the hot leg elevation. When the level dropped below the bottom of the hot leg at 11.6 hours, the flow was increased to 65 gpm for the remainder of the transient (see Figure 5-14). The emergency diesel pump restored the vessel water level to ~8 inches above the bottom of the hot leg by 14 hours. Because of the relatively low level in the vessel, there was minimal excess spillage of the injected water into the cold leg, which would eventually be lost due to seal leakage.

The lessons learned that were described in Section 5.1.2 are also applicable in the mitigated early RCP failure case. There are the following quantitative and timing differences for the early RCP seal failure case versus the late RCP seal failure case insights that were presented in Section 5.1.2. First, the reduction of the primary system pressure reduced the total RCP seal leakage flow from a nominal value of 182 gpm per pump to approximately the pumping capacity of the high-head emergency diesel pump (i.e., 65 gpm) after 4 hours. The reduction in RCP leakage delays core damage and increases the likelihood that the operators will be able to prevent core damage. The depressurization also allows use of a lower head pump to provide RCS make-up. Second, operator actions were required to replenish the water supply to the ECST for the TD-AFW (i.e., exhausted after 5.8 hours and required 420,000 gal for 72 hours) and the

RWST for the emergency RCS injection (i.e., exhausted after 57 hours). These actions were necessary to maintain primary and secondary coolant injection.

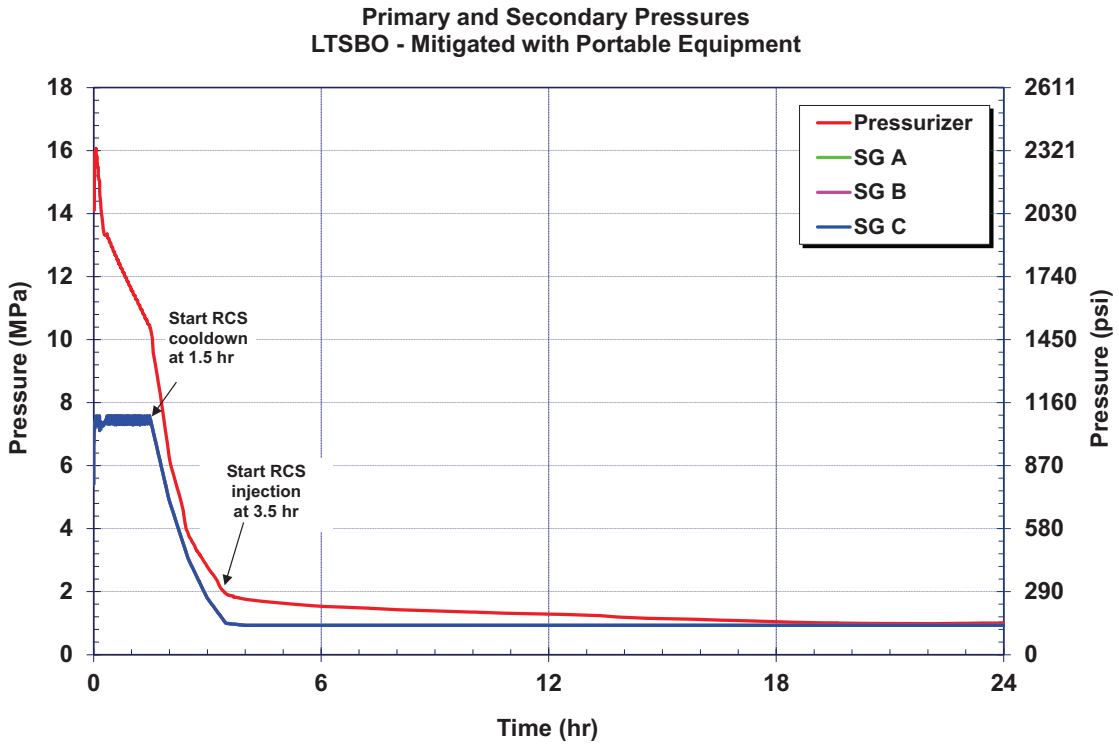

Figure 5-23 Primary and secondary pressure responses for the mitigated long-term station blackout with early RCP seal failure

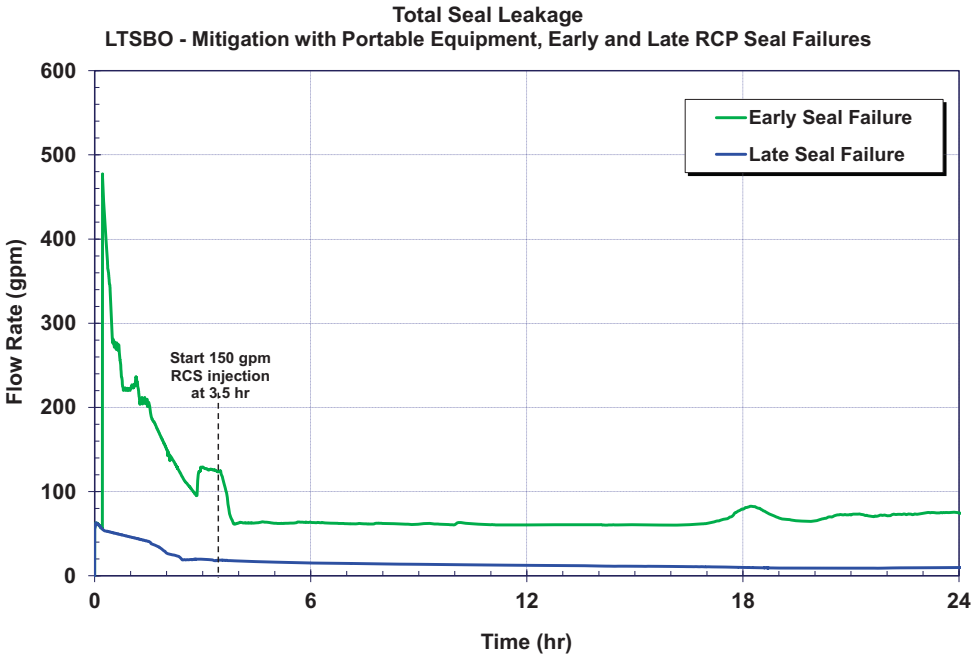

Figure 5-24 Comparison of the mitigated long-term station blackout RCP seal leakages with and without early RCP seal failures

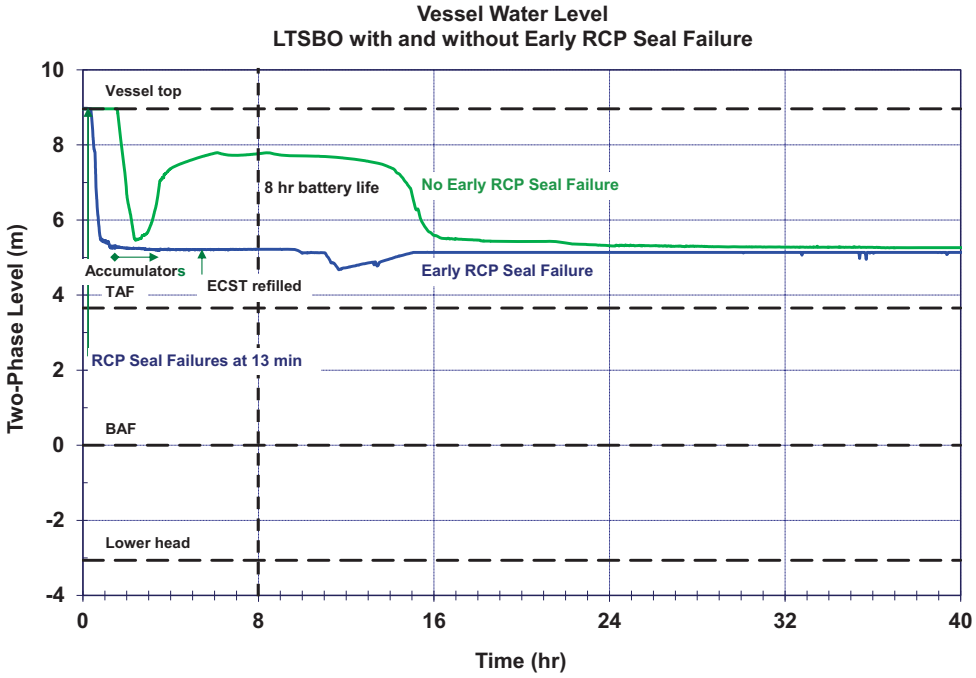

Figure 5-25 Comparison of the mitigated long-term station blackout vessel level with and without early RCP seal failures

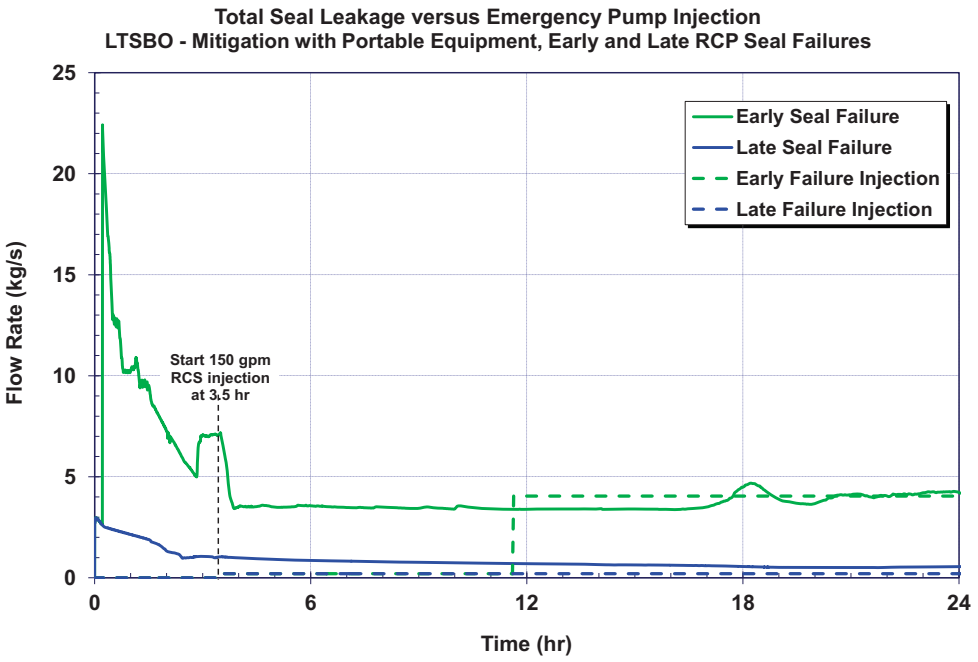

Figure 5-26 Comparison of the mitigated long-term station blackout portable pump injection rates with and without early RCP seal failures

5.1.4.2 Radionuclide Release

There was no fission product release for the mitigated LTSBO scenario with early RCP failures.

5.2 Short-Term Station Blackout

The STSBO is assumed to be initiated by a seismic event. Section 5.2.1 presents the results of an unmitigated scenario with no successful operator actions. For the mitigated scenario in Section 5.2.2, a portable emergency pump is connected to the containment spray system at 8 hours and available to inject 1,000,000 gallons.

5.2.1 Unmitigated Short-Term Station Blackout

Table 5-5 summarizes the timing of the key events in the unmitigated STSBO. As described in Section 3.2.1, the accident scenario initiates with a complete loss of all onsite and offsite power and failure of the ECST. The reactor successfully trips and the containment isolates but all powered safety systems are unavailable. The timings of the key events are discussed further in Sections 5.2.1.1 and 5.2.2.1. However, it is worth noting that fission product releases from the fuel do not begin until 2 hr 57 min and significant fission product releases to the environment do not begin until 25 hr 32 min. Section 5.2.1.1 summarizes the thermal-hydraulic response of the reactor and containment while Section 5.2.2.2 summarizes the associated radionuclide release from the fuel to the environment.

Table 5-5 Timing of key events for unmitigated STSBO

Event Description	Time (hh:mm)
Initiating event Station blackout – loss of all onsite and offsite AC and DC power	00:00
MSIVs close Reactor trip RCP seals initially leak at 21 gpm/pump TD-AFW starts but fails to inject due to ECST rupture	00:00
First SG SRV opening	00:03
SG dryout	01:16
Pressurizer SRV opens	01:27
Pressurizer relief tank rupture disk opens	01:46
Start of fuel heatup	02:19
RCP seal failures	02:45
First fission product gap releases	02:57
Creep rupture failure of the C loop hot leg nozzle	03:45
Accumulators start discharging	03:45
Accumulators are empty	03:45
Vessel lower head failure by creep rupture	07:16
Debris discharge to reactor cavity	07:16
Cavity dryout	07:27
Containment at design pressure (45 psig)	11:00
Start of increased leakage of containment ($P/P_{design} = 2.18$)	25:32
Containment pressure increase slows	32:00
Containment pressure stops decreasing	44:14
End of calculation	48:00

5.2.1.1 Thermal-Hydraulic Response

The responses of the primary and secondary pressure systems are shown in Figure 5-27. At the start of the accident sequence, the reactor successfully scrams in response to the loss of power. The main steam line isolation and containment isolation valves close in response due to the loss of power. The reactor coolant and main feedwater pumps also trip to the loss of power. Once the main steam lines close, the normal mechanism of heat removal from the primary system is unavailable. Consequently, both the primary and secondary system pressures rise.
The secondary system quickly pressurizes to the safety relief valve opening pressure, which results in the safety relief valves to open and then subsequently close when the closing pressure

criterion is achieved. The relief flow through the SG SRVs is the principle primary system energy removal mechanism in the first hour. There is also energy removal through the RCP seal leakage, but the energy flow is small relative to the SG SRV flow.

Due to the complete loss of all feedwater at the start of the calculation, the water inventory in the steam generators decreased very rapidly and was completely boiled away by 1 hr 16 min. Although the steam generators relief valves continue to cycle and release steam, the associated heat removal is inadequate and the primary system sharply increases to the pressurizer safety relief valve opening pressure. The safety valves on the pressurizer begin opening and closing to remove excess energy. However, the pressurizer relief valve flow causes a steady decrease in the primary system coolant inventory (see Figure 5-28). The fuel starts to uncover at 2 hr 19 min (see Figure 5-29). The fuel cladding fails at 2 hr 59 min, which starts the release of fission products from the fuel. The fuel rods starts to degrade above 2400 K as the molten zirconium breaks through the oxidized shell of the cladding on the fuel rods and eventually collapse due a thermal-mechanical weakening of the remaining oxide shell at high temperature. As shown in Figure 5-29, the peak fuel-debris temperature reaches the fuel-zirconium oxide eutectic melting temperature of 2800 K.

Following the uncovery of the fuel, an in-vessel natural circulation flow develops between the hot fuel in the core and the cooler structures in the upper plenum. Hot gases rise out of the center of the core rise into the upper plenum and return down the cooler peripheral sections of the core. Simultaneously, a natural circulation circuit develops between the hot gases in the vessel and the steam generator [7]. Hot gases from inside the vessel flow along the top of the hot leg and into the steam generator. The hot gases flow through the steam generator in approximately half the tubes and return through the remaining tubes. The large masses of the hot leg nozzle, hot leg piping, and the steam generator tubes absorb the heat from the gases exiting the vessel. The cooler gases leaving the steam generator return to the vessel along the bottom of the hot leg. Due to its close proximity to the hot gases exiting in the vessel, the hot leg nozzle at the carbon steel interface region to the stainless steel piping was predicted to fail by creep rupture at 3 hr 45 min.[22]

Upon creep failure of the hot leg nozzle, a large hole opened that rapidly depressurized the RCS (i.e., like a large break loss-of-coolant accident). The RCS depressurization permitted a complete accumulator injection at low-pressure (i.e., water level rise at 3 hr 45 min on Figure 5-28). Although the water filled above the core region, the hottest fuel in the core remained in film boiling and continued to collapse and degrade (see Figure 5-29). The lower temperature regions on the periphery of the core quenched but subsequently reheated once the water level decreased into the core.

[22] Alternate failure locations could include the pressurizer surge line and the steam generator tubes. There was some residual water in the pressurizer that cooled the surge line. Due to the relatively high pressure in the steam generator secondary side, the resultant thermal-mechanical stresses across the steam generator tubes were less severe than the hot leg nozzle. Consequently, the most vulnerable location was calculated to be the hot leg nozzle. The variation of the scenario was evaluated assuming a SG tube was the initial failure location.

Following the accumulator injection at 3 hr 45 minute, the decay heat from the fuel boiled away the injected water. By 4.3 hr, a large debris bed had formed in the center of the core. The debris continued to expand until 5.8 hr when all the fuel had collapsed and was resting on the core plate. The hot debris failed the core support plate and fell onto the lower core support plate, which failed at 6.6 hr. Following the lower core support plate failure, the debris bed relocated onto the lower head. The small amount of remaining water in the lower head was quickly boiled away. As shown in Figure 5-31, the hot debris quickly heated the lower head to above the melting temperature of stainless steel (i.e., 1700 K) on the inside surface. As the heat transferred through the lower head, it eventually failed at 7 hr 16 min due to the creep rupture failure criterion (i.e., primarily due to the thermal stress component and the low differential pressure).

By 7.5 hr, nearly all the hot debris relocated from the vessel into the reactor cavity in the containment under the reactor vessel. The hot debris boiled away the water in the reactor cavity started to ablate the concrete. The ex-vessel core-concrete interactions (CCI) continued for the remainder of the calculation, which generated non-condensable gases. In addition, the hot gases exiting the reactor cavity and the radioactive heating from airborne and settled fission products steadily evaporated the water on the containment floor outside the reactor cavity from 7.3 hr to 44 hr. The resultant non-condensable gas and steam generation pressurized the containment (see Figure 5-32). At 25.5 hr, the containment failed due to liner tearing near the containment equipment hatch at mid-height in the cylindrical region of the containment (i.e., containment leakage area in Figure 5-30). The containment continues to pressurize until the leakage flow balanced the steam and non-condensable gas generation (see Figure 5-33). By 44 hr, all the water on the floor has evaporated. The containment depressurized thereafter due to only a smaller gas loading from the non-condensable gas generation.

The containment failure location was around the equipment hatch, which is located on the side of the containment without a surrounding building (e.g., not adjacent to the auxiliary or safeguards buildings). Consequently, all released fission products are released directly to the environment.

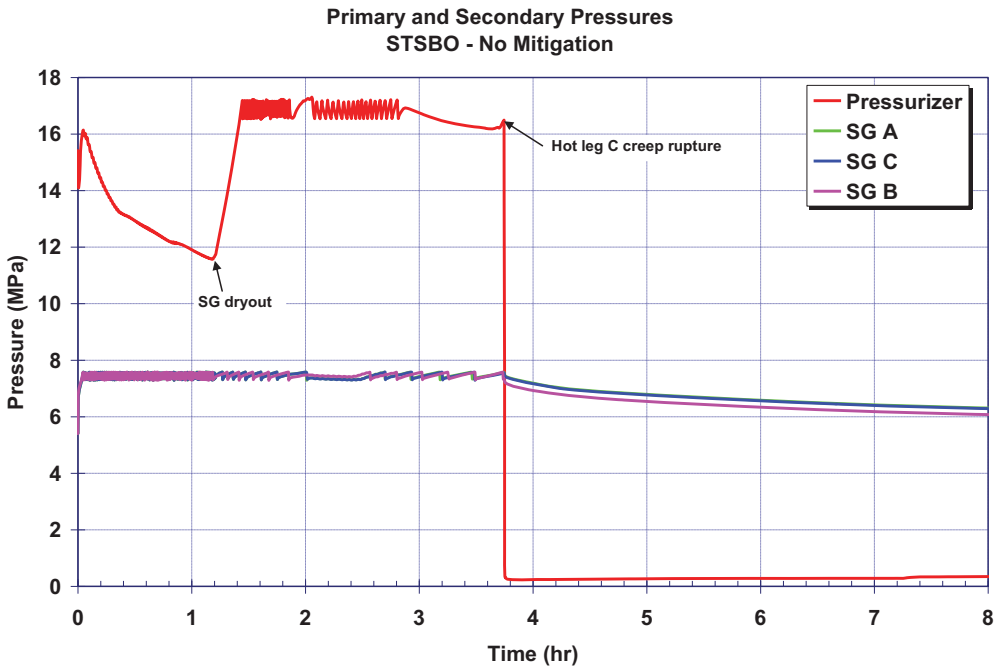

Figure 5-27 Unmitigated STSBO primary and secondary pressures history

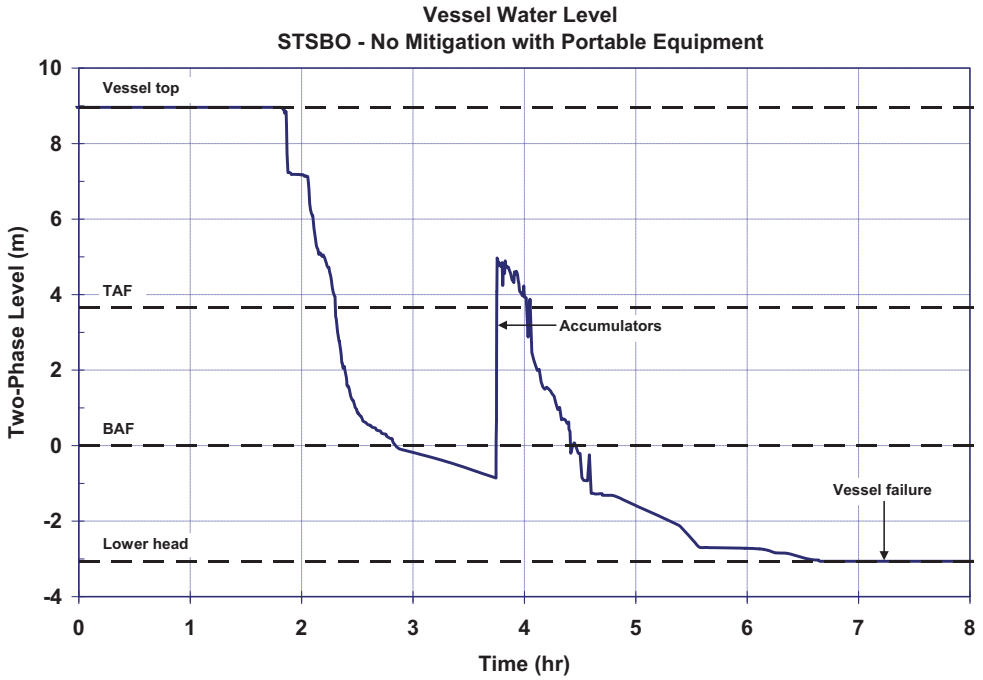

Figure 5-28 Unmitigated short-term station blackout vessel two-phase coolant level

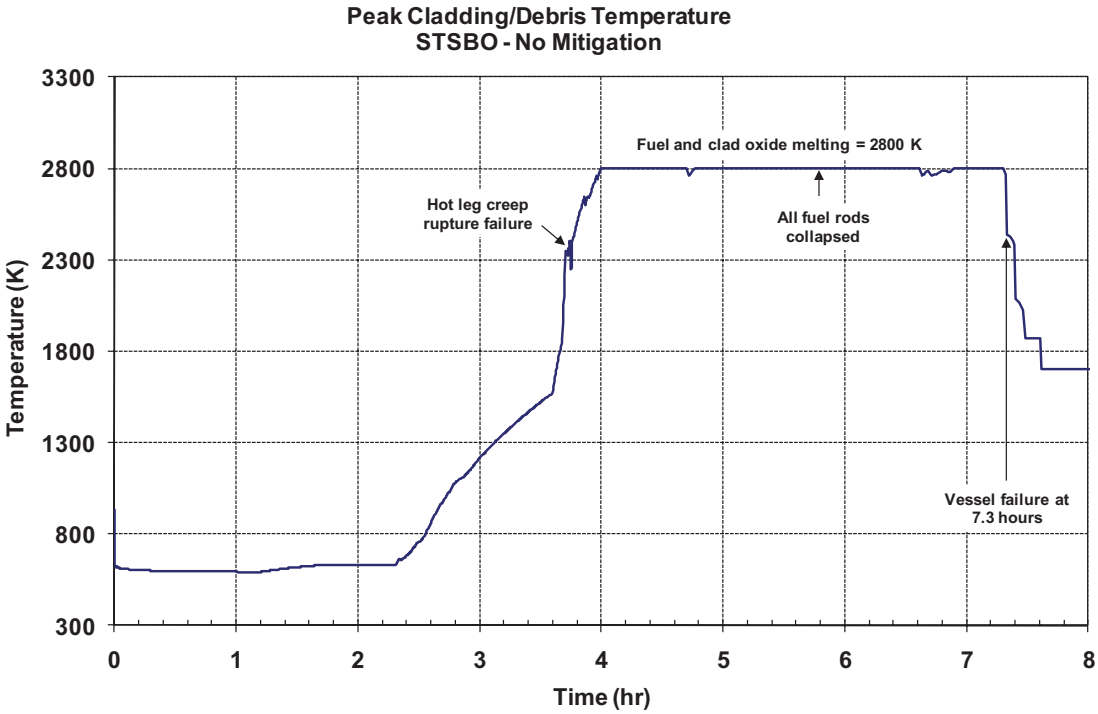

Figure 5-29 Unmitigated STSBO core temperature history

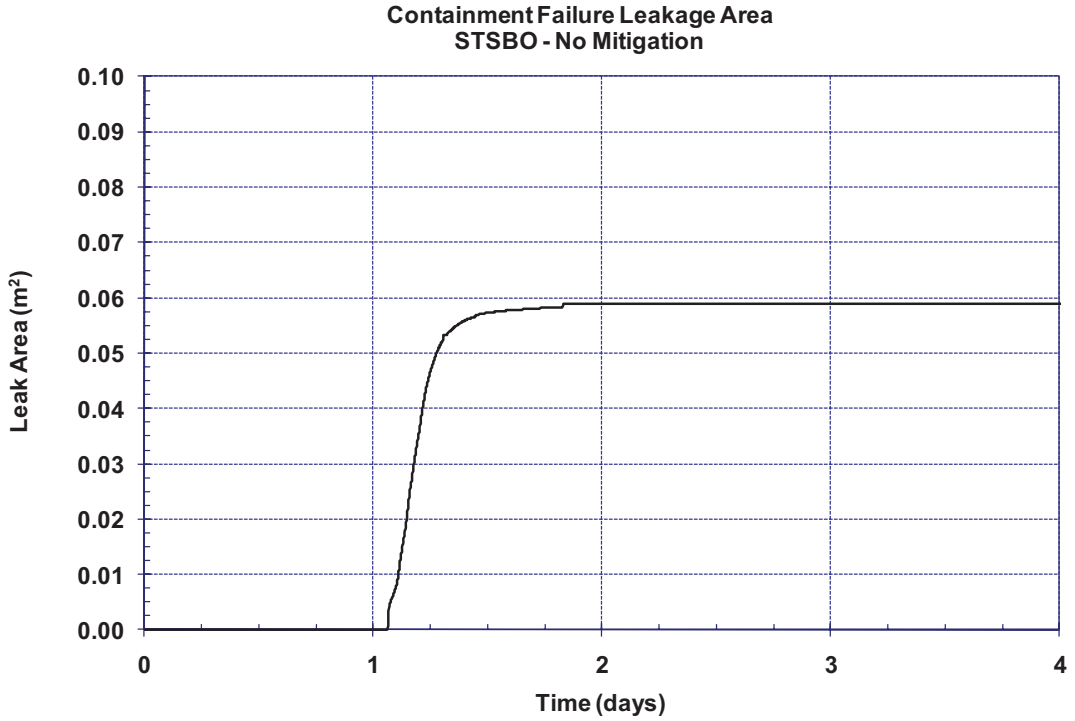

Figure 5-30 Unmitigated STSBO containment leakage area

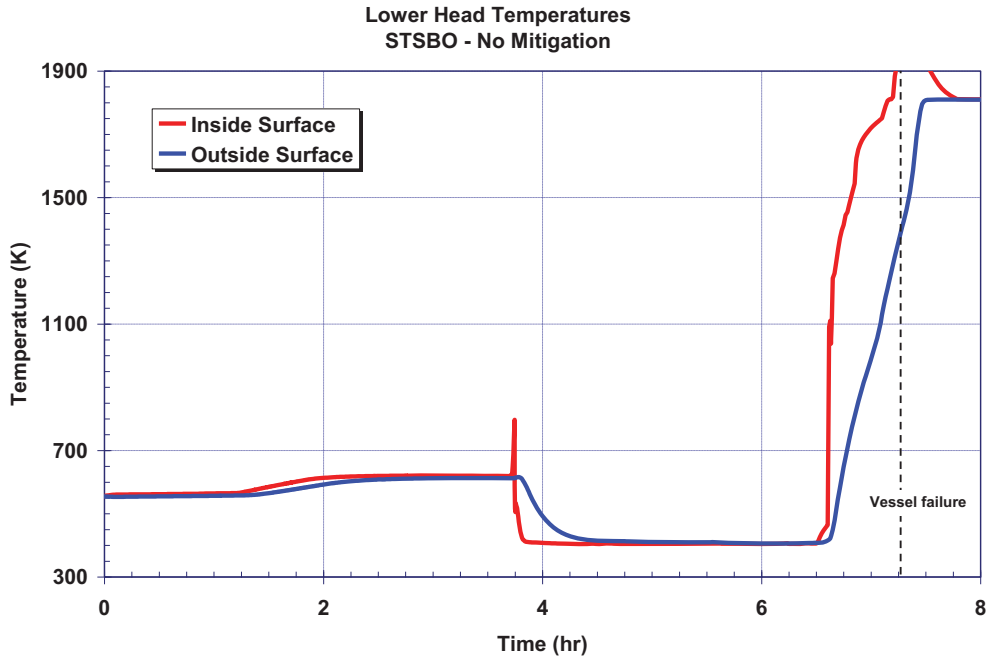

Figure 5-31 Unmitigated STSBO lower head inner and outer temperature history

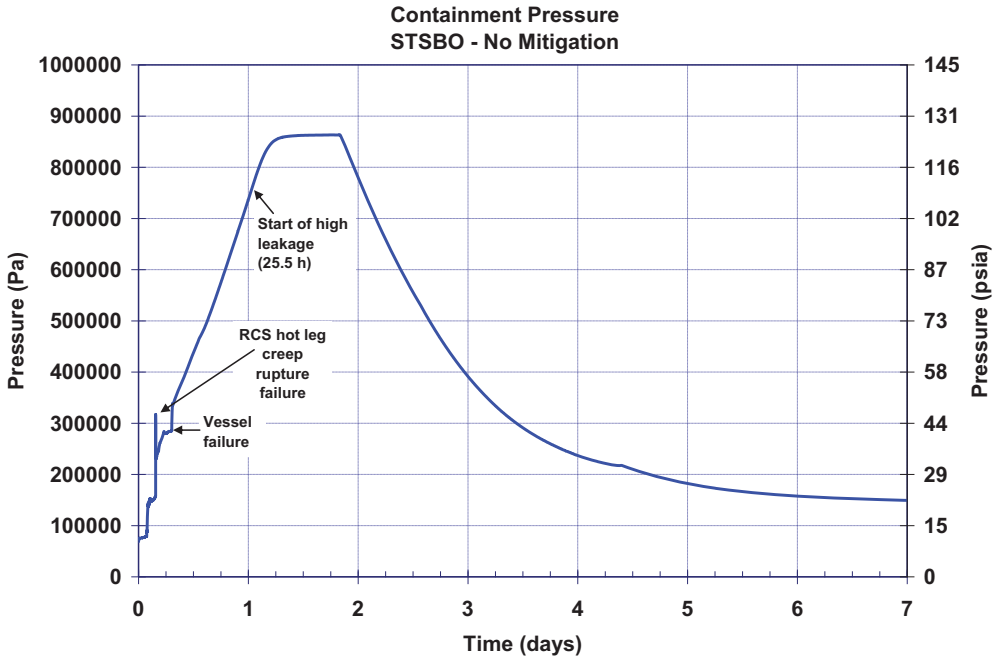

Figure 5-32 Unmitigated short-term station blackout containment pressure history

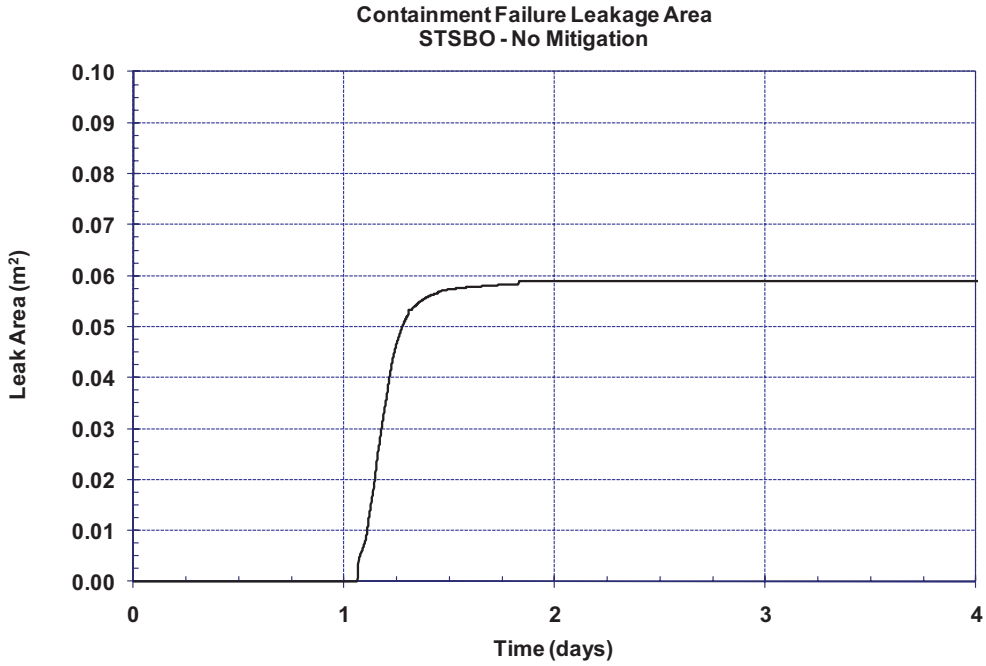

Figure 5-33 Unmitigated short-term station blackout containment leakage area

5.2.1.2 Radionuclide Release

The fission product releases from the fuel started following the first thermal-mechanical failures of the fuel cladding in the hottest rods at 2 hr 57 min, or about 38 min after the uncovery of the top of the fuel rods. The in-vessel fission product release phase continued through vessel failure at 7.3 hr. Initially, the fission product releases from the fuel circulated through the primary system as well as being released to the containment through the pressurizer safety relief valves. The PRT rupture disk opened about 1 hour before the start of the start of the fission product releases. Subsequently, the fission product releases exiting through the pressurizer relief valves were not well retained in the PRT because the pool was nearly saturated and in the PRT rupture disk was open. Following vessel failure, the fission product releases continued from the ex-vessel fuel in the reactor cavity.

Figure 5-34 and Figure 5-35 show the fission product distributions of the iodine and cesium radionuclides that were released from the fuel, respectively (see Appendix B for a detailed radionuclide core inventory). Approximately 97% and 98% of the iodine and cesium, respectively, were released from the fuel prior to vessel failure while the remaining amount was released ex-vessel. At the time of the hot leg failure, approximately 40% of these volatile radionuclides had been released. The resultant blowdown of the vessel immediately discharged the airborne fission products to the containment. However, about 6% of the iodine and 5% of the cesium remained in the vessel. Most of the radionuclides retained in the RCS were deposited in the steam generators during the natural circulation phase of the accident. Following the RCS blowdown after the hot leg nozzle failure, more radionuclides were released from the fuel as the core further degraded. At low pressure conditions, the fission products continued to circulate within the vessel and to the steam generators with a substantial portion being depositing on the structural surfaces. However, as shown in the figures, the majority of the released radionuclides

were transported to the containment. Within the first day, most of the airborne fission products in the containment settled on surfaces. This was significant because the containment failure occurred at 25 hr 32 min. Consequently, there was little airborne mass that could be released to the environment.

The chemical form of the released iodine was cesium-iodine, which was more volatile than the predominant form of the released cesium, which was cesium-molybdate (Cs_2MoO_4). As shown in the iodine history figure (see Figure 5-34), the in-vessel iodine mass was decreasing following vessel failure until approximately 2.9 days. The decrease of mass represents a vaporization process of previously deposited radionuclides. The late in-vessel vaporization release was significant because it continued after containment failure and had a significant contribution to the overall environmental release. The thermal mechanisms for the vaporization of the iodine were from two sources. First, the fission product decay of the settled radionuclides heated the structures. Second, a natural circulation flow of very hot gases (i.e., from 1050 K to >1600 K) flowed from the reactor cavity, through the failed vessel lower head, through the reactor vessel, and out the failed hot leg nozzle. As the deposited cesium-iodine heated, gaseous iodine was released and the cesium remained chemisorbed to the stainless steel surfaces. The natural circulation flow pattern also effectively vented the gaseous iodine from the RCS to the containment.

In contrast to the iodine response in Figure 5-34, the deposited cesium molybdate was less volatile and remained deposited in the RCS (see Figure 5-35). Except for inside the reactor cavity, the containment was cooler than vessel and well below conditions that would vaporize settled radionuclides. Consequently, none of the deposited radionuclides (i.e., including iodine) in the containment vaporized.

Finally, Figure 5-36 summarizes the releases of the radionuclides to the environment. At 4 days, 92% of the noble gases, 1.7% of the tellurium, 1.0% if the iodine, 0.75% of the radioactive cadmium, 0.4% of the cesium, and 0.1% of the barium and radioactive tin had been released to the environment. All other releases were less than 0.1% of the initial inventory. There were some environmental releases prior to the containment failure at 25.5 hr due to nominal leakages (i.e., design specification of 0.1% vol/day at the design pressure). The releases to the environment increased sharply after the failure of the containment. Between 25.5 hr, 48 hr, 53% of the airborne noble gases in the containment were released. Over the next 2 days, ~40% more was released.

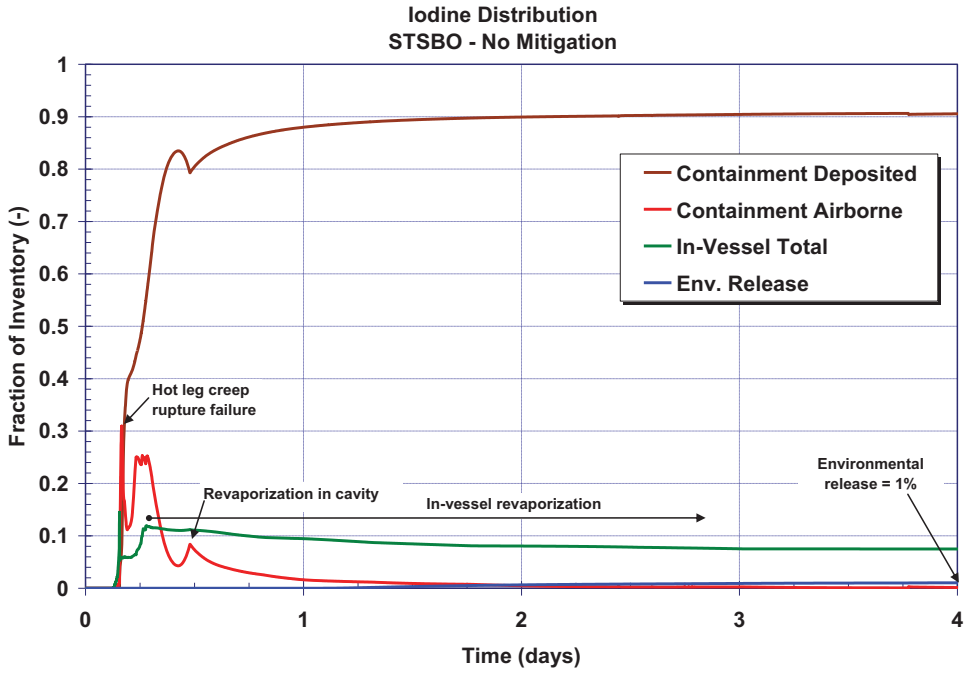

Figure 5-34 Unmitigated STSBO iodine fission product distribution history[23]

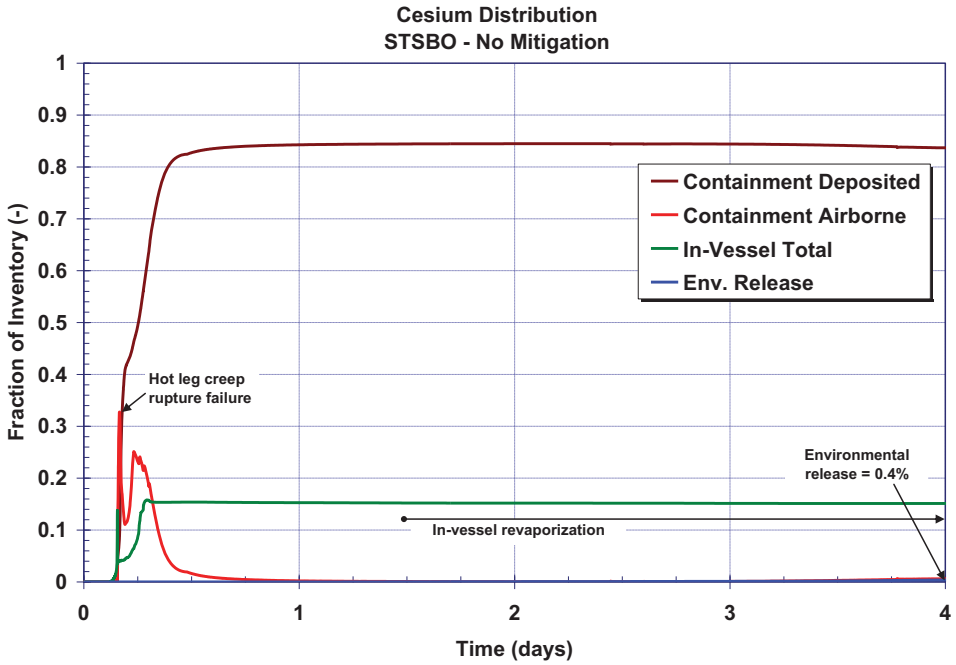

Figure 5-35 Unmitigated STSBO cesium fission product distribution history [24]

[23] In-vessel refers to the entire primary-side of the RCS.
[24] In-vessel refers to the entire primary-side of the RCS.

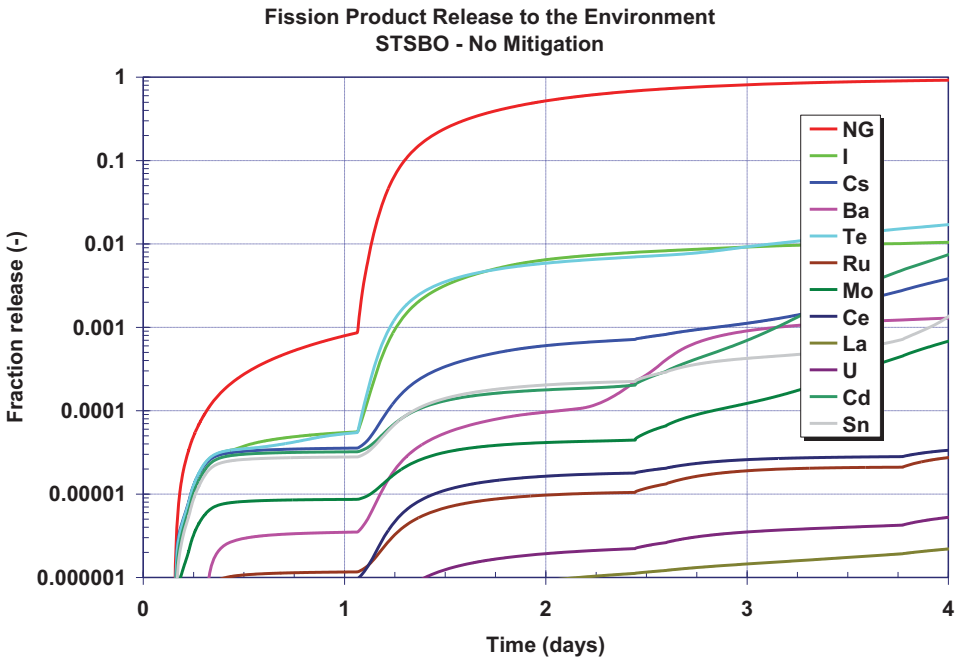

Figure 5-36 Unmitigated STSBO environmental release history of all fission products

5.2.2 Mitigated Short-Term Station Blackout

Table 5-6 summarizes the timing of the key events in the mitigated STSBO. As described in Section 3.2, the accident scenario initiates with a complete lost of all onsite and offsite power. The reactor successfully trips and the containment isolates, but all powered safety styems are unavailable. The timing of key events are discussed further in Sections 5.2.2.1 and 5.2.2.2. Unlike the unmitigated STSBO described in Section 5.2.1, the mitigated STSBO credits the successful connection of the portable, low-pressure, diesel-driven (Godwin) pump to the containment spray system at 8 hours. The Godwin pump is a high-flow, low-head pump with a design capacity of 2,000 gpm at 120 psi.[25] A reliable source of water is maintained while 1,000,000 gallons is injected into the containment through the containment sprays. In particular, the core has degraded and failed the vessel lower head prior to the spray actuation (see Table 5-6). The emergency containment sprays are effective at reducing the containment pressure and knocking down airborne fission products while they are operating. However, the containment subsequenctly pressurizes after the sprays are terminated to the failure pressure. While not investigated, intermitten operation of the sprays and deeper flooding could have further delyed failure of the containment.

[25] The rated containment pump spray flowrate was 3,200 gpm. It was judged that the portable Godwin pump would pressurize the system and develop the spray droplet flow patter.

Table 5-6 Timing of key events for mitigated STSBO

Event Description	Time (hh:mm)
Initiating event Station blackout – loss of all onsite and offsite AC and DC power	00:00
MSIVs close Reactor trip RCP seals initially leak at 21 gpm/pump TD-AFW starts but fails to inject due to ECST rupture	00:00
First SG SRV opening	00:03
SG dryout	01:16
Pressurizer SRV opens	01:27
Pressurizer relief tank rupture disk opens	01:46
Start of fuel heatup	02:19
RCP seal failures	02:45
First fission product gap releases	02:57
Creep rupture failure of the C loop hot leg nozzle	03:45
Accumulators start discharging	03:45
Accumulators are empty	03:45
Vessel lower head failure by creep rupture	07:16
Debris discharge to reactor cavity	07:16
Cavity dryout	07:27
Start of containment sprays	8:00
End of containment sprays (1,000,000 gal)	15:02
Containment at design pressure (45 psig)	40:00
Start of increased leakage of containment ($P/P_{design} = 2.18$)	66:30

5.2.2.1 Thermal-Hydraulic Response

The progression of events in the mitigated STSBO is identical to the unmitigated STSBO as described in Section 5.2.1 through the first 8 hr, which includes core degradation and vessel failure. Consequently, the system pressure and peak fuel temperature responses though the first 8 hr is identical between the two sequences (i.e., compare Figure 5-37 and Figure 5-27, Figure 5-39 and Figure 5-29, and Figure 5-40 and Figure 5-31). However, after 8 hr, there are some key differences. For example, the long-term reactor vessel level shows different behavior after 8 hr. Although the water in the vessel boils away by 6.6 hr when the core relocates onto the lower head, the vessel water level starts to recover at 13.7 hr as shown in Figure 5-38. After 5.7 hr of containment spray operation, the water level in the containment was calculated to fill

above the bottom of the vessel.[26] At 15 hr when the containment spray was terminated, the containment water had flooded ~1.3 m into the vessel.

The reactor cavity of Unit 1 of the Surry containment connects to the surrounding lower regions of the containment through: (a) a 12" hole in the reactor cavity wall at 2'-7" above the bottom of the floor, (b) a penetration at 24'-3" above the floor, and (c) the holes in the cavity wall for the RCS piping (i.e., nearly 40' above the bottom of the floor). In the case of this scenario, the lower hole into the reactor cavity was flooded whereas the upper openings were well above the water level. Hence, there was no natural circulation of water from the containment basement into the reactor cavity and out the gaps for the RCS piping penetrations. While the containment sprays were operating, a significant portion of the spray water drained into the reactor cavity from refueling pool. The resultant water flow through the reactor cavity removed the heat from the fuel debris. Once the spray flow stopped, the water in the cavity heated to saturation conditions and started to boil. The resulting steam load from the boiling pressurized the containment to the failure pressure (see Figure 5-41). Although there was 1,000,000 gallons of water in the containment, the core debris was only in thermal contact with ~40,000 gallons in the reactor cavity. Consequently, the containment pressurized to failure conditions much faster than if all 1,000,000 gallons were being heated. As stated in Section 4.2, intermittent spray operation and/or flooding above the RCS piping penetrations would have substantially delayed containment failure. Although the containment sprays did not prevent containment failure, they delayed containment failure by over 40 hr relative to the unmitigated case.

Although the exact conditions following a severe seismic event were not known, it was estimated that portable sprays could be started by 8 hr. Based on the pressure response of the unmitigated STSBO, the containment sprays must be started before 15.6 hr while the containment pressure was below the shutoff head of the portable pump. Once the containment sprays are initiated, they are effective in quickly reducing the containment pressure. Consequently, there was almost eight additional hours from the assumed starting time to establish containment sprays, or 15.6 hr after the start of the scenario.

The selection of the containment sprays as a mitigation technique for this scenario was particularly beneficial for several reasons. First, the containment sprays were extremely effective in knocking down the airborne aerosols into the large containment pool. Second, the sprays delayed containment failure for an additional 41 hr. In contrast, the alternate strategies of containment flooding or vessel injection would not be expected to be as beneficial for this scenario (i.e., assuming an initiation time after vessel failure). The high-head portable pump used for vessel injection can only provide 65 gpm versus 2000 gpm for the portable containment spray pump. Consequently, the time to deep flood the containment would be significantly longer. More importantly, the water would merely fall out of the failed vessel and not reduce the containment pressure (i.e., versus the highly effective heat and mass transfer from the containment spray system). In fact, the small amount of water flooding onto the ex-vessel core debris would enhance the pressurization of the containment versus a dry reactor cavity.

[26] At the time of the calculation, the exact flooding water level characteristics of the Surry containment were not known. Subsequently, information was obtained from the plant that shows ~1,160,000 gal are needed to fill to the bottom of the vessel. Consequently, the calculated water level response of this scenario is actually consistent with a slightly higher integrated spray flow.

Furthermore, the injection flow would not directly knockdown the airborne aerosol radionuclides. Similarly, direct containment injection using the high flow pump would not depressurize the containment nor reduce any airborne fission products.

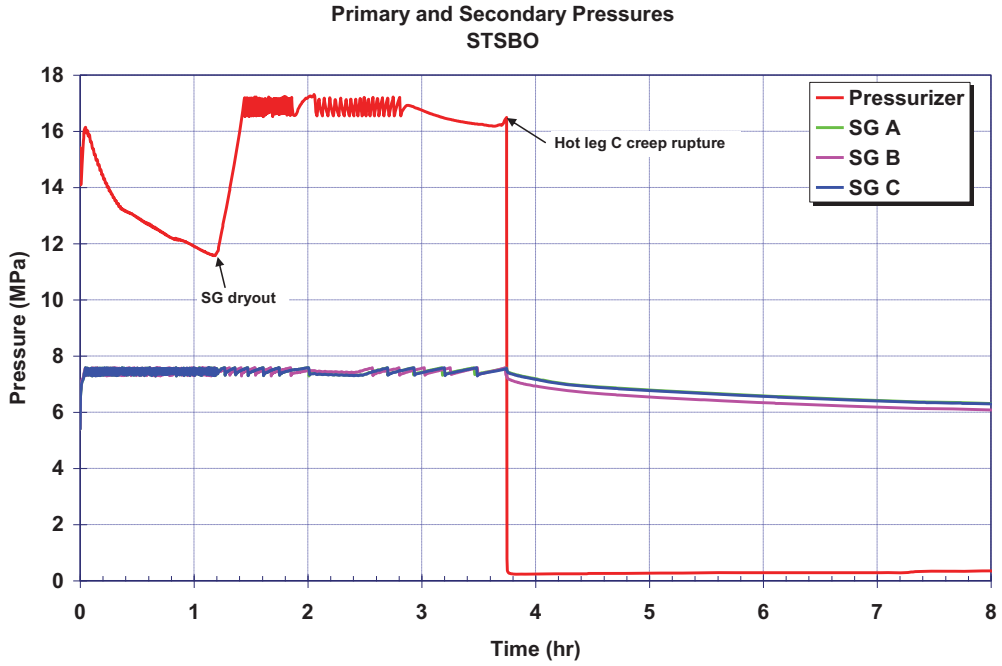

Figure 5-37 Mitigated STSBO primary and secondary pressure history

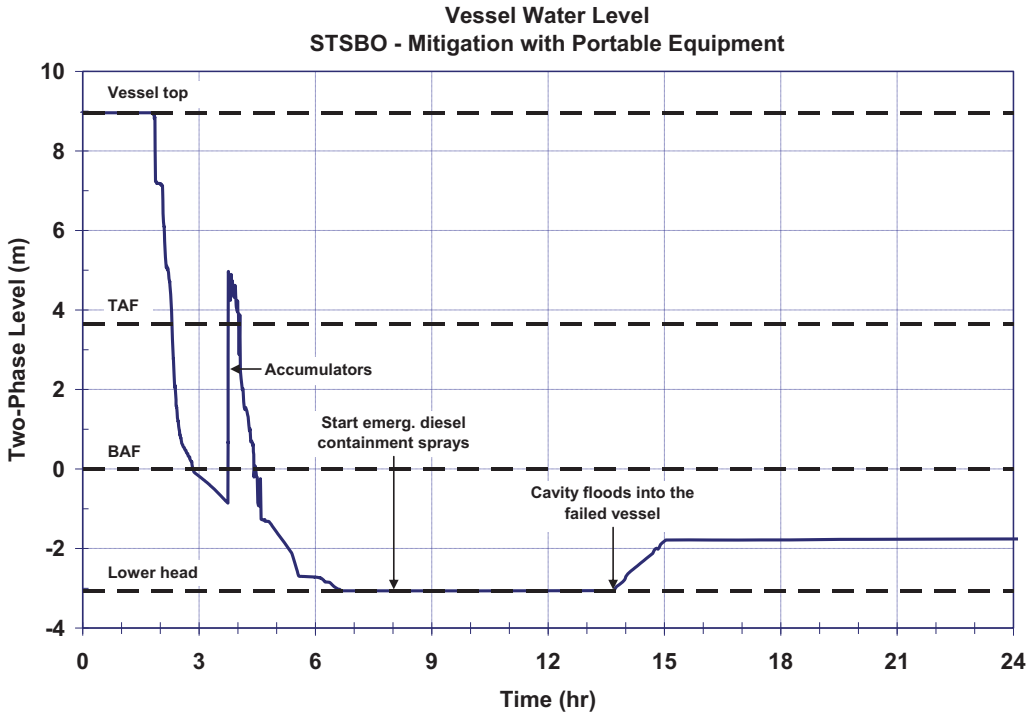

Figure 5-38 Mitigated short-term station blackout vessel two-phase coolant level

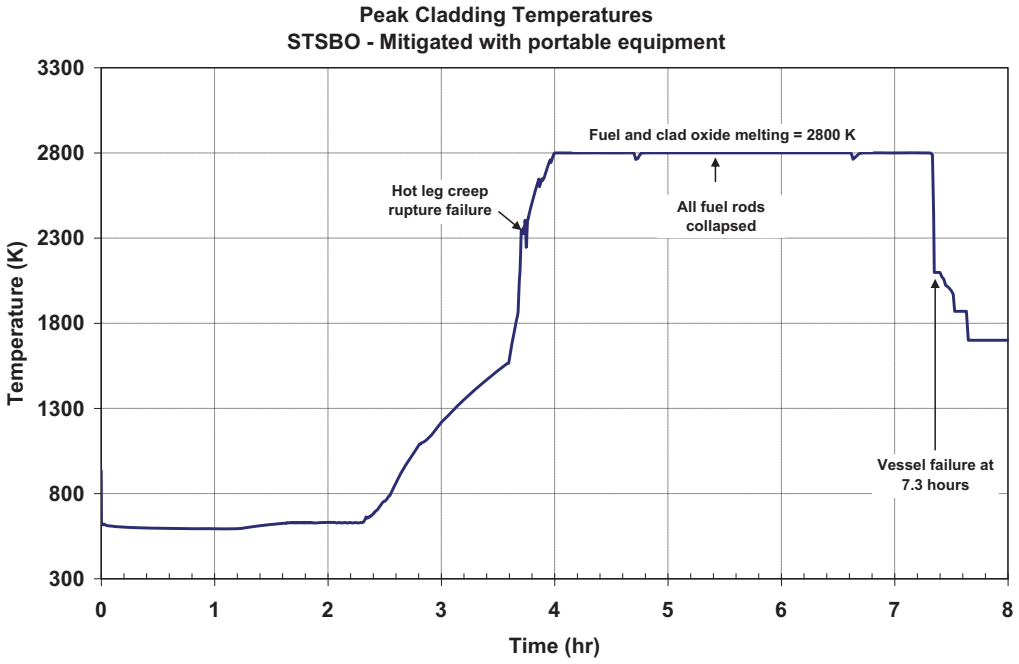

Figure 5-39 Mitigated short-term station blackout core temperature history

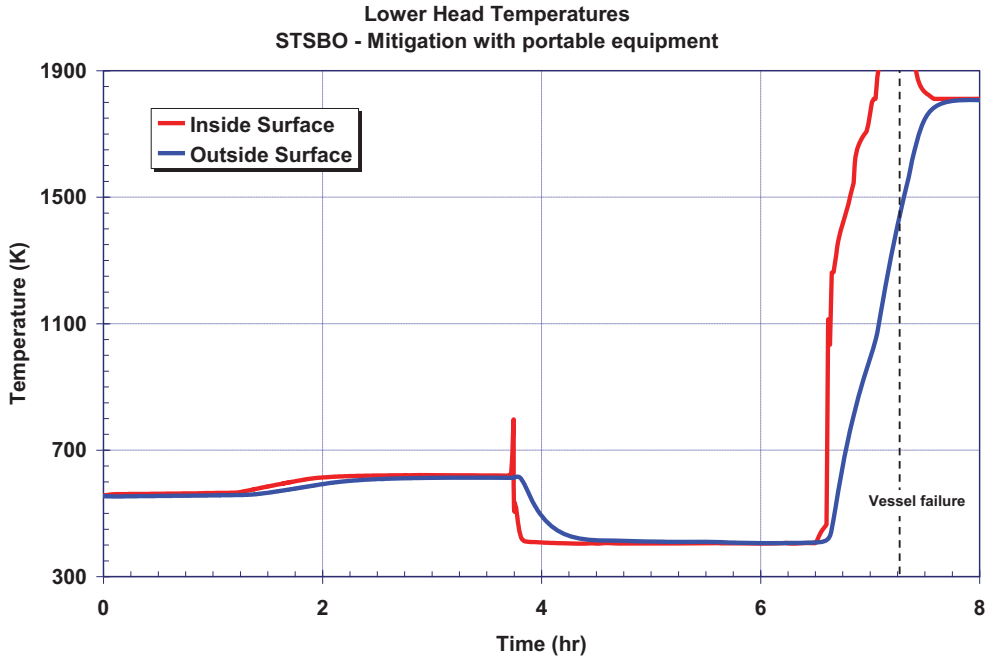

Figure 5-40 Mitigated STSBO lower head inner and outer temperature history

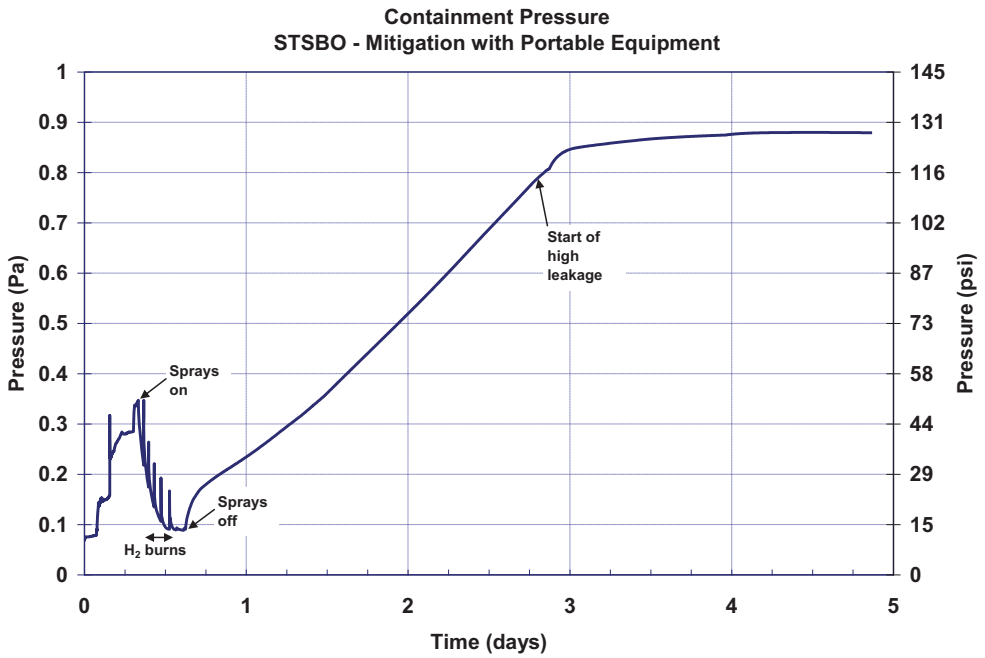

Figure 5-41 Mitigated short-term station blackout containment pressure history

5.2.2.2 Radionuclide Release

The radionuclide response of the mitigated STSBO is identical to the unmitigated response described in Section 4.1.2 for the first 8 hr, or through vessel failure until the start of the containment sprays. Following the start of the emergency containment sprays at 8 hr (0.25 days), the airborne aerosols of iodine and cesium rapidly decease (see Figure 5-42 and Figure 5-43, respectively). By the time the sprays are terminated at 15 hr (0.63 days), almost all of the airborne aerosols have been captured in the pool on the containment floor. Since the containment failure was delayed until 66 hr 30 min (2.8 days), the amount of airborne mass available for release was insignificant. The environmental release of iodine and cesium was very small (i.e., 0.007% and 0.003%, respectively).

Due to the deep flooding in the reactor cavity by the spray operation, the bottom of the failed vessel lower head is submerged in water. Therefore, the natural hot circulation flow that promoted vaporization of deposited radionuclides in the unmitigated STSBO is not present. Instead, the water pool in the reactor cavity cools the bottom of the vessel. Due to the boiling in the cavity, relatively cool steam flows through the vessel and out the failed hot leg nozzle location, which removes heat and inhibits vaporization of deposited radionuclides in the upper vessel and hot leg. Consequently, the vaporization of the in-vessel deposited fission products (i.e., especially cesium-iodine) that was seen in the unmitigated STSBO (i.e., characteristic of vaporization), was negligible in the mitigated case through 4 days.

Finally, Figure 5-44 summarizes the releases of the radionuclides to the environment. At 4 days, 60% of the noble gases, 0.0046% of the tellurium, 0.0065% of the iodine and cadmium, 0.0027% of the cesium had been released to the environment. Except for the noble gases, all the releases were less than 0.01% of the initial inventory. As shown in the figure, the initial releases to the

environment were due to the nominal leakages (i.e., design specification of 0.1% vol/day at the design pressure) prior to the containment failure at 66 hr 30 min (2.8 days). Following containment failure at 2.8 days until 4 days, the noble gas release went from 0.24% to 60%, which represents a significant flushing of the containment gas space to the environment. There is some evidence of increased leakage of the other radionuclides after containment failure. However, the response is exaggerated in the figure due to the semi-logarithmic scale. The absolute magnitude of the releases was small relative to the unmitigated response.

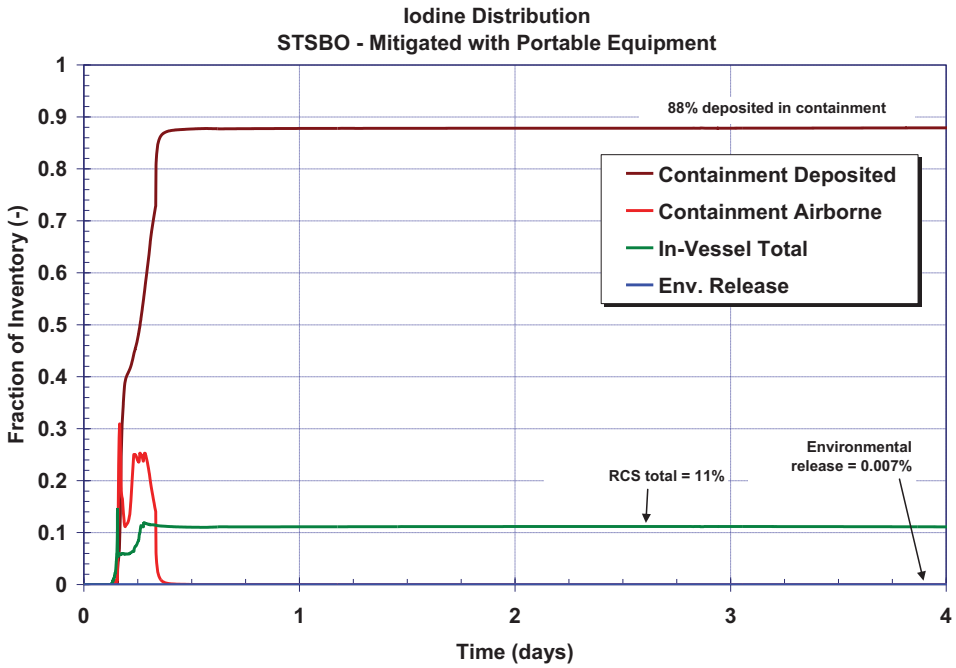

Figure 5-42 Mitigated short-term station blackout iodine fission product distribution history [27]

[27] In-vessel refers to the entire primary-side of the RCS.

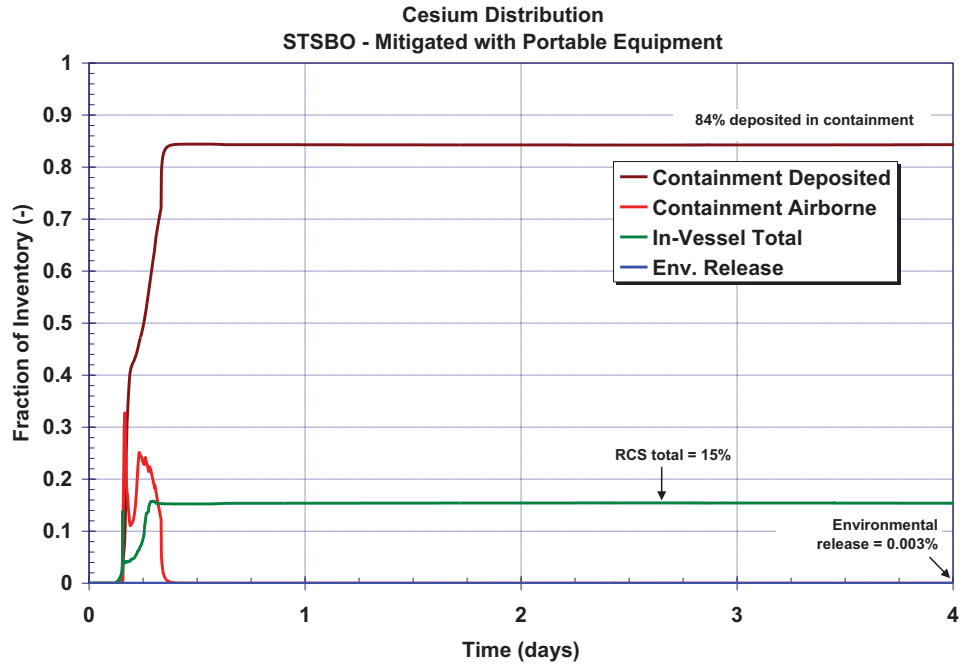

Figure 5-43 Mitigated STSBO cesium fission product distribution history [28]

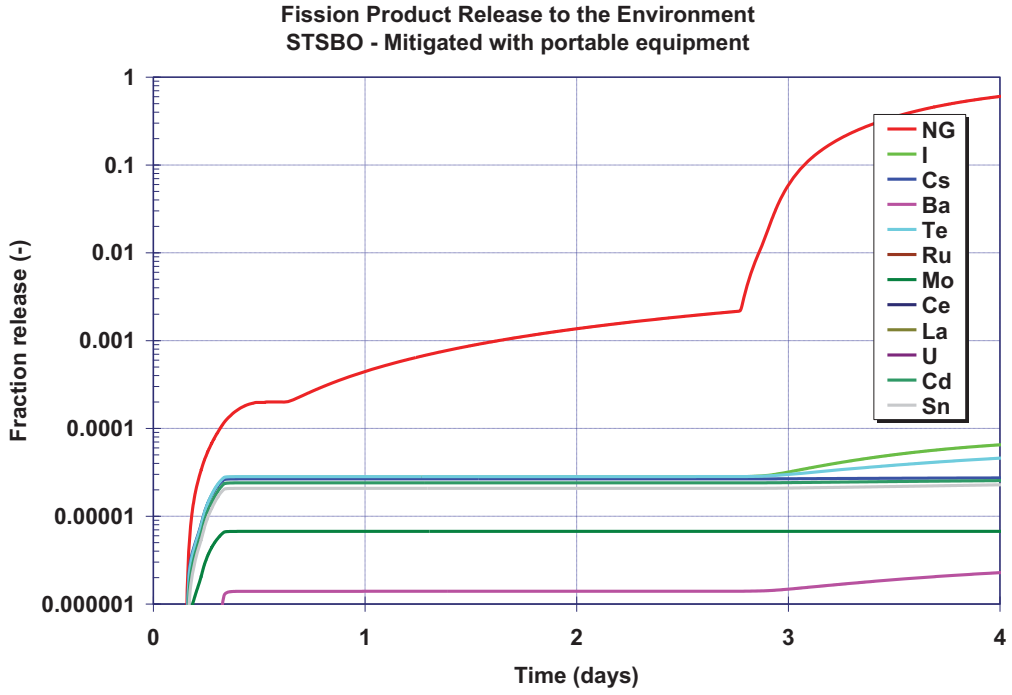

Figure 5-44 Mitigated STSBO environmental release history of all fission products

[28] In-vessel refers to the entire primary-side of the RCS.

5.2.3 Uncertainties in the Hydrogen Combustion in the Mitigated Short-Term Station Blackout

During the peer review of the mitigated STSBO, there was concern about the undesirable effects of combustion following an emergency spray actuation in the containment. Although emergency sprays mitigated the accident, there was severe damage to the fuel with considerable hydrogen production. On the other hand, another peer review comment concerned the time it took to transport a diesel-driven pump and connect it to plant piping following a large seismic event. The peer reviewer noted that while the licensee estimated 2 hours would be required, SOARCA assumed that 8 hours would be required. This comment also supports the idea that the mitigated case could have involved injection into the RCS resulting in no core damage and therefore no hydrogen combustion. It should be noted that further discussion with the plant staff revealed that the decision to install and operate the emergency sprays is made by the TSC and is also uncertain. The TSC will use calculation aids to assess the benefits of containment sprays versus the adverse effects of enhancing conditions for hydrogen burns. Consequently, the mitigated STSBO calculation described in Section 3.2.3 and the following sensitivity calculations examine the potential system responses assuming the use of emergency sprays as a mitigative action, which is uncertain. Alternate responses include: (a) no successful mitigative actions (i.e., the unmitigated response described in Section 5.1.1), (b) emergency RCS injection prior to vessel failure, (c) emergency AFW injection that greatly delays core damage, and (d) containment flooding, which does not enhance hydrogen combustion.

In the mitigated case described in Section 3.2.3, there was severe damage to the fuel with considerable hydrogen production due to the delay in connecting the diesel-driven pump to plant piping. However, the severity of the accident was reduced by covering the core debris with water, scrubbing airborne fission products, and reducing containment pressure. As shown in Figure 5-45, 200 kg of hydrogen was produced by the time of the hot leg failure (i.e., 3:45 hr). There was a hydrogen burn coincident with hot leg rupture. Subsequently, the hydrogen production continued and an additional 150 kg of hydrogen was produced by vessel lower head rupture failure (i.e., 7:16 hr).

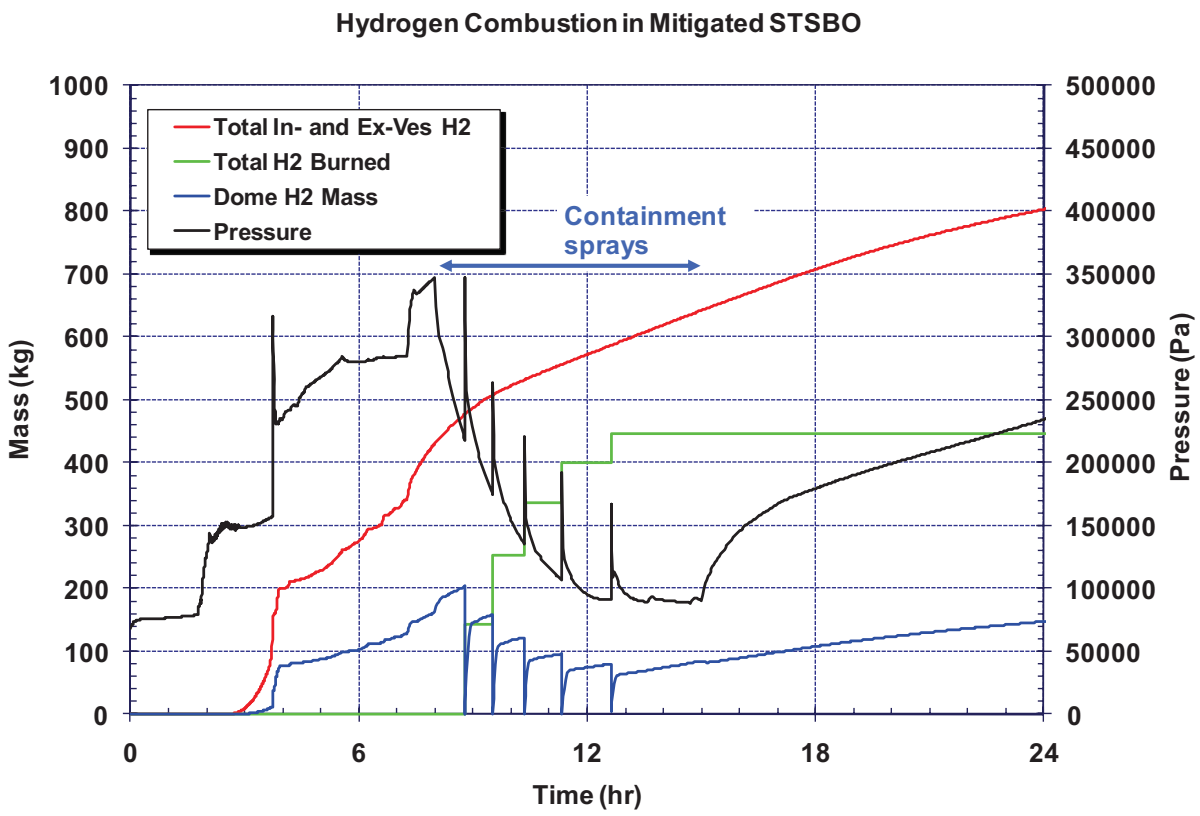

Figure 5-45 Comparison of the mitigated short-term station blackout containment pressure history versus the dome hydrogen mass and total hydrogen production

Following vessel failure, steam production by debris falling into water on the containment floor kept the containment steam-inerted.[29] Consequently, there were no further hydrogen burns in the unmitigated case. In the mitigated case, emergency containment sprays subsequently condensed the steam in the containment atmosphere and reduced the containment pressure. The net effects of the emergency spray operation between 8 to 15 hours were high hydrogen and oxygen concentrations, good mixing, and a low steam concentration (i.e., conditions suitable for combustion). Hydrogen combustion was modeled whenever the gaseous concentrations reached the specified levels in MELCOR's default combustion model (i.e., χ_{steam} <55%, $\chi_{hydrogen}$>10%, and χ_{oxygen} >5%). This resulted in several smaller burns as shown in Figure 5-45. Due the uncertainty of the ignition source, SOARCA peer reviewers inquired about the consequences of a later but larger burn.

Several facets were investigated relative to the SOARCA peer reviewer's comments. First, the potential ignition sources were reviewed. The most likely sources are the hot gases exiting the failed hot leg (i.e., a hot jet or hot pipe) and debris when the vessel fails. Two locations were examined, the containment cavity (see Figure 5-46) and the containment dome (i.e., see Figure 5-47, representative of the bulk conditions due to high mixing during spray operation).

[29] As described in Section 4.9, MELCOR's default hydrogen combustion model was used, which identifies steam concentrations greater than 55% to be steam-inerted and unable to support a hydrogen burn. Following vessel failure, the ex-vessel debris boiled water on the containment floor to maintain a high steam concentration.

Hot, hydrogen-rich gases discharge into the cavity following hot leg failure. The temperature of the gases is well above the auto-ignition temperature for a hydrogen jet (i.e., 950-1100 K), as shown in Figure 5-46. Hence, ignition is likely, which occurred in the base calculation. The specific conditions at the hot leg failure are summarized in the figure. However, due to the subsequent discharge of the accumulators and full depressurization of the primary system, the high temperature jet flow stopped shortly thereafter. Furthermore, steam from the vessel quickly inerted the cavity atmosphere to >90%.[30] Following vessel failure, very hot debris fell from the vessel into the cavity, which also created a likely ignition source. However, once the hot debris reached the water pool on the cavity floor, there was a sustained, rapid steam production. The additional steaming re-inerted the containment and increased the containment pressure, which lowered the relative hydrogen concentration.

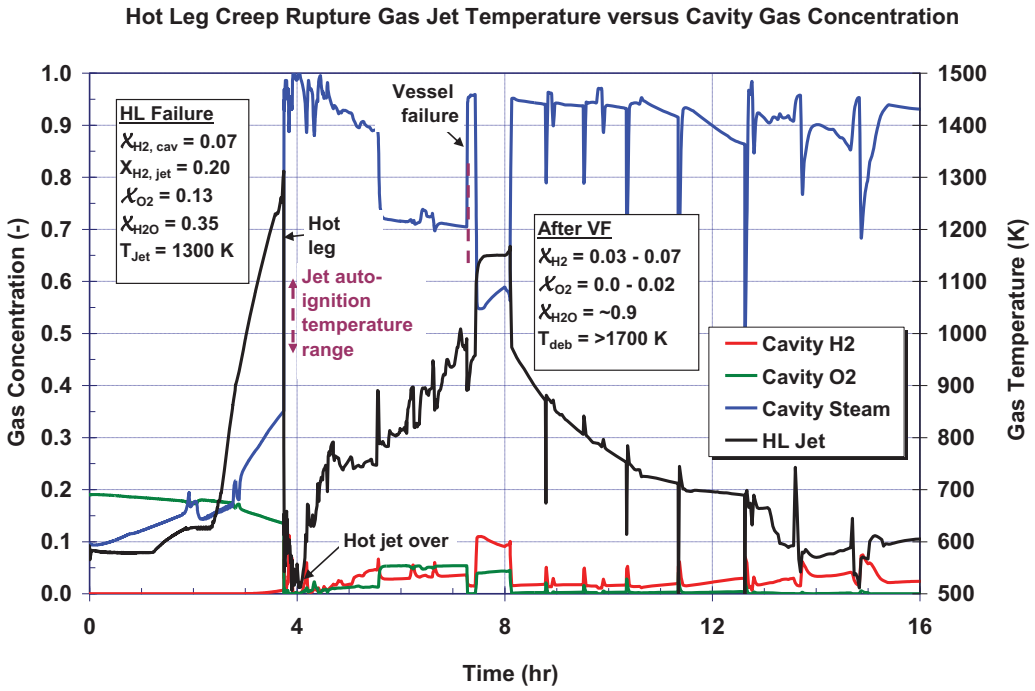

Figure 5-46 Comparison of the mitigated short-term station blackout containment cavity gas concentration history and potential ignition source temperatures

[30] The high steam source through the hot leg failure location into the containment occurred as accumulator water boiled in the hot vessel debris.

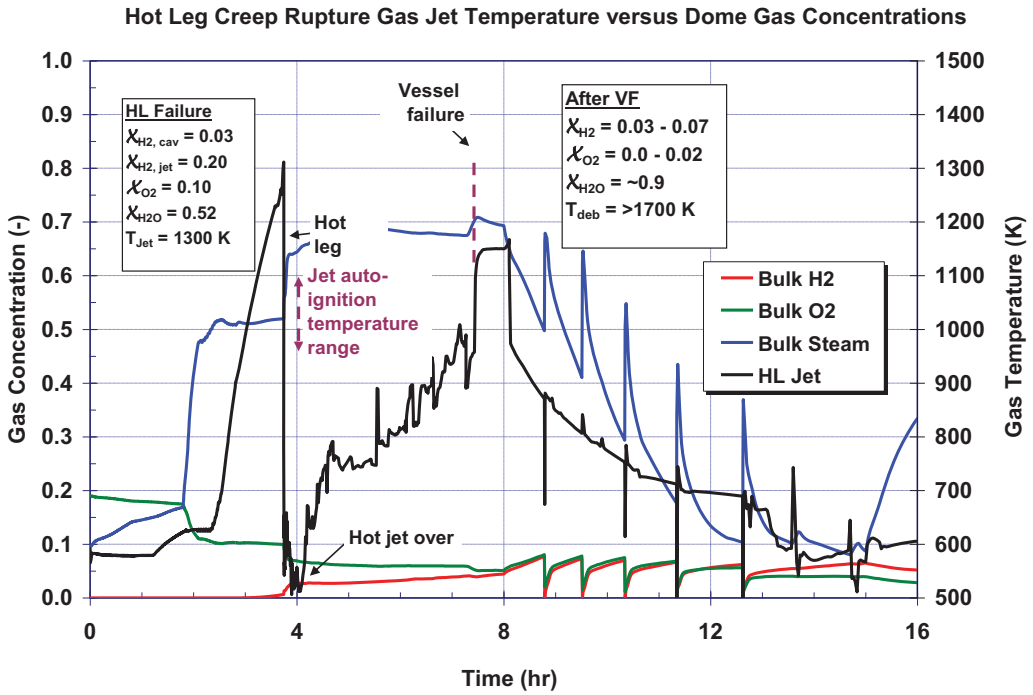

Figure 5-47 Comparison of the mitigated short-term station blackout containment dome gas concentration history and potential ignition source temperature

For the regions outside the cavity (i.e., characterized by the dome region in Figure 5-47), the response was similar to the cavity at hot leg failure. A high temperature, hydrogen-rich gas jet exited into the dome for a short period until the accumulators discharged. Hence, ignition is likely in the dome within the jet. However, as shown in both the cavity and dome figures, the steam concentration rapidly increased to inerting conditions (i.e., χ_{steam}>55%) once the accumulators discharged. Subsequently, the debris exiting the vessel after vessel failure could entrain hot debris particles and small aerosols outside the cavity or a burn in the cavity could propagate into the surrounding regions. As indicated in Figure 5-47, the hydrogen concentration is above the default ignition criterion when an ignition source is present (i.e., >7%). However, the oxygen concentration is low (i.e., below the default ignition criterion) and the steam concentration is high (i.e., above the default ignition criterion).

In summary, ignition would be expected at hot leg failure, which occurred. However, the amount of hydrogen available for combustion is limited at this phase of the accident and the pressurization during the burn was well below the pressure capacity of the containment. An ignition later than hot leg creep rupture failure (e.g., following vessel creep rupture failure, which is the next clear ignition source) is unlikely due to high steam inerting throughout the containment.

In the second facet of hydrogen uncertainty examined, the variability in the timing of the combustion was examined. The spray operation led to conditions where hydrogen combustion was possible (i.e., see multiple burns during the spray operation in Figure 5-45). However, the presence of a clear ignition source after hot leg failure is uncertain. Consequently, a sensitivity

case was run to investigate a delayed burn with a larger amount of hydrogen accumulation. In this case, three conservatisms were applied relative to the base case. First, all combustion in the containment was prevented until the emergency spray operation completed (i.e., ~15 hr). This includes preventing combustion at the time of hot leg failure when an ignition source is present. Second, ignition sources were assumed to be present in the containment at 15 hr, even though station blackout conditions existed. Third, ignition sources were activated simultaneously in all regions of the containment at 15 hr, which initiated burns without any propagation delay. The pressure response in the sensitivity case is shown in Figure 5-48. Due to robust circulation flows during spray operation, the hydrogen concentration was relatively uniform between 18-20% throughout the various regions in contamination. Following the specified deflagration at 15 hours, the peak pressure was 60 kPa (8.7 psi) above the containment pressure that would result in increased containment leakage (i.e., 779 kPa, 113 psi).

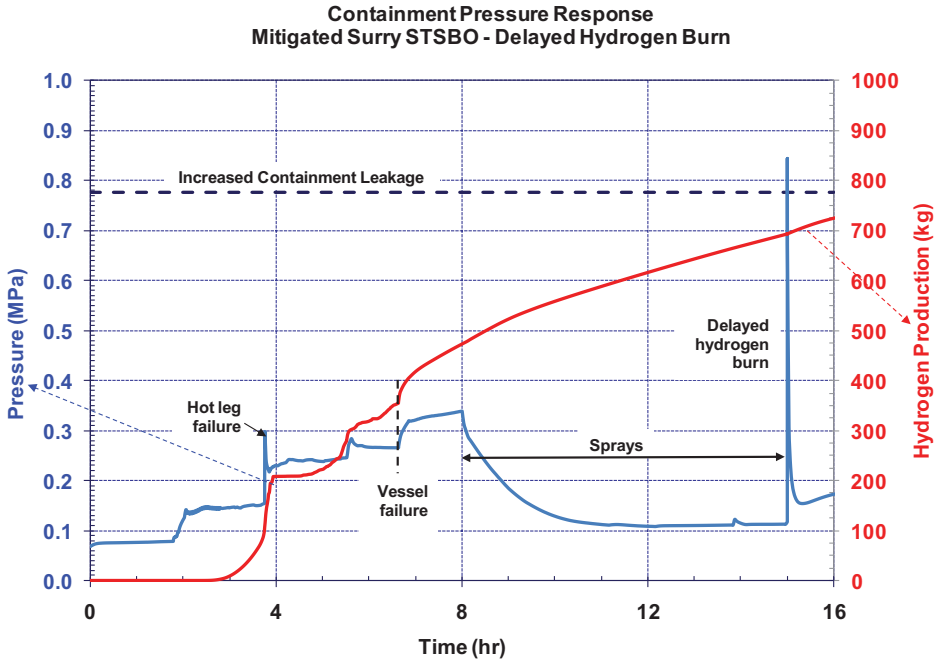

Figure 5-48 Mitigated short-term station blackout containment pressure history for the sensitivity calculation with delayed ignition

In the sensitivity calculation, MELCOR's default deflagration model considers the relative gas concentrations and the overall geometry for a best-estimate calculation. It not only includes combustion of hydrogen, but also combustion of carbon monoxide from the ex-vessel core-concrete interactions. The conditions at the start of the burn at 15 hours are shown in Table 5-7.

Table 5-7 Containment conditions at start of hydrogen and carbon monoxide burn

Condition in the Containment Dome	Value
Pressure	118.2 kPa
Temperature	314 K
Hydrogen mole fraction	19.0%
Carbon monoxide mole fraction	14.6%
Steam mole fraction	4.5%
Oxygen mole fraction	12.7%
Nitrogen mole fraction	49.2%

As shown in Figure 5-49, the combined concentration of the hydrogen and carbon monoxide exceeded the stoichiometric amount of oxygen after 10.3 hours. Hence, the deflagration was oxygen limited. Since the heat of combustion of hydrogen with oxygen and carbon dioxide with oxygen is approximately the same, any additional hydrogen gas generation would not substantially change the maximum peak pressure from deflagration.

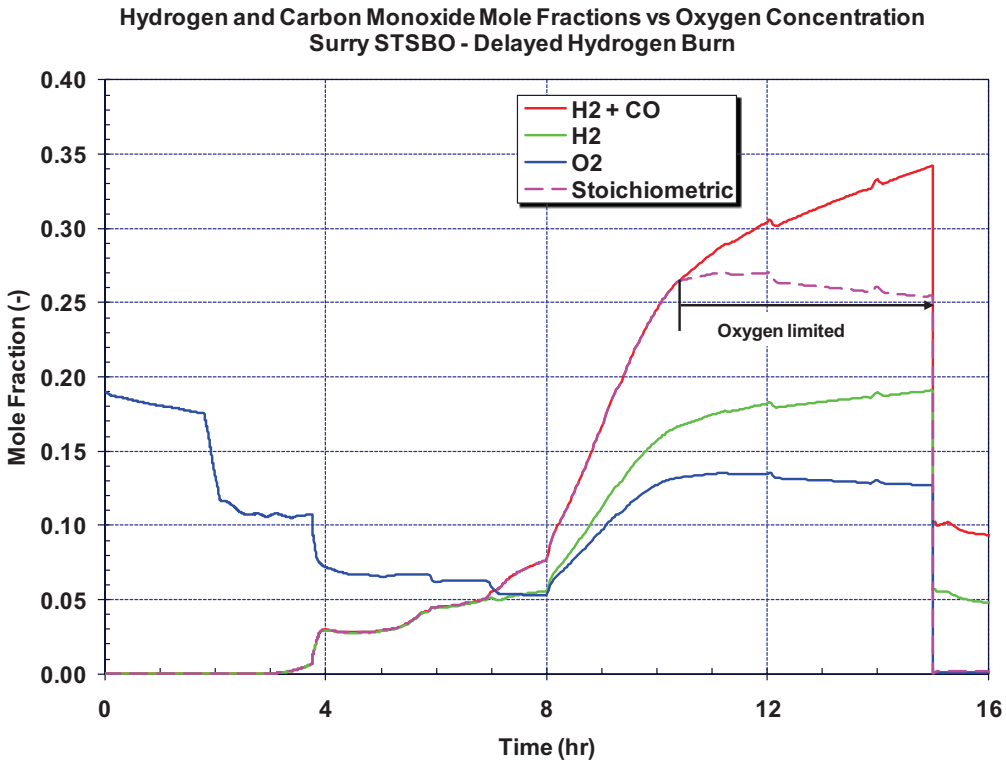

Figure 5-49 Mitigated short-term station blackout containment dome gas concentrations versus stoichiometric

A set of six other delayed burn sensitivity calculation were performed. In addition to delaying combustion until 15 hours, additional sensitivity cases were performed delaying combustion to 9.5 and 11.5 hours. As described earlier, a hydrogen burn due to jet auto-ignition following the hot leg failure and then further burns were suppressed until 9.5, 11.5, and 15 hours. These

calculations were performed to investigate the benefit of pre-burning some of the hydrogen at a low concentration. Finally, a sensitivity case was calculated with the spray initiation and termination occurring 2 hours earlier (i.e., the emergency sprays ran from 6 hr to 13 hr). the hydrogen burn was delayed until 13 hr. in all the delayed combustion sensitivity calculations, ignition source was simultaneously applied at the control volumes at the specified time.

The containment pressure histories for all the delayed combustion sensitivity calculations are shown in Figure 5-50. Only the cases where combustion was delayed to the end of the spray operation (i.e., 15 hours, or 13 hours in the 6 hr start case) was the pressure criterion for increased leakage exceeded.[31] Hence, three of the sensitivity cases resulted in increased containment leakage and four cases remained below the failure pressure criterion through 24 hours. The resultant environmental source term of cesium and iodine are summarized in Figure 5-51 and Figure 5-52, respectively. Through 24 hr, the cesium and iodine environmental source terms were very small (i.e., <0.01%). It is difficult to distinguish the nominal leakage from cases with increased containment leakage from the cases with some increased leakage. In summary, the containment sprays were very effective at reducing the source term and the driving pressure leakage. The negative consequences of possible burns due to a spray operation were offset by the scrubbing of containment sprays.

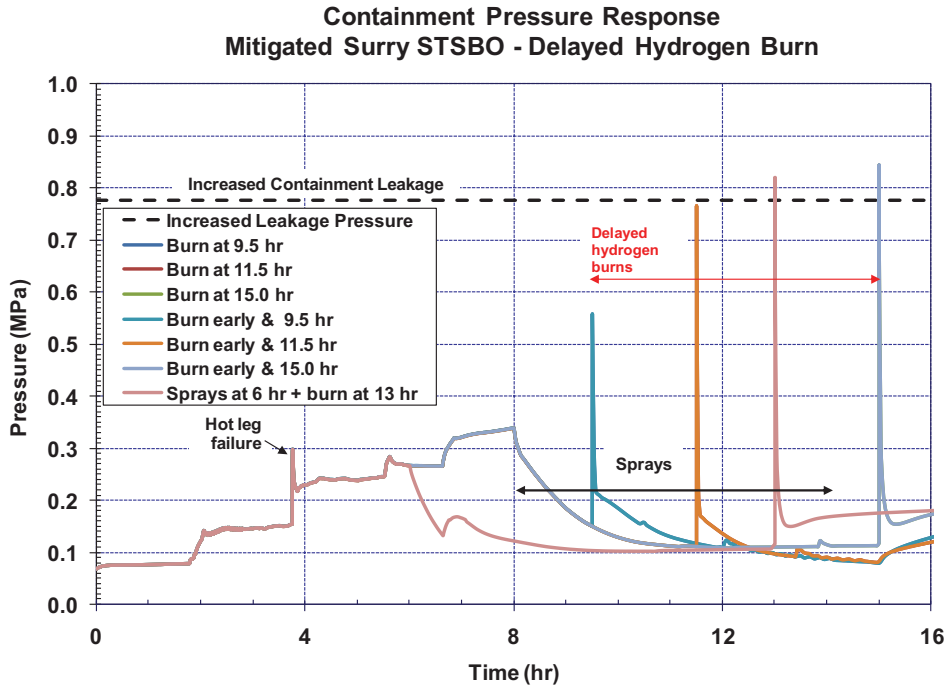

Figure 5-50 Comparison of the containment pressure responses for the sensitivity calculations with delayed ignition

[31] Although Figure 5-49 shows the containment dome exceeds the stochiometric concentration of oxygen by 10.3 hours, the combustible gas concentration in the lower reigons of the containment was still increasing until 15 hours. Hence, a larger and more uniform burn occurred.

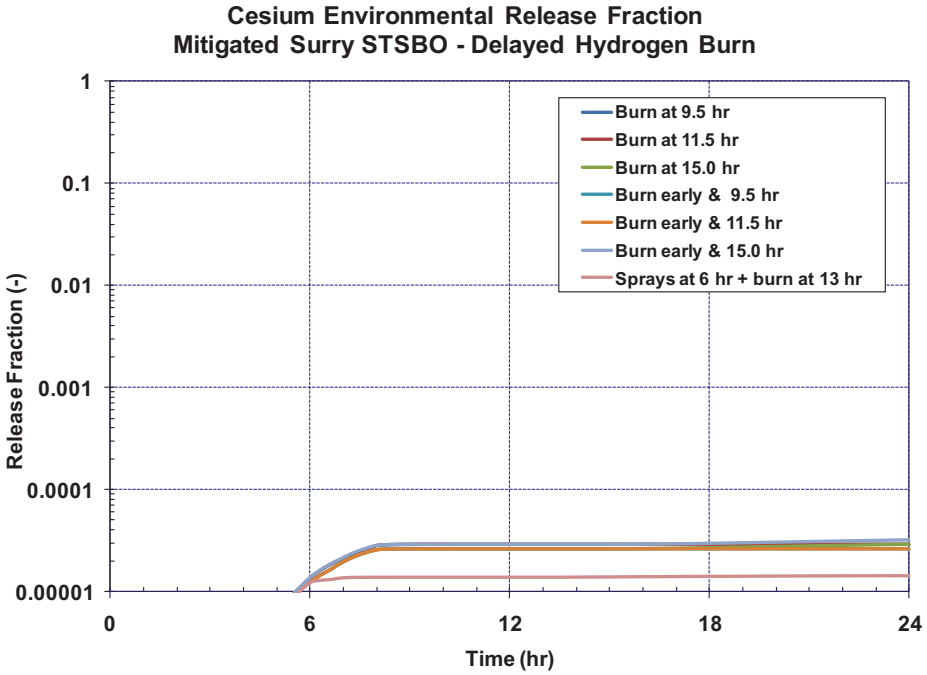

Figure 5-51 Comparison of the cesium release to the environment for the sensitivity calculations with delayed ignition

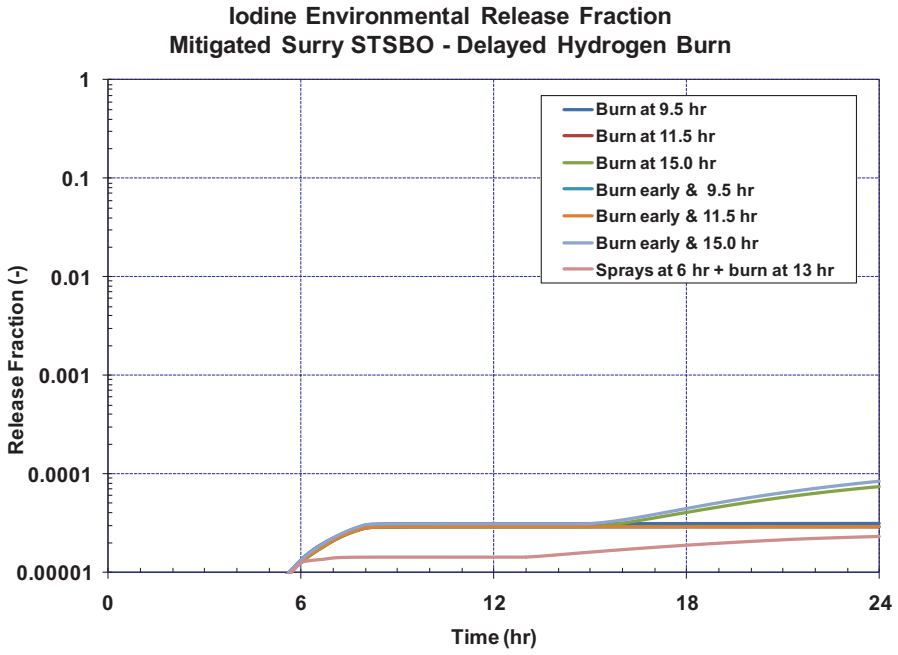

Figure 5-52 Comparison of the iodine release to the environment for the sensitivity calculations with delayed ignition

To confirm the MELCOR estimate of peak pressure, the adiabatic, isochoric, complete combustion (AICC) pressure was calculated [31]. The complete combustion assumption refers to the participation of the reactants only (i.e., hydrogen, carbon monoxide, oxygen). Some small fraction of the fuel will always exist in equilibrium with the combustion products. The AICC assumptions result in the highest possible equilibrium pressures. Inclusion of best-estimate heat transfer, volume expansion, and incomplete combustion will result in lower pressures (e.g., the default MELCOR combustion model). If the AICC process assumptions are met, then at equilibrium, simple deflagrations, accelerated flames, and detonations reach the same final AICC pressure.[32] A number of hydrogen deflagration and detonation studies were conducted as part of this analysis. Delayed hydrogen deflagration and detonation were shown to be a threat to containment integrity.

Figure 5-53 shows the bulk hydrogen and oxygen concentrations in the containment. At 15 hr, the peak hydrogen concentration was ~20% and the peak oxygen concentration was 12%. The AICC pressure for a 20% hydrogen concentration shown in Figure 5-54. The peak pressure was just slightly below the containment pressure that would result in increased containment leakage. However, since both hydrogen and carbon monoxide were present in the containment, the maximum equivalent hydrogen concentration for stoichiometric burn for the available oxygen would be a 24% hydrogen concentration. The peak AICC pressure from a 24% equivalent hydrogen concentration was slightly above the containment pressure that would result in increased containment leakage and approximately equal to the peak pressure calculated in the MELCOR delayed burn sensitivity calculation.

[32] The difference between deflagrations and detonations in a confined volume is the transient pressure-time histories between ignition and final equilibrium.

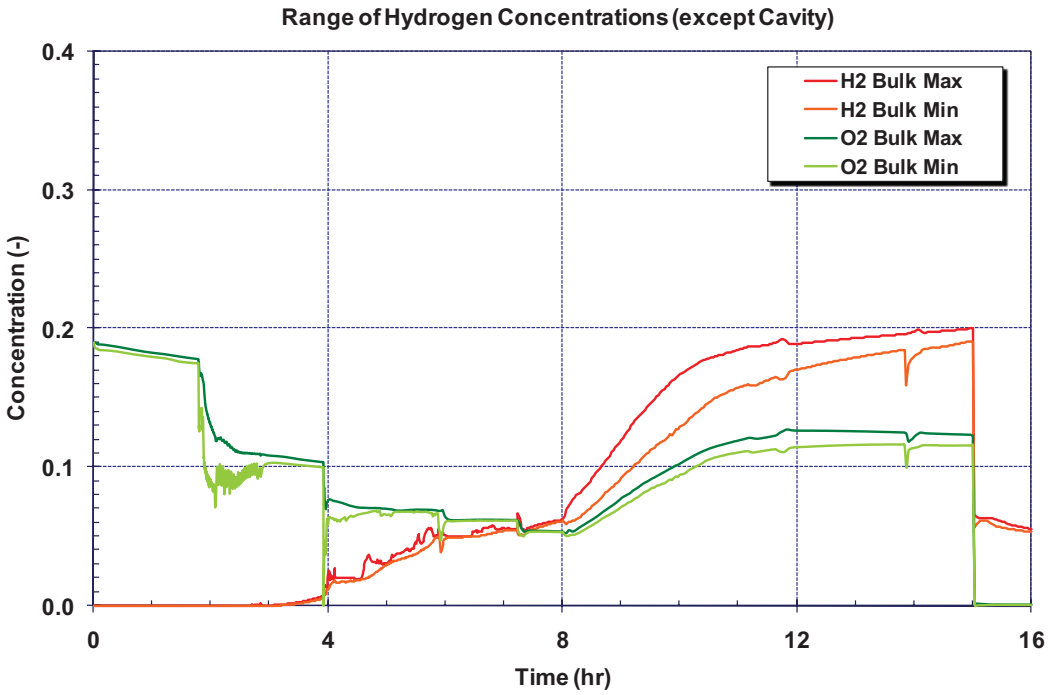

Figure 5-53 Mitigated short-term station blackout containment gas concentration history for the sensitivity calculation with delayed ignition

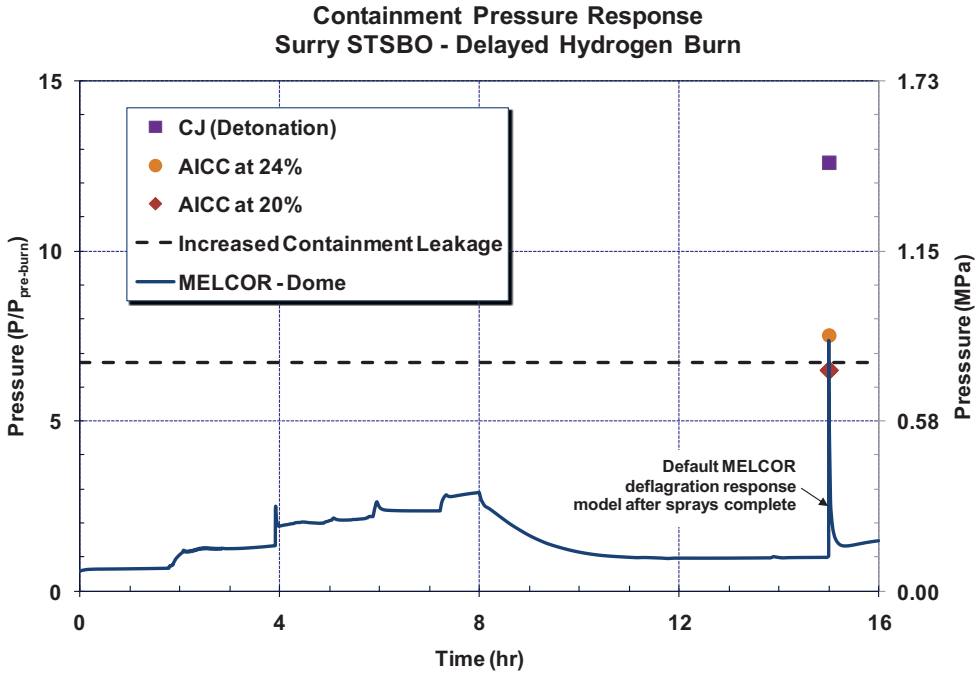

Figure 5-54 Mitigated short-term station blackout containment pressure history for the sensitivity calculation with delayed ignition

The potential for a detonation event was also raised by the peer review committee. While the dynamics pressure of a freely propagating detonation would exceed the equilibrium AICC pressure, this dynamic pressure load may not be large enough to damage a reinforced concrete containment. The detonation pressure can be estimated using the Chapman-Jouguet (CJ) model [32]. The CJ model is derived from conservation of mass, momentum, and energy across a one-dimensional flow discontinuity. The shock wave is assumed to be sonic. It is known that gaseous detonation waves are three-dimensional and are not discontinuously thin. However, the CJ model predicts the measured detonation pressure within about 15%. The CJ pressure represents the one-dimensional average of the actual pressure in a detonation wave. At 15 hours, the CJ pressure ratio (i.e., $P_{cj}/P_{pre\text{-}burn}$, or the peak detonation pressure divided by the pre-burn pressure) was calculated to be 12.5, or slightly less than twice the AICC pressure. Consequently, a detonation would momentarily exceed the pressure which increased containment leakage would be predicted for a static load. As stated above, the final equilibrium pressure following the detonation wave is the AICC pressure.

To assess the impact of the increased containment leakage from an earlier combustion event, the timing of the burn and the benefits of the emergency spray airborne radionuclide scrubbing should be simultaneously considered. Figure 5-55 shows the airborne concentration of cesium and iodine aerosols as a function of the containment hydrogen concentration. Following the actuation of the sprays, the airborne aerosol mass decreases rapidly. Before the hydrogen concentration reaches a quantity that, if combusted, could result in increased containment leakage, there is a negligible mass of airborne aerosols for release.

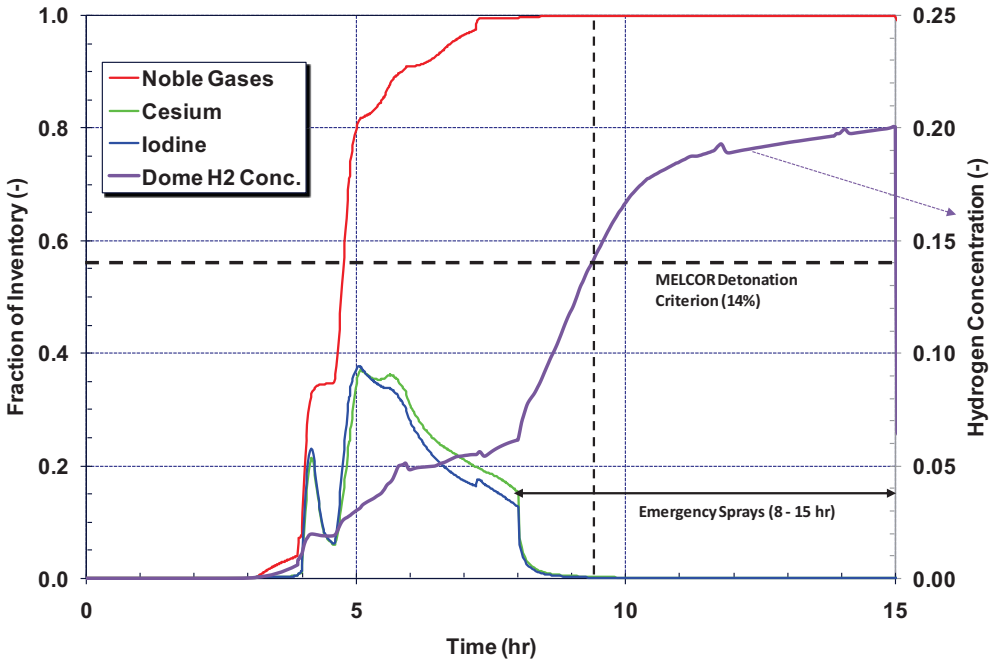

Figure 5-55 Mitigated short-term station blackout containment airborne radionuclide history versus hydrogen concentrations for the sensitivity calculation with delayed ignition

In summary, spray operation for an extended period with no early deflagration is needed to achieve a combustible or detonable mixture potentially capable of causing increased containment leakage. However, if ignition is delayed until the spray termination (i.e., 15 hours, then both MELCOR and the AICC model predict a peak pressure above the containment pressure criterion for increased leakage. Similarly, the CJ model was used to estimate the detonation pressure. The peak pressure predicted by the CJ model is approximately twice as large as the AICC value. The precise criteria for detonation are difficult to determine. However, detonations have been experimentally achieved at hydrogen concentrations as low as 14%, then the release of fission products could occur as early as 9.3 hours. However, the sprays are effective at settling airborne aerosols before detonable quantities could be formed that could fail the containment. The resulting fission product release would consist of only noble gases and would not be expected to substantially increase the offsite health consequences relative to the base case calculation. The conditions that potentially lead to severe combustion or detonable events (i.e., emergency spray operation) also include enhanced scrubbing of the airborne aerosols, which minimizes the impact of increased containment leakage due to a combustion event. Consequently, the best-estimate response reported in Section 5.2.2 is a reasonable representation of the source term for this scenario.

5.3 Short-Term Station Blackout with Thermally-Induced SGTR

The STSBO with thermally-induced SGTR scenario is assumed to be initiated by a large seismic event. Section 5.3.1 presents the results of an unmitigated scenario with no successful operator actions. For the mitigated scenario in Section 5.3.2, a portable emergency pump is connected to the containment spray system at 8 hours and available to inject 1,000,000 gallons.

The SOARCA sequences were selected based on screening criteria applied to SPAR evaluations for Surry. While hot leg rupture is generally predicted deterministically prior to thermally-induced SGTR (TI-SGTR), an induced tube rupture sequence was selected as a variant of the Surry STSBO analysis. The most significant competing challenges occur between hot leg (HL) creep rupture failure versus a TI-SGTR; the parameters that govern the timing of HL creep rupture relative to the TI-SGTR were examined. Section 5.3.3 examines the sensitivity of the timing of HL creep rupture failure to the TI-SGTR. NUREG/CR-6995 shows that a TI-SGTR is only likely if the reactor coolant pump seals do not fail and there is failure of the steam generator safety valves or the main steam isolation valve leaks to depressurize the secondary.

Based on the calculated MELCOR results, the requirement for other failures, and the extensive research in NUREG/CR-6995, high-pressure reactor pressure vessel failure was not included as representative accident signature for SOARCA. Based on many analyses of STSBO sequences, the lower head failure prior to hot leg failure is rarely if ever observed based on current best modeling practices. Based on a considerable number of analysis performed by the NRC in the context of the STGR integrity studies (i.e., see NUREG/CR-6995), it has been a consistent finding that HL creep rupture precedes lower head failure by a significant margin. It is recognized that the lower head failure at high pressure may retain some residual low likelihood in current PRA practice; however, this is considered to be of such low likelihood that it should not be considered in the context of the SOARCA process for best estimate analysis.

A considerable amount of work has been done by the NRC analyzing the potential for thermally induced steam generator tube rupture (e.g., NUREG/CR-6995). The SOARCA project incorporated the findings from these studies to include the potential for TI-SGTR. Two cases were considered; a single tube rupture and two tubes. The failures were assumed to occur near the steam generator inlet plenum tube sheet where the high temperature stream enters the tube bundle. The one and two tube TI-SGTR cases showed interesting and divergent effects of enhancing oxidation and providing additional core cooling, respectively. It was assumed that the most vulnerable defect(s) was exposed to the highest temperature gas stream entering the steam generator. Since the high temperature stream cools rapidly as it flows through the steam generator, the timing of the failure for other locations would only decrease the timing between the subsequent HL creep rupture failure. It was believed that the SOARCA approach was conservative in this respect but could have benefitted from additional realism by considering inspection experience. Additional realism could be introduced by reviewing data from plant inspections to examine the location and magnitudes of defects. This data could be cross-correlated against the CFD work done by the NRC (i.e., NUREG-1788) against the likelihood of those tubes receiving the highest temperature flow stream from the inlet plenum.

5.3.1 Unmitigated Short-Term Station Blackout with Thermally-Induced Steam Generator Tube Rupture

Table 5-8 summarizes the timings of the key events for the unmitigated STSBO with a TI-SGTR scenarios. Unlike the unmitigated STSBO described in Section 5.2.1, either one (i.e., equivalent of 100% flow area) or two (i.e., equivalent of 200% flow area) steam generator tubes fail prior to any other RCS creep rupture failures along with a stuck open secondary safety relief valve. Consequently, there is a containment bypass pathway for fission products once the steam generator tubes fail. As described in Section 3.2, the accident scenario initiates with a complete loss of all onsite and offsite power. The reactor successfully trips and the containment isolates but all powered safety systems are unavailable. The timings of the key events are discussed further in Sections 5.3.1.1 and 5.3.1.2. Similar to the unmitigated STSBO, the fission product releases from the fuel do not begin until 2 hr 57 min. However, since a steam generator SRV sticks open at 3 hr and the tubes fail at 3 hr 33 min, fission product releases to the environment can begin earlier than the unmitigated STSBO described in Section 5.2.1 (i.e., 3 hr 33 min versus 25 hr 32 min). Two cases were performed to examine the sensitivity of the tube failure size to the magnitude of the fission product release to the environment and the potential for preventing hot leg creep rupture failure. Section 5.3.1.1 summarizes the thermal-hydraulic response of the reactor and containment while Section 5.3.1.2 summarizes the associated radionuclide release from the fuel to the environment.

Table 5-8 Timing of key events for unmitigated STSBO TI-SGTR

Event Description	100% TI-SGTR Time (hh:mm)	200% TI-SGTR Time (hh:mm)
Station blackout – loss of all onsite and offsite AC and DC power MSIVs close Reactor trip RCP seal leak at 21 gpm/pump TD-AFW fails	00:00	00:00
First SG SRV opening	00:03	00:03
SG dryout	01:14	01:14
Pressurizer SRV opens	01:27	01:27
PRT failure	01:47	01:47
Start of fuel heatup	02:19	02:19
RCP seal failures	02:46	02:46
First fission product gap releases	02:57	02:57
Stuck open SG SRV	03:00	03:00
SGTR	03:33	03:33
Creep rupture failure of the Loop C hot leg nozzle	03:47	03:49
Accumulator discharges	03:47	03:49
Accumulator empty	03:47	03:49
Vessel lower head failure by creep rupture	07:30	06:51
Debris discharge to reactor cavity	07:30	06:51
Cavity dryout	07:54	07:21
Containment at design pressure (45 psig)	12:34	13:36
Start of increased leakage of containment ($P/P_{design} = 2.18$)	27.54	30:14
Containment pressure stops decreasing	40:18	40:20

5.3.1.1 Thermal-hydraulic Response

The responses of the primary and secondary pressure systems are shown in Figure 5-56 for the 100% and 200% TI-SGTR cases. The initial response through 3 hr is identical to the unmitigated STSBO (see Section 5.2.1). At 3 hr, a safety valve on steam generator C (SG-C) fails open.[33] SG-C subsequently depressurizes to near atmospheric conditions and creates a large

[33] The valve failure was a specified boundary condition to develop a high differential pressure drop across the steam generator tubes and a direct bypass flow path to the environment. The valve failure occurred after the majority of

differential pressure across the steam generator tubes. During the core damage phase, hot gases circulate through the steam generator and increase the thermal stress across the tubes. The equivalent of a 100% or 200% tube area failure occurs at 3 hr and 33 min (see Figure 5-57), or about 12 min before the previously predicted creep rupture failure of the hot leg in the unmitigated STSBO (see Section 5.2.1). The combination of the TI-SGTR and the leakage through the failed RCP seals (2 hr and 45 min) causes a slow depressurization of the primary system. At 3 hr 45 min and 3 hr 47 min, respectively for the 100% and 200% TI-SGTR cases, the hot leg nozzle also fails due to a thermally-induced creep rupture. The failure of the hot leg nozzle leads to a rapid depressurization of the primary system and injection of the accumulator water. Following the depressurization of the RCS, the TI-SGTR flowrate drops to <0.2 kg/s through vessel failure at 7 hr 30 min and 6 hr 61 min, for the 100% and 200% TI-SGTR cases respectively.

There were some differences in the timing of events for the 100% versus the 200% TI-SGTR cases following the opening of the TI-SGTR. As shown in Figure 5-57, the flowrate through the 200% tube rupture case was approximately twice as large as the flow through the 100% tube rupture case. The net effect was: (a) increased heat removal from the core (see Figure 5-58), (b) a higher flow of gas past the hot leg nozzle, (c) a reduction in the zirconium oxidation rate in the 200% case (see Figure 5-59), and (d) a slightly faster depressurization rate in the 200% case versus the 100% case. The first two effects increased the heat flow past hot leg nozzle while the second two effects reduced the core exit temperature and the mechanical stress across the hot leg nozzle. The net effect was a slightly later hot leg creep rupture failure in the 200% case relative to the 100% case. Hence, the 100% case represented a condition that enhanced the core rate oxidation and accelerated core damage whereas the 200% case increased core cooling and decreased oxidation.

The vessel water level is shown in Figure 5-60. In response to flow out of the pressurizer safety relief valve, the pump seal leakage, and leakage flow through the TI-SGTR, the vessel water level drops into the core and uncovers the fuel. The fuel heatup leads to a natural circulation phase that fails a steam generator tube(s) and eventually a hot leg nozzle creep rupture failure. The RCS pressure drops rapidly once the hot leg nozzle fails and the accumulators dump to refill the core with water. As discussed above, the timing to the RCS hot leg failure is not significantly different between the 100% and 200% cases.

Prior to the quench of the fuel by the accumulator water, the 100% case had more oxidation than the 200% case. Hence, the oxide layer thickness and potential for further oxidation following the core accumulator reflood was lower in 100% case than the 200% case. As shown in Figure 5-61, the zirconium cladding in the 200% case oxidizes at a higher rate than the 100% following the hot leg failure. Due to higher oxidation power in the 200% case in the post-reflood phase, the fuel degradation, the debris relocation to the lower head, and the failure of the vessel occurred faster in the 200% case. The fuel relocated to the lower plenum at 6.5 hr and 6 hr in the 100% and 200% cases, respectively. The vessel failure occurred at 7 hr 30 min and 6 hr 51 min in the 100% and 200% cases, respectively (see Figure 5-62).

---

the safety valve cycles but before the predicted time of the hot leg failure (i.e., to promote a steam generator tube failure).

Following vessel failure, the debris dropped into the reactor cavity under the reactor vessel. The hot debris immediately boiled away the water in the reactor cavity and started to ablate the concrete. The ex-vessel core-concrete interactions (CCI) continued for the remainder of the calculation, which generated non-condensable gases. In addition, the hot gases exiting the reactor cavity and the radioactive heating from settled fission products steadily evaporated the water on the containment floor outside the reactor cavity from the time of vessel failure to 1.7 days (i.e., 41 hr in both cases). The resultant non-condensable and steam production pressurized the containment (see Figure 5-63). However, due to the TI-SGTR, there was a leakage pathway from the containment through the vessel. The TI-SGTR slowed the pressurization of the containment relative to the unmitigated STSBO. Due to the larger TI-SGTR leakage area in the 200% case, the containment failure area in the 200% case was smaller than the 100% case (see relative leakage areas in Figure 5-64). In both cases, the containment continued to pressurize until the leakage flow balanced the steam and non-condensable gas generation. Hence, the containment failure leakage area increased in each case until the sum of the TI-SGTR and containment failure leakage areas balanced the gas generation. By 44 hr, all the water on the floor was evaporated and the steam generation stopped. The containment depressurized thereafter without any steam generation.

The conservatively assumed containment failure location was around the equipment hatch, which is located on the side of the containment without a surrounding building (e.g., the auxiliary or safeguards buildings); other location, such as personnel airlocks and penetrations, would result in lower releases due to transport and deposition inside adjacent buildings. Consequently, the fission products that leaked from the containment are released directly to the environment.

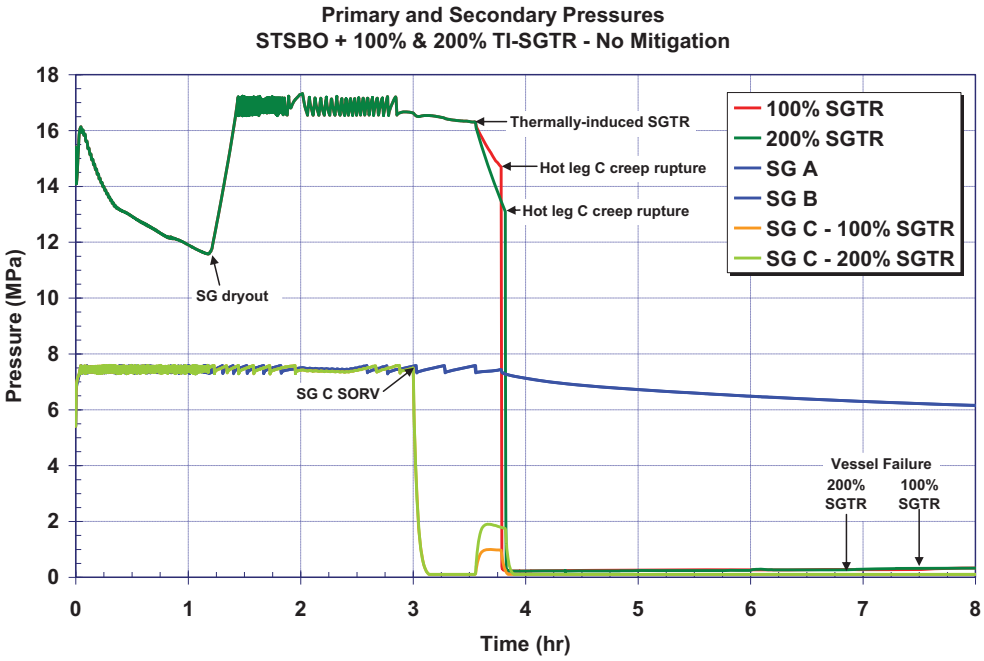

Figure 5-56 Unmitigated 100% and 200% TI-SGTR STSBO primary and secondary pressures histories

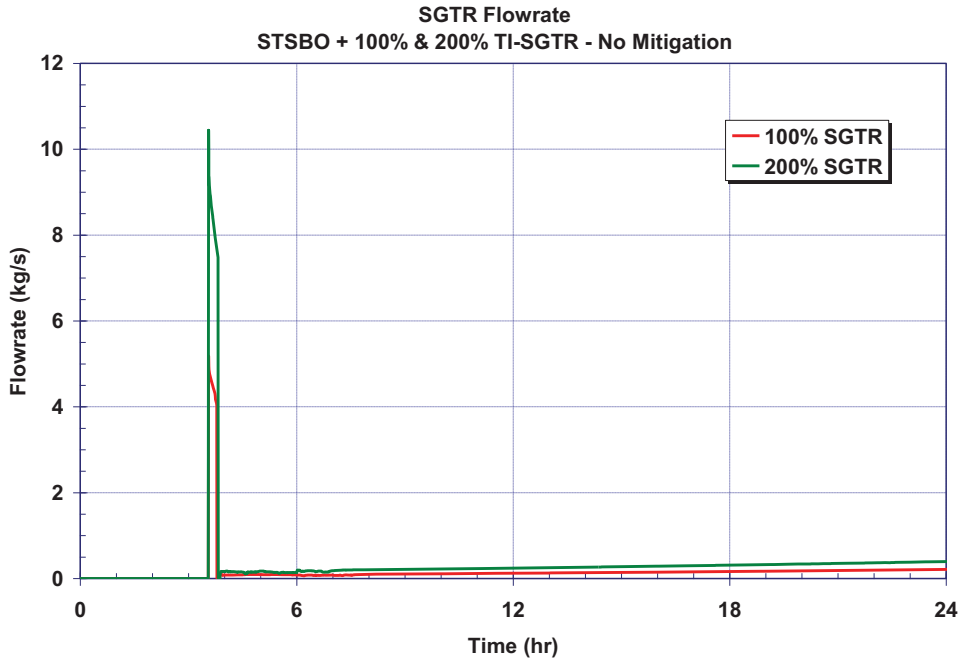

Figure 5-57 Unmitigated 100% and 200% TI-SGTR STSBO primary and TI-SGTR flowrate histories

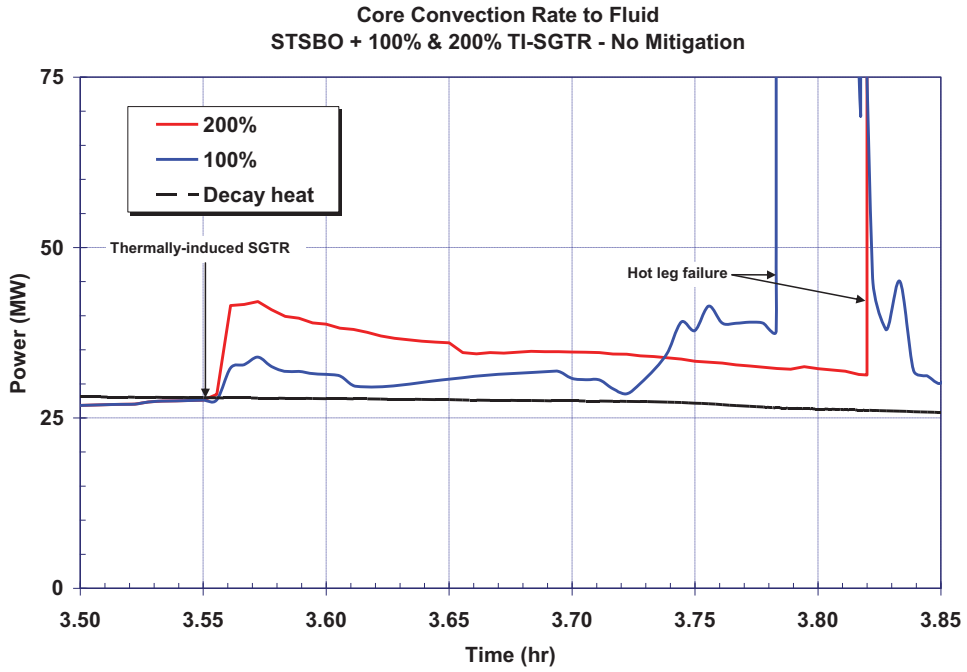

Figure 5-58 Unmitigated 100% and 200% TI-SGTR STSBO vessel convective heat removal rate from the fuel

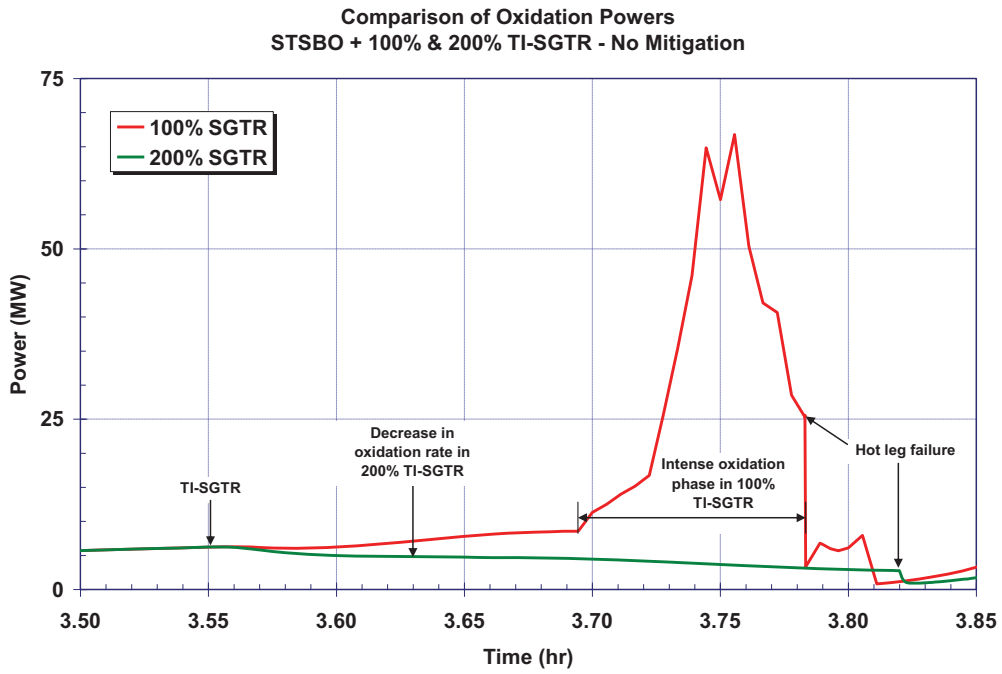

Figure 5-59 Unmitigated 100% and 200% TI-SGTR STSBO fuel oxidation power before the RCS hot leg failure

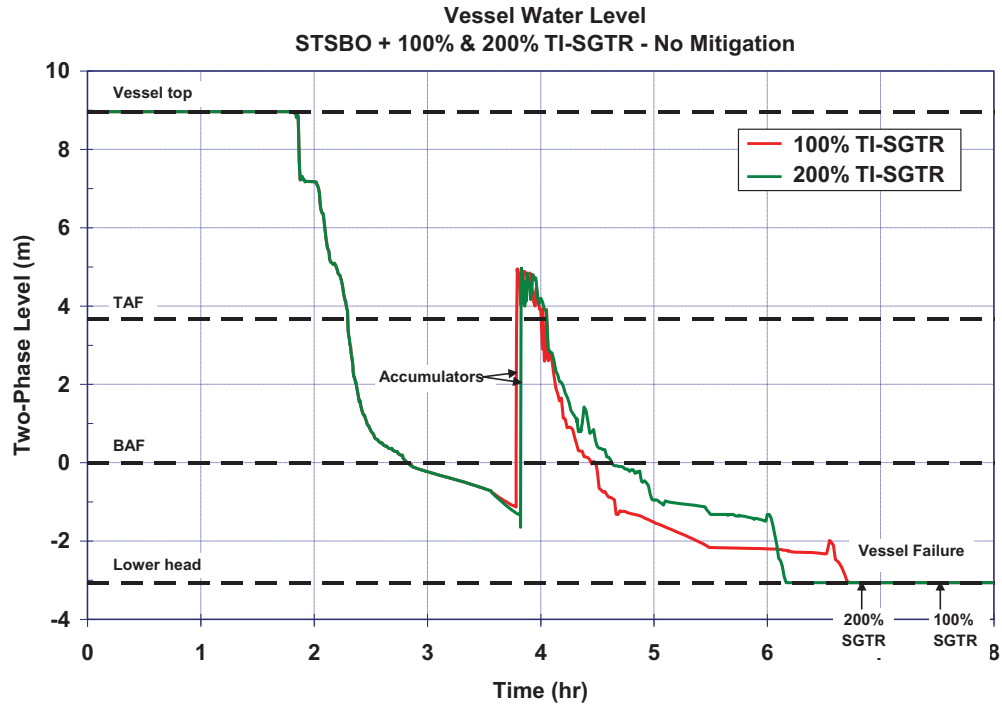

Figure 5-60 Unmitigated 100% and 200% TI-SGTR short-term station blackout vessel two-phase coolant level

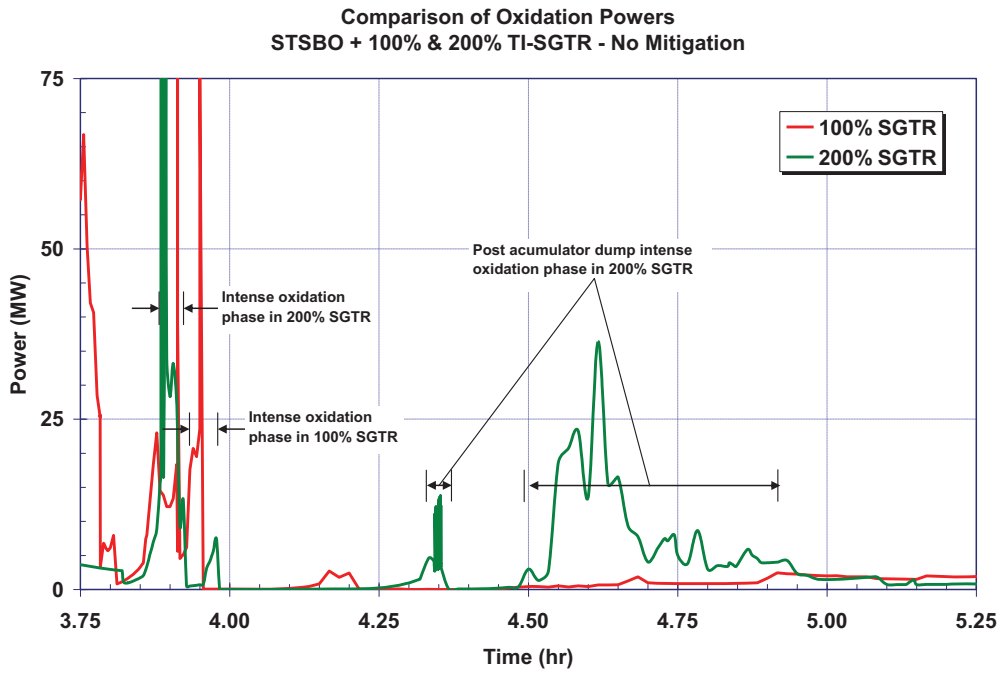

Figure 5-61 Unmitigated 100% and 200% TI-SGTR short-term station blackout fuel oxidation power after the RCS hot leg failure

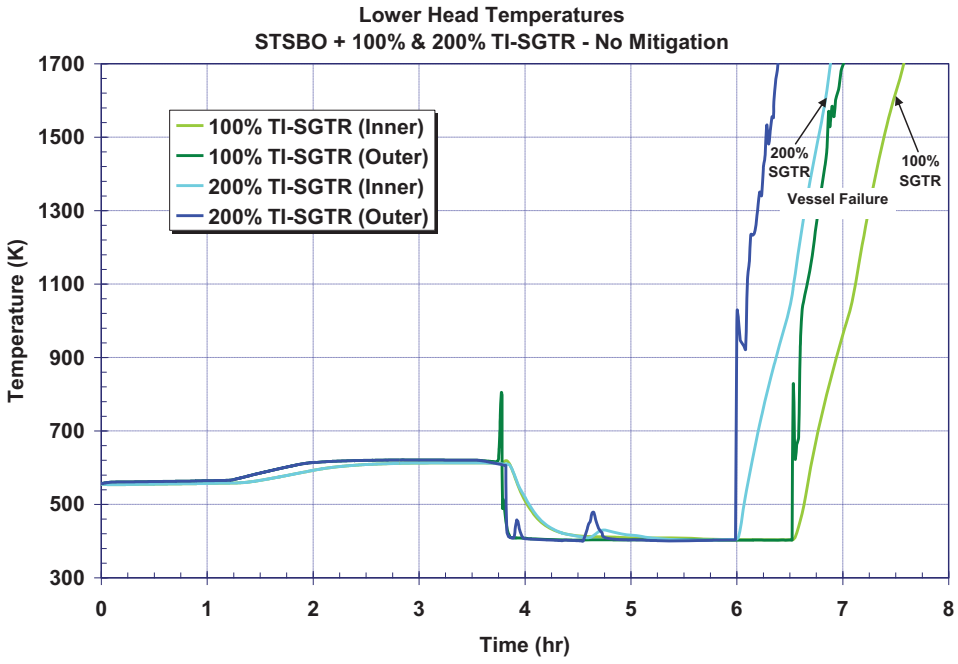

Figure 5-62 Unmitigated 100% and 200% TI-SGTR short-term station blackout lower head inner and outer temperature histories

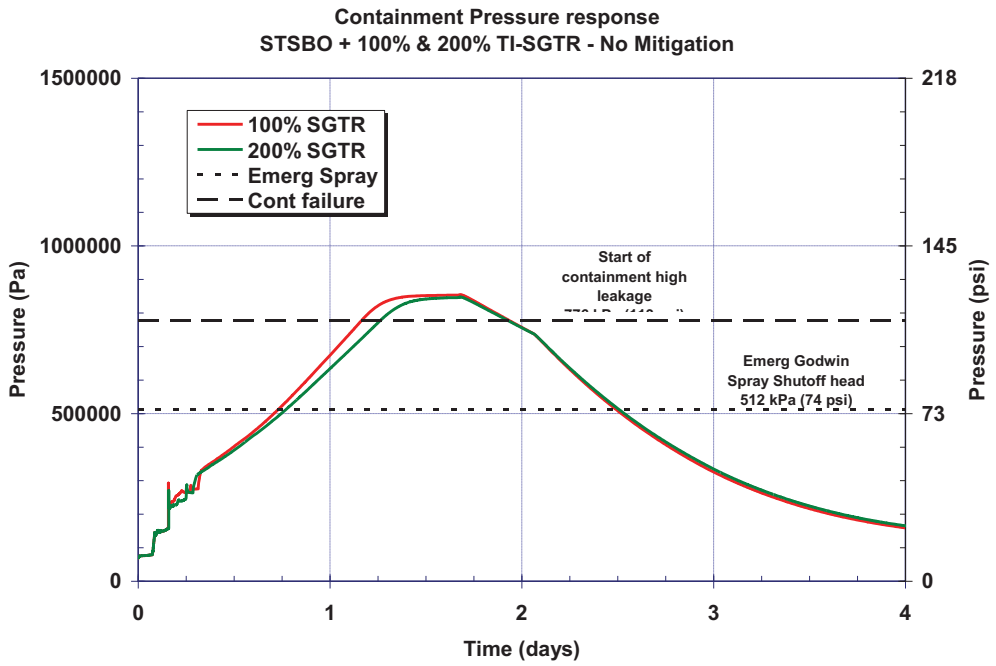

Figure 5-63 Unmitigated 100% and 200% TI-SGTR short-term station blackout containment pressure histories

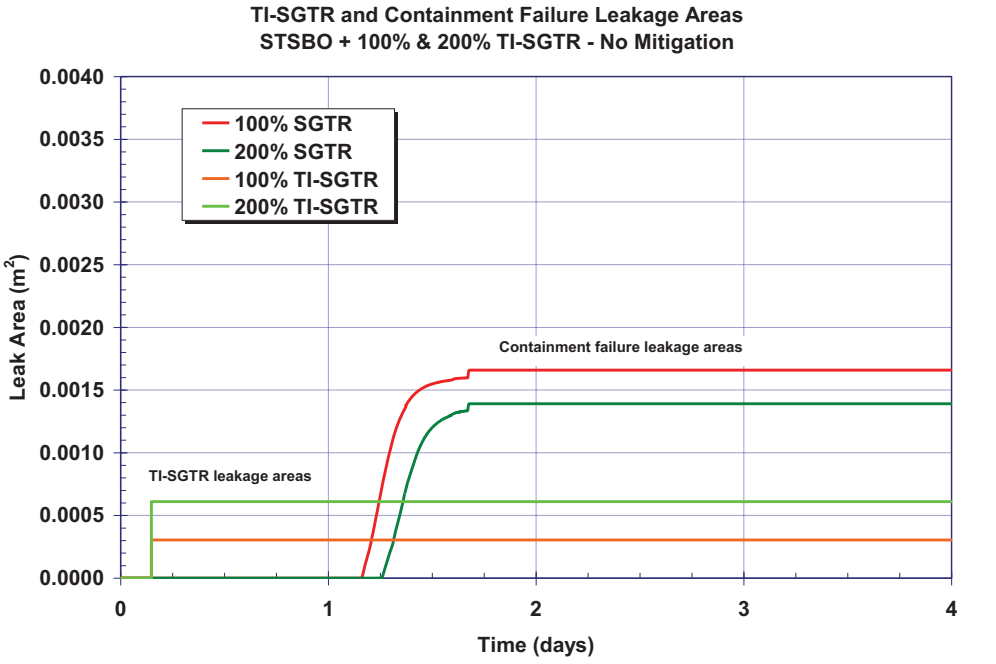

Figure 5-64 Unmitigated 100% and 200% TI-SGTR short-term station blackout containment and TI-SGTR leakage areas

5.3.1.2 Radionuclide Release

The fission product releases from the fuel started following the first thermal-mechanical failure of the fuel cladding in the hottest rods at 2 hr 57 min, or 38 min after the uncovery of the top of

the fuel rods. At 3 hr, the secondary safety relief valve on SG-C sticks open and allows the steam generator to depressurize to near atmospheric conditions. Prior to the TI-SGTR, any fission products leaving the RCS would flow out the pressurizer safety relief valve to the pressurizer relief tank in the containment. However, the PRT over-pressurized and failed prior to the start of the fission product releases. Hence, any fission products vented to the containment were not scrubbed in the PRT.

Due to the complete loss of all feedwater at the start of the calculation, the water inventory in the steam generators decreased very rapidly and was completely boiled away by 1 hr 16 min. Consequently, there is no water on the secondary side of the steam generator after the TI-SGTR at 3 hr 33 min. Furthermore, since the steam generator relief valve stuck open at 3 hr, the released fission products can flow directly out the failed generator tube and through the stuck open relief valve to the environment. The flow of fission products through the tube rupture into the steam generator is very complicated and beyond the current modeling capabilities in MELCOR. Several decontamination mechanisms such as: (a) impaction, vena contracta effects at the tube rupture, (b) deposition in bends, and (c) capture by the secondary side tube grid spacers are not addressed by the MELCOR aerosol deposition models. It was estimated from ARTIST tests that the steam generator aerosol decontamination in a full-scale steam generator would be between 4.7 and 9 [33]. The normal aerosol capture and settling models were disabled on the secondary side in MELCOR and the secondary side decontamination factor was prescribed to be seven (i.e., approximately the average of 4.7 and 9).

Figure 5-65 and Figure 5-66 show the fission product distributions of the iodine radionuclides for the 100% and 200% TI-SGTR cases, respectively. The basic trends of the two cases were similar. The resultant distribution of iodine was partitioned between the RCS (i.e., including the vessel and the primary side of the steam generator tubes), the secondary side of the steam generators, the containment, and the environment. During the high release phase of the accident, the iodine is simultaneously released to the containment via the pressurizer safety relief valve, the secondary side of the steam generator and the environment via the TI-SGTR, or retained in the RCS. At the time of the TI-SGTR at 3 hr 33 min (0.15 days), only 8.4% of the iodine had been released from the fuel. About 1% was discharged to the containment via the pressurizer safety relief valve with the 7.4% retained in the RCS.

Between the timing of the 100% TI-SGTR and vessel failure, 98% of the iodine was released with 80% in the containment, 15% retained in the RCS, 3.1% in the SG secondary, and 0.5% in the environment. The overall steam generator and steam line decontamination factor was ~7 (i.e., the specified value). Eighty percent of the iodine transported to the containment versus only 3.6% in the steam generator secondary or the environment. The numbers were similar for the 200% TI-SGTR case with 97% released, 80% in the containment, 10% in the RCS, 5.3% in the steam generator secondary, and 0.8% in the environment. Due to the larger leak rate through the TI-SGTR, the 200% case had about twice the environmental release by vessel failure. The trends are similar for cesium, which are shown in Figure 5-67 and Figure 5-68.

The flow rate through the TI-SGTR decreased rapidly following hot leg failure at ~3.8 hr (see Figure 5-57), which slowed the release of the fission products to the faulted steam generator. Subsequently, the fission products moved from the reactor coolant system via the TI-SGTR

rupture and the failed hot leg piping via natural circulation processes until the vessel lower head failure. As shown in Figure 5-65 through Figure 5-68, the releases to the containment or retention in the RCS increased most rapidly following hot leg failure. Prior to vessel failure, the fission product releases to the environment through the failed SGTR tube was roughly proportional to the size of the TI-SGTR leakage hole for the two cases (see Figure 5-69 and Figure 5-70).

After the lower head vessel failure, the releases to the environment for the 100% TI-SGTR were faster than the 200% case. By 4 days, the iodine releases to the environment were almost identical between the two cases (see Figure 5-69) and the cesium releases were much closer than at vessel failure (Figure 5-70). As shown in Figure 5-64, the TI-SGTR leakage areas were smaller than the containment leakage areas. However, the 100% TI-SGTR case needed a larger containment failure area to remove energy than the 200% case. Consequently, there was more leakage from the containment in the 100% TI-SGTR case than the 200% TI-SGTR case. Most of the releases through the TI-SGTR rupture were retained in the secondary side of the steam generator (i.e., a DF~7). In contrast, the fission products released through the containment failure went directly to the environment without any local retention or deposition in the leakage pathway through the tear in the containment wall. Since the 100% TI-SGTR case had more flow out the containment failure, the releases to the environment after the containment failure in the 100% case were higher than the 200% case. This non-intuitive trend eventually led to similar environmental releases for the two cases, which is evident in Figure 5-69 and Figure 5-70.

Finally, Figure 5-71 and Figure 5-72 summarize the releases of the radionuclides to the environment for the 100% and 200% cases, respectively. At 4 days, 95% of the noble gases, 4.2% of the molybdenum, 1.5% of the iodine, 0.7-0.8% of the cesium, 2.7% (100%) and 1.5% (200%) of the tellurium, and 0.2% of the barium had been released to the environment.

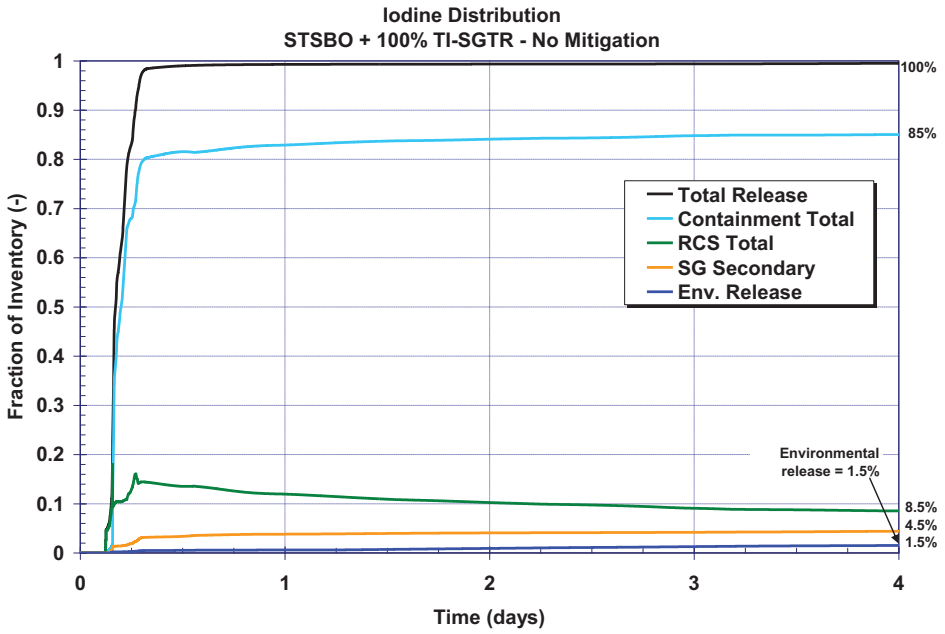

Figure 5-65 Unmitigated 100% TI-SGTR STSBO iodine fission product distribution history

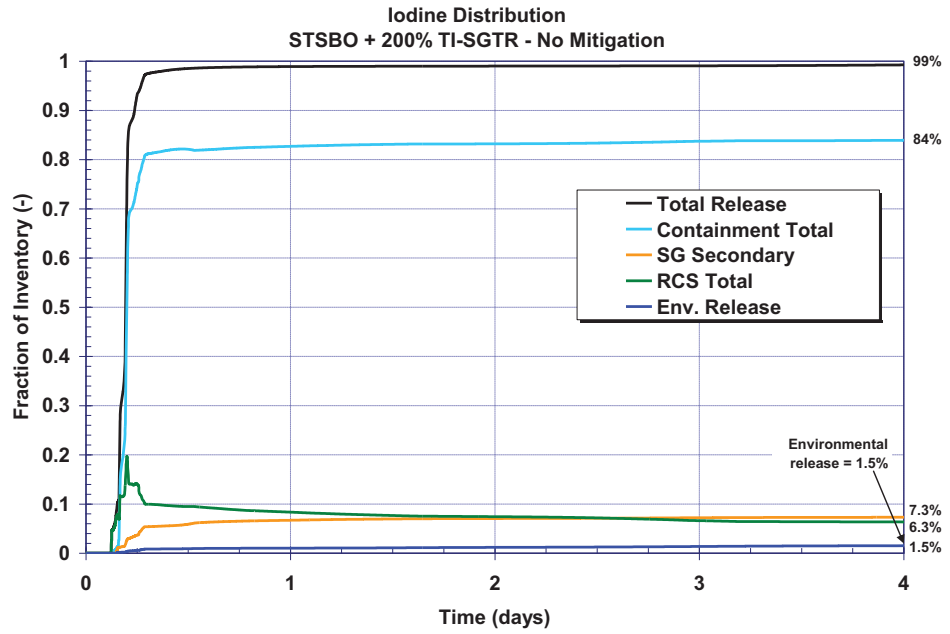

Figure 5-66 The unmitigated 200% TI-SGTR short-term station blackout iodine fission product distribution history

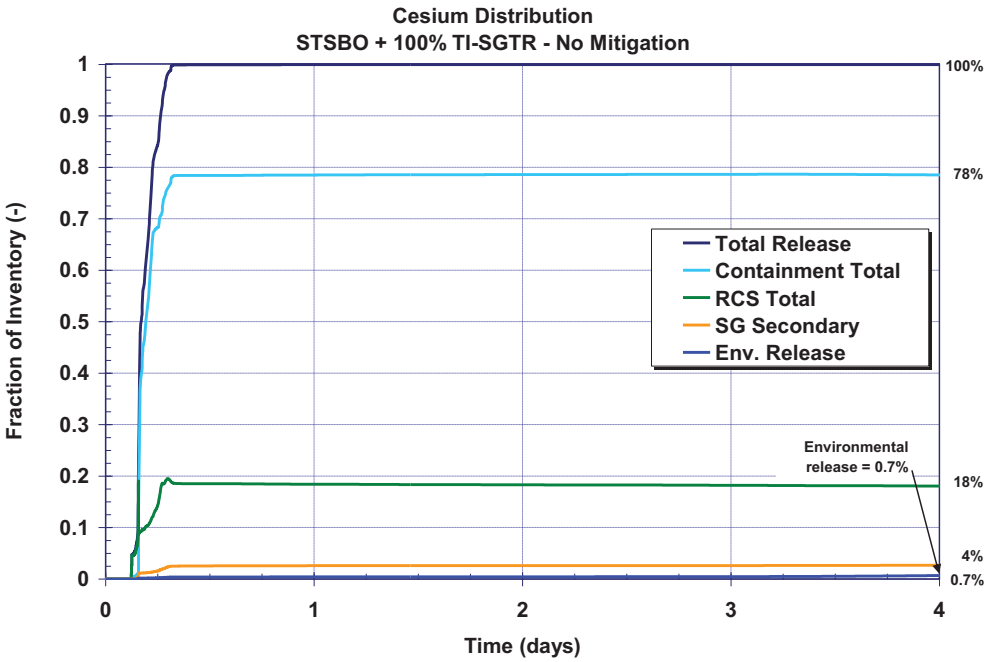

Figure 5-67 The unmitigated 100% TI-SGTR short-term station blackout cesium fission product distribution history

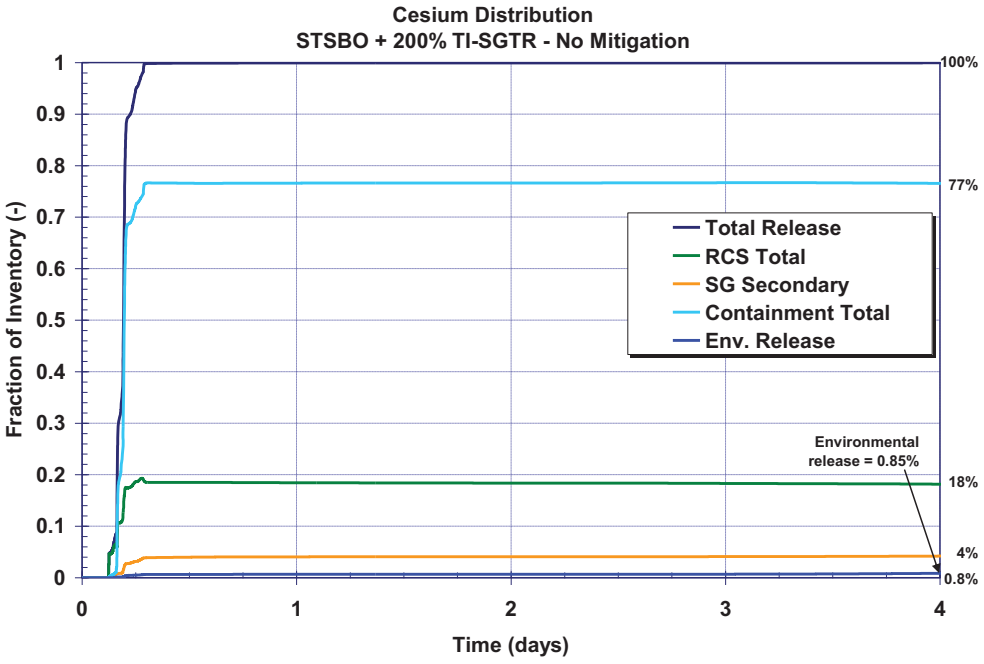

Figure 5-68 The unmitigated 200% TI-SGTR short-term station blackout cesium fission product distribution history

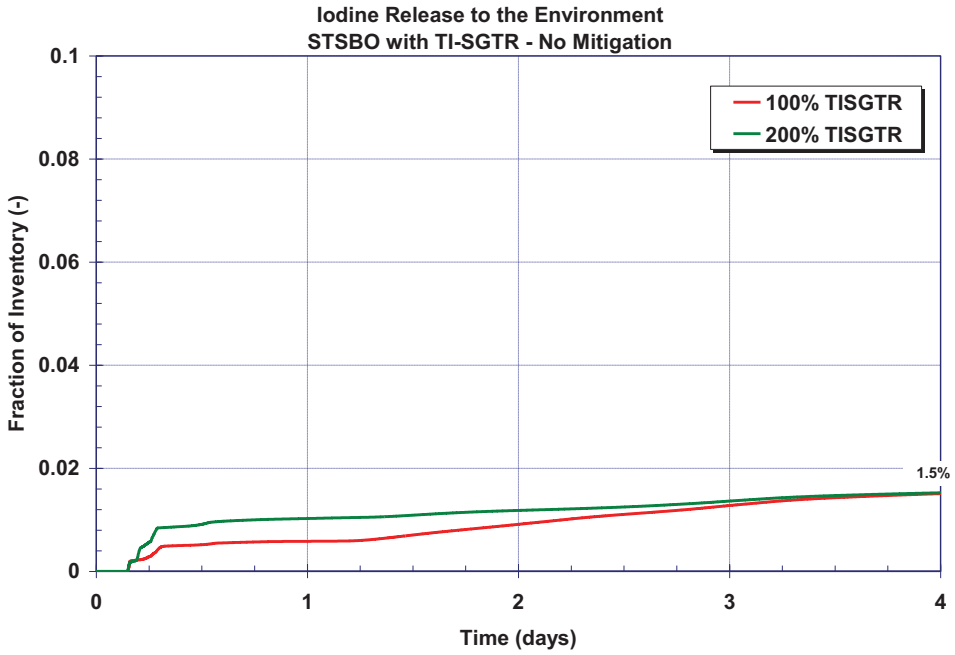

Figure 5-69 The unmitigated 100% and 200% TI-SGTR short-term station blackout iodine fission product distribution history

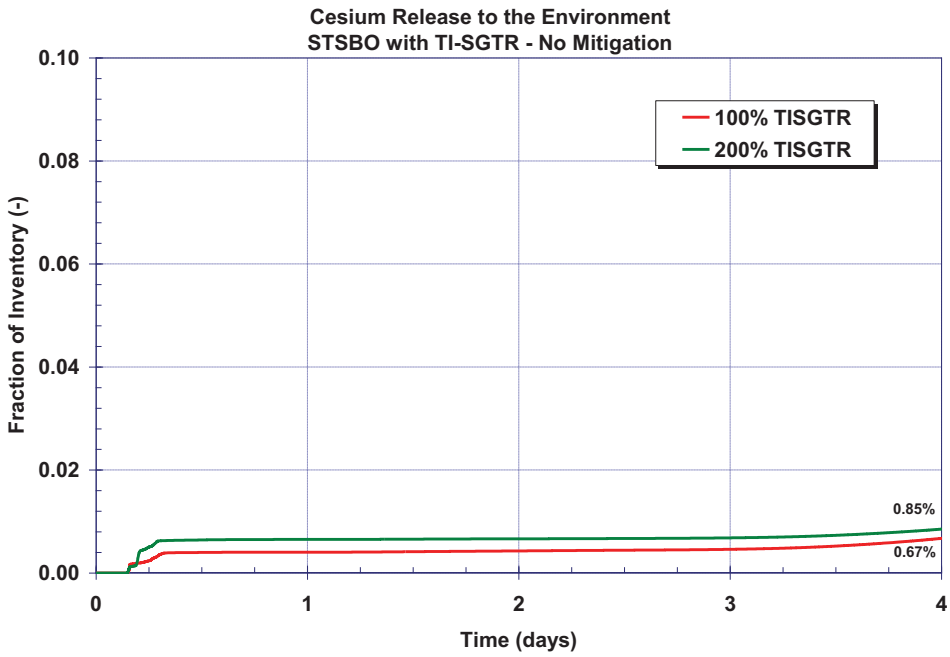

Figure 5-70 The unmitigated 100% and 200% TI-SGTR short-term station blackout cesium fission product distribution history

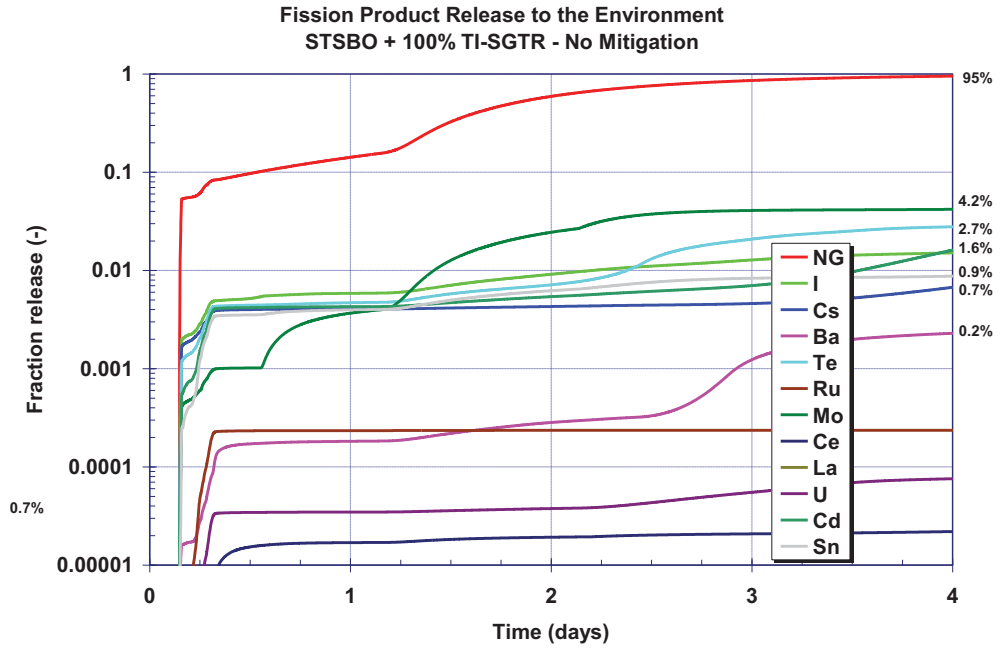

Figure 5-71 The unmitigated 100% TI-SGTR short-term station blackout environmental release history of all fission products

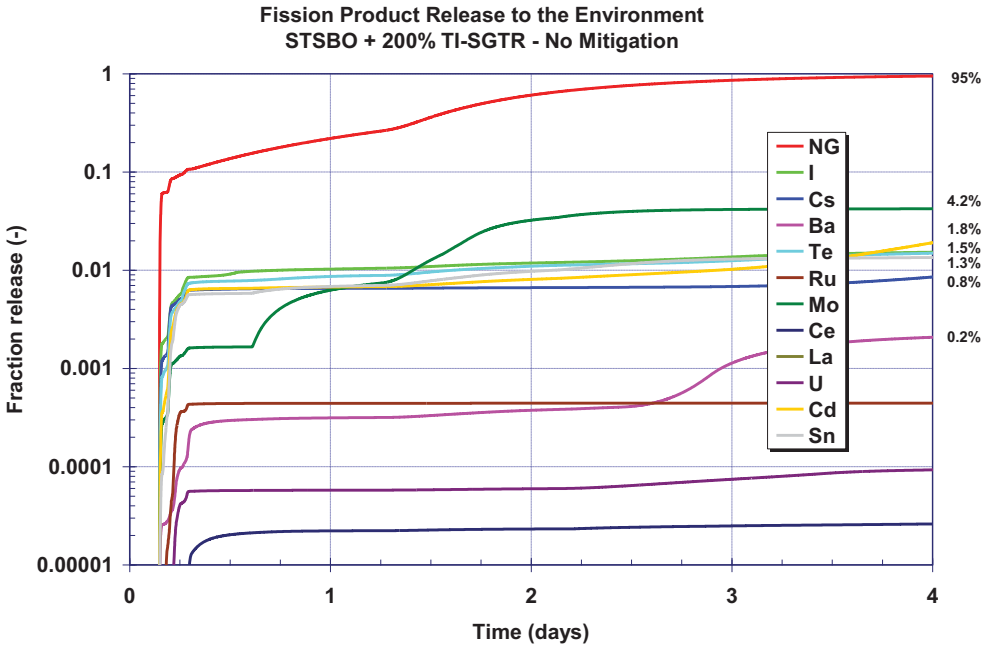

Figure 5-72 The unmitigated 200% TI-SGTR short-term station blackout environmental release history of all fission products

5.3.2 Mitigated Short-Term Station Blackout with Thermally Induced Steam Generator Tube Rupture

Table 5-9 summarizes the timings of the key events in the mitigated STSBO with a TI-SGTR. One (i.e., equivalent of 100% flow area) steam generator tube failed prior to any other RCS creep rupture failures along with a stuck open secondary safety relief valve. Consequently, there is a containment bypass pathway for fission products once the steam generator tube fails. As described in Section 3.2, the accident scenario initiates with a complete loss of all onsite and offsite power. The reactor successfully trips and the containment isolates but all powered safety systems are unavailable. The mitigated STSBO credits the successful connection of the portable, low-pressure, diesel-driven (Godwin) pump to the containment spray system at 8 hr. The Godwin pump is a high-flow, low-head pump with a design capacity of 2000 gpm at 120 psi. A reliable source of water is maintained while 1,000,000 gallons is injected into the containment through the containment sprays. At the time of the analysis, there was no guidance in the emergency procedures for the duration of the spray operation or termination, so the 1,000,000 gallons amount was somewhat arbitrarily selected. The sequence of events is identical to the unmitigated STSBO with a TI-SGTR until 8 hr. In particular, the core has degraded and failed the vessel lower head prior to the spray actuation (see Table 5-9). The emergency containment sprays are effective at reducing the containment pressure and knocking down airborne fission products while they are operating. However, the containment subsequently pressurizes after the sprays are terminated to the failure pressure. While not investigated, intermittent operation of the sprays and deeper flooding could have further delayed failure of the containment. Section 5.3.2.1 summarizes the thermal-hydraulic response of the reactor and containment while Section 5.3.2.2 summarizes the associated radionuclide release from the fuel to the environment.

Table 5-9 The timing of key events for mitigated STSBO with TI-SGTR

Event Description	Time (hh:mm)
Station blackout – loss of all onsite and offsite AC and DC power MSIVs close Reactor trip RCP seal leak at 21 gpm/pump TD-AFW starts but fails to inject due to ECST rupture	00:00
First SG SRV opening	00:03
SG dryout	01:14
Pressurizer SRV opens	01:27
PRT failure	01:47
Start of fuel heatup	02:19
RCP seal failures	02:46
First fission product gap releases	02:57
Stuck open SG PORV	03:00
SGTR	03:33
Creep rupture failure of the Loop C hot leg nozzle	03:47
Accumulator discharges	03:47
Accumulator empty	03:47
Vessel lower head failure by creep rupture	07:30
Debris discharge to reactor cavity	07:30
Cavity dryout (temporary)	07:54
Start of containment sprays	8:00
End of containment sprays (1,000,000 gal)	15:02
Containment at design pressure (45 psig)	44:10
Start of increased leakage of containment ($P/P_{design} = 2.18$)	74:48

5.3.2.1 Thermal-Hydraulic Response

The progression of events in the mitigated STSBO with TI-SGTR is identical to the unmitigated STSBO with TI-SGTR as described in Section 5.3.1 through the first 8 hr, which includes core degradation and vessel failure (e.g., compare the system pressure from Figure 5-73 and the 100% case in Figure 5-56 or the vessel level from Figure 5-74 and the 100% case in Figure 5-60). The portable emergency pump was connected to the containment spray system at 8 hours and begins injection. By 15 hours, 1,000,000 gallons were sprayed into the containment and the emergency

injection was terminated. There was no guidance in the emergency procedures for the duration of the spray operation or termination; therefore, 1,000,000 gallons was an assumed value.

After the containment sprays terminated at 15 hours, the containment water was flooded to ~0.1 m below the bottom of the vessel (see Figure 5-74). The water levels in the reactor cavity and the containment basement were approximately equal due to the hydraulic connection through the 12" hole in the reactor cavity wall at 2'-7" above the bottom of the floor. The reactor cavity also connects to the containment basement via a penetration at 24'-3" above the floor and the holes in the cavity wall for the RCS piping (i.e., nearly 40' above the bottom of the floor). Similar to the response seen in mitigated STSBO (Section 5.2.23.2.4.2), the water level was too low to allow natural circulation from the containment basement into the reactor cavity and out the gaps and RCS piping penetrations present. Since the reactor cavity contains the fuel debris from the failed reactor vessel, the water heated to boiling once the sprays terminated. Intermittent spray operation and/or flooding above the RCS piping penetrations would have substantially delayed containment failure. Although the containment sprays did not prevent containment failure, they delayed containment failure by over ~46 hr relative to the unmitigated case.

The containment sprays are effective in quickly reducing the containment pressure. As shown in Figure 5-75, the containment pressure would reach the shutoff head of the emergency portable pump by 17.5 hours. Based on the containment pressurization rate, it is estimated that there would be considerable additional time to connect the spray system. However, without additional spray flow above the initial 1,000,000 gal, the containment will pressurize above the emergency pump shutoff head by 2.2 days (52 hours) and to failure conditions by 3.1 days (74.8 hours). See the long-term containment pressure response in Figure 5-76.

The selection of the containment sprays as a mitigation technique for this scenario was particularly beneficial for several reasons, as previously discussed in Section 3.2.4.2. These benefits included aerosol knockdown in the containment, delaying containment failure by almost 2 days, and deep flooding and cooling the ex-vessel debris. The spray operation reduced the flow out the failed steam generator tube to the environment (i.e., a containment bypass leakage path prior to containment failure). The impact of these benefits on the source term is discussed in Section 5.3.2.2.

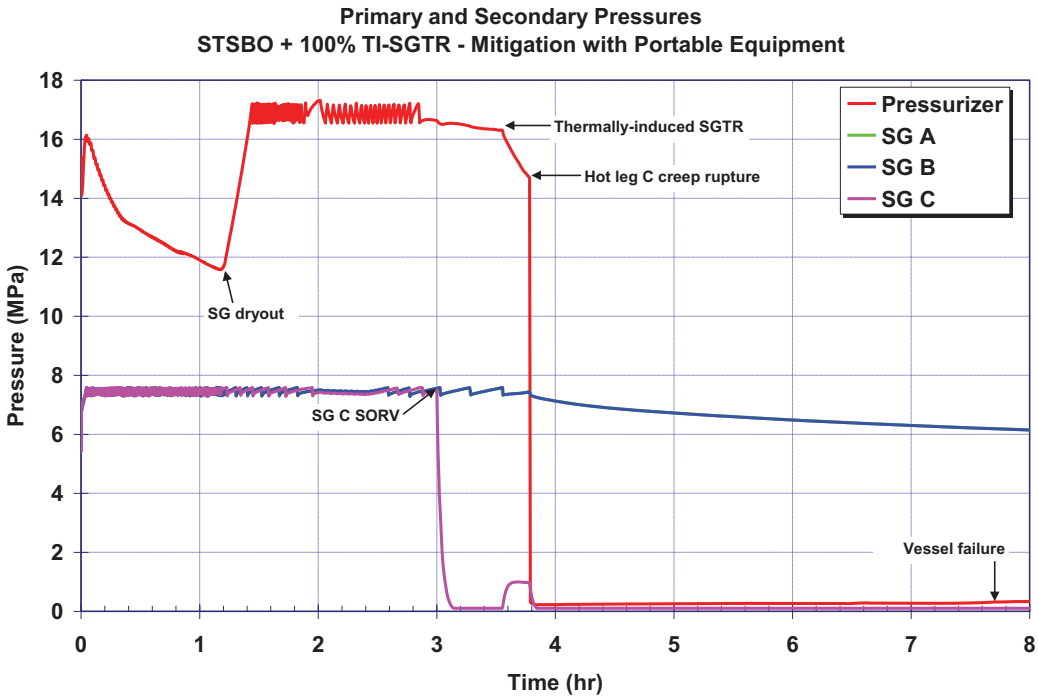

Figure 5-73 The mitigated STSBO primary and secondary pressure history

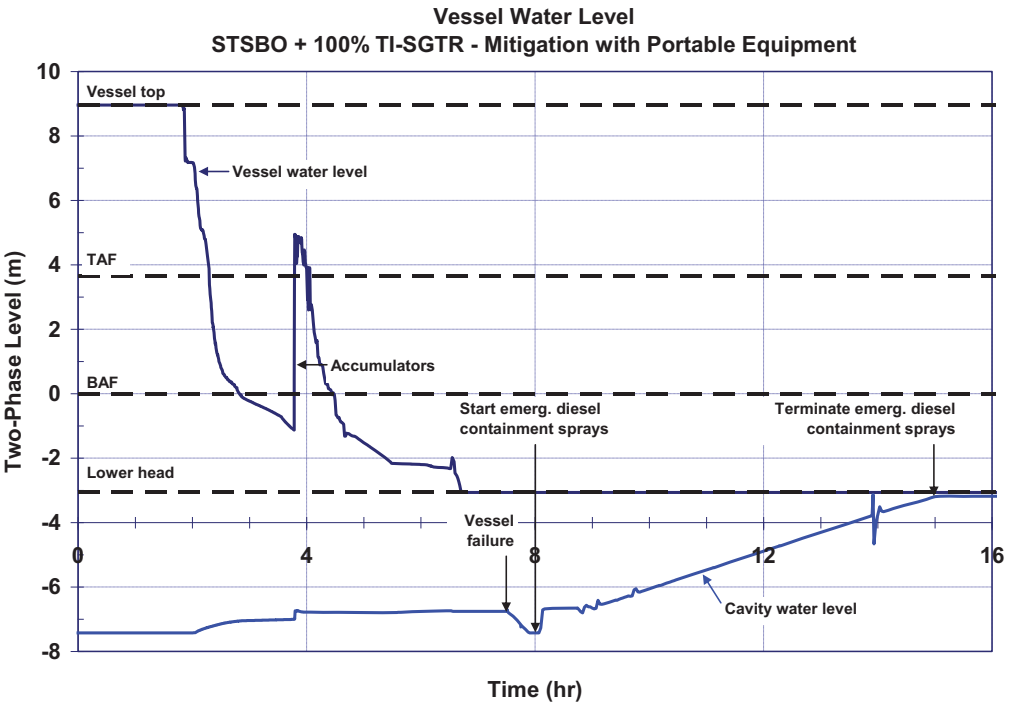

Figure 5-74 The mitigated short-term station blackout vessel two-phase coolant level

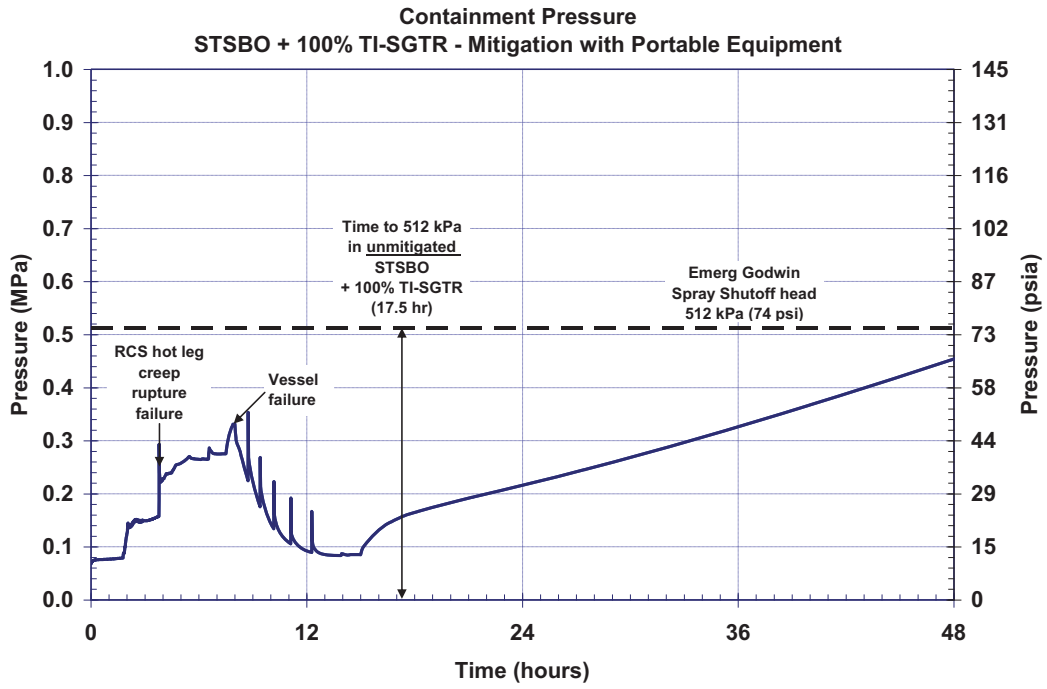

Figure 5-75 The mitigated short-term station blackout containment pressure history

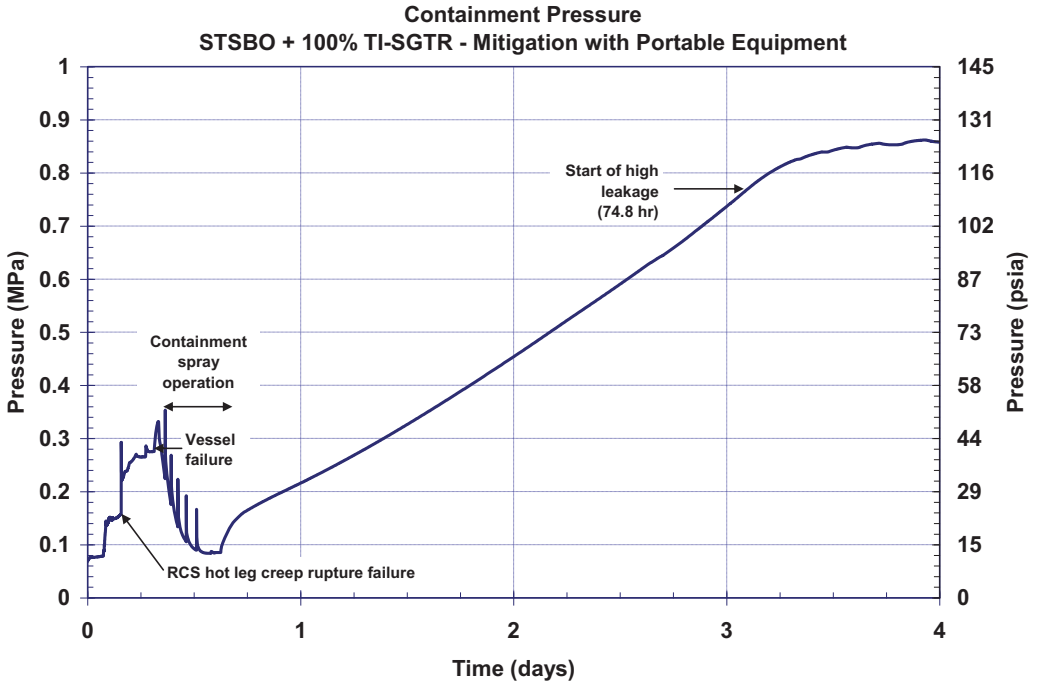

Figure 5-76 The mitigated short-term station blackout containment pressure history

5.3.2.2 Radionuclide Release

The radionuclide response of the mitigated STSBO with a TI-SGTR is identical to the unmitigated response described in Section 5.3.1.2 for the first 8 hr, or through vessel failure until the start of the containment sprays. Following the start of the emergency containment sprays at 8 hr (0.33 days), the airborne aerosols of iodine and cesium rapidly decease (see Figure 5-77 and Figure 5-78, respectively). By the time the sprays are terminated at 15 hr (0.63 days), almost all of the airborne aerosols have been captured in the pool on the containment floor. Since the containment failure was delayed until 74 hr 48 min (3.1 days), natural settling of the airborne mass in the containment was also significant, which is reflected in the small environmental release of iodine and cesium (i.e., 0.5% and 0.4%, respectively). However, natural settling was also effective in the unmitigated case, which does not occur until 27 hr 54 min. As will be discussed next, the spray water was important in preventing revaporization. This was the most significant difference between the mitigated and unmitigated cases.

Due to the deep flooding in the reactor cavity by the spray operation, the bottom of the failed vessel lower head is at the top of the water level in the reactor cavity.[34] Therefore, the natural hot circulation flow that promoted revaporization in the unmitigated STSBO is not present. Instead, the water pool in the reactor cavity cools the bottom of the vessel. Due to some boiling in the cavity, a relatively cool flow of steam passes through the vessel and out the failed hot leg nozzle location, which also removes heat and inhibits revaporization of deposited radionuclides in the upper vessel and hot leg. Consequently, the revaporization of the in-vessel deposited fission products (i.e., especially cesium-iodine) that was seen in the unmitigated STSBO with a TI-SGTR is characteristic of revaporization) was negligible in the mitigated case through 4 days (see Figure 5-79 and Figure 5-80).

[34] Although the level is 0.1 m below the inside of reactor vessel, the level covers the bottom of the outside surface of the lower head, which is 0.13 m thick. Hence, the water blocks the flow of air into the reactor vessel through the lower head failure hole.

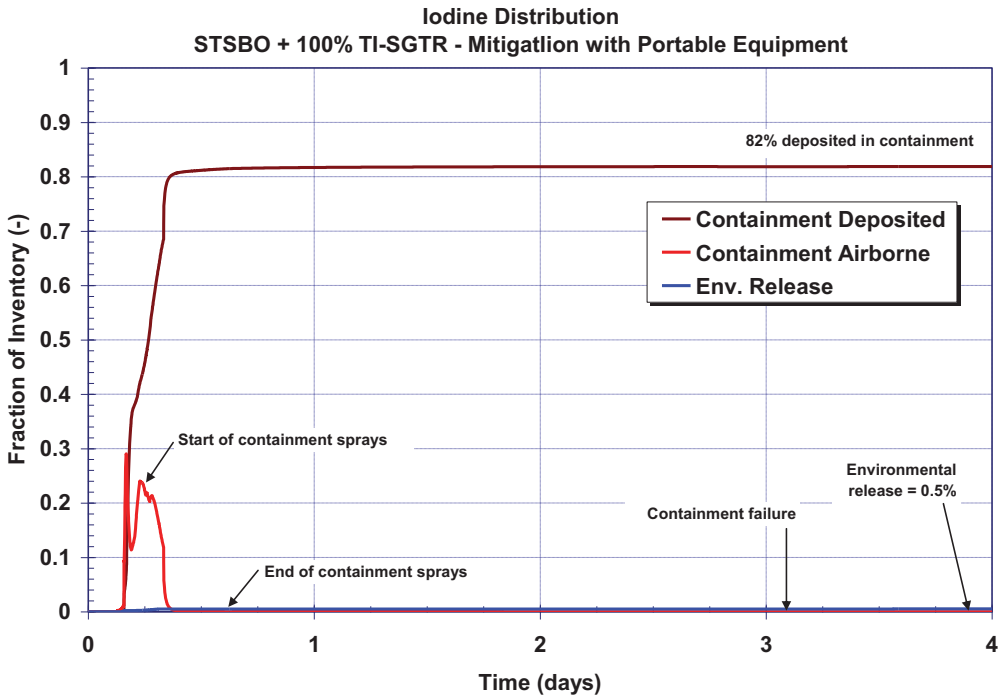

Figure 5-77 The iodine distribution in the containment for short-term station blackout with a 100% thermally-induced SGTR with spray mitigation

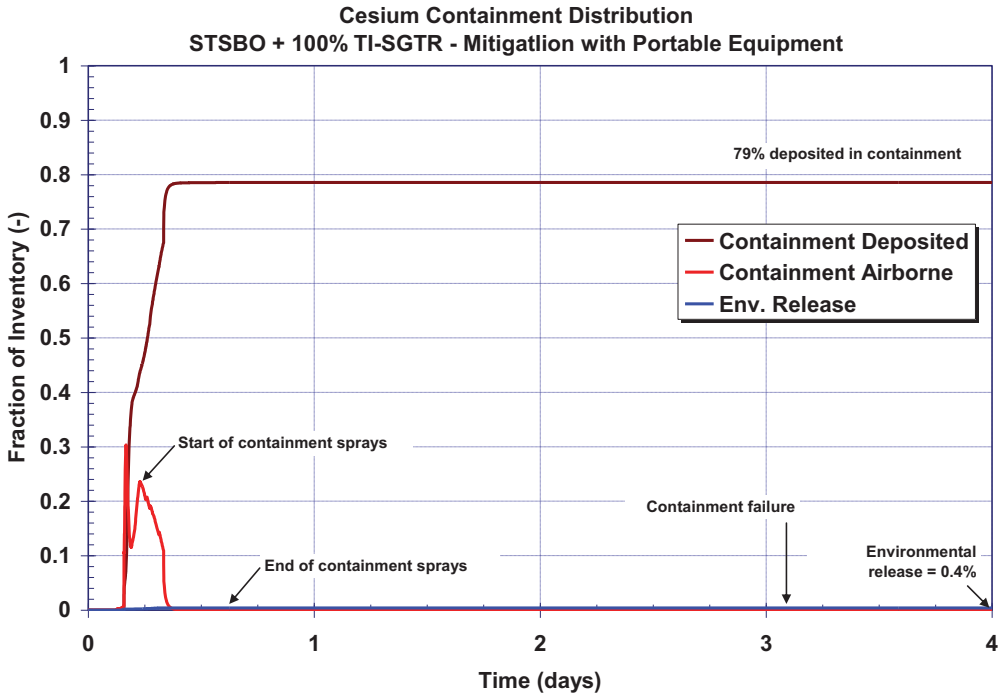

Figure 5-78 The cesium distribution in the containment for short-term station blackout with a 100% thermally-induced SGTR with spray mitigation

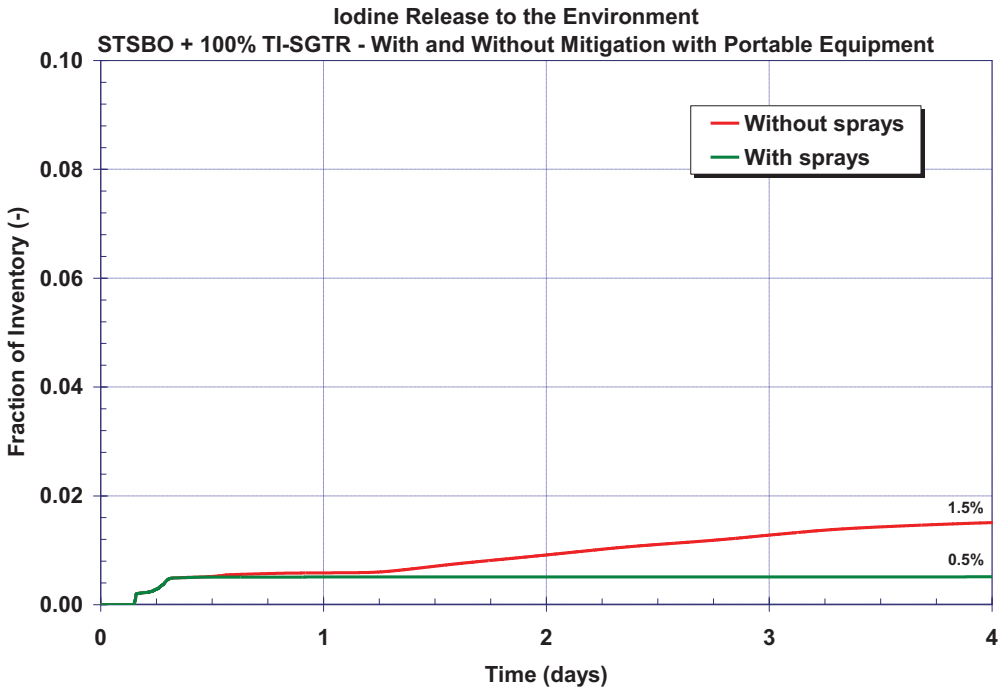

Figure 5-79 The short-term station blackout with a 100% thermally-induced SGTR with and without spray mitigation iodine environmental release

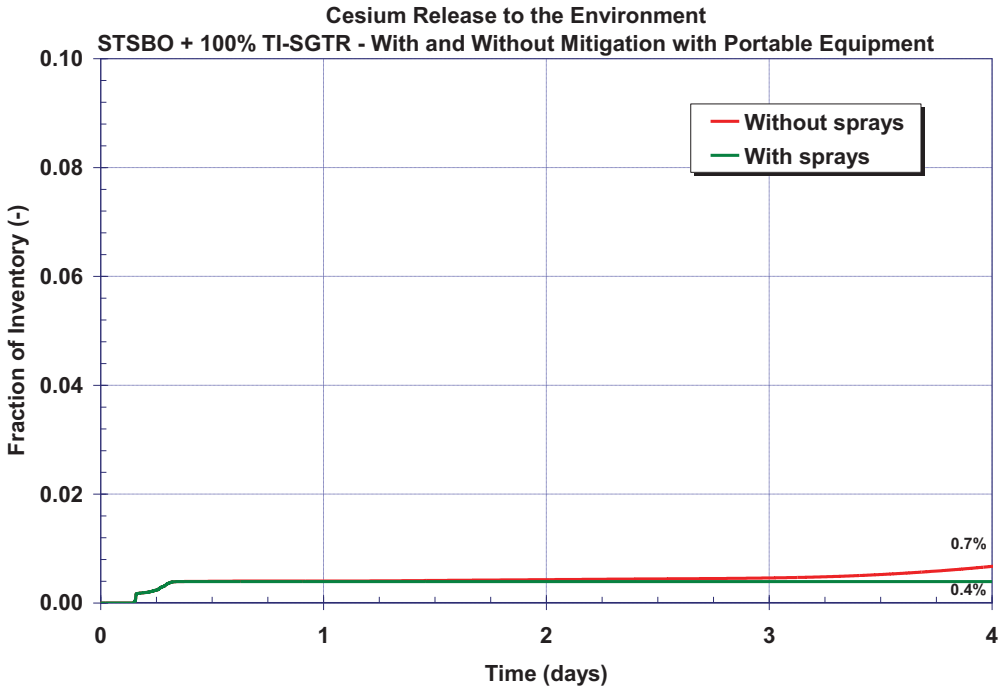

Figure 5-80 The short-term station blackout with a 100% thermally-induced SGTR with and without spray mitigation cesium environmental release

5.3.3 Uncertainties in the Failure of the Thermally-Induced Steam Generator Tube versus the Hot Leg

During the peer review of the unmitigated STSBO with a thermally-induced tube rupture, there were questions about the competing events of a thermally-induced steam generator tube versus the hot leg creep rupture failure. The probability of a TI-SGTR has previously been assessed to be 0.25 [34]. Consequently, calculations were performed in Section 5.3 with a TI-SGTR to supplement the calculations described in Section 5.2 without tube failures. More recent research has investigated the relative timing of the TI-SGTR relative to creep rupture failure of the hot leg with mechanistic simulations of natural circulation flow patterns[19][20][36][37]. The results of the research show comparable timings for hot leg creep rupture failure and thermally-induced steam generator tube failure, for a flawed tube at maximum thermal stress conditions, with the former slightly proceeding the later for most conditions.

MELCOR also predicts failure of a hot leg prior to any steam generator tubes (i.e., potential failures are monitored at both locations). Consequently, the calculations presented previously in Section 5.3 increased the mechanical stress across the tubes by prescribing a stuck-open safety relief valve and an increase in the thermal stress by inducing tube failure at a lower criterion than the default model. Subsequent to the failure of the steam generator tube, the hot leg failed and mitigated the magnitude of the potential release of radionuclides that bypass the containment.

To investigate the relative vulnerability of the hot leg to a TI-SGTR, a sensitivity calculation was performed with MELCOR where the failure of the hot leg was prevented. Figure 5-81 shows the creep rupture damage index of the hot leg. The steam generator tube failed at 3.55 hr. Hot leg failure was predicted 14 min later at 3.8 hr when the failure index reached a lifetime value of 1. Vessel failure was calculated to occur at 5.3 hr in the sensitivity calculation. Between 3.8 and 5.3 hr, the damage index increased from 1 to greater than four orders of magnitude larger. The creep index is highly sensitive to the thermal response of the hot leg nozzle as very hot gases continue to flow from the core (see hot leg temperature responses in Figure 5-82).

Figure 5-83 includes the iodine release to the environment for the failure and no failure case. As discussed in Section 5.3.1.2, there is a direct pathway for radionuclide releases to the environment through the failed steam generator tube prior to hot leg failure. However, the iodine release to the environment essentially stopped once the hot leg failed. Between 3.8 hours and 4 hours, the hot leg creep failure index in the no hot leg failure sensitivity case increased more than an order of magnitude (i.e., a factor of 18) above the best-estimate failure value. The iodine release to the environment increased by a factor of three during this time to a 0.6% release. Consequently, there is a high sensitivity to the creep failure damage index at high temperatures that quickly increases the index above the failure threshold.

In summary, it is not credible that the hot leg would not fail by creep rupture in the examined scenarios. The conditions that lead to the TI-SGTR are the same conditions that promote hot leg failure. As discussed in Section 5.3.1, the TI-SGTR increased heat removal from the core and the heat flow past the hot leg nozzle. The best-estimate creep rupture damage index is rapidly increasing near the time of the TI-SGTR. Within 10 minutes after the best-estimate failure time of the hot leg nozzle, the creep rupture damage index has increased by an order of magnitude due

to the strong dependence of the nozzle strength to temperature. There is a factor of three increase in the iodine release to the environment while the creep rupture index increases to an order of magnitude larger. However, the release of iodine to the environment was only 0.6% at the order-of-magnitude higher damage value.

Three sensitivity calculations were also performed using the SCDAP/RELAP5 code and associated natural circulation severe accident model [19][20][36]. The best-estimate parameters in the SCDAP/RELAP5 calculation were based on the latest FLUENT CFD research [37]. Unlike the MELCOR calculation, which used a specified criterion to create the TI-SGTR (i.e., specified to occur ~10 min prior hot leg failure timing from the STSBO in Section 5.2.1), the SCDAP/RELAP5 simulation tied the TI-SGTR to stress enhancing vulnerabilities due to flaws developed during in-service operation. The three SCDAP/RELAP5 cases examined: (1) a TI-SGTR in the hottest portion of the natural circulation plume and a stress multiplier of two, (2) a TI-SGTR in the hottest portion of the natural circulation plume and a stress multiplier of three, and (3) multiple tube failures with a stress multiplier of two. The results of the SCDAP/RELAP5 study (i.e., shown in Table 5-10) confirmed that: (a) TI-SGTR will not preclude hot leg creep rupture failure, and (b) hot leg creep rupture failure occurs within minutes of the TI-SGTR for a range of tube stress conditions.

Table 5-10 The timing of hot leg failure for SCDAP/RELAP5 simulations with TI-SGTR

Case	**Delay of Hot Leg Failure after TI-SGTR (min)**
1. Steam generator tube stress multiplier of 2	1.2
2. Steam generator tube stress multiplier of 3	8.8
3. Multiple steam generator tubes w/stress multiplier of 2	1.3

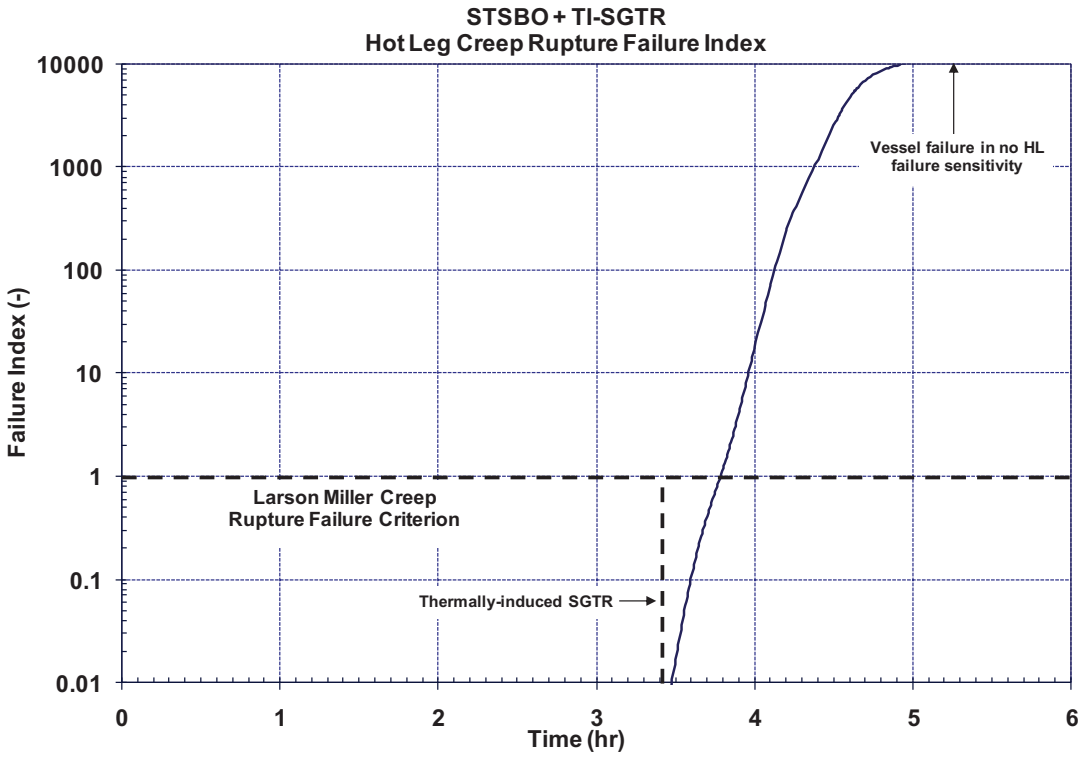

Figure 5-81 The hot leg creep rupture failure index in the short-term station blackout sensitivity case with a 100% thermally-induced SGTR and no hot leg failure

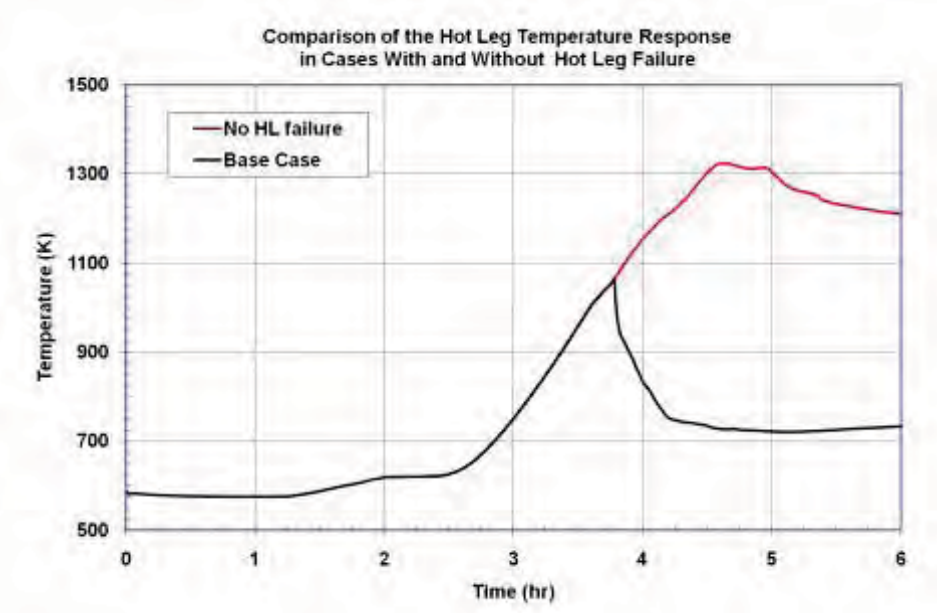

Figure 5-82 The hot leg temperature response in the thermally-induced steam generator tube rupture cases with and without hot leg failure

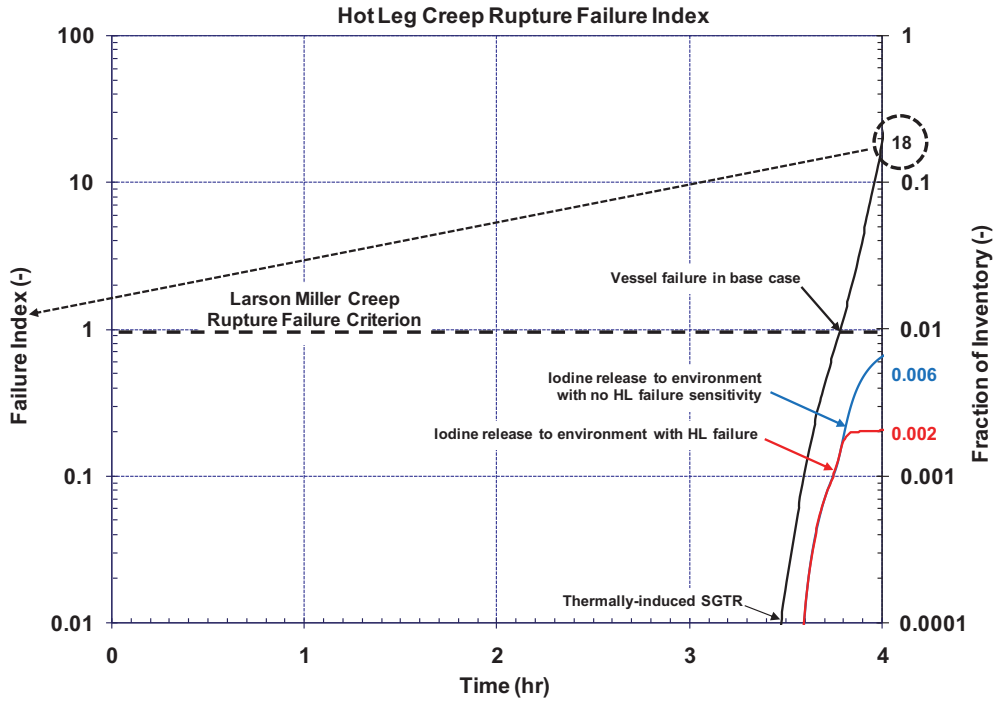

Figure 5-83 The hot leg creep rupture failure index and iodine release to environment for the thermally-induced steam generator tube rupture cases with and without hot leg failure

5.4 Spontaneous SGTR

The spontaneous SGTR sequence is a double-ended-guillotine rupture of a single steam generator tube occurring while the reactor system is operating at normal conditions. Section 5.4.1 presents the results of a mitigated scenario where the expected operator actions are successful. For the unmitigated scenario in Section 5.4.2, the operator fails to isolate the faulted steam generator or cooldown the RCS using the two intact generators. Finally, the unmitigated scenario in Section 5.4.3 has the same failed operator actions as the previous unmitigated scenario. In addition, the relief valve on the faulted generator is assumed to fail open when water from the SGTR fills the steam generator and flows through the valve.

5.4.1 Mitigated Spontaneous Steam Generator Tube Rupture

Table 5-11 summarizes the timing of the key events in the mitigated spontaneous steam generator tube rupture with expected operator actions. As described in Section 3.3.1, the accident scenario initiates with a spontaneous double-ended guillotine rupture of one steam generator tube. After about three minutes, the reactor successfully trips and the containment isolates. The full complement of systems at Surry Power Station is considered functional in this scenario including all systems associated with engineered safeguards and instrumentation and control as well as all auxiliary and emergency systems. Operator actions are successful at isolating the faulted steam generator and cooling the reactor system to permit operation of the residual heat removal (RHR) system. Section 5.4.1.1 summarizes the thermal-hydraulic response of the reactor and containment while Section 5.4.1.2 summarizes the associated radionuclide release from the fuel to the environment.

Table 5-11 Timing of key events for the Spontaneous SGTR with Expected Operator Action

Event Description	Time (hh:mm)
Spontaneous SGTR	00:00
Reactor scram	00:03
Turbine stop valves close	00:03
Steam dump valves open and modulate	Not accomplished*
Steam dump valves close (RCS temperature < 547 °F)	Not accomplished*
HHSI initiated (3 pumps)	00:03
First AFW delivery	00:03
Operators take control of AFW (as the SGs are overfilling)	00:15
AFW delivery to faulted steam generator secured**	00:15
1 of 3 HHSI pumps secured	00:15
Faulted steam generator flooded	00:20
TDAFW fails (turbine floods)	00:20
Faulted steam generator PORV 1st lifts	00:23
Faulted steam generator isolated	02:30
HHSI secured	02:30
Leakage through faulted steam generator PORV stopped***	02:30
100 °F/hr cool-down initiated	02:30
RHR entry pressure (400 – 450 psig) achieved	03:18 (450 psig)
RHR entry temperature (350°F) achieved	03:43

* The automatic operation of steam dump valves was not represented in the Surry MELCOR model. The thermal-hydraulic signature in the subject calculation suggests that the valves might be active for the first 6 min following scram but at no other time. Valve action would reduce RCS temperature by ~25 °F for the first few min and by a few °F in the next few min. The differences are thought to be inconsequential.

** AFW to the faulted steam generator is stopped on account of runaway high level in the generator.

*** Isolating the faulted steam generator, i.e., closing the MSIVs serving it, in combination with securing HHSI, stops the leakage through the faulted steam generator PORV.

5.4.1.1 Thermal-hydraulic Response

Figure 5-84 through Figure 5-90 present the thermal hydraulic response predicted by MELCOR for spontaneous SGTR at Surry where reactor systems operate as designed and reactor operators respond as expected per training and procedure. System pressure histories are shown in Figure 5-84. Figure 5-85 shows RCS conditions relative to RHR entry conditions. Figure 5-86 and Figure 5-87 show reactor pressure vessel level and fuel cladding and reactor vessel lower head temperatures, respectively. RWST and ECST inventories are tracked in Figure 5-88 while containment pressure is tracked in Figure 5-89. Steam generator level is tracked in Figure 5-90. Operator actions in this scenario are those expected per training and procedure. Specifically, the operators:

- Secure AFW delivery to the steam generator with the broken tube (the faulted steam generator) at 00:15:00, i.e., 15 min after the SGTR event, in response to runaway high level in the generator.
- Secure 1 of the 3 total HHSI pumps at 00:15:00
- Isolate the faulted steam generator, i.e., close the MSIVs serving the faulted steam generator at 2:30:00
- Secure HHSI at 2:30:00 (which in combination with the above actions ends the RCS leakage)
- Initiate a 100° F/hr cool-down of the RCS at 2:30:00
- Accomplish RHR entry at 03:43:00 (predicted)

The spontaneous SGTR quickly leads to a reactor scram, turbine stop valve closure, HHSI actuation, and AFW delivery. The flow of primary system coolant through the tube rupture into the secondary side of the faulted steam generator results in a fairly sustained leak to the environment beginning at 23 min when the PORV serving the generator first lifts.

Once level control of AFW is initiated in the MELCOR calculation (i.e., at 15 min simulating the operators taking control), HHSI stably removes core decay heat up to the time when operator action to end the leakage of coolant to the environment is represented (i.e., at 2.5 hr) and operator actions to depressurize and cool down the RCS are modeled to begin (i.e., also at 2.5 hr). There is no heat removal by the intact steam generators during this time as evidenced in Figure 5-88 where no drawdown on ECST inventory shows to occur. Note that pressure in the intact steam generators during this period is low relative to the setpoint of the main steam line PORVs such that no venting of the generators occurs and hence no heat removal is accomplished by them. Coinciding flow out the tube rupture is governed by the head-versus-flow characteristics of the HHSI pumps, the flow resistance at the tube rupture, and the set point of the PORV on the faulted steam generator. Operator action to secure HHSI, modeled to occur at 2.5 hrs, allows the PORV to reseat shortly thereafter ending leakage through the tube rupture. The 100°F/hr cool-down initiated at 2.5 hrs gradually brings the temperature of the RCS down to RHR entry temperature. RHR entry pressure is reached somewhat earlier, however, the timing

may be accelerated given that no active pressure control was represented in the MELCOR calculation, i.e., no pressurizer heater operation was modeled. The 100°F/hr cool-down in the MELCOR calculation was accomplished realistically in that the intact steam generators were vented in a controlled fashion while AFW was delivered as needed to maintain level.

The results of the MELCOR calculation simulating an SGTR with expected operator action show that RHR entry conditions would be achieved without challenging the RWST inventory and without immoderately draining the ECST. No uncovering or overheating of the reactor core would occur and no damage to the core would result.

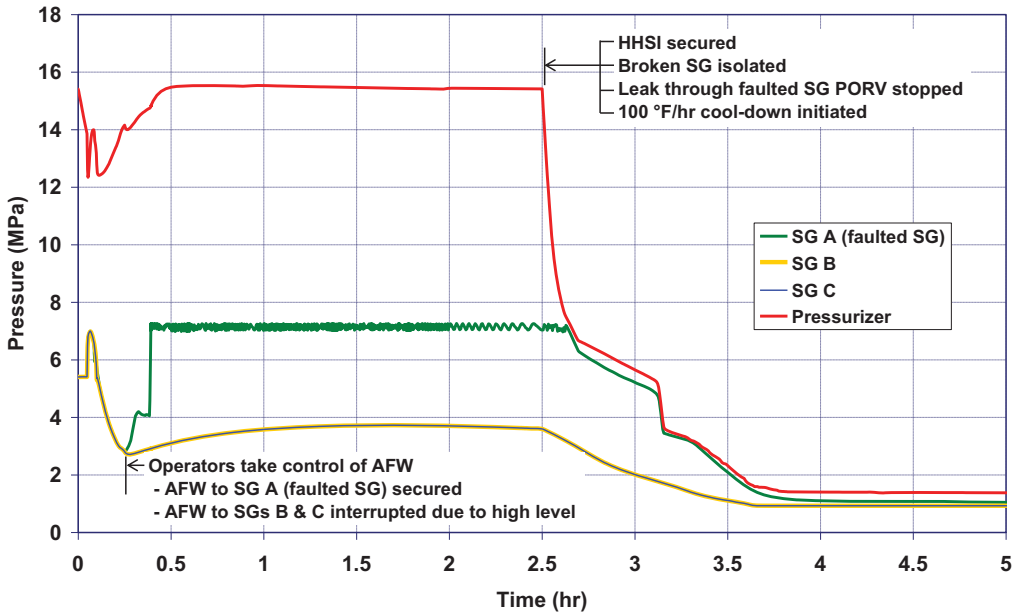

Figure 5-84 SGTR with Operator Action – System Pressures

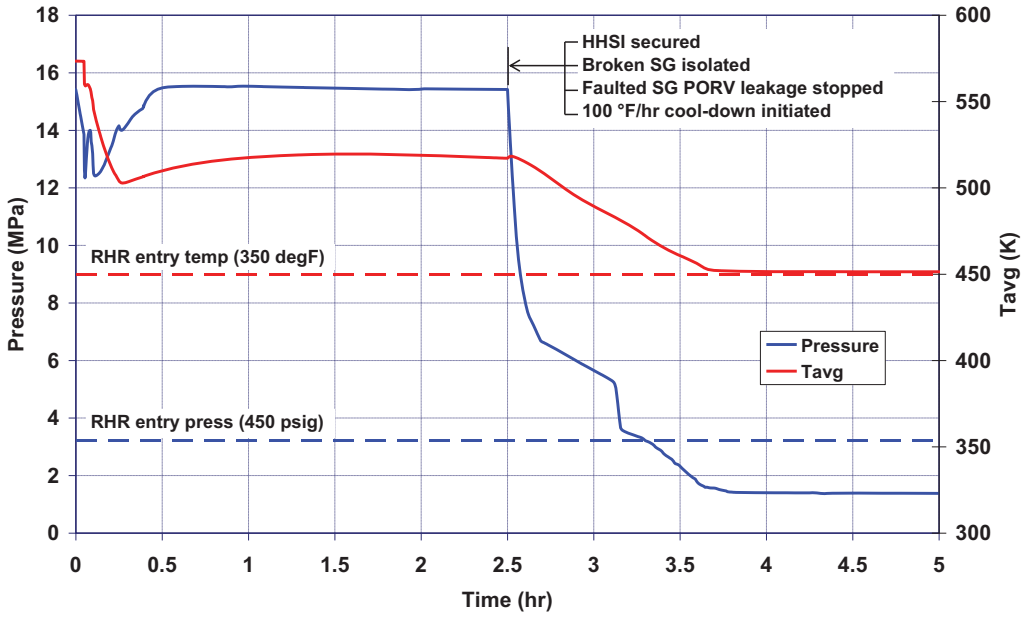

Figure 5-85 SGTR with Operator Action – RCS Conditions Relative to RHR Entry Conditions

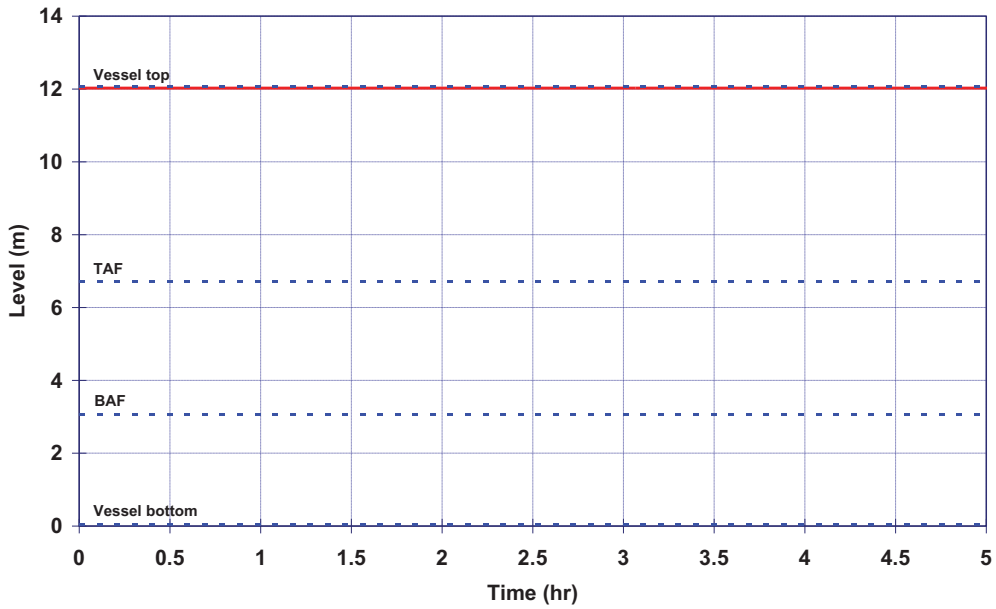

Figure 5-86 SGTR with Operator Action – RPV Level

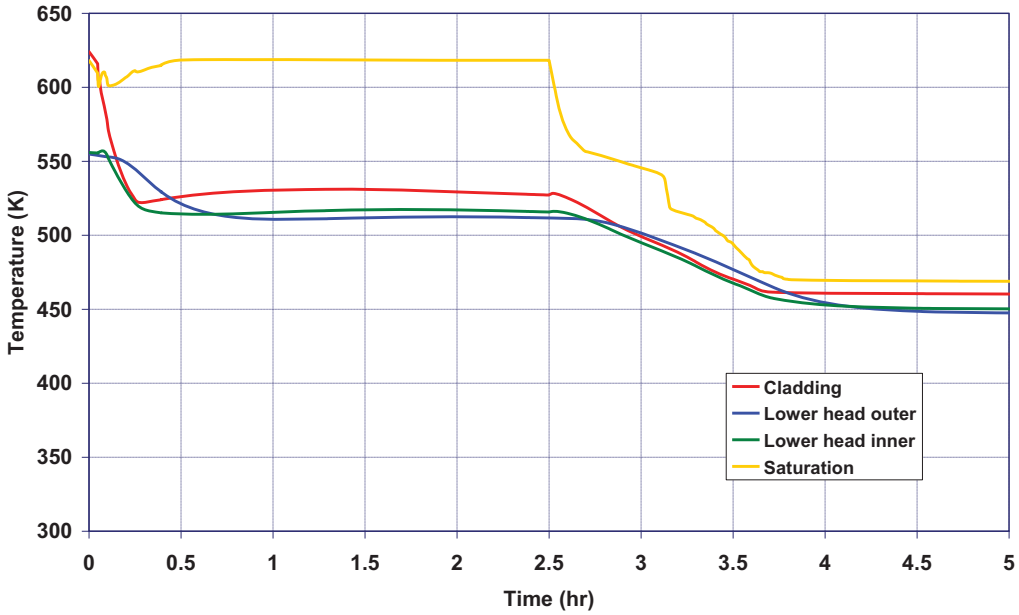

Figure 5-87 SGTR with Operator Action – Maximum Cladding and Lower Head Temperatures

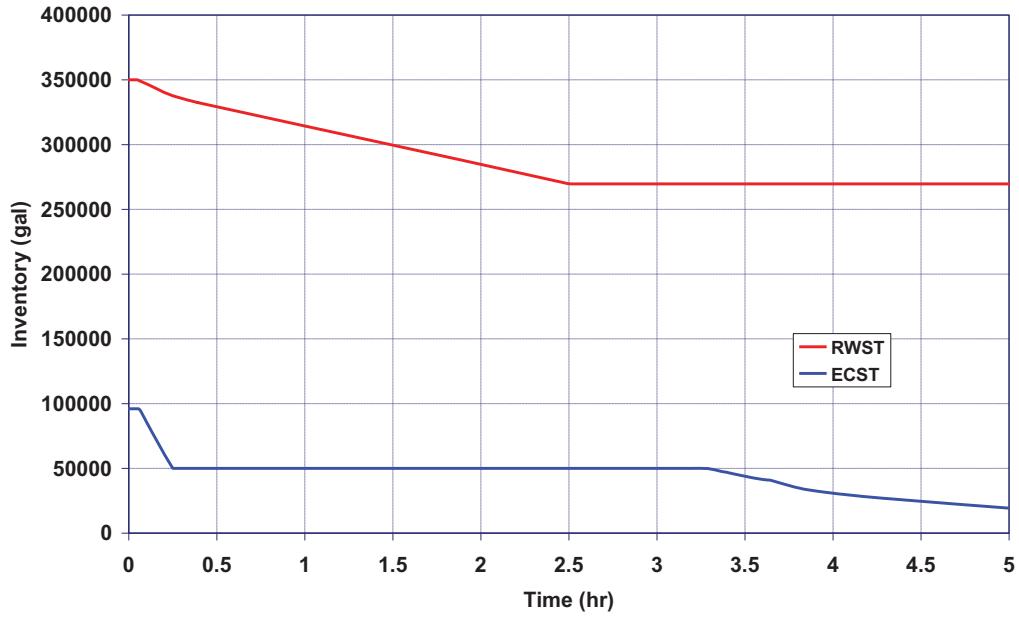

Figure 5-88 SGTR with Operator Action – RWST and ECST Inventories

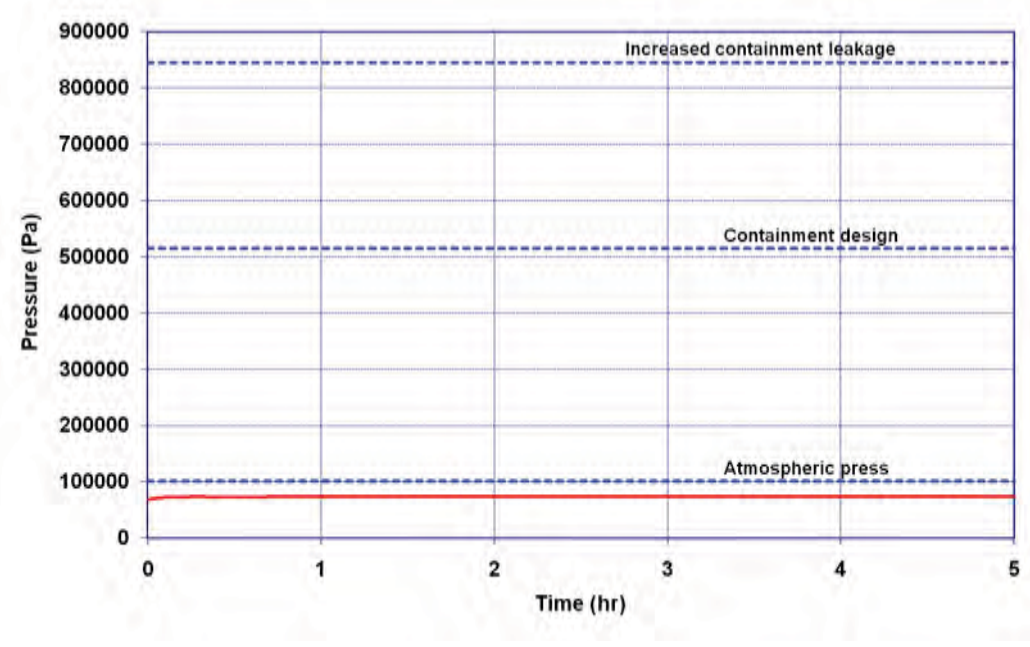

Figure 5-89 SGTR with Operator Action- Containment Pressure

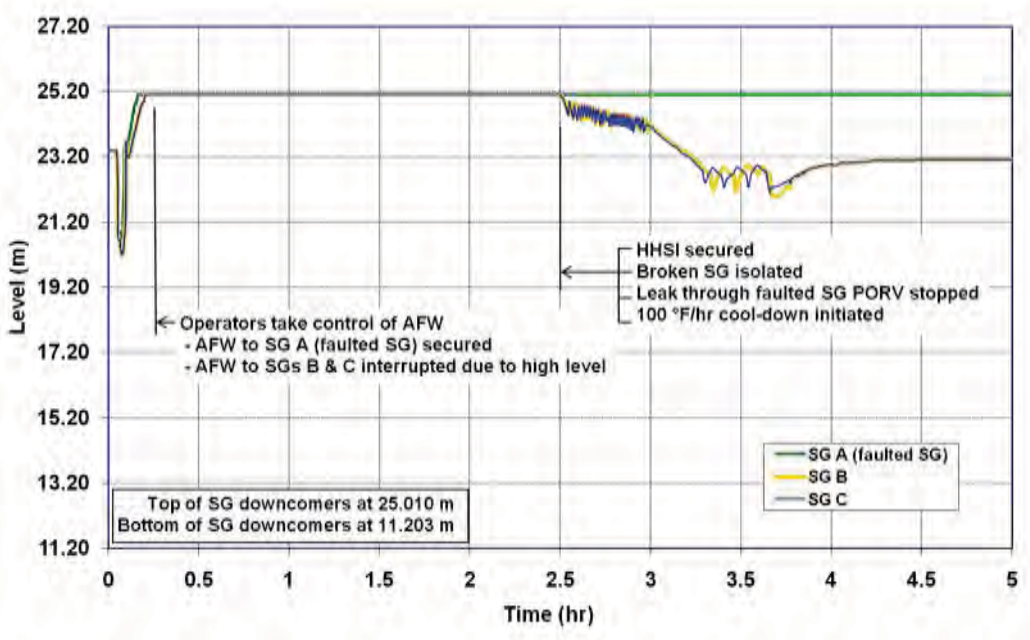

Figure 5-90 SGTR with Operator Action- Steam Generator Level

5.4.1.2 Radionuclide Release

No fission product releases from the reactor core occurred in the spontaneous SGTR with expected operator actions.

5.4.2 Unmitigated - Spontaneous SGTR with Failed Operator Action

Table 5-12 summarizes the timing of the key events in the spontaneous steam generator tube rupture with failed operator actions. As described in Section 3.3.1, the accident scenario initiates with a spontaneous double-ended-guillotine rupture of one steam generator tube. After about three minutes, the reactor successfully trips and the containment isolates. The full complement of systems at Surry Power Station is considered functional in this scenario including all systems associated with engineered safeguards and instrumentation and control as well as all auxiliary and emergency systems. However, the operator actions are not successful at isolating the faulted steam generator or cooling the reactor system to permit operation of the RHR system. Eventually, the refueling water storage tank and the ECST are exhausted (i.e., after ~11 hr and ~33.5 hr, respectively) leading to core uncover (i.e., beginning at ~43.75 hr) and core damage. Due to the long amount of time to core damage, it was judged unlikely that the operators would not correct missed actions (i.e., failure to isolate the faulted SG, failure to cool down and depressurize, and failure to refill the RWST or connect to the unaffected unit's RWST). Section 5.4.2.1 summarizes the thermal-hydraulic response of the reactor and containment while Section 5.4.2.2 summarizes the associated radionuclide release from the fuel to the environment.

Table 5-12 Timing of key events for the Spontaneous SGTR with Failed Operator Action

Event Description	Time (hh:mm)
Spontaneous SGTR	00:00
Reactor scram	00:03
Turbine stop valves close	00:03
Steam dump valves open and modulate	Not accomplished*
Steam dump valves close (RCS temperature < 547 °F)	Not accomplished*
HHSI initiated (3 pumps)	00:03
First AFW delivery	00:03
Operators take control of AFW as the SGs are overfilling	00:10**
AFW delivery to faulted steam generator secured	00:12***
1 of 3 HHSI pumps secured	00:15
Faulted steam generator PORV 1st lifts	00:32
Faulted steam generator flooded	00:42
TDAFW fails (turbine floods)	00:42
Faulted steam generator isolated	Not accomplished by operators
HHSI secured	Not accomplished by operators
Leakage through faulted steam generator PORV stopped	Not accomplished by operators
100 °F/hr cool-down initiated	Not accomplished by operators
RWST exhausted (safety injection ends)	11:03
RCPs trip	18:22
Steam Generator C PORV fails open due to excessive cycling	31:00
First accumulator discharge	31:16
ECST exhausted (AFW delivery ends)	33:29
Steam Generator B PORV fails open due to excessive cycling	38:20
Core uncovering begins	43:48
First fission product gap release	45:46

* The automatic operation of steam dump valves was not represented in the Surry MELCOR model. The thermal-hydraulic signature in the subject calculation suggests that the valves might be active for the first 6 min following scram but at no other time. Valve action would reduce RCS temperature by ~25 °F for the first few min and by a few °F in the next few min. The differences are thought to be inconsequential.

** Best-estimate timing for operators assuming manual control of AFW is 15 min. A discrepancy in the MELCOR input initiated level control of AFW at 10 min.

*** Best-estimate timing for operators securing AFW delivery to the faulted steam generator is 15 min. A discrepancy in the MELCOR input interrupted AFW to the steam generator at 12 min and 30 sec. AFW to the faulted steam generator is stopped on account of runaway high level in the generator

5.4.2.1 Thermal-hydraulic Response

Figure 5-91 through Figure 5-96 present the thermal hydraulic response predicted by the MELCOR for a spontaneous SGTR at Surry where reactor systems operate as designed but reactor operators fail to accomplish key actions per training and procedure. Specifically, the operators fail to depressurize and cool down the RCS. System pressure histories are shown in Figure 5-91. Figure 5-92 and Figure 5-93 show reactor pressure vessel level and fuel cladding and reactor vessel lower head temperatures, respectively. RWST and ECST inventories are tracked in Figure 5-94 while containment pressure is tracked in Figure 5-95. Steam generator level is tracked in Figure 5-96.

Operator actions are remiss in this scenario with respect to training and procedure in that the operators:

- Fail to isolate the faulted steam generator
- Fail to depressurize and cool down the RCS
- Fail to extend the available duration of ECCS injection by refilling the RWST or cross connecting to the other Surry unit's RWST.

The tube rupture quickly leads to a reactor scram, turbine stop valve closure, HHSI actuation, and AFW delivery. The flow of primary system coolant through the tube rupture into the secondary side of the faulted steam generator results in a fairly sustained leak to the environment beginning at 32 min when the PORV serving the generator first lifts.

Once level control of AFW is initiated in the MELCOR calculation (at 10 min simulation the operators taking control), HHSI stably removes core decay heat and reduces core temperatures up to the time when the useable inventory of the RWST is exhausted thereby ending injection. There is no heat removal by the intact steam generators during this time as evidenced in Figure 5-94 where no drawdown on ECST inventory shows to occur. Note that pressure in the intact steam generators during this period is low relative to the setpoint of the main steam line PORVs such that no venting of the generators occurs and hence no heat removal is accomplished by them. Coinciding flow out the tube rupture is governed by the head-versus-flow characteristics of the HHSI pumps, the flow resistance at the tube rupture, and the set point of the PORV in the faulted steam generator. The RCS heats to saturation over the course of several hours following the RWST being exhausted and an extended boil-off of the RCS inventory begins. The RCPs are stopped in the MELCOR calculation at the first occurrence of void in the RCS simulating the pumps tripping on their own or the operators shutting them down on account of erratic performance. As the RCS heats to saturation, the intact steam generators pressurize up to the setpoint on the main steam line PORVs and the generators function to remove heat from the RCS. This remains the case until the ECST is exhausted. (Note that once the RCS begins to void and the RCPs stop, heat rejection to the steam generators is by reflux cooling only.) Late in the course of the boil-off of the RCS inventory, the pressure history of the system is influenced strongly by failures of the PORVs serving the intact steam generators. The PORVs are modeled to fail open due to excessive cycling for a particular per-demand failure probability and a particular cumulative distribution function value according to the relation:

$$P(n) = 1-(1-Pd)^n$$

where *P(n)* is the cumulative distribution function value, *Pd* is the per-demand failure probability, and *n* is the number of cycles. Given a per-demand failure probability of 0.0058 (i.e., per Surry's response to a SOARCA information request) and an assumed cumulative distribution function value of 0.5, the valves fail open after 119 cycles. Following failure of the PORVs serving the intact steam generators, dramatic reductions in system pressure result as the steam generators blow down. Note that over-cycle failure of the PORV serving the faulted steam generator was prevented in the subject MELCOR calculation. If this had not been done, inordinate cycling of the simplistically-modeled valve would have occurred as liquid entered it from the flooded generator and the valve would have failed open at 70 min. The sensitivity of the progression of the accident to the status of this PORV is addressed by the calculation of the next Section where the valve is failed open when liquid first flows through it.

The MELCOR calculation predicts that core uncovering initiates at 43 hr and 48 min. The first release of fission products from a fuel/cladding gap is seen at 45 hr and 46 min. Traces in Figures 99 through 104 end at first gap release and figures of fission product tracking are not presented for the subject scenario on account of the great unlikelihood that operators would fail to depressurize and cool down the reactor system for some 43 hours.

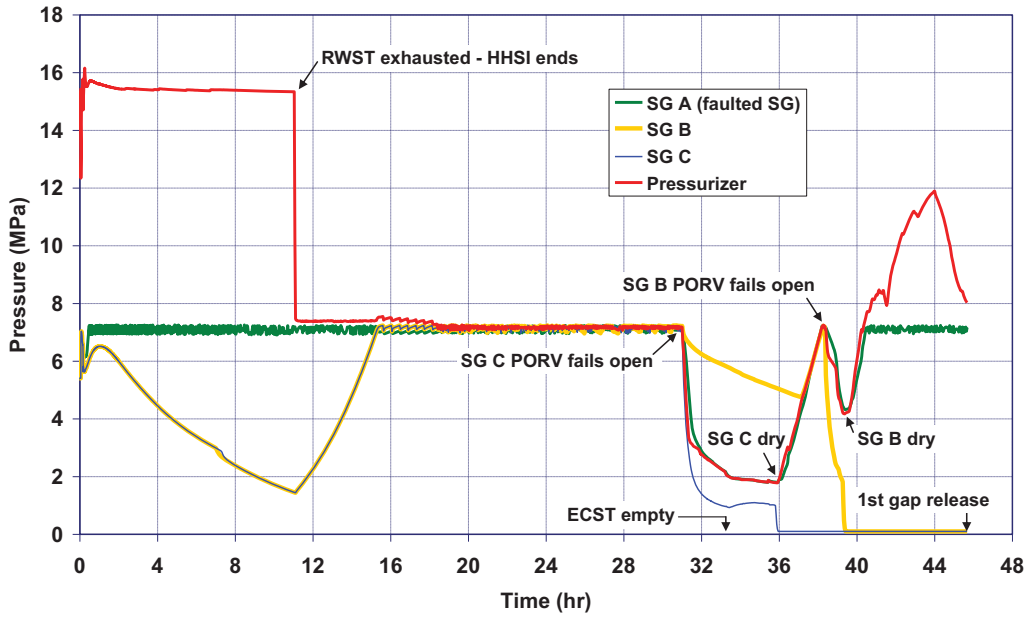

Figure 5-91 SGTR with Failed Operator Action – System Pressures

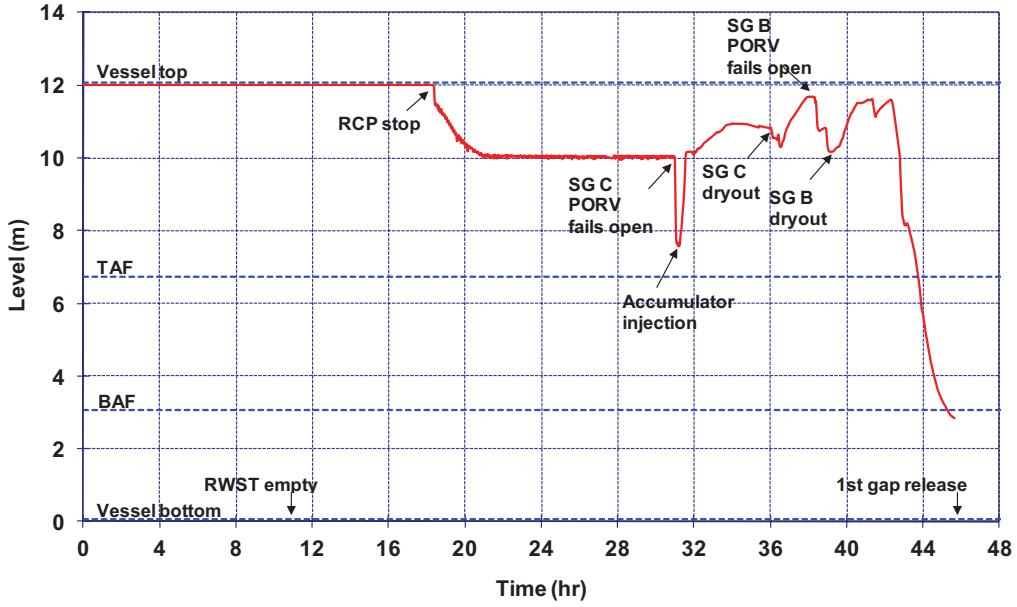

Figure 5-92 SGTR with Failed Operator Action – RPV Water Level

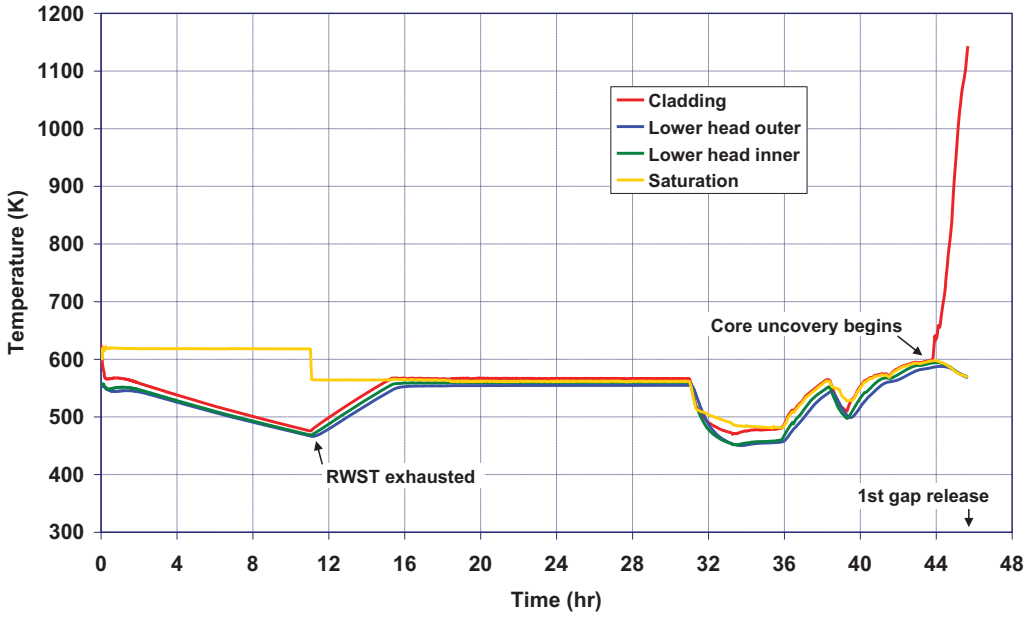

Figure 5-93 SGTR with Failed Operator Action – Maximum Cladding and Lower Head Temperatures

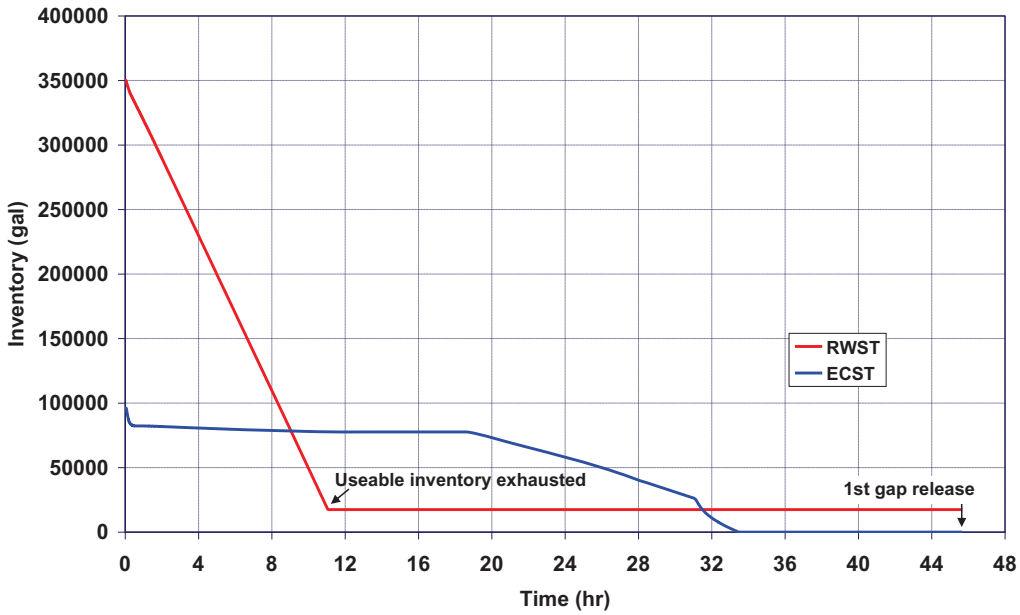

Figure 5-94 SGTR with Failed Operator Action – RWST and ECST Inventories

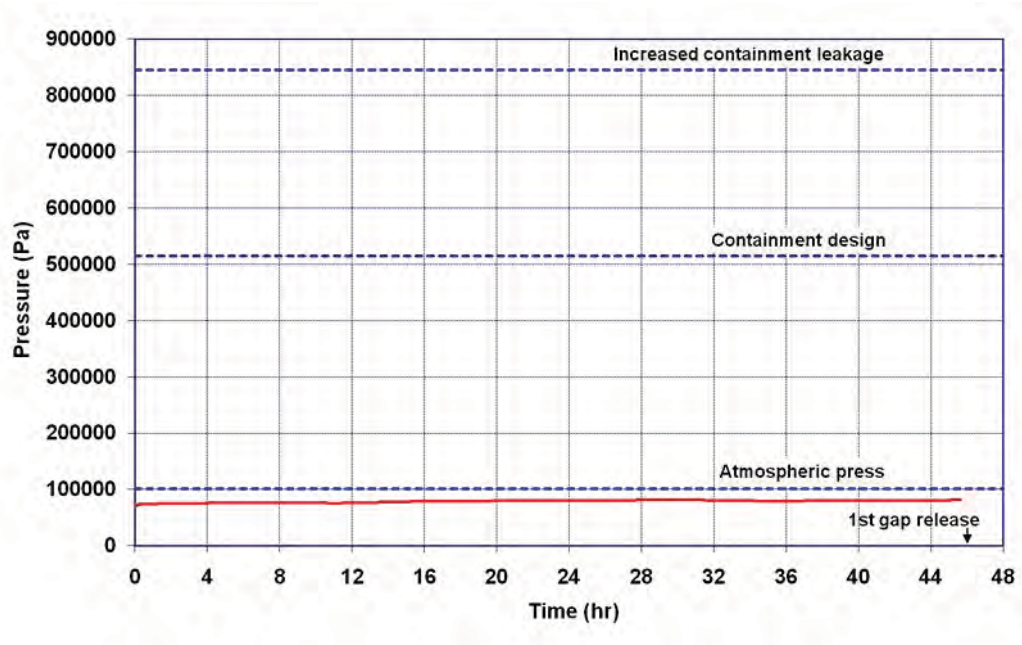

Figure 5-95 SGTR with Failed Operator Action-Containment Pressure

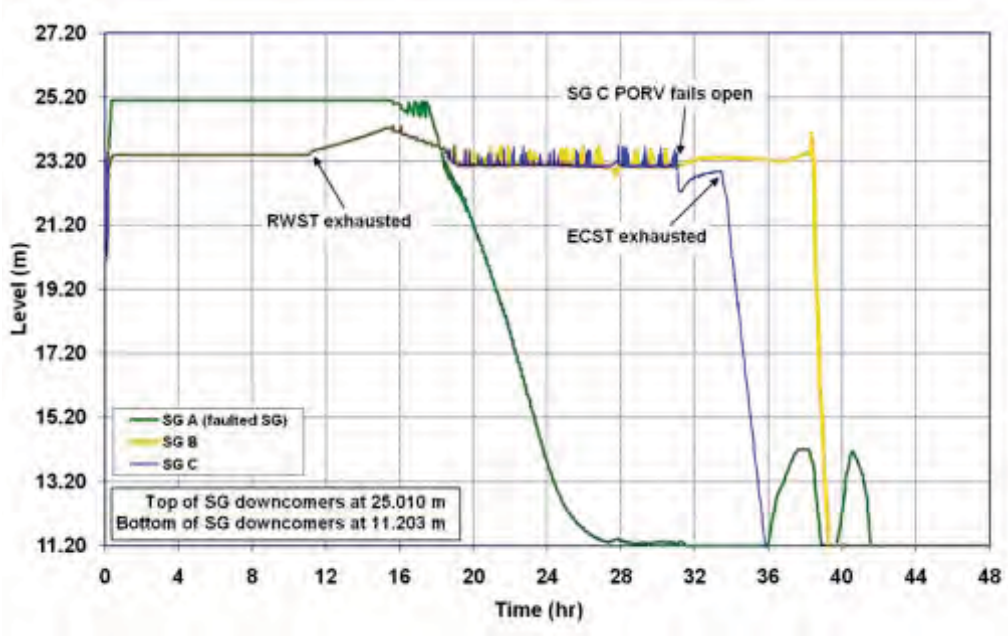

Figure 5-96 STGR with Failed Operator Action- Steam Generator Level

5.4.2.2 Radionuclide Release

The radionuclide release analysis is not presented for this scenario due to the low likelihood that operators would fail to depressurize and cool down the reactor system for the 43 hr necessary for the reactor core to begin to uncover (i.e., predicted by MELCOR). Table-top exercises performed with operators during site visits substantiate the low likelihood that operators would fail to depressurize and cool down the reactor system especially given the ample time for TSC and EOF intervention.

5.4.3 Unmitigated - Spontaneous SGTR with Failed Operator Action and Faulted Steam Generator SORV

Table 5-13 summarizes the timing of the key events in the SGTR with failed operator actions, and as a resultant SORV on the faulted steam generator (unmitigated). As described in Section 3.3.1, the accident scenario initiates with a spontaneous double-ended-guillotine rupture of one steam generator tube. After about three minutes, the reactor successfully trips and the containment isolates. The full complement of systems at Surry Power Station is considered functional in this scenario including all systems associated with engineered safeguards and instrumentation and control as well as all auxiliary and emergency systems. However, operator actions are not successful at isolating the faulted steam generator or at cooling the reactor system (i.e., to permit operation of the RHR system) and the PORV on the faulted steam generator fails open when liquid first flows through it. Eventually the RWST is exhausted (i.e., after ~8.75 hr) leading to core uncover (i.e., beginning at ~22.75 hr) and core damage. Due to the long amount of time to core damage, it was judged unlikely that the operators would not correct missed actions (i.e., failure to isolate the faulted SG, failure to cool down and depressurize, and failure to refill the RWST or connect to the unaffected unit's RWST). Section 5.4.3.1 summarizes the thermal-hydraulic response of the reactor and containment while Section 5.4.3.2 summarizes the associated radionuclide release from the fuel to the environment.

Table 5-13 The timing of key events for the Spontaneous SGTR with Failed Operator Action and Faulted Steam Generator SORV

Event Description	Time (hh:mm)
Spontaneous SGTR	00:00
Reactor scram	00:03
Turbine stop valves close	00:03
Steam dump valves open and modulate	Not accomplished*
Steam dump valves close (RCS temperature < 547 °F)	Not accomplished*
HHSI initiated (3 pumps)	00:03
First AFW delivery	00:03
Operators take control of AFW (as the SGs are overfilling)	00:10**
AFW delivery to faulted steam generator secured	00:12***
1 of 3 HHSI pumps secured	00:15
Faulted steam generator PORV 1st lifts	00:32
Faulted steam generator flooded	00:42
TDAFW fails (turbine floods)	00:42
Faulted steam generator PORV fails open (1st liquid flow through valve)	00:44
Faulted steam generator isolated	Not accomplished by operators
HHSI secured	Not accomplished by operators
Leakage through faulted steam generator PORV stopped	Not accomplished by operators
100 °F/hr cool-down initiated	Not accomplished by operators
RWST exhausted (safety injection ends)	08:43
First accumulator discharge	08:53
RCPs trip	12:43
Core uncovering begins	22:48
First fission product gap release	26:44

* The automatic operation of steam dump valves was not represented in the Surry MELCOR model. The thermal-hydraulic signature in the subject calculation suggests that the valves might be active for the first 6 min following scram but at no other time. Valve action would reduce RCS temperature by ~25 °F for the first few min and by a few °F in the next few min. The differences are thought to be inconsequential.

** Best-estimate timing for operators assuming manual control of AFW is 15 min. A discrepancy in the MELCOR modeling initiated level control of AFW at 10 min.

*** Best-estimate timing for operators securing AFW delivery to the faulted steam generator is 15 min. A discrepancy in the MELCOR modeling interrupted AFW to the steam generator at 12 min and 30 sec. AFW to the faulted steam generator is stopped on account of runaway high level in the generator.

5.4.3.1 Thermal-hydraulic Response

Figure 5-97 through Figure 5-102 present the thermal hydraulic response predicted by MELCOR for an accident with the same initiation event, system availabilities, and mitigative actions as the accident of the preceding Section with one distinction. The distinction is the inclusion of an additional mechanism for the PORV serving the faulted steam generator where the valve is failed open when liquid first flows through it. System pressure histories are shown in Figure 5-97. Figure 5-98 and Figure 5-99 show reactor pressure vessel level and fuel cladding and reactor vessel lower head temperatures, respectively. RWST and ECST inventories are tracked in Figure 5-100, while containment pressure is tracked in Figure 5-101. Steam generator level is tracked in Figure 5-102.

As in the accident of the preceding section, the SGTR quickly leads to a reactor scram, turbine stop valve closure, HHSI actuation, and AFW delivery. The flow of primary system coolant through the tube rupture into the secondary side of the faulted steam generator results in a fairly sustained leak to the environment beginning at 32 min when the PORV serving the generator first lifts. The faulted steam generator floods at 42 min and liquid first flows through the PORV serving the generator at 44.5 min. The PORV is failed open at this time in the MELCOR calculation instituting a sustained leak from the RCS to the environment. The assumption here is that the valve is not designed to pass violent critical flows of flashing liquid and would hence fail.

Once level control of AFW is initiated in the MELCOR calculation (at 10 min simulating the operators taking control), HHSI stably removes core decay heat and reduces core temperatures up to the time when the useable inventory of the RWST is exhausted thereby ending injection. There is no heat removal by the intact steam generators during this time as evidenced in Figure 5-100 where no drawdown on ECST inventory shows to occur. Note that pressure in the intact steam generators during this period is low relative to the setpoint of the main steam line PORVs such that no venting of the generators occurs and hence no heat removal is accomplished by them. Coinciding flow out the tube rupture is governed by the head-versus-flow characteristics of the HHSI pumps, the flow resistance at the tube rupture, and by either the set point of the PORV on the faulted steam generator (i.e., until the PORV fails open) or by the relief capacity of the PORV (i.e., once it fails open). The RCS heats to saturation over the course of a few hours following the RWST being exhausted and an extended boil-off of the RCS inventory begins. Note that the RWST empties ~2.25 hr earlier in this scenario (i.e., failed operator action and SORV) than in the previous scenario (i.e., failed operator action). This is simply because more water is pumped by the HHSI system through the RCS, out the SGTR, and out the relief valve given a stuck-open valve than given a cycling valve. The RCPs are stopped in the MELCOR calculation at the first occurrence of void in the RCS simulating the pumps tripping on their own or the operators shutting them down on account of erratic performance. Unlike in the calculation of the previous section, the intact steam generators pressurize up the setpoint of the main steam line PORVs very late in the calculation close to the time when the core starts uncovering. Consequently, the generators do not serve in any meaningful heat removal as the accident progresses to core damage. The core uncovers with nominal level in the steam generators and most of the original ECST inventory unused.

The MELCOR calculation predicts that core uncovering initiates at 22 hr and 48 min. The first release of fission products from a fuel/cladding gap is seen at 26 hr and 44 min. Traces in Figure 5-97 through Figure 5-102 end at first gap release and figures of fission product tracking are not presented for the subject scenario on account of the great unlikelihood that operators would fail to depressurize and cool down the reactor system for some 22 hours.

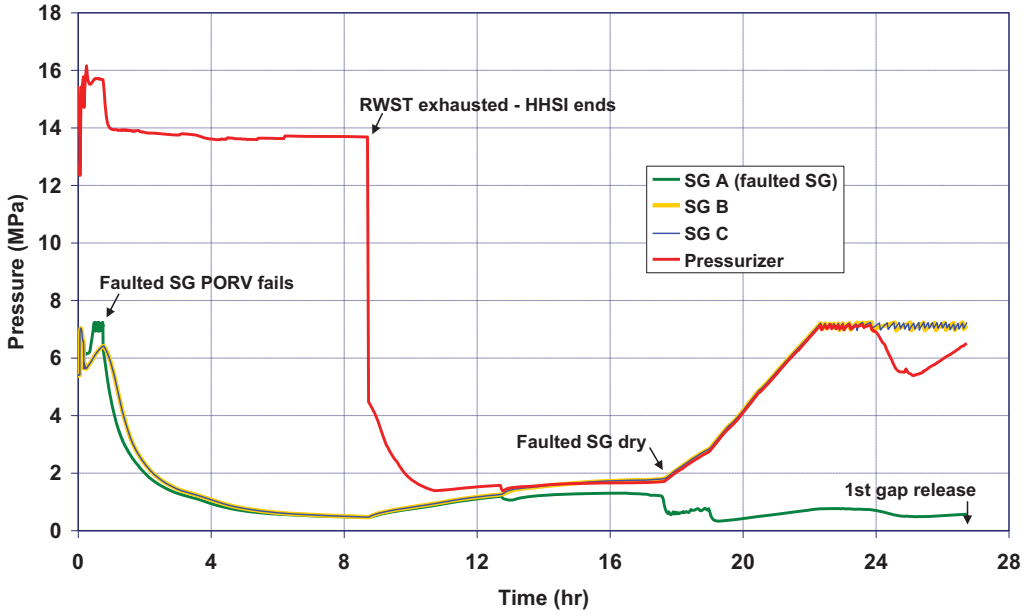

Figure 5-97 SGTR with Failed Operator Action and SORV – System Pressures

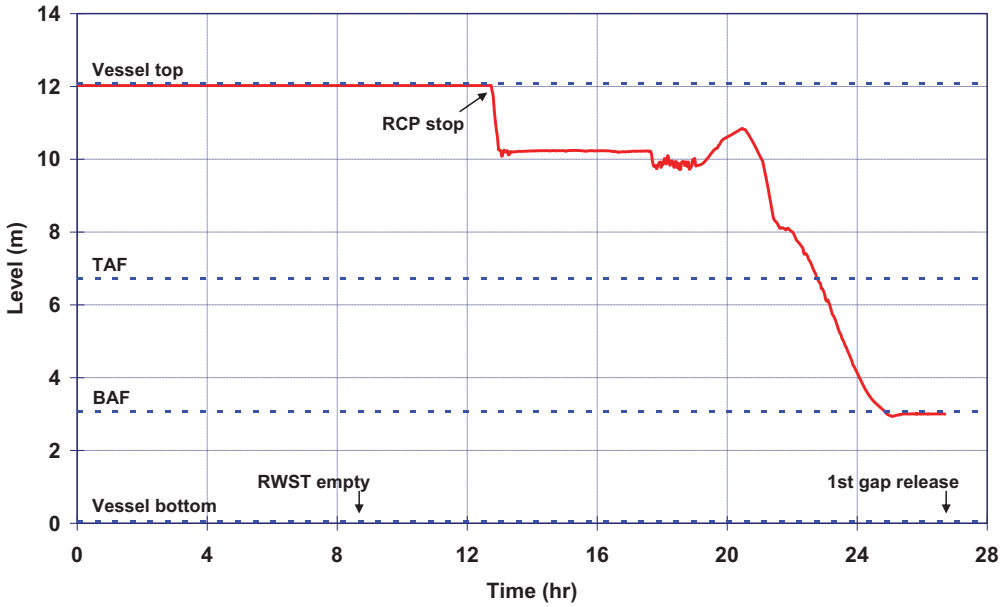

Figure 5-98 SGTR with Failed Operator Action and SORV – RPV Water Level

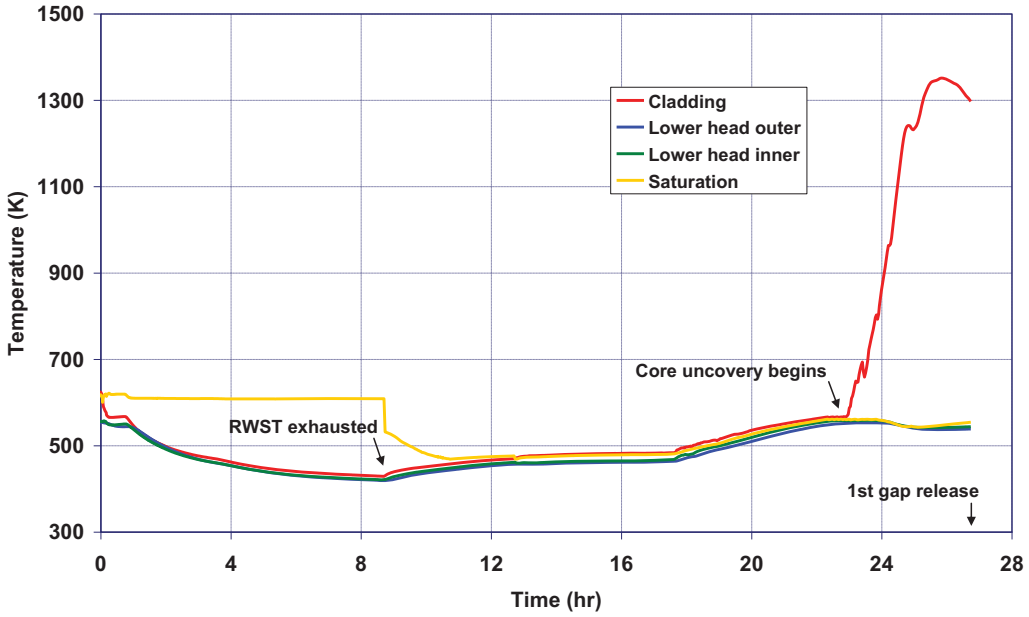

Figure 5-99 SGTR with Failed Operator Action and SORV – Max Clad and Lower Head Temperature

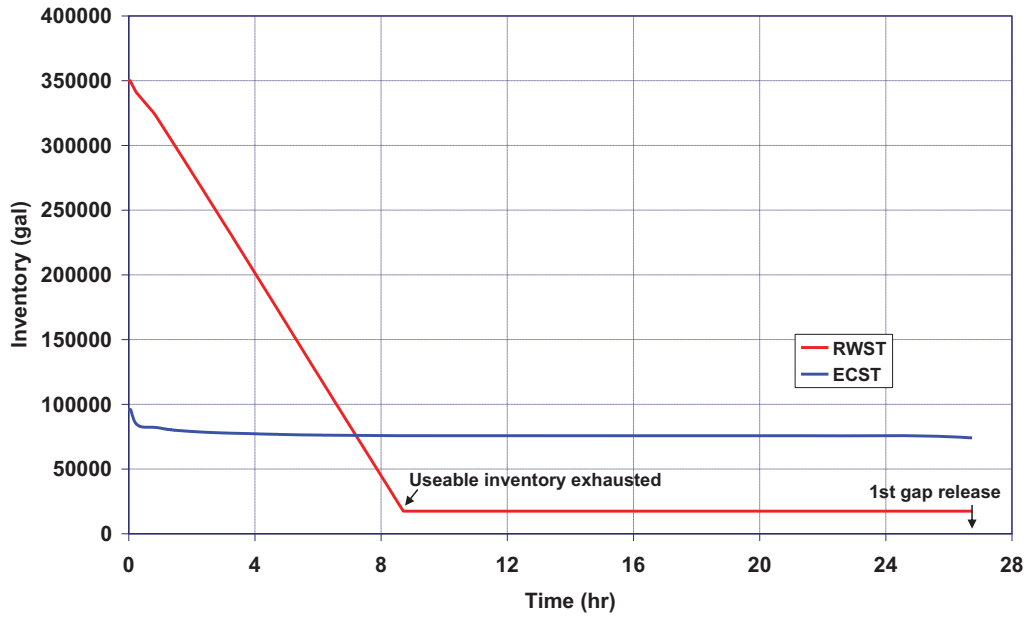

Figure 5-100 SGTR with Failed Operator Action with SORV – RWST and ECST Inventories

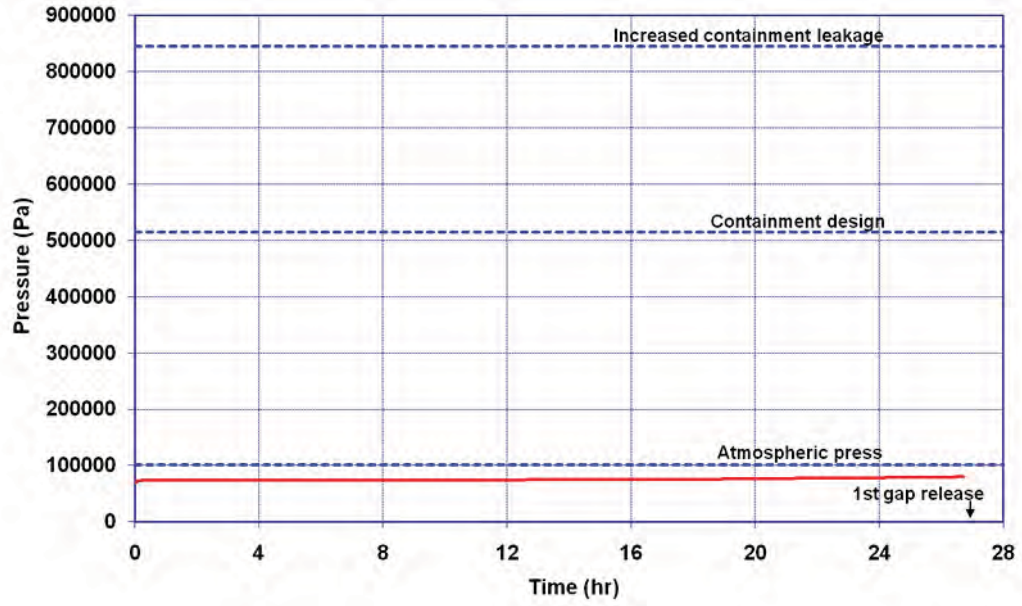

Figure 5-101 SGTR with Failed Operator Action and SORV- Containment Pressure

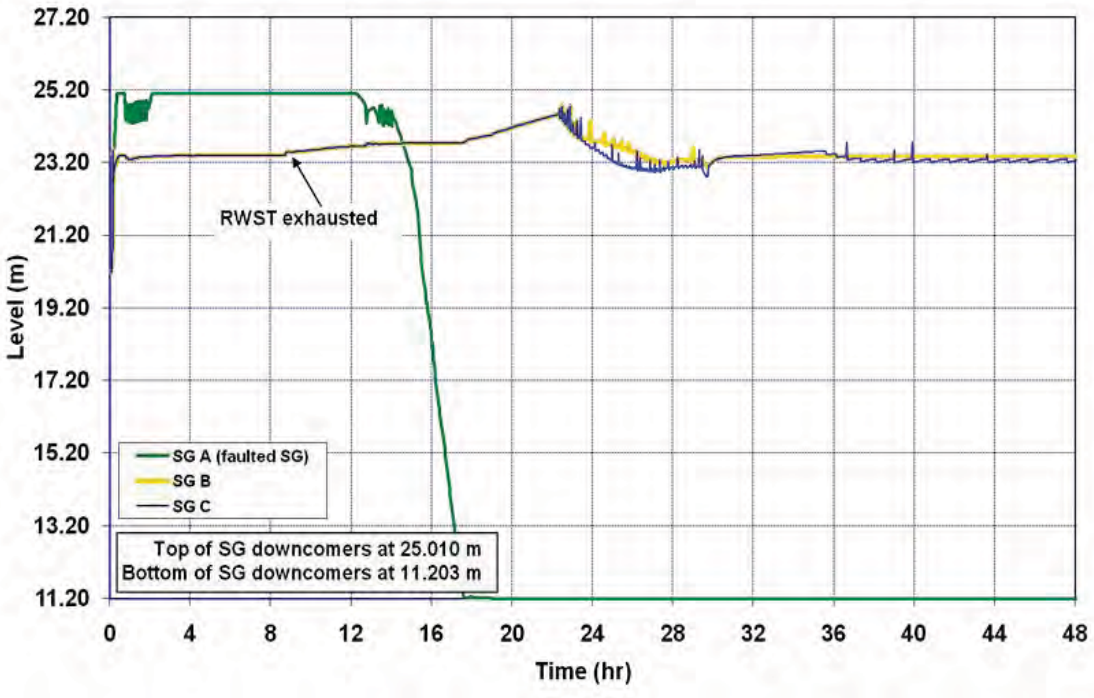

Figure 5-102 STGR with Failed Operator Action and SORV- Steam Generator Level

5.4.3.2 Radionuclide Release

The radionuclide release analysis is not presented for this scenario due to the low likelihood that operators would fail to depressurize and cool down the reactor system for the 22 hr necessary for the reactor core to begin to uncover (i.e., predicted by MELCOR). Table-top exercises performed with operators during site visits substantiate the low likelihood that operators would fail to depressurize and cool down the reactor system especially given the ample time for TSC and EOF intervention.

5.5 Interfacing System Loss of Coolant Accident

The ISLOCA scenario initiates with a common mode failure of both inboard isolation check valves in one leg of safety injection piping. The LHSI piping in the Safeguards outside of containment pressurizes to failure initiating a loss-of-coolant accident with containment bypass.

5.5.1 Unmitigated ISLOCA

The thermal hydraulic responses resulting for the unmitigated ISLOCA sequence are presented initially followed by the associated radionuclide migration. Table 5-14 summarizes the timing of the key events in the unmitigated ISLOCA.

Table 5-14 Sequence of Events for the Unmitigated ISLOCA

Event Description	Time (hh:mm:ss)
LHSI check valves fail	00:00:00
LHSI piping ruptures in Safeguards Area (outside Containment)	00:00:00+
Safeguards Area personnel door opens	00:00:16
SCRAM	00:00:22
ECCS initiates	00:00:26
Safeguards Area filtered exhaust ventilation system starts	00:00:26
Safeguards Area roof flashing tears	00:00:36
LHSI isolation valve MOV 1890C motor floods (valve inoperable)	00:02:41
RCP trip	00:03:11
MSVH/Aux. Bldg. pipe tunnel opens (penetration sealant dislodges)	00:04:13
Operators stop LHSI Pump A	00:06:17
Operators secure 1 of 3 HHSI pumps	00:15:00
Operators stop LHSI Pump B	00:15:44
Operators isolate LHSI pump suctions (RWST spillage to Safeguards Area ends)	00:16:18
Accumulators begin discharging	00:28:27
Switchover to hot leg injection	00:45:00
Operators begin cooldown	01:00:00
Accumulators exhausted	01:12:00
Operators secure 2 of 3 HHSI pumps	01:45:00
RWST exhausted, HHSI ends	06:12:00
Water level at TAF	10:15:00
First fuel rod gap release	12:49:00
First hydrogen burn	13:29:00
Release of 1% of core inventory of iodine to environment	13:39:00
Safeguards roof fails grossly (from hydrogen burn)	13:54:00
Reactor lower head fails	18:34:00

The operator actions identified in this table are critical to delaying the onset of core damage, those actions being:

1. Stopping LHSI Pump A at 6 min and 17 sec
2. Stopping LHSI Pump B at 15 min and 44 sec
3. Isolating the LHSI pump suctions from the RWST at 16 min and 18 sec
4. Stopping two of the three total HHSI pumps to conserve RWST inventory

With these actions accomplished, MELCOR predicts the onset of core damage at 12 hr and 49 min. Without these actions accomplished, MELCOR predicts the onset of core damage much earlier.

The thermal hydraulic responses and releases of radionuclides predicted by MELCOR in the unmitigated ISLOCA calculation and related separate-effects (deposition) calculation are presented below.

5.5.1.1 Thermal Hydraulic Response

The thermal hydraulic response in the MELCOR ISLOCA calculation is illustrated in Figure 5-103 through Figure 5-125. Presentation of these figures is grouped by RCS, Containment, Safeguards, and Safeguards ventilation response.

RCS Response:
Figure 5-103 shows the pressure response of the RCS and steam generators to the ISLOCA. Figure 5-104 shows the flow through the break expressed as an equivalent volumetric flow of cold water. The pressure response to the 2.57" diameter break is dramatic. RCS inventory loss is severe to the point where the primary and secondary systems decouple. Timing comparisons with Figure 5-108 and Figure 5-109 indicate that pressure approaches atmospheric once steam and hydrogen production in the reactor vessel subside and especially after the reactor vessel lower head fails.

Figure 5-105 shows ECCS flow rates. LHSI flows are to the Safeguards Area through the ISLOCA pipe break. The shutoffs of LHSI Pump A at 6 min and 17 sec and of LHSI Pump B at 15 min and 44 sec are evident in the combined LHSI trace. HHSI is to the RCS cold legs initially. RWST drainage to the Safeguards Area ends with the operator action at 16 min and 18 sec of isolating the LHSI pump inlets. The shutoff of one HHSI pump at 15 min is evident in the combined HHSI trace as is the manual transition from cold leg injection to hot leg injection at 45 min. The step drop at 1 hr and 45 min reflects the manual shutoff of another HHSI pump (leaving just one of three total HHSI pumps running). HHSI ends at 6 hr and 12 min when the RWST is exhausted. RWST inventory is shown in Figure 5-106. The inflections in the trace in this figure reflect the various LHSI and HHSI pump shutoffs.

Accumulator discharge is illustrated in Figure 5-107. Discharge initiates when RCS pressure drops to 600 psig. The accumulators discharge at an approximately uniform rate until exhausted.

Reactor vessel water level is shown in Figure 5-108. With the exception of some early fluctuations accentuated by shutting off one HHSI pump at 15 min, level is maintained well above TAF until HHSI ends at 6 hr and 12 min. Level begins receding at this time. Hydrogen production from fuel cladding oxidation is shown in Figure 5-109. Hydrogen production flattens in Figure 5-109 when the reactor vessel lower head fails dropping the disintegrated reactor core to the reactor cavity in Containment. Maximum reactor core temperature, intact fuel and fuel debris considered, is shown in Figure 5-110. The temperatures of the inner and outer surfaces of the reactor lower head (in Radial Ring 1) are shown in Figure 5-111. The sharp decrease in this figure beginning at 18 hr and 34 min is coincident with the lower head failing.

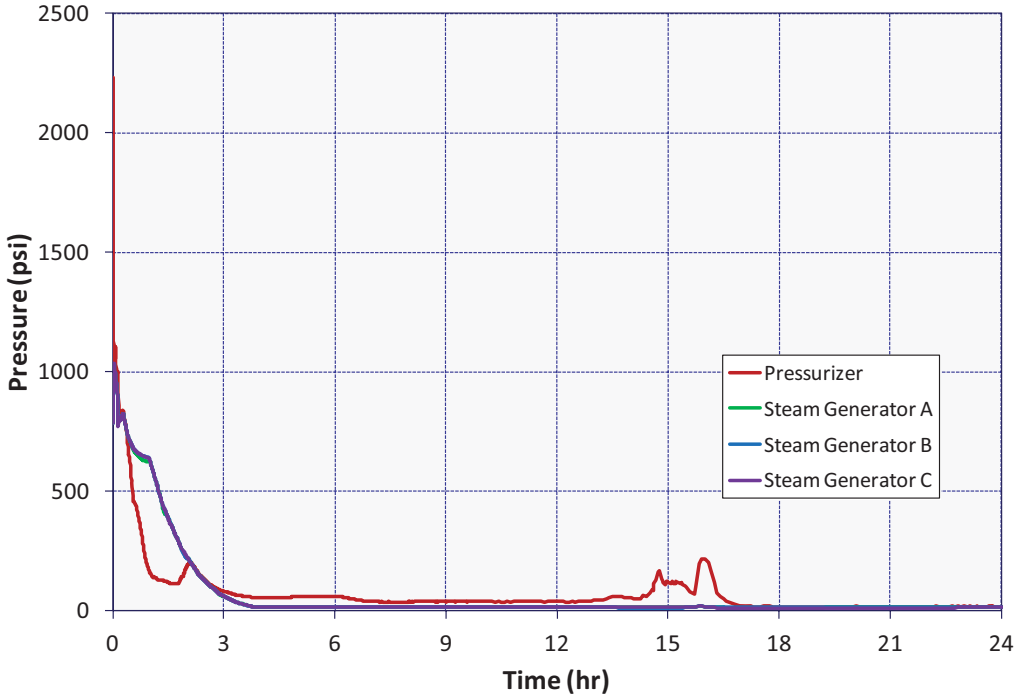

Figure 5-103 ISLOCA Reactor System Pressure

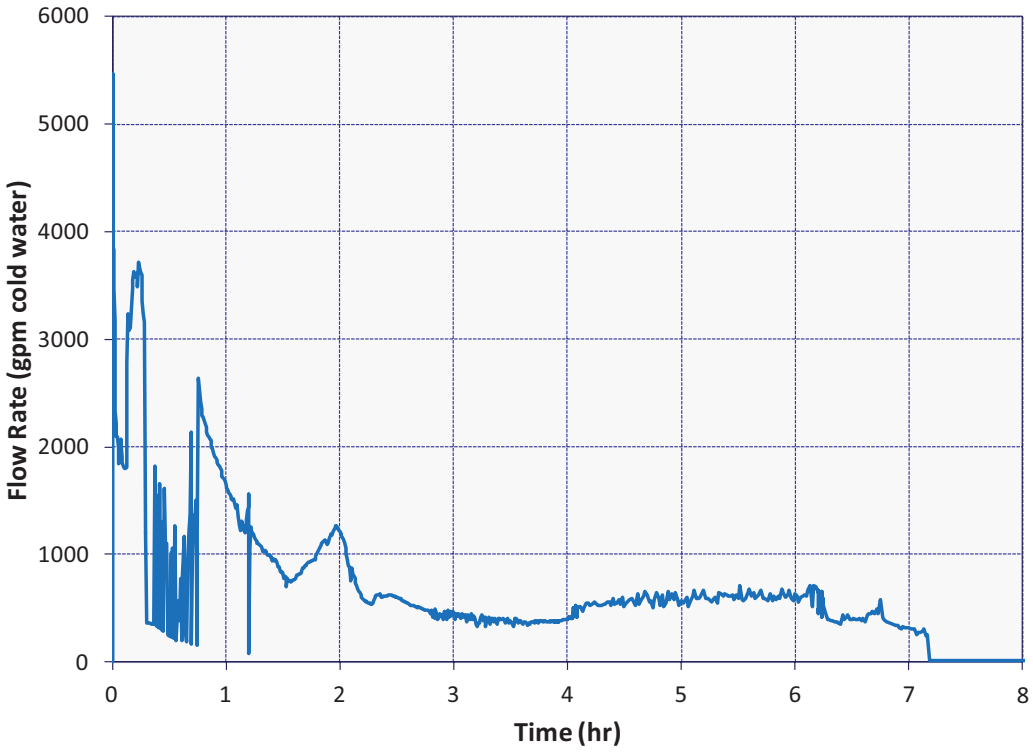

Figure 5-104 ISLOCA Break Flow (RCS to Safeguards)

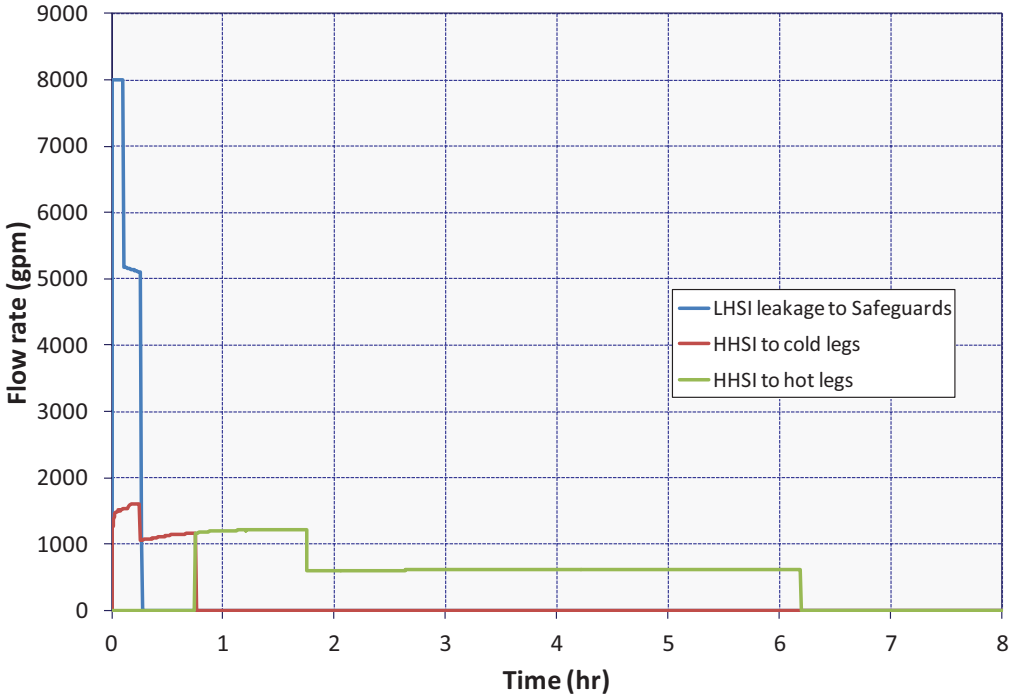

Figure 5-105 ISLOCA ECCS Flow

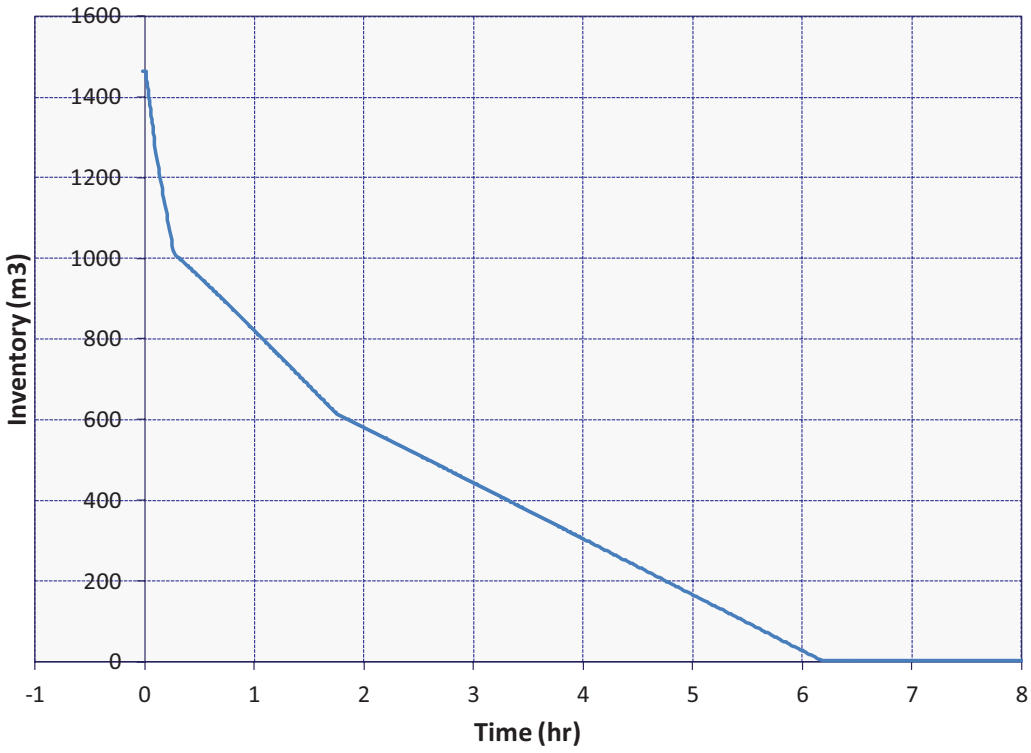

Figure 5-106 ISLOCA RWST Inventory

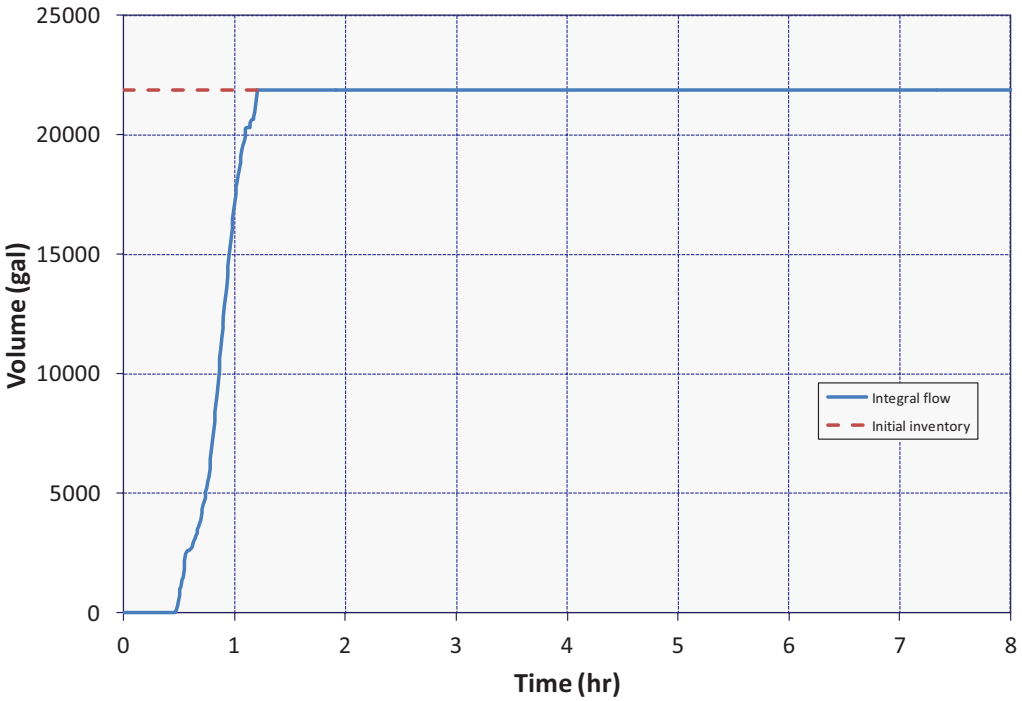

Figure 5-107 ISLOCA Integral Accumulator Flow

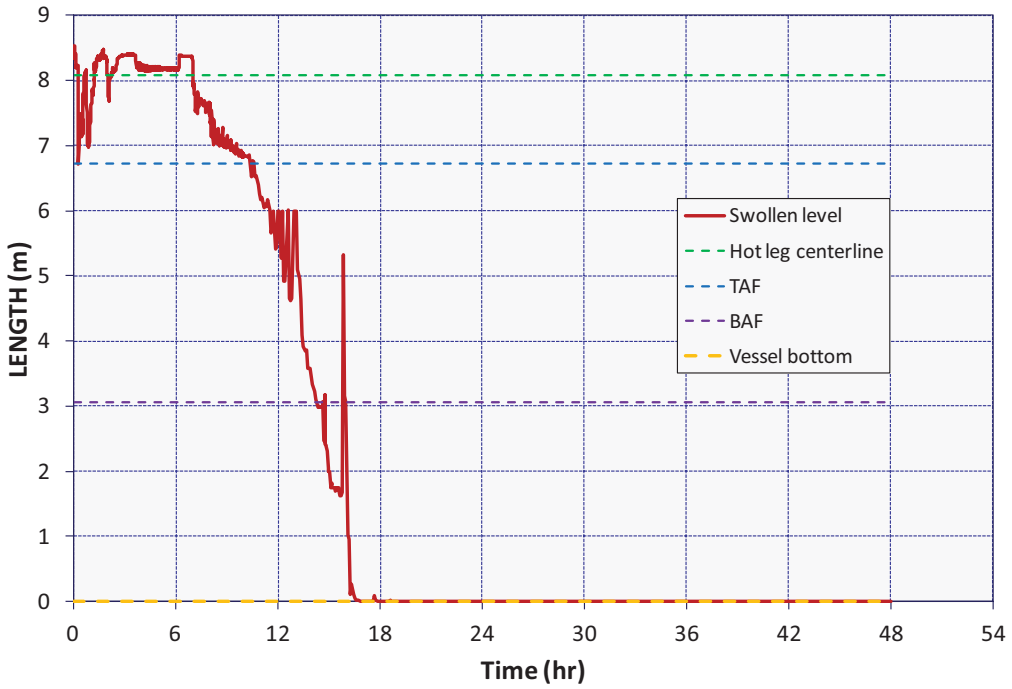

Figure 5-108 ISLOCA Reactor Vessel Water Level

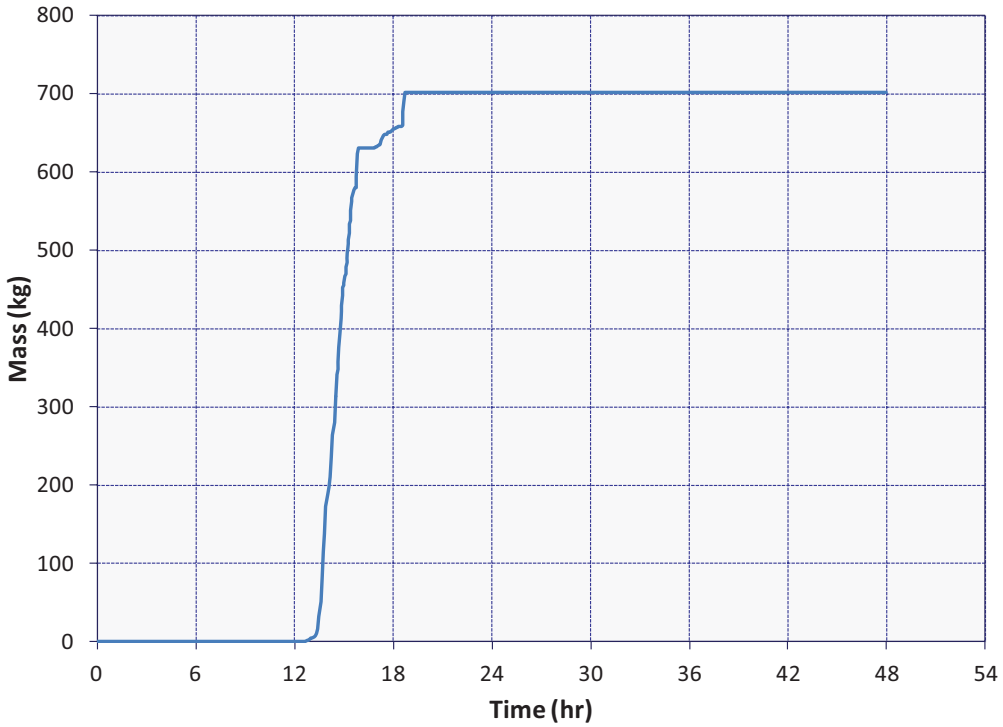

Figure 5-109 ISLOCA In-Vessel Hydrogen Production

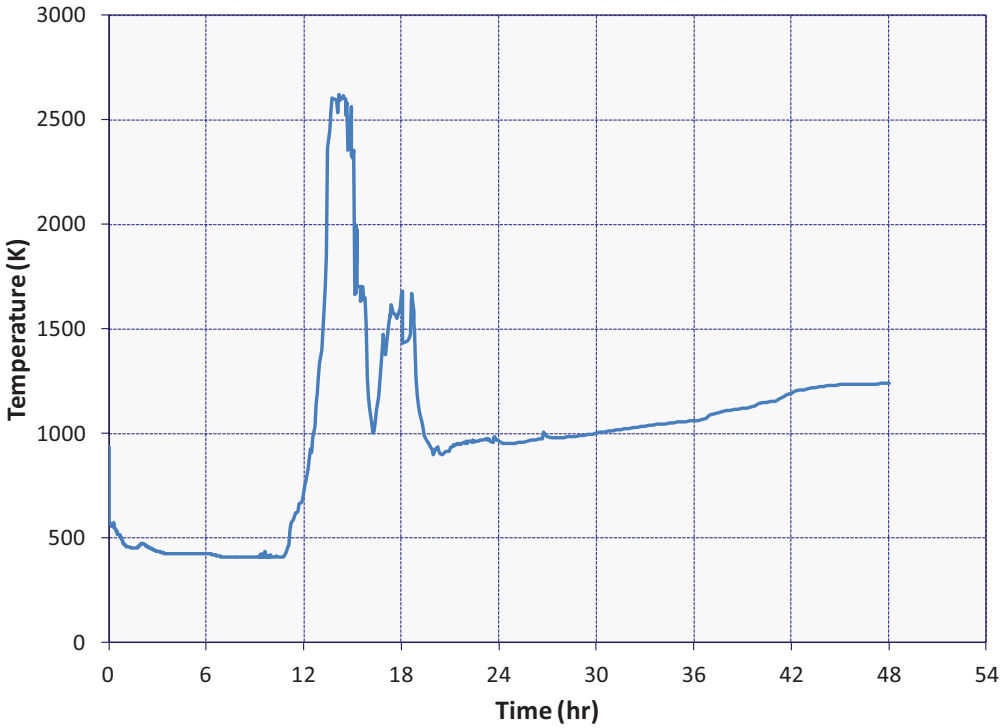

Figure 5-110 ISLOCA Maximum Core Temperature

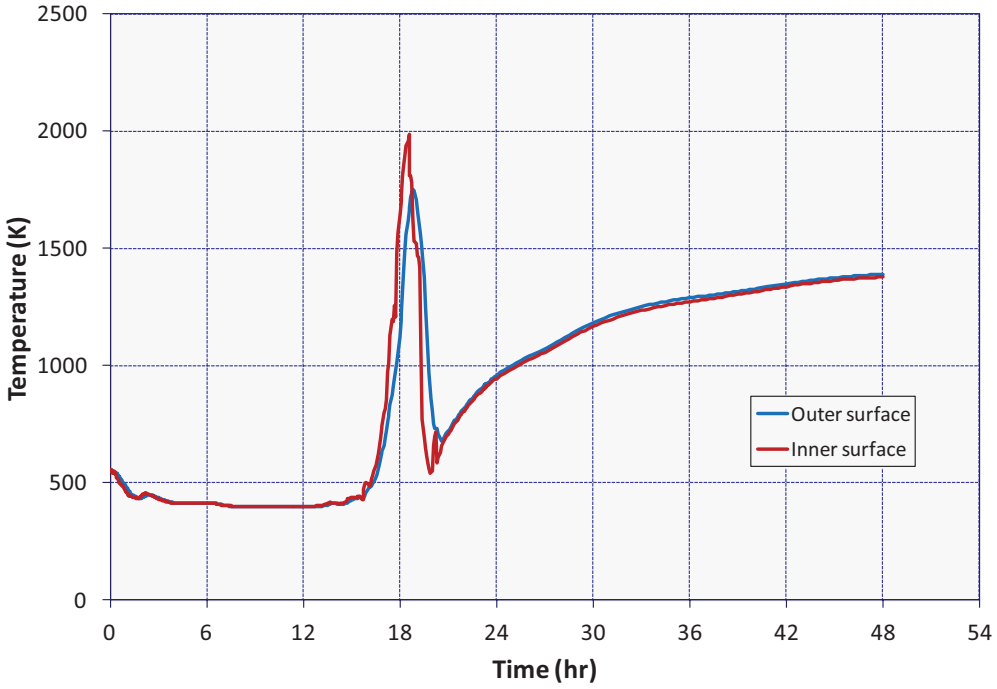

Figure 5-111 ISLOCA Reactor Vessel Lower Head Temperature

Containment Response:

Containment pressure is shown in Figure 5-112. Pressure is sub atmospheric (i.e., by design) until reactor lower head failure at 18 hr and 34 min. Spikes in the figure are attributable to hydrogen and carbon monoxide burns. Temperatures in Containment are illustrated in Figure 5-113.

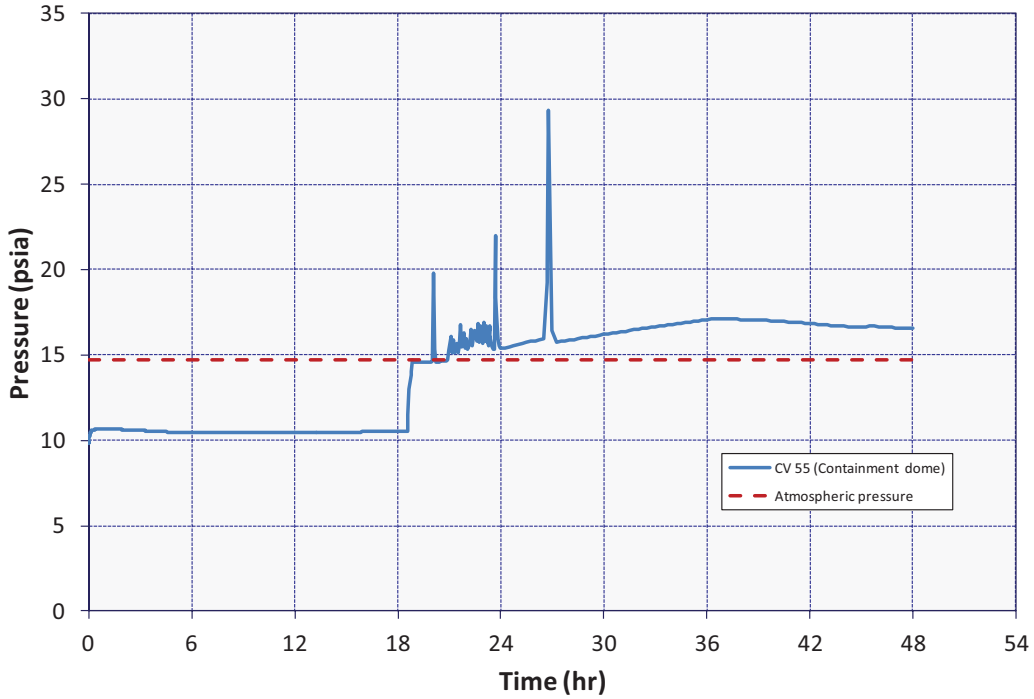

Figure 5-112 ISLOCA Containment Pressure

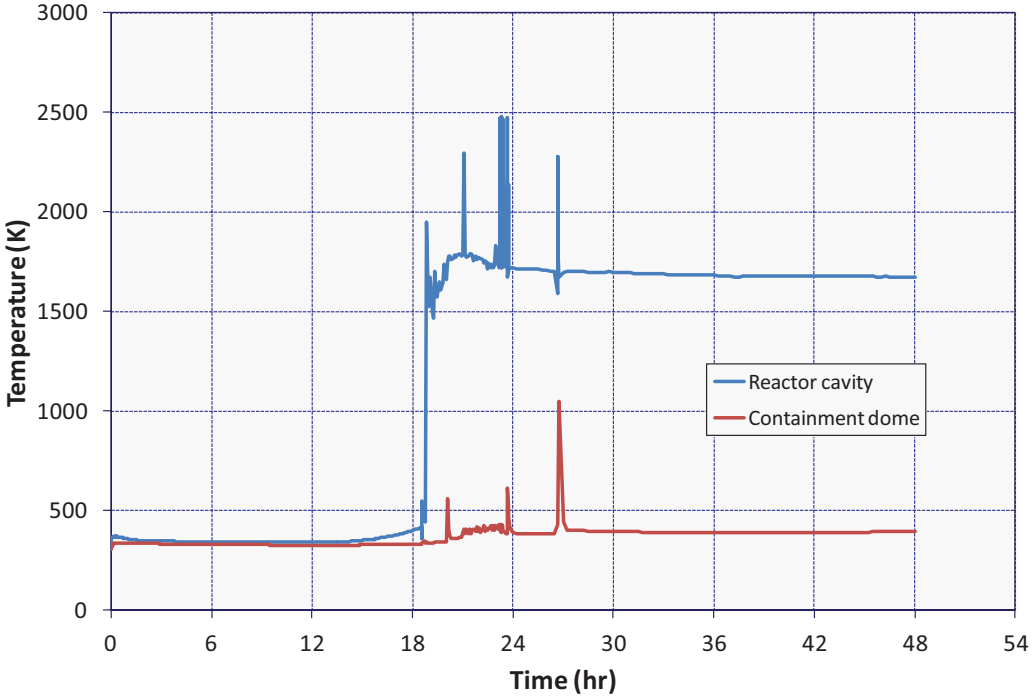

Figure 5-113 ISLOCA Containment Temperature

Safeguards Response:
The initial pressure response of the Safeguards buildings to the blowdown of the RCS is illustrated in Figure 5-114. While pressure increases are highest in the lower regions of the Safeguards Area, these regions are below grade and therefore reinforced. With respect to building boundary integrity, the pressure increase seen in the level of the Safeguards Area above grade (CV 860) is most important. The pressure response of this level can be seen in Figure 5-114 relative to the pressure necessary to fail the roof, (i.e., relative to the pressure estimated as necessary to tear the flashing spanning from the edge of the steel roofing to the containment cylinder).

Figure 5-115 illustrates the temperature (i.e., atmospheric) response of the Safeguards buildings. Spikes in this figure reflect hydrogen and carbon monoxide burns.

The depth of the pool formed in the Safeguards Area in the short term is shown in Figure 5-116 relative to the elevation estimated to flood the LHSI pump motors and the motor of LHSI isolation valve MOV 1890C. Based on this figure, it was concluded that the Safeguards flooding caused by the postulated ISLOCA would not threaten the LHSI pump motors but would short out the motor on MOV 1890C making it inoperable at 2 min and 41 sec. The “Pipe penetration” elevations labeled in the figure pertains to the 21” high by 5’ wide piping penetration in the 12” thick concrete wall between the Safeguards Area and the Containment Spray Pump Area. This penetration governs how deep flooding would get in the Safeguards Area. Long term flooding in the Safeguards buildings is presented in Figure 5-117. The continual drop in level from 6 or 7 hr to reactor lower head failure at 18 hr and 34 min is due primarily to leakage through the shaker space (FL 636) between the Recirculation Spray Pump B cubicle (CV 853) and the Containment Spray Pump Area (CV 861). The sudden level drop at lower head failure is because of water in the Safeguards pool being drawn back through the LHSI piping, through the breach in the lower head, and into containment. The driver for this flow is the initial sub atmospheric pressure of containment. With the exception of this water drawn into containment the eventual destination of all water lost through the ISLOCA pipe break is the Auxiliary Building.

The burning in the Safeguards buildings of hydrogen produced by fuel cladding oxidation and core-concrete interaction and of carbon monoxide produced by core-concrete interaction is illustrated in Figure 5-118. The associated energy release is shown in Figure 5-119 with annotations of the power related to two sections of the trace. Noteworthy is how continual the energy release from burning is during much of the calculation.

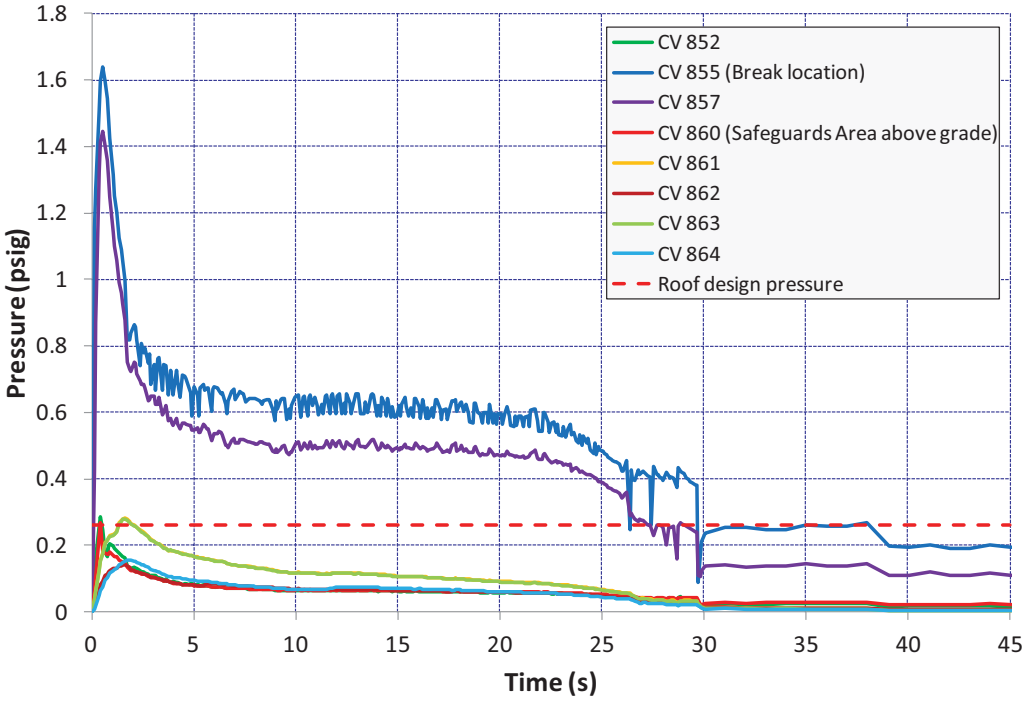

Figure 5-114 ISLOCA Safeguards Pressure

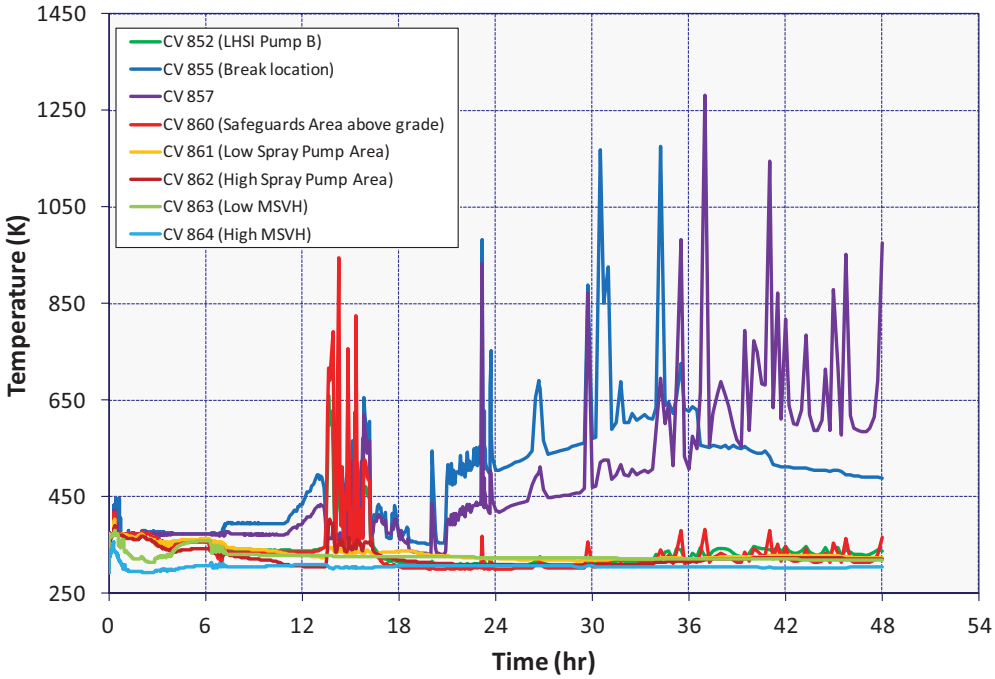

Figure 5-115 ISLOCA Safeguards Temperature

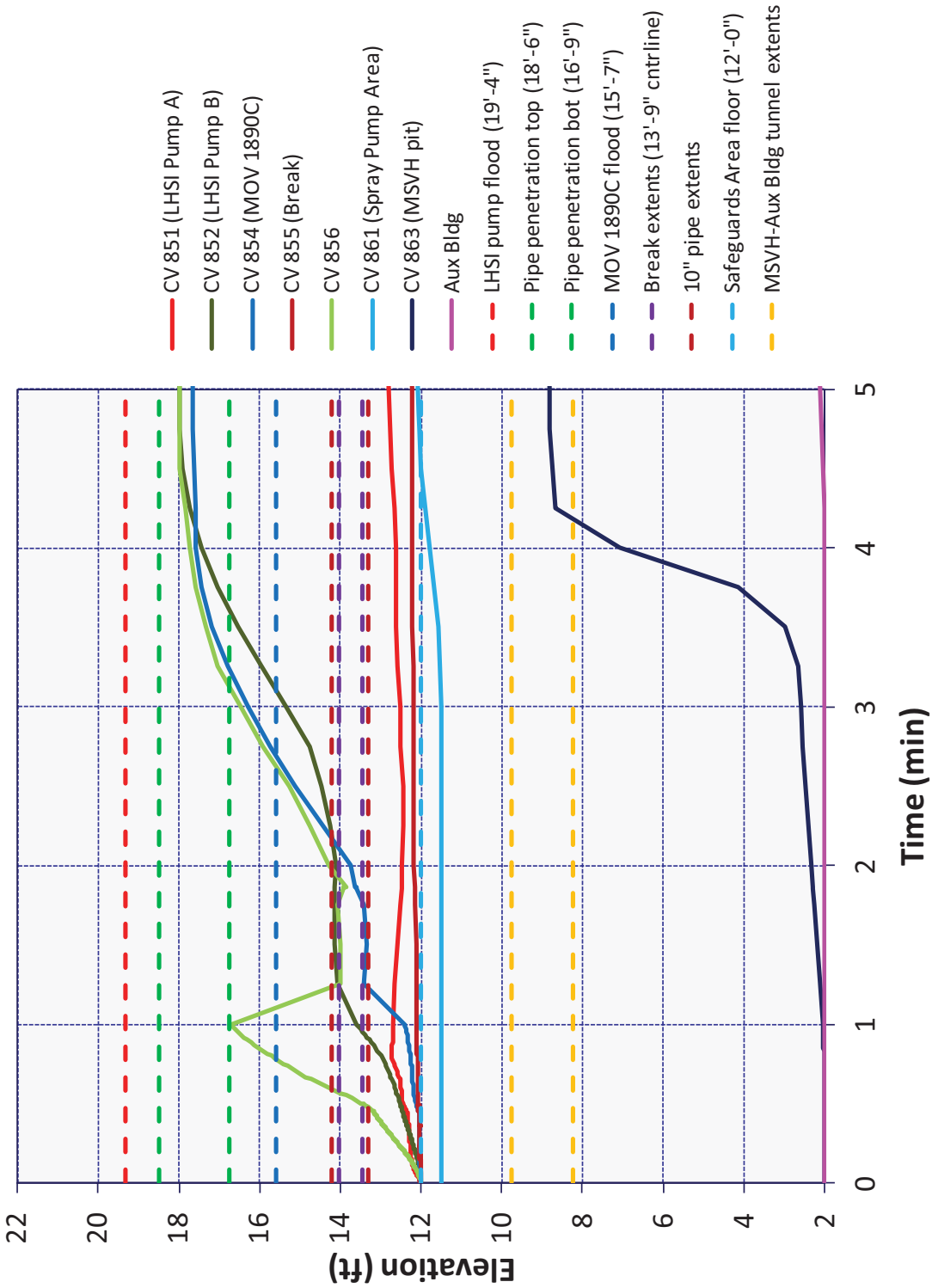

Figure 5-116 ISLOCA Safeguards Level Short Term

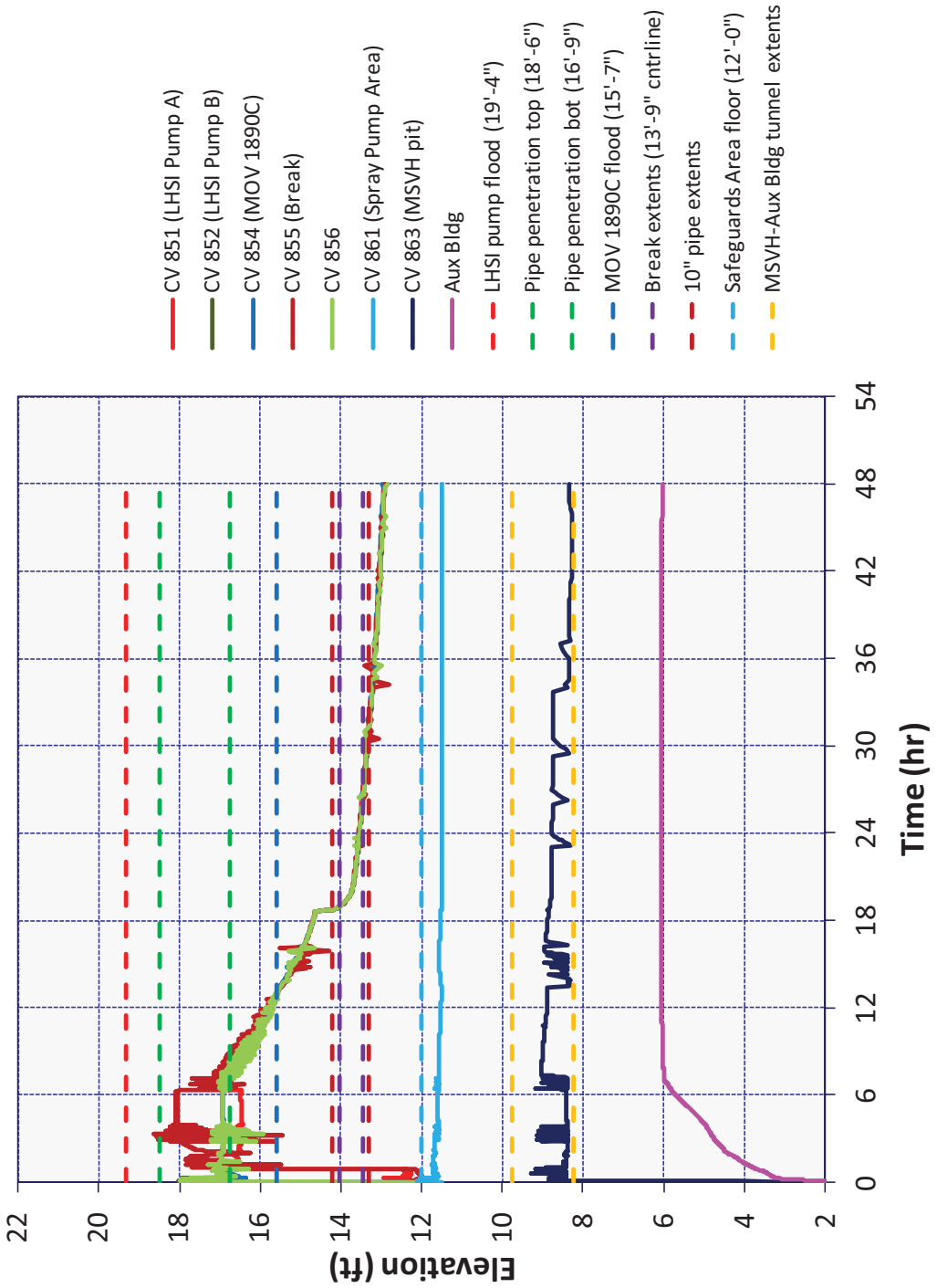

Figure 5-117 ISLOCA Safeguards Level Long Term

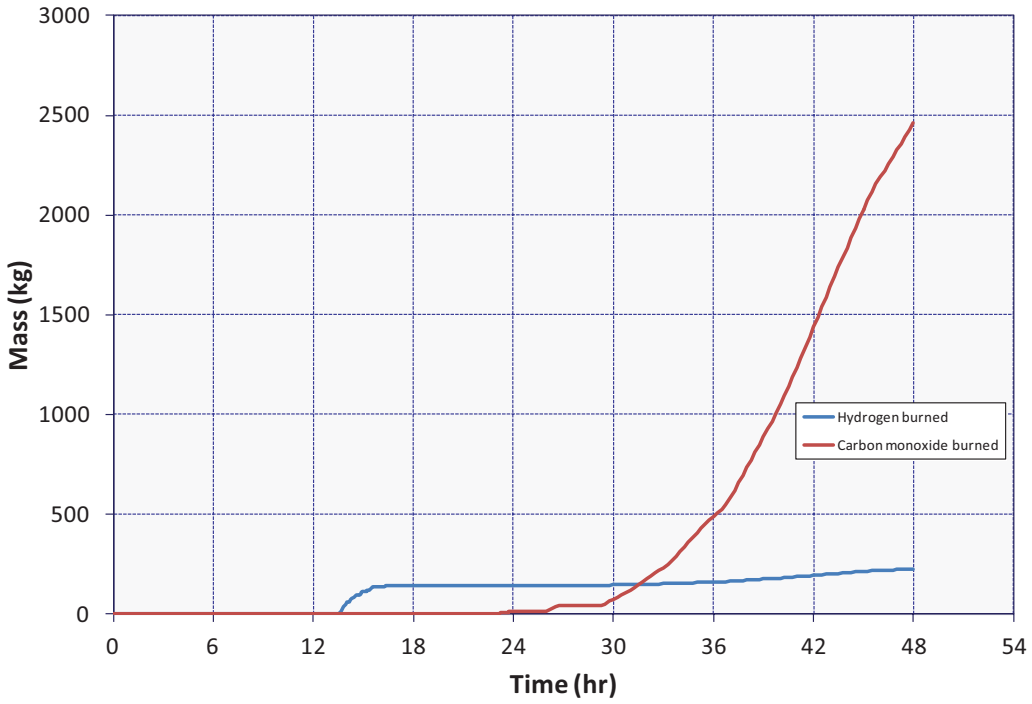

Figure 5-118 ISLOCA Integral Mass of H_2 & CO Burned in Safeguards Area

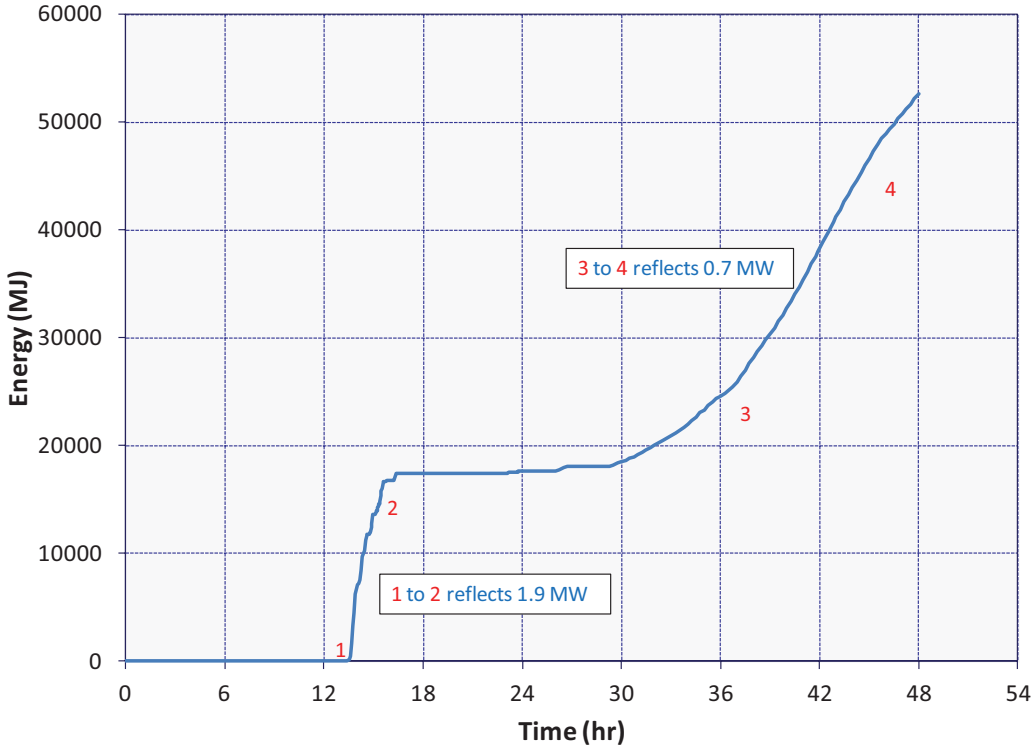

Figure 5-119 ISLOCA Energy Release from H_2 and CO Burns in Safeguards Area

Safeguards Ventilation System Response:

The head developed by the safety-related exhaust ventilation fans serving Safeguards is shown in Figure 5-120. The fans started upon generation of a safety injection signal. The head increased as the HEPA filters upstream of the fans loaded with particulate. The line at 21 inches of H_2O gauge in Figure 5-120, indicates the threshold that would result in the fans tripping in the calculation. The threshold in the calculation mimics the actual threshold at Surry. It could be reached given extensive filter loading.

Figure 5-121 shows the flow drawn by the exhaust ventilation fans, the portion of the flow drawn by the fans from Safeguards, and the "Central" portion of the flow drawn by the fans from other regions of the plant. Noteworthy is that the flow drawn by the fans is largely from areas of the plant other than Safeguards. Flow gradually decreases as the HEPA filters load.

Particulate loading on the HEPA filters is shown in Figure 5-122. Loading from the onset of core damage to the time of lower head failure is largely comprised of radionuclides released from the core. Later loading is made up of radionuclides and concrete from core-concrete interactions. Figure 5-123 shows the increasing differential pressure across the filter units and the HEPA filters load with aerosol. The traces in this figure include clean filter losses across the prefilters, HEPA filters, and charcoal filters.

Figure 5-124 shows temperatures along the Safeguard exhaust ventilation ducting relative to the maximum continuous service temperature rating for the HEPA filters (250 ºF). While the temperature of the flow drawn from Safeguards continually exceeds the filter temperature rating, the temperature in the filter inlet plenum does not. This is because of the mixing in the plenum of the hot Safeguards flow with the much larger cold flows (68 °F) drawn from other areas of the plant.

The power associated with the decay of fission products captured in the HEPA filters is presented in Figure 5-125. The airflow through the filters could easily remove the heat generation indicated.

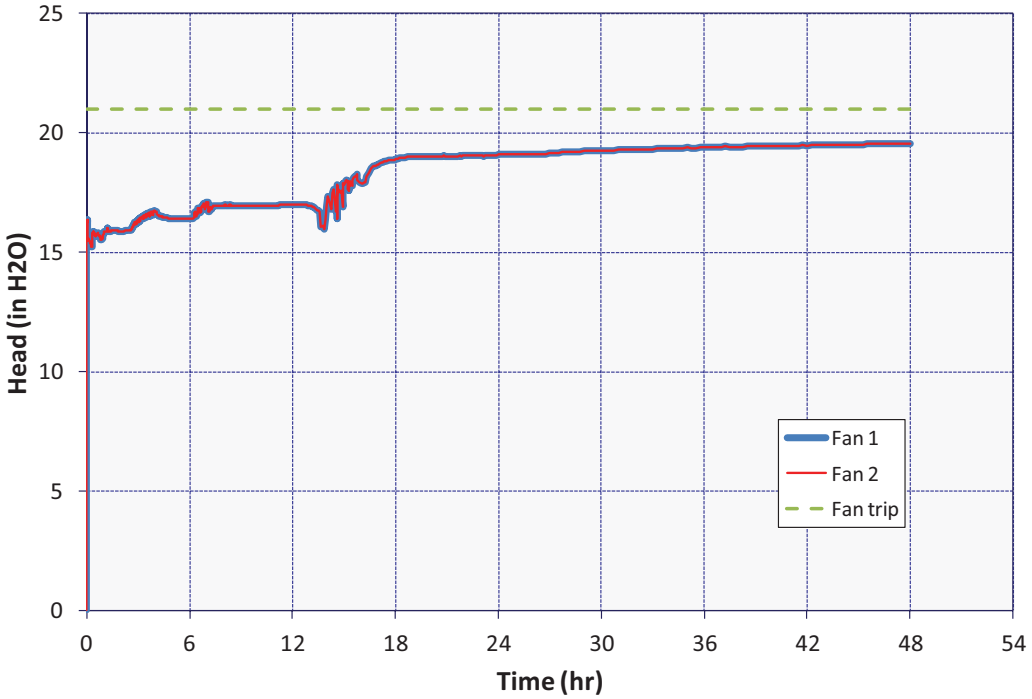

Figure 5-120 ISLOCA Safeguards Exhaust Ventilation Fan Head

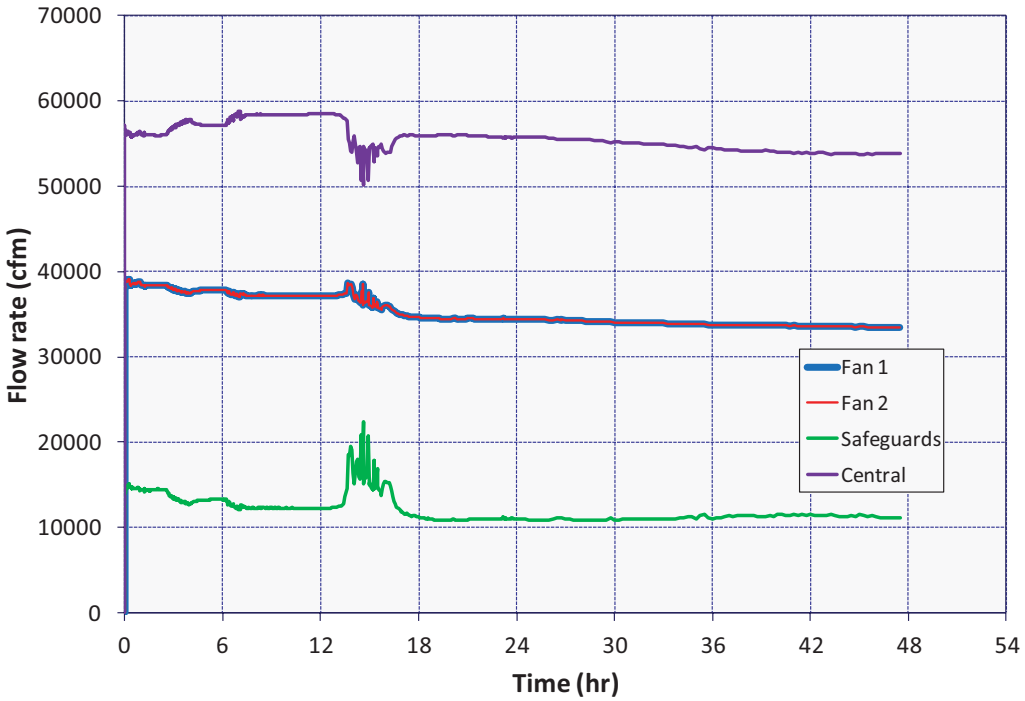

Figure 5-121 ISLOCA Safeguards Exhaust Ventilation Flows

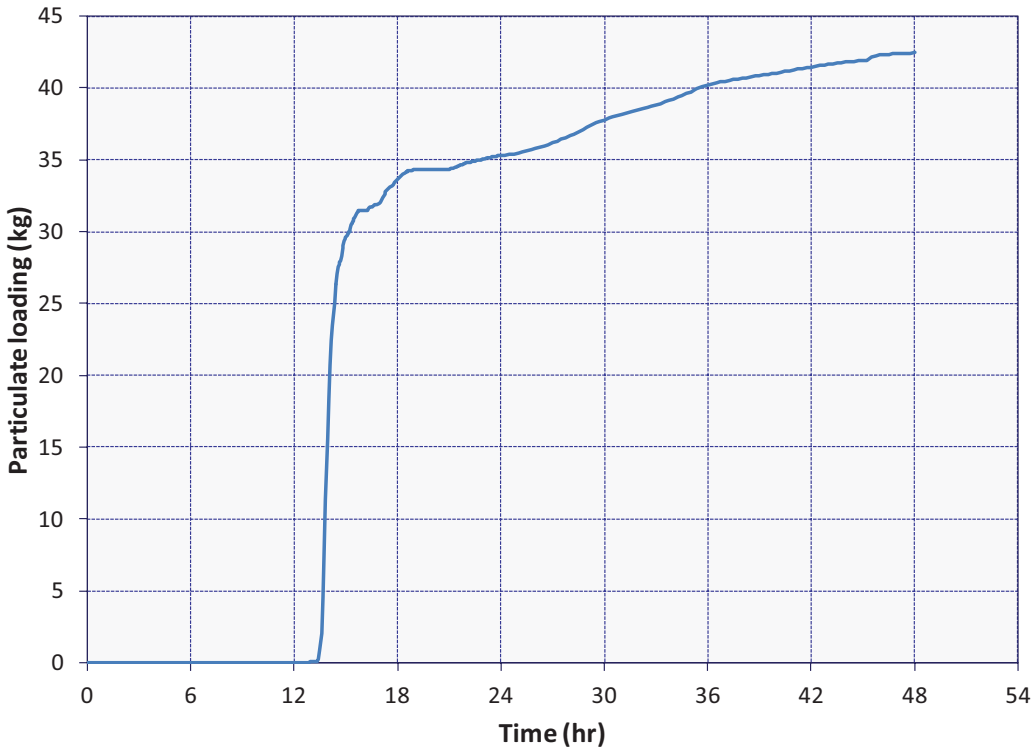

Figure 5-122 ISLOCA Safeguards Exhaust Ventilation Filter Aerosol Loading

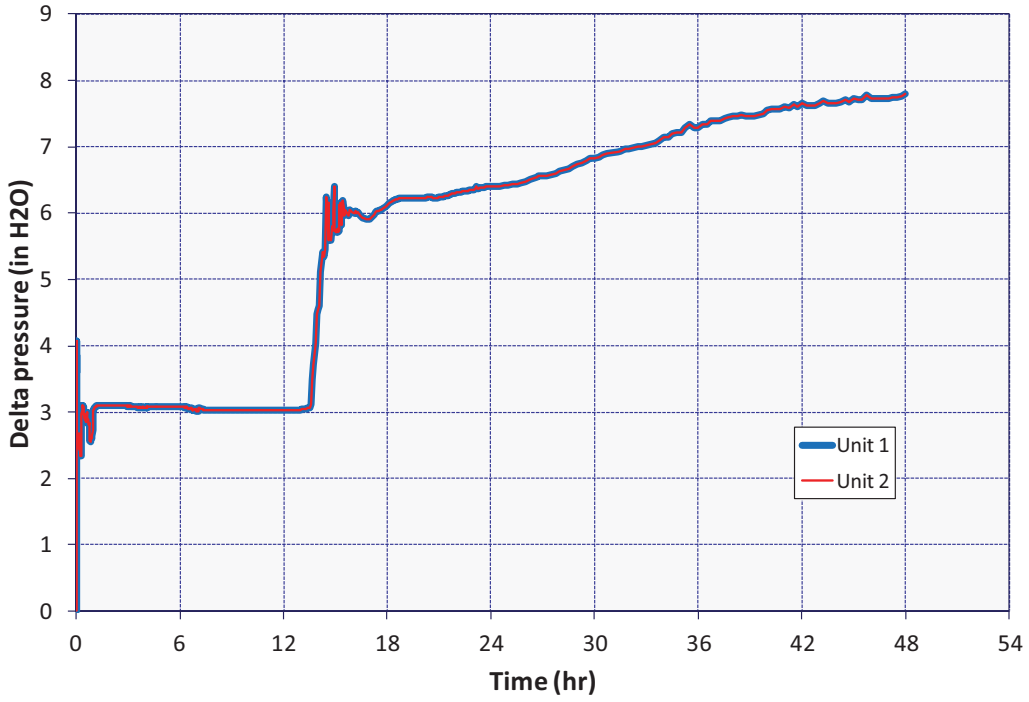

Figure 5-123 ISLOCA Safeguards Exhaust Ventilation Filter Unit Pressure Differential

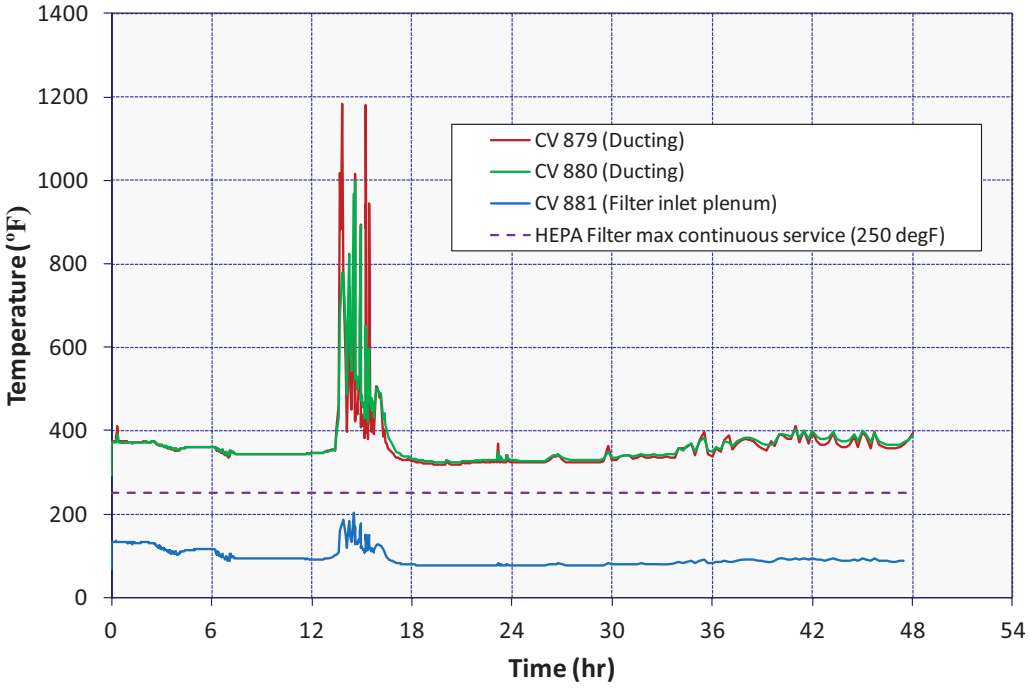

Figure 5-124 ISLOCA Safeguards Exhaust Ventilation Duct and Filter Inlet Temperature

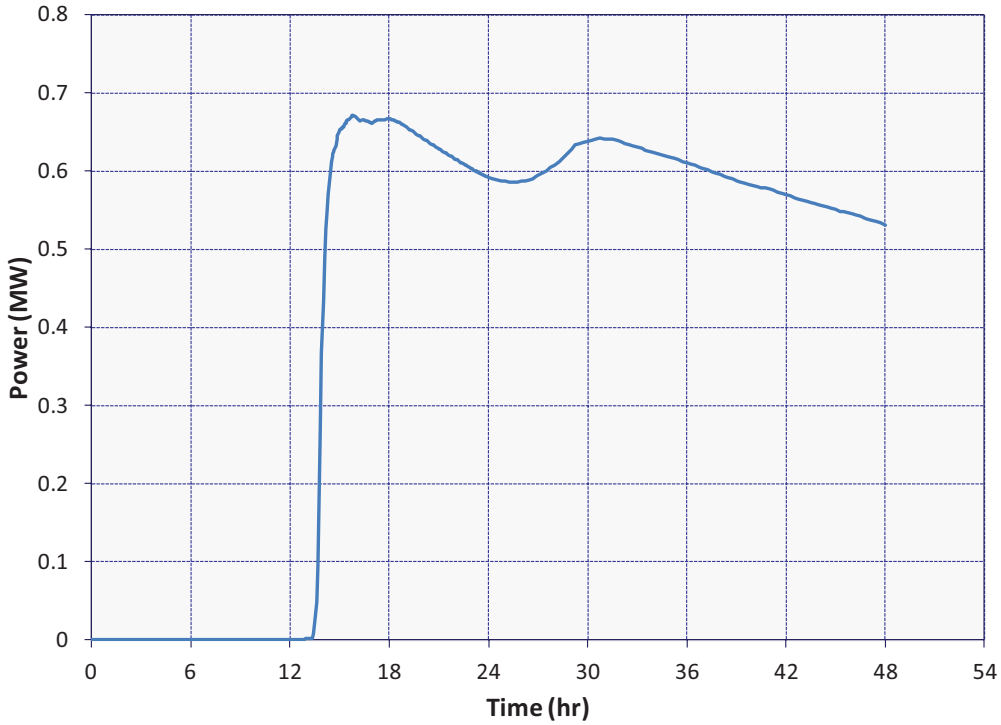

Figure 5-125 ISLOCA Decay Power of Fission Products Captured in Safeguards Exhaust Ventilation HEPA Filters

5.5.1.2 Radionuclide Release

The migration of radionuclides released from the core in the MELCOR ISLOCA calculation is illustrated in Figure 5-126 through Figure 5-129.

Figure 5-126 shows the fractional release to the environment of the original core inventory of the different radionuclide classes. The static conditions suggested in this figure after 18 hr are deceiving for some of the radionuclide classes because of the scale of the drawing and because of the time dependence of revaporization of radionuclide deposits in the LHSI piping not being captured in the overall ISLOCA calculation. The time dependence of this revaporization can only be seen in the separate-effects calculation. The results of the separate-effects calculation are presented in Section 5.5.2. Note that although the time dependence of revaporization of radionuclide deposits in the LHSI piping is missing from the overall ISLOCA results, the amounts of materials revaporized are accounted for. The migrations of the materials to the Safeguards Area do, however, come earlier in the overall calculation than they should.

The distribution of cesium throughout the MELCOR model is presented in Figure 5-127. The step change seen at 16 hr and 15 min is coincident with the reactor vessel lower plenum drying out. When a pool within a MELCOR control volume evaporates entirely, the hydrosols suspended within it are introduced as aerosols to the atmosphere in the same control volume. This happened in the control volume representing the lower plenum at the subject time and at least some of the aerosols introduced were swept into the LHSI piping where they promptly deposited by means of turbulent deposition and/or impaction.

The distribution of iodine throughout the MELCOR model is presented in Figure 5-128. The sudden increase in iodine in containment and the sudden decrease in iodine in Safeguards, coincident with reactor lower head failure at 18 hr and 34 min, is due to water being drawn into containment from Safeguards. The driver for this was the initial sub atmospheric pressure in containment. The gradual reduction in the RCS portion of the distribution between 25 hr and 31 hr is cesium iodide vapor evolving from aerosol deposits in the RCS. The vapor later condensed and the resulting aerosol was drawn into the HEPA filters of the Safeguards exhaust ventilation system.

The releases of cesium iodide to the environment through the various release pathways represented in the MELCOR model are plotted in Figure 5-129. Each trace in Figure 5-129 shows the release through a particular pathway as a percentage of the current (i.e., instantaneous) total release through all pathways. Since release rates through the various pathways peak at different times, some of the traces in the figure do not increase continually. Pathways through which less than 0.5% of the total release ultimately passed have been excluded.

Of interest in the MELCOR calculation were the amounts of radionuclides scrubbed by the pool formed on the Safeguards floor as gas laden with radionuclides bubbled up from the ISLOCA pipe break through the pool. Amounts were trivial compared to amounts deposited in the LHSI piping or captured in the HEPA filters (e.g., 3.31 kg (pool) versus 550 kg (piping) and 42.45 kg (HEPA filters), respectively).

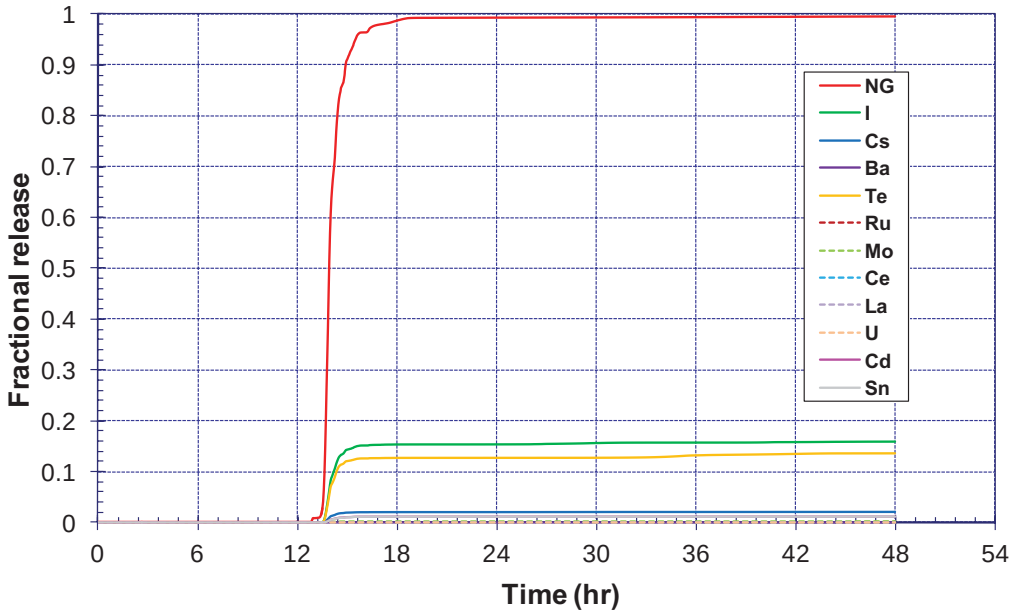

Figure 5-126 ISLOCA Fission Product Release to the Environment

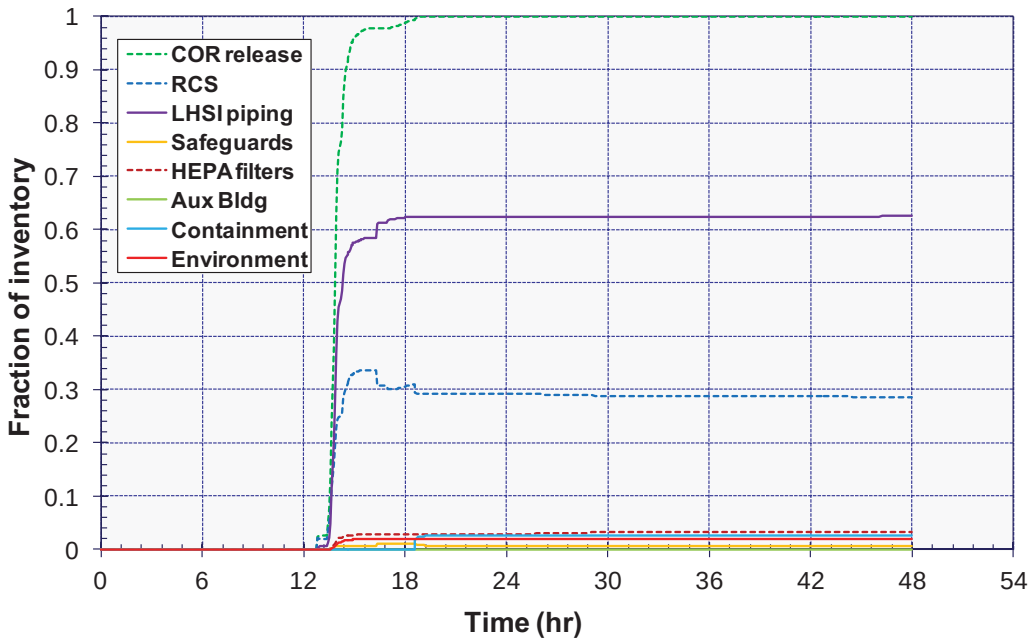

Figure 5-127 ISLOCA Cesium Distribution

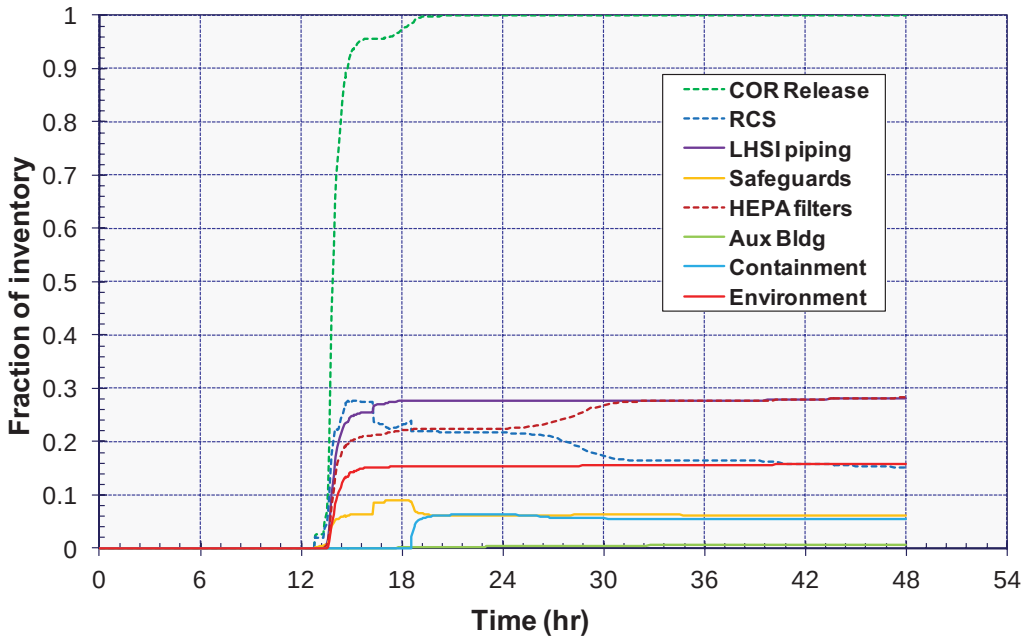

Figure 5-128 ISLOCA Iodine Distribution

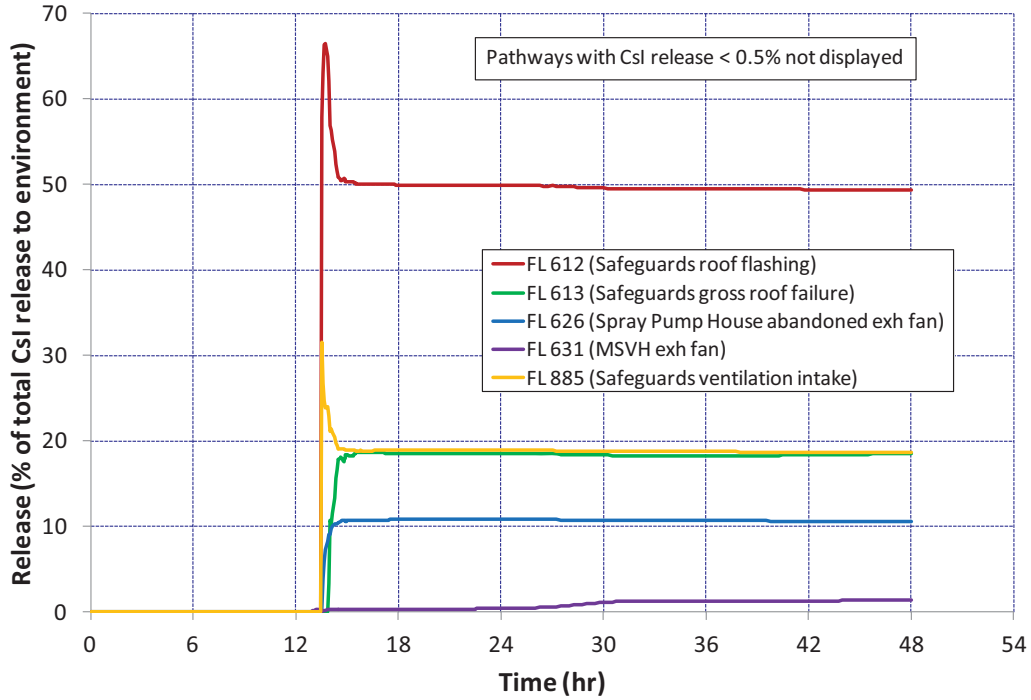

Figure 5-129 ISLOCA CsI Releases by Available Pathways (% of Instantaneous Total)

5.5.2 ISLOCA Separate-effects Calculation

The thermal hydraulic responses resulting from the ISLOCA separate-effects calculation are presented initially followed by the associated radionuclide migration.

5.5.2.1 Thermal Hydraulic Response

The thermal hydraulic response in the MELCOR ISLOCA separate-effects (i.e., deposition) calculation is illustrated in Figure 5-130 through Figure 5-133. In considering these figures, note that the separate-effects calculation was started 12 hr into the ISLOCA scenario somewhat before (i.e., 49 minutes before) the onset of core damage in the initial MELCOR overall ISLOCA calculation. This was sufficiently early for pipe wall temperatures to begin tracking the temperature of the vapor flowing through the LHSI piping before the first release of fission products from the core. The separate-effects calculation was carried out to 48 hr consistent with the duration of the initial and final overall ISLOCA calculations.

Figure 5-130 shows the pressure response along the LHSI piping. Pressure is higher upstream of the cavitating flow venturi from 12 to 17 hr suggesting choked flow conditions in the venturi.

Figure 5-131 and Figure 5-132 show vapor temperature and pipe wall inside surface temperature along the LHSI piping, respectively. Pipe wall temperatures exceed vapor temperatures due to the pipe walls absorbing gamma radiation emitted by fission product deposits accumulated in the piping. The LHSI piping in the Safeguards Area (i.e., the CV 301 trace in Figure 5-132), remains relatively cold for a number of hours because it is submerged in the water pool formed in the Safeguards Area. The eventual heat-up of the piping is in response to the piping uncovering as the pool recedes. The marked temperature decreases seen in these figures at 36 hr result when the low point in the cold leg piping dries out, i.e., when the loop seal clears. Clearing of the loop seal promotes cooling full-loop convective flow through the steam generator.

Vapor velocity along the LHSI piping is shown in Figure 5-133. Negative velocities exist for a period following reactor vessel lower head failure. This is because of the normally sub-atmospheric state of the Surry containments. Flow is from Safeguards to containment during this period of negative velocities. Velocity is greatest at the cavitating venturi as this is the minimum flow area in the LHSI piping. Velocities are relatively low in the 6” piping upstream of the venturi and relatively high in the 6” piping downstream of it. This is because of the higher pressures and hence higher densities upstream of the venturi. Velocity through the ISLOCA pipe break is lower than velocities in the 6” piping downstream of the venturi because the break in the 10” piping is larger than the 6” piping.

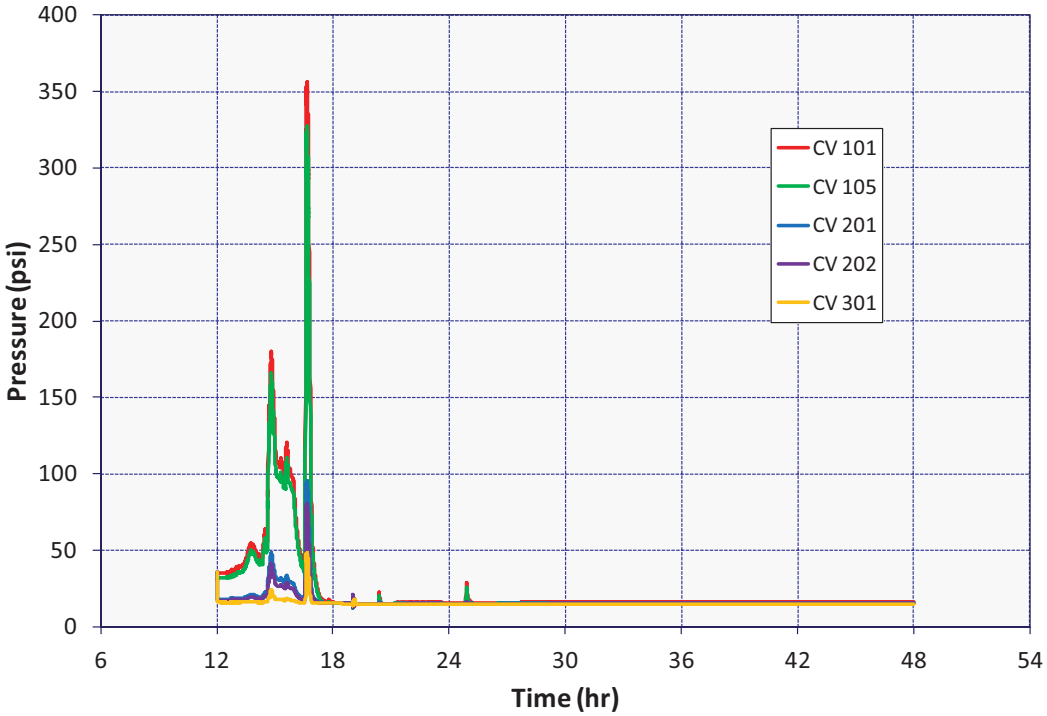

Figure 5-130 Pressure Along LHSI Piping in ISLOCA Deposition Calculation

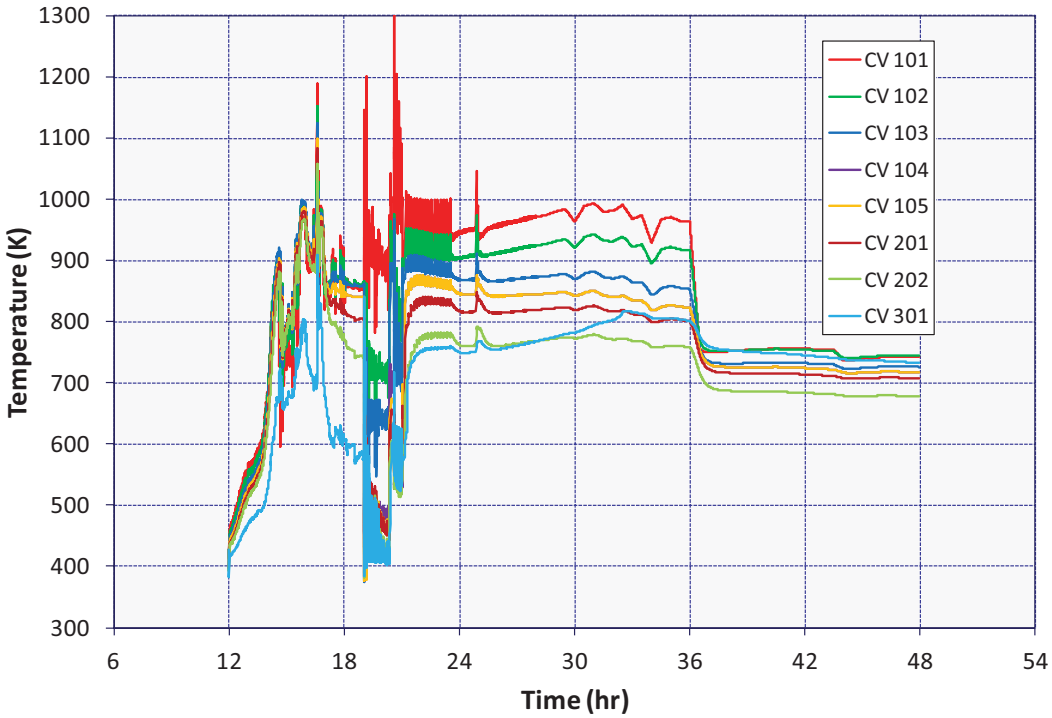

Figure 5-131 Vapor Temperature Along LHSI Piping in ISLOCA Deposition Calculation

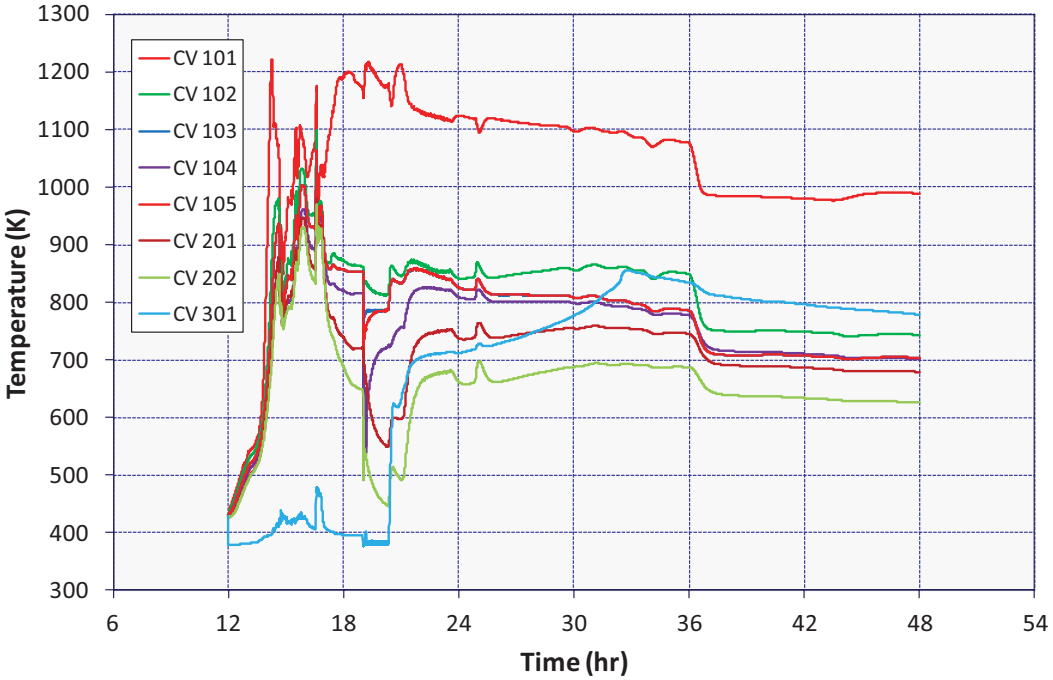

Figure 5-132 Pipe Wall Inside Surface Temperature Along LHSI Piping in ISLOCA Deposition Calculation

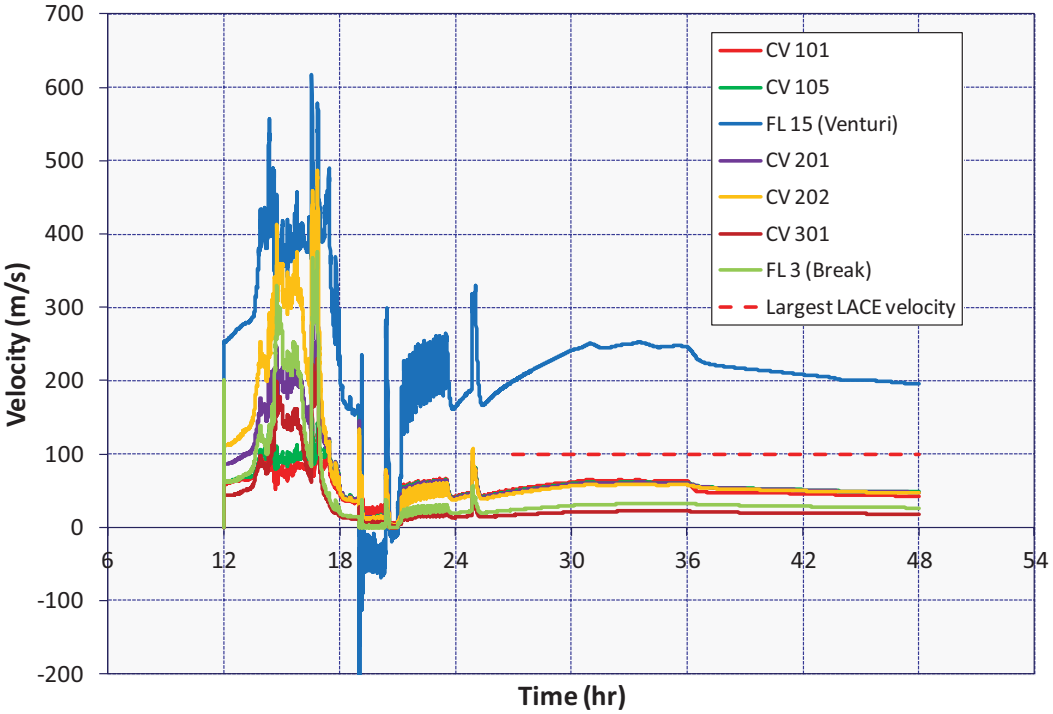

Figure 5-133 Vapor Velocity Along LHSI Piping in ISLOCA Deposition Calculation

5.5.2.2 Radionuclide Response

The capture of aerosolized fission products by LHSI piping in the MELCOR ISLOCA separate effects (deposition) calculation is illustrated in Figure 5-134 through Figure 5-139. These figures address only cesium iodide, cesium molybdate, barium, and tellurium, but illustrate well the competing influences of deposition (i.e., via turbulent deposition and impaction) and vaporization of radionuclide deposits.

Figure 5-134 identifies that most all of the cesium molybdate introduced to the LHSI piping deposited in the piping and remained there. At the same time, the figure identifies that more than half of the cesium iodide that deposited in the piping subsequently revaporized and left the piping. Figure 5-135 identifies analogous information for the barium and tellurium radionuclide classes. Note that the results for the barium class are for a metallic as opposed to an oxidic form. The step changes in these plots at 16 hr and 48 min are the result of the water pool in the reactor lower plenum disappearing. When an evaporating pool in a MELCOR control volume disappears, the hydrosols it suspended are introduced to the atmosphere of the control volume as aerosols. When the pool in the lower plenum disappeared in the initial overall ISLOCA MELCOR calculation, such introduction of aerosols occurred, and some of the aerosols were swept into the LHSI piping.

Figure 5-136 shows, for cesium iodide, the capture of aerosol along the LHSI piping through reactor lower head failure at 18 hr 34 min. Standing out in this figure is the relatively large amount of cesium iodide retained in the section of piping in the Safeguards Area. The large retention is attributable to the early relatively cold temperature of this piping associated with its being under water. Figure 5-137 shows the capture of cesium iodide for the entire duration of the anlaysis. Figure 5-138 shows information analogous to Figure 5-137 but for cesium molybdate. Clear in this figure is that cesium molybdate deposits in the LHSI piping are not susceptible to vaporization driven by fission product decay heating.

Illustrated in Figure 5-139 is the volume of radionuclide deposits relative to physical piping volume along the LHSI piping. MELCOR does not formulate a material volume associated with radionuclide deposits, so, Figure 5-139 presents volume estimates based on an average mass-weighted density determined from the masses of all radionuclide classes captured in the LHSI piping as a whole. The resulting average density was 6,043 kg/m^3. Additionally, Figure 5-139 is based on a packing factor of 0.5. Noteworthy is that radionuclide deposits exceed physical pipe volume in the section of piping closest to the RCS cold leg. This section of 6” Schedule 160 piping is 18’-1” long. The overfilled condition in the MELCOR calculation is not perceived as an indication that the piping would become blocked to fluid flow, as the radionuclide deposits of this nature are not envisioned to have the structural rigidity necessary to cause such. Instead, the perception is that such deposits would break loose and carry further down the piping towards Safeguards in a form not readily aerosolized (i.e., the assumption has been made that such relocated radionuclide deposits would not release to the environment in dispersible form). To emphasize in context, MELCOR does not address aerosol resuspension. Aerosols deposited by turbulent deposition, impaction, or by other means in a MELCOR calculation, remain deposited indefinitely unless evolved by revaporization. Additionally noteworthy with respect to Figure 5-139 is that the capture of concrete dust evolved from core concrete interaction in containment is not accounted for in the separate-effects calculation.

Consideration of concrete dust in the final overall MELCOR ISLOCA calculation suggests a 0.0062-m^3 capture of this material in the LHSI piping.

In considering the implications of volumetrically significant deposits of aerosols, it may be important to realize that feedback to the MELCOR thermal hydraulic solution from aerosol deposits is limited to energy addition from fission product decay. Energy associated with gamma radiation is deposited locally in the heat structure upon which the fission product aerosols reside and in the liquid water in the control volume to which the heat structure is coupled. The energy associated with beta particles is deposited in the heat structure and the fluid in the control volume. There is no other feedback to the thermal hydraulic solution (e.g., a reduction in available fluid flow area due to the buildup of aerosol deposits that is not taken ino account).

Table 5-15 presents the results of the MELCOR ISLOCA separate-effects calculation. The DFs identified in this table were placed on the flow path representing the LHSI piping in the final overall MELCOR ISLOCA calculation. Additionally, a DF of 10 was placed on the flow path associated with concrete dust. Concrete aerosol was not treated in the separate-effects calculation but was assumed fairly represented by the uranium, which had a resultant DF of 11.

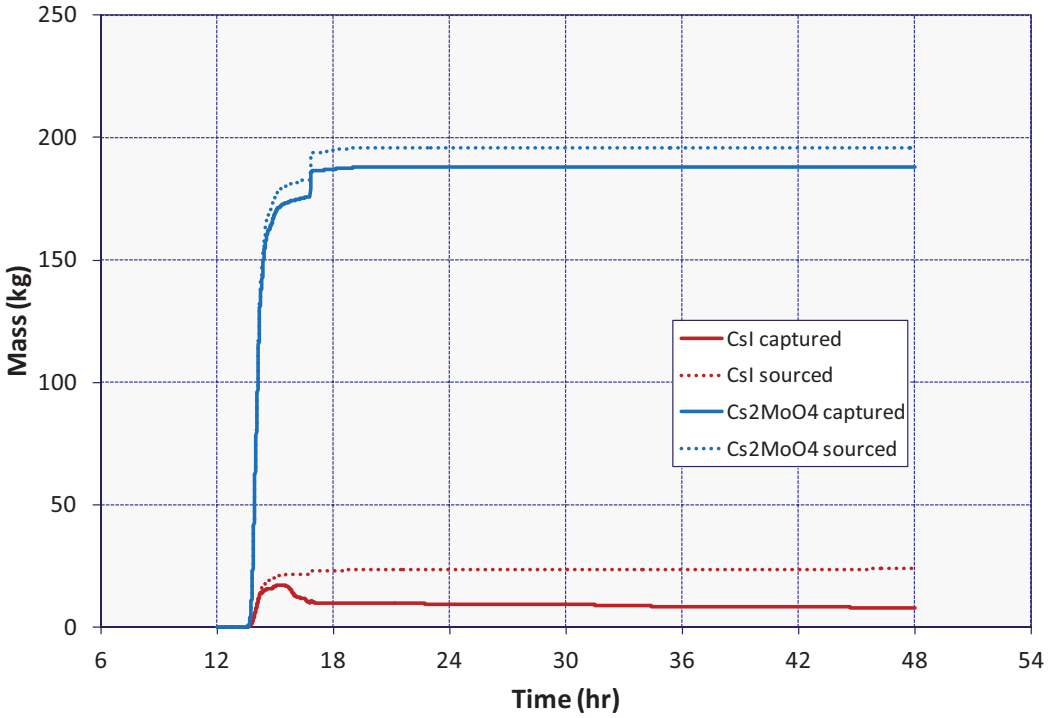

Figure 5-134 LHSI Piping CsI and Cs_2MoO_4 Capture in ISLOCA Deposition Calculation

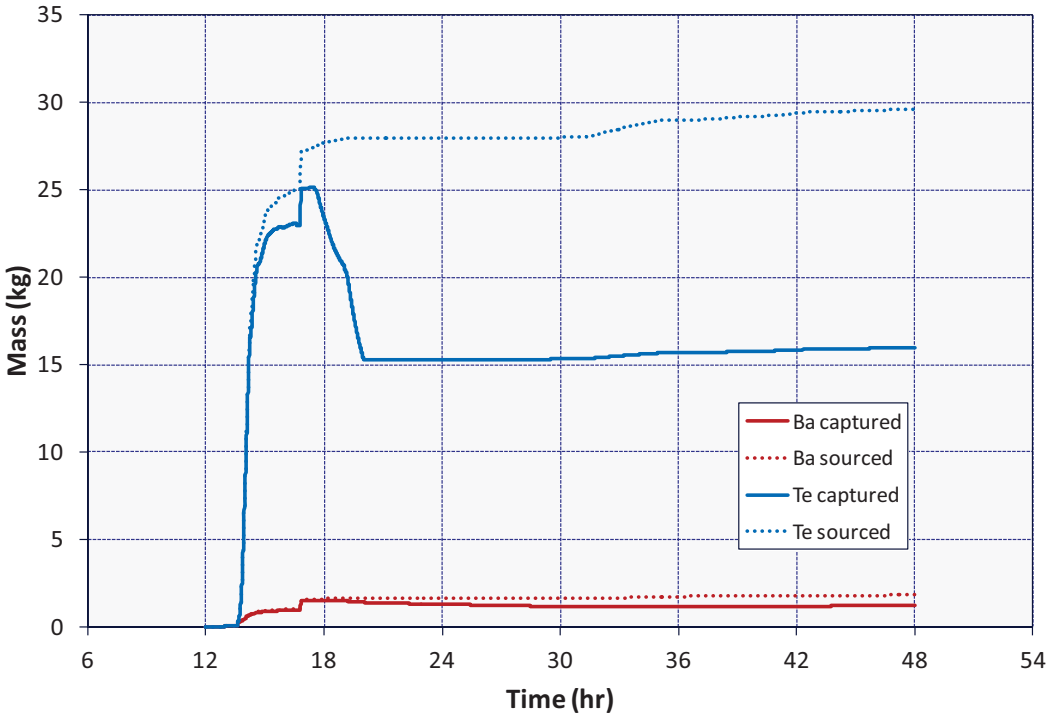

Figure 5-135 LHSI Piping Ba and Te Capture in ISLOCA Deposition Calculation

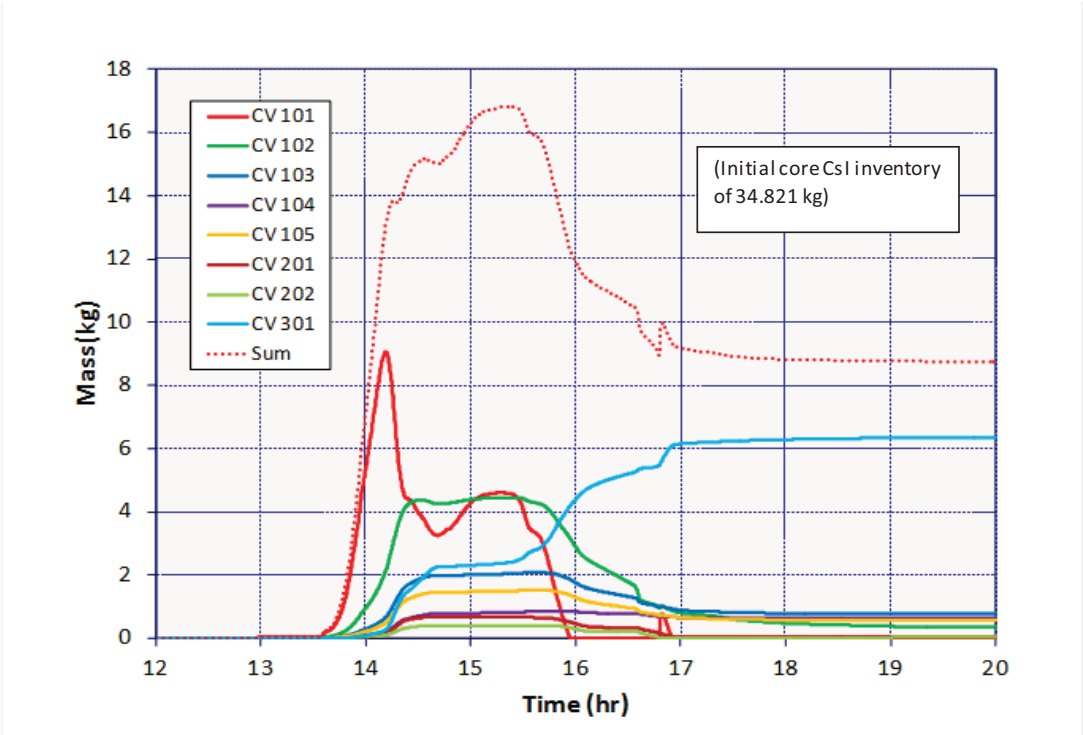

Figure 5-136 CsI Capture along LHSI Piping in ISLOCA Deposition Calculation (Early)

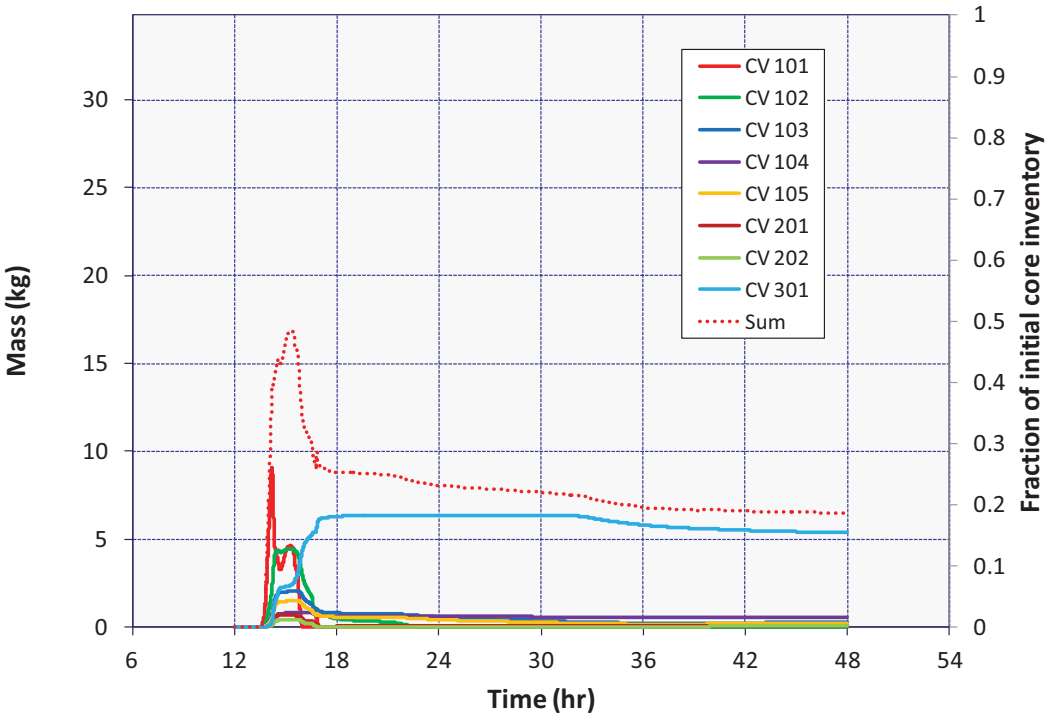

Figure 5-137 CsI Capture along LHSI Piping in ISLOCA Deposition Calculation

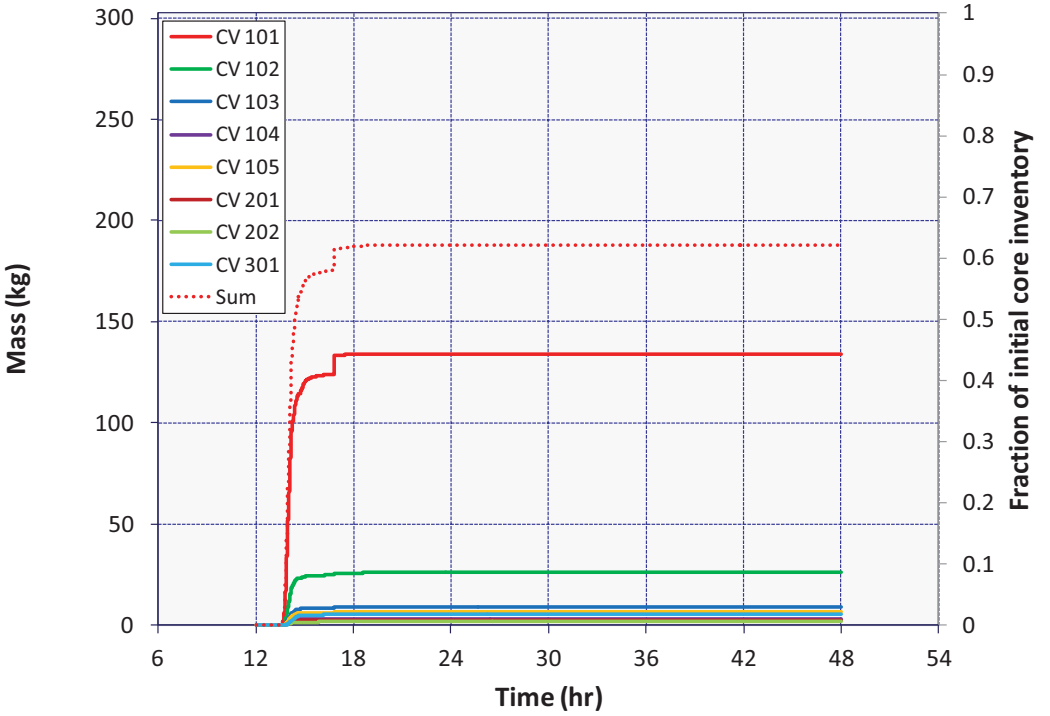

Figure 5-138 Cs_2MoO_4 Capture along LHSI Piping in ISLOCA Deposition Calculation

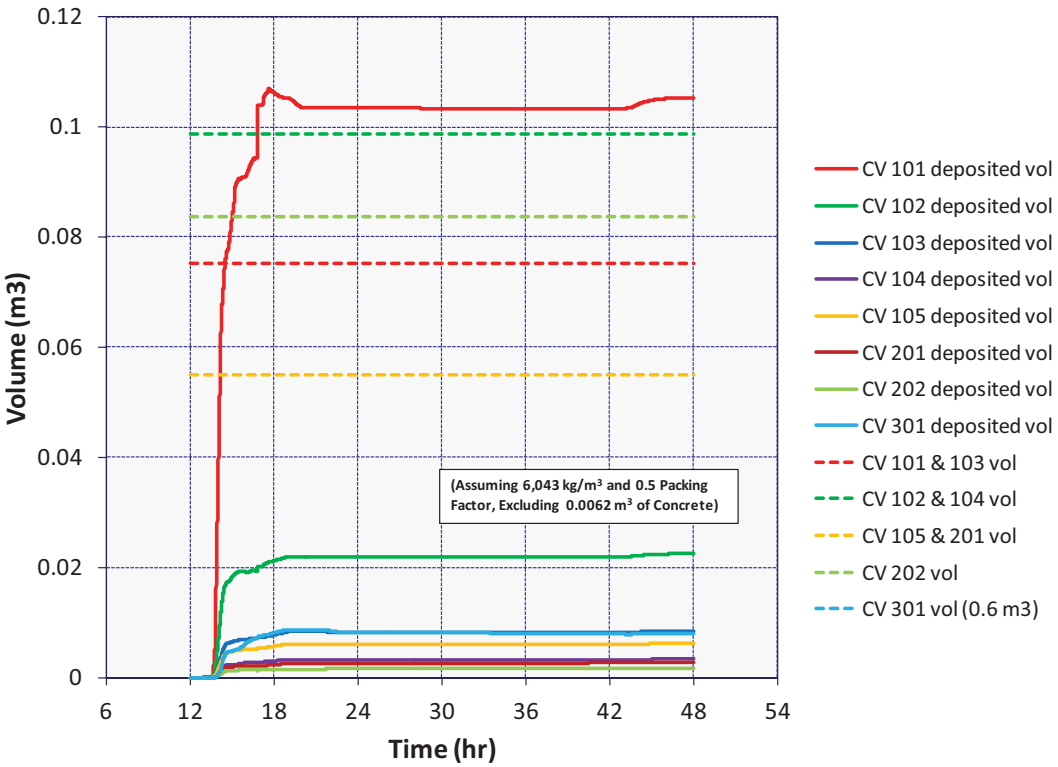

Figure 5-139 Captured Particulate Volume versus Pipe Volume in ISLOCA Deposition Calculation

Table 5-15 LHSI Piping Aerosol Capture in the ISLOCA Separate-effects Calculation and Associated DFs

Radionuclide class	Aerosol mass entering LHSI piping (kg)	Aerosol and vapor mass exiting LHSI piping (kg)	Fractional capture	Associated DF	Initial core inventory (kg)	Fraction of initial core inventory retained in LHSI piping
Cesium[1]	6.2	0.1	0.98	50	11.7	0.52
Barium[2]	1.6	0.1	0.96	24	187.6	0.01
Tellurium	29.6	13.6	0.54	2.2	40.9	0.39
Rubidium	2.7	0.2	0.92	13	309.5	0.01
Molybdenum	10.8	1.3	0.88	8.4	243.3	0.04
Cerium	0.0	0.0	0.60	2.5	1226.0	0.00
Lanthanum	0.0	0.0	0.50	2.0	621.2	0.00
Uranium	76.8	6.9	0.91	11	66770.0	0.00
Cadmium	3.9	0.3	0.94	15	7.3	0.50
Tin	4.0	0.3	0.93	14	9.2	0.40
Cesium iodide	23.7	15.8	0.33	1.5	34.8	0.23
Cesium molybdate	195.9	8.0	0.96	24	302.5	0.62
Control rod silver	75.5	2.9	0.96	26	102.9	0.71
Control rod indium	13.5	0.5	0.96	25	18.1	0.72
Control rod cadmium	6.8	6.8	0.00	1.0	6.2	0.00
Structural tin[3]	91.8	8.3	0.91	11	177.4	0.47

[1] Initial fuel-cladding gap inventory of cesium assumed by MELCOR 1.8.6 default to have the vapor pressure attributes of cesium molybdate.

[2] In deriving the DF for the barium class, it was assumed that the form of the material would be oxidic as opposed to metallic (i.e., it was assumed that deposits would not be susceptible to revaporization).

[3] The aerosol accounted for here is the tin that would be released by the melting of zircaloy fuel cladding. The zircaloy was assumed 1.45% tin by mass.

5.5.3 Mitigation of the ISLOCA

The unmitigated ISLOCA scenario analyzed in SOARCA is a catastrophic failure of both of the inboard isolation check valve disks within the LHSI piping together with failure to refill the RWST or to cross-connect to the unaffected unit's RWST. Detailed analysis of this scenario using MELCOR provides insight into conservatisms in the PRA models and leads to identification of additional mitigation measures that are practical.

The MELCOR analysis of the unmitigated ISLOCA scenario predicts that that the RWST becomes empty at 6 hrs and the fission product release begins at 13 hours. Assuming failure to refill or cross-connect RWSTs for 13 hours is a significant conservatism.

The unmitigated ISLOCA scenario analyzed in SOARCA includes operator actions to stop and isolate both LHSI pumps and to stop two of the three HHSI pumps to preserve RWST inventory. During a Surry site visit on October 26, 2011, NRC staff learned that the operators would stop the second HHSI pump earlier (i.e., at 1 hr instead of at 1.75 hrs) and throttle HHSI flow starting between 1.5 and 2 hrs. Based on these more realistic assumptions, our additional MELCOR analysis shows that the RWST becomes empty at 30 hours and 40 minutes.

Based on the MELCOR analysis of the unmitigated ISLOCA scenario and a review of emergency procedures, it was identified that there was an additional procedure, which would establish core cooling and prevent core damage. It was concluded that core damage could be averted by starting the RHR system before the RWST becomes empty. By 2 hours and 40 minutes, RHR entry conditions are satisfied. Thus, RHR initiation can establish adequate core cooling without the need for RCS inventory loss. This is discussed further in Section 5.5.3.1 and Section 5.5.3.2.

For the unmitigated ISLOCA scenario, MELCOR sensitivity analysis showed that opening pressurizer PORVs and any other RCS-to-containment valves diverts some of the fission product release into the containment where it deposits on surfaces. This sensitivity analysis is described in Section 5.5.3.3.

Finally, a discussion with the utility provided further insights into expected operator actions associated with the HHSI pumps during an ISLOCA. To preserve RWST inventory, operators would secure (i.e., stop) two HHSI pumps and throttle the remaining running pump as necessary to maintain water level in the reactor. This is further discussed in Section 5.5.3.4.

5.5.3.1 Review of Mitigation Measures for the ISLOCA

The expected operator actions for the ISLOCA were confirmed over several visits, numerous conference calls, review of the applicable procedures, a full-scope simulator run for key event timings, and some independent analysis (i.e., see Section 3.4). The initial review of operator actions was performed in 2007. Then in 2011, the latest version of the procedures were obtained. Surry also performed a full-scope simulator exercise in 2011 using an operations crew to obtain the timings of some of the initial events.

The expected operator actions and timing obtained from the activities cited above allowed specification of the events for the unmitigated scenario previously described in Section 5.5.1. The unmitigated scenario arises from failure of the operators to perform the following actions: (a) failure to successfully establish RHR, (b) refill the RWST, and (c) cross connect to the unaffected unit's RWST. The purpose of this section is to review the specific actions cited in the emergency procedures that would lead to mitigation of the ISLOCA without the assumed operator failures.

Upon identification of the reactor trip and ECCS actuation, the operators quickly transition to Emergency Procedure E-0, "Reactor Trip or Safety Injection." Both a reactor trip and safety injection initiate normally in the ISLOCA. The procedure methodically goes through the annunciator alarms and plant signals to identify the confirm operation of safety systems and then identify the cause of the transient. At a specific step, a LOCA into the containment is ruled out because of normal containment radiation, pressure, and sump conditions. In a following step, abnormal conditions would be identified in the control areas outside containment (i.e., sump annunciator signals in the Safeguards Building). The Emergency Procedure E-0 directs the operators to Emergency Procedure ECA-1.2, "LOCA Outside of the Containment."

In Emergency Procedure ECA-1.2, the critical valve alignments are confirmed. Next, the operator attempts to identify the location of the leak. First, it would be determined that the RCS pressure could not be stabilized through the identified valve isolation actions. Next, confirmation of sump annunciator signals in the safeguards and auxiliary building leads to the following actions: (a) local inspection of the piping in the auxiliary and safeguards buildings, (b) notification to the TSC of water in those locations, and (c) directions to proceed to Emergency Procedure ECA-1.1, "Loss of Emergency Coolant Recirculation."

Emergency Procedure ECA-1.1 includes the critical steps for mitigation of the ISLOCA. The purposes of the procedure are defined as follows:

> "To provide guidance to restore emergency coolant recirculation capability, to delay RWST depletion by adding makeup and reducing outflow, and to depressurize the RCS to minimize break flow."

The highlights of the key steps in ECA-1.1 that would lead to modeling actions in the MELCOR simulation include:

- Start make-up of the RWST
- Initiate RCS cooldown at no more than 100 °F/hr
- Raise RCS make-up flow to maintain RVLIS at >63% (i.e., top of the active fuel)
- Depressurize RCS using one pressurizer PORV. If RCS subcooling is <30 ^{o}F, raise RCS make-up flow to restore subcooling
- Check if RHR system can be placed in service
- If RWST < 3%, use RWST crosstie, establish charging pump crosstie as needed
- Depressurize all intact SGs to atmospheric
- Use RHR system if in service

Consequently, as evidenced above, the three operator failures assumed in the unmitigated ISLOCA are identified as procedural steps in ECA-1.1 (i.e., failure to refill the RWST, failure to establish a RWST crosstie to the other unit, and RHR operation, respectively).

5.5.3.2 Analysis of RHR Operation

Mitigation of the ISLOCA would be achieved through actuation of the RHR system. The RHR system removes water out of the Loop A hot leg and returns it into the Loop B and C cold legs after cooling it in a heat exchanger. The RHR system is a relatively high flow system (i.e., ~3700 gpm/pump versus 550 gpm/pump HHSI at runout conditions), which quickly subcools the core and leads to complete depressurization of the primary system. The entry conditions for the RHR include a RCS pressure below 450 psig and T_{ave} below 350 ºF. The water level must be at least mid-height in the hot leg to prevent vortexing vapor into the pump. Following Surry procedures and confirmed by the EOF and TSC, the operators would attempt to establish RHR as soon as possible to mitigate the accident.

Figure 5-140 shows the RCS pressure and T_{ave} with the RHR pressure and temperature entry criteria. After 2 hours and 40 minutes, the RHR pressure and temperature entry criteria are established. The vessel swollen level is shown in Figure 5-141. The swollen vessel level is above the hot leg centerline after 2 hours and 40 minutes. Hence, after 2 hours and 40 minutes, the operators could establish RHR based on the entry criteria.

There are several challenges to be considered. First, water will need to be added to the RCS until the break flow is terminated. The RHR system will fully depressurizes the RCS, which terminates the break flow. The break flow from the unmitigated ISLOCA is shown in Figure 5-142. At 2 hours and 40 minutes, the break flow is less than 40 kg/s and steady due to the successful operator actions to reduce HHSI injection to only one pump. There is sufficient inventory in the RWST to maintain HHSI injection for more than 3 hours (see Figure 5-143). Previous experience in modeling RHR operation for a similar, mitigated ISLOCA shows that the RCS will depressurize to atmospheric conditions in about 30 minutes after the start of RHR. Since the LHSI piping with the ISLOCA connects to the top of the cold leg piping and immediately rises vertically 4 ft upon leaving the cold leg,[35] the break flow will terminate once the RCS pressure drops below the head of the piping rise (~1.7 psig).

A second challenge is maintenance of the HHSI flow while the RHR is depressurizing the RCS. The HHSI pumps are vulnerable to flooding due to drainage of the effluent from the ISLOCA into the basement of the Auxiliary Building. Surry has done a flooding analysis of the Auxiliary Building and concluded the HHSI pumps will begin to flood when the water volume exceeds 530,000 gallons in the basement. As shown in Figure 5-144, the water volume in the basement of the auxiliary building is ~235,000 gal at 2 hours and 40 minutes. Therefore, there is considerable margin before the HHSI pumps are flooded. As illustrated in the unmitigated ISLOCA Auxiliary Building water volume response (see Figure 5-144), there is insufficient water to flood the HHSI pumps. Consequently, they have some margin to use additional water from a RWST crosstie (i.e., ECA-1.1) or by refilling the RWST (i.e., ECA-1.1).

[35] Normal, forward flow for the LHSI piping is into the cold leg. Leaving the top of the cold leg in this context is the direction of the ISLOCA break flow, which is backwards through the LHSI piping.

The final challenge is maintenance of available Net Positive Suction Head (NPSH) of the RHR pumps. The NPSH is the pressure head difference between the actual pressure of a liquid in a pipeline and the liquid's vapor pressure at the liquid temperature. If the liquid pressure drops below the vapor pressure, then vapor bubbles will form. The vapor bubbles cause cavitation and reduce the efficiency of the pumps. The collapse of the cavitation bubble in the pump impeller creates a pressure wave that can destroy the internal pump components (usually the leading edge of the impeller). Additionally, the inevitable increase in vibration can cause other mechanical faults in the pump and associated equipment [MCP, 2009].

There are two aspects of the NPSH: the available NPSH and the required NPSH. The available NPSH is the suction pressure at the pump inlet. The available NPSH is defined as follows:

$$\boldsymbol{Available\ NPSH = \frac{p_0 - p_v}{\rho g} + \Delta z - h_L}$$

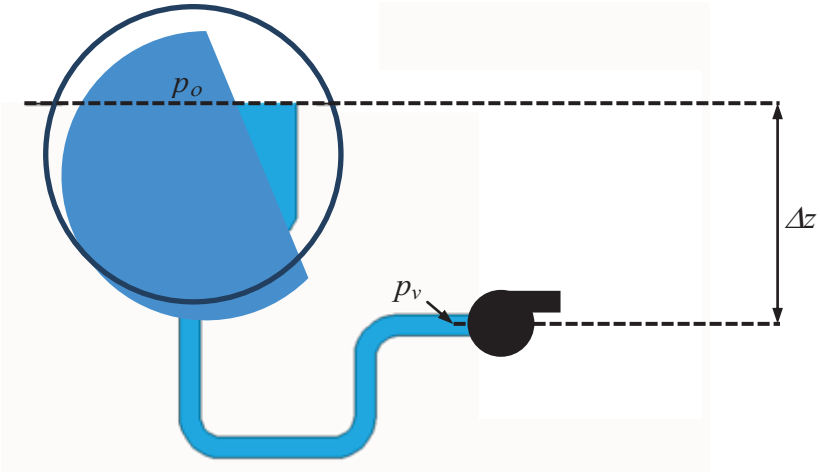

where:

h_L	is the head loss from the hot leg to the pump inlet, [m]
p_0	is the pressure in the hot leg, [Pa]
$p_v(T_{liq})$	is the saturation pressure at the temperature of the liquid in the piping, [Pa]
Δz	is the difference in height, [m]
ρ	is density of the liquid, [kg/m^3]
g	is gravitational acceleration, [m/s^2]

The required NPSH is experimentally determined by the pump manufacturer. It represents the head needed before the pump's total differential head performance is reduced by 3% due to cavitation. Cavitation occurs at suction pressure levels below the required NPSH and pump damage can occur from cavitation even though the pump may continue to provide injection flow.

At 3 hours in the Surry ISLOCA sequence, $p_v(T_{liq})$ is near saturation conditions. Setting $T_{liq} = T_{sat}$ in the previous equation, the available NPSH reduces to the following expression:

$$Available\ NPSH = \frac{p_0 - \overset{0}{\cancel{p_v}}}{\rho g} + \Delta z - h_L$$

$$Available\ NPSH = \Delta z - h_L$$

The difference in height between the hot leg and the RHR pump (Δz) was determined from plant drawings to be 25-ft. The head loss h_L is a function of the flow rate, fluid state, and the losses in the piping. Surry provide the results from engineering RHR NPSH calculations. The RHR NPSH calculations that indicated there was adequate (no less than 7" and no more than 20") NPSH margin (i.e., $NPSH_{margin} = NPSH_{available} - NPSH_{required}$) at saturated conditions with 8" of water in the hot leg with one RHR pump running. The Surry NPSH calculations imply that the RHR must be started gradually (i.e., only one of the two pumps) until additional subcooling was achieved.[36] In addition, as indicated in ECA-1.1, additional make-up flow should be initiated to increase the subcooling. Since only HHSI pump was running in the results presented in Figure 5-140 through Figure 5-142 there are additional resources and procedural direction to increase the RCS water level and the subcooling, which will further reduce the potential for inadequate NPSH margin.

In summary, RHR could be established after 2 hours and 40 minutes to provide closed loop cooling of the RCS and terminate the break flow. There is adequate water in the RWST for 3 hours to complete this action. The available NPSH is adequate to start the pumps, especially if the operators followed procedural steps to increase subcooling (i.e., starting additional HHSI pumps). Once RHR is established, the core will become subcooled. This allows the RCS pressure to decrease to atmospheric conditions, which will terminate the ISLOCA break flow.

[36] Following discussions with Surry operations, there is plant experience in cavitating the RHR pumps during mid-loop operations. There are identifiable signals in the control room of the condition. The operator would monitor the flow rate of the RHR system and secure one or both RHR pumps if inadequate flow is developed. The plant operations staff shared that there are ample control room signals to identify when two pumps could be operated. The plant experience demonstrates that the pumps were robust enough to tolerate cavitation during RHR startup.

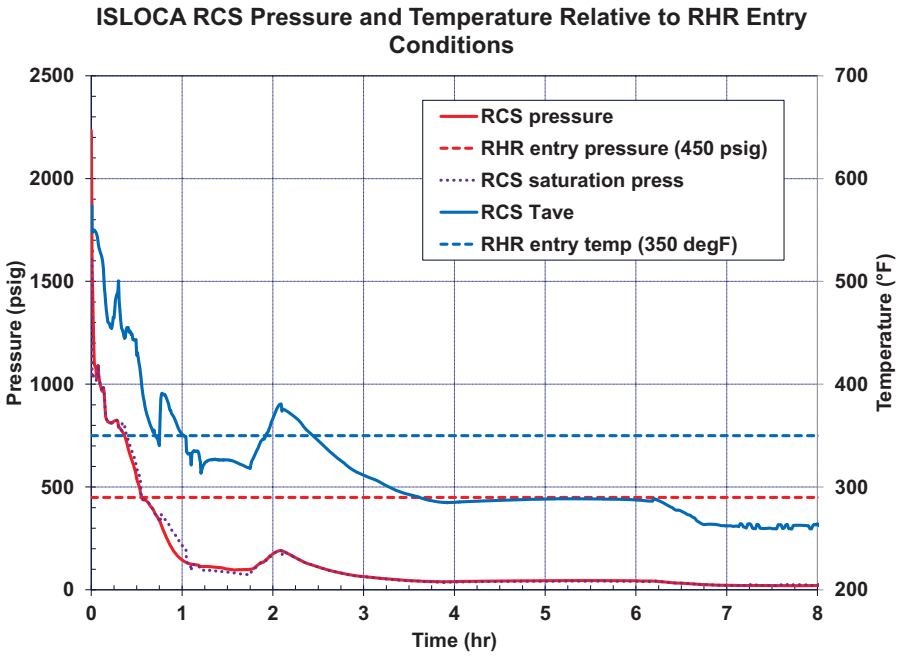

Figure 5-140 ISLOCA RCS Pressure and Temperature Relative to the RHR Entry Pressure and Temperature Criteria for the Unmitigated ISLOCA

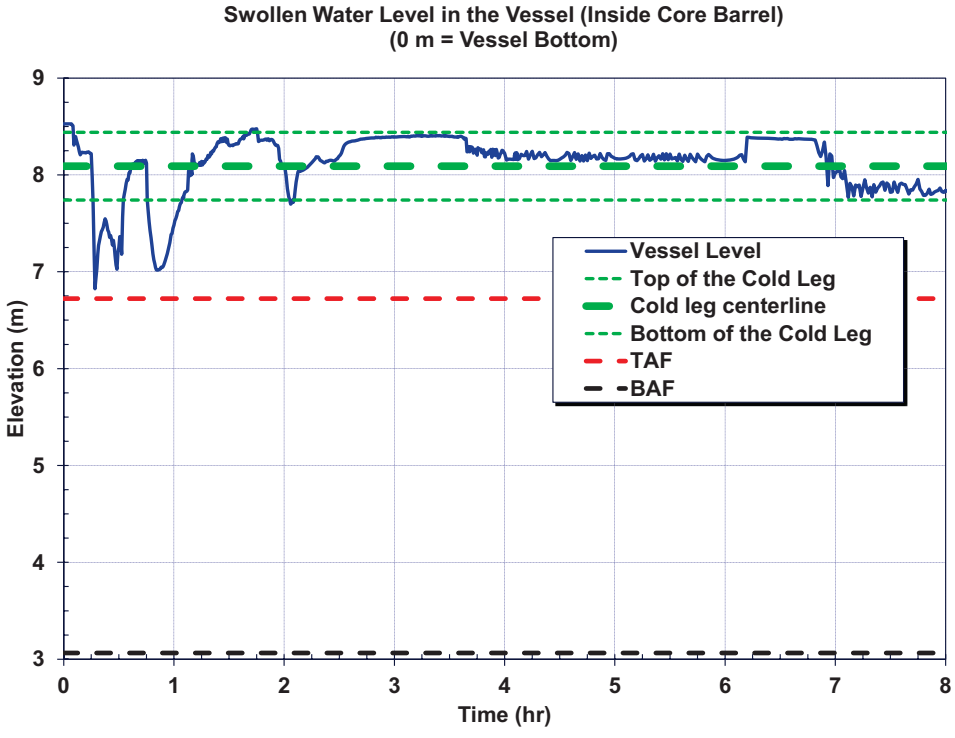

Figure 5-141 ISLOCA Vessel Swollen Water Level for the Unmitigated ISLOCA

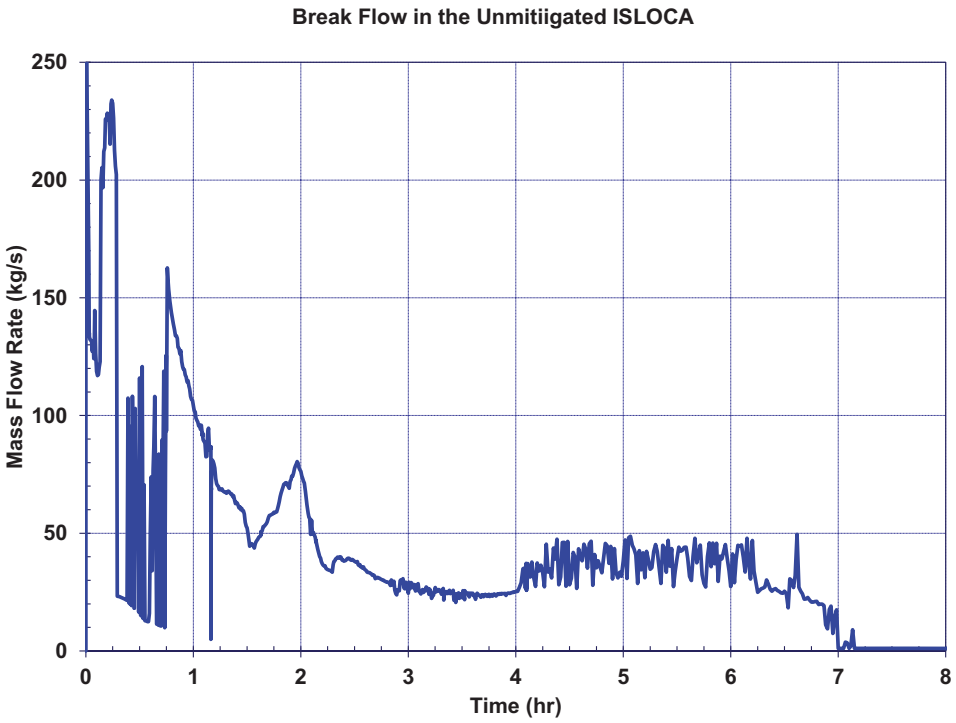

Figure 5-142 ISLOCA Break Flow for the Unmitigated ISLOCA

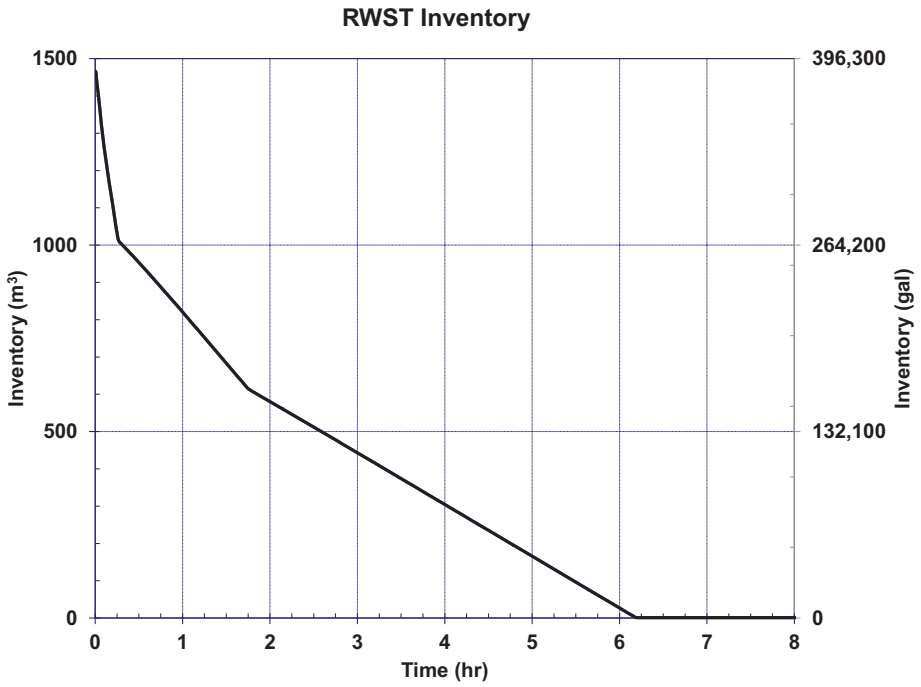

Figure 5-143 RWST Volume for the Unmitigated ISLOCA

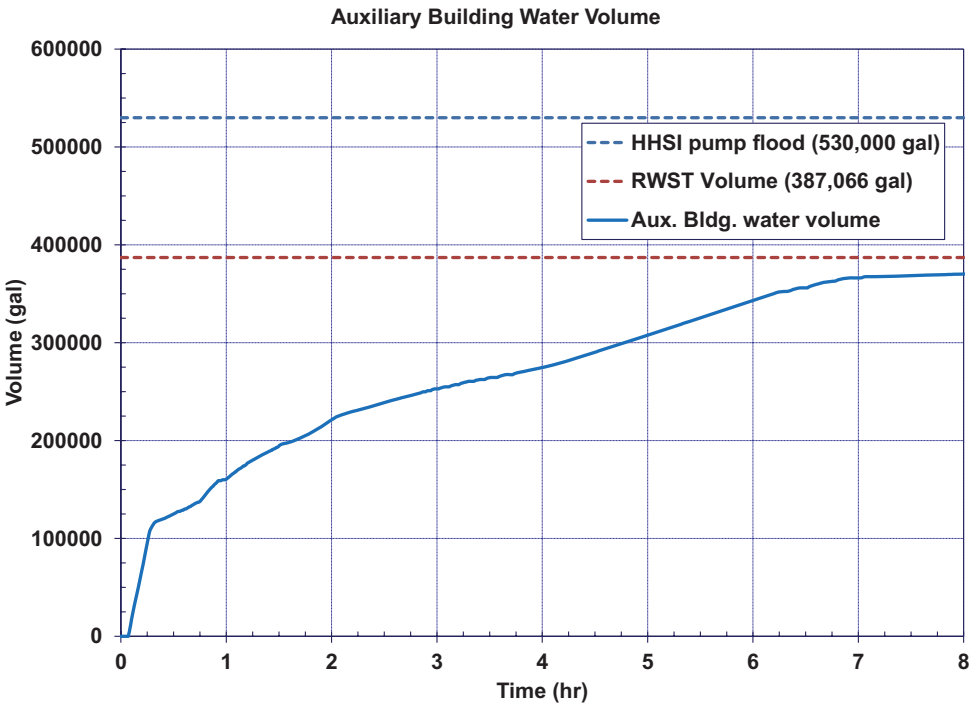

Figure 5-144 Auxiliary Building Water Volume for the Unmitigated ISLOCA

5.5.3.3 Analysis of Mitigation Using Pressurizer PORVs

Mitigation of the ISLOCA also could be achieved by opening valves between the RCS and containment, potentially diverting flow of fission products into the containment where fission products could deposit and the eventual release to the environment could be delayed. A review of the Surry plant design showed that paths between the RCS and containment could be opened by opening the pressurizer PORVs to reduce RCS subcooling (i.e., ECA-1.1). This section demonstrates the potential benefits of reducing fission product released to the safeguards area should conditions permit PORV actuation. Similarly, the RCS vent and drain system could allow venting to containment.

Opening the pressurizer PORVs allows steam, hydrogen, and fission products to reach the pressurizer relief tank. Once the pressurizer relief tank pressure reaches 100 psi above containment pressure, the PRT rupture disks will open providing a flow path from the pressurizer relief tank to the containment. This section investigates the effectiveness of opening pressurizer PORVs in reducing the offsite release.

As noted above, a pressure difference of 100 psi is needed to open the PRT rupture disks. Figure 5-103 and Figure 5-112 shows the pressure in the RCS and containment, respectively. Pressure in the RCS appears sufficient to open the PRT rupture disks at two different phases: The first couple of hours of RCS depressurization and during the in-vessel core degradation. Several calculations were performed to estimate the time interval, post scram, when the PORVs must be opened to burst the rupture disks prior to in-vessel release. The variations were performed at half hour intervals. The longest delay in pressurizer PORV actuation that resulted

in PRT rupture disk opening prior to in-vessel release was 2 hrs. PORV actuation following 2.5 hrs resulted in PRT rupture disk opening during core degradation.

Two sensitivities were performed to investigate the effectiveness of PORV actuation in mitigating fission product release to the environment: (1) PORV actuation at 0.5 hrs after scram, and (2) PORV actuation at the start of the in-vessel core degradation (i.e., when water level is at core mid-plane). Each sensitivity is a variation of the unmitigated ISLOCA, described in Section 5.5.1.

Facility pressure response to the actuation of the pressurizer PORVs at 0.5 hrs is presented in Figure 5-145. The PRT rupture disks opened at 0.74 hrs. The pressurizer level increases in response to PORV actuation, as shown in Figure 5-146. Initial flow is predominantly vapor, Figure 5-147. Once the level reaches the base of the PORVs at 1.1 hrs, the flow transitions to two-phase. At 6.6 hrs the flow returns to single phase vapor for the duration of the in-vessel release.

Given the rupture disks are open, the differential pressure between the RCS and the containment atmosphere, established during the boildown, sustains vapor flow through the PORVs during the in-vessel release phase of the accident. Therefore, vapor released from the RCS is partitioned between the safeguards area and containment as well as the transported fission products, shown in Figure 5-148. The flow through the PORVs is diverting a significant portion of fission products into containment. Using the containment volume during the in-vessel release reduced the cesium and iodine released to the environment, presented in Figure 5-149 and Figure 5-150, respectively. Flow through the pressurizer PORVs terminates due to lower head failure.

The sensitivity characterizing late actuation of the pressurizer PORVs was performed coinciding with core degradation at 12.8 hrs. It is postulated that given PORV actuation occurs between the initiation of core degradation and 2.5 hrs, post scram, the result will be late PRT rupture disk opening. Upon PORV actuation, flow through the PORVs occurs for a short time but terminates prior to fission product release; subsequently, fission products released evacuate the RCS through the LHSI piping. In Figure 5-151, the pressure excursion at 14.5 hrs resulted from the failure of the flow distributor element. This failure provides a pathway for core debris to relocate into the pooled water below the distributor, generating an increase in steam production and a corresponding pressure rise. The pressure rises above the rupture disks set point which opens the rupture disks. This decreases flow through the LHSI line as release paths are now established to the containment as well as the safeguards area. CsI released in-vessel is overlaid with the LHSI and PORV flow rates in Figure 5-152. The resulting reductions in cesium and iodine released to the environment are presented in Figure 5-153 and Figure 5-154, respectively.

From the results presented, reductions to the environmental release were achieved through PORV actuation. PORV actuation resulted in PRT pressurization and eventually the PRT rupture disks to burst. Once the rupture disks were open, steam, vapor, and fission products produced in the core were partially diverted to containment. Observations from the two sensitivities demonstrated a strong dependency between the PRT rupture disk actuation with the back-pressure of the RCS. Two time periods were indentified when RCS pressure was great enough to induce rupture disk actuation. The first period was during early depressurization and

the second was post depressurization and prior to core degradation. Early actuation established continual flow from the RCS to containment during the in-vessel release, until lower head failure. Actuation of the PORVs after depressurization resulted in PRT rupture disks remaining intact for the majority of the in-vessel release.

The percent of iodine released to the environment was reduced from 15.8% to 11.3% and 14.4% and the percent of cesium released to the environment was reduced from 2.03% to 1.37% and 1.97%, for PORV actuation at 0.5 hrs after scram and at the beginning of core degradation, respectively.

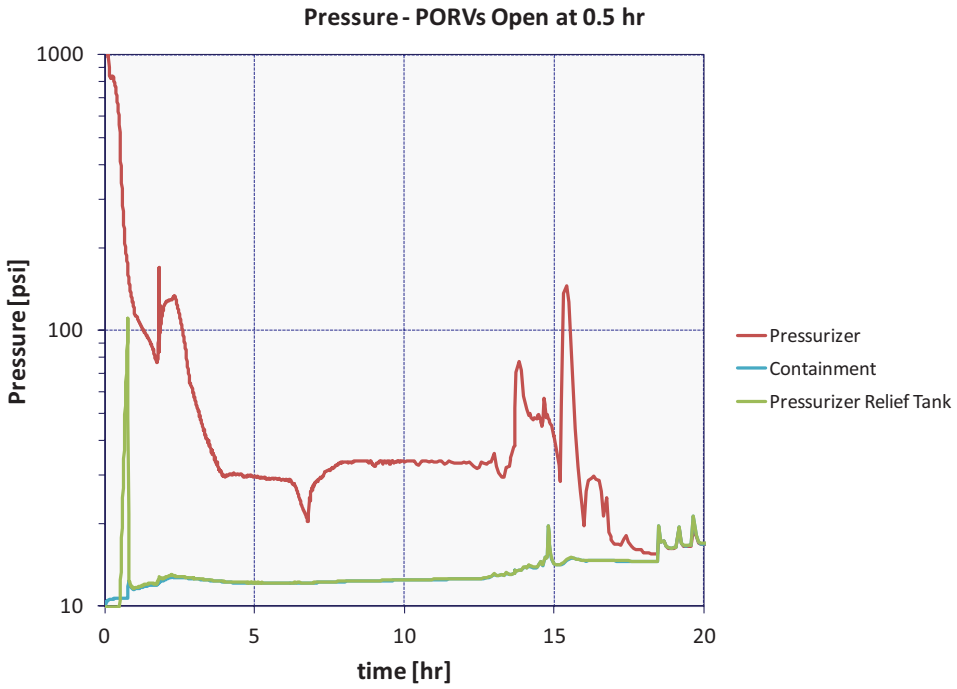

Figure 5-145 Facility pressure response to PORV actuation at 0.5hrs

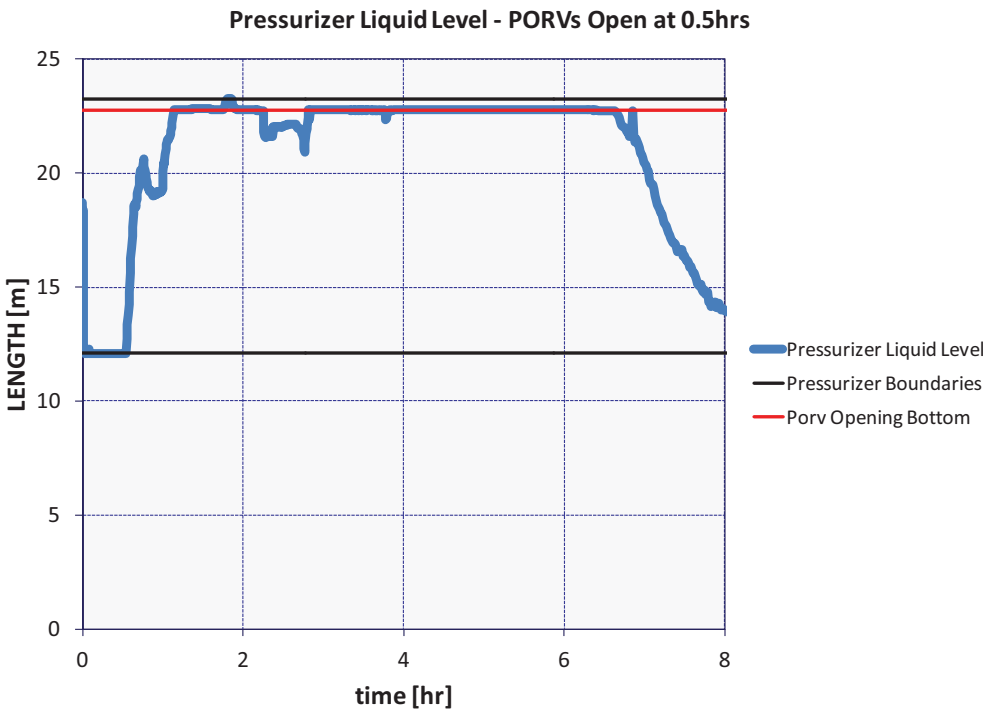

Figure 5-146 Pressurizer liquid level response to PORV actuation at 0.5hrs

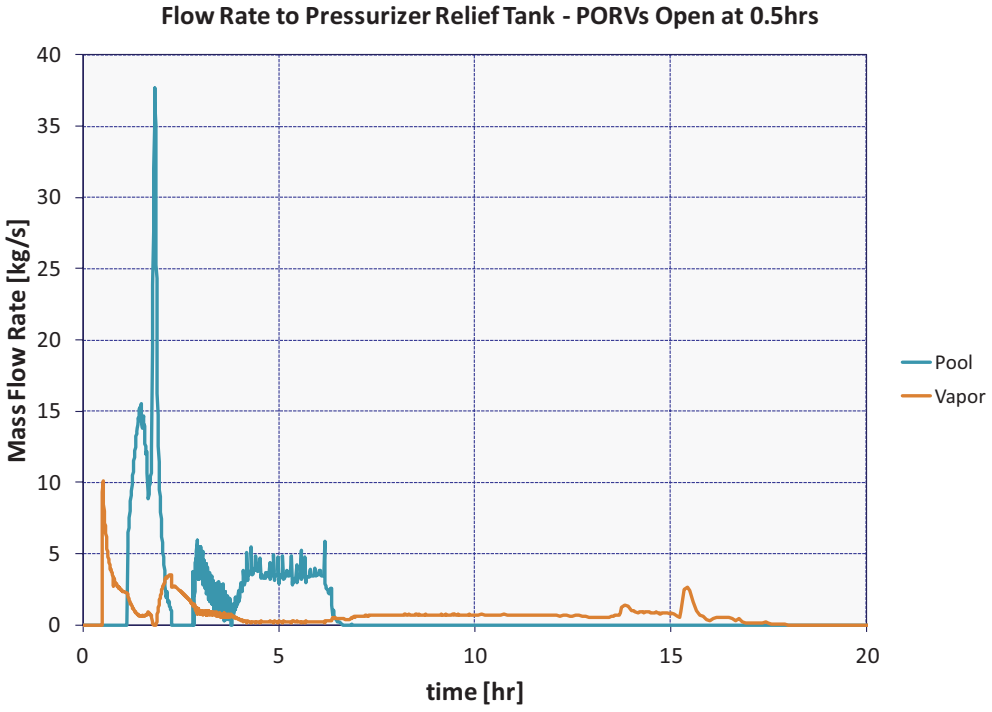

Figure 5-147 Flow Rate to Pressurizer Relief Tank – PORVs Open at 0.5 hrs

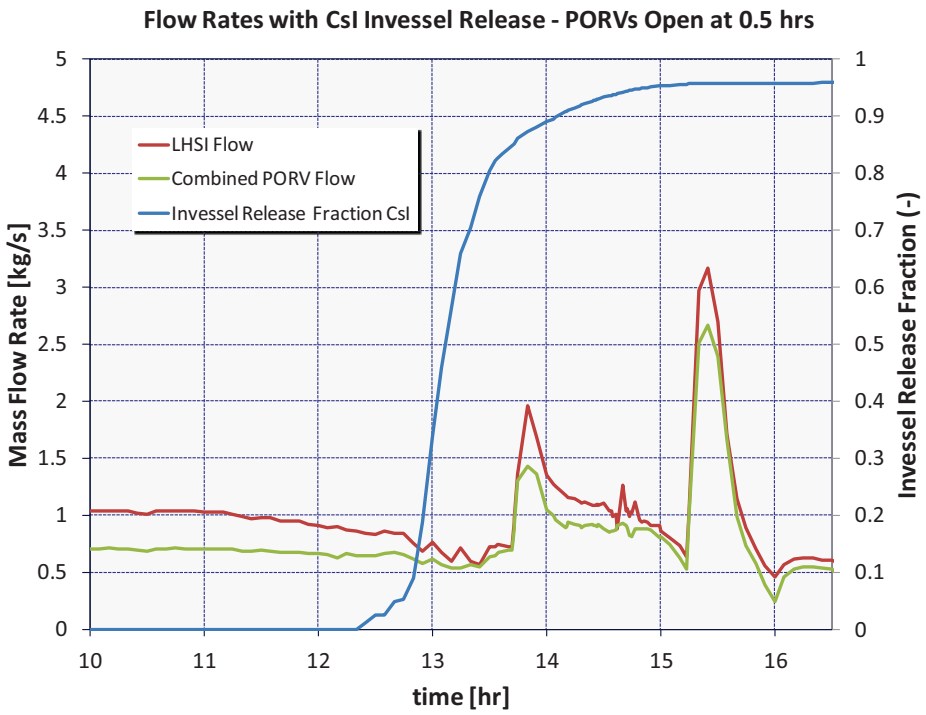

Figure 5-148 Flow Rates with CsI Invessel Release – PORVs Open at 0.5 hrs

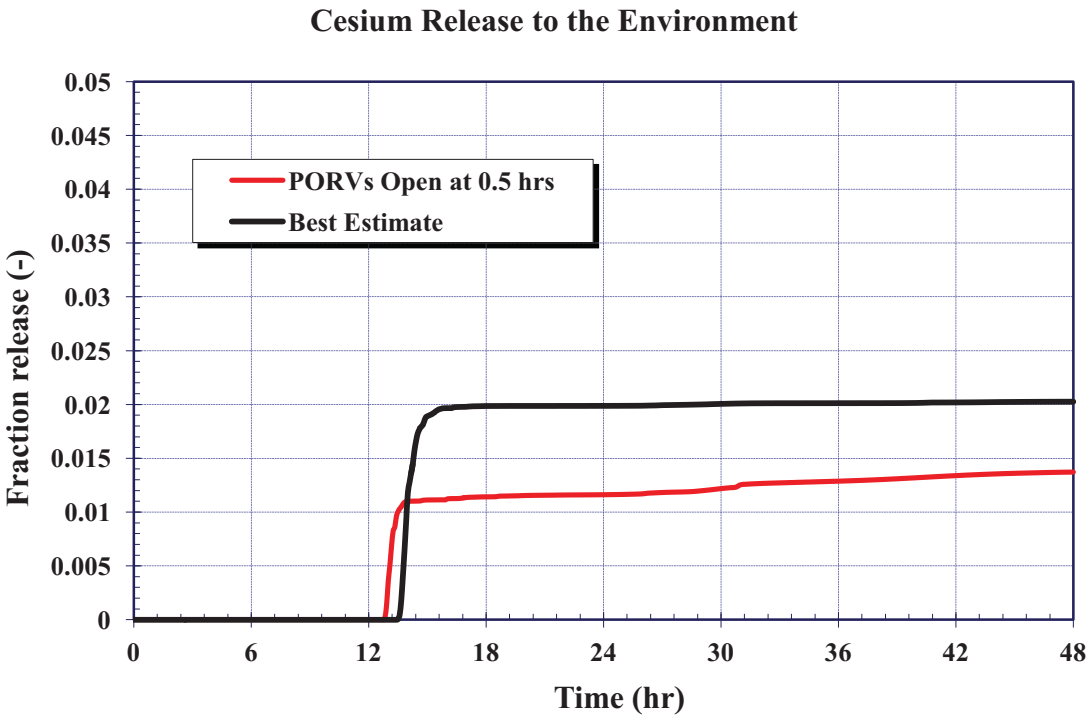

Figure 5-149 Cesium Release to the Environment – PORVs Open at 0.5 hrs

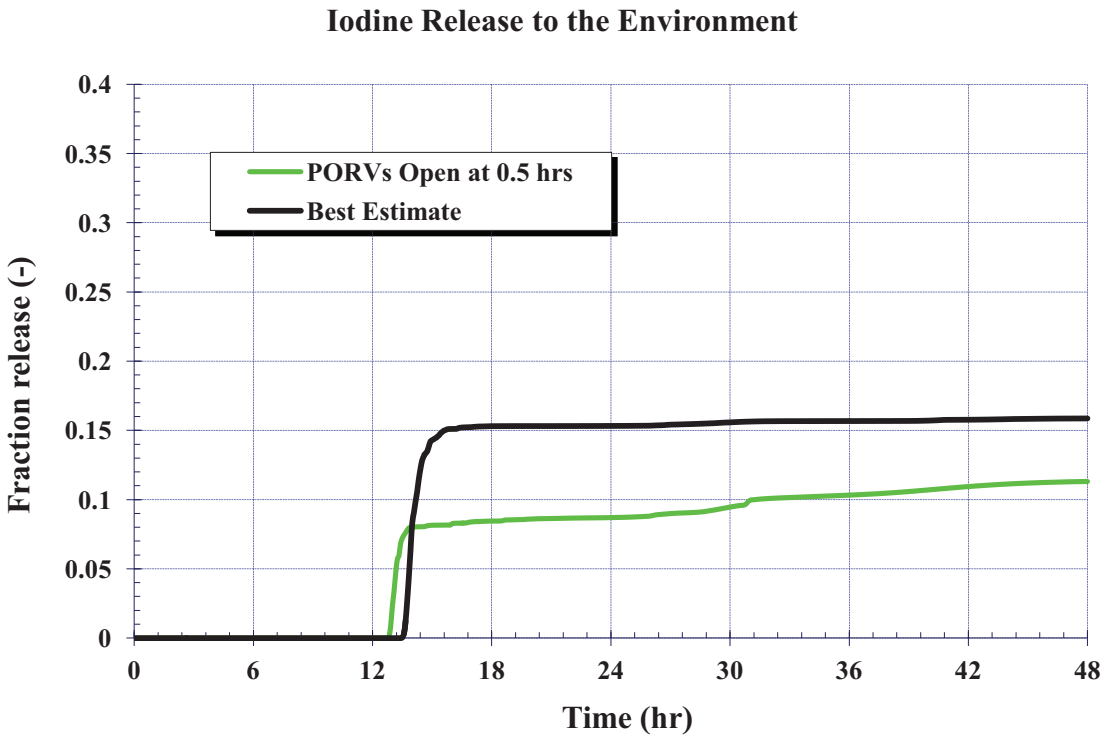

Figure 5-150 Iodine Release to the Environment – PORVs Open at 0.5 hrs

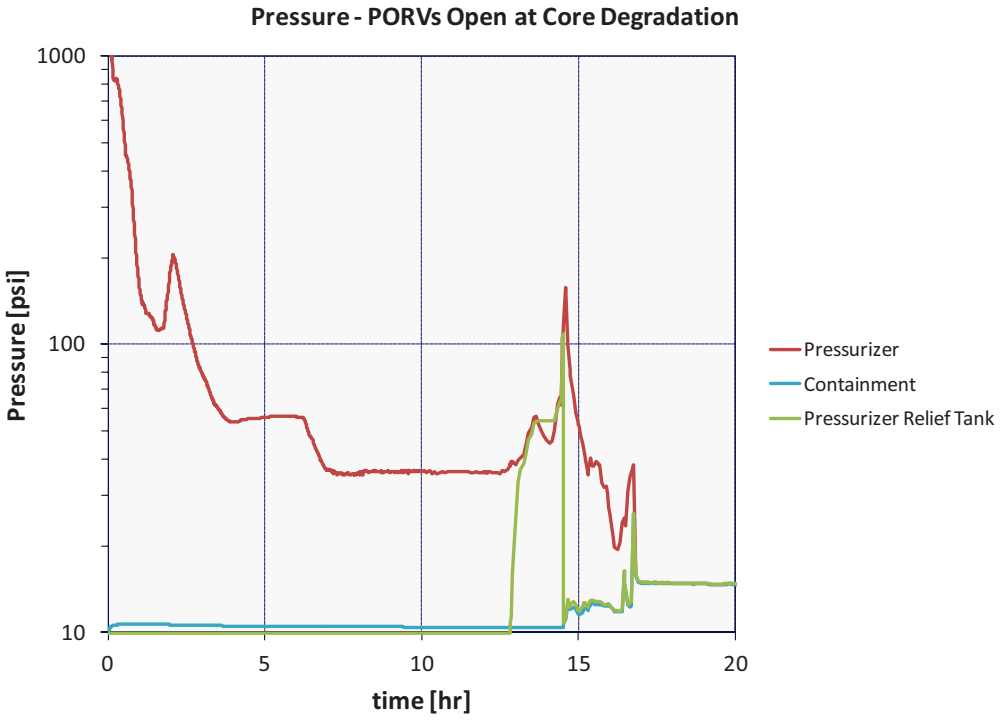

Figure 5-151 Facility pressure response to PORV actuation at Core Degradation

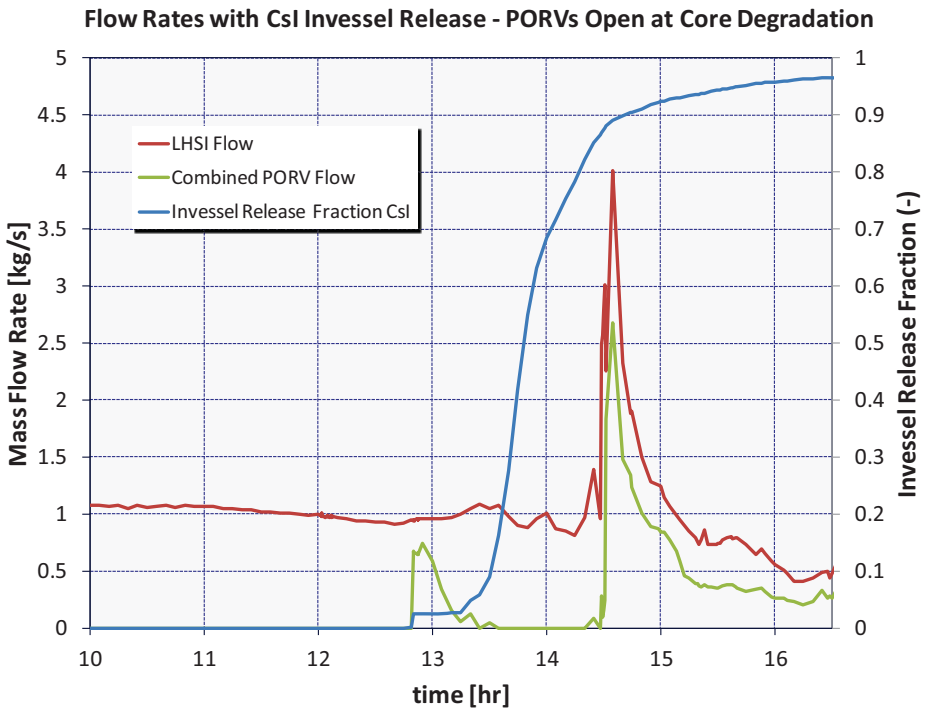

Figure 5-152 Flow Rates with CsI Invessel Release – PORVs Open at Core Degradation

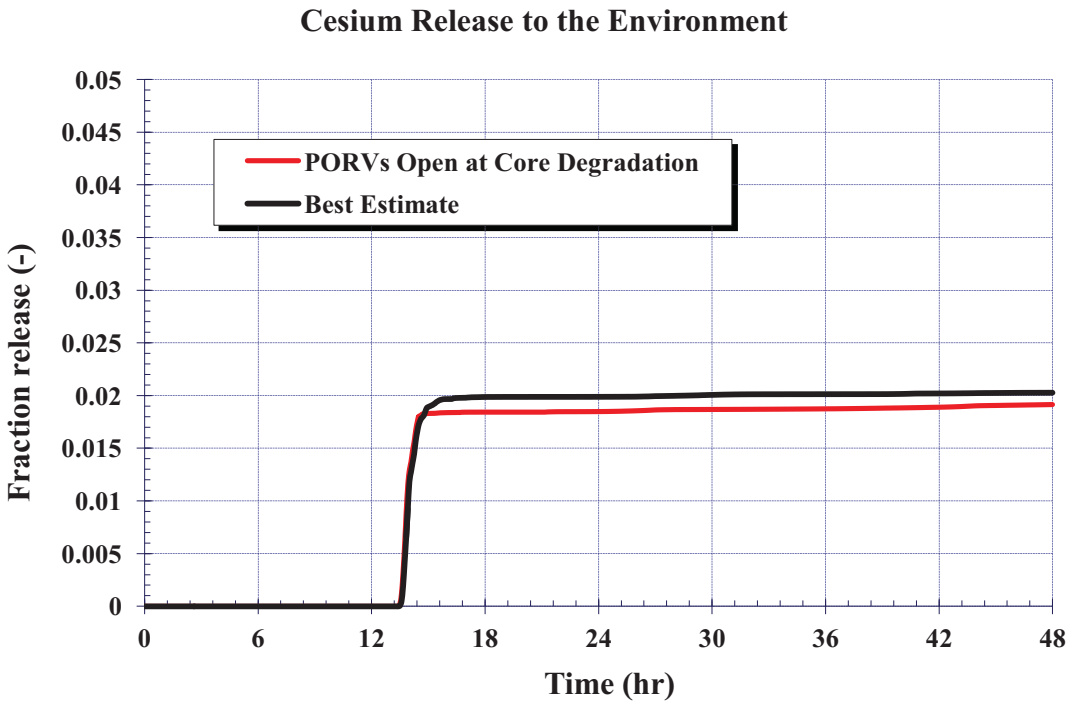

Figure 5-153 Cesium Release to the Environment – PORVs Open at Core Degradation

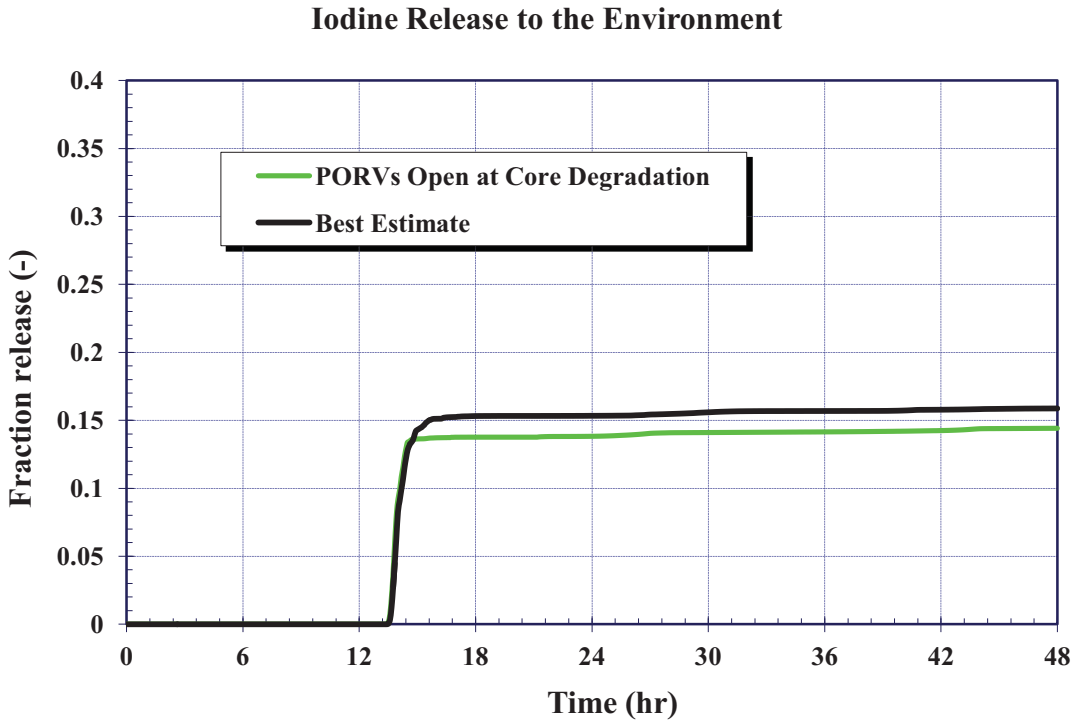

Figure 5-154 Iodine Release to the Environment – PORVs Open at Core Degradation

5.5.3.4 Effect of Throttling HHSI Flow

Discussion with the utility provided further insights into expected operator actions associated with the HHSI pumps during an ISLOCA. To preserve RWST inventory, operators would secure (i.e., stop) two HHSI pumps and throttle the remaining running pump as necessary to maintain water level in the reactor above TAF.

A timeline provided by the utility demonstrated that one HHSI pump would be secured 15 min after scram and another 1 hr after scram. Throttling of the third pump would commence at 1 hr and 45 min. Core water level would be maintained above TAF. A quasi-steady balance would be achieved between HHSI flow rate and the rate of steam production in the core.

The timeline described above was instituted in a MELCOR ISLOCA sensitivity calculation. 1 hr and 45 min into the calculation, when throttling of the remaining running HHSI pump began, roughly 190,000 gallons or 49% of the original 388,000 gallons in the RWST remained. This can be seen in Figure 5-155. Fission product decay power at this time had reduced to 32.5 MW as seen in Figure 5-156. By 4 hr, the reactor had depressurized to atmospheric pressure and the calculation had become uneventful. Figure 5-157, Figure 5-158, and Figure 5-159 show reactor pressure, water level, and maximum fuel cladding temperature in the calculation, respectively. Since the MELCOR calculation had become uneventful and was time consuming, a side calculation was performed to estimate how long it would take decay power to consume the remaining inventory in the RWST. Consuming the inventory was taken to involve heating the water to saturation and transforming it to steam. The decreasing trend of decay power was

accounted for. The side calculation predicted that the RWST would be exhausted 30 hr and 40 min after the onset of the ISLOCA.

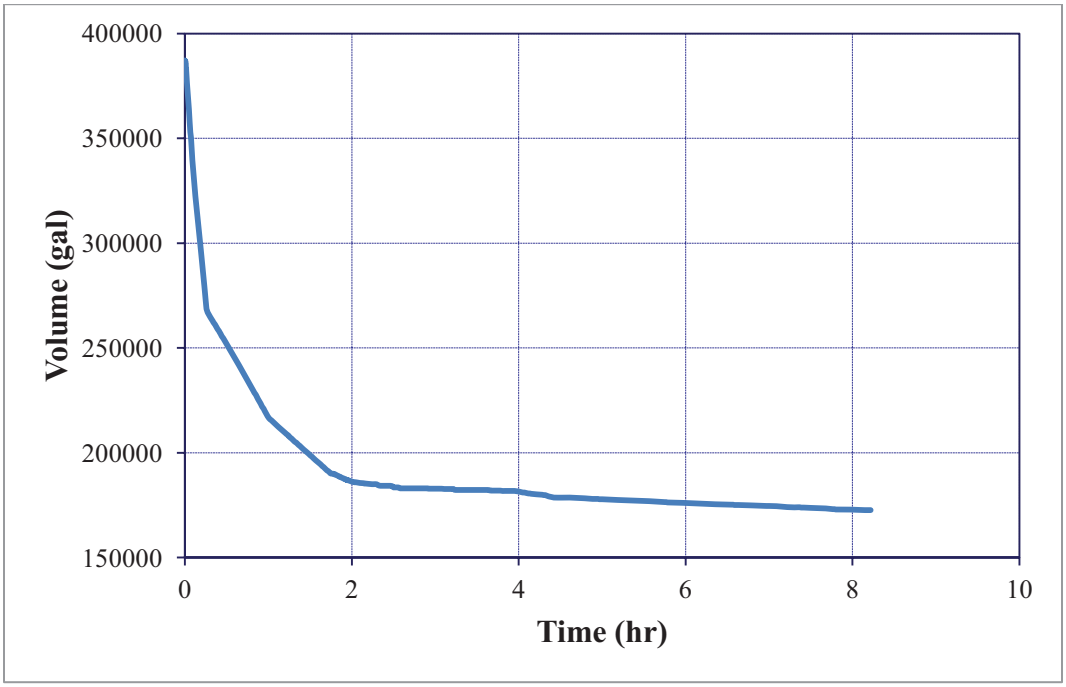

Figure 5-155 ISLOCA HHSI Throttling Sensitivity - RWST Inventory

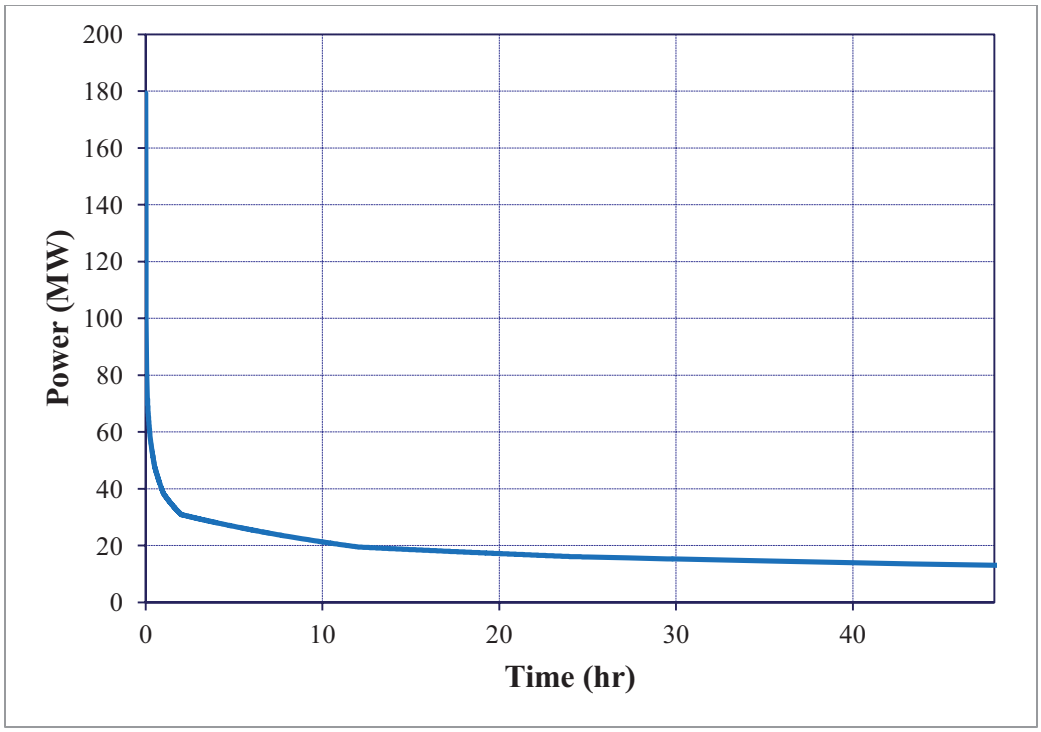

Figure 5-156 ISLOCA HHSI Throttling Sensitivity - Fission Product Decay Power

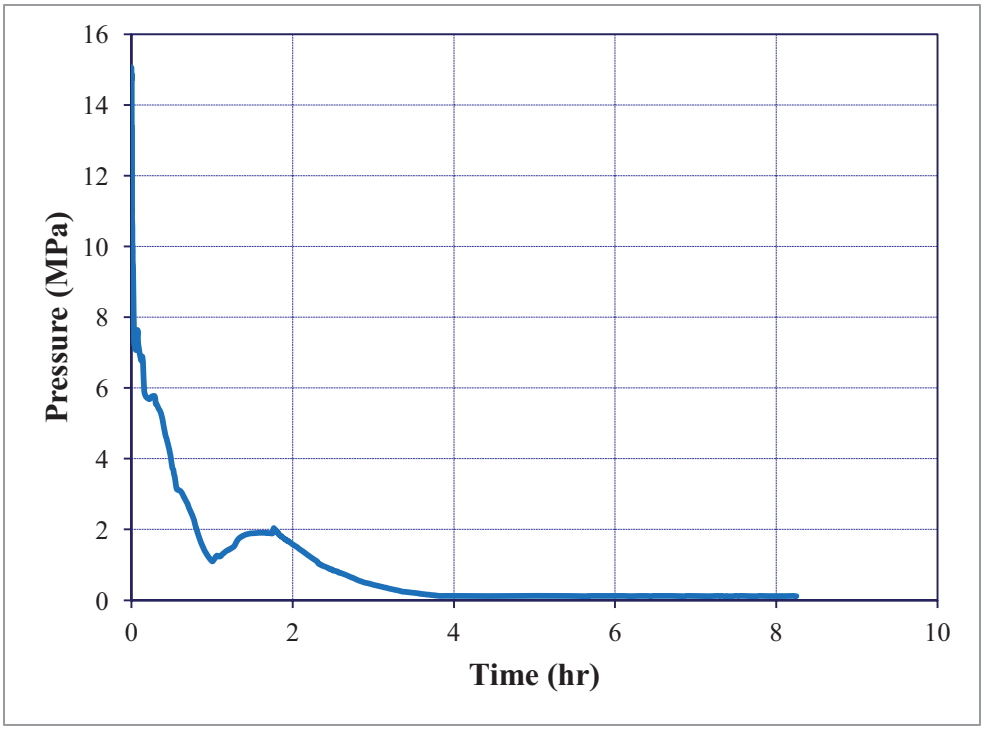

Figure 5-157 ISLOCA HHSI Throttling Sensitivity - RCS Pressure

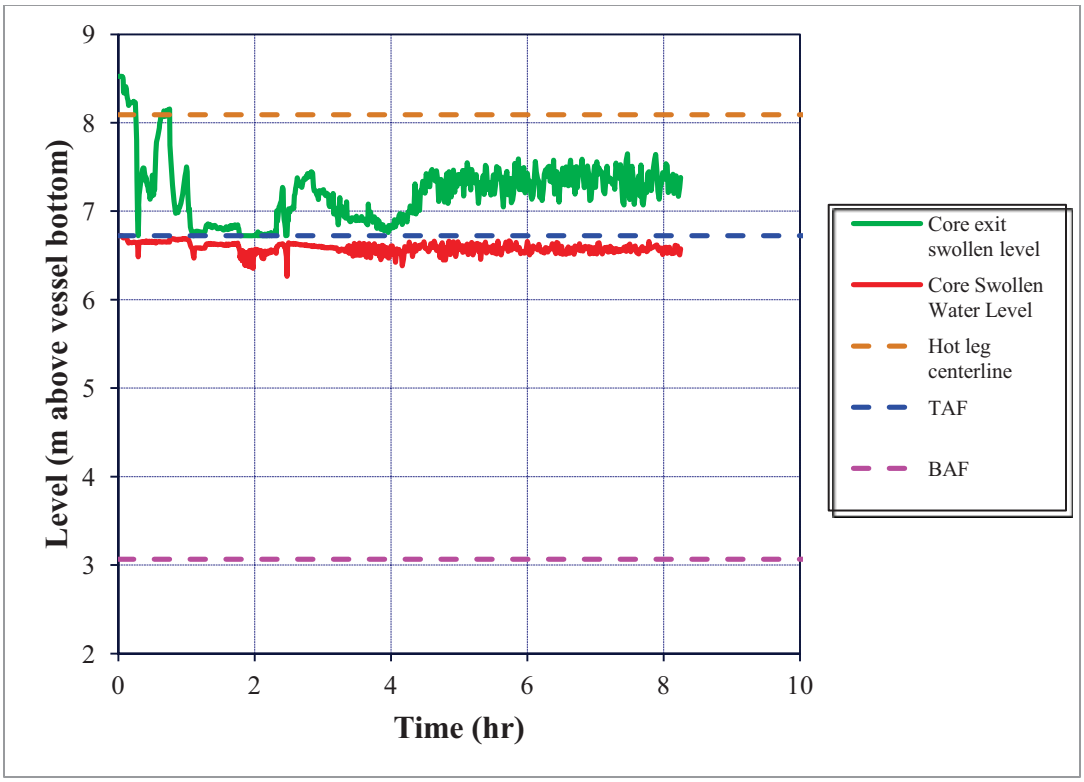

Figure 5-158 ISLOCA HHSI Throttling Sensitivity - Core Water Level

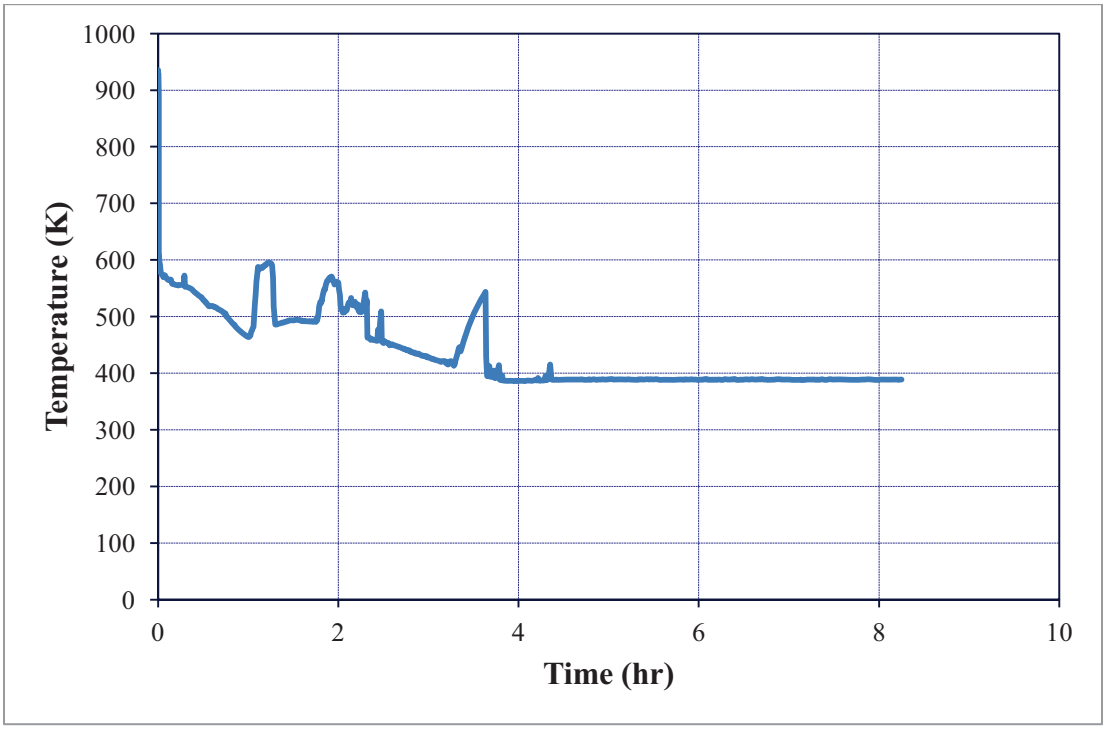

Figure 5-159 ISLOCA HHSI Throttling Sensitivity - Maximum Core Temperature

5.6 Other Sensitivity Studies

During the peer review of the MELCOR calculations, several other more generic issues were identified relative to the ones already discussed in Sections 5.2.3 and 5.3.3. They include uncertainties in the chemical form of iodine, iodine spiking, uncertainties of the impact of air ingression into the vessel, and uncertainties in the aerosol deposition rate in containment.

5.6.1 Chemical Form of Iodine

The chemical forms and quantities of gaseous iodine are an active research topic as new information is still being evaluated in existing and planned tests. The SOARCA calculations did not include gaseous iodine. All iodine was assumed to be combined with cesium to form cesium iodine and remain in that chemical form. New data from Phebus suggests some iodine is released in elemental form yet undergoes complex chemical reactions in the containment to form organic compounds unless liberated by the chemosorption process. MELCOR does not include a model for surface chemistry with paint. Furthermore, MELCOR's ex-vessel iodine pool model is very slow running and not fully validated. Consequently, all the iodine was modeled as a cesium iodine compound and the pool iodine model was not used. It should be noted that the uncertainty study will investigate the influence of different fixed amounts of gaseous iodine (i.e., elemental and organic forms).

Relative to the current results, it is worth making some simple evaluations using recent interpretations of Phebus data [40]. Phebus Test FTP-1 shows that the concentration of iodine reaches a steady state in the containment that is independent of the pool pH and condensing or evaporating conditions. In particular, the prototypical Phebus configuration shows a steady state exchange between the painted surfaces where the iodine is absorbed and released to maintain a steady concentration.

Two evaluations were performed to assess the impact of gaseous iodine on the source term using Phebus FTP1 data. In the first evaluation using the STSBO, a range of gaseous iodine concentrations were considered with the calculated containment leakage rate to estimate the additional iodine source term. The measured Phebus gaseous iodine containment concentrations are shown in Figure 5-160 with the conversion to an iodine release fractions based on the containment release rate. The calculated iodine release magnitude was 0.65% in the unmitigated STSBO at 48 hours (see Section 5.2.1). Assuming gaseous iodine concentrations of 0.05%, 0.10%, and 0.15%, the additional source term would be less than 0.10%. Given the small absolute and relative magnitude of the iodine release, the impact of a 0.10% additional gaseous iodine release was judged as not significant.

The second evaluation examined the additional source term to the environment through the failed steam generator tube, which occurred earlier in the accident progression. The measured Phebus gaseous iodine containment concentrations are shown in Figure 5-161. The higher short-term values were used to estimate the additional gaseous release to the environment. Using the noble gas leakage rate into the environment through the steam generator secondary and the early,

higher concentrations from Phebus containment, the gaseous iodine leak rate was calculated.[37] The calculated iodine release rate was 0.6% in the first 24 hours when the dominant releases through the TI-SGTR occurred (see Section 5.3.1.2). Assuming gaseous iodine concentrations of 0.10%, 0.15%, and 0.20%, the additional source term would be <<0.10%, respectively. Given the small absolute and relative magnitude of the iodine release, the impact of gaseous iodine on the source term was also judged small. Following vessel failure, any remaining gaseous iodine in the reactor vessel was discharged into the containment. All further releases through the failed TI-SGTR were diluted by the volume of the containment.

In summary, gaseous forms of iodine have the potential to increase the severity of the environmental source term because they do not settle like other aerosol radionuclides. Gaseous iodine remains an important source term issue, especially with respect to long-term containment performance issues after the comparatively much larger airborne radioactivity has settled from the atmosphere. The mechanistic modeling treatment for gaseous iodine behavior is a technology still under development with important international research programs underway to determine the dynamic behavior of iodine chemistry with respect to paints, wetted surfaces, buffered and unbuffered water pools undergoing radiolysis, and gas phase chemistry. In SOARCA, gaseous iodine was not specifically included except as a revaporization gas from deposited cesium iodine that had chemisorbed onto stainless steel surfaces. The magnitude of the revaporization release was generally very small. A review of Phebus data suggests that gaseous iodine is released from the fuel and complex surface and pool reactions take place in the containment. Based on the analysis of the early and the long-term behavior from Phebus for two of the SOARCA calculations, it does not significantly change the magnitude or the timing of the overall iodine release. It was judged that the small additional source term of gaseous in the other sequences would also not change the overall conclusions of the study. Nevertheless, it should be noted that on-going and future NRC research is dedicated to better understanding iodine behavior.

Gaseous iodine remains an important source term issue, especially with respect to long-term containment performance issues after the comparatively much larger airborne radioactivity has settled from the atmosphere. The mechanistic modeling treatment for gaseous iodine behavior is a technology still under development with important international research programs underway to determine the dynamic behavior of iodine chemistry with respect to paints, wetted surfaces, buffered and unbuffered water pools undergoing radiolysis, and gas phase chemistry. The base case treatment under the best practices recommendation are sufficient for the mean effects addressed in SOARCA.

[37] The gaseous iodine release was estimated by examining the noble gas release from the fuel and the fraction subsequently transported through the failed steam generator tube. Since the release of the noble gases occurred roughly coincidental with the expected gaseous iodine release (i.e., both considered highly volatile), the subsequent accumulation and transport of the non-condensable noble gas would be a good surrogate for gaseous iodine. In particular, the portion transported out the failed tube versus the amount discharged in the containment could be assessed. As described above, the magnitude of the gaseous iodine release from the fuel was scaled based on the short-term estimates from Phebus FPT1.

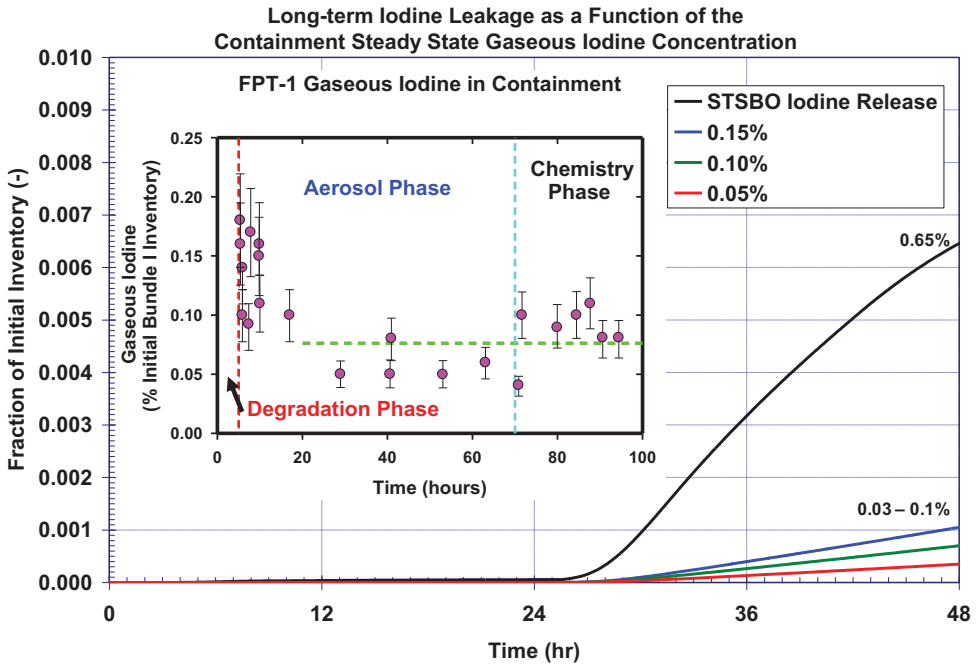

Figure 5-160 The additional gaseous iodine source term using Phebus data is compared to the iodine source term for the unmitigated short-term station blackout

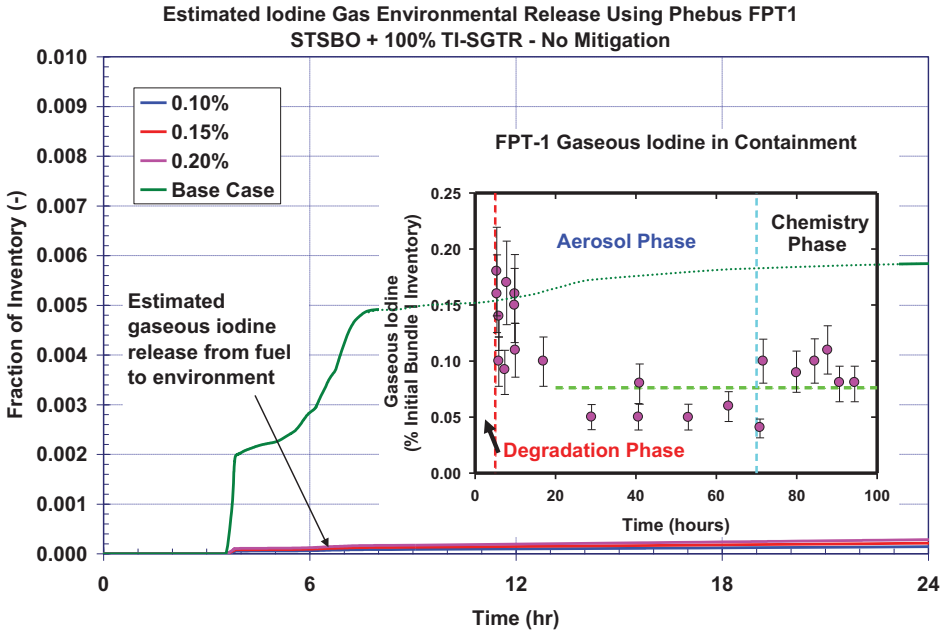

Figure 5-161 The additional gaseous iodine source term using Phebus data is compared to the iodine source term for the unmitigated short-term station blackout with a thermally-induced steam generator tube rupture

5.6.2 Additional Source Term from Iodine Spiking

Iodine spiking was identified by one of the review committee members as a possible alternate source of iodine to the environment for an early release in the spontaneous SGTR. Using the water leakage from the unmitigated SGTR, the maximum recorded iodine spike (18 μCi/g), and the recommended partition factor from Regulatory Guide 1.83 (i.e., 100)[38], the fractional iodine release was 10^{-6} [42]. While an iodine spike might be an operational concern, it is not significant relative to the magnitude of release fractions from the other considered severe accidents (see Table 5-16).

Table 5-16 Comparison of Iodine Spike Source Term to Iodine Source Terms from the Other Unmitigated Accidents

Unmitigated Scenario	Core fraction of iodine released to environment
Long-term SBO	0.003
Short-term SBO	0.006
Short-term SBO with thermally induced SGTR	0.009
ISLOCA	0.158
Spontaneous SGTR (Iodine Spike)	10^{-6}

5.6.3 Air Ingression into the Vessel

Air ingression into the vessel was identified by one of the peer review committee members as an important concern for enhanced air oxidation of metals and enhanced ruthenium releases. There are two events in the Surry SOARCA sequences where air ingression into the reactor could occur.[39] First, while the fuel is degrading, natural circulation into the RCS could lead to creep rupture of the hot leg. Since there was a large decay heat source in the reactor vessel, all cases showed a slight pressurization of the reactor coolant system relative to the containment (or auxiliary building) that maintained a steady flow outward of the pipe breaks. Consequently, inward flow of air during this time was not expected.

Later in the accident progression, the fuel will collapse onto the lower head and fail the reactor vessel. Following failure of reactor vessel, the hot contents in the lower plenum poured into the reactor cavity. In the progression of events calculated in the unmitigated scenarios, all injection

[38] Although Regulatory Guide 1.83 was withdrawn on November 12, 2009 (Federal Register Volume 74, Number 217, 58324), the use of the recommended partition factor remains appropriate for the purposes of this analysis.

[39] A pipe break in the reactor coolant system for a loss-of-coolant accident (LOCA) could be another event. The ISLOCA was the only LOCA examined for Surry. It is incredible to imagine any significant air ingression upstream through 30 m of LHSI piping against sonic two-phase flow in the ISLOCA. However, if a large break LOCA of the RCS piping had been considered , there is a potential for air ingression.

had terminated and the entire core had degraded and collapsed prior to vessel failure. Consequently, all the debris relocated to the cavity prior to any significant air-ingression (e.g., see Figure 5-162).

Finally, MELCOR includes models for both steam and air oxidation of metals in the core package. Consequently, air oxidation is considered if any air ingression occurs. However, there are no models for automatically changing the ruthenium release model in an air-oxidizing environment. Consequently, each calculation must be reviewed for the presence of high air concentration conditions, which was done.

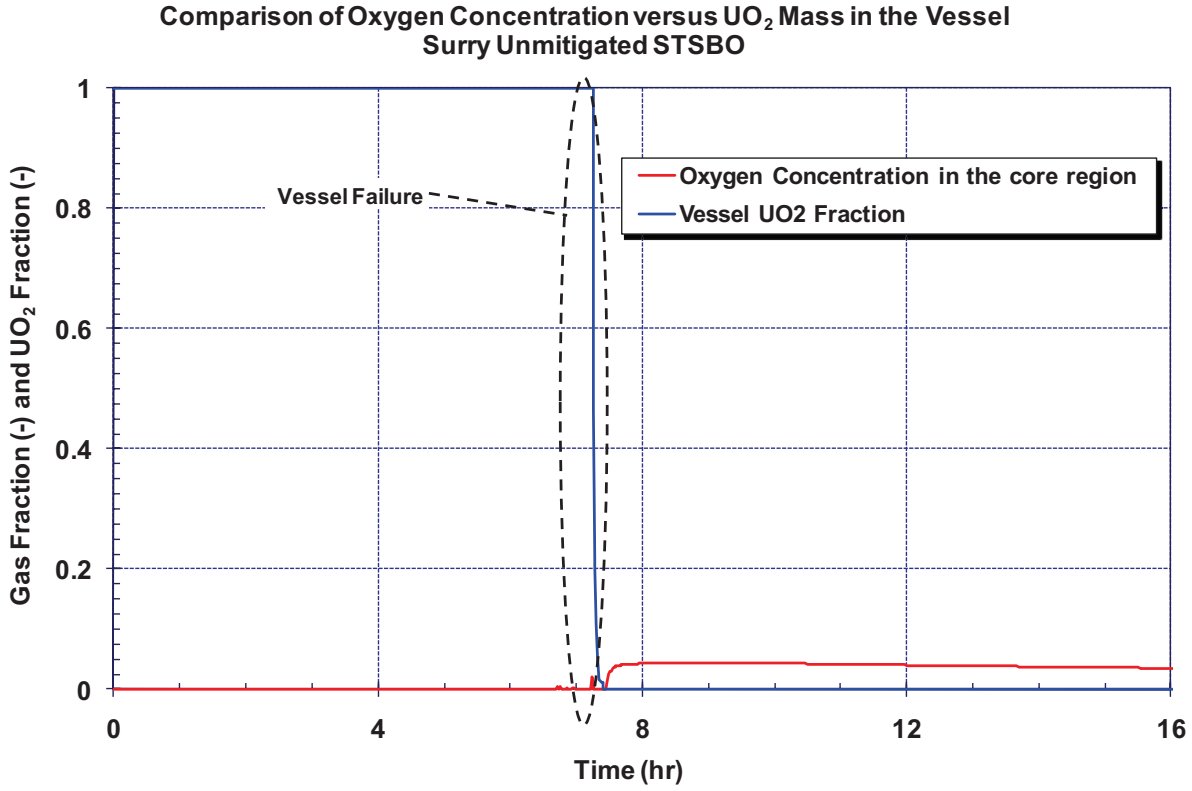

Figure 5-162 Comparison of the oxygen concentration and UO_2 mass in the vessel during the unmitigated STSBO

5.6.4 Aerosol Settling Rate in the Containment

A peer review committee member thought the aerosol settling rate in the containment looked high (e.g., Figure 5-34) for the STSBO scenario without B.5.b mitigation. To address this issue, two time phases were investigated. The first time phase occurred after the hot leg failure. Following hot leg failure, co-dispersing and flashing water from accumulator injection with the aerosols immediately led to a very high mass median diameter of the airborne aerosols (>10 μm), which caused them to settle very quickly. The condescending steam helped increase agglomeration enhanced deposition. Within one hour after hot leg failure, over 50% of the airborne aerosols had settled.

The second phase occurred with the releases following prior to and at vessel failure. To analyze the settling rate, the mass of airborne aerosols in the STSBO at vessel failure were normalized to one (see Figure 5-163). Following vessel failure, the airborne aerosol concentration decreased steadily. The airborne decay constant, λ, was calculated and compared to Phebus FTP0 data [41]. The calculated decay constant is a strong function of the mass-median diameter of the airborne aerosols. However, the results in Figure 5-163 show the settling rate was comparable to the test data and actually slightly slower.

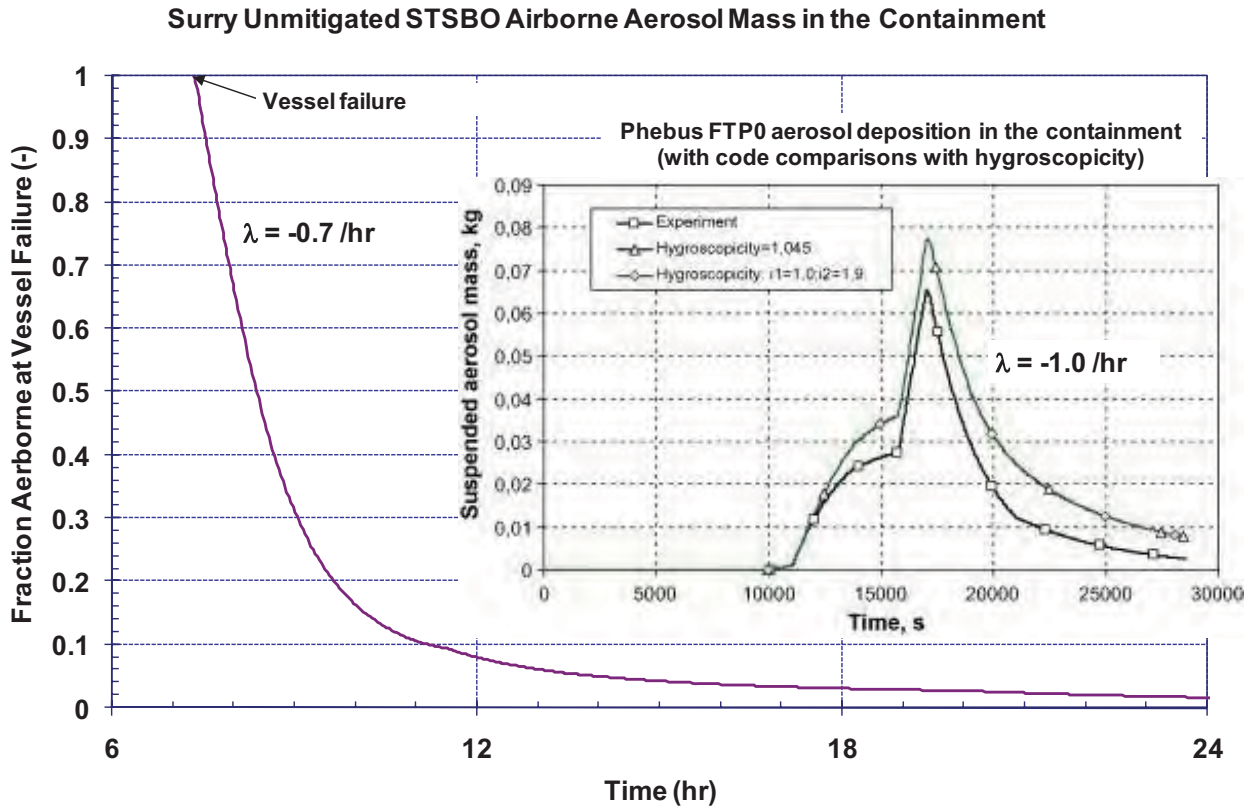

Figure 5-163 Unmitigated STSBO airborne aerosol mass in the containment following vessel failure

6. EMERGENCY RESPONSE

Advancements in consequence modeling now allow more detailed and more realistic treatment of emergency response when performing consequence analyses. This includes the ability to model protective action decisions from offsite response organizations (OROs) and the implementation of protective actions by individual population segments. To best utilize these advancements, detailed information was obtained from local sources and OROs. Through a user interface added to the consequence model, this detailed information was input to account for differences in the implementation of protective actions by individual population segments. These advancements are significant because they facilitate more realistic modeling of response activities, timing of decisions, and implementation of protective actions across different population segments.

Emergency response programs for nuclear power plants (NPPs) are designed to protect public health and safety in the event of a radiological accident. These emergency response programs are developed, tested, and evaluated and are in place as defense in depth to respond in the unlikely event of an accident. To support a state of the art approach and integrate realism in the analyses, the modeling of the emergency response was based on the site-specific emergency planning documentation and on research of public response to non-nuclear emergencies. The information developed in this Emergency Response Section was used to support the MACCS2 consequence analyses for the accident scenarios. These analyses are conducted for the unmitigated accident sequences only. Many of these response actions would be similar for the mitigated case because response officials initiate protective actions upon notification, which as described herein occurs very early in the incident, even before mitigation actions have been implemented. This is because emergency planning is designed to be proactive to remove the public prior to plume arrival when possible. For each accident scenario, evacuation of the plume exposure pathway emergency planning zone (EPZ) was assessed. This included consideration of a shadow evacuation to a distance of 20 miles from the plant. Including a shadow evacuation, which occurs when members of the public evacuate from areas that are not under official evacuation orders, provides realism because these are observed in large-scale evacuations [51] and have the potential to slow down the evacuation from the affected area. Also, for each scenario, members of the public were modeled as being relocated from any area where doses are projected, based on the consequence analysis model, to exceed established criteria. Figure 6-1 identifies the location of the Surry plant and radial distances of 10 and 20 miles from the plant.

Sensitivity analyses were completed for one of the accident scenarios to evaluate evacuation distances of 16 miles and 20 miles from the plant. The sensitivity analysis of an evacuation to 20 miles is different than the shadow evacuation to 20 miles described above, because the sensitivity analysis evaluates the conditions under which residents of the entire 20 mile area are notified to evacuate and leave the area. A sensitivity analysis was performed to assess the effect of a delay in the implementation of protective actions, as suggested by the peer review committee. An analysis was also conducted that included consideration of the effects on infrastructure, emergency response, and response of the public due to a seismic event.

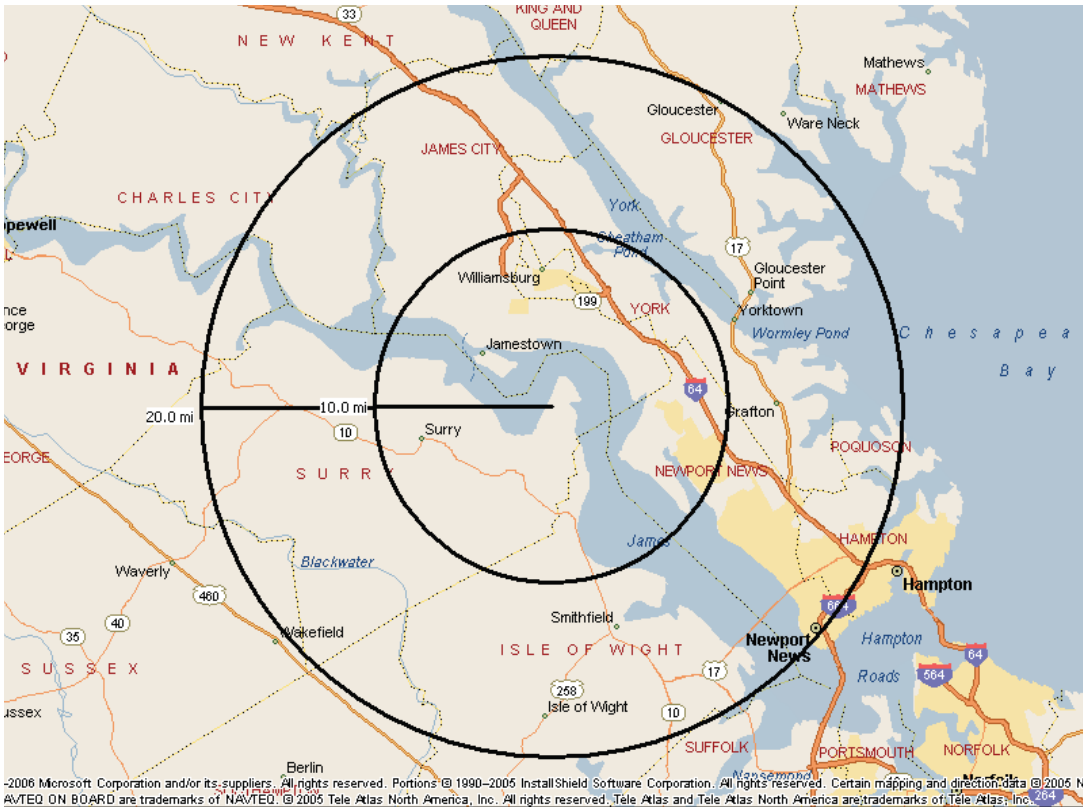

Figure 6-1 Surry 10 and 20 Mile Areas

As required by 10 CFR 50, OROs develop emergency response plans for implementation in the event of an NPP accident. These plans are regularly drilled and are inspected biennially, through a demonstration exercise performed in conjunction with the licensee. In biennial exercises, ORO personnel demonstrate timely decision making and the ability to implement public protective actions. Emergency plans escalate response activities in accordance with a classification scheme based on emergency action levels (EALs). Preplanned actions are implemented at each classification level including Unusual Event, Alert, Site Area Emergency (SAE), and General Emergency (GE). Public protective actions are required at the GE level, but ORO plans commonly include precautionary protective actions at the SAE level and sometimes at an Alert.

The plume exposure pathway EPZ is identified in NUREG-0654 / FEMA – REP-1, Rev. 1, [26] as the area around an NPP of about 10 miles. Within the EPZ, detailed emergency plans are in place to reduce the risk of public health consequences in the unlikely event of an accident. Emergency planning within the EPZ provides a substantial basis for expansion of response efforts should it be necessary. ORO personnel have repeatedly demonstrated the ability to implement protective actions within the EPZ during inspected biennial exercises. Modeling of expected protective action response is described in this section. Analyses were conducted for accident scenarios identified in Table 6-1.

Table 6-1 Scenarios Assessed for Emergency Response

Report Section Number	Scenario
6.3.1	Unmitigated STSBO
6.3.2	Unmitigated STSBO with TI-SGTR
6.3.3	Mitigated STSBO with TI-SGTR
6.3.4	Unmitigated LTSBO
6.3.5	Unmitigated ISLOCA
6.4.1	Sensitivity 1 Unmitigated ISLOCA and evacuation to 16 miles
6.4.2	Sensitivity 2 Unmitigated ISLOCA and evacuation to 20 miles
6.4.3	Sensitivity 3 Unmitigated ISLOCA with a Delay in Implementation of Protective Actions
6.5.6	Seismic Analysis - Unmitigated STSBO with TI-SGTR

6.1 Population Attributes

The population near the Surry plant was modeled using six cohorts. A cohort is a population group that mobilizes or moves differently from other population groups. Modeling includes members of the public who evacuate early, evacuate late, those who refuse to evacuate, and those who evacuate from areas not under an evacuation order (e.g., the shadow evacuation). The consequence model does not constrain the number of cohorts but there is no benefit to defining an excessive number of cohorts with little difference in response characteristics. The following cohorts were established for SOARCA analyses:

Cohort 1: 0 to 10 Public:
This cohort includes the public residing within the EPZ.

Cohort 2: 10 to 20 Shadow:
This cohort includes the shadow evacuation from the 10 to 20 mile area beyond the EPZ. A shadow evacuation occurs when members of the public evacuate from areas that are not under official evacuation orders and generally begins when a large scale evacuation is ordered [51]. Shadow evacuations are often reported and observed, although there is little quantitative data available. In a national telephone survey of residents of EPZs, more than 20 percent of people that had been asked to evacuate for emergencies such as hurricanes, had also evacuated for similar emergencies in which they were asked not to evacuate (e.g., they were shadow evacuees) [51]. Additional information used to develop a value for use in the SOARCA analysis included a review of more than 20 NPP evacuation time estimate (ETE) studies. Although not currently required, most of these ETE studies included an analysis of a shadow evacuation. Typically, a shadow evacuation of 30 percent of the public outside the EPZ to a distance of 15 miles was included in the analysis and often sensitivity analyses were provided that varied the shadow evacuation percentage to values as high as 60 percent. Review of the ETE values

showed that increasing the percentage of public participating in the shadow evacuation did not affect the ETE in 11 of 16 studies that included a sensitivity analysis. Using the above information, combined with the early decision in the SOARCA project to consider effects beyond the EPZ to a distance of 20 miles, a shadow evacuation of 20 percent of the public from the area 10 to 20 miles from the plant was modeled. The shadow evacuation was determined to have no effect on the evacuation of the Surry EPZ because much of the area beyond the EPZ is lightly populated.

Cohort 3: 0 to 10 Schools:
This cohort includes elementary, middle and high school student populations within the EPZ. Schools receive early and direct warning from OROs and have response plans in place to support busing of students out of the EPZ, but sirens are not sounded as SAE.

Cohort 4: 0 to 10 Special Facilities:
The Special Facilities population includes residents of hospitals, nursing homes, assisted living communities and prisons. Special facility residents are assumed to reside in robust facilities such as hospitals, nursing homes, or similar structures, which provide additional shielding. Shielding factors for this population group consider this fact. In an emergency, Special Facilities would be evacuated individually over a period of time based upon available transportation.

Cohort 5: 0 to 10 Tail:
The 0 to 10 Tail is defined as the last 10 percent of the public to evacuate from the EPZ. The approach to modeling the Tail is an analysis simplification to support inclusion of this population group. The Tail takes longer to evacuate for many valid reasons such as the need to return home from work to evacuate with the family, pick up children, shut down farming or manufacturing operations or performing other actions prior to evacuating as well as those who may miss the initial notification.

Cohort 6: Non-evacuating public:
This cohort represents a portion of the public from 0 to 10 miles who may refuse to evacuate and is assumed to be 0.5 percent of the population. The cohort is modeled as though they are performing normal activities. Research of large scale evacuations has shown that a small percentage of the public refuse to evacuate [51] and this cohort accounts for this potential group. It is important to note that emergency planning is in place to support evacuation of 100 percent of the public.

6.1.1 Population Distribution

The Surry 2001 ETE was used to develop the population fractions for the cohorts within the EPZ. The populations provided in the Surry 2001 ETE [27] present a detailed estimate of the population of the 0 to 10 mile region.

A separate estimate was developed for the permanent residents and special facilities population beyond the EPZ to support development of the shadow population cohort and sensitivity analyses. SECPOP2000 was used to estimate the population within 20 miles of the plant. The population was projected to 2005 using a multiplier of 1.0533 obtained from Census Bureau information. The population of the 10 to 20 mile area outside the EPZ was then calculated as the

difference between the total estimated population within 20 miles and the 10 mile EPZ population. School children are not a separate cohort in the 10 to 20 mile area because it is assumed there is ample time for schools to close and children to go home and evacuate with families; therefore they are included in the 10 to 20 public. Special facilities data for hospitals, nursing homes, and detention facilities in the 10 to 20 mile area was developed by researching available public information.

To establish the population distributions, the Shadow population was assessed first and defined as 20 percent of the total population within 10 to 20 miles from the plant. This value for the Shadow was then combined with non-evacuee, special facilities, and schools and then subtracted from the remaining total to establish the general public. Ten percent of the general public defines the evacuation tail, and the remainder was used as the total for the general public. The non-evacuating population is 0.5 percent of the total population in each region. Cohort populations are provided in Table 6-2.

Table 6-2 Surry Cohort Population Values

Cohort	Description	Population
1	0 to 10 Public	88,590
2	10 to 20 Shadow	63,171
3	0 to 10 Schools	23,262
4	0 to 10 Special Facilities	844
5	0 to 10 Tail	7,232
6	0 to 10 Non-evacuating	603

6.1.2 Evacuation Time Estimates

As provided in 10 CFR 50.47 Appendix E, each licensee is required to estimate the time to evacuate the EPZ. Appendix 4 of NUREG-0654/FEMA-REP-1, Revision 1 [26] provides information on the requirements of ETEs, and NUREG/CR-6863, "Development of Evacuation Time Estimate Studies for Nuclear Power Plants," [28] provides detailed guidance on development of ETEs. A typical ETE includes many scenarios to help identify the combination of events for normal and off-normal conditions and provides emergency planners with estimates of the time to evacuate the EPZ under varying conditions [28]. The ETE study provides information regarding population characteristics, mobilization of the public, special facilities, transportation infrastructure, and other information used to estimate the time to evacuate the EPZ.

The SOARCA project used a normal weather weekday scenario that includes schools in session. This scenario was selected because it presents several challenges to timely protective action implementation including evacuating while residents are at work and mobilizing buses to evacuate children at school. The Surry 2001 ETE report [27] provides the following regarding evacuation of the general public:

East of the James River- The densely populated area.

- 100 percent evacuation: 13 hours; and
- 90 percent evacuation: 10 hours and 50 minutes (rounded to 11 hours).

West of the James River- The rural low population area.

- 100 percent ETE: 3 hours 10 minutes; and
- 90 percent ETE: Not provided.

These values were used to develop the speeds for the cohorts used in the analysis. The Surry study [27] describes the ETE scenario used as a 'worst case' because it includes the high number of transients in the area and schools in session. This scenario can be considered the bounding ETE case for the analysis and alternative seasonal evaluations and time of day are not necessary.

For the evacuation scenarios, a speed is input into the consequence model. The evacuation speed is developed from the ETE and is primarily influenced by population density and roadway capacity. When using ETE information, it is important to understand the components of the time estimate. The ETE includes mobilization activities the public undertakes upon receiving the initial notification of the incident [26], [28]. These actions include receiving the warning, verifying information, gathering children, pets, belongings, etc., packing, securing the home, and other evacuation preparations. Thus, a 13 hour ETE does not indicate that all of the vehicles are en route for 13 hours, but is the end of a 13 hour period in which the public mobilizes and evacuates the area. An evacuating population does not enter the roadway system at once. Rather an ideal model would include a "road loading function" that represents the expected movement. Most ETE studies use such a model. However, MACCS2 does not currently have the capability to move populations in this manner. This being the case, cohorts are modeled to begin moving together at a specific time after notification. To represent this movement of the cohort evacuating together, a single linear value based on distance divided by time (i.e., the ETE) was used for the speed. This distance over ETE ratio provides a slightly slower average speed than would be expected in an evacuation and adds some conservatism to the analysis.

Evacuations can therefore be represented as a curve that is relatively steep at the beginning and tends to flatten as the last members of the public exit the area. Through review of more than 20 existing ETE studies, the point at which the curve tends to flatten occurs where approximately 90 percent of the population has evacuated. This is consistent with research that has shown that a small portion of the population that takes a longer time to evacuate than the rest of the general public and is the last to leave the evacuation area [26]. This last 10 percent of the population is identified as the evacuation tail. A goal of emergency preparedness is to protect the public health and safety of the public. To best achieve this goal, new guidance from the NRC [89] suggests the 90 percent ETE be used when making protective action recommendations and decisions; therefore, for the analyses in this study, the 90 percent ETE value was used to develop evacuation speeds.

6.2 WinMACCS

WinMACCS is a user interface for the MACCS2 code and was used to generate input for MACCS2 model runs. WinMACCS has the ability to integrate the information described above into the consequence analysis. The entire evacuation area was mapped onto a radial sector grid network around the plant. The roadway network was reviewed against site-specific evacuation plans to determine likely evacuation direction in each grid element. The results of the ETE were reviewed to determine localized areas of congestion and areas where no congestion would be expected. Using this information, speed adjustment factors ranging from one to three were applied at the grid element level to speed up vehicles in the rural uncongested areas and to slow down vehicles in more urban settings.

6.2.1 Hotspot and Normal Relocation and Habitability

In the unlikely case of a severe accident and radiological release, protective actions in addition to evacuation may be implemented. For instance, residents would be relocated if their potential dose exceeds protective action criteria. OROs would base this determination on dose projections using state, utility, and Federal agency computer models as well as measurements taken in the field. Hotspot relocation and normal relocation models are included in the MACCS2 code to treat this contingency. Total dose commitment pathways for the relocation models are cloudshine, groundshine, direct inhalation, and resuspension inhalation. Relocated individuals are removed from the calculation for the remainder of the emergency phase and receive no additional dose during that phase. The dose criteria are applied after plume arrival at the affected area.

Hotspot relocation of individuals beyond ten miles occurs 24 hours after plume arrival if the total lifetime dose commitment for the weeklong emergency phase exceeds 0.05 Sv (5 rem). Normal relocation of individuals occurs 36 hours after plume arrival if the total lifetime dose commitment exceeds 0.01 Sv (1 rem). The relocation times of 24 hours for hotspot and 36 hours for normal relocation were established based on review of the emergency response timelines, which suggest that because of the high population density in some areas off the EPZ, OROs would not likely be available earlier to assist with relocation due to higher priority tasks in the evacuation area. Relocation is a process that requires identification of the affected areas and notification of residents within those areas. The time values represent the average time expected to implement each action.

The hotspot value used in NUREG-1150 [2] was 0.5 Sv (50 rem) and the relocation value was 0.25 Sv (25 rem). The long term habitability criteria used in NUREG-1150 was 0.04 Sv (4 rem) over a 5 year period. The NUREG-1150 long term habitability criterion is the same as the site specific value used for the Surry analysis. It should be noted that the non-evacuating cohort is still subject to the Hotspot and Normal Relocation criterion. It is assumed these individuals will evacuate when they understand a release has in fact occurred and they are informed they are located in high dose areas.

6.2.2 Shielding Factors

Shielding factors vary by geographical region across the United States, and those used in the Surry analysis are shown in Table 6-3. The factors represent the fraction of dose that a person

would be exposed to when performing normal activities, evacuating, or staying in a shelter in comparison to a person outside with full exposure and are applied to all cohorts. Special Facilities are typically larger and more robust structures than housing stock and therefore have better shielding factors as identified in the table. Special facilities have the same factor for normal and shelter indicating these individuals are all indoors.

Table 6-3 Surry Shielding Factors

	Ground Shine			Cloud Shine			Inhalation/Skin		
	Normal	**Evac.**	**Shelter**	**Normal**	**Evac.**	**Shelter**	**Normal**	**Evac.**	**Shelter**
Cohorts	0.26	0.50	0.20	0.68	1.00	0.60	0.46	0.98	0.33
Special Facilities	0.05	0.50	0.05	0.31	1.00	0.31	0.33	0.98	0.33

The shielding factors provided in Table 6-3 were obtained from a variety of sources. Where appropriate, site specific values for sheltering were obtained from NUREG-1150 [2]. An updated inhalation/skin evacuation shielding factor was obtained from NUREG/CR-6953, Vol. 1, [52]. The normal activity shielding factors have been adjusted to account for the understanding that people do not spend a great deal of time outdoors. The normal activity values are all weighted averages of indoor and outdoor values based on being indoors 81 percent of the time and outdoors 19 percent of the time [90]. Indoor values are assumed to be the same as sheltering.

6.2.3 Potassium Iodide

The State of Virginia implements a potassium iodide (KI) program. The Virginia Department of Health provides potassium iodide to people who live, work or visit within 10 miles of the Surry NPP. Potassium iodide also is available to the public for purchase without a prescription at pharmacies and from manufacturers.

The purpose of the KI is to saturate the thyroid gland with stable iodine so that further uptake of radioactive iodine by the thyroid is diminished. If taken at the right time and in the appropriate dosage, KI can nearly eliminate doses to the thyroid gland from inhaled radioiodine. Factors that contribute to the effectiveness of KI include the availability (i.e., whether residents can find their KI), the timing of ingestion, and the degree of pre-existing stable iodine saturation of the thyroid gland. It is considered that some residents will not remember where they have placed their KI or may not have it available and will therefore not take KI. It is also assumed some residents will not take their KI when directed (i.e., they may take it early or late which reduces the efficacy). To account for this, KI was turned on in the model for approximately 50 percent of the public, and the efficacy of the KI was set at 70 percent.

6.2.4 Adverse Weather

Adverse weather is typically defined as rain, ice, or snow that affects the response of the public during an emergency. The affect of adverse weather on the mobilization of the public is not directly considered in establishing emergency planning parameters for this project because such a consideration approximates a worst case evacuation scenario. However, adverse weather was

addressed in the movement of cohorts within the analysis. The evacuation speed multiplier (ESPMUL) parameter in WinMACCS is used to reduce travel speed when precipitation is occurring as indicated from the meteorological weather file. The ESPMUL factor was set at 0.7, which effectively slows down the evacuating public to 70 percent of the established travel speed when precipitation exists.

6.2.5 Modeling using Evacuation Time Estimates

The purpose of using the ETE as a parameter in consequence modeling is to better approximate the real time actions expected of the public. Although consequence modeling has evolved to allow use of many cohorts and can address many individual aspects of each cohort, the approach to modeling evacuations is not direct. As stated earlier, evacuations include mobilizing and evacuating the public over a period of time, which is best modeled as a distribution. To use WinMACCS, this distribution of data must be converted into discrete events. For instance, upon the sounding of the sirens and issuance of the Emergency Alert System messaging, it is assumed all members of the public shelter and one hour later all members of the public enter the roadway network together at the same time and begin to evacuate. In research of existing evacuations for technological hazards, it is shown that most members of the public would enter the roadway network over a period of about an hour. It is not realistic that all vehicles would load simultaneously; however, this treatment within the model is necessary due to the current modeling abilities of WinMACCS.

Although WinMACCS can accommodate more cohorts, expert judgment was used to balance the number of cohorts with model run time. The speeds for each cohort are developed from the ETE, and the elements that factor into the speeds include:

- Time to receive notification and prepare to evacuate (i.e., mobilization time);
- Time to evacuate; and
- Distance of travel.

The time to receive notification requires assurance that sirens sound when needed. In review of the Reactor Oversight Program data regarding sirens for Surry, the average siren performance indicator was 99.9 percent, indicating that sirens will perform when needed. With few exceptions, travel speeds were established as whole numbers. A simple ratio of distance to time would show that evacuation of the 0 to 10 public from the 10 mile EPZ at Surry, which has an ETE of 10 hours 50 minutes, would provide a speed of 0.92 mph. However, as indicated above, notification and preparation to evacuate are included in the ETE.

For the general public, a one hour delay to shelter is assigned to reflect the mobilization time when residents receive the warning and prepare to evacuate. If the one hour mobilization time is subtracted from the ETE (10:50 – 1 hour) there remains 9 hours and 50 minutes to travel a maximum of 10 miles. As observed in actual evacuations due to technological or other hazards, people perform these mobilization activities at varying times with some residents ready to evacuate quickly while others can take up to an hour or longer. While this cohort is sheltered, a greater shielding factor is applied, and while en route during the evacuation, a lower shielding factor is applied.

During the evacuation, roadway congestion occurs rather quickly and traffic exiting the EPZ begins to slow. In review of over 20 ETE studies, this congestion typically occurs in 1 to 2 hours depending upon the population density and roadway capacity of the EPZ. In the SOARCA analysis, the 0-10 public is sheltered and preparing to evacuate for one hour. The public is then loaded onto the roadway and congestion is assumed to occur within 15 minutes. This total time of 1 hour 15 minutes for congestion to occur was established to be consistent with ETE studies.

The calculation of the speed of evacuees includes the first 15 minutes to the point when congestion occurs. For this first 15 minutes, evacuees are assumed to travel at 5 mph. The slow initial speed was set to account for the model loading all members of a cohort at one time. In the first 15 minutes at 5 mph, a distance of 1.25 miles has been traveled. At that time congestion is heavy and speeds slow for the next 8.75 miles.

The ETE is 10 hours 50 minutes for this cohort. Having sheltered and prepared to evacuate for 1 hour and then traveled the first 15 minutes at 5 mph, the remaining time is 9 hours and 35 minutes (10:50 - 1 hour shelter - 15 minutes at 5 mph). To determine the speed of travel for the remaining 8.75 miles, the distance is divided by the time (8.75 miles / 9 hours and 35 minutes) which provides a speed of 0.9 mph. The calculated speed used in the analysis for this cohort was rounded to 1 mph for this cohort. This approach applies to evacuees travelling 10 miles. Most evacuees would travel less distance and some travel a greater distance because the roadways are not radial away from the plant. Adjustments were made to the speeds based on review of population densities and aerial photos of roadways. The baseline speed of 1 mph was assigned to the general public cohort Because this represents the slowest speed expected, the speed was increased using a speed adjustment factor of 3 in the rural areas where no congestion is expected.

6.2.6 Establishing the Initial Cohort in the Calculation

The WinMACCS parameters for the cohorts are stored in multi-dimensional arrays, and the dimensions of the arrays are defined by geographical area for the analysis. WinMACCS requires the dimensions be established with the first cohort. All subsequent cohorts must be defined within these array dimensions, meaning they can extend from the origin to any distance equal to or less than the maximum distance established with the first cohort.

Cohort 1 was defined as the 0 to 10 mile public and has the same response characteristics as Cohort 2. The cohort that extends the greatest distance and defines the limits of the array is the Shadow Evacuation, which is Cohort 2. Thus, in the WinMACCS model, Cohorts 1 and 2 had to be redefined to meet the above requirement. The model input parameters for Cohort 1 were extended from the plant out to the maximum array distance of 20 miles, and Cohort 2 extends from the plant out to 10 miles. Cohort 1 is input as 20 percent of the population from 0 to 20 miles. This captures the 20 percent of the population between 10 and 20 miles involved in the shadow evacuation beyond the EPZ. As noted earlier, for this site the shadow evacuation has no effect on the evacuation of the residents of the EPZ. The combination of Cohorts 1 and 2 from 0 to 10 miles in the WinMACCS model represent the Public (0 – 10) Cohort defined above. For the remaining cohorts, application of parameters in the WinMACCS model is direct, and the population fractions directly correspond to the cohort descriptions.

6.3 Accident Scenarios

An emergency response timeline was developed for each accident scenario using information from the MELCOR analyses, expected timing of Emergency Classification declarations, and information from the ETE. The timeline identifies points at which cohorts would receive instruction from OROs to implement protective actions. In practice, initial evacuation orders are based on the severity of the accident and in Virginia would likely include an evacuation of the 2 mile zone and a 5 mile downwind keyhole consistent with the guidance in Supplement 3 to NUREG-0654/FEMA-REP-1, Revision 1 [26]. The distance would be expanded to 10 miles based on dose projections. Because WinMACCS does not readily support modeling a keyhole area, the SOARCA project modeled evacuation of the full EPZ and a shadow evacuation from the 10 to 20 mile area.

6.3.1 Unmitigated LTSBO

The emergency response timeline for the unmitigated LTSBO scenario is shown in Figure 6-2. The timing of emergency classification declarations was based on the EALs contained in site emergency plan implementing procedures. Protective actions were assumed to be recommended by OROs in accordance with approved emergency plans and procedures. Discussions were held with site representatives to help ensure proper understanding of EALs for each accident scenario and emergency response practices. Discussions with OROs confirmed that sirens are only sounded for a GE at Surry. Siren systems are tested routinely within all EPZs and the results of the Response Oversight Program indicate a 99.9 percent performance rating for sirens at Surry. Therefore, it is assumed that sirens do not fail and in the event one or two do fail, societal notification and route alerting by OROs would alert residents in these areas within the same mobilization time period as estimated for the EPZ.

For this scenario, EAL SS1.1 specifies that if all offsite power and all onsite AC power is lost for greater than 15 minutes an SAE is declared. If restoration of power is not likely within 4 hours, EAL SG1.1 establishes that a GE be declared. It is expected the SAE is declared in about 15 minutes, and plant operators would recognize rather soon that restoration of power within 4 hours is unlikely. A 2 hour period from loss of power was selected as a reasonable time for declaration of a GE. It is expected that notification to OROs is timely and the sounding of sirens and broadcast of EAS messages occurs approximately 45 minutes after declaration of GE. From the MELCOR analysis, the first fission product gap release occurs 16 hours into the event with a significant radioactive release to the environment occurring 45.5 hours into the event. The duration of specific protective actions for each cohort are summarized in Figure 6-3.

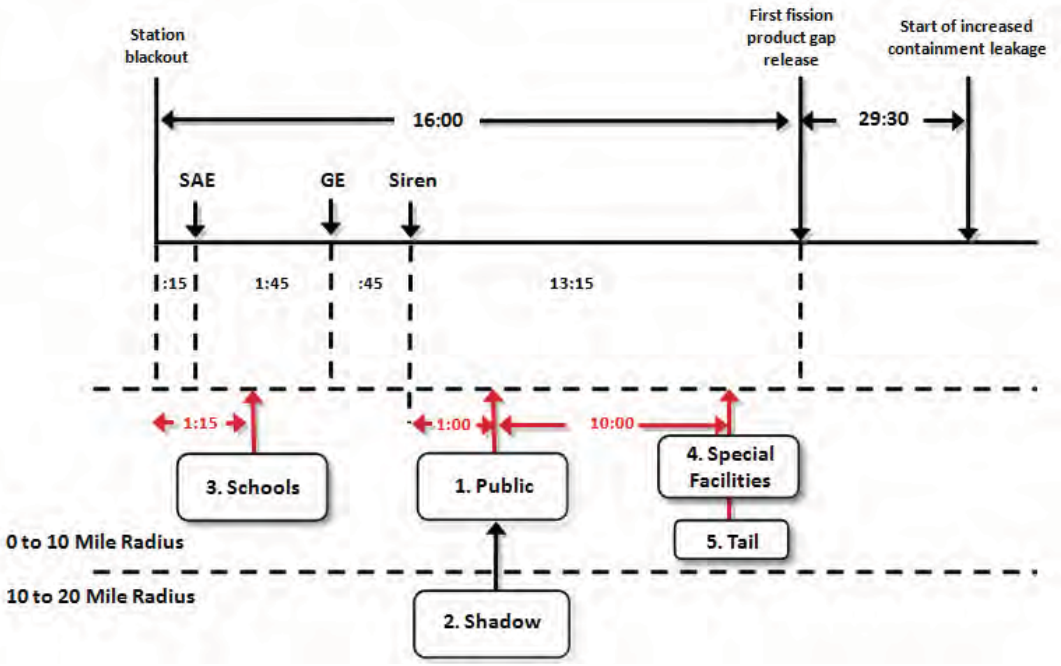

Figure 6-2 Unmitigated LTSBO Emergency Response Timeline

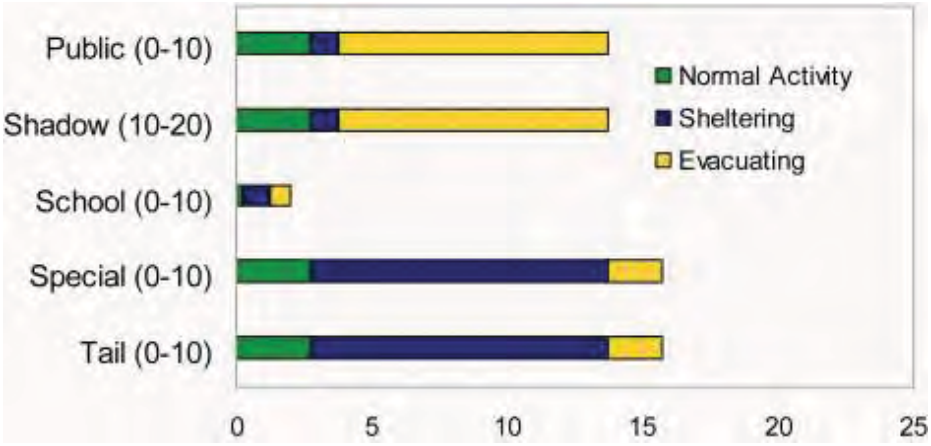

Figure 6-3 Duration of Protective Actions - Unmitigated LTSBO

The Virginia Department of Emergency Management will directly communicate with schools upon receiving the declaration of SAE. This allows for the preparation and early response of schools, but the public is largely unaware at this time. It could be noted that there would be a societal communication process as members of the public become aware of the school evacuation. Sirens are sounded at an SAE in many states, but Virginia only sounds sirens in response to declaration of a GE. Although there could potentially be some shadow evacuation due to societal communication, it is assumed that there would be no significant movement of the general public. The initiating event for the Unmitigated STSBO, Unmitigated STSBO with

TI-SGTR, Mitigated STSBO with TI-SGTR, and Unmitigated LTSBO scenarios is a station blackout and EAL SS1.1 and SG1.1 are reached. Therefore, the cohort actions are identical for each of these scenarios:

Cohort 1: 0 to 10 Public:
Following declaration of a GE, sirens are sounded and an evacuation order would be issued via an EAS message for affected areas within the EPZ. Cohort 1 is assumed to shelter when the sirens sound. The time to receive the warning and prepare to mobilize is assumed to be 1 hour after the siren. One hour is based on evacuation research, which shows the public mobilizes over a period of time with some members of the public moving soon after hearing the sirens, while most take some time to prepare and then evacuate. One hour was selected as a reasonable centroid of an evacuation curve for this cohort, which is consistent with empirical data from previous large scale evacuations [30].

Cohort 2: 10 to 20 Shadow:
This cohort is assumed to begin movement at the same time as the 0 to 10 Public after sirens have sounded within the EPZ and when widespread media broadcasts are underway. Residents in the 10 to 20 area begin seeing large numbers of people evacuating and initiate a shadow evacuation. There is no warning or notification for the public residing in this area, which is not under an evacuation order.

Cohort 3: 0 to 10 Schools:
Schools are the first to take action. Upon receipt of the declaration of SAE by the site, the Virginia Department of Emergency Management would notify the schools in accordance with the offsite emergency response plan. It is assumed schools are notified at SAE and begin sheltering in about 15 minutes. Buses would be mobilized, and it is assumed schools begin evacuating 1 hour after the start of the incident. At this time in the event, roads are uncongested and school buses are able to exit the EPZ quickly.

Cohort 4: 0 to 10 Special Facilities:
Special Facilities can take longer to evacuate than the general public because transportation resources, some of which are very specialized, must be mobilized. Special Facilities would be evacuated individually over a period of time based upon available transportation and the number of return trips needed. Special Facilities provide better shielding for the residents, thus while residents are in the facility, they are better protected than when they are evacuating. It was determined that the best representation of this cohort in the modeling is to evacuate with the tail and apply shielding factors consistent with the types of structures within which these residents reside. The Special Facilities cohort is assumed to depart at the same time as the evacuation tail, although it is recognized this cohort would begin mobilization about the same time as the schools.

Cohort 5: 0 to 10 Tail:
Using the evacuation data provided in the Surry ETE study [27], 90 percent of the evacuation of the EPZ is complete at approximately 11 hours into the evacuation, and this corresponds to the departure time for the 0 to 10 Tail.

Cohort 6: Non-evacuating public:
This cohort group represents the portion of the public who may refuse to evacuate and is assumed to be 0.5 percent of the population. Any member of the public who does not evacuate is still subject to the Hotspot and Normal Relocation criterion discussed earlier.

Selected input parameters for WinMACCS are provided to support detailed use of this study. More detailed information regarding modeling parameters is available in the MACCS2 User's Guide [48]. A brief description of the parameters is provided below:

- Delay to Shelter (DLTSHL) represents a delay from the time of the start of the accident until cohorts enter the shelter.

- Delay to Evacuation (DLTEVA) represents the length of the sheltering period from the time a cohort enters the shelter until the point at which they begin to evacuate.

- The speed (ESPEED) is assigned for each of the three phases used in WinMACCS including Early, Middle, and Late. Average evacuation speeds were developed from the Surry 2001 ETE report. Speed adjustment factors were then utilized in the WinMACCS application to represent free flow in rural areas and congested flow in urban areas.

- Duration of Beginning phase (DURBEG) is the duration assigned to the beginning phase of the evacuation and may be assigned uniquely for each cohort.

- Duration of Middle phase (DURMID) is the duration assigned to the middle phase of the evacuation and may also be assigned uniquely for each cohort.

For the 0 to 10 Public and the 0 to 10 Tail cohorts, by definition the sum of the DLTEVA, DURBEG and DURMID is equal to the ETE. This is because the ETE does not include shelter time. Table 6-4 provides a summary of the evacuation timing actions for each cohort. The MACCS2 variable names are included at the top of each column.

Table 6-4 Unmitigated LTSBO cohort timing

Cohort	Delay to Shelter DLTSHL (hr)	Delay to Evacuation DLTEVA (hr)	Duration of beginning phase DURBEG (hr)	Duration of middle phase DURMID (hr)	Speed of early phase ESPEED† (early) mph	Speed of middle phase ESPEED† (mid) mph
0 to 10 Public	2.75	1	0.25	9.75	5	1
10 to 20 Shadow	2.75	1	0.25	9.75	5	1
0 to 10 Schools	0.25	1	0.25	0.5	10	10
0 to 10 Special Facilities	2.75	11	1	1	1	10
0 to 10 Tail	2.75	11	1	1	1	10
Non-Evac	NA	NA	NA	NA	0	0

† Values represent speeds east of the James River. Speeds west of the river are increased through use of multipliers in the WinMACCS model.

Departure speeds and durations of the beginning and middle periods for the WinMACCS runs were developed from the Surry ETE study. Adjustments were made to individual elements of the WinMACCS grid to reflect differences in vehicle direction and speed of travel through the network. The timeline identifies the point at which it is assumed that cohorts begin to take action. The actions taken by each cohort last for a given period as indicated in Table 6-4.

6.3.2 Unmitigated STSBO

The emergency response timeline for the unmitigated STSBO scenario is shown in Figure 6-4. The timing of emergency classification declarations was based on the EALs contained in site emergency plan implementing procedures. Protective actions were expected to be recommended by OROs in accordance with approved emergency plans and procedures. Discussions were held with site representatives to help ensure proper understanding of EALs for each accident scenario and emergency response practices. Discussions with OROs confirmed that sirens are only sounded for a GE at Surry. Siren systems are tested routinely within all EPZs and the results of the Response Oversight Program indicate a 99.9 percent performance rating for sirens at Surry. Therefore, it is assumed that sirens do not fail and in the event one or two do fail, societal notification and route alerting by OROs would alert residents in these areas within the same mobilization time period as estimated for the EPZ. Figure 6-5 summarizes the duration of specific protective actions for each cohort.

For this scenario, EAL SS1.1 specifies that if all offsite power and all onsite AC power is lost for greater than 15 minutes an SAE is declared. If restoration of power is not likely within 4 hours, EAL SG1.1 establishes that a GE be declared. It is expected the SAE is declared in about 15 minutes as shown in Figure 6-4 and that plant operators would recognize rather soon that restoration of power within 4 hours is unlikely. A 2 hour period from loss of power was selected as a reasonable time for declaration of a GE. It is expected that notification to OROs is timely

and the sounding of sirens and broadcasting the EAS message occurs approximately 45 minutes after declaration of GE. From the MELCOR analysis, the first fission product gap release occurs about three hours into the event with a significant radioactive release occurring 25.5 hours into the event.

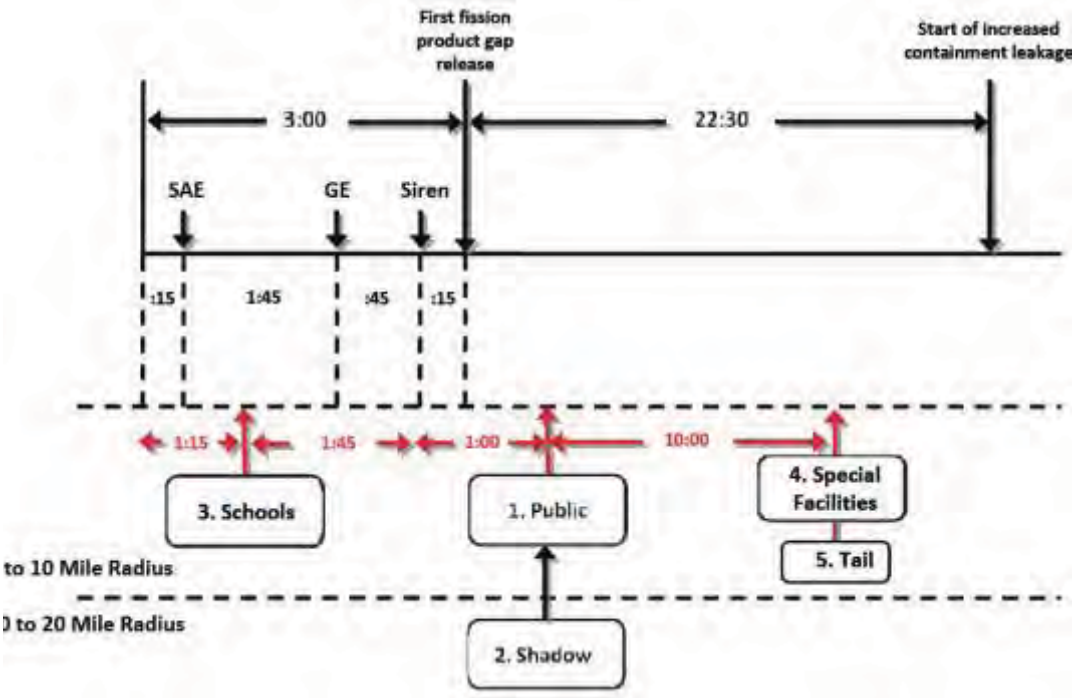

Figure 6-4 Unmitigated STSBO emergency response timeline

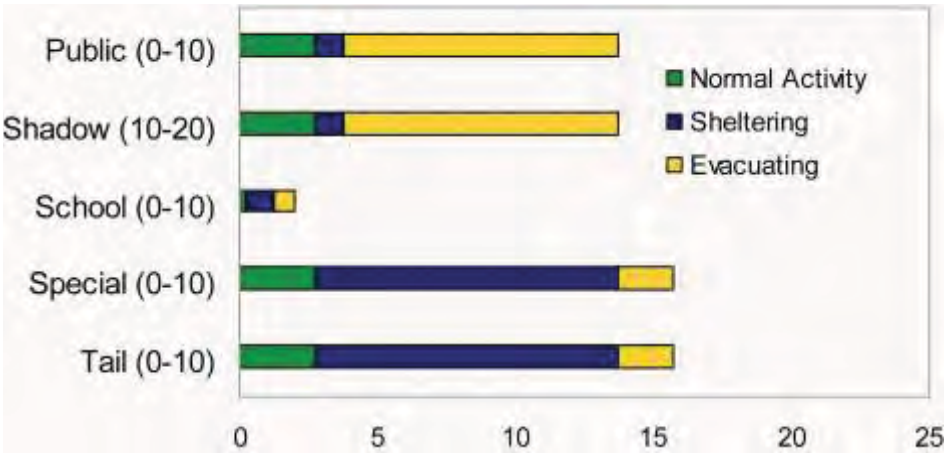

Figure 6-5 Duration of Protective Actions - Unmitigated STSBO

The Virginia Department of Emergency Management will directly communicate with schools upon receiving the declaration of SAE. This allows for the preparation and early response of schools, but the public is largely unaware at this time. It could be noted that there would be a societal communication process as members of the public become aware of the school evacuation. Sirens are sounded at an SAE in many states, but Virginia only sounds sirens in response to declaration of a GE. Although there could potentially be some shadow evacuation due to societal communication, it is assumed that there would be no significant movement of the general public. The initiating event for the Unmitigated STSBO, Unmitigated STSBO with TI-SGTR, Mitigated STSBO with TI-SGTR, and Unmitigated LTSBO scenarios is a station blackout and EAL SS1.1 and SG1.1 are reached. Therefore, the cohort actions are identical for each of these scenarios. The cohorts are expected to respond to the EAS messages as described below:

Cohort 1: 0 to 10 Public:
Following declaration of a GE, sirens are sounded and an evacuation order would be issued via an EAS message for affected areas within the EPZ. Cohort 1 is assumed to shelter when the sirens sound. The time to receive the warning and prepare to mobilize is assumed to be 1 hour after the siren. One hour is based on evacuation research, which shows the public mobilizes over a period of time with some members of the public moving soon after hearing the sirens, while most take some time to prepare and then evacuate. One hour was selected as a reasonable centroid of an evacuation curve for this cohort, which is consistent with empirical data from previous large scale evacuations [30].

Cohort 2: 10 to 20 Shadow:
This cohort is assumed to begin movement at the same time as the 0 to 10 Public after sirens have sounded within the EPZ and when widespread media broadcasts are underway. Residents in the 10 to 20 area begin seeing large numbers of people evacuating and initiate a shadow evacuation. There is no warning or notification for the public residing in this area, which is not under an evacuation order.

Cohort 3: 0 to 10 Schools:
Schools are the first to take action. Upon receipt of the declaration of SAE by the site, the Virginia Department of Emergency Management would notify the schools in accordance with the offsite emergency response plan. It is assumed schools are notified at SAE and begin sheltering in about 15 minutes. Buses would be mobilized, and it is assumed schools begin evacuating 1 hour after the start of the incident. At this time in the event, roads are uncongested and school buses are able to exit the EPZ quickly.

Cohort 4: 0 to 10 Special Facilities:
Special Facilities can take longer to evacuate than the general public because transportation resources, some of which are very specialized, must be mobilized. Special Facilities would be evacuated individually over a period of time based upon available transportation and the number of return trips needed. Special Facilities provide better shielding for the residents, thus while residents are in the facility, they are better protected than when they are evacuating. It was determined that the best representation of this cohort in the modeling is to evacuate with the tail and apply shielding factors consistent with the types of structures within which these residents

reside. The Special Facilities cohort is assumed to depart at the same time as the evacuation tail, although it is recognized this cohort would begin mobilization about the same time as the schools.

Cohort 5: 0 to 10 Tail:
Using the evacuation data provided in the Surry ETE study [27], 90 percent of the evacuation of the EPZ is complete at approximately 11 hours into the evacuation, and this corresponds to the departure time for the 0 to 10 Tail.

Cohort 6: Non-evacuating public:
This cohort group represents the portion of the public who may refuse to evacuate and is assumed to be 0.5 percent of the population. Any member of the public who does not evacuate is still subject to the Hotspot and Normal Relocation criterion discussed earlier.

The evacuation timing for each cohort is presented in Table 6-5. Selected input parameters for WinMACCS are provided to support detailed use of this study. More detailed information regarding modeling parameters is available in the MACCS2 User's Guide [48]. A brief description of the parameters is provided below:

- Delay to Shelter (DLTSHL) represents a delay from the time of the start of the accident until cohorts enter the shelter.

- Delay to Evacuation (DLTEVA) represents the length of the sheltering period from the time a cohort enters the shelter until the point at which they begin to evacuate.

- The speed (ESPEED) is assigned for each of the three phases used in WinMACCS including Early, Middle, and Late. Average evacuation speeds were developed from the Surry 2001 ETE report. Speed adjustment factors were then utilized in the WinMACCS application to represent free flow in rural areas and congested flow in urban areas.

- Duration of Beginning phase (DURBEG) is the duration assigned to the beginning phase of the evacuation and may be assigned uniquely for each cohort.

- Duration of Middle phase (DURMID) is the duration assigned to the middle phase of the evacuation and may also be assigned uniquely for each cohort.

For the 0 to 10 Public and the 0 to 10 Tail cohorts, by definition the sum of the DLTEVA, DURBEG and DURMID is equal to the ETE. This is because the ETE does not include shelter time.

Table 6-5 Unmitigated STSBO cohort timing

Cohort	Delay to Shelter DLTSHL (hr)	Delay to Evacuation DLTEVA (hr)	Duration of beginning phase DURBEG (hr)	Duration of middle phase DURMID (hr)	Speed of early phase ESPEED† (early) mph	Speed of middle phase ESPEED† (mid) mph
0 to 10 Public	2.75	1	0.25	9.75	5	1
10 to 20 Shadow	2.75	1	0.25	9.75	5	1
0 to 10 Schools	0.25	1	0.25	0.5	10	10
0 to 10 Special Facilities	2.75	11	1	1	1	10
0 to 10 Tail	2.75	11	1	1	1	10
Non-Evac	NA	NA	NA	NA	0	0

† Values represent speeds east of the James River. Speeds west of the river are increased through use of multipliers in the WinMACCS model.

6.3.3 Unmitigated STSBO with TI-SGTR

The emergency response timeline for the unmitigated STSBO with TI-SGTR scenario is shown in Figure 6-6. For this scenario, EAL SS1.1 specifies that if all offsite power and all onsite AC power is lost for greater than 15 minutes an SAE is declared. If restoration of power is not likely within 4 hours, EAL SG1.1 establishes that a GE be declared. It is expected the SAE is declared in about 15 minutes, and plant operators would recognize rather soon that restoration of power within 4 hours is unlikely. A 2 hour period from loss of power was selected as a reasonable time for declaration of a GE. It is expected that notification to OROs is timely and the sounding of sirens and broadcast of an EAS message occurs approximately 45 minutes after declaration of GE. From the MELCOR analysis, the first fission product gap release occurs about three hours into the event with the SGTR occurring 30 minutes later. The duration of specific protective actions for each cohort in this scenario is described in Figure 6-7.

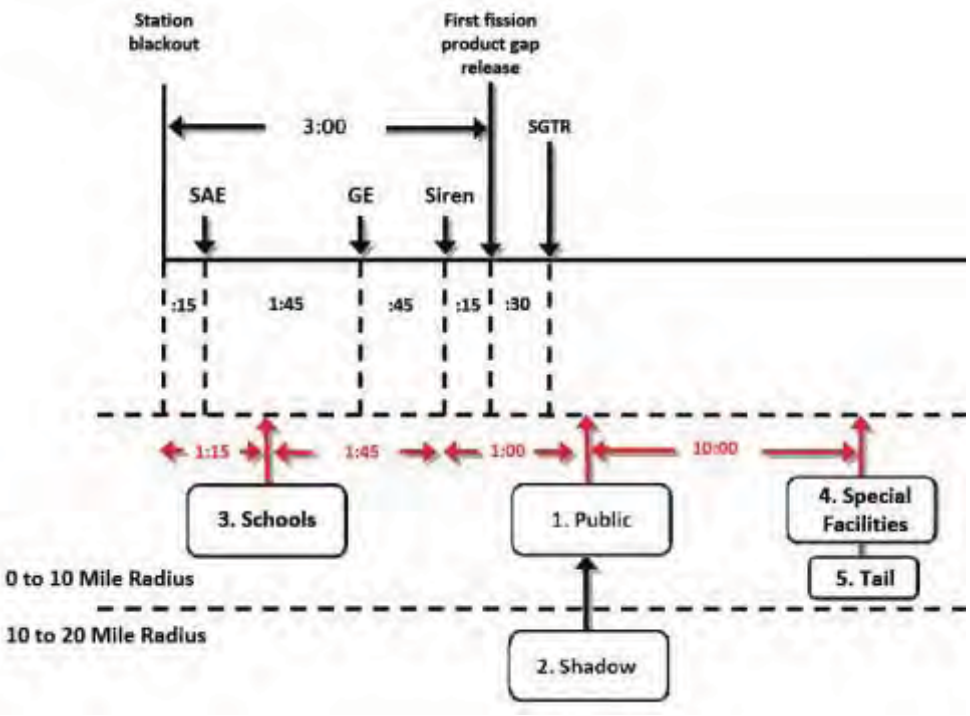

Figure 6-6 Unmitigated STSBO with TI-SGTR emergency response timeline

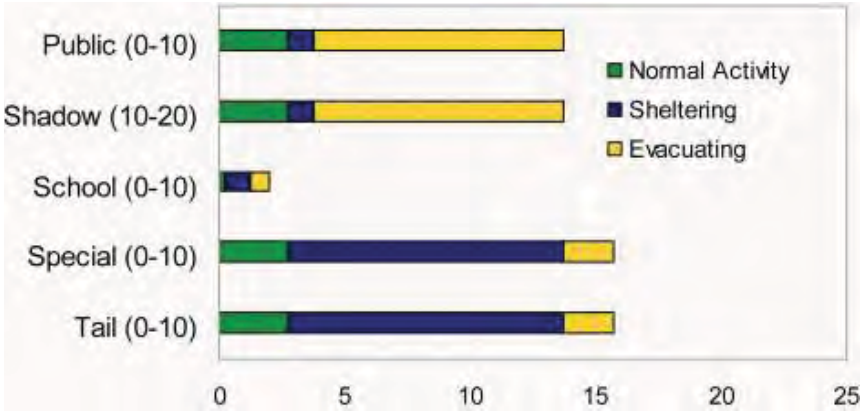

Figure 6-7 Duration of Protective Actions - Unmitigated STSBO with TI-SGTR

The initiating event for the Unmitigated STSBO, Unmitigated STSBO with TI-SGTR, Mitigated STSBO with TI-SGTR, and Unmitigated LTSBO scenarios is a station blackout and EAL SS1.1 and SG1.1 are reached. Therefore, the cohort actions are identical for each of these scenarios as described below:

Cohort 1: 0 to 10 Public:
Following declaration of a GE, sirens are sounded and an evacuation order would be issued via an EAS message for affected areas within the EPZ. Cohort 1 is assumed to shelter when the sirens sound. The time to receive the warning and prepare to mobilize is assumed to be 1 hour

after the siren. One hour is based on evacuation research, which shows the public mobilizes over a period of time with some members of the public moving soon after hearing the sirens, while most take some time to prepare and then evacuate. One hour was selected as a reasonable centroid of an evacuation curve for this cohort, which is consistent with empirical data from previous large scale evacuations [30].

Cohort 2: 10 to 20 Shadow:
This cohort is assumed to begin movement at the same time as the 0 to 10 Public after sirens have sounded within the EPZ and when widespread media broadcasts are underway. Residents in the 10 to 20 area begin seeing large numbers of people evacuating and initiate a shadow evacuation. There is no warning or notification for the public residing in this area, which is not under an evacuation order.

Cohort 3: 0 to 10 Schools:
Schools are the first to take action. Upon receipt of the declaration of SAE by the site, the Virginia Department of Emergency Management would notify the schools in accordance with the offsite emergency response plan. It is assumed schools are notified at SAE and begin sheltering in about 15 minutes. Buses would be mobilized, and it is assumed schools begin evacuating 1 hour after the start of the incident. At this time in the event, roads are uncongested and school buses are able to exit the EPZ quickly.

Cohort 4: 0 to 10 Special Facilities:
Special Facilities can take longer to evacuate than the general public because transportation resources, some of which are very specialized, must be mobilized. Special Facilities would be evacuated individually over a period of time based upon available transportation and the number of return trips needed. Special Facilities provide better shielding for the residents, thus while residents are in the facility, they are better protected than when they are evacuating. It was determined that the best representation of this cohort in the modeling is to evacuate with the tail and apply shielding factors consistent with the types of structures within which these residents reside. Special Facilities are assumed to depart at the same time as the evacuation tail, although it is recognized this cohort would begin mobilization about the same time as the schools.

Cohort 5: 0 to 10 Tail:
Using the evacuation data provided in the Surry ETE study [27], 90 percent of the evacuation of the EPZ is complete at approximately 11 hours into the evacuation, and this corresponds to the departure time for the 0 to 10 Tail.

Cohort 6: Non-evacuating public:
This cohort group represents the portion of the public who may refuse to evacuate and is assumed to be 0.5 percent of the population. Any member of the public who does not evacuate is still subject to the Hotspot and Normal Relocation criterion discussed earlier.

Table 6-6 provides a summary of the evacuation timing activities for each cohort.

Table 6-6 Unmitigated STSBO with TI-SGTR cohort timing

Cohort	Delay to Shelter DLTSHL (hr)	Delay to Evacuation DLTEVA (hr)	Duration of beginning phase DURBEG (hr)	Duration of middle phase DURMID (hr)	Speed of early phase ESPEED† (early) mph	Speed of middle phase ESPEED† (mid) mph
0 to 10 Public	2.75	1	0.25	9.75	5	1
10 to 20 Shadow	2.75	1	0.25	9.75	5	1
0 to 10 Schools	0.25	1	0.25	0.5	10	10
0 to 10 Special Facilities	2.75	11	1	1	1	10
0 to 10 Tail	2.75	11	1	1	1	10
Non-Evac	NA	NA	NA	NA	0	0

† Values represent speeds east of the James River. Speeds west of the river are increased through use of multipliers in the WinMACCS model.

6.3.4 Mitigated STSBO with TI-SGTR

The accident scenario timeline for the Mitigated STSBO with TI-SGTR is identical to the unmitigated STSBO with TI-SGTR as shown in Figure 6-8 and Figure 6-9. The values identified in Table 6-6 were used to support the consequence analyses for the Mitigated STSBO with TI-SGTR.

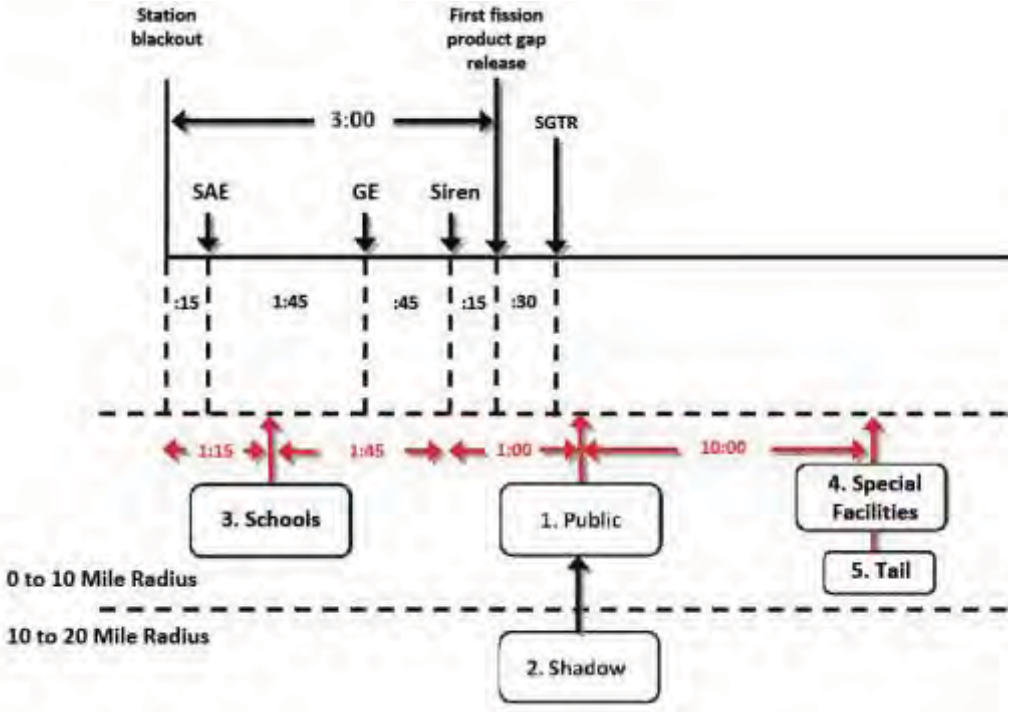

Figure 6-8 Mitigated STSBO with TI-SGTR emergency response timeline

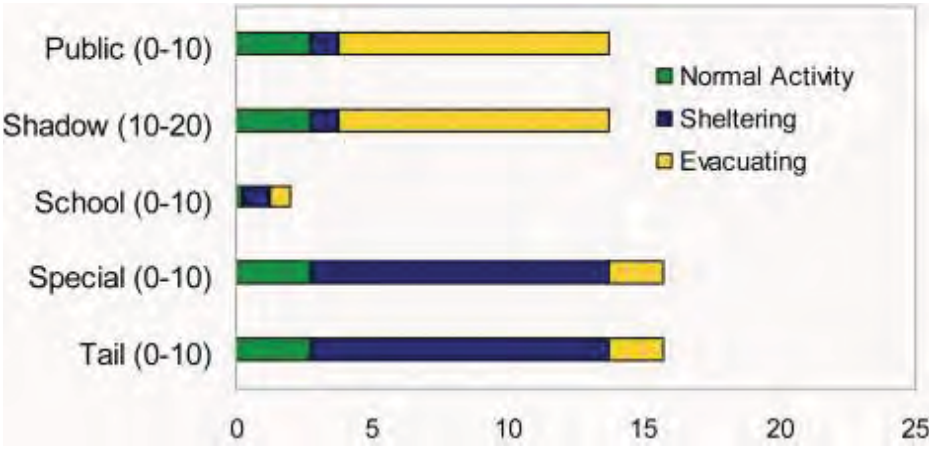

Figure 6-9 Duration of Protective Actions - Mitigated STSBO with TI-SGTR

The initiating event for the Unmitigated STSBO, Unmitigated STSBO with TI-SGTR, Mitigated STSBO with TI-SGTR, and Unmitigated LTSBO scenarios is a station blackout and EAL SS1.1 and SG1.1 are reached. Therefore, the cohort actions are identical for each of these scenarios.

Cohort 1: 0 to 10 Public:
Following declaration of a GE, sirens are sounded and an evacuation order would be issued via an EAS message for affected areas within the EPZ. Cohort 1 is assumed to shelter when the sirens sound. The time to receive the warning and prepare to mobilize is assumed to be 1 hour after the siren. One hour is based on evacuation research, which shows the public mobilizes over a period of time with some members of the public moving soon after hearing the sirens, while most take some time to prepare and then evacuate. One hour was selected as a reasonable centroid of an evacuation curve for this cohort, which is consistent with empirical data from previous large scale evacuations [30].

Cohort 2: 10 to 20 Shadow:
This cohort is assumed to begin movement at the same time as the 0 to 10 Public after sirens have sounded within the EPZ and when widespread media broadcasts are underway. Residents in the 10 to 20 area begin seeing large numbers of people evacuating and initiate a shadow evacuation. There is no warning or notification for the public residing in this area, which is not under an evacuation order.

Cohort 3: 0 to 10 Schools:
Schools are the first to take action. Upon receipt of the declaration of SAE by the site, the Virginia Department of Emergency Management would notify the schools in accordance with the offsite emergency response plan. It is assumed schools are notified at SAE and begin sheltering in about 15 minutes. Buses would be mobilized, and it is assumed schools begin evacuating 1 hour after the start of the incident. At this time in the event, roads are uncongested and school buses are able to exit the EPZ quickly.

Cohort 4: 0 to 10 Special Facilities:
Special Facilities can take longer to evacuate than the general public because transportation resources, some of which are very specialized, must be mobilized. Special Facilities would be evacuated individually over a period of time based upon available transportation and the number of return trips needed. Special Facilities provide better shielding for the residents, thus while residents are in the facility, they are better protected than when they are evacuating. It was determined that the best representation of this cohort in the modeling is to evacuate with the tail and apply shielding factors consistent with the types of structures within which these residents reside. The Special Facilities cohort is assumed to depart at the same time as the evacuation tail, although it is recognized this cohort would begin mobilization about the same time as the schools.

Cohort 5: 0 to 10 Tail:
Using the evacuation data provided in the Surry ETE study [27], 90 percent of the evacuation of the EPZ is complete at approximately 11 hours into the evacuation, and this corresponds to the departure time for the 0 to 10 Tail.

Cohort 6: Non-evacuating public:
This cohort group represents the portion of the public who may refuse to evacuate and is assumed to be 0.5 percent of the population. Any member of the public who does not evacuate is still subject to the Hotspot and Normal Relocation criterion discussed earlier.

Table 6-7 provides a summary of the evacuation timing activities for each cohort.

Table 6-7 Unmitigated STSBO with TI-SGTR cohort timing

Cohort	Delay to Shelter DLTSHL (hr)	Delay to Evacuation DLTEVA (hr)	Duration of beginning phase DURBEG (hr)	Duration of middle phase DURMID (hr)	Speed of early phase ESPEED† (early) mph	Speed of middle phase ESPEED† (mid) mph
0 to 10 Public	2.75	1	0.25	9.75	5	1
10 to 20 Shadow	2.75	1	0.25	9.75	5	1
0 to 10 Schools	0.25	1	0.25	0.5	10	10
0 to 10 Special Facilities	2.75	11	1	1	1	10
0 to 10 Tail	2.75	11	1	1	1	10
Non-Evac	NA	NA	NA	NA	0	0

† Values represent speeds east of the James River. Speeds west of the river are increased through use of multipliers in the WinMACCS model.

6.3.5 Unmitigated ISLOCA

The emergency response timeline for the unmitigated ISLOCA scenario is shown in Figure 6-10. As shown in the figure, SAE is declared 15 minutes after the initiating event based on EAL FS1.1. A GE is declared 2 hours after the start of the event, the basis of which is discussed below. Sirens sound and EAS messages are broadcast approximately 45 minutes after declaration of GE. The durations of specific protective actions for each cohort are summarized in Figure 6-11.

Establishing the response timing for the Surry ISLOCA scenario required review of affected systems and expected operator actions. For this scenario, procedures would direct plant personnel to add water to the RWST. If water injection to the RWST is not possible, procedures identify use of a cross connect to the RWST of the unaffected unit. However, the boundary conditions for this accident scenario include failure to refill the RWST or crossconnect to the unaffected units RWST.

Within the bounds of the above constraint, staff discussed the response timing of this scenario with cognizant licensee technical staff. Following procedures, the licensee stated declaration of SAE would occur within about 15 minutes. Direct interpretation of response procedures for the declaration of a GE was not as straightforward.

The ISLOCA affects multiple plant systems, which require evaluation to determine whether the change in status requires declaration of a GE. For instance, MELCOR results indicate the reactor vessel water level approaches TAF in about 15 minutes, however, the water level is quickly recovered. The procedure calls for a GE if RVLIS indicates 46 percent (TAF), so a GE may not be warranted due to the brief uncovery of TAF. Another path to a GE would be radiation dose. Because the core is not exposed, radiation monitors may not show dose rates high enough to warrant declaration of a GE. Following the orange path of plant procedures, a GE would be declared when there is no injection or when core thermocouples indicate potential loss of fuel clad integrity. The orange path would be entered when the RWST is empty and water is no longer available for core injection. A GE would be declared based on a potential loss of fuel clad. As shown in Figure 5-106, ISLOCA RWST Inventory, the RWST empties in just over 6 hours.

From a system status perspective, the GE would be declared at 6 hours. However, emergency plan implementing procedures instruct operators to declare an emergency classification when it is determined that the emergency action level will be reached. In this case, when operators become aware that there will be no source of injection after the tank is empty, they would likely declare a GE. The timing of the declaration would be dependent upon the situation and the efforts to refill the tank or provide another source. Following declaration of an SAE, all licensee, offsite response organization and federal emergency response organizations and centers would be activated. These organizations would provide response support to the control room and execution of mitigation efforts. In particular, TSC management would provide onsite engineering and management resources to determine the likelihood of successful mitigative action. When those efforts are determined to be unsuccessful with the RWST level falling below 50 percent capacity and continuing to fall, emergency response management would be expected to declare the GE. The licensee would use the ETE in support of a protective action

recommendation. It was determined that a GE would be declared in about 2 hours. A response timeline was therefore developed assuming a GE would be declared at 2 hours.

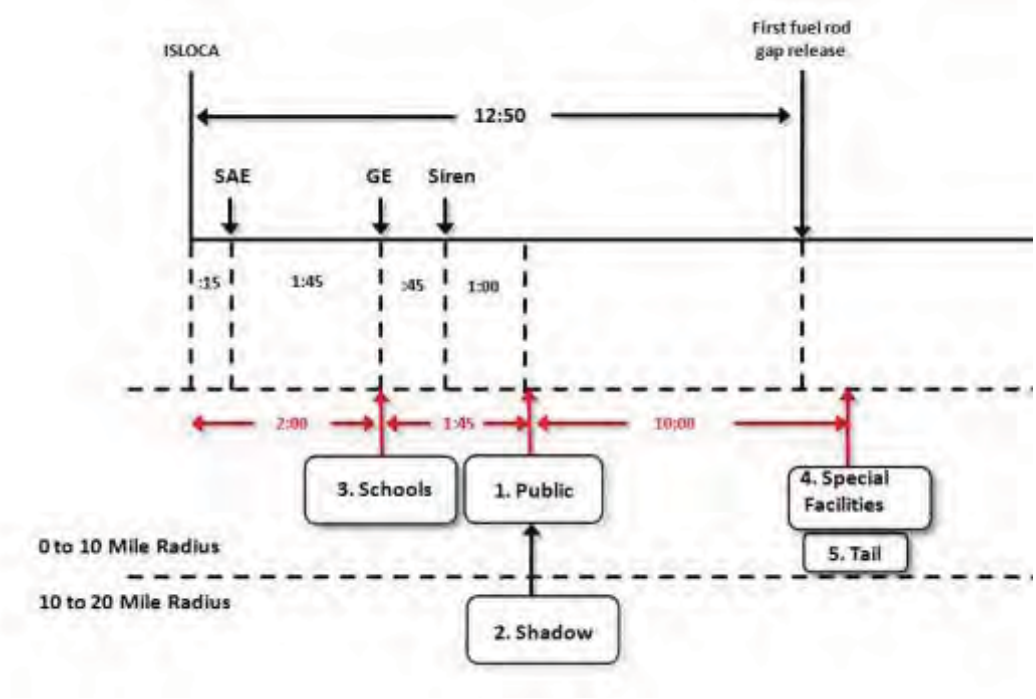

Figure 6-10 Unmitigated ISLOCA Emergency Response Timeline

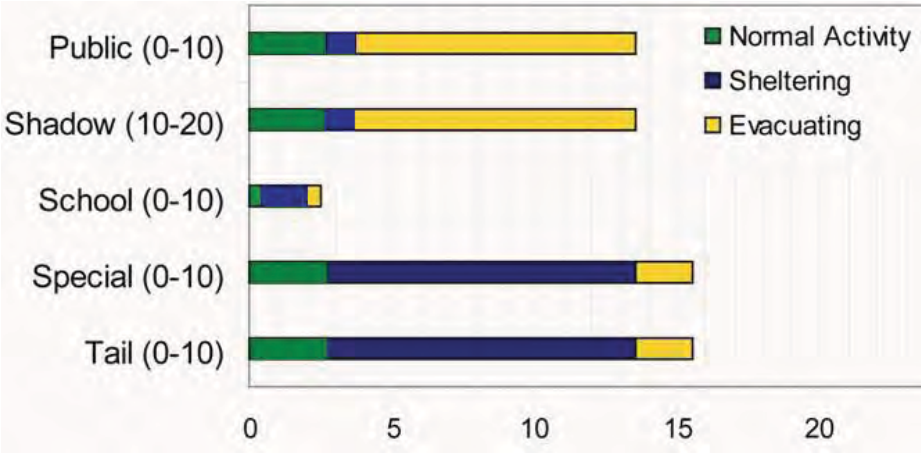

Figure 6-11 Duration of Protective Actions - Unmitigated ISLOCA

The timing of these EALs and cohort actions are different than the scenarios where the initiating event is a station blackout.

Cohort 1: 0 to 10 Public:
Cohort 1 is assumed to shelter when the sirens sound, and the time to receive the warning and prepare to mobilize is assumed to be 1 hour after the siren at which time this cohort begins to evacuate.

Cohort 2: 10 to 20 Shadow:
This cohort is assumed to begin movement at the same time as the 0 to 10 Public after sirens have sounded within the EPZ and when widespread media broadcasts are underway. Residents in the 10 to 20 area begin seeing large numbers of people evacuating and initiate a shadow evacuation. There is no warning or notification for the public residing in this area, which is not under an evacuation order.

Cohort 3: 0 to 10 Schools:
Upon notification of the declaration of SAE by the site, the Virginia Department of Emergency Management would notify the schools promptly in accordance with the emergency response plan. This is a slowly developing accident and although it is assumed that notifications are prompt, extra time is included for drivers and buses to be mobilized. It is assumed schools begin evacuating 1.5 hours after receipt of notification at SAE, which is shown as 2 hours after start of the accident in the emergency response timeline.

Cohort 4: 0 to 10 Special Facilities:
The Special Facilities cohort is assumed to depart at the same time as the evacuation tail.

Cohort 5: 0 to 10 Tail:
The Tail evacuates 11 hours after notification to evacuate.

Cohort 6: Non-evacuating public:
This cohort group represents the portion of the public who may refuse to evacuate and is assumed to be 0.5 percent of the population.

Table 6-8 provides a summary of the evacuation timing actions for each cohort.

Table 6-8 Unmitigated ISLOCA cohort timing

Cohort	Delay to Shelter DLTSHL (hr)	Delay to Evacuation DLTEVA (hr)	Duration of beginning phase DURBEG (hr)	Duration of middle phase DURMID (hr)	Speed of early phase ESPEED† (early) mph	Speed of middle phase ESPEED† (mid) mph
0 to 10 Public	2.75	1	0.25	9.75	5	1
10 to 20 Shadow	2.75	1	0.25	9.75	5	1
0 to 10 Schools	0.25	1.75	0.25	0.5	10	10
0 to 10 Special Facilities	2.75	11	1	1	1	10
0 to 10 Tail	2.75	11	1	1	1	10
Non-Evac	NA	NA	NA	NA	0	0

† Values represent speeds east of the James River. Speeds west of the river are increased through use of multipliers in the WinMACCS model.

Departure speeds and durations of the beginning and middle periods for the WinMACCS runs were developed from the Surry ETE study. Adjustments made to individual elements of the WinMACCS grid to reflect differences in vehicle direction and speed of travel through the network remained the same for this scenario. The timeline identifies the point at which it is assumed cohorts begin to take action. The actions taken by each cohort last for a given period as indicated in the timing table.

6.4 Sensitivity Studies

Analysis of emergency preparedness and response parameters such as demographics, infrastructure, timing, etc., provide opportunity for further evaluation through sensitivity studies. The project team selected three additional calculations to assess variations in the implementation of protective actions. Each of the sensitivity studies was conducted using the ISLOCA accident scenario.

Sensitivity 1 - Evacuation of a 16 mile area including a shadow evacuation from within the 16 to 20 mile area.

Sensitivity 2 – Evacuation of the 0 to 20 mile area.

Sensitivity 3 – Delay in implementation of protective actions for the public within the EPZ.

Sensitivities 1 and 2 assessed the effects of expanding the initial protective actions to distances of 16 and 20 miles respectively. The objective of this sensitivity analysis was to determine whether consequences might be reduced if the initial evacuation area was larger. Twenty miles was selected because it is twice the distance of the EPZ. A middle distance was also desired and

16 miles was selected because a 'ring' had been established in the underlying nodalization network in WinMACCS. A ring was not available at 15 miles.

A full scale evacuation model was developed to assess the sensitivity of consequences to changes in protective action strategies. Although the modeling of the area beyond the EPZ includes a full scale evacuation for the sensitivity analysis, this does not reflect likely protective action recommendations. To support the assessment of implementing protective actions beyond the EPZ, data was obtained for the 10 to 20 mile area around the NPP. Evacuation speeds for the area 10 to 20 miles beyond the EPZ were developed using OREMS Version 2.6. OREMS is a Windows-based application used to simulate traffic flow and was designed specifically for emergency evacuation modeling [29]. The main features of OREMS utilized in the analysis include:

- Determining the length of time associated with complete or partial evacuation of the population at risk within an emergency zone, or for specific sections of highway network or sub-zones;

- Determining potential congestion areas in terms of traffic operations within the emergency zone.

The OREMS model considers special conditions which may be imposed during an emergency evacuation. For example, intersections that normally have pre-timed controllers are assumed to be manned by emergency personnel to facilitate traffic flow [29]. This function is consistent with the emergency response actions that may be expected during an evacuation. Detail for roadway networks was obtained from aerial mapping and was input into OREMS using the standard intersection functions available in the model. Judgment and experience were necessary in determining the number of nodes that are established for the model. OREMS can manage hundreds of nodes, but there is a point at which the addition of nodes and links provides little change in the results. The nodal network established for the Surry plant is a moderately populated network for this code because about half of the EPZ is rural, southwest of the James River, and half is more urban, northeast of the river. With fewer nodes needed in rural areas, the mix of rural and urban areas results in a moderately populated nodal network.

The population values for the 10 to 20 mile area were developed using SECPOP 2000. A total of 171,182 vehicles were loaded onto 47 nodes distributed over 5 one-hour time periods. Vehicle data from the Surry 2001 ETE was also loaded onto the 10 to 20 mile area evacuation network consistent with the Surry ETE. The following evacuation times were produced from the OREMS calculation:

- 100 percent evacuation to a distance of 20 miles: 17 hours and 30 minutes; and
- 90 percent evacuation to a distance of 20 miles: 13 hours and 15 minutes.

These times were used to develop the evacuation speeds for input into the WinMACCS model. The evacuation modeling conducted for the Surry plant was developed consistent with the characteristics observed in prior evacuations conducted for non-nuclear incidents. Most notably, the analysis includes the common phenomenon of evacuations in which travelers who depart the

threat zone the earliest experience lower amounts of delay. This occurs because the routes have yet to become fully utilized during the emergency and the traffic volume and corresponding route congestion is generally lower. Evacuees who depart during the middle part of the evacuation, when the greatest number of people are seeking to depart, generally experience the highest amount of congestion and delay. This is because the demand on the roadway network is at its greatest, exceeding the available capacity in many areas. Evacuees who depart the hazard zone later, while potentially putting themselves at greater risk, enter the transportation network as the demand is near or even less than the roadway capacity. This means that this group, the tail, generally avoids the delays associated with the peak evacuation demand period. The OREMS output evacuation curve for the 20 mile evacuation is provided in Figure 6-12.

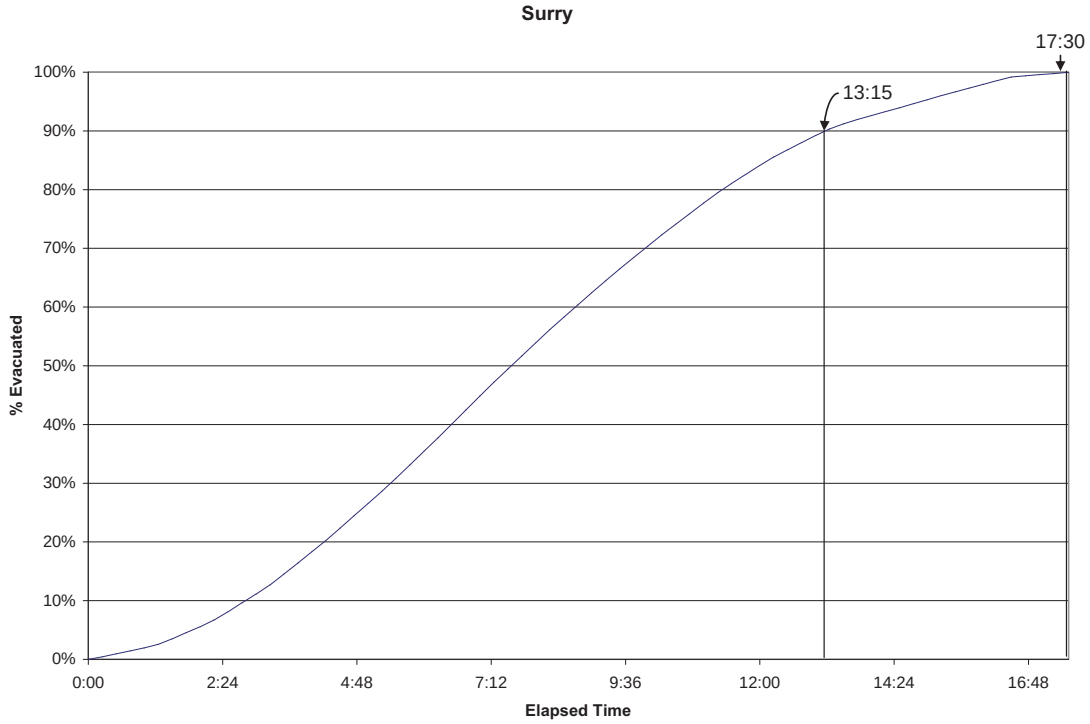

Figure 6-12 Evacuation Timeline from Surry for the 10 to 20 Mile Region

The initial accident scenarios were evaluated for protective actions within the EPZ. Expanding the protective actions to distances beyond the EPZ is not readily accommodated using the modeling approach selected for these analyses. For instance, although OROs may request the 10 to 20 population shelter, this population group is treated within the modeling as performing normal activities throughout the emergency. The normal activity shielding factors are weighted averages of indoor and outdoor values based on being indoors 81 percent of the time and outdoors 19 percent of the time [90]. The hotspot and normal relocation model within MACCS2 will move affected individuals out of the area if the dose criteria apply.

6.4.1 Sensitivity 1 ISLOCA

For sensitivity 1, evacuation of a 16 mile area around the NPP is assessed. In addition, a shadow evacuation occurs from within the 16 to 20 mile area, and the remaining members of the public in the 16 to 20 mile area were assumed to shelter. Figure 6-13, Figure 6-14, and Table 6-9 summarize the cohort timing for sensitivity 1.

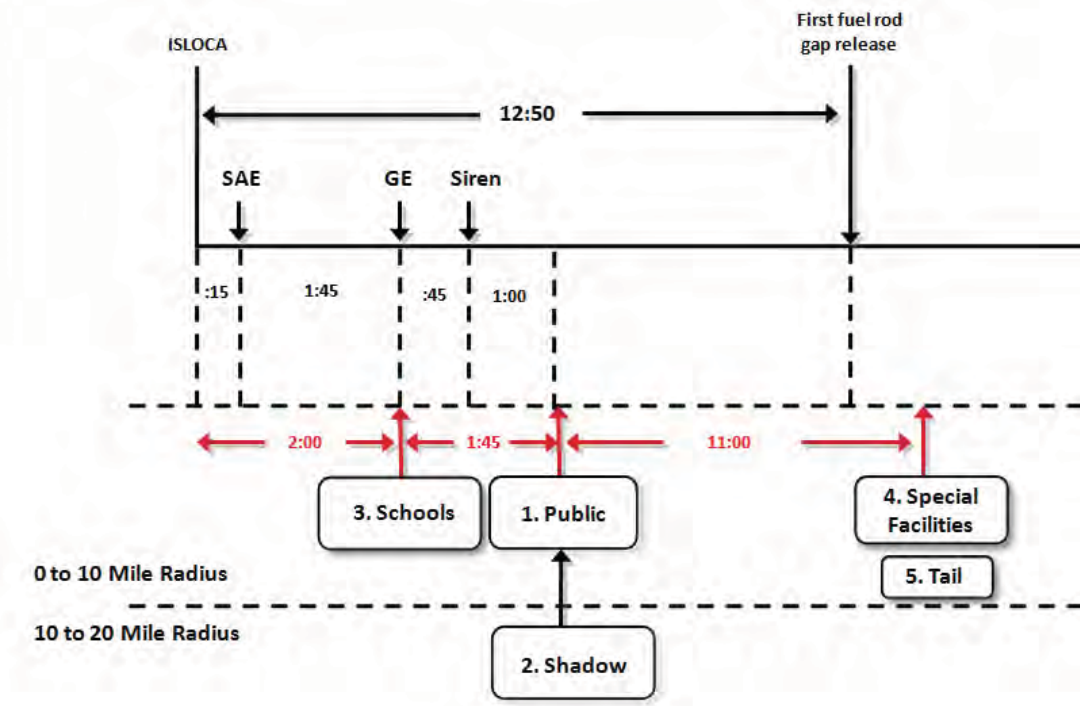

Figure 6-13 Unmitigated ISLOCA Timeline for Sensitivity 1

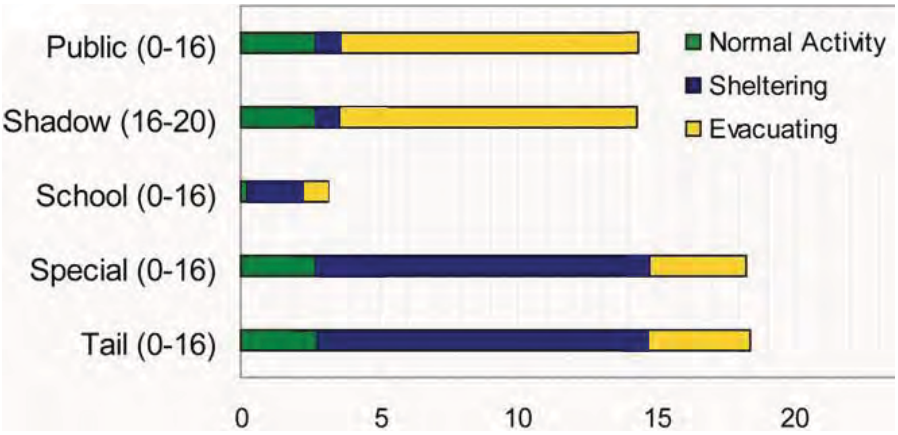

Figure 6-14 Duration of Protective Actions - Unmitigated ISLOCA Sensitivity 1

Cohort 1: 0 to 16 Public:
Following declaration of a GE, sirens are sounded and an EAS message is broadcast that includes an evacuation order for affected areas within the EPZ. The public is assumed to shelter upon receipt of the EAS message, and the time to receive the warning and prepare to mobilize is assumed to be 1 hour. An assumption in this sensitivity analysis is the 10 to 16 public would be notified at the same time as the EPZ via EAS messaging and route alerting. The ETE for the public was estimated as a linear projection between the Surry 2001 ETE Study and the 10 to 20 mile ETE developed for the sensitivity 2 analysis.

Cohort 2: 16 to 20 Shadow:
This cohort is assumed to begin movement at the same time as the 0 to 16 Public after sirens have sounded within the EPZ, EAS messages are broadcast, and when widespread media broadcasts are underway. Residents in the 16 to 20 area begin seeing large numbers of people evacuating and initiate a shadow evacuation.

Cohort 3: 0 to 16 Schools:
Schools are the first to take action. Upon receipt of the declaration of SAE by the site, the Virginia Department of Emergency Management would notify the schools within the EPZ in accordance with the emergency response plan. For this scenario, it is assumed schools within the 10 mile to 16 mile area would evacuate beginning 1.5 hours after receipt of notification. For this sensitivity study, it is assumed schools beyond the EPZ would decide, based upon media information, that it is prudent to evacuate or close schools immediately.

Cohort 4: 0 to 16 Special Facilities:
For this sensitivity study, it is assumed Special Facilities beyond the EPZ would decide, based upon media information that it is prudent to evacuate. Special Facilities can take longer to evacuate than the general public because transportation resources must be mobilized, some of which are very specialized; therefore, the Special Facilities cohort is assumed to depart at the same time as the evacuation tail.

Cohort 5: 0 to 16 Tail:
An estimate of the departure for the evacuation tail is established as a linear projection between the Surry 2001 ETE Study and the OREMS 10 to 20 mile ETE developed for evacuation to a distance of 20 miles from the plant.

Cohort 6: Non-evacuating public:
This cohort group represents the portion of the 0 to 16 mile public who may refuse to evacuate and is assumed to be 0.5 percent of the population.

Table 6-9 Sensitivity Case 1 cohort timing

Cohort	Delay to Shelter DLTSHL (hr)	Delay to Evacuation DLTEVA (hr)	Duration of beginning phase DURBEG (hr)	Duration of middle phase DURMID (hr)	Speed of early phase ESPEED† (early) mph	Speed of middle phase ESPEED† (mid) mph
0 to 16 Public	2.75	1	0.25	10.75	5	1.5
16 to 20 Shadow	2.75	1	0.25	10.75	5	1.5
0 to 16 Schools	0.25	1.75	0.25	0.5	10	10
0 to 16 Special Facilities	2.75	12	2	2	1.5	10
0 to 16 Tail	2.75	12	2	2	1.5	10
Non-Evac	NA	NA	NA	NA	0	0

† Values represent speeds east of the James River. Speeds west of the river are increased through use of multipliers in the WinMACCS model.

The timeline identifies the point at which it is assumed that cohorts begin to take action. The actions taken by each cohort last for a given period as indicated in the timing table.

6.4.2 Sensitivity 2 ISLOCA

For Sensitivity Case 2, evacuation of a 20 mile area around the NPP is assessed. It is not expected that evacuation would be required beyond the EPZ; however, this sensitivity analysis considers the possibility. Because the limit of the evacuation in this sensitivity analysis extends a considerable distance away from the plant, it was determined that adding a shadow evacuation beyond 20 miles would not be realistic. Therefore, no shadow evacuation is assumed in this calculation. Figure 6-15, Figure 6-16, and Table 6-10 summarize the cohort timing for sensitivity 2.

The WinMACCS model structure requires the first cohort to extend to the limits of the calculation, and for earlier calculations this was the limit of the shadow evacuation. In this sensitivity analysis, because there is no shadow evacuation, the limit of the first cohort is 20 miles and represents the 0 to 20 public.

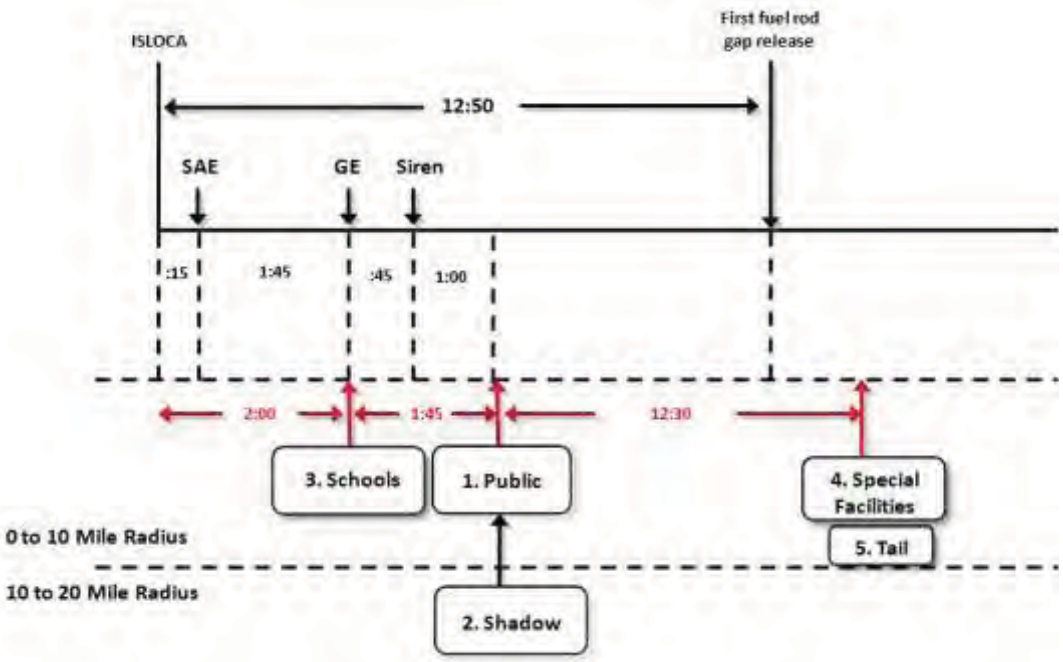

Figure 6-15 Unmitigated ISLOCA Timeline for Sensitivity 2

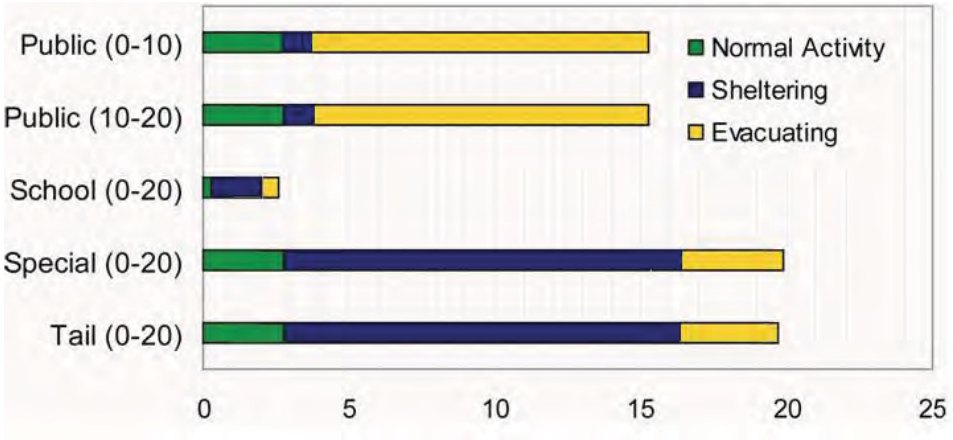

Figure 6-16 Protective Action Durations - Unmitigated ISLOCA Sensitivity 2

Cohort 1: 0 to 10 Public:
Cohort 1 is assumed to shelter when the sirens sound and the EAS message is broadcast. The time to receive the warning and prepare to mobilize is assumed to be 1 hour after the siren at which time this cohort begins to evacuate.

Cohort 2: 10 to 20 Public:
There are no sirens in the 10 to 20 mile area and no preplanned EAS messages; therefore, notification is assumed to be media broadcasts to residents in this area. The time to receive the warning and prepare to mobilize is still assumed to be 1 hour after the initial notification. The ETE for the 10 to 20 public was estimated using OREMS.

Cohort 3: 0 to 20 Schools:
Upon receipt of the declaration of SAE by the site, the Virginia Department of Emergency Management would notify the schools within the EPZ in accordance with the emergency response plan. For this sensitivity study, it is assumed schools beyond the EPZ would decide, based upon media information, that it is prudent to evacuate or close schools immediately.

Cohort 4: 0 to 20 Special Facilities:
For this sensitivity study, it is assumed Special Facilities beyond the EPZ would decide, based upon media information that it is prudent to evacuate. Special Facilities can take longer to evacuate than the general public because transportation resources must be mobilized, some of which are very specialized; therefore, the Special Facilities cohort is assumed to depart at the same time as the evacuation tail.

Cohort 5: 0 to 20 Tail:
The ETE for the evacuation tail was estimated based on the OREMS analysis.

Cohort 6: Non-evacuating public:
This cohort group represents the portion of the 0 to 20 mile public who may refuse to evacuate and is assumed to be 0.5 percent of the population.

Table 6-10 Sensitivity Case 2 cohort timing

Cohort	Delay to Shelter DLTSHL (hr)	Delay to Evacuation DLTEVA (hr)	Duration of beginning phase DURBEG (hr)	Duration of middle phase DURMID (hr)	Speed of early phase ESPEED† (early) mph	Speed of middle phase ESPEED† (mid) mph
0 to 10 Public	2.75	1	0.25	12	5	1.6
10 to 20 Public	2.75	1	0.25	12	5	1.6
0 to 20 Schools	0.25	1.75	0.25	0.5	10	10
0 to 20 Special Facilities	2.75	13.5	2	2	1.6	10
0 to 20 Tail	2.75	13.5	2	2	1.6	10
Non-Evac	NA	NA	NA	NA	0	0

† Values represent speeds east of the James River. Speeds west of the river are increased through use of multipliers in the WinMACCS model.

The timeline identifies the point at which it is assumed that cohorts begin to take action. The actions taken by each cohort last for a given period as indicated in the timing table.

6.4.3 Sensitivity 3 ISLOCA with Delay of Implementation of Protective Actions

There is a high level of confidence regarding the actions expected from control room operators in the event of accident scenarios identified for analysis in the SOARCA project. The initiating conditions provide clear indication to these operators and the response actions of the control room are prescribed. The Peer Review committee suggested that analysis consider a delay of the implementation of protective actions. Such a delay could be due to delay in control room declaration of an incident, delay in the decision process of OROs, delay in communication to the public regarding implementation of protective actions or other reasons. To address the potential for delay, an additional protective action timeline has been developed for the ISLOCA. This timeline reflects a delay in the implementation of protective actions by the public within the EPZ. Because protocols and procedures are in place, exercised and tested frequently, it is assumed that a delay of 30 minutes is adequate for this sensitivity study. Figure 6-17, Figure 6-18, and Table 6-11 summarize cohort timing for sensitivity 3.

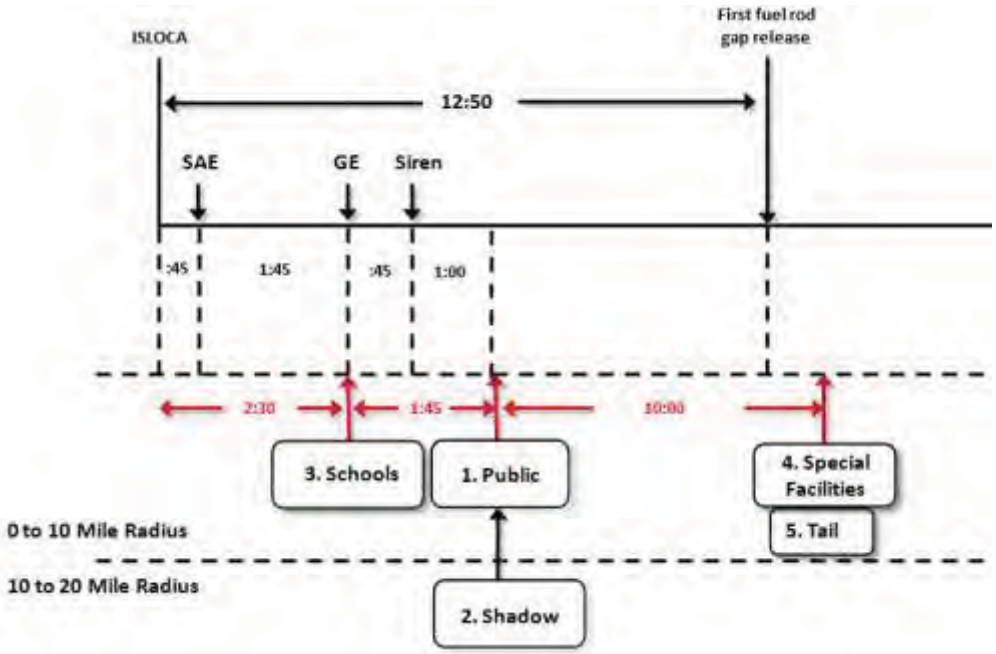

Figure 6-17 Unmitigated ISLOCA Timing for Sensitivity 3

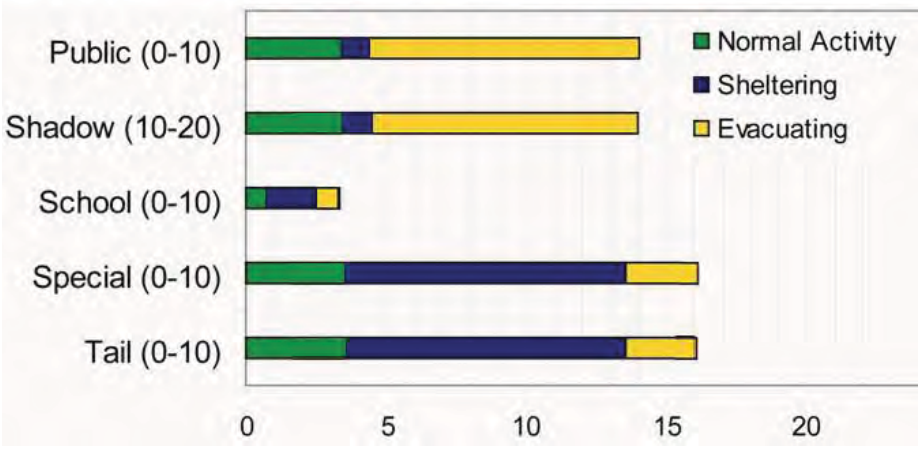

Figure 6-18 Protective Action Durations - Unmitigated ISLOCA Sensitivity 3

The timing of these EALs and cohort actions are different than the scenarios where the initiating event is a station blackout. This sensitivity study includes a delay of 30 minutes in the implementation of protective actions. This delay is accounted for by delaying declaration of SAE by 30 minutes.

Cohort 1: 0 to 10 Public:
Cohort 1 is assumed to shelter when the sirens sound and the initial EAS message is broadcast. The time to receive the warning and prepare to mobilize is assumed to be 1 hour after the receipt of the EAS message at which time this cohort begins to evacuate.

Cohort 2: 10 to 20 Shadow:
This cohort is assumed to begin movement at the same time as the 0 to 10 Public after sirens have sounded within the EPZ and when widespread media broadcasts are underway. Residents in the 10 to 20 area begin seeing large numbers of people evacuating and initiate a shadow evacuation. There is no warning or notification for the public residing in this area which is not under an evacuation order.

Cohort 3: 0 to 10 Schools:
Upon receipt of the declaration of SAE by the site, the Virginia Department of Emergency Management would notify the schools in accordance with the emergency response plan. Buses would be mobilized, and it is assumed schools begin evacuating 1.75 hours after notification.

Cohort 4: 0 to 10 Special Facilities:
The Special Facilities cohort is assumed to depart at the same time as the evacuation tail.

Cohort 5: 0 to 10 Tail:
The Tail evacuates 11 hours after the public has been notified to evacuate.

Cohort 6: Non-evacuating public:
This cohort group represents the portion of the public who may refuse to evacuate and is assumed to be 0.5 percent of the population.

Table 6-11 Sensitivity Case 3 cohort timing

Cohort	Delay to Shelter DLTSHL (hr)	Delay to Evacuation DLTEVA (hr)	Duration of beginning phase DURBEG (hr)	Duration of middle phase DURMID (hr)	Speed of early phase ESPEED† (early) mph	Speed of middle phase ESPEED† (mid) mph
0 to 10 Public	3.25	1	0.25	9.75	5	1
10 to 20 Public	3.25	1	0.25	9.75	5	1
0 to 10 Schools	0.75	1.75	0.25	0.5	10	10
0 to 10 Special Facilities	3.25	11	1	1	1	10
0 to 10 Tail	3.25	11	1	1	1	10
Non-Evac	NA	NA	NA	NA	0	0

† Values represent speeds east of the James River. Speeds west of the river are increased through use of multipliers in the WinMACCS model.

6.5 Analysis of Earthquake Impact

A seismic analysis was developed to assess the potential effects on local infrastructure, communications, and emergency response in the event of a large scale earthquake. The accident used in the earthquake analysis is the STSBO with TI-SGTR. Integrating the effects of the earthquake into the analysis required assessing the damage potential of the earthquake, identification of parameters that would be affected, and determining the adjusted values for affected parameters.

The potential for an earthquake is largely identified by the occurrence of previous earthquakes in the region. Understanding of where earthquake faults exist in the eastern United States is not robust; whereas, in the west geological fault lines can be identified on the surface. Faults in the east are usually buried below layers of soil and rock and are not identifiable making prediction of earthquake location and magnitude difficult. The earthquakes hypothesized in SOARCA are assumed to be close to the plant site, and it may be assumed that severe damage is generally localized. Housing stock would generally survive the earthquake with some damage. The local electrical grid is assumed out of service due to the failure of lines, switch yard equipment, or other impacts. There is a backup power system for the sirens at Surry, and it is expected sirens would function. Under these postulated conditions, the potential for such an earthquake to affect emergency response and public evacuation is considered.

6.5.1 Soils Review

To approximate the extent of damage, an evaluation of the potential failure of infrastructure was conducted by NRC seismic experts to determine which, if any, roadways or bridges may fail under the postulated earthquake conditions. The assessment was performed using readily available information and professional judgment. Existing information on basic bedrock geology of the region was developed from reports and papers from the United States Geological Service.

Soils of this region are formed from unconsolidated sediments deposited when the ocean level was much higher than at present. As sea levels lowered, many of these deposits were reworked by meandering rivers and streams that originated in the western part of the state and flowed to the east. In general, the closer to the coast, the nearer the water table is to the soil surface. Soils in the coastal plain are acidic, infertile, highly weathered, and vary from sandy textures to very clayey textures. Soil types are mostly silts and sands deposited in low energy environments, which make them potentially susceptible to liquefaction in an earthquake; however, site specific liquefaction potential is highly variable.

Most landscapes are nearly level to gently sloping and because of this feature, the soils are not as susceptible to erosion.

6.5.2 Infrastructure Analysis

The seismic evaluation of the potential failure of roadway infrastructure identified 40 bridges and roadway segments that could fail under the postulated conditions. The major areas where problems occur are in and around the urban area of Williamsburg, Virginia. Figure 6-19 shows an example of a bridge that could potentially fail under the earthquake conditions. Figure 6-20 shows the transportation network and the locations of the affected roadway segments and bridges. Table 6-12 provides a description of each of the roadway segments and bridges that could fail.

Figure 6-19 Highway 199 Over Highway 321
(Bridge 13 on Figure 6-20)

Figure 6-20 Roadway Network Identifying Potentially Affected Roadways and Bridges

The earthquake may cause structural damage in other areas of the EPZ. The structures within the EPZ are primarily light commercial and residential housing, both of which would largely be expected to stay intact. However, there are areas of larger commercial facilities and theme parks, which could sustain damage. The urban setting is also likely to experience localized fires caused by ruptured gas lines.

Table 6-12 Description of the Potential Evacuation Failure Locations

Location	Description
1	Small bridge on Highway 10 across pond
2	Overpass on Highway 10 near Smithfield
3	Bridge on Highway 10 near Smithfield
4	Stream culvert and boggy area under Highway 10
5	Road 617 (Whitemarsh Rd) culvert and bog beneath roadway
6	Highway 31 south of Highway 10- Bridge over pond
7	Road 621 (Burwell Bay Rd) pond and bog
8	Bridge over Route 5 (John Tyler Highway)
9	Bridge on Route 31 (Jamestown Rd)
10	Bridge over small lake on Route 31
11	Route 31 across small dam
12	Bridge over river on Highway 199-2 bridges in this area
13	Highway 199-overpass over Route 321 (Monticello Ave)
14	Highway 199-overpass over Longhill road
15	Highway 199-overpass Old Towne Rd
16	Route 321 (Monticello Ave) adjacent to Lake Powhaton, Potential slope failure/slumping
17	Route 321 (Monticello Ave) bridge over bog
18	Highway 60 in Williamsburg-Overpass over rail tracks
19	Overpass US 199 over US 60 in Williamsburg
20	US 199/I-64 Interchange in Williamsburg
21	I-64/US 60 Interchange in Williamsburg
22	I-64 overpass near Williamsburg
23	I-64 Bridges over Colonial Parkway, edge of Williamsburg
24	I-64 Bridge over river and swampy area
25	I-64/Route 143 overpass
26	Route 143 ridge over river and swampy area
27	US 60-Dike over lake, southwest of Williamsburg
28	US 60 and SR 105 interchange
29	Small dam above US 60
30	I-64 overpass with SR 143 (Jefferson Ave)
31	I-64 overpass - Bland Ave.
32	I-64 Overpass, SR 173 (Denbigh Ave)
33	I-64 bridges over Industrial Park Drive
34	I-64 bridge over lake
35	I-64 and SR 238 (Old Williamsburg Rd) overpass
36	SR 105 (Ft. Eustis Blvd) bridge over lake
37	Colonial Historic Parkway- road on dam
38	Colonial Historic Parkway- bridge over creek
39	Highway 17 bridge across York River
40	Highway 17/258 across James River

6.5.3 Electrical and Communications

There are many high voltage power lines traversing the Surry EPZ. It is assumed transformers and switchgear fail; however, power lines and related structures are assumed to not fail to a degree that they affect the emergency response (i.e., it is assumed that power lines do not fall across roadways potentially affecting evacuation routes). The siren system at Surry includes backup batteries, which would be sufficient to sound the sirens upon declaration of a GE.

Loss of power limits the potential for residents to receive instructions via the Emergency Alert System (EAS) messaging. Televisions, household radios, and some telephones will not operate; although battery operated radios and car radios will operate. It is expected that the public will utilize these means of communication as well as societal forms, such as neighbor to neighbor, propagating the EAS message throughout the EPZ. The alert and notification would be supplemented by route alerting conducted by OROs. This is a planned back up form of communication for the EPZ, and research shows this is effective and can be conducted in a timely manner. As observed in other large scale disasters, calls can inundate the emergency telecommunications systems with questions and requests for help, many of which will require emergency responder support [51]. This may cause cell phone service to be overloaded and may delay communications. However, for a localized event such as an earthquake, it is assumed that cell phone service is restored quickly.

The loss of power will affect traffic signalization within the EPZ. Typically, traffic signals default to flashing red in both directions in a power outage requiring all directions to stop prior to entering an intersection. This effectively turns signalized intersections into four-way stop signs. Four-way stop, as an intersection control, is less effective signalization for moving large numbers of vehicles, particularly when traffic is present on multiple approaches [53].

6.5.4 Emergency Response

The assumption on the event timing is a mid-week winter day in which the public is at work and children are at school. The primary shift of emergency responders would be on duty and immediately available at the time of the incident. These initial priorities for emergency response personnel may delay implementation of traffic control to support an evacuation. It is expected that alerting the public would not be appreciably delayed, because Surry has backup batteries for the siren system. Route alerting may supplement alert and notification in localized areas.

During large scale emergencies, OROs routinely supplement staff with on-call and off-duty personnel. Although communications are assumed to be initially limited, radios are available to contact needed staff, and off-duty responders are expected to report for duty during such emergencies. By the time an evacuation is ordered, it is expected that OROs would have been augmented with additional staff; however, the effect on the infrastructure within the EPZ will require that OROs initially support activities that are protective of health and safety.

6.5.4.1 Evacuation Time Estimate

Evacuation times are affected by bridges and roadways that fail, traffic signalization, and EAS messaging is not disseminated timely to inform evacuees of protective actions and evacuation routes. There are 40 locations identified as potential failures of infrastructure. Although evacuations are planned and conducted to move the public radially away from the NPP, evacuation following this postulated earthquake will be constrained to the few unobstructed access routes out of the EPZ. West of the James River, the population is sparse and infrastructure failures are relatively isolated. The result is a negligible affect on the evacuation time for this area. However, the infrastructure failures north and east of the river will have a pronounced affect on the movement of vehicles and requires that an ETE for this area be developed to reflect the conditions.

In review of the Surry 2001 ETE report [27], no significant traffic congestion was noted in the areas west of the James River. The ETE analysis does indicate significant traffic congestion in all zones that are north and east of the James River. The James River varies in width from about 1.5 to 5.5 miles with only three crossings along a 50-mile stretch between Hopewell and Portsmouth. For this reason, the evacuation network north and east of the James River is essentially disconnected from the network west of the river.

The major road system on the east side of the river, as discussed in the Surry 2001 ETE report [27], is oriented northwesterly and southeasterly, parallel with the peninsula. Primary evacuation routes east of the river include U.S. Highway 17, Interstate 64, U.S. Highway 60, and Route 143 and the Surry ETE report identifies all of these roadways as congested under evacuation conditions. These roadways are further affected by the seismic event.

As indicated in Figure 6-20, 32 of the 40 affected roadways and bridges are located east of the James River and are clustered in and around Williamsburg, Virginia. Of particular importance is the major affect on Interstate 64 through this section of the EPZ. Most of the bridges and overpasses on this interstate are assumed to fail which causes some very difficult issues with an assessment of the evacuation time. To truly understand the effect of such damage on the ETE, the roadway system should be modeled. A basic vehicle/capacity approach was applied to develop a reasonable ETE and associated evacuation speeds. This assessment considers the timing and activities of residents, but may not fully account for factors such as driver confusion over which routes are accessible.

This scenario is a mid-day mid-week event where the interstate can be assumed to be moderately traveled. A priority for emergency response personnel will be assisting those who are in life threatening conditions such as occupants of vehicles that are stranded on or under the sections of Interstate 64 between the failed bridge segments. The assistance in removing the vehicles has a two fold effect of tying up emergency response personnel and creating additional congestion around the roadways leading to the interstate.

Even before an SAE has been declared, the failure of the interstate bridges will affect traffic and cause a gridlock within the area. The interstate is unusable, and the underpasses to the interstate also become unusable which are major impediments to an evacuation. The significant failure of infrastructure causes the limiting factor of the ETE to be the queuing and loading of the

evacuating vehicles at the points at which evacuation routes are available near the edge of the EPZ. At approximately the point at which Interstate 64 crosses the 10 mile EPZ boundary, there is no further damage to the Interstate. This is true at both the north and south ends of the EPZ, and at this point Interstate 64 is available to support the evacuation with 3 lanes northbound and 5 lanes southbound.

Theoretical lane capacity for the Interstate would approximate 2,400 passenger cars per lane per hour; however, studies of lane capacity during planned evacuations, such as the evacuation in response to Hurricane Katrina, concluded that observed peak interstate flows were between 1,350 and 1,500 passenger cars per lane per hour [50]. There are an estimated 90,000 evacuating vehicles, as developed from the Surry ETE report [27]. Applying a rate of 1,500 passenger cars per lane per hour, the 8 available lanes would support all of the vehicles in approximately 7.5 hours; however, vehicles cannot simply access the interstate, so this simple Interstate capacity analysis only confirms that once on the Interstate, traffic will be in a free-flow state.

The controlling point in the evacuation is the access capacity to Interstate 64. As vehicles travel to the available Interstate onramps, the lines of traffic, or queue, saturate the roadway network. To evaluate onramp capacity, the segment-flow density function is applied for oversaturated conditions following the procedure in Chapter 22 of the Highway Capacity Manual [53]. Using a saturated traffic density estimated at 160 passenger cars per mile per lane, which is appropriate for gridlock conditions, a corresponding onramp capacity of 500 passenger cars per hour per lane is obtained. Using aerial mapping, there are an estimated 10 onramps to Interstate 64 within a short distance of the EPZ boundary. Ten onramps with 500 passenger cars per hour per lane can load 90,000 in 18 hours. Because outbound capacity once on the Interstate is not a limiting factor and the loading points are beyond the limits of the EPZ, it is assumed that the time to load the vehicles is effectively the ETE.

This is a simplified approach to evacuation under the seismic conditions identified. However, for purposes of understanding the effects of protective actions, the value of 18 hours to complete the evacuation of areas east of the James River appears reasonable. The evacuation of residents west of the river evacuate much quicker and speed adjustment factors were used in modeling this area.

6.5.5 Development of WinMACCS parameters

Traffic movement was approximated in each grid element by assigning a direction and speed for the vehicles within the grid. To account for the potential loss of bridges and roadway sections, the routing patterns in the WinMACCS model were adjusted to divert traffic around the locations identified.

6.5.5.1 Relocation Outside the Evacuation Area

In the event of a significant release, the population in the region outside the evacuation area would be moved if their potential dose exceeds protective action criteria based on field measurements. The MACCS2 code uses hotspot and normal relocation, which is a dose based rather than distance based protective action. The values used in the earthquake analysis are the same as those used in the baseline analysis.

For hotspot relocation, individuals beyond twenty miles are relocated 24 hours after plume arrival if the total lifetime dose commitment for the weeklong emergency phase exceeds 0.05 Sv (5 rem). For the normal relocation, individuals are relocated 36 hours after plume arrival if the total lifetime dose commitment exceeds 0.01 Sv (1 rem). Review of the accident sequence timelines suggest that OROs would not be available earlier to assist with relocation due to higher priority tasks in the evacuation area.

6.5.5.2 Shielding Factors

Shielding factors are the same as those used in the baseline analyses. It may be expected that the damage to structures caused by an earthquake of this magnitude would include broken windows and some structural damage. However, because residents within the seismic area are assumed to shelter only a short period of time, no adjustments in the modeling were made.

6.5.6 Seismic Analysis STSBO with TI-SGTR

The emergency response timeline for the unmitigated STSBO with TI-SGTR seismic scenario is shown in Figure 6-21. For this scenario, EAL SS1.1 specifies that if all offsite power and all onsite AC power is lost for greater than 15 minutes an SAE is declared. If restoration of power is not likely within 4 hours, EAL SG1.1 establishes that a GE be declared. It is expected the SAE is declared in about 15 minutes, and plant operators would recognize rather soon that restoration of power within 4 hours is unlikely. A 2 hour period from loss of power was selected as a reasonable time for declaration of a GE. It is expected that notification to OROs is timely and sounding of sirens occurs approximately 45 minutes after declaration of GE. From the MELCOR analysis, the first fission product gap release about three hours into the event with the SGTR occurring 30 minutes later. The duration of specific protective actions for each cohort is summarized in Figure 6-22.

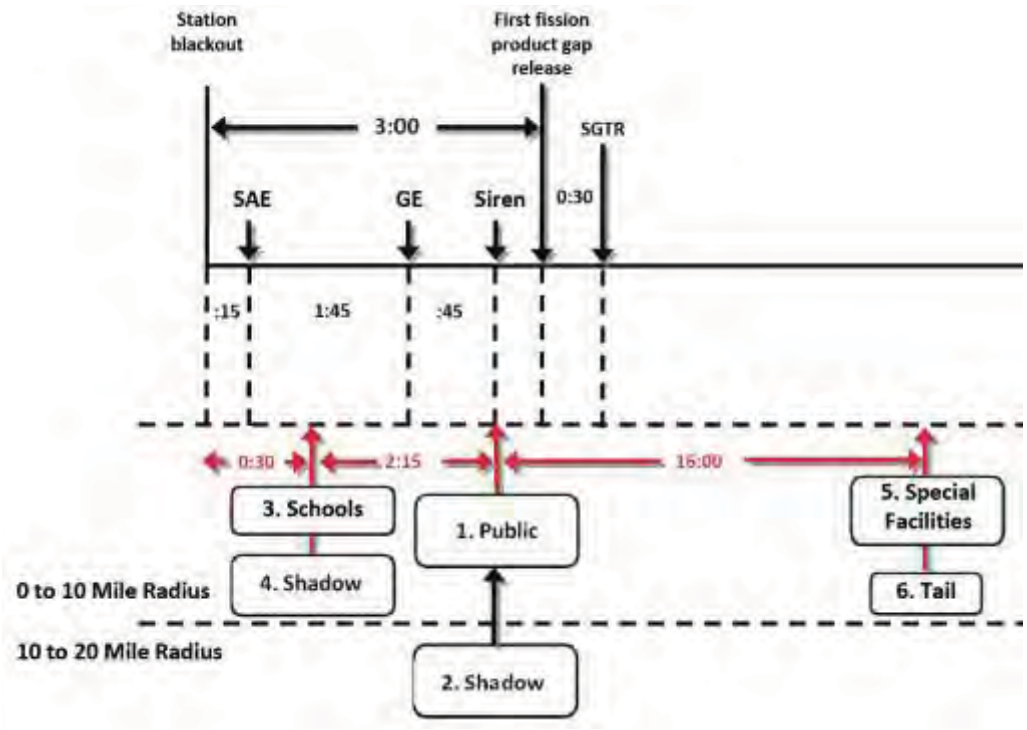

Figure 6-21 STSBO with TI-SGTR Emergency Response Timeline (Seismic Scenario)

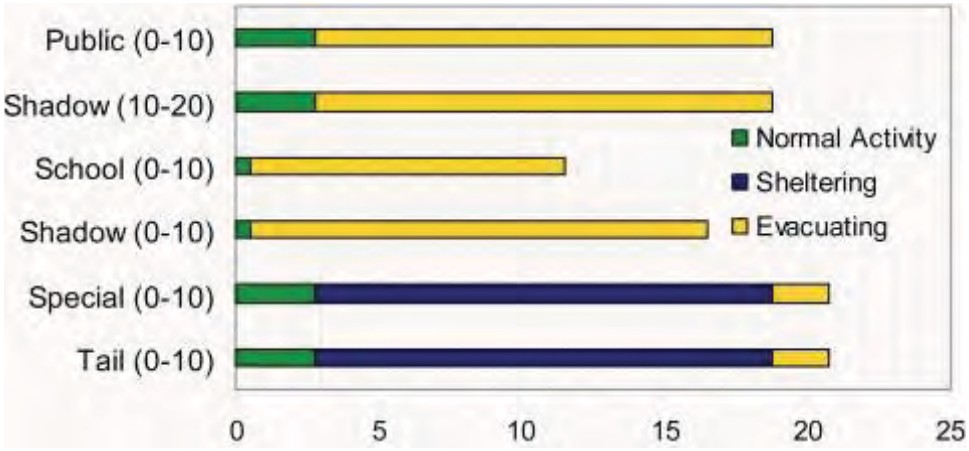

Figure 6-22 Protective Action Durations - STSBO with TI-SGTR (Seismic Scenario)

The timeline identifies points at which cohorts would receive instruction from OROs to implement protective actions. While protective actions within the EPZ can be modeled in accordance with procedures, assumptions were made that reasonably approximate those actions that could be taken due to the effects of the earthquake; however, the actual decisions made by OROs could differ.

The emergency response procedures for Surry provide for the sounding of sirens for a declaration of General Emergency. Backup batteries are available to support the sounding of sirens. It is assumed the large earthquake will be felt by everyone within the EPZ, and individuals will begin to prepare for an evacuation prior to receiving official notice.

Cohort 1: 0 to 10 Public:
The 0 to 10 Public is assumed to begin evacuating when the sirens sound. OROs would prepare and broadcast an EAS message, but the loss of power and infrastructure may limit the range of the broadcast. It is assumed that the effects of the earthquake are severe such that members of the public, knowing they live within an EPZ, begin preparations for evacuation shortly after the earthquake and are ready to leave when sirens sound.

Cohort 2: 10 to 20 Shadow:
This cohort is assumed to begin movement at the same time as the 0 to 10 Public after sirens have sounded within the EPZ and when widespread media broadcasts are underway. Residents in the 10 to 20 area begin seeing large numbers of people evacuating and initiate a shadow evacuation. There is no warning or notification for the public residing in this area which is not under an evacuation order. It is assumed that the shadow population increases to 30 percent of the public in the area beyond the EPZ.

Cohort 3: 0 to 10 Schools:
It is assumed schools take the initiative to prepare to evacuate prior to notification from the Virginia Department of Emergency Management. Buses would be mobilized, and it is assumed schools begin evacuating 30 minutes after the start of the incident; however, traffic congestion resulting from infrastructure failure causes a very slow evacuation speed. The analysis also considers that some drivers may not report due to an inability to get to the bus depot or need to address other immediate concerns. It is also assumed that given the magnitude of the earthquake, parents in the vicinity of the schools will pick up their children, reducing the need for a full complement of buses. In addition, it is expected schools will respond as needed and make do with the resources that arrive to evacuate the children in a single wave. This may include placing more than the normal 50 to 70 children on a bus and / or using school administrator's and teacher's vehicles to augment transportation needs.

Cohort 4: 0 to 10 Shadow:
This cohort is assumed to begin movement first. They experience the earthquake and quickly begin to evacuate avoiding the congestion.

Cohort 5: 0 to 10 Special Facilities:
The Special Facilities cohort is assumed to depart at the same time as the evacuation tail. Special Facilities need to have transportation resources mobilized, some of which are very specialized. Inbound lanes on roadways will be useable for emergency support vehicles, but traffic congestion will delay the arrival of specialized vehicles. Special Facilities are assumed to leave at the same time as the evacuation tail; however, as discussed earlier, this is a simplification of the analysis because Special Facilities would realistically evacuate individually as resources are available.

Cohort 6: 0 to 10 Tail:
The Tail takes longer to evacuate for many valid reasons such as the need to return home from work to evacuate with the family; the need to shut down farming or manufacturing operations prior to evacuating; and for the earthquake, the need to move rubble or other items prior to evacuating. However, with the extent of damage within the Surry EPZ, the tail simply becomes a continuous extension of the evacuating public.

Cohort 7: Non-evacuating public:
This cohort group represents the portion of the 0 to 10 public who may refuse to evacuate and is assumed to be 0.5 percent of the population.

Table 6-13 provides a summary of the evacuation timing for each cohort. The values in the table represent the minimum evacuation speeds corresponding to the area north and east of the site. In general, the cohorts in the seismic study have faster mobilization times but significantly slower evacuation speeds. The delay to shelter represents a delay before people get to the shelter, and delay to evacuation represents the length of the sheltering period prior to evacuation. These delays correspond to the different shielding factors that were applied to each cohort during these timeframes. Speed values are adjusted within each grid element of the WinMACCS model.

Table 6-13 Cohort Timing STSBO with TI-SGTR Including Speeds

Cohort	Delay to Shelter DLTSHL (hr)	Delay to Evacuation DLTEVA (hr)	DURBEG (hr)	DURMID (hr)	ESPEED early (mph)		ESPEED middle (mph)	
					E	W	E	W
0-10 Public	2.75	0	0.25	15.75	5	15	0.7	2.1
10 to 20 Shadow	2.75	0	0.25	15.75	5	15	0.7	2.1
0-10 Schools	0.50	0	1.00	10.00	5	15	0.7	2.1
0 to 10 Shadow	0.50	0	0.25	10.00	10.0	30	0.7	2.1
0-10 Special Facilities	2.75	16	1.00	1.00	0.7	2.1	10.0	30.0
0-10 Tail	2.75	16	1.00	1.00	0.7	2.1	10.0	30.0
Non-evac	NA	NA	NA	NA	NA	NA	NA	NA

As indicated in Table 6-13, the evacuation speeds east of the James River are significantly slower than the speeds west of the river. The actions taken by each cohort last for a given period as indicated in the timing table. To model the difference in speeds between the east and west sides of the river, the speeds were developed for the east side and the WinMACCS multipliers were applied to the west side.

6.6 Accident Response and Mitigation of Source Terms

The Surry SOARCA study has concluded that scenarios can be mitigated by the licensee through the use of safety and security enhancements, including most of the SAMGs and 10 CFR 50.54(hh) mitigation measures. Analyses were conducted of the consequences that may result if the onsite emergency response organization (ERO) is unable to prevent core damage and radiological release to the environment. It is expected that mitigative actions would be attempted. However, a human reliability assessment and a detailed seismic damage assessment were not performed for implementation of mitigative measures. The staff believed it appropriate to perform the consequence analyses to develop an understanding of core melt sequences, source term evolution, and offsite response dynamics to compare to previous studies. Perhaps the most important objective of these analyses is to quantify the benefit of mitigation enhancements. The following analysis describes an expected national level response to a severe nuclear power plant accident and provides a basis for truncating the release no later than 48 hours after the accident begins. Note that past studies, including PRAs such as NUREG-1150, typically truncated releases after 24 hours.

Mitigative actions taken during an accident are intended to:

- prevent the accident from progressing;
- terminate core damage if it begins;
- maintain the integrity of the containment as long as possible; and
- minimize the effects of offsite releases.

Response to a General Emergency would begin with the onsite ERO and would expand as needed to include utility corporate resources, State and local resources, and resources available from the Federal government, should these be necessary. If plant personnel efforts were unsuccessful, the national level response would provide resources to support mitigation of the source term. The discussion below presents a timeline for bringing resources onto the Surry site in order to flood containment to a level above a hypothetical hole in the reactor vessel to minimize the effects of an offsite release. Flooding containment would jeopardize vital equipment and monitoring capabilities and is considered a last resort option. Such an option would not begin until all other efforts have been exhausted. The approach described herein also discusses, to the extent practical at this time, the NRC Task Force review of the response to the nuclear power plant accidents at the Fukushima Dia-ichi facility in Japan.

On March 11, 2011, the Great East Japan Earthquake caused a large tsunami estimated to have exceeded 14 meters (45 feet) in height at the Fukushima Daiichi nuclear power plant site. The earthquake and tsunami produced widespread devastation across northeastern Japan, resulting in approximately 25,000 people dead or missing, displacing tens of thousands of people, and significantly impacting the infrastructure and industry in the northeastern coastal areas of Japan. The earthquake and tsunami caused accidents at Units 1, 2 and 3 of the Fukushima Daiichi nuclear power plant facility and caused concern for the remaining units and spent fuel pools at the site. Amid the vast devastation and competing health and safety priorities in the region, onsite and offsite response agencies worked diligently to bring the accidents under control.

Shortly after the nuclear accident, the NRC established a task force to conduct a methodical and systematic review of the NRC's processes and regulations to determine whether the agency

should make additional improvements to its regulatory system. The Task Force report, "Recommendations for Enhancing Reactor Safety in the 21st Century," [76] identified that prolonged SBO and multiunit events present challenges to Emergency Preparedness facilities that were not considered when the NRC issued NUREG – 0696, "Functional Criteria for Emergency Response Facilities," in 1981. The Task Force report also states that an overarching lesson is that major damage to infrastructure in the area surrounding the plant might challenge an effective emergency response. A number of recommendations are presented in the report that address physical, administrative, and regulatory enhancements to further reduce the risk of similar challenges occurring among the US fleet of NPPs. As a state-of-art analyses, the SOARCA project included a degree of depth in the analyses beyond the scope of many previous studies. In this regard, some of the recommendations of the Task Force report had already been considered in SOARCA.

For instance, SOARCA investigated the challenges of potential damage to infrastructure within and beyond the EPZ as a result of an earthquake. The site specific analysis showed that 40 bridges and/or roadway segments may fail. Review of the locations of the affected roadways showed that there would be a significant impact on the evacuation of the public from the area east of the James River, while the effects on infrastructure west of the river were shown to be relatively minor. The seismic analysis described in Section 6.5 quantified the offsite effects of challenges to both infrastructure and resources within the Surry EPZ. The Task Force report also recommends further enhancement of current capabilities for onsite emergency actions by requiring licensee's modify the EOP technical guidelines to include SAMGs. This would enhance current capabilities, but would not change the manner in which SAMGs have already been considered in SOARCA.

With regard to the emergency response, the Surry analyses applied the site specific EALs. For Surry, an SAE would be declared within 15 minutes for all of the accident scenarios. A GE would be declared about 1 hour 45 minutes hours after SAE for all scenarios. Licensees are required by regulation to notify OROs within 15 minutes of declaring an emergency, and the OROs then initiate a planned response by offsite agencies who are able to direct necessary resources upon request, such as fire trucks, to support mitigation of the accident. The declaration by the licensee is not only a notification; this declaration initiates an ongoing communication between the control room, licensee staff, OROs, NRC, and other response agencies.

As supported by the SOARCA analyses, it is shown that the accidents evaluated could be mitigated through the actions of the onsite and offsite response agencies. The evaluation of the mitigation of source term and truncation of the accident at 48 hours further expands upon the response resources through identification of corporate, State, local and Federal offsite resources. The responsibilities and resources of each of these organizations are described in onsite and offsite emergency response plans. These response organizations would mobilize upon request and as needed to support a severe nuclear power plant accident. These resources are in addition to the mitigative actions by the licensee through the use of safety and security enhancements, including SAMGs and 10 CFR 50.54(hh) mitigation measures.

Although the response to the Fukushima Daiichi has taken much time and challenges still remain, it is expected that the regulatory structure, protocols, and resources available to support a

response in the US are sufficient to mitigate the release of the accident scenarios identified in this study within 48 hours. Implementation of recommendations from the Task Force report would further improve the capabilities to mitigate the accident itself in a timely manner, to help prevent a release from occurring.

The NRC has onsite inspectors that are available to provide firsthand knowledge of accident conditions. NRC would be notified, following plant procedures, within one hour of the declaration; although, for a seismic event, it is likely that the NRC would be informed sooner than one hour by the onsite NRC resident inspectors, if not the licensee. Upon receipt of notification of the emergency classification, the NRC would activate the Headquarters Operations Center (HOC). NRC response teams reporting to the HOC include the Reactor Safety Team, Protective Measures Team, Executive Team, and other teams that support response related activities. Plant drawings and procedures are available in the HOC. Data that is typically communicated to the HOC via the Emergency Response Data System (ERDS), the Emergency Notification System bridge line, and other communication bridges, would likely be communicated via the resident inspectors satellite phones and via site battery operated systems. Licensees are required to provide guaranteed power to the emergency communications equipment per NRC Bulletin 80-15, "Possible Loss of Emergency Notification System (ENS) with Loss of Offsite Power." The NRC region office would activate with similar response teams and would deploy a Site Team to the licensee's EOF to support the response. A Site Team would include reactor safety engineers and protective measures specialists to review actions taken to mitigate the accident and to review protective action decisions that will be recommended to the public to assure the most appropriate actions are taken. Arrival of the Site Team may take several hours. The HOC, Regional Operations Center, and Site Team include liaisons to support coordination of resources when requested by the licensee.

Surry is part of the Dominion fleet which includes a remote EOF that would be activated and has access to fleet wide emergency response personnel and equipment, including equipment from sister plants following 10 CFR 50.54(hh) reactor security requirements to mitigate the effects of large fires and explosions. Significant resources would be made available to the site to mitigate the accident. The equipment would support multiple response needs and include such items as generators, pumps, compressed gas, etc. In addition to those directly involved in the incident and those agencies that fully test and exercise response plans, the Institute for Nuclear Power Operations and the Nuclear Energy Institute would activate their emergency response centers to assist the site. These efforts would provide knowledgeable personnel and an extensive array of equipment would be available and as such are considered in the decision to truncate the release at 48 hours.

Concurrently with the NRC and industry response, the National Response Framework (NRF) establishes a coordinated response of national assets and would be implemented for an accident that progresses to a General Emergency. As described in the Nuclear/Radiological Incident Annex to the NRF, NRC is the Coordinating Agency for incidents occurring at NRC-licensed facilities. As Coordinating Agency, NRC has technical leadership for the Federal Government's response to the incident. Under established agreement, if the severity of an emergency rises to the level of General Emergency, overall coordination of the incident would be conducted by the DHS. In this case, NRC retains the Federal technical leadership role but does not coordinate

overall Federal response. Some of the other agencies cooperating in an incident include the EPA, FEMA, Health and Human Services, and any other Federal agency that may be needed. The assets of the Department of Energy (DOE) would be activated and brought to bear on the accident. Every licensee participates with many of these organizations in a full onsite and offsite exercise biennially. The NRC has an extensive, well-trained and exercised emergency response capability that would support, and under unusual circumstances, direct licensee efforts. Communications systems require battery backup in accordance with 10 CFR 50.54 Appendix E, and multiple communication bridge lines would be established to facilitate structured communication among the various response teams. Satellite phones, cell phones, radios, and other means are available for those instances where communications have been affected.

The above organizations would be developing onsite and offsite mitigation strategies with different objectives. These strategies would be implemented concurrently. An onsite mitigation strategy relies upon onsite resources and is expected to be immediate in order to prevent core melt and radiological release. Offsite mitigation strategies would bring national resources to the site and take more time to develop than onsite measures.

6.6.1 External Resources

The primary focus of the site and utility ERO would be mitigating core damage, and State and local resources would focus on the public evacuation. However, it is typical, as demonstrated in drills and exercises, for EROs to develop contingency plans in case initial onsite mitigative actions are not successful. The NRC ERO would focus on protection of the public and methods to reduce consequences reviewing the licensee and ORO information, actions, and decisions while performing independent analyses. If the site ERO is not successful with the onsite mitigative actions, as the unmitigated cases assume, various EROs would be considering in parallel the availability of portable power and pumping capacity from offsite locations. Virginia has a statewide mutual aid agreement for assistance from every fire department in the commonwealth.

The Surry volunteer fire department and Rushmere volunteer fire department are both 15 miles from the site. The fire departments are in opposite directions, but they share a six mile stretch of road to the power plant. Figure 6-23 shows Surry and Rushmere Volunteer Fire Departments in relation to Surry Nuclear Power Plant.

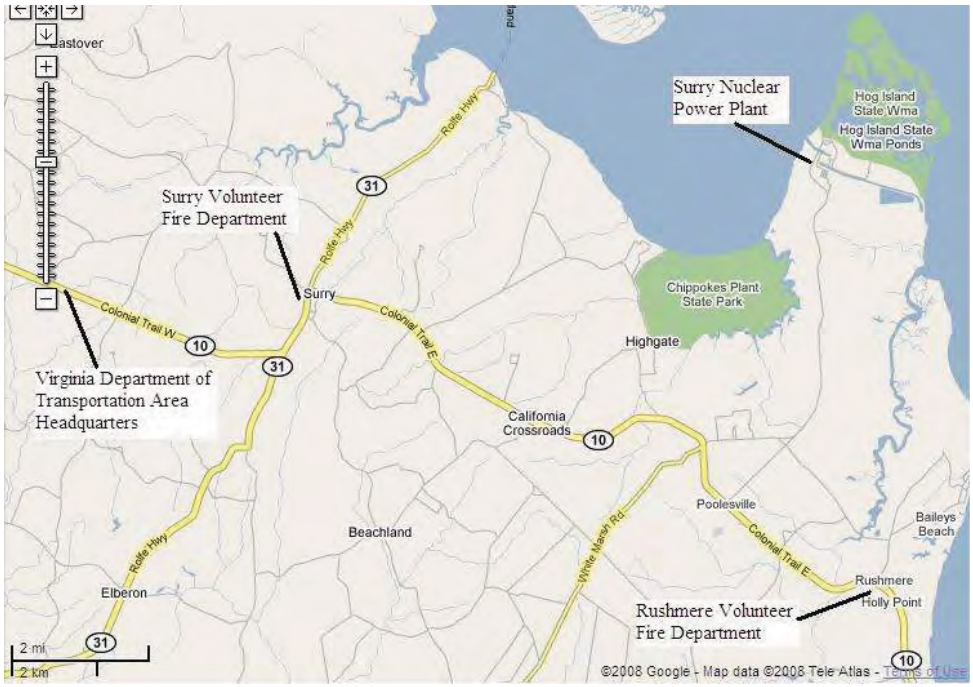

Figure 6-23 Surry and Rushmere Fire Departments

The Surry volunteer fire department practices annual response drills with Surry Nuclear Power Plant. This fire department has five pumper trucks, each with a capability to pump 500 to 1000 gpm and has the ability to draft water directly from the river. A fire truck typically provides a pressure of up to 125 psi when limited by the firefighter controlling the nozzle. Fire hoses have a test pressure of at least 300 psi and a burst pressure of between 600 and 1000 psi. To obtain an Underwriter's Laboratory (U.L.) Certification, a fire pump inside the truck must meet the following rated capacity shown in Table 6-14.

Table 6-14 Rated Flowrate of Fire Pumps

Pressure (psi)	Rated Flowrate
150	100%
165	100%
200	70%
250	50%

Additional resources are available through the State of Virginia Office of Emergency Management (OEM) which has an emergency services contract for the delivery of significant amounts of equipment within eight hours. OEM has access to high-pressure, high capacity pumps with 8 and 12 inch flanges that could readily move the water necessary for containment flooding. Such equipment is available for immediate State emergency use from many locations including Norfolk, Elizabeth City, and Raleigh.

The initiating event for the reactor accident is an earthquake in close proximity to the plant. This event causes significant ground motion and damage to certain types of structures. The impact to

infrastructure, including the loss of some highway bridges within the EPZ, is described in Section 6.5. However, the loss of these bridges would not affect the ability to truck equipment into the site, because roads west of the James River were shown to be largely unaffected.

The EPZ environment is generally rural west of the river, and the roadway system is substantial. There are small bridges and culvert crossings on the plant access route that could be damaged, but these would not prevent passage by heavy trucks. A Virginia department of transportation area headquarters is 3 miles from the Surry fire department and has six dump trucks, two front-end loaders, a road grader, and other heavy equipment. Staff at the area headquarters have the capability to open roads and could immediately respond. Even if the culverts were to collapse, personnel at the transportation facility believe they could fix the road so that equipment could pass in less than 10 hours. In addition, Norfolk Naval Station has airlift resources that could be used to bring equipment into the plant. Fire trucks, which can weigh 35,000 lbs, are too heavy for air lift with MH-53 Helicopters which have a lift capacity of about 13,000 pounds. Airlift is not expected to be necessary, but if it was, the EROs would work together to identify appropriate pump and electrical equipment resources. The State has access to fire pumps and diesel generators that range from 15 kW to 15 MW and electrical generators are also available from commercial sources. These fire pumps and generators could be on site within about 10 hours.

In addition, there are six fireboats in the Newport News/Norfolk area each with the pumping capacity of 1500 to 3000 gpm, and a marine fire fighting capability exists for three more boats equipped for firefighting, if needed. These fireboats have tremendous pumping capacity but may need to use long lengths of hose to support the site. It is likely that fire trucks and other portable equipment can be trucked onto the site more rapidly than the fire boats can be deployed, but they are a viable option should they be needed. EROs may pursue several options to ensure success.

The timing of the hypothetical radiological release is scenario dependent, but when it occurs the site would be contaminated and working conditions more difficult. However, plant staff are trained in radiological work and the full staff of health physics technicians would be available. Within about 12 hours, staff from Dominion fleet plants could be at the site as well as staff from the DOE. Additional radiological technicians could likely be obtained from neighboring plants or perhaps from the Norfolk Naval Shipyard approximately 40 miles away should they be needed.

6.6.2 Mitigation Strategies

Strategies initially focus on injection of water into the reactor vessel. If all efforts in this regard fail, flooding of containment might be attempted to reduce the release potential through the cooling and scrubbing action of water. The site, utility and NRC EROs would identify various water injection methods corresponding to the damage circumstances. An effective option may be to inject water via the containment spray system. The two containment spray systems at Surry each have the capacity to inject more than 3,000 gpm into containment. This would have an immediate effect of lowering pressure and scrubbing radionuclides from the air and would suppress the release. The containment spray system has 8 inch flanges which can accept a milled flange and fire hose arrangement. The containment spray system has two sections: the containment spray (CS) subsystem and the recirculation spray (RS) subsystem. The recirculation

spray subsystem also has two sections, inside and outside. Both the inside recirculation spray (ISRS) and the outside recirculation spray (OSRS) are designed for 100 percent capacity.

There are several water sources but earthquake based scenarios assume that most water supply tanks fail. If nothing else is available, the intake or discharge canals would provide a water source. The site ERO would perform a damage survey to determine tank status and either find usable tanks or make repairs. The utility would connect a water tank to a containment spray connection and make up to the water tank from the river if necessary. Local fire departments are experienced in drafting water directly from the river if needed. The availability of portable electrical power sources was discussed above, and portable power would likely be available at about the same time tank repairs and pumping capacity would be arranged.

Mitigation of the ISLOCA scenario is different from the SBO scenarios in this volume because it is not seismically induced. There is no widespread onsite damage to prevent the use of normal systems and water sources. Actually, most ECCSs would be available to prevent core damage or truncate the release. As described in the site procedure key steps in Section 5.5.3, the utility has established at lease three proceduralized steps to align different water sources to one of many injection systems for truncating a release.

In addition to the proceduralized steps described in Section 5.5.3, Surry has a portable low-pressure pump with a capacity of ~2000 gpm, and two portable high-pressure diesel-driven (Kerr) pumps. There is also a diesel-driven fire pump available at the Surry site. The utility has procedures to align installed pumps, portable pumps or the fire pump to the containment spray system and would use this strategy for the LTSBO and STSBO accident sequences. ISLOCA and STSBO TI-SGTR on the other hand are bypass events, so this strategy would not stop the release of radioactive material. However, connecting the fire pump to the containment spray system could be effective for any sequence after the molten core falls into the lower plenum or breaches the vessel.

A high-pressure pump would be more effective because of the elevation of the containment spray nozzles and containment pressure. A high-pressure, high capacity fire pump (i.e., available from the State) connected to either the CS or the OSRS subsystems would immediately start to lower the pressure, scrub the volatiles, and eventually cover the molten core on the drywell floor. Figure 6-24 shows the analyzed pressure of the unmitigated STSBO accident.

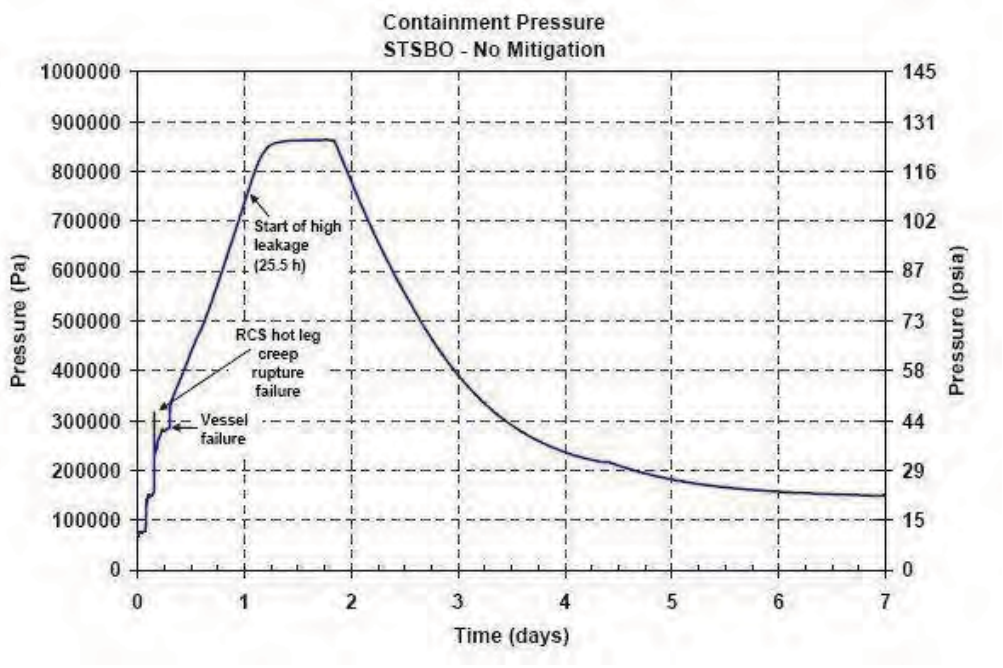

Figure 6-24 Containment Pressure for Unmitigated STSBO

The ERO could also use a fire truck for pumping capacity. The utility has guidelines for using a fire truck to feed plant systems such as auxiliary feed water. However, to obtain a desirable flow rate in containment spray it would be necessary to gang fire trucks, and high capacity high-pressure portable pumps may be a better solution.

Another method for release truncation would be to inject water directly into the primary system. This may be preferred because there is little elevation head to overcome and water would flow directly to the breach in the containment vessel and cover the molten core on the drywell floor scrubbing volatiles from the release. Containment pressure would continue to increase due to decay heat and the site ERO would need a means to remove heat (e.g., air coolers or heat exchangers via containment spray system). As necessary, all EROs would work together to identify other measures for mitigation interacting with plant personnel who know the plant well and may identify innovative solutions to inject water into containment.

In Unit-2 the water cannot overflow into the reactor cavity until it reaches a level 25 feet from the bottom of the sump. In Unit-2 about 1.75 million gallons of water, as extrapolated from Figure 6-25, would be necessary. Table 6-15 provides the data used to extrapolate the level from the bottom of the sump with respect to cumulative water volume.

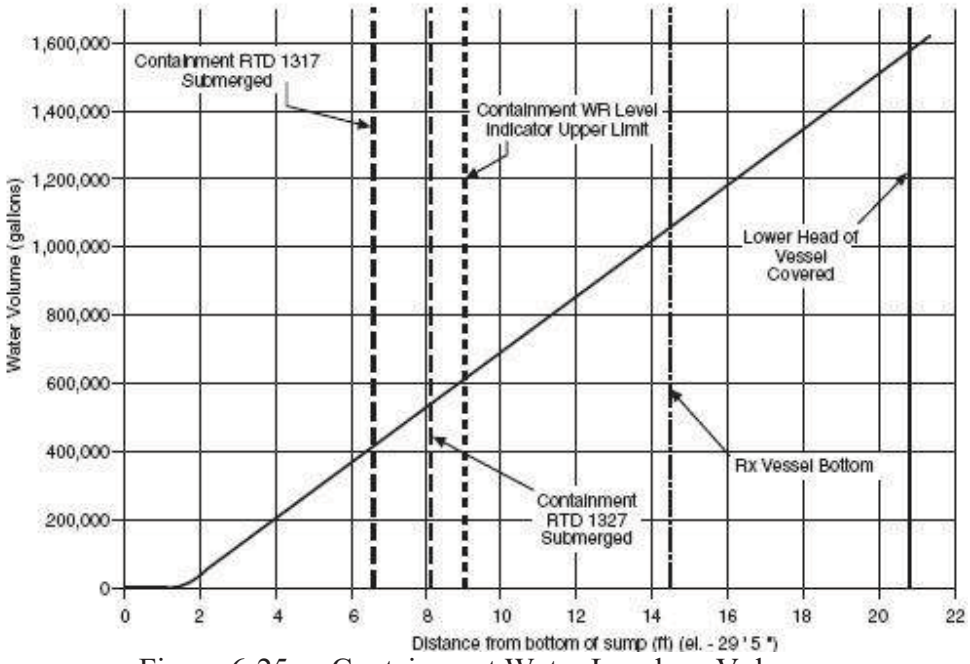

Figure 6-25 Containment Water Level vs. Volume

Table 6-15 Cumulative Water Volume vs. Elevation for Unit 1

ELEVATION (sea level)	**Distance from bottom of sump (ft)**	**Water volume (gal)**	**Water volume (ft^3)**
-29' 4 7/8"	0	0	0
-29' 4"	0.07	52	7
-29' 3"	0.16	108	14.4
-29' 3"	0.24	164	21.9
-29' 3"	0.41	277	37
-28' 7"	0.82	558	74.6
-28' 2"	1.24	965	129
-27' 10"	1.57	1,831	244.8
-27' 7"	1.82	9,113	1,218.2
-26' 7"	2.82	87,990	11,762.6
-25' 7"	3.82	166,867	22,306.9
-24' 7"	4.82	245,744	32,851.3
-23' 7"	5.82	324,620	43,395.5
-22' 7"	6.82	404,997	54,140.4
-21' 10 1/2"	7.53	461,933	61,751.6
-20' 1"	9.32	600,688	80,300.5
-10' **	19.41	1,381,588	184,692.0

** Last data point extrapolated

The location of radiological release from containment may be expected in the vicinity of the equipment hatch, but the location of the increased leakage is not expected to depressurize the containment immediately. Therefore, in the unlikely event that the increased leakage is at or below the level of the water, the containment would still be capable of retaining water. In any case, if water is injected into containment through containment spray or primary injection it would suppress the release.

Figure 6-26 shows the Surry containment system elevations. Figure 6-27 shows the time it would take to pump 2 million gallons of water at various pumping capacities. At 3,000 gpm, it would take about 11 hours and at 6,000 gpm it would take about 5.5 hours.

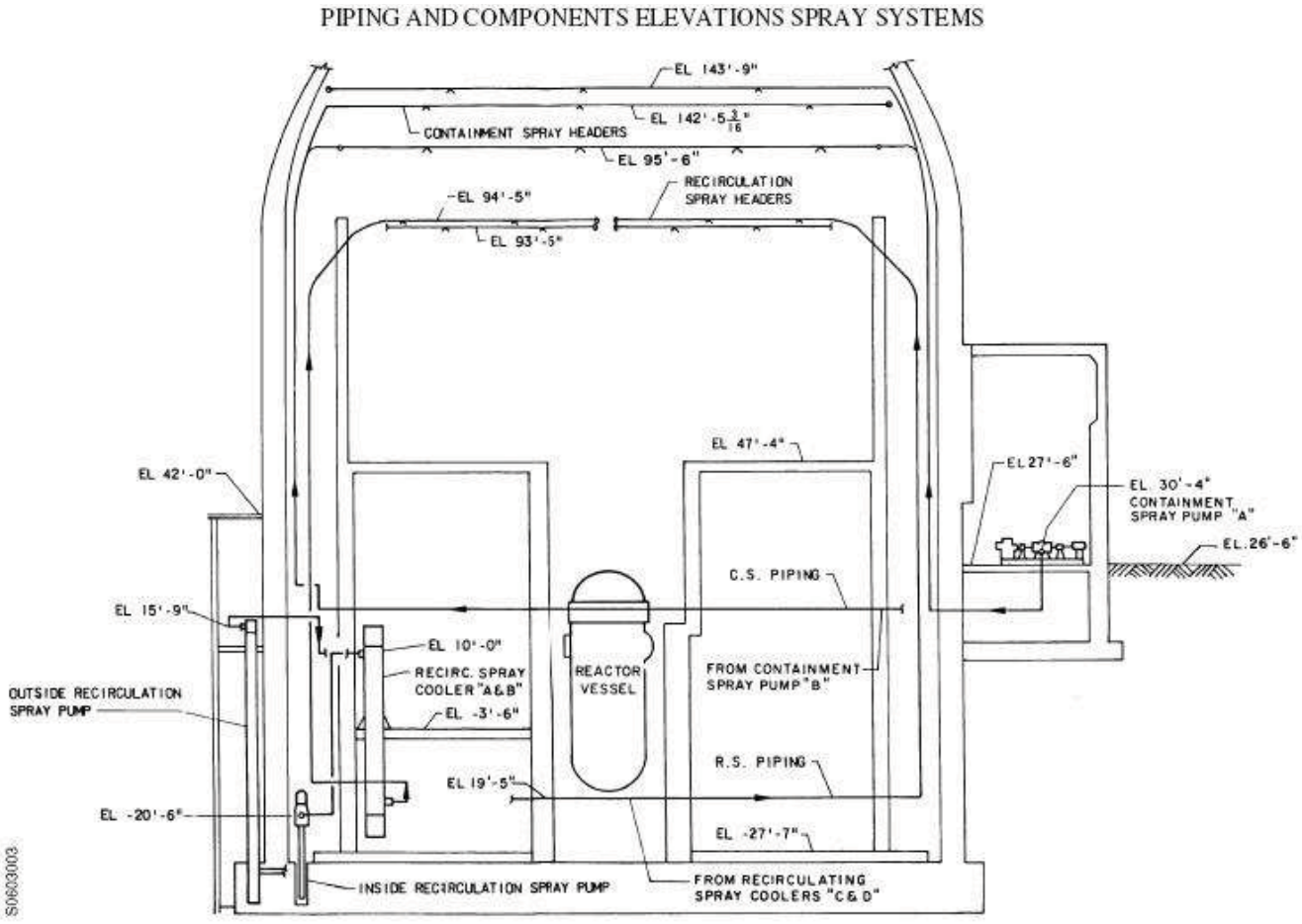

Figure 6-26 Surry Containment System

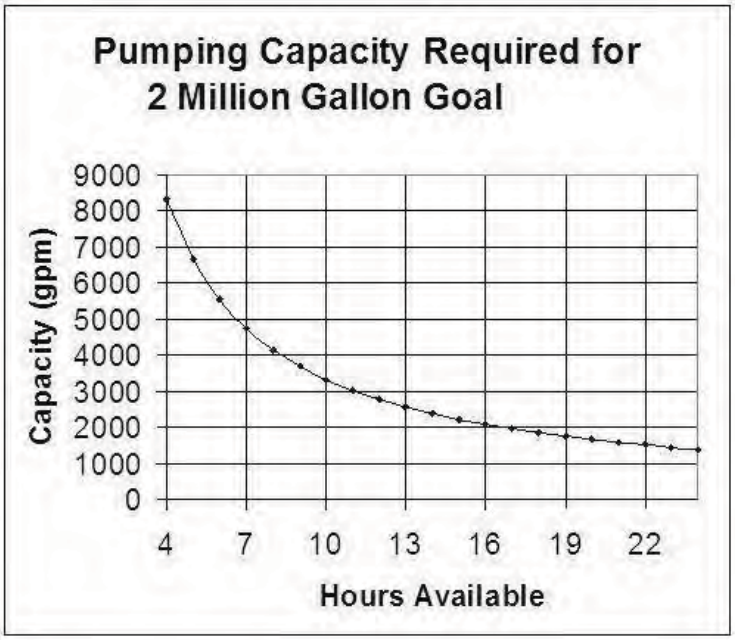

Figure 6-27 Pumping Capacity

6.6.3 Truncation Summary

The types of resources needed are multi-use and would begin being acquired or established early in the response to support restoration of cooling, depressurizing the RCS, injecting into the RCS, etc. Based on the above, flooding of containment would need to begin about 40 hours after the start of the accident. This would allow 8 hours to fill the containment to an appropriate depth, which would require a pumping rate of about 4,000 gpm. It is reasonable to assume that within 40 hours response personnel would be prepared to make a decision to flood the containment. The approach described provides a supporting basis for truncating the release at 48 hours. It is expected that onsite mitigative actions would limit core damage and reduce the release magnitude; however, this analysis is not definitive. Some of the actions identified are described within emergency response plans and some are ad hoc. The availability of the equipment is likely but not certain. If core damage is not prevented from the onsite mitigative measures, this truncation analysis demonstrates the offsite mitigative measures would likely take no more than 48 hours from accident initiation to truncate the radiological release. Based on the approach provided, which considers in detail the timing of many activities underway during an event, it is reasonable to bound the truncation of the accidents at 48 hours.

6.7 Emergency Preparedness Summary and Conclusions

Advancements in consequence modeling provide an opportunity to integrate more detail and realism in the application of protective action decisions applied for discrete population segments to represent implementation of protective actions. To best utilize these advancements, detailed information was developed and / or obtained from response of OROs to assure the quality of input data. Consequence modeling now provides for analysis of individual population segments and a user interface has been added to the consequence model to facilitate input detailed information that incorporates differences in the response to protective actions by various population segments. These advancements are significant because they now allow more detailed

modeling of response activities, timing of decisions, and implementation of protective actions across a wide range of population segments.

Licensees develop ETEs to support emergency planning and help assure the most appropriate protective actions are implemented in an emergency. These ETEs provide detailed information regarding the evacuation of the general public, schools, special facilities and the evacuation tail. The improvements to consequence modeling and improved understanding of implementation of protective actions now allows use of this detailed information when modeling potential consequences of reactor accidents. For the first time, consequence modeling can represent the actions of OROs and the timing of public response to an emergency with a clearer and more defensible basis provided for the timing of these actions.

In this analysis, six cohorts were modeled for each of the accident scenarios and a seventh cohort was added for the seismic analysis. Protective action factors were applied to each specific cohort.

- For the general public, shielding factors appropriate for the region were applied during normal, sheltering, and evacuation and response times and speeds were developed from the Surry 2001 ETE.

- Schools are notified directly in accordance with offsite emergency response plans and buses are mobilized to support expedited evacuation of schoolchildren. Mobilizing school resources early allows the evacuation of schools to occur first, prior to roadways becoming congested from evacuation of the general public. Therefore, the speed of the school cohort was established based on relatively little traffic on the roadways at the time.

- Special facilities are also notified early, but respond quite differently than schools. Transportation resources for special facilities are quite specialized, can be limited, and typically take extra time to mobilize. Evacuation of these facilities starts later than schools and continues longer than the evacuation of the general public. This is because transportation resources take longer to mobilize and make return trips to evacuate each facility independently. A benefit of special facilities is the robust nature of the structures of these nursing homes, hospitals, etc. The shielding protection values are increased for these facilities. For this analysis, this cohort is sheltered until the point at which evacuation begins which for calculation purposes was set at the same time as the evacuation tail begins.

- The evacuation tail was treated as a separate cohort and includes those members of the public who take longer to evacuate and are the last to leave the area. Indoor shielding values were applied to this cohort and it was evacuated late in the emergency moving at faster speeds because of the lower volume of traffic on the roadways at this time. The timing of the evacuation tail was developed from the ETE as the time when the last 10 percent of the public begin to evacuate.

- A shadow evacuation, which occurs when people evacuate from areas that are not under an evacuation order, was represented in the area beyond the EPZ in the analysis to account for additional vehicles on the roadway network. Including a shadow evacuation adds realism to the analysis and allows consideration of the impact of the shadow evacuation vehicles on the evacuation of the EPZ.

- Consistent with NUREG-1150, evacuees received a dose until they traveled to a point 10 miles beyond the analysis area, which for SOARCA was 30 miles.

- For the seismic analysis, it may be expected that a shadow evacuation of residents from within the EPZ may occur prior to the issuance of an evacuation order. This additional shadow evacuation was included in the analysis.

- A non-evacuating cohort was also included in the analysis assuming that a small percentage of the public may refuse to evacuate. Normal activity shielding values were applied to this cohort.

The Surry EALs were obtained for each of the accident scenarios modeled to reflect the timing of the declaration of SAE and GE.

The following accident scenarios were modeled:

1. Unmitigated STSBO
2. Unmitigated STSBO with TI-SGTR
3. Mitigated STSBO with TI-SGTR
4. Unmitigated LTSBO
5. Unmitigated ISLOCA
6. Sensitivity 1, Unmitigated ISLOCA with evacuation to 16 miles
7. Sensitivity 2, Unmitigated ISLOCA with evacuation to 20 miles
8. Sensitivity 3, Unmitigated ISLOCA with a delay in implementation of protective actions
9. Seismic Unmitigated STSBO with TI-SGTR

For each of these accident scenarios, the specific EAL information and cohort movement was applied and the WinMACCS files were complied for the consequence analysis.

The sensitivity analyses were performed to identify differences when varying selected parameters. This included expanding the limits of the evacuation and adjusting the timing of implementation of protective actions. In the first sensitivity analysis, the limits of the evacuation were extended to 16 miles. In order to evaluate evacuation to this distance, an ETE was developed using OREMS. A second sensitivity analysis was conducted modeling evacuation to a distance of 20 miles from the plant. An ETE was developed using OREMS, and for this case, there was no shadow evacuation assumed due to the extreme distance from the point of the accident.

An additional sensitivity analysis was conducted to assess the sensitivity of the timing of ORO decisions to consequences. This required increasing the delay times for cohorts to take action.

As supported by the SOARCA analyses, it is expected that the accidents evaluated would be mitigated through the actions of the onsite and offsite response agencies. The evaluation of the mitigation of source term and truncation of the accident at 48 hours further expands upon the response resources through identification of corporate, local, State, and Federal offsite resources. The responsibilities and resources of each of these organizations are described in onsite and offsite emergency response plans. These response organizations would mobilize upon request and as needed to support a severe nuclear power plant accident. These resources are in addition to the mitigative actions by the licensee through the use of safety and security enhancements, including SAMGs and 10 CFR 50.54(hh) mitigation measures.

The parameters developed in this section provide input to the MACCS2 consequence model presented in Section 7.

7. OFF-SITE CONSEQUENCES

7.1 Introduction

The MACCS2 consequence model (Version 2.5) was used to calculate offsite doses and their effect on members of the public. MACCS2 was developed at Sandia National Laboratories for the NRC for use in PRAs for commercial nuclear reactors to simulate the impact of accidental atmospheric releases of radiological materials on humans and on the surrounding environment. The principal phenomena considered in MACCS2 are atmospheric transport using a straight-line Gaussian plume model, short-term and long-term dose accumulation through several pathways including cloudshine, groundshine, inhalation, deposition onto the skin, and food and water ingestion. The ingestion pathway was not treated in the analyses reported here because uncontaminated food and water supplies are abundant within the United States and it is unlikely that the public would consume radioactively contaminated food or water. The following doses are included in the reported risk metrics:

* Cloudshine during plume passage

* Groundshine during the emergency and long-term phases from deposited aerosols

* Inhalation during plume passage and following plume passage from resuspension of deposited aerosols. Resuspension is treated during both the emergency and long-term phases.

The SOARCA project made additional enhancements to MACCS2 [24]. In general, these enhancements reflect recommendations obtained during the SOARCA external review and also reflect needs identified by the broader consequence analysis community. The code enhancements done for SOARCA were primarily to improve fidelity and code performance, and to enhance existing functionality. These enhancements are anticipated to have a significant effect on the fidelity of the analyses performed under the SOARCA project.

MACCS2 previously allowed up to three emergency-phase cohorts. Each emergency-phase cohort represents a fraction of the population who behave in a similar manner, although response times can be a function of radius. For example, a cohort might represent a fraction of the population who rapidly evacuate after officials instruct them to do so. To create a high fidelity model for SOARCA, the number of emergency-phase cohorts was increased, as described in Section 6 of this report. This allowed significantly more variations in emergency response, (e.g., variations in preparation time prior to evacuation to more accurately reflect the movement of the public during an emergency). In a similar way, modeling evacuation routes using the network-evacuation model added a greater degree of realism than in previous analyses that used the simpler radial evacuation model.

7.2 Surry Source Terms

Brief descriptions of the source terms for the Surry accident scenarios are provided in Table 7-1. For comparison, the largest source term (SST1) from the 1982 NUREG/CR-2239, "Technical Guidance for Siting Criteria Development" (referred to hereafter as the 'The 1982 Siting Study'

or just 'The Siting Study') [49] is also shown. Of the Surry source terms shown in the table, the unmitigated interfacing-systems loss-of-coolant accident (ISLOCA) is the largest in terms of release magnitude, but the release begins at 12.8 hours after accident initiation. Release begins earliest for the two thermally induced steam generator tube rupture scenarios (TISGTR), only 3.6 hours after accident initiation, but the magnitudes are very small. The unmitigated STSBO and LTSBO scenarios begin very late in time and have very small release magnitudes.

In comparison, the SST1 source term is significantly larger in magnitude, especially for the cesium class, than any of the Surry source terms. Moreover, it begins only 1.5 hours after accident initiation, about 2 hours earlier than the fastest release of the set of Surry source terms. The current understanding of accident progression has lead to a very different characterization of release signatures than was assumed for the 1982 Siting Study.

Table 7-1 Brief Source-Term Description for Unmitigated Surry Accident Scenarios and the SST1 Source Term from the 1982 Siting Study

		Integral Release Fractions by Chemical Class									Atmospheric Release Timing	
Scenario	**CDF (Events/yr)**	**Xe**	**Cs**	**Ba**	**I***	**Te**	**Ru**	**Mo**	**Ce**	**La**	**Start (hr)**	**End (hr)**
Surry STSBO	$2x10^{-6}$	0.518	0.001	0.000	0.006	0.006	0.000	0.000	0.000	0.000	25.5	48.0
Surry STSBO w/ TISGTR	$4x10^{-7}$	0.592	0.004	0.000	0.009	0.007	0.000	0.001	0.000	0.000	3.6	48.0
Surry Mitigated STSBO w/ TISGTR	$4x10^{-7}$	0.085	0.004	0.000	0.005	0.004	0.000	0.001	0.000	0.000	3.6	48.0
Surry LTSBO	$2x10^{-5}$	0.537	0.000	0.000	0.003	0.006	0.000	0.000	0.000	0.000	45.3	72.0
Surry ISLOCA	$3x10^{-8}$	0.983	0.020	0.000	0.154	0.132	0.000	0.003	0.000	0.000	12.8	48.0
SST1	$1x10^{-5}$	1.000	0.670	0.070	0.450	0.640	0.050	0.050	0.009	0.009	1.5	3.5

* The Iodine release fraction for the ISLOCA is less than that presented in Section 5.5 (0.158) due to the plume segment limitations of MACCS2. A MACCS2 analysis is limited to a maximum of 200 plume segments. In order to fully capture the ISLOCA Iodine release fraction and retain the one-hour plume segment durations, it would have taken ~300 plume segments in the analysis. Thus, the 200 plume segments that represented the majority of the release were used.

For comparison purposes, a consequence analysis using the old SST1 source term is presented in this chapter. This allows a direct comparison, using the same modeling options and result metrics, of the SST1 source term and the current, best-estimate source terms. An attempt to replicate the results of the 1982 Siting Study and comparison with SOARCA results is also presented.

7.3 Consequence Analyses

The results of the consequence analyses are presented in terms of risk to the public for each of the five accident scenarios identified for Surry. Both conditional and absolute risks are tabulated. The conditional risks are per reactor event. The absolute risks are likelihood of receiving a fatal cancer or early fatality for an average individual living within a specified radius of the plant per year of reactor operation from a potential plant accident.

The risk metrics are latent-cancer-fatality and early-fatality risks to residents in circular regions surrounding the plant. Population and economic data used in these analyses are projected for the year 2005. They are averaged over the entire residential population within the circular region. The risk values represent the predicted number of fatalities divided by the population for three choices of dose-truncation level. These risk metrics account for the distribution of the population within the circular region and for the interplay between the population distribution and the wind rose probabilities.

LCF risk results are presented for three dose-response assumptions: linear no threshold (LNT); US average natural background dose rate combined with average annual medical exposure as a dose truncation level (US BGR), which is 620 mrem/yr; and a dose truncation level based on the Health Physics Society's Position that there is a dose below which, due to uncertainties, a quantified risk should not be assigned (HPS), which is 5 rem/yr with a lifetime dose limit of 10 rem. A 10 mrem/yr dose truncation level was investigated, but it produced results that were just slightly lower than with the LNT assumption and thus these results were not included in the final version of this document.

In addition to the base-case mitigated and unmitigated accident scenarios, several sensitivity analyses are reported in this chapter. A sensitivity analysis for the unmitigated STSBO scenario shows the influence of the size of the evacuation zone or a delay in evacuation on predicted risk. Another sensitivity analysis considers the effect of seismic activity on emergency response. This sensitivity is considered because the base case results account for the effect of the seismic event on the plant but do not account for its effects on evacuation. This sensitivity analysis takes the latter effects into account as well. A separate analysis of the SST1 source term (shown in Table 7-1) allows older source-term assumptions to be compared with the current state-of-the-art methods for source term evaluation using otherwise equivalent assumptions and models. This analysis does not try to reproduce the 1982 Siting Study results; it merely overlays the older source term onto what are otherwise SOARCA assumptions for dose-response modeling, emergency response, and other factors. The final analyses show the relative contributions of each of the chemical classes included in the MELCOR source term analysis.

In this section, the risk tables represent rounded values obtained from the full data sets. The plots were developed from the full data sets and slight differences may be noticed due to this rounding.

7.3.1 Unmitigated Long-Term Station Blackout

The unmitigated LTSBO scenario is similar to the STSBO scenario except that cooling of the primary system is maintained until the batteries die, so degradation of the fuel and subsequent

failure of the containment are delayed in the LTSBO scenario. As a result, the source term is later and smaller for this scenario than for the STSBO. In fact, the source term for this scenario begins more than 45 hr after accident initiation. This source term is also unique in that it was truncated at 72 hr rather than 48 hr, the time that was used for all of the other source terms.

Table 7-2 displays the conditional, mean, latent-cancer-fatality (LCF) risks to residents within a set of concentric circular areas centered at the Surry site for the unmitigated LTSBO scenario. Three values of dose-truncation level are shown in the table: Linear, no threshold (LNT), i.e., a dose-truncation level of zero; the average, annual, US-background radiation (including average medical radiation) of 620 mrem/yr; and a dose-truncation level based on the Health Physics Society (HPS) Position, i.e., 5 rem/yr with a lifetime limit of 10 rem.

The truncation based on the HPS Position is more complex than the others because it involves both annual and lifetime limits. According to the recommendation, annual doses below the 5 rem truncation level do not need to be counted toward health effects; however, if the lifetime dose exceeds 10 rem, all annual doses, no matter how small, count toward health effects. Because of the 10 rem lifetime limit, risks predicted with the truncation based on the HPS Position can sometimes exceed those using the background radiation level for dose truncation.

Table 7-3 is analogous to Table 7-2, but displays absolute rather than conditional risks. In the case of the Surry LTSBO scenario, the mean CDF is $2x10^{-5}$ pry, a frequency that is based on the assumption that B.5.b mitigation does not succeed.

The values in Figure 7-3 are shown in Figure 7-1. The plot shows that for all dose-truncation levels, the risk is greatest for those closest to the plant and diminishes monotonically as distance increases. The trends shown in this figure are the same as those shown below in Figure 7-3 for the unmitigated STSBO.

Table 7-2 Mean, Individual LCF Risk per Event (Dimensionless) for Residents within the Specified Radii of the Surry Site for the Unmitigated LTSBO for a Mean CDF of $2x10^{-5}$ pry

Radius of Circular Area (mi)	LNT	US BGR	HPS
10	4.7E-05	4.0E-07	1.5E-09
20	2.6E-05	1.4E-07	4.1E-10
30	1.7E-05	7.8E-08	2.3E-10
40	1.1E-05	4.0E-08	1.2E-10
50	8.1E-06	2.7E-08	7.9E-11

Table 7-3 Mean, Individual LCF Risk per Reactor Year for Residents within the Specified Radii of the Surry Site for the Unmitigated LTSBO Scenario for a Mean CDF of $2x10^{-5}$ pry

Radius of Circular Area (mi)	LNT	US BGR	HPS
10	7.1E-10	6.0E-12	2.2E-14
20	3.8E-10	2.1E-12	6.2E-15
30	2.6E-10	1.2E-12	3.4E-15
40	1.6E-10	6.0E-13	1.8E-15
50	1.2E-10	4.1E-13	1.2E-15

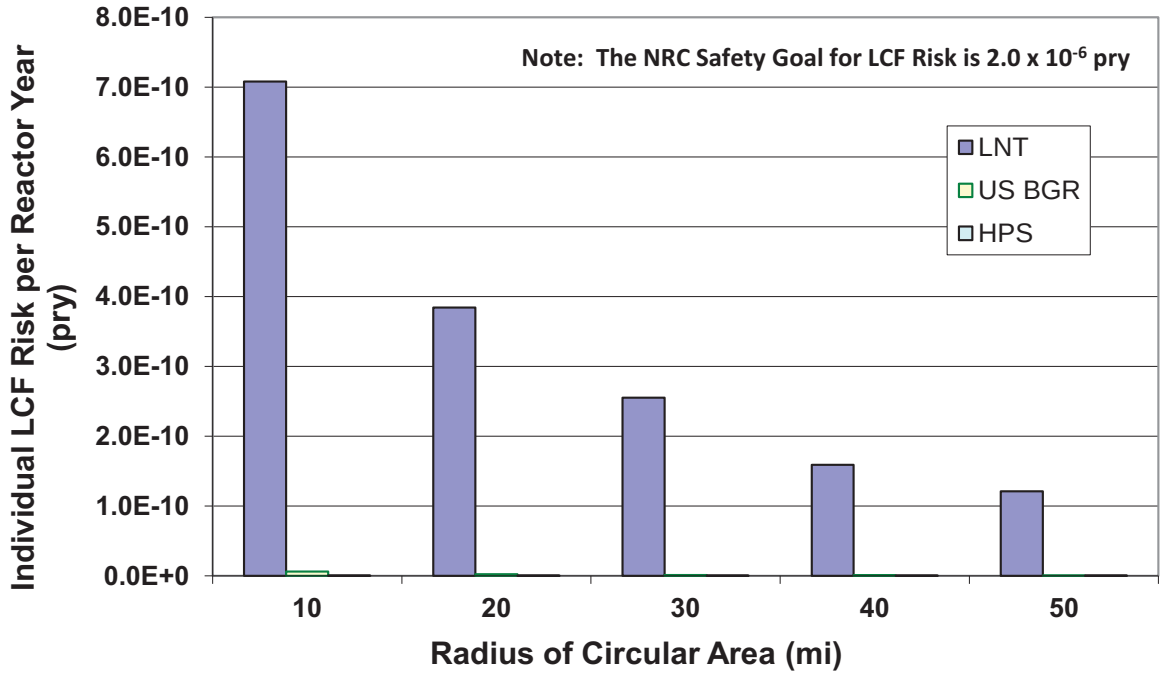

Figure 7-1 Mean, individual LCF risk per Reactor Year from the Surry unmitigated LTSBO scenario for residents within a circular area of specified radius from the plant for three values of dose-truncation level

Figure 7-2 shows absolute LNT risks for the Surry unmitigated LTSBO for the emergency and long-term phases. The entire height of each column shows the combined (total) risk for the two phases. The figure shows that the emergency response is very effective within the EPZ and that the long-term phase dominates the overall risks. The habitability (i.e., return) criterion, which is implemented as a limit of 4 rem in the first 5 years after returning to live in a residential area, controls the overall risk to the public for this accident scenario. The trends shown in this figure are the same as those shown in Figure 7-4 for the unmitigated STSBO. In both cases, evacuees have ample time to evacuate before release begins.

All of the emergency-phase risk within the 10-mile EPZ is for the non-evacuating cohort. This is because all of the other cohorts avoid exposure to the plume. Thus, for this accident scenario, the residents within the EPZ who comply with the request to evacuate have no increased risk prior to the long-term phase. The peak emergency-phase risk is at 20 miles, which is the first location in the plot outside of the evacuation zone.

The prompt-fatality risks are identically zero for this accident scenario. This is because the release fractions (shown in Table 7-1) are too small to produce doses large enough to exceed the dose thresholds for early fatalities, even for the 0.5% of the population that does not evacuate. Estimated risks below 1×10^{-7} per reactor year should be viewed with caution because of the potential impact of events not studied in the analyses and the inherent uncertainty in very small calculated numbers.

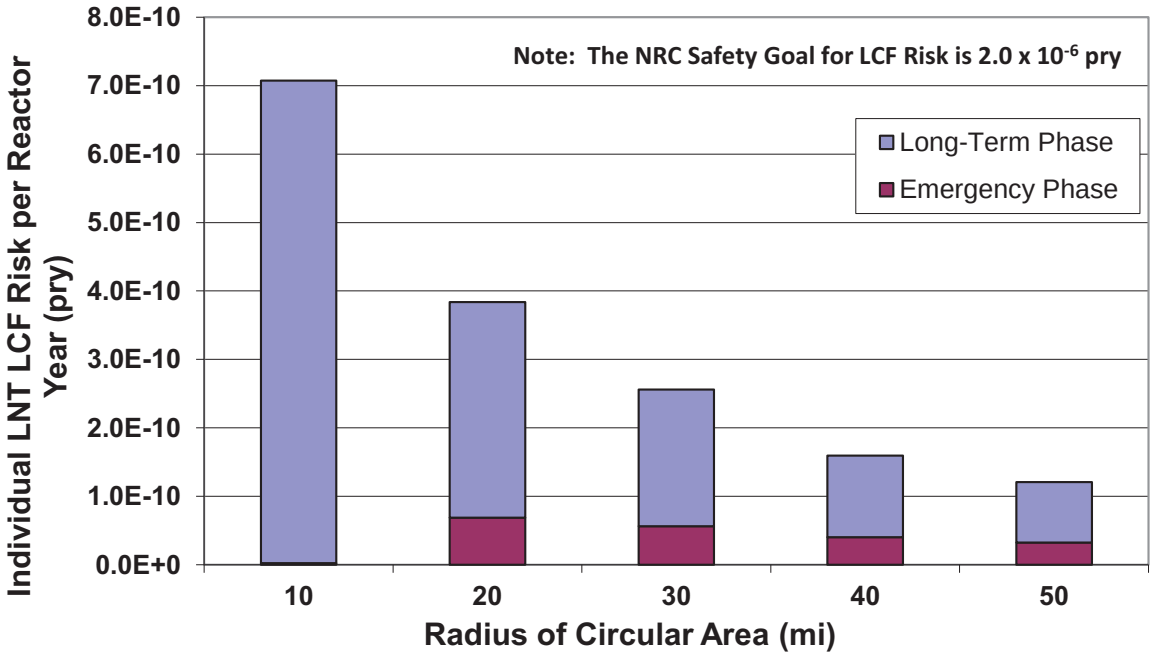

Figure 7-2 Mean, individual LNT, LCF risk per Reactor Year from the Surry unmitigated LTSBO scenario for residents within a circular area of specified radius from the plant for the emergency and long-term phases

7.3.2 Unmitigated Short-Term Station Blackout

Table 7-4 displays the conditional, mean, latent-cancer-fatality risks to residents within a set of concentric circular areas centered at the Surry site for the unmitigated STSBO scenario.

Table 7-4 Mean, Individual, LCF Risk per Event (Dimensionless) for Residents within the Specified Radii of the Surry Site for the Unmitigated STSBO Scenario, for a Mean CDF of $1.5x10^{-6}$/pry

Radius of Circular Area (mi)	LNT	US BGR	HPS
10	9.4E-05	3.4E-06	1.4E-08
20	4.8E-05	1.5E-06	4.9E-09
30	3.2E-05	8.4E-07	2.7E-09
40	2.0E-05	4.3E-07	1.4E-09
50	1.5E-05	2.9E-07	9.4E-10

Table 7-5 is analogous to Table 7-4 but shows absolute rather than conditional risks. In the case of the Surry unmitigated STSBO, the mean CDF of $1.5x10^{-6}$ per year is used, a frequency that is based on the assumption that B.5.b mitigation does not succeed. These risks are shown graphically in Figure 7-3. The plot shows that for all dose-truncation levels, the risk is greatest for those closest to the plant and diminishes monotonically with distance.

Table 7-5 Mean, Individual, LCF Risk per Reactor Year for Residents within the Specified Radii of the Surry Site for the Unmitigated STSBO Scenario for a Mean CDF of $1.5x10^{-6}$ pry

Radius of Circular Area (mi)	LNT	US BGR	HPS
10	1.4E-10	5.1E-12	2.1E-14
20	7.2E-11	2.3E-12	7.3E-15
30	4.8E-11	1.3E-12	4.0E-15
40	2.9E-11	6.5E-13	2.1E-15
50	2.2E-11	4.4E-13	1.4E-15

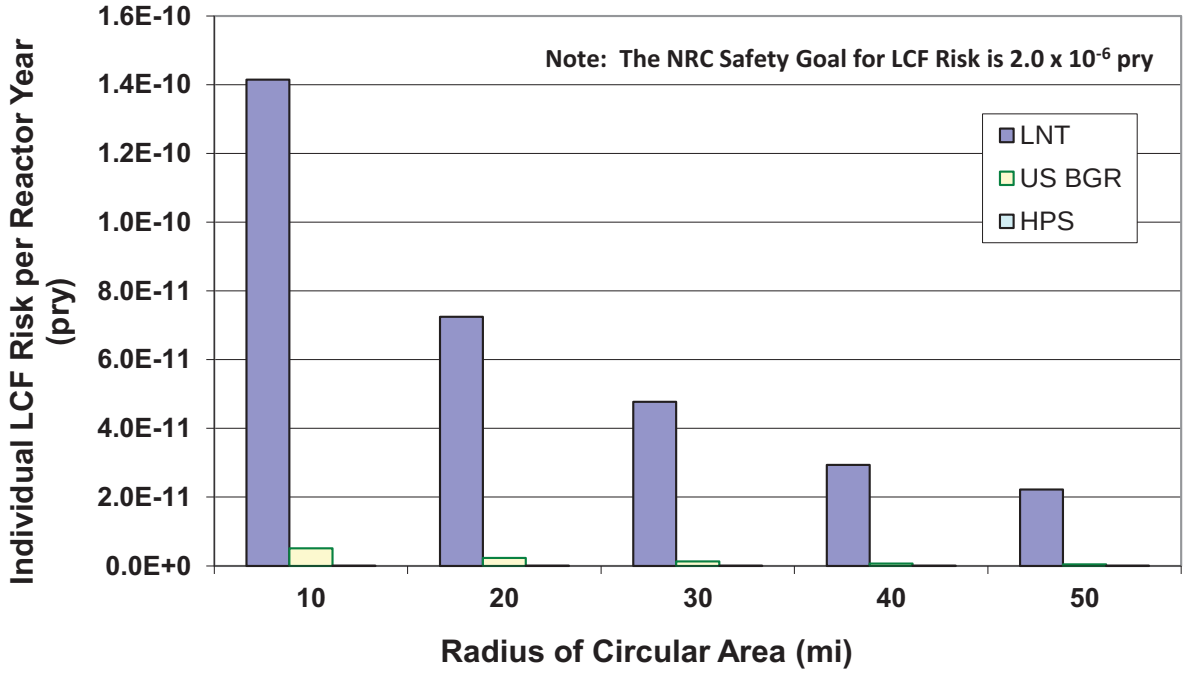

Figure 7-3 Mean, Individual, LCF Risk per Reactor Year from the Surry unmitigated STSBO scenario for residents within a circular area of specified radius from the plant for three values of dose-truncation level

Figure 7-4 shows the mean, individual, LNT, LCF risk for the Surry unmitigated STSBO for the emergency and the long-term phases. The height of each column indicates the combined (total) risk for the two phases. The figure shows that the emergency response is very effective within the EPZ, so those risks are very small and entirely represent the 0.5 percent of the population that does not evacuate. Thus, for this accident scenario, the residents within the EPZ who comply with the request to evacuate have no increased risk prior to the long-term phase. The peak in the emergency-phase risk is at 20 miles, which is the first location outside of the evacuation zone.

The long-term phase dominates the overall risks under the LNT assumption. The habitability (i.e., return) criterion, which is implemented as a limit of 4 rem in the first 5 years after returning to live in a residential area, controls the overall risk to the public.

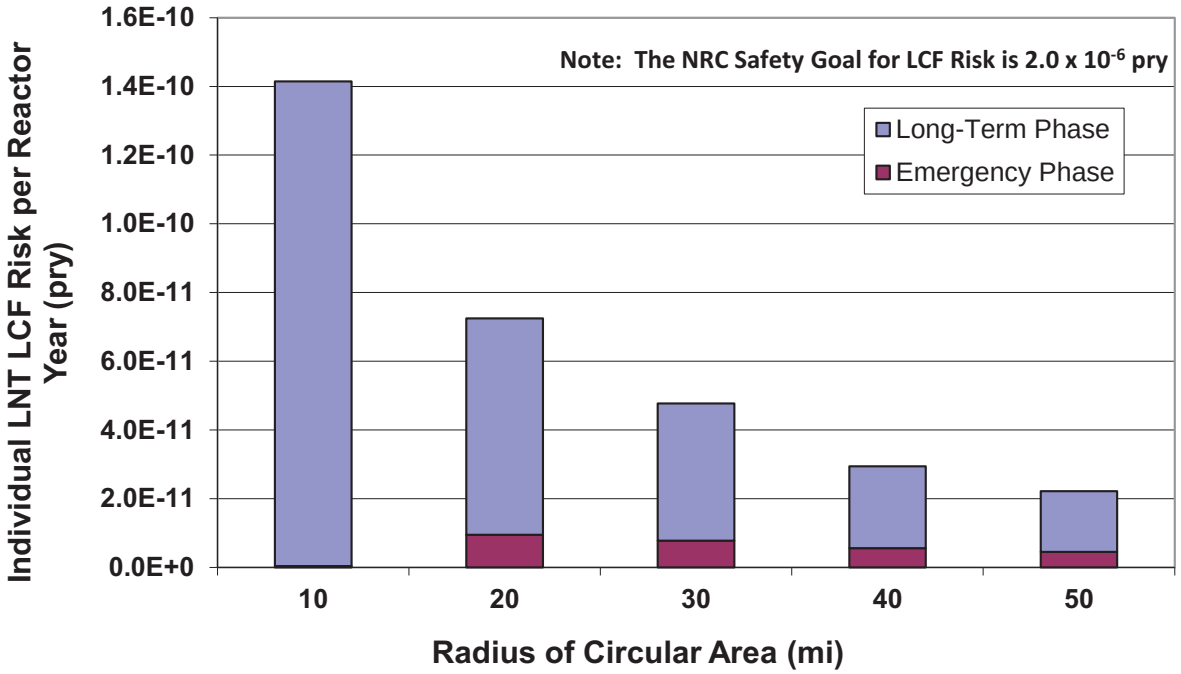

Figure 7-4 Mean, Individual, LNT, LCF Risk per Reactor Year from the Surry unmitigated STSBO scenario for residents within a circular area of specified radius from the plant for the emergency and long-term phases

The prompt-fatality risks are identically zero for this accident scenario. This is because the release fractions (shown in Table 7-1) are too small to produce doses large enough to exceed the dose thresholds for early fatalities, even for the 0.5% of the population that does not evacuate.

7.3.3 Unmitigated Short-Term Station Blackout with TI-SGTR

Table 7-6 displays the conditional, mean, latent-cancer-fatality risks to residents within a set of concentric circular areas centered at the Surry site for the unmitigated STSBO initiated, thermally induced, steam-generator-tube rupture (TISGTR) scenario.

Table 7-7 is analogous to Table 7-6, but shows absolute rather than the conditional risks. In the case of the Surry unmitigated STSBO with TISGTR scenario, the mean CDF of 3.75×10^{-7} pry is used[40]. This frequency is based on the assumption that B.5.b mitigation does not succeed.

[40] The frequency of the Surry short-term station blackout is 1×10^{-6} to 2×10^{-6}/yr. The conditional probability of a thermally induced steam generator tube rupture is 0.1 to 0.4. The mean core damage frequency of 3.75×10^{-7}/yr represents the product of the mid points of these two ranges, (i.e., $0.25 * 1.5 \times 10^{-6}$/yr).

Table 7-6 Mean, Individual, LCF Risk per Event (Dimensionless) for Residents within the Specified Radii of the Surry Site for the Unmitigated STSBO with TISGTR With a Mean CDF of $4x10^{-7}$ pry

Radius of Circular Area (mi)	LNT	US BGR	HPS
10	3.2E-04	7.4E-05	1.3E-05
20	1.9E-04	4.0E-05	4.5E-06
30	1.3E-04	2.5E-05	2.5E-06
40	8.4E-05	1.4E-05	1.3E-06
50	6.5E-05	9.9E-06	8.6E-07

Table 7-7 Mean, Individual, LCF Risk per Reactor Year for Residents within the Specified Radii of the Surry Site for the Unmitigated STSBO with TISGTR With a Mean CDF of $4x10^{-7}$ pry

Radius of Circular Area (mi)	LNT	US BGR	HPS
10	1.2E-10	2.8E-11	5.0E-12
20	7.2E-11	1.5E-11	1.7E-12
30	4.9E-11	9.5E-12	9.2E-13
40	3.2E-11	5.3E-12	4.7E-13
50	2.4E-11	3.7E-12	3.2E-13

The values in Figure 7-7 are shown in Figure 7-5. The plot shows that for all dose-truncation levels, the risk is greatest for those closest to the plant and diminishes monotonically with distance. The general trends in this figure are very similar to those shown in Figure 7-3 in the previous subsection.

Figure 7-6 shows the LNT latent-cancer-fatality risks for the Surry unmitigated STSBO with TISGTR for the emergency and long-term phases. The figure shows that the emergency response does not entirely eliminate doses within the EPZ, but nonetheless, the risks are very small compared with the long-term phase risks. The doses received during the early phase stem from the relatively early release, which begins 3.6 hr after accident initiation (as shown in Table 7-1). The habitability (i.e., return) criterion, which is implemented as a limit of 4 rem in the first 5 years after returning home, controls the overall risk to the public for this accident scenario. The general trends in this figure are very similar to those shown in Figure 7-4 in the previous subsection, with one exception. The risk from exposure during the emergency phase within a 10-mile radius is very small compared with the other distances shown in Figure 7-4; it is larger within a 10-mile radius than it is for the larger radii in Figure 7-6. The difference is directly related to the source-term characteristics, particularly the initiation of release, as discussed in the following paragraph.

Most of the emergency-phase risk within the 10-mile EPZ is for the evacuees. This is because release begins at 3.6 hr after accident initiation; the public begins to evacuate at 3.75 hr. Thus,

some of the evacuees travel through the plume. By comparison, release begins 25.5 hours after accident initiation in the unmitigated STSBO discussed in the previous subsection while evacuation begins at the same time for both sequences.

The nonevacuating cohort represents 1.4% of the overall emergency-phase risk using the LNT hypothesis. This is a larger percentage of the overall risk than the population fraction represented by this cohort, which is 0.5%. This is expected, i.e., that the nonevacuating cohort should represent a greater risk than the cohorts that evacuate.

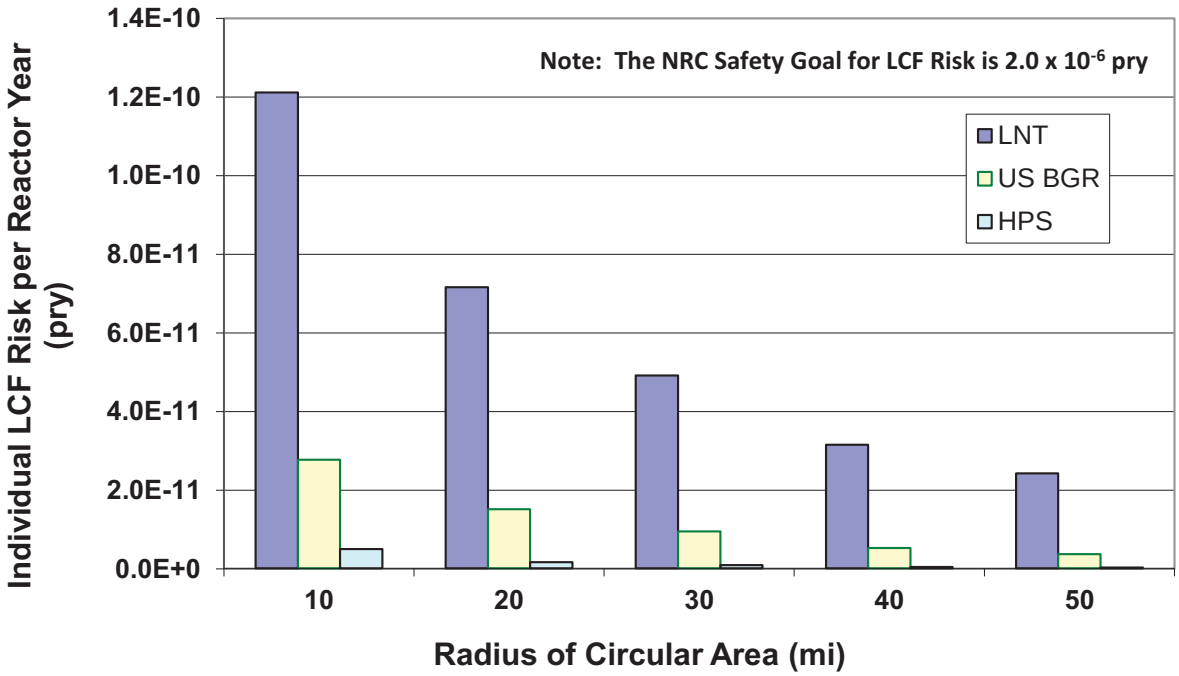

Figure 7-5 Mean, Individual, LCF Risk per Reactor Year from the Surry, unmitigated STSBO with TISGTR scenario for residents within a circular area of specified radius from the plant for three choices of dose-truncation level

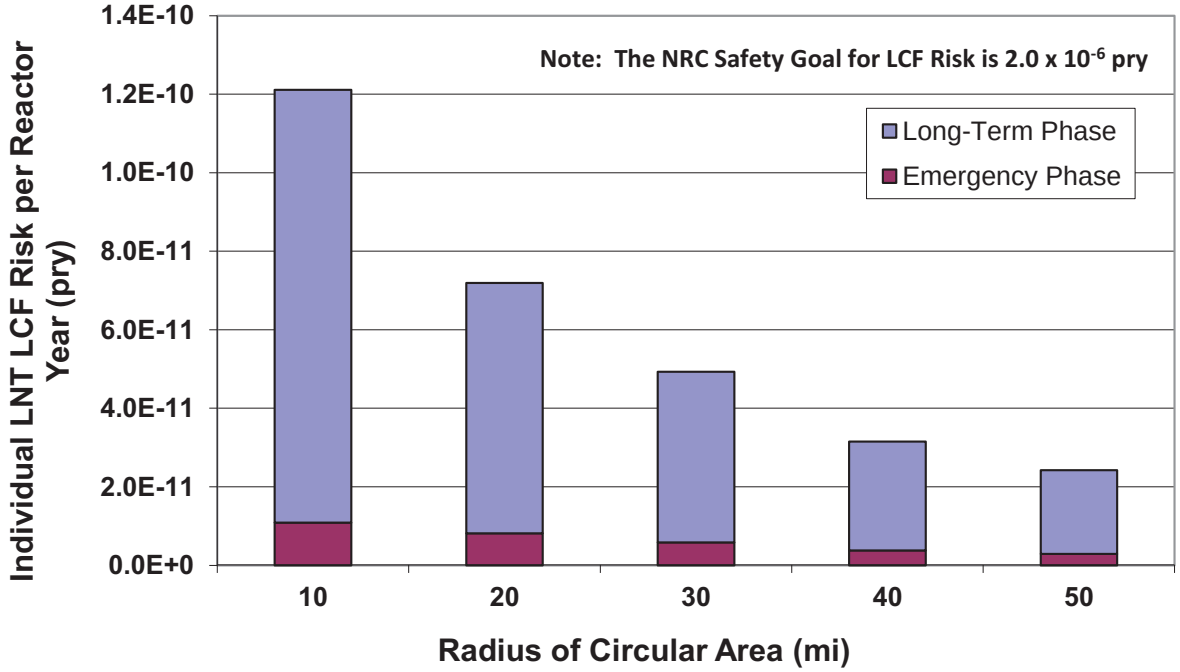

Figure 7-6 Mean, Individual, LNT, LCF Risk per Reactor Year from the Surry, unmitigated, STSBO with TISGTR scenario for residents within a circular area of specified radius from the plant for the emergency and long-term phases.

The prompt-fatality risks are zero for this accident scenario. This is because the release fractions (shown in Table 7-1) are too small to produce doses large enough to exceed the dose thresholds for early fatalities, even for the 0.5% of the population that does not evacuate.

7.3.4 Mitigated Short-Term Station Blackout with TI-SGTR Rupture

Table 7-8 displays the conditional, mean, latent-cancer-fatality risks to residents within a set of concentric circular areas centered at the Surry site for the mitigated STSBO with TISGTR scenario. This scenario is similar to the one in the previous Section except that it is mitigated by operator actions to restore containment sprays. Because of the restored containment sprays, the risks are slightly lower than those shown in the previous subsection.

Table 7-9 is analogous to Table 7-8, but displays absolute rather than the conditional risk. In the case of the Surry mitigated STSBO with TISGTR scenario, the mean core damage frequency is $4x10^{-7}$ pry a frequency that is based on the assumption that B.5.b mitigation does not succeed. The values in this table are plotted in Figure 7-7. The trends are identical to those shown in the previous subsection for the unmitigated STSBO with TISGTR.

Table 7-8 Mean, Individual, LCF Risk per Event (Dimensionless) for Residents within the Specified Radii of the Surry Site for the Mitigated STSBO with TISGTR Scenario with a CDF of $4x10^{-7}$ pry

Radius of Circular Area (mi)	LNT	US BGR	HPS
10	2.8E-04	7.1E-05	1.4E-05
20	1.7E-04	3.8E-05	4.5E-06
30	1.1E-04	2.4E-05	2.5E-06
40	7.3E-05	1.3E-05	1.3E-06
50	5.6E-05	9.3E-06	8.7E-07

Table 7-9 Mean, Individual, LCF Risk per Reactor-Year for Residents within the Specified Radii of the Surry Site for the Mitigated STSBO with TISGTR Scenario with a CDF of $4x10^{-7}$ pry

Radius of Circular Area (mi)	LNT	US BGR	HPS
10	1.0E-10	2.7E-11	5.1E-12
20	6.2E-11	1.4E-11	1.7E-12
30	4.3E-11	8.9E-12	9.3E-13
40	2.7E-11	4.9E-12	4.8E-13
50	2.1E-11	3.5E-12	3.3E-13

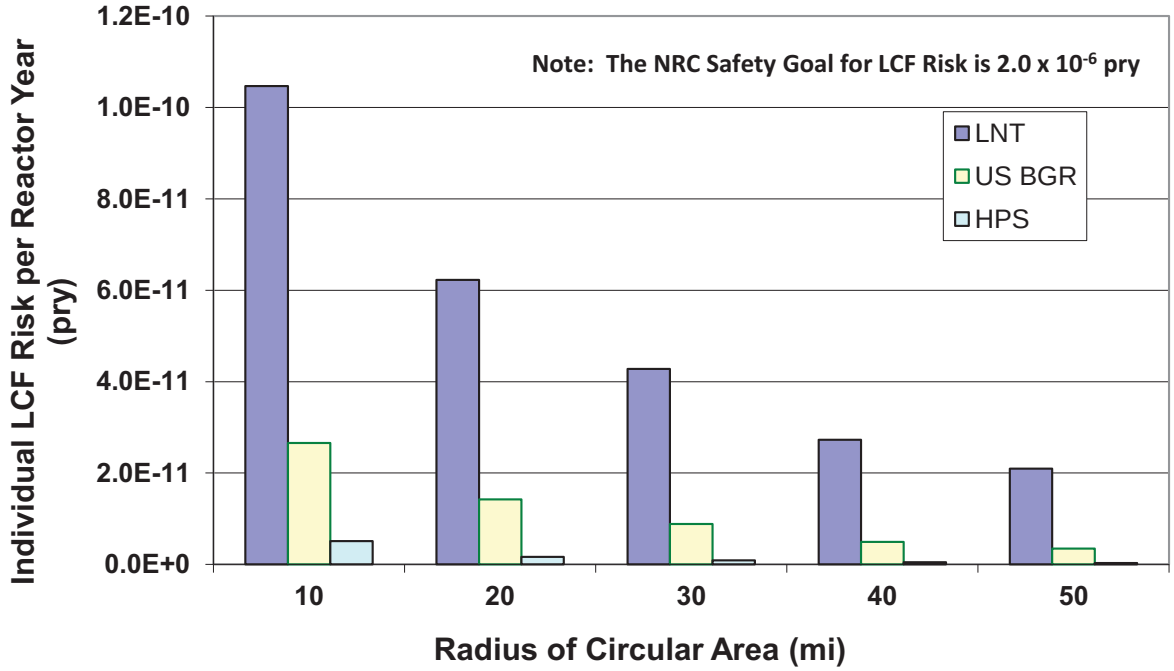

Figure 7-7 Mean, Individual, LCF Risk per Reactor Year from the Surry, mitigated, STSBO with TISGTR scenario for residents within a circular area of specified radius from the plant for three choices of dose-truncation level

Figure 7-8 shows the LCF risk for the Surry mitigated STSBO with TISGTR scenario for the emergency and long-term phases. The figure shows that the emergency response does not entirely eliminate doses within the EPZ, but nonetheless, the risks are very small compared with the long-term risks. The doses received during the emergency phase stem from the relatively early release, which begins just 3.6 hr after accident initiation (cf., shown in Table 7-1). The habitability (i.e., return) criterion, which is implemented as a limit of 4 rem in the first 5 years after returning home, controls the overall risk to the public for this accident scenario. The trends shown in Figure 7-8 are identical to those shown in Figure 7-6 for the unmitigated scenario, but the magnitudes are slightly smaller.

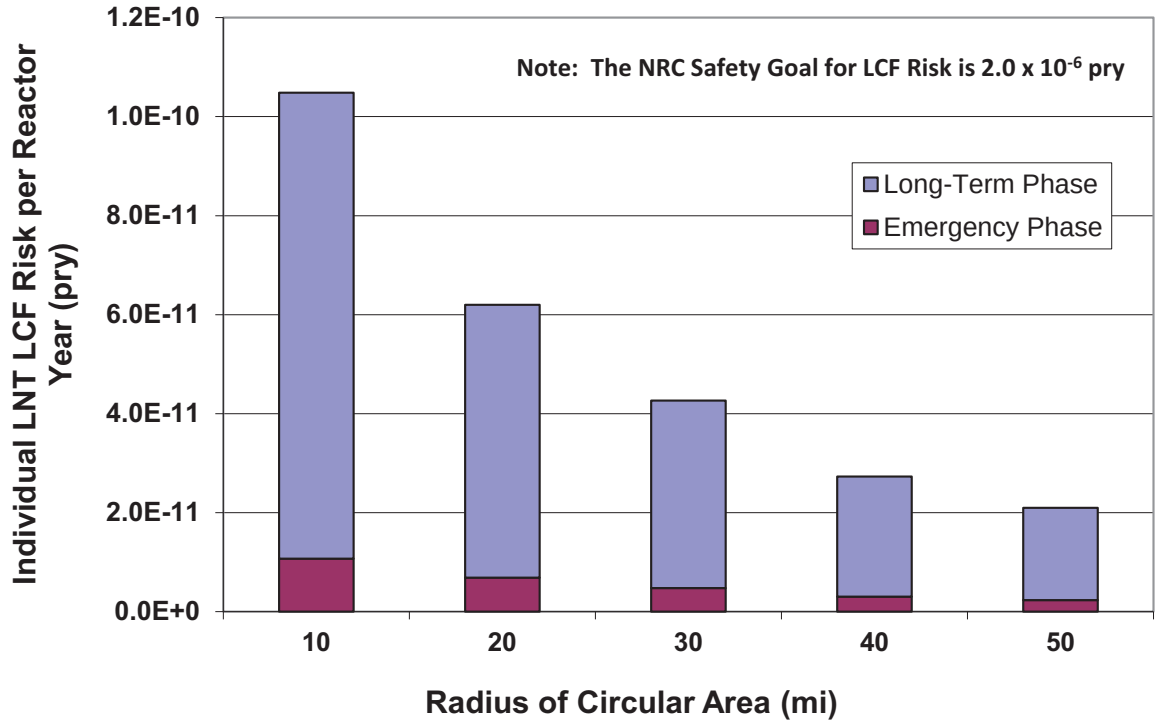

Figure 7-8 Mean, Individual, LNT, LCF Risk per Reactor Year from the Surry mitigated STSBO with TISGTR scenario for residents within a circular area of specified radius from the plant for the emergency and long-term phases

The prompt-fatality risks are zero for this accident scenario. This is because the release fractions (shown in Table 7-1) are too low to produce doses large enough to exceed the dose thresholds for early fatalities, even for the 0.5% of the population that does not evacuate.

Most of the emergency-phase risk within the 10-mile EPZ is for the evacuees. This is because release begins at 3.6 hr and, as a result, most of the evacuees are unable to avoid exposure to the plume. The nonevacuating cohort represents 1.1% of the overall emergency-phase risk using the LNT hypothesis. This is clearly a larger percentage of the overall risk than the population fraction represented by this cohort, which is 0.5%. It is expected that the nonevacuating cohort should have a greater risk than the cohorts who evacuate.

7.3.5 Unmitigated ISLOCA

The unmitigated interfacing systems loss of coolant accident (ISLOCA) has the largest predicted release and it begins earlier than for the SBO scenarios without TISGTR. The release for this scenario begins at 12.8 hours after accident initiation. Emergency response is very effective and essentially no early fatalities are predicted to occur. However, predicted latent cancer fatality risk is larger than it is for the scenarios described in the previous subsections.

Table 7-10 displays the conditional, mean, latent cancer fatality risks to residents within a set of concentric circular areas centered at the Surry site for the unmitigated ISLOCA scenario.

Table 7-11 is analogous to Table 7-10, but displays absolute rather than the conditional risks. In the case of the Surry unmitigated ISLOCA scenario, the mean CDF is $3x10^{-8}$/yr. This frequency is used to multiply the results in Table 7-10, as described above.

The values in Figure 7-11 are plotted in Figure 7-9. The plot shows that for all dose truncation levels, the risk is greatest at the 20-mile radius. This trend is due to evacuation in the 10-mile EPZ and only a partial shadow evacuation between 10 and 20 miles. Predicted LCF risk is larger in this scenario than it is in the scenarios described in the preceding subsections.

Figure 7-10 shows the latent cancer fatality risks as a function of the radius from the plant for the emergency phase (EARLY), the long-term phase (CHRONC), and the combined phases (sum of the two). The figure shows that the emergency response does not entirely eliminate risks within the EPZ. This is because release begins at 12.8 hours after accident initiation, which is before evacuation is complete. Figure 6-10 shows that the public evacuates from 3 hr to 13 hr after accident initiation and the Special Facilities and Tail Cohorts only begin to evacuate at 13 hr after accident initiation. Therefore, there is a potential for exposure to the plume during evacuation for this accident scenario. This accounts for the emergency-phase risk within the 10-mile EPZ shown in Figure 7-10.

Nonetheless, the long-term phase dominates the overall risks, even within the EPZ. The habitability (i.e., return) criterion, which is implemented as a limit of 4 rem in the first 5 years after returning home, controls the overall risk to the public for this accident scenario.

Most of the emergency-phase risk within the 10-mile EPZ is for the evacuees. The nonevacuating cohort represents 29.8% of the overall emergency-phase risk using the LNT hypothesis. This is more than an order-of-magnitude larger percentage of the overall risk than the population fraction represented by this cohort, which is 0.5%. This result is expected, that is, that the individual risk for the cohort that does not evacuate should be greater than for the cohorts who do evacuate.

Table 7-10 Mean, Individual LCF Risk per Event (Dimensionless) for Residents within the Specified Radii of the Surry Site for the Unmitigated ISLOCA Scenario with a CDF of $3x10^{-8}$ pry

Radius of Circular Area (mi)	LNT	US BGR	HPS
10	3.0E-04	6.5E-05	3.3E-05
20	3.4E-04	1.7E-04	1.5E-04
30	2.7E-04	1.4E-04	1.1E-04
40	2.0E-04	9.4E-05	6.6E-05
50	1.6E-04	7.5E-05	4.9E-05

Table 7-11 Mean, Individual, LCF Risk per Reactor-Year for Residents within the Specified Radii of the Surry Site for the Unmitigated ISLOCA Scenario with a CDF of $3x10^{-8}$ pry

Radius of Circular Area (mi)	LNT	US BGR	HPS
10	9.1E-12	1.9E-12	1.0E-12
20	1.0E-11	5.2E-12	4.5E-12
30	8.1E-12	4.1E-12	3.2E-12
40	5.9E-12	2.8E-12	2.0E-12
50	4.9E-12	2.2E-12	1.5E-12

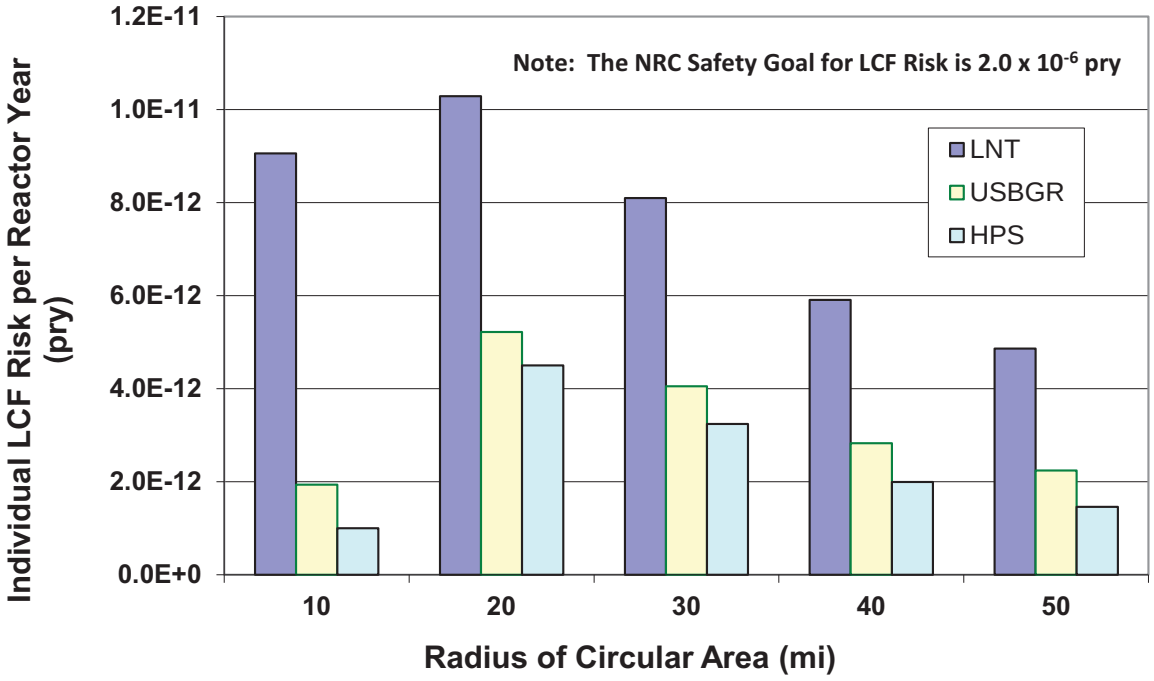

Figure 7-9 Mean, Individual, LCF Risk per Reactor Year from the Surry, unmitigated, ISLOCA scenario for residents within a circular area of specified radius from the plant for three choices of dose truncation level

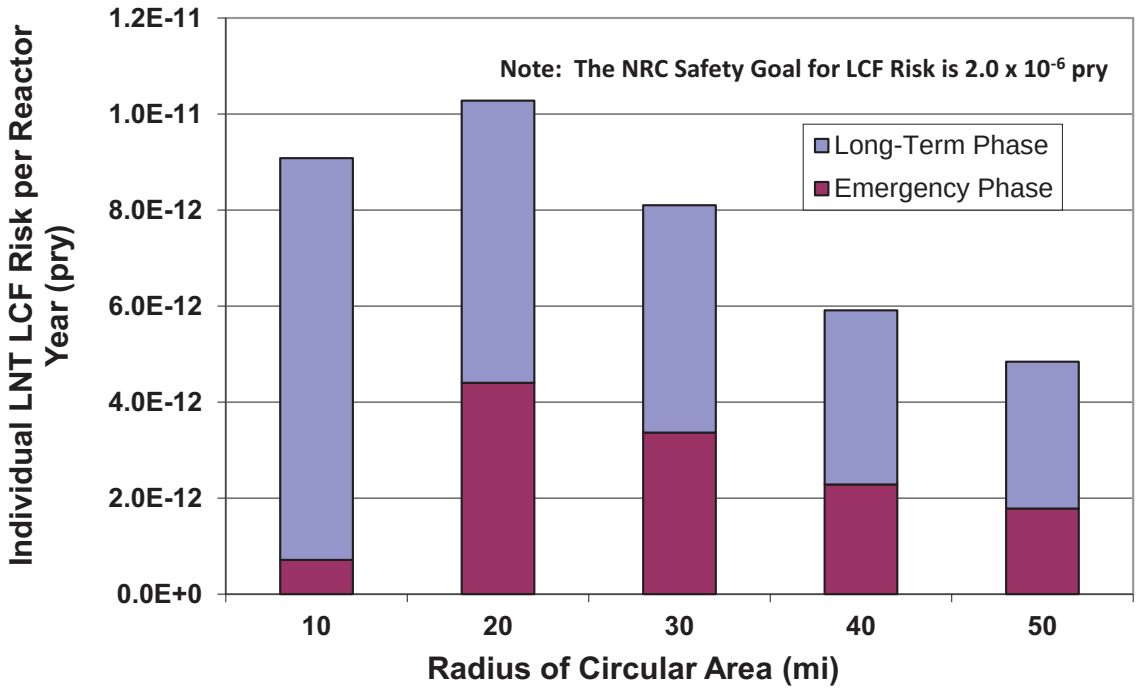

Figure 7-10 Mean, Individual, LNT, LCF Risk per Reactor Year from the Surry, unmitigated, ISLOCA scenario for residents within a circular area of specified radius from the plant for the emergency and long-term phases

The prompt fatality risks are essentially zero for this accident scenario. The releases are close to the threshold for early fatalities. There is no prompt fatality risk for the cohorts that evacuate. Conditional prompt fatality risks are shown in Table 7-12 as a function of distance from the plant. Absolute prompt fatality risks are shown in Table 7-13.

Table 7-12 Mean, Individual, Prompt Fatality Risk per Event (Dimensionless) for Residents within the Specified Radii of the Surry Site for the ISLOCA Scenario with a Mean CDF of $3x10^{-8}$ pry

Radius of Circular Area (mi)	Prompt Fatality Risk
1.3	1.5E-06
2.0	6.4E-07
2.5	4.0E-07

Table 7-13 Mean, Individual Prompt-Fatality Risk per Reactor-Year for Residents within the Specified Radii of the Surry Site for the ISLOCA Scenario with a Mean CDF of $3x10^{-8}$ pry

Radius of Circular Area (mi)	Prompt Fatality Risk
1.3	4.4E-14
2.0	1.9E-14
2.5	1.2E-14

The NRC quantitative health objective (QHO) for prompt fatalities is generally interpreted as the absolute risk within 1 mile of the exclusion area boundary. For Surry, the exclusion area boundary is 0.35 miles from the reactor building from which release occurs, so the outer boundary of this 1-mile zone is at 1.35 miles. The closest MACCS2 grid boundary to 1.35 miles used in this set of calculations is at 1.3 miles. Using the risk within 1.3 miles should reasonably approximate the risk within 1 mile of the exclusion area boundary. The absolute risk of a prompt fatality to an individual for this source term is approximately $4.4x10^{-14}$ per reactor year, which is well below the QHO. In fact, this risk is so low that for practical purposes it is zero.

7.3.6 Sensitivity Analyses on Size of the Evacuation Zone and Evacuation Start Time

The baseline analyses included evacuation of the 10-mile EPZ, a partial shadow evacuation between 10 and 20 miles, and relocations of the remaining members of the public. For the unmitigated ISLOCA scenario, three additional calculations were performed to assess variations in the protective actions.

Sensitivity 1: Evacuation of a 16-Mile Circular Area:
In this calculation, the evacuation zone is expanded to 16 miles. Shadow evacuation occurs from within the 16- to 20-mile area.

Sensitivity 2: Evacuation of a 20-Mile Circular Area:
In this calculation, the evacuation zone is expanded to 20 miles. No shadow evacuation beyond the evacuation zone is considered.

Sensitivity 3: Delayed Evacuation of a 10-Mile Circular Area:
This calculation is identical to the baseline case described above except that implementation of protective action is delayed by 30 minutes.

The results of all three sensitivity analyses are compared with the base case in Table 7-14, which shows that very little benefit results from increasing the size of the evacuation zone beyond the standard 10 miles. A delay in evacuation timing also has little impact on the results.

Table 7-14 Effect of Size of Evacuation Zone on Mean, LNT, LCF Risks for Residents within the Specified Radii of the Surry Site for the Unmitigated ISLOCA Scenario

Radius of Circular Area (mi)	Base Case 10-Mile Evacuation	Sensitivity 1 16-Mile Evacuation	Sensitivity 2 20-Mile Evacuation	Sensitivity 3 10-Mile Delayed Protective Action
10	3.0E-04	3.9E-04	4.1E-04	3.2E-04
20	3.4E-04	2.7E-04	2.5E-04	3.5E-04
30	2.7E-04	2.3E-04	2.2E-04	2.7E-04
40	2.0E-04	1.8E-04	1.7E-04	2.0E-04
50	1.6E-04	1.5E-04	1.4E-04	1.6E-04

7.3.7 Evaluation of the Effect of the Seismic Activity on Emergency Response

The effects of seismic activity on emergency response are evaluated in this subsection for the unmitigated TISGTR scenario. Several impacts of the seismic activity are considered. One of these is the effect of collapsed bridges and impassible roadways on the evacuation itself, which is expected to increase risk. Another effect is on the size of the shadow evacuation, which is expected to decrease risk. The overall impact of the seismic activity on emergency response at the Surry site is insignificant, as shown in Table 7-15. Prompt fatality risk remains zero for this scenario.

Table 7-15 Mean, Individual, LNT, LCF Risk per Event (Dimensionless) for Residents within the Specified Radii of the Surry Site for the unmitigated TISGTR Scenario and Comparing the Unmodified Emergency Response (ER) and ER Adjusted to Account for the Effect of Seismic Activity on Evacuation Routes and Human Response

Radius of Circular Area (mi)	Unmodified ER	ER Adjusted for Seismic Effects
10	3.2×10^{-4}	3.3×10^{-4}
20	1.9×10^{-4}	1.9×10^{-4}
30	1.3×10^{-4}	1.3×10^{-4}
40	8.4×10^{-5}	8.4×10^{-5}
50	6.5×10^{-5}	6.5×10^{-5}

7.3.8 Evaluation of SST1 Source Term

One of the differences between the SOARCA study and the 1982 Siting Study is the character of the radiological releases in terms of magnitude and timing. Because of this difference, it is useful to characterize and compare the risk to the public that derives from these releases.

The approach used in this section is to substitute the SST1 source term for the SOARCA source term into the MACCS2 input files for the unmitigated STSBO with TISGTR scenario. These

sensitivity analyses show the impact of the improvements made in the source term methods and practices on the consequence results.

The characteristics of the SST1 source term are described in the 1982 Siting Study report as follows:

- Severe core damage
- Essentially involves loss of all installed safety features
- Severe direct breach of containment

An exact scenario and containment failure mechanism (e.g., hydrogen detonation, direct containment heating, or alpha-mode failure) are not specified in the report.

Notification time (i.e., sounding a siren to notify the public that a GE has been declared) for the unmitigated STSBO with TISGTR occurs at 2.75 hr, as shown in Figure 6-4. Declaration of a general emergency occurs at 2 hr and it takes an additional 45 min to notify the public. Notification of the public is thus after the beginning of release for the SST1 source term (cf., Table 7-1), which occurs 1.5 hr after accident initiation. Evacuation of the general public begins one hour after notification, or 3.75 hr after accident initiation. The start of evacuation here for this scenario is slightly earlier, but comparable to that for the largest segment of the population in the 1982 Siting Study, which occurred 4 hr after accident initiation.

While the 1982 Siting Study treated emergency response very simplistically, a major emphasis of the SOARCA project is to treat all aspects of the consequence analysis as realistically as possible. No attempt was made in this sensitivity analysis to reproduce the treatment of emergency response used in the 1982 Siting Study.

Table 7-16 shows the latent-cancer-fatality risks for a release corresponding to the SST1 source term occurring at Surry based on the unmitigated STSBO with TISGTR ER. Table 7-17 compares the LNT risks with those for the unmitigated ISLOCA and the unmitigated STSBO with TISGTR scenarios discussed in preceding subsections. The LNT risk within 10 miles is about a factor of 30 higher than for the largest Surry source term considered in this study, which is for the ISLOCA. The 10-mile risk using a 620 mrem/yr dose truncation criterion is a factor of 150 higher (cf., Table 7-10). At 50 miles the LNT risk is about a factor of 10 higher.

Table 7-16 Mean, Individual, LCF Risk per Event (Dimensionless) for Residents within the Specified Radii of the Surry Site for the SST1 Source Term from the 1982 Siting Study with All Parameters Other than for Source Terms Are Taken from the Unmitigated STSBO Scenario

Radius of Circular Area (mi)	LNT	US BGR	HPS
10	1.0E-02	9.8E-03	1.0E-02
20	5.1E-03	4.9E-03	5.1E-03
50	1.5E-03	1.3E-03	1.4E-03

Table 7-17 Mean, Individual, LNT, LCF Risk per Event (Dimensionless) for Residents within the Specified Radii of the Surry Site for the SST1 Source Term from the 1982 Siting Study Using Emergency Response Parameters from the STSBO Scenario. Results are Compared with the Unmitigated ISLOCA and the Unmitigated STSBO with TISGTR Scenarios

Radius of Circular Area (mi)	SST1 Using Unmitigated STSBO ER	Unmitigated ISLOCA	Unmitigated STSBO with TISGTR
10	1.0E-02	3.0E-04	3.2E-04
20	5.1E-03	3.4E-04	1.9E-04
30	3.3E-03	2.7E-04	1.3E-04
40	2.0E-03	2.0E-04	8.4E-05
50	1.5E-03	1.6E-04	6.5E-05

The maximum risk for the SST1 source term is within 10 miles, which is partially due to the fact that emergency response is not rapid enough to prevent exposures within the EPZ during the emergency phase. This is expected since release begins before notification of the public and, therefore, before evacuation begins.

A notable feature of the risks presented in Table 7-16 is that the choice of dose truncation criterion has a minor influence on risk. This is very different from the SOARCA accident scenarios discussed in preceding subsections. Figure 7-11 provides some insights into this behavior. Figure 7-11 shows the risk per event for the population living near the Surry site. For the SST1 source term, nearly all of the risk, especially at short distances from the plant, is from exposures that occur during the emergency phase. Because a significant fraction of these doses are received over a short period of time and the doses are large due to the large source term, the level used for the dose truncation criterion has little influence on predicted risks. Again, this is a very different trend than is observed for the current, state-of-the-art source terms.

Table 7-18 shows the risk of prompt fatalities for several circular areas of specified radii centered at the plant. Unlike the source terms presented above, the predicted prompt-fatality risks are significantly greater than zero. Furthermore, the maximum distance at which prompt fatalities occur is more than 10 miles for this calculation. The SST1 release fractions are more than large enough to induce prompt fatalities for members of the public who live close to the plant and who do not evacuate quickly.

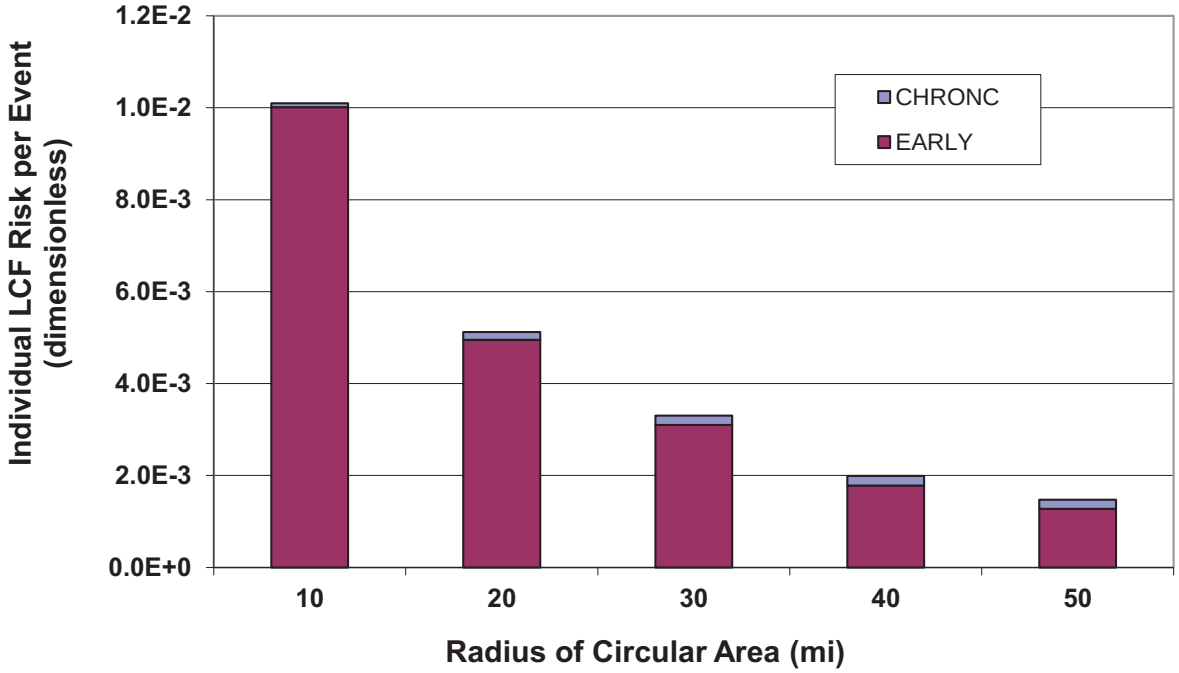

Figure 7-11 Mean, LNT, latent cancer fatality risks from the SST1 source term for residents within a circular area of specified radius from the Surry plant for the emergency and long-term phases.

Table 7-18 Mean, Individual, Prompt-Fatality Risk per Event (Dimensionless) for Residents within the Specified Radii of the Surry Site for the SST1 Source Term from the 1982 Siting Study Using Emergency Response Parameters from the Unmitigated STSBO Scenario

Radius of Circular Area (mi)	Prompt-Fatality Risk per Event Using STSBO ER (dimensionless)
1.3	1.3E-02
2.0	1.5E-02
2.5	1.1E-02
3.0	8.4E-03
3.5	5.4E-03
5.0	3.7E-04
7.0	5.0E-05
10.0	1.5E-05

The NRC QHO for prompt fatality risk is generally interpreted as the absolute risk within 1 mile of the exclusion area boundary. For Surry, the exclusion area boundary is 0.35 miles from the reactor building from which release occurs, so the outer boundary of this 1-mile zone is at 1.35 miles. The closest MACCS2 grid boundary to 1.35 miles used in this set of calculations is at 1.3 miles. Using the risk within 1.3 miles should reasonably approximate the risk within 1 mile of the exclusion area boundary. The frequency stated for the SST1 source term in the 1982 Siting

Study is 10^{-5} pry, so the absolute risk of a prompt fatality to an individual for this source term is approximately 1.3×10^{-7} pry, which is well below the QHO. The actual risk of a prompt fatality (cf., Table 7-13), using current best-estimate practices for calculating source terms, is about five orders of magnitude lower than using the SST1 source term would imply (cf., Table 7-13 and Table 7-18).

The acute-fatality risks presented in Table 7-18 are lower than the risks that would have been calculated in the 1982 Siting Study. There are two primary reasons for this difference. One is that 30% of the population within the EPZ is assumed to evacuate a full 6 hr after accident initiation in the 1982 Siting Study; here, 97.4% of the population within the EPZ begin to evacuate at least by 3.75 hr after accident initiation. A second reason is that the coefficients in the equations for acute health effects have been updated since the 1982 Siting Study based on more recent expert data [41]. The updated coefficients result in lower predicted acute fatalities across most of the exposure range for which these health effects can occur.

7.3.9 Surface Roughness

All of the SOARCA analyses presented above use a surface roughness length that represents a typical value for the US, which is 10 cm. This value was used in the 1982 Siting Study and in NUREG-1150 and has become a de facto default for most if not all license-related consequence analyses (e.g., severe accident mitigation alternatives (SAMA) analyses for license extension). However, this value of surface roughness is not necessarily the best choice for all regions of the country. In this section, we consider a site-specific value of surface roughness.

The effect of increased surface roughness is twofold: It increases vertical mixing of the plume and it increases deposition velocities for all aerosol sizes. Both effects are treated in this sensitivity analysis and are discussed in the subsequent paragraphs.

Surry is located on the James River and the area surrounding the plant may be characterized by a mosaic of surface water, forests, farmland, suburban areas, and urban areas. The James River covers a large fraction of the EPZ. Land-use types correspond to a typical surface roughness or a range of surface roughness, some of which are shown in Table 7-19 [85].

Table 7-19 Surface roughness for various land-use categories for the area surrounding the Surry site

Land-Use Category	Surface Roughness (cm)
Farmland recently plowed	1
Farmland with mature corn	10
Suburban housing	5 to 20
Suburban institutional buildings	70
Woodland forests	20 to 100
Urban Areas	100 to 600

Determining the best choice of surface roughness to represent the range of land-use categories is not a simple task. The value of 10 cm used in the base case is representative of the farmland and river that make up a significant fraction of the countryside surrounding the plant. Woodland

forests and urban areas also make up a large fraction of the area and have a mean surface roughness of about 100 cm. An intermediate choice representing the average between cornfields and woodland forest, about 50 to 60 cm, might also have been a reasonable choice for this area. But the proximity of the surface features must also be considered. Because the river dominates the landscape and the urban areas are across the river, which is 2 to 3 miles wide in some areas, the lower value of 10 cm was chosen for this site. Additional discussion regarding surface roughness, including a sensitivity analyses, are provided in NUREG/CR-7110, Volume 1.

The effect on vertical mixing has traditionally been modeled by means of a multiplicative factor on vertical dispersion. The empirical expression for this factor is the ratio of surface roughness at the site in question to a standard value of surface roughness to the 1/5th power. Most of the data upon which empirical dispersion models have been based were taken at a site characterized by prairie grass [86], which was estimated to have a surface roughness of 3 cm. Thus, the empirical equation used to scale vertical dispersion uses the actual surface roughness divided by 3 cm to the 1/5th power. The standard multiplicative factor corresponding to a 10-cm surface roughness is $(10 / 3)^{0.2} = 1.27$, which is the value used in all of the calculations presented above. A surface roughness length of 60 cm corresponds to a multiplicative factor of 1.82.

The effect of surface roughness on deposition velocity has been characterized by Bixler et al. [88] and is based on expert elicitation data [87]. Bixler et al. provides a set of correlations for estimating deposition velocity as a function of aerosol diameter, wind speed, surface roughness, and percentile representing degree of belief by the experts. Here, we use the 50th percentile from the experts to get a best estimate deposition velocity. The 50th percentile correlation is as follows:

$$\ln(v_d) = -3.112 + 0.992 \cdot ln(d_p) + 0.190 \cdot [ln(d_p)]^2 - 0.072 \cdot [ln(d_p)]^3 + 5.922 \cdot z_0 - 6.314 \cdot {z_0}^2 + 0.169 \cdot v$$

where

v_d = deposition velocity (cm/s)
d_p = aerosol diameter (μm)
z_0 = surface roughness (m)
v = mean wind speed (m/s)

Table 7-20 shows the aerosol deposition velocities calculated with the above equation that were used in this study for each aerosol bin in the MELCOR model. A mean wind speed of 2.2 m/s was used to obtain the results in the table. The column of deposition velocities corresponding to a surface roughness of 10 cm were used for all of the results shown in the preceding subsections. Increasing surface roughness from 10 to 60 cm roughly doubles the deposition velocity. The effect of surface roughness on deposition velocity was also investigated in the sensitivity study in NUREG/CR-7110, Vol. 1.

Table 7-20 Deposition Velocities Used for the Base Case Calculations and for the Surface Roughness Sensitivity Study for Each of the Ten Aerosol Bins in the MELCOR Model

Mass Median Aerosol Diameter (μm)	Deposition Velocity (cm/s) for Specified Surface Roughness	
	10 cm	60 cm
0.15	0.053	0.11
0.29	0.049	0.10
0.53	0.064	0.14
0.99	0.11	0.23
1.8	0.21	0.45
3.4	0.43	0.92
6.4	0.84	1.8
11.9	1.4	2.9
22.1	1.7	3.7
41.2	1.7	3.7

7.3.10 Importance of Chemical Classes

Each isotope present in the core of a nuclear reactor contributes to the overall risk of an accident; however, the release of some isotopes contributes to risk much more than others. There are three reasons some isotopes are more important than others:

- Abundance of an isotope in the inventory in the core at the beginning of an accident,
- Release fraction of an isotope into the atmosphere, and
- The dose conversion factors for an isotope, which depends on the type and energy of the radiation produced, the half life of the isotope, and for internal pathways, the biokinetics of the isotope.

There are 69 isotopes in the treatment of consequences considered in the MACCS2 analysis, as described in Appendix B. These isotopes are grouped into a set of 9 chemical classes in the MELCOR analyses that generated the source terms used in the SOARCA analyses. Since release fractions are calculated by MELCOR at the level of chemical classes, it is both reasonable and useful to examine how these same chemical classes influence the evaluation of risk.

One approach to estimate the relative importance of each chemical class on risk is to release one chemical class at a time and evaluate the fraction of the overall risk that results, where overall risk is evaluated by releasing all chemical classes simultaneously. The problem with this approach is that the contributions from the individual chemical classes add up to more than the overall risk. The difference results from the amount of remedial action that is taken to reduce doses to the public. For example, much less remedial action is taken when doses are small, which may be the case when only one chemical class is released at a time, than when doses are

large. Because less remedial action is taken, the contribution of an individual chemical group to risk is greater when it is released on its own than when it is part of a larger release. To make the fractional contributions from individual chemical classes add to unity, the contribution from a single chemical class must be normalized by the sum of the individual contributions of the chemical classes rather than the risk calculated for the combined effect of all chemical classes. This inherent nonlinearity tends to diminish the effect of the major contributors and exaggerate the effect of the minor contributors.

To minimize the effect of the nonlinearities described in the previous paragraph, an alternative approach is adopted here. That is to evaluate the contribution of a chemical class by performing calculations with all but that one chemical class. The effect of that chemical class is then calculated by taking the difference between the risk when all chemical classes are included and the risk for all but that one chemical class (i.e., setting the release fractions for that chemical class to zero).

The relative importance of each chemical class was evaluated for the unmitigated ISLOCA accident sequence, for each dose truncation level: LNT, US BGR, and HPS. The results for the population within 10 miles are shown in Figure 7-12, Figure 7-13, and Figure 7-14. Results at longer distances are shown in subsequent figures.

The first of these, Figure 7-12, is for LNT for the population within 10 miles. It shows the importance of each chemical group on total risk, on just the emergency-phase risk, and on just the long-term-phase risk. The cesium group dominates the total risk and the long-term phase risk, but contributes only a few percent to the emergency-phase risk owing to the relatively long half lives of the cesium isotopes (e.g., ^{137}Cs has a half life of 30 yrs). Tellurium and iodine contribute most of the emergency-phase risk owing to the short half-lives of the isotopes represented by these chemical classes. However, the emergency phase contributes very little to the total risk because 99.5% of the population within 10 miles evacuate and do not receive any dose during the emergency phase.

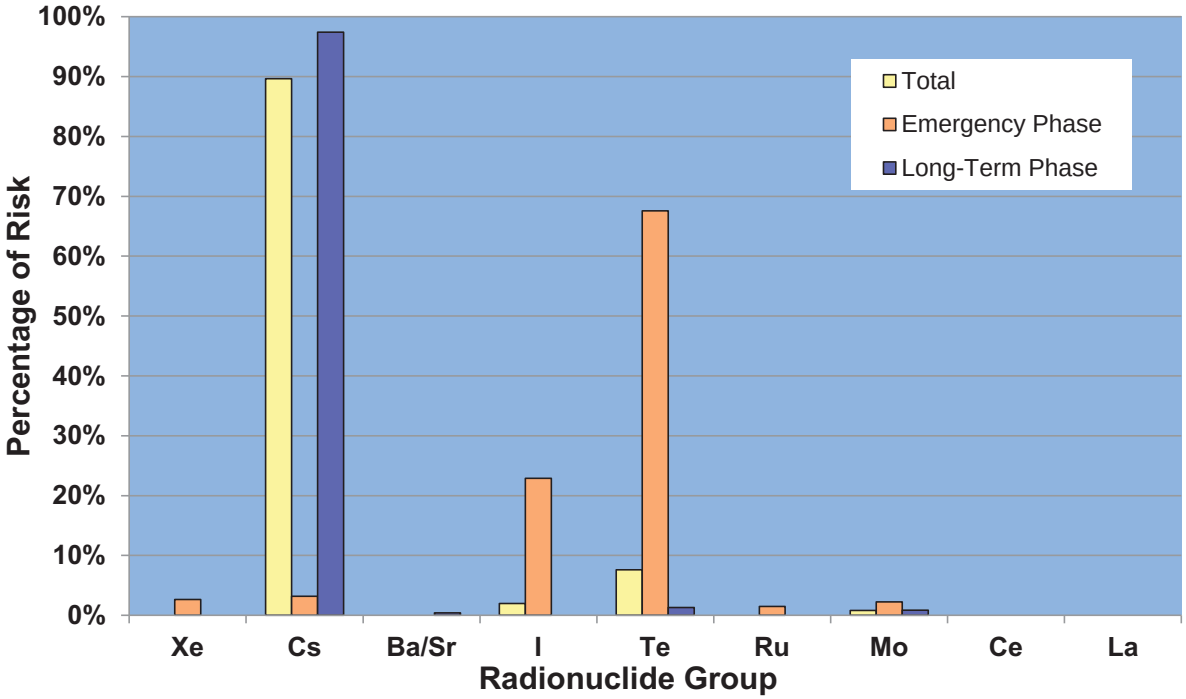

Figure 7-12 Percentage contribution to total, emergency-phase, and long-term-phase, mean, individual risk for the population within 10 miles by chemical class for the Surry unmitigated ISLOCA based on the LNT hypothesis

Figure 7-13 and Figure 7-14 show the total risk contributions of each chemical class for the unmitigated ISLOCA using US BGR dose truncation and truncation based on the HPS Position, respectively. These plots also show risk to the population living within 10 miles of the plant. They only show the total risk contribution because annual doses in the first year are combinations of emergency- and long-term-phase doses. Because of the overlapping contributions to the first year, the individual contributions of the two phases cannot be easily deconvolved from the whole. These figures show that the tellurium, cesium, and iodine chemical classes contribute most of the risk for these dose truncation criteria, with the same order of importance in the two figures. Isotopes with relatively short half-lives tend to be more dominant than those with longer half-lives because most of the risk is from doses received during the first year for the US BGR and truncation based on the HPS Position. Longer-term annual doses are limited by the habitability criterion to values below the dose truncation levels.

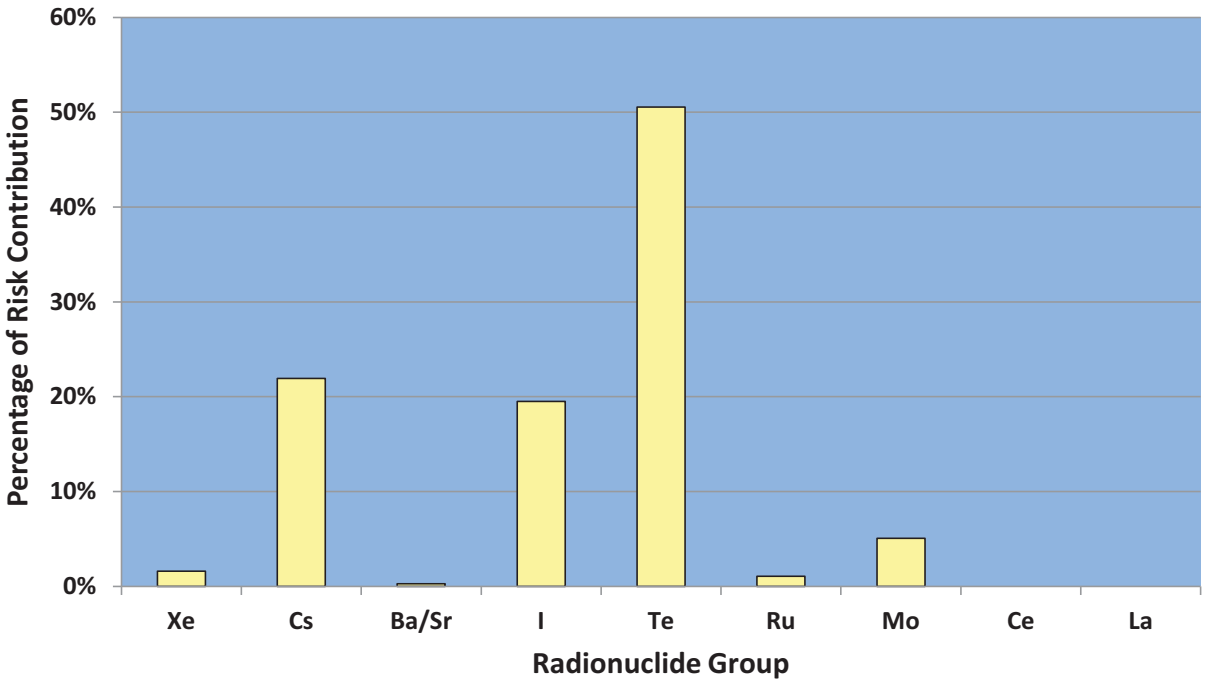

Figure 7-13 Percentage contribution to total, mean, individual risk for the population within 10 miles by chemical class for the Surry unmitigated ISLOCA based on US BGR dose truncation

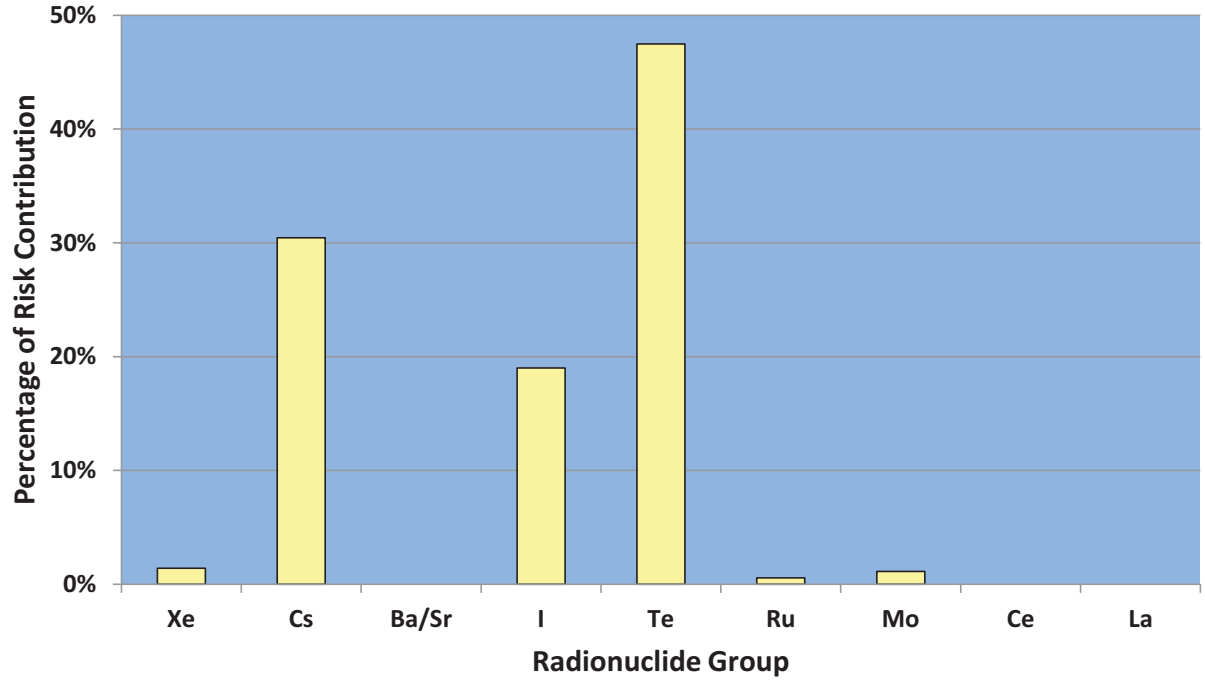

Figure 7-14 Percentage contribution to total, mean, individual risk for the population within 10 miles by chemical class for the Surry unmitigated ISLOCA based on a truncation level reflecting the HPS Position for quantifying health effects

Figure 7-15 through Figure 7-20 are analogous to those above but show the relative importance of the chemical classes for the population within 20 and 50 miles. The trends are similar, but the emergency phase plays a larger role because significant portions of the population do not evacuate before the plume arrives and, thereby, receive a dose during the emergency phase. The most important set of chemical classes using the LNT hypothesis is cesium, tellurium, and iodine in that order. For the two dose truncation criteria, cesium is less important because of the relatively long half-lives of the dominant isotopes.

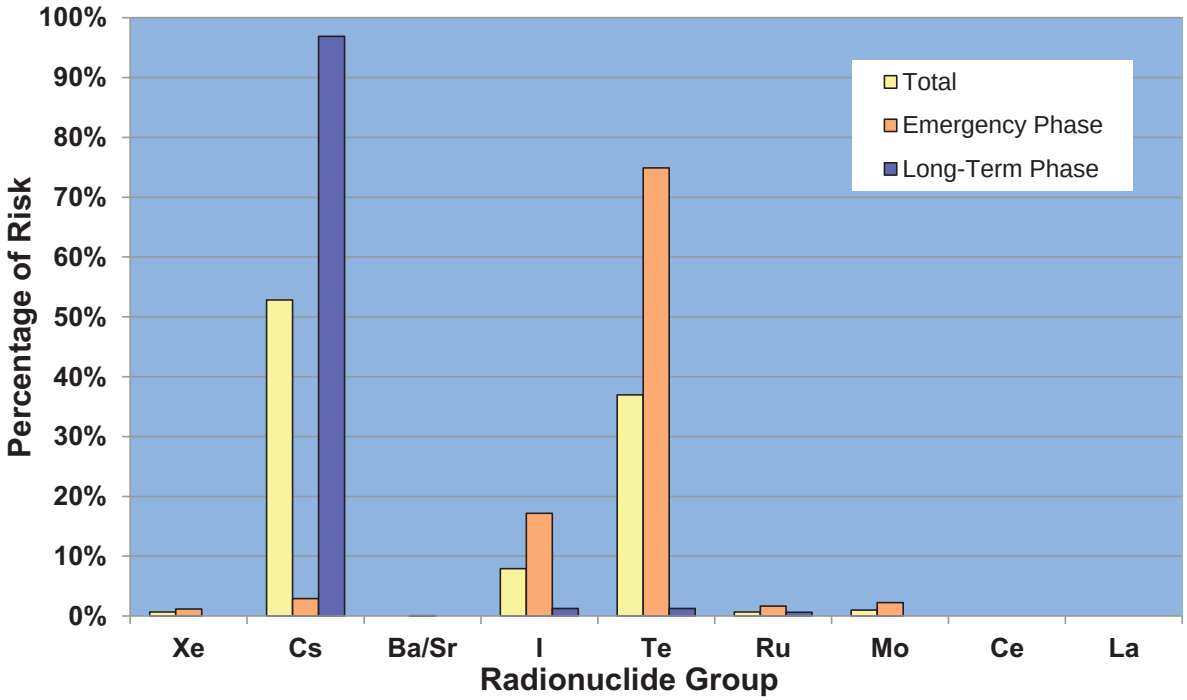

Figure 7-15 Percentage contribution to total, emergency-phase, and long-term-phase, mean, individual risk for the population within 20 miles by chemical class for the Surry unmitigated ISLOCA based on LNT hypothesis

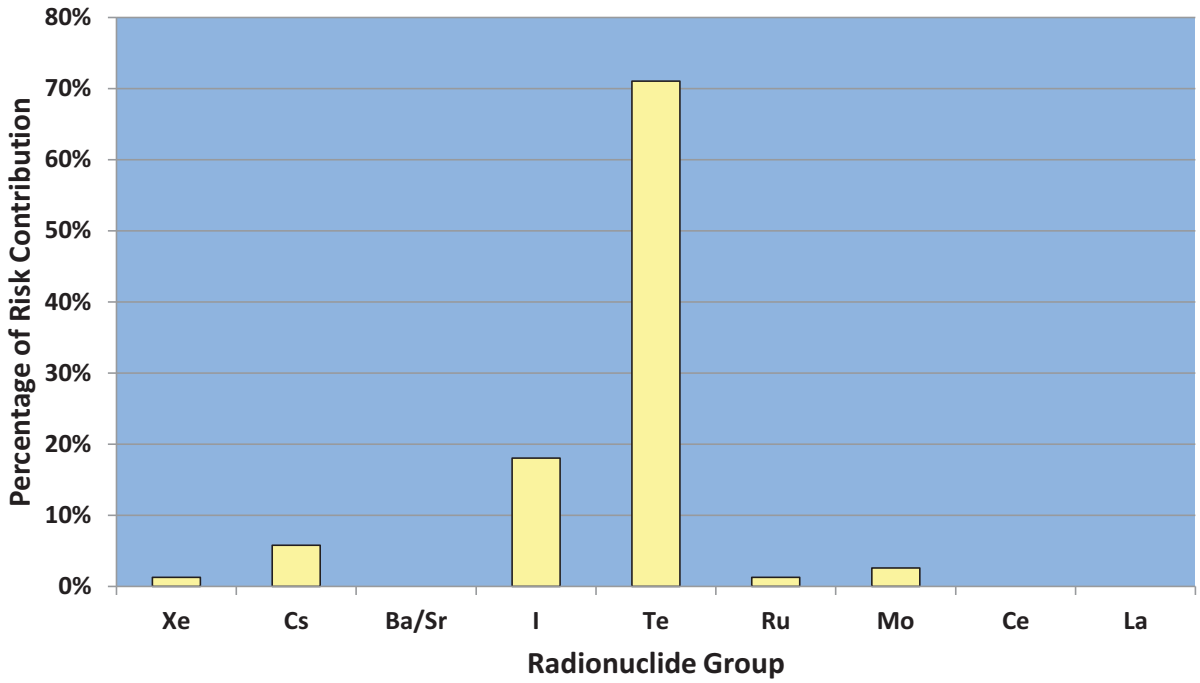

Figure 7-16 Percentage contribution to total, mean, individual risk for the population within 20 miles by chemical class for the Surry unmitigated ISLOCA based on US BGR dose truncation

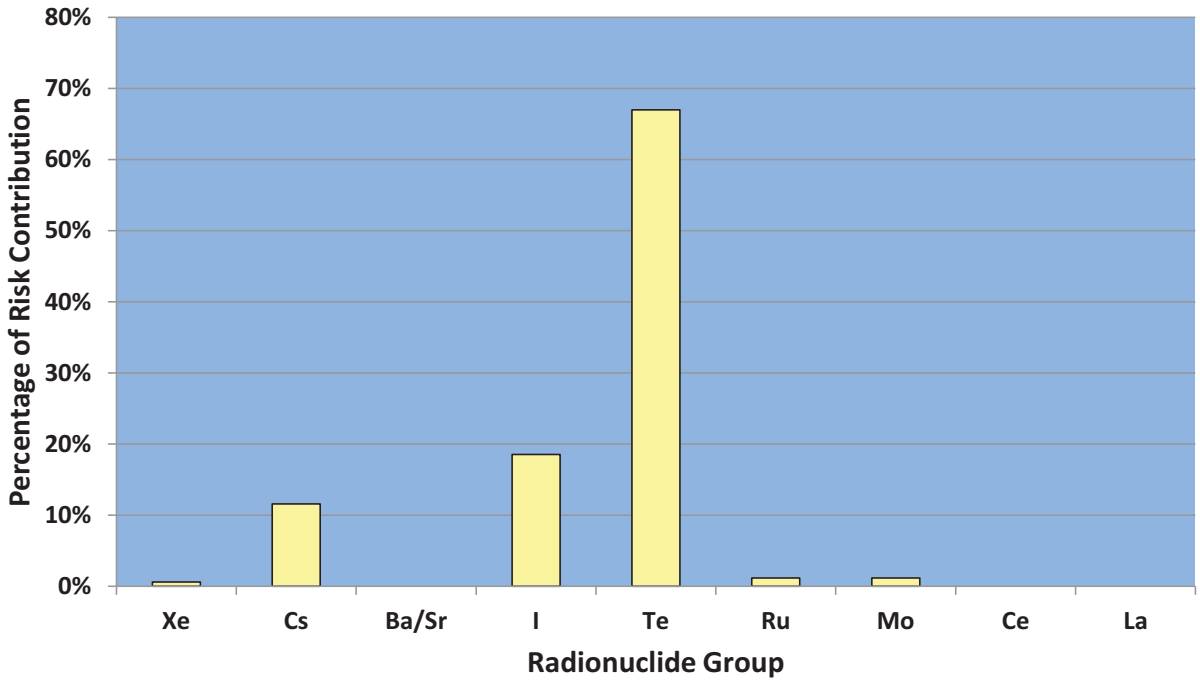

Figure 7-17 Percentage of contribution to total, mean, individual risk for the population within 20 miles by chemical class for the Surry unmitigated ISLOCA based on a truncation level reflecting the HPS Position for quantifying health effects

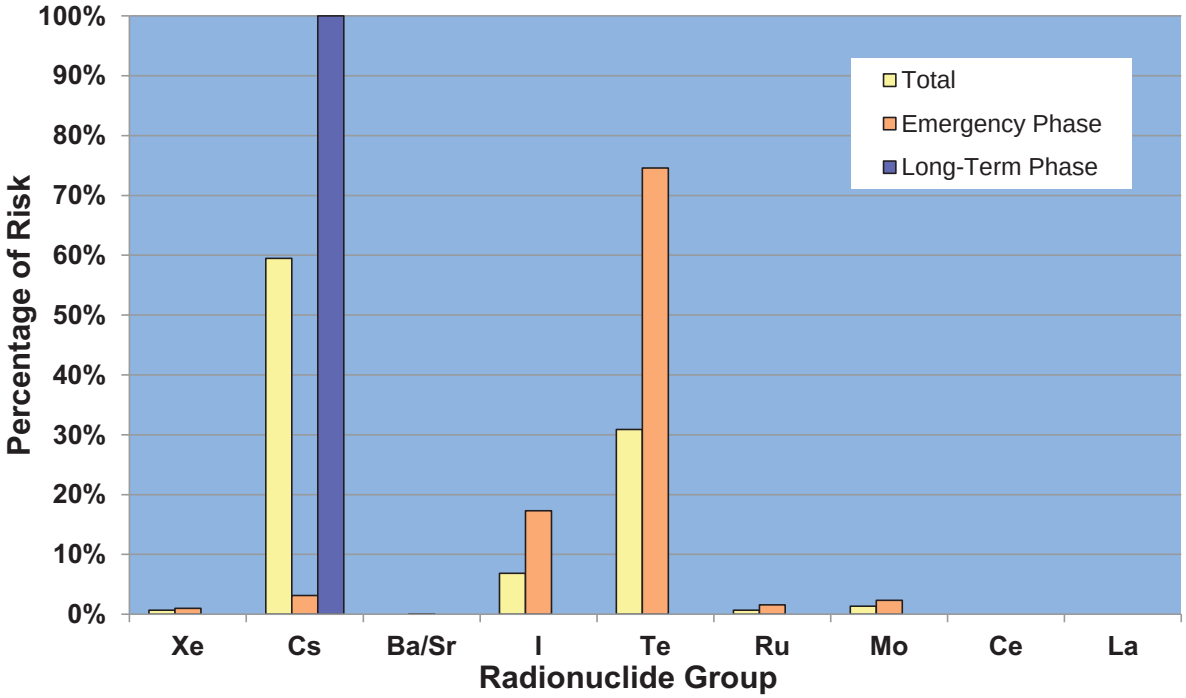

Figure 7-18 Percentage contribution to total, emergency-phase, and long-term-phase, mean, individual risk for the population within 50 miles by chemical class for the Surry unmitigated ISLOCA based on the LNT hypothesis

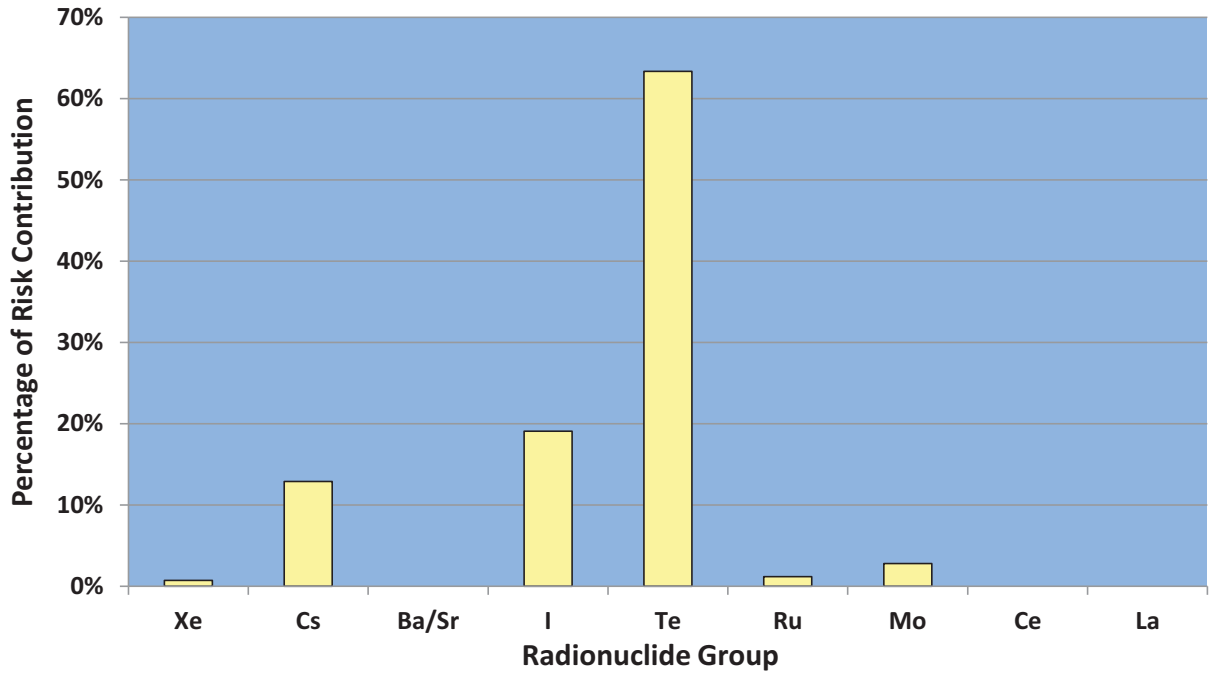

Figure 7-19 Percentage contribution to total, mean, individual risk for the population within 50 miles by chemical class for the Surry unmitigated ISLOCA based on US BGR dose truncation

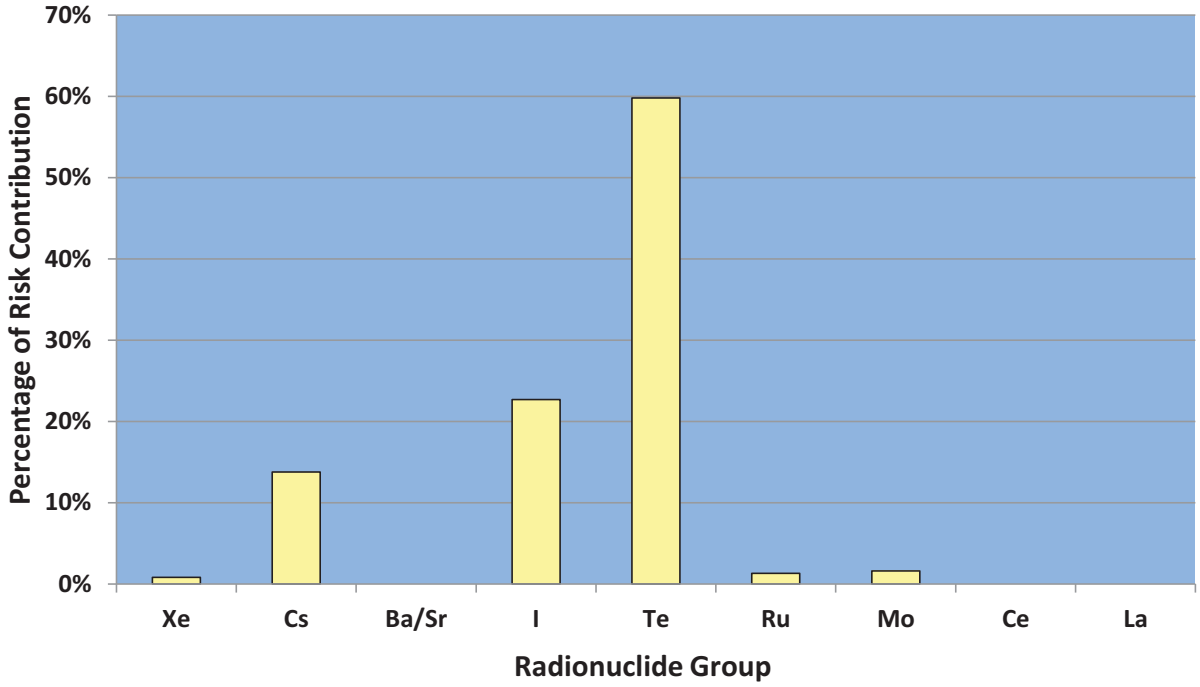

Figure 7-20 Percentage contribution to total, mean, individual risk for the population within 50 miles by chemical class for the Surry unmitigated ISLOCA based on a truncation level reflecting the HPS Position for quantifying health effects

8. REFERENCES

[1] NUREG/CR-2239, Technical Guidance for Siting Criteria Development. 1982, Sandia National Laboratories: Albuquerque, NM.

[2] NUREG-1150, V., Severe Accident Risks: An Assessment for Five U.S. Nuclear Power Plants. 1990, U.S. Nuclear Regulatory Commission: Washington, D.C.

[3] Safety Goals for the Operation of Nuclear Power Plants, in Federal Register, 51 FR 28044. 1986.

[4] RG-1.174, An approach for using probabilistic risk assessment in risk-informed decisions on plant-specific changes to the licensing basis. 2002, U.S. Nuclear Regulatory Commission: Washington, D.C.

[5] NUREG/CR-7008, "Best Practices for Simulation of Severe Accident Progression at Nuclear Power Plants," U.S. Nuclear Regulatory Commission, Washington, D.C., 2010 (To be published)

[6] Nuclear Regulatory Commission, 1990, "Severe Accident Risks: An Assessment for Five U.S. Nuclear Power Plants," NUREG 1150, U.S. Nuclear Regulatory Agency, Washington, DC.

[7] P.D. Bayless et al., "Severe Accident Natural Circulation Studies at the INEL," NUREG/CR 6285, INEL 94/0016, February 1995.

[8] C.F. Boyd, K. Hardesty, "CFD Analysis of 1/7th Scale Steam Generator Inlet Plenum Mixing During a PWR Severe Accident," NUREG 1781, October 2003.

[9] C.F. Boyd, D.M. Helton, K. Hardesty, "CFD Analysis of Full Scale Steam Generator Inlet Plenum Mixing During a PWR Severe Accident," NUREG 1788, U.S. Nuclear Regulatory Commission, May 2004.

[10] C.A. Dobbe, Letter to Dr. J.E. Kelly (Sandia National Laboratories), "Transmittal of Floppy Disk Containing the MELCOR Input Decks of the Surry PWR - CAD-2-88," Idaho National Engineering Laboratory, May 17, 1988.

[11] P. B. Bayless, "Analysis of Natural Circulation During A Surry Station Blackout Using SCDAP/RELAP5," NUREG/CR-5214, EGG-2547, Idaho National Engineering Laboratory, Idaho Falls, Idaho, September 1988.

[12] “State-of-the-Art Reactor Consequence Analysis Project, MELCOR Best Modeling Practices,” NUREG/CR-7008, U.S. Nuclear Regulatory Commission, Washington, DC (to be published 2010)

[13] Gauntt, R. O., Cash, J.E., Cole, R. K.,. Erickson, C. M, Humphries, L.L., Rodriguez, S. B., Young, M. F., 2005, "MELCOR Computer Code Manuals, Vol. 1: Primer and User's Guide, Version 1.8.6," NUREG/CR 6119, Vol. 1, Rev. 3, U.S. Nuclear Regulatory Commission, Washington, DC.

[14] Laur, M.N., 2006, "Meeting with Sandia National Laboratories and an Expert Panel on MELCOR/MACCS Codes in Support of the State of the Art Reactor Consequence Analysis Project," Memo to J.T. Yerokun, Agency Document Access and Management System Accession Number ML062500078, U.S. Nuclear Regulatory Agency, Washington, DC, September.

[15] Surry Updated Final Safey Analysis Report, Revision 38, 05/31/07.

[16] Surry response to SOARCA information request, August 9, 2007, Email from Gary Miller, Dominion to Robert Prato, NRC.

[17] Stewart, W.A., Pieczynski, A.T., and Srinivar, V., "Natural Circulation Experiments for PWR Degraded Core Accidents," EPRI Report NP 6324 D, 1989.

[18] Stewart, W.A., Pieczynski, A.T., and Srinivar, V., "Natural Circulation Experiments for PWR High Pressure Accidents," EPRI Report TR 102815, 1993.

[19] Fletcher, C. D., and Beaton, R. M., "SCDAP/RELAP5 Base Case Calculation for the Station Blackout Uncertainty Study," Letter report to D. M. Helton, US NRC, August 2006.

[20] Fletcher, C. D., and Beaton, R. M., "Evaluation of Uncertainties in SCDAP/RELAP5 Station Blackout Simulations," Letter report to D. M. Helton, US NRC, August 2006.

[21] Wagner, K. C., Wagner, KC, "MELCOR 1.8.5 Analysis of Natural Circulation Flow in the Westinghouse High-Pressure SF6 Experiments," Draft SAND Report, Sandia National Laboratories, June 2001.

[22] Dominion, “Operator Response Times for a Total Loss of RCP Seal Cooling,” ET-CME-05-0020, Revision 2, December 5, 2006.

[23] Virginia Electric Power Company, “Individual Plant Examination Submittal for Surry.”

[24] Gieseke J. A., et al., “Radionuclide Release under Specific LWR Accident Conditions,” Battelle Memorial Institute Report, BMI-2104, February 1985.

[25] Pilch, M. M., H. Yan, and T.G. Theofanous, “The Probability of Containment Failure by Direct Containment Heating in Zion,” NUREG/CR-6075, SAND93-1535, December 1994.

[26] Nuclear Regulatory Commission (U.S.) (NRC). NUREG-0654/FEMA-REP-1, Rev. 1, "Criteria for Preparation and Evaluation of Radiological Emergency Response Plans and Preparedness in Support of Nuclear Power Plants." Washington D.C.: NRC. 1980.

[27] Innovative Emergency Management (IEM). "Evacuation Time Estimates for the Surry Power Station and Surrounding Jurisdictions." Baton Rouge, LA. November 28, 2001.

[28] Nuclear Regulatory Commission (U.S.) (NRC). NUREG/CR-6863, SAND2004-5900. "Development of Evacuation Time Estimate Studies for Nuclear Power Plants." Washington D.C.: NRC. January 2005.

[29] Oak Ridge Evacuation Modeling System, Oak Ridge National Laboratory, 2008. Available from http://www.emc.ornl.gov/CSEPPweb/data/html/software.html.

[30] Rogers, G.O., A.P. Watson, J.H. Sorensen, R.D. Sharp, and S.A. Carnes, "Evaluating Protective Actions for Chemical Agent Emergencies." Oak Ridge National Laboratory (U.S.) (ORNL). ORNL-6615. Oak Ridge, Tennessee: ORNL. April 1990.

[31] Camp, A. L., et al., "Light Water Reactor Hydrogen Manual," NUREG/CR-2726, SAND82-1137, August 1983.

[32] Boyak, K. W., Tieszen, S. R., and Stamps, D. W., "Loads from the Detonation of Hydrogen-Air-Steam Mixtures, SAND92-0541, July 1992.

[33] "Action Item on Secondary Side Retention of Fission Products in a Steam Generator Tube Rupture Accident," Email Memo from D. Powers, Sandia National Laboratories to US NRC, May 2008.

[34] SGTR Severe Accident Working Group, "Risk Assessment of Severe Accident-Induced Steam Generator Tube Rupture;' NUREG-1570, U.S. Nuclear Regulatory Commission, Washington DC, 1998.

[35] Liao, Y. and Guentay, S., "Potential steam generator tube rupture in the presence of severe accident thermal challenge and tube flaws due to foreign object wear," Nuclear Engineering and Design 239, pp. 1128–1135, 2009.

[36] Fletcher, C. D., et al, "SCDAP/RELAP5 Thermal-Hydraulic Evaluations of the Potential for Containment Bypass During Extended Station Blackout Severe Accident Sequences in a Westinghouse Four-Loop PWR," NUREG/CR to be published.

[37] Boyd, C. F., and Armstrong, K., "Computational Fluid Dynamics Analysis of Natural Circulation Flows in a Pressurized Water Reactor Loop under Severe Accident Conditions," NUREG to be published.

[38] Powers, D. A., "Aerosol Penetration of Leak Pathways – An Examination of the Available Data and Models," SAND2009-1701, Sandia National Laboratories, April 2009.

[39] Soffer, L., et al., "Accident Source Terms for Light-Water Nuclear Power Plants," NUREG-1465, U.S. Nuclear Regulatory Commission, 1995.

[40] Birchley, J. Haste, T., Bruchertseifer, H., Cripps, R., Güntay, S., and Jäckel, B., "PHÉBUS-FP: Results and significance for plant safety in Switzerland", Nuclear Engineering and Design, 235 (2005) 1607-1633.

[41] Jacquemain, D., S. Bourdon, A. de Braemaeker, M. Barrachin (2000) PHEBUS FPT1 Final Report, IPSN/CRS/SEA/PEPF Report SEA1/00, IP/00/479, Institut de protection et de surete nucleare (IPSN), Cadarache, France.

[42] USNRC, "Alternate Radiological Source Terms for Evaluating Design Basis Accidents at Nuclear Power Reactors," Draft Regulatory Guide DG 1081, December 1999.

[43] Hessheimer, M. F., and Dameron, R. A., "Containment Integrity Research at Sandia National Laboratories," NUREG/CR–6906, 2006.

[44] Dameron, R. A., Rashid, Y. R., and Sullaway, M. F., "Pretest Prediction Analysis and Posttest Correlation of the Sizewell-B 1;10 Scale Prestressed Concrete Containment Model Test," NUREG/CR–5671, 1998.

[45] Dameron, R. A., Rashid, Y. R., and Tang, H. T., "Leak Area and Leakage Rate Prediction for Probabilistic Risk Assessment of Concrete Containments under Severe Core Conditions," Nuclear Engineering and Design, 1995.

[46] Horschell, D. S., "Experimental Results From Pressure Testing a 1:6 – Scale Nuclear Power Plant Containment," NUREG/CR–5121, 1992.

[47] USNRC NUREG/CR-4334, "An Approach to the Quantification of Seismic Margins in Nuclear Power Plants," Lawrence Livermore National Laboratory, August 1985.

[48] Chanin, D. I., and M. L. Young, "Code Manual for MACCS2: Volume 1, User's Guide," NUREG/CR-6613, 1998.

[49] Aldrich, D. C., et al., "Technical Guidance for Siting Criteria Development," NUREG/CR-2239, 1982.

[50] Wolshon, Brian. Ben McArdle. "Temporospatial Analysis of Hurricane Katrina Regional Evacuation Traffic Patters." American Society of Civil Engineers (ASCE) . ASCE Journal of Infrastructure Systems – Special Issue on "Infrastructure Planning, Design, and Management for Big Events." 2008.

[51] Nuclear Regulatory Commission (U.S.) (NRC). NUREG/CR - 6864, SAND2004-5901. "Identification and Analysis of Factors Affecting Emergency Evacuations." Washington D.C.: NRC. January 2005.

[52] Nuclear Regulatory Commission (U.S.) (NRC). NUREG/CR-6953, Vol. I. SAND2007-5448P. "Review of NUREG-0654, Supplement 3, " Criteria for Protective Action Recommendations for Severe Accidents." Washington D.C.: NRC. December 2007.

[53] Transportation Research Board (2000). "Highway Capacity Manual," National Research Council, Washington D.C.

[54] "Surry Power Station Updated Final Safety Analysis Report," Revision 36, September 30,2004

[55] Nuclear Regulatory Commission (U.S.) (NRC). NUREG/CR-6953, Vol. 2. SAND2008-4195P. "Review of NUREG-0654, Supplement 3, " Criteria for Protective Action Recommendations for Severe Accidents: Focus Groups and Telephone Survey" Washington D.C.: NRC. December 2007.

[56] Dennis Atkinson and Russell F. Lee, "Procedures for Substituting Values for Missing NWS Meteorological Data for Use in Regulatory Air Quality Models," July 7, 1992, http://www.rflee.com/RFL_Pages/missdata.pdf

[57] NUREG-0917, NUREG-0917: Nuclear Regulatory Commission Staff Computer Programs for Use With Meteorological Data. 1982, U.S. Nuclear Regulatory Commission: Washington, D.C.

[58] RG-1.23, Regulatory Guide 1.23, Rev. 1: Meteorological Monitoring Programs for Nuclear Power Plants. 2007, U.S. Nuclear Regulatory Commission: Washington, DC.

[59] McFadden, K.L., N.E. Bixler, and R.O. Gauntt, MELMACCS System Documentation (MELCOR to MACCS2 interface definition). 2005, Sandia National Laboratories: Albuquerque, NM.

[60] Bixler, N.E., E. Clause, C. W. Morrow, and J. A. Mitchell, Evaluation of Distributions Representing Important Non-Site Specific Parameters in Off-Site Consequence Analyses, to be published as a NUREG Report, Sandia National Laboratories: Albuquerque, NM, 2010.

[61] Bixler, N.E., et al., NUREG/ER-6525, Rev. 1, SAND2003-1648P: SECPOP2000: Sector Population, Land Fraction, and Economic Estimation Program. 2003, Sandia National Laboratories: Albuquerque, NM.

[62] EPA (2002) Federal Guidance Report No. 13 CD Supplement, E.-C.-.-., Rev. 1. 2002, Prepared by Oak Ridge National Laboratory, Oak Ridge, TN for Office of Air and Radiation, U. S. Environmental Protection Agency: Washington, DC.

[63] EPA (1994). Estimating Radiogenic Cancer Risk. EPA 402-R-93-076 (U.S. Environmental Protection Agency, Washington, D.C.)

[64] Eckerman, K. F., Risk Coefficients for SOARCA Project, memo, Oak Ridge National Laboratory, May 2008.

[65] NAS, Health Effects of Exposure to Low Levels of Ionizing Radiaiton: BEIR V. 1990, National Academy of Sciences, National Research Council, National Academy Press: Washington, DC.

[66] Aurengo, A., et al., French National Academy of Medicine report: Dose-effect relationships and estimation of the carcinogenic effects of low doses of ionizing radiation. 2005, French Academy of Sciences, French National Academy of Medicine.

[67] ICRP, The 2007 Recommendations of the International Commission on Radiological Protection. Annals of the ICRP, 2007. 37(Nos. 2-4).

[68] ICRP, Scope of Radiological Protection Control Measures. Annals of the ICRP, 2007. 37(Nos. 5).

[69] HPS, PS010-1: Position Statement of the Health Physics Society -- Radiation Risk in Perspective. 2004, Health Physics Society: McLean, VA.

[70] Scott G. Ashbaugh, Mark T. Leonard, Pamela Longmire, Randall O. Gauntt, Andrew Goldmann, and Dana A. Powers, "Accident Source Terms for Pressurized Water Reactors with High Burnup Cores Calculated Using MELCOR 1.8.5," SAND 2008-6664, 2008.

[71] "Surry Unit 2, Cycle 16 Startup Physics Tests Report," NE-1206, Revision 0, Virginia Electric and Power Company, 1999.

[72] "Surry Unit 2, Cycle 17 Startup Physics Tests Report," NE-1261, Revision 0, Virginia Electric and Power Company, December 2000.

[73] "Surry Unit 2, Cycle 18 Startup Physics Tests Report," NE-1326, Revision 0, Virginia Electric and Power Company, July 2002.

[74] SCALE: A Modular Code System for Performing Standardized Computer Analyses for Licensing Evaluations, ORNL/TM-2005/39, Version 5.1, Vols. I-III, November 2006.

[75] ASME/ANS, "Addenda to ASME/ANS RA-S-2008 Standard for Level 1 / Large Early Release Frequency Probabilistic Risk Assessment for Nuclear Power Plant Applications," ASME/ANS RA-Sa-2009, The American Society of Mechancial Engineers, 2009.

[76] Miller, C. L., et al., "Recommendations for Enhancing Reactor Safety in the 21st Century – The Near-Term Task Force Review of Insights From the Fukushima Dai-Ichi Accident," U.S. Nuclear Regulatory Commission, Washington D.C., July 2011.

[77] B. Shleien, "The Health Physics and Radiological Health Handbook, Revised Edition", Scinta, Inc. 2421 Homestead Drive, Silver Spring Md. 20902, 1992.

[78] MELCOR Aerosol Transport Module Modification for NSSR-1, INEL-96/0081, March 1996

[79] VICTORIA 2.0: A Mechanistic Model for Radionuclide Behavior in a Nuclear Reactor Coolant System Under Severe Accident Conditions, NUREG/CR-6131, December 1998

[80] "The LWR Aerosol Containment Experiments (LACE) Project, Summary Report, EPRI NP-6094-D, November 1988

[81] N.B. Wood, "A Simple Method for the Calculation of Turbulent Deposition to Smooth and Rough Surfaces", J. Aerosol Sci. Vol. 12. No 3 (1981), 275-290.

[82] B.Y. H. Liu and J.K. Agarwal, "Experimental Observation of Aerosol Deposition in Turbulent Flow", J. Aerosol Science, *5* (1974) 145-155.

[83] S.K. Friedlander and H.F. Johnstone, "Deposition of Suspended Particles from Turbulent Gas Streams", Ind. Eng. Chem., *49* (1957) 1151-1156.

[84] G.A. Sehmel, "Particle Deposition from Turbulent Air Flow", J. Geophysical Research, *75* (1970) 1766-1781.

[85] Whelan, G., D.L. Strenge, J.G. Droppo Jr., B.L. Steelman, and J.W. Buck, "The Remedial Action Priority System (RAPS): Mathematical Formulations," DOE/RL-87-09, Pacific Northwest Laboratory: Richland, WA. August 1987.

[86] Haugen, D. A. (Ed.), "Project Prairie Grass: A Field Program in Diffusion." No. 59, Vol. III, Report AFCRC-TR-58-235, Air Force Cambridge Research Center. 1959.

[87] Harper, F. T., et al., "Probabilistic Accident Consequence Uncertainty Analysis, Dispersion and Deposition Uncertainty Analysis," NUREG/CR-6244, U.S. Nuclear Regulatory Commission: Washington DC. 1994.

[88] Bixler, N. E., E. Clauss, C.W. Morrow, and J.A. Mitchell, "Evaluation of Distributions Representing Important Non-Site-Specific Parameters in Offsite Consequence Analysis," to be published as a NUREG Report, U.S. Nuclear Regulatory Commission: Washington, DC. 2011.

[89] Nuclear Regulatory Commission (U.S.) (NRC). NUREG/CR-7002, "Criteria for Development of Evacuation Time Estimate Studies." Washington D.C. NRC. (NRC, 2011).

[90] Wheeler, T., G. Wyss, and F. Harper, "Cassini Spacecraft Uncertainty Analysis Data and Methodology Review and Update Volume 1: Updated Parameter Uncertainty Models for the Consequence Analysis," SAND2000-2719/1, Sandia National Laboratories: Albuquerque, NM. November, 2000.

APPENDIX A
SURRY CONTAINMENT PERFORMANCE

This Page Intentionally Left Blank

1.0 INTRODUCTION

Containment performance at beyond design basis accident internal pressure and temperature is required as an input for determining the offsite consequences and accident progression of a nuclear power plant during a severe accident. This appendix documents the analysis and assessment of Surry Nuclear Power Plant (SNPP) containment at beyond design basis internal pressures and temperatures developed during a severe accident. The design-specific SNPP containment failure pressure, leakage area, and leakage location as documented is used as an input for the State of-the-Art Reactor Consequences Analysis (SOARCA) of the SNPP.

2.0 APPROACH

Extensive research and scale model testing of reinforced and prestressed concrete containments to determine behavior at beyond design basis accident pressure has been performed in the last 25 years at SNL [2] and CEGB [3]. Concrete containments start to leak before a complete rupture or failure. It is extremely difficult to accurately predict the location and leakage rate of the concrete containment due to beyond design basis internal pressure and temperature. Hessheimer and Dameron [2], and Dameron, Rashid, and Tang [4] provide guidance for predicting leak area and leak rate in containments. Hessheimer and Dameron [2] recommend a non-linear finite element analysis of the concrete containment to predict containment performance and leakage. In the past, reactor severe accident progression analysis has often assumed that the concrete containment starts to leak through a small hole as soon as containment is pressurized. The area of the small hole is calculated based on nominal design leakage rate of 0.10 to 0.20 percent of containment free volume mass per day at the design internal pressure. The area of the hole is assumed to remain constant until containment failure in the accident progression analysis. Results of concrete containment model tests [5, 6] indicate that leakage area increases appreciably with internal pressure. In addition, if the rate of pressurization is gradual and does not exceed the leakage rate, catastrophic failure of the concrete containment is not possible.

2.1 Concrete Containment Performance under Internal Pressure

A 1:6 scale model of a representative PWR concrete containment was tested at the Sandia National Laboratories (SNL) in July 1987 [5]. Prior to performing the test, 10 international organizations performed an independent and separate (round robin) pretest analyses of the containment [7] to predict containment behavior. A summary of the round robin analyses and test results is presented in Table A-1 .

Hessheimer and Dameron [2] have concluded that global, free field strain of 1.5 to 2.0% for reinforced and 0.5 to 1.0% for prestressed concrete can be achieved before failure or rupture. In addition, leakage in concrete containment increases appreciably after the rebars and liner plate yield. Furthermore, under gradual increase in internal pressure, containment leakage continues to grow without failure and rupture. Using these criteria, failure and yield pressure for the 1:6 scale model concrete containment were calculated using the following equations.

The results of these simple calculations, as shown in Table A-1 , are quite consistent with detailed finite element analyses using state of the art computer codes and test data.

$$P_{fail} = (A_{hoop} * Y_{rebar@2\%} + A_{liner} * Y_{liner@2\%}) / R$$

$$P_{yield} = (A_{hoop} * Y_{rebar} + A_{liner} * Y_{liner}) / R$$

where:

P_{fail} = Containment failure pressure
P_{yield} = Containment pressure at which hoop rebars and liner plate yield
A_{hoop} = Area of the hoop rebars
A_{liner} = Area of the liner plate
Y_{rebar} = Yield stress of the rebar
Y_{liner} = Yield stress of the liner plate
$Y_{rebar@2\%}$ = Stress in the rebar at 2% strain
$Y_{liner@2\%}$ = Stress in the rebar at 2% strain
R = Radius of the containment

Table A-1 Internal Pressure in 1:6-Scale Reinforced Concrete Containment

Source	Hoop Rebar and Liner Plate Yield MPa (psig)	Containment Failure MPa (psig)
Round Robin Analyses (Maximum)	0.951 (138)	1.276 (185)
Round Robin Analyses (Minimum)	0.827 (120)	0.883 (128)
Round Robin Analyses (Average)	0.869 (126)	1.076 (156)
Test Data	0.820 (119)	1.00 (145)
Proposed Simplified Analysis	0.876 (127)	0.986 (143)

The simplified analysis approach was then used to determine the behavior of three existing reinforced concrete PWR containments. The comparison of results using the simplified approach with information provided by the three plant licensees in their Individual Plant Examination (IPE) reports is presented in Table A-2. A review of this table indicates that failure pressure predicted in the IPE reports for all three containments is 10 to 25 percent higher than the one obtained by simplified approach. Similarly, the pressure at which rebars in the three containments yield, as reported in the IPE reports, varies from the simplified analysis by 4 to 40 percent. These differences in the predictions are similar to the ones reported by the round robin analysts for the 1:6 scale containment, and are essentially due to the use of different criteria for postulated failure. For instance, the licensees have used strains greater than 2 percent to determine failure pressure reported in the IPEs.

Table A-2 Internal Pressure at Yield and Failure in Reinforced Concrete PWR Containments

Item	Containment #1	Containment #2	Containment #3
Internal Pressure at Rebar Yield from IPE Report MPa (psig)	0.758 (110)	1.000 (145)	1.248 (181)
Internal Pressure at Failure from IPE Report MPa (psig)	1.062 (154)	1.048 (152)	1.489 (216)*
Internal Pressure at Rebar Yield from Simplified Analysis MPa (psig)	0.779 (113)	0.848 (123)	1.062 (154)
Internal Pressure at from the Proposed Simplified Analysis MPa (psig)	0.855 (124)	0.958 (139)	1.200 (174)

* IPE confirmatory analysis determined the failure pressure as 158 psi at 1% strain.

To further confirm the validity of the simplified analysis approach, it was applied to the ¼ scale model of a PWR prestressed concrete containment that was tested at Sandia National Laboratories in 2000 [6]. Prior to performing the test, a round robin pretest analysis of the containment [8] was performed by 17 international organizations to predict containment behavior. A summary of the round robin analysis, test results, and results of simplified analysis based on free field strain of 1.0% for failure is presented in Table A-3. The simplified approach for prestressed containment is similar to the one described above for reinforced concrete except that effect of prestressing steel is included in the calculations.

Table A-3 Internal Pressure at Yield and Failure in the 1:4-Scale Prestressed Concrete Containment

Source	**Hoop Reinforcement Yield MPa(psig)**	**Containment Failure MPa (psig) (Leakage >100%)**
Round Robin Analyses (Maximum)	1.248 (181)	1.979 (287)
Round Robin Analyses (Minimum)	0.855 (124)	0.814 (118)
Round Robin Analyses (Average)	1.034 (150)	1.413 (205)
Test Data	1.055 (153)	1.296 (188)
Proposed Simplified Analysis	1.062 (154)	1.331(193)

A review of the Table A-3 indicates that there is a wide variation in predicted pressures by 17 organizations. The maximum predicted failure pressure is 2.4 times more than the minimum predicted failure pressure. However, the average round robin and the proposed simplified analysis predicted pressures are quite close to the pressures recorded during the test.

The simplified approach described above was also applied to the 1:10 Scale Sizewell B model. The results of proposed simplified analysis are compared with the 3-D finite element analysis and pressure test data in Table A-4. The proposed simplified approach results closely match with detailed 3-dimensional non-linear finite element analysis and test data.

Table A-4 Internal Pressure at Yield and Failure in the 1:10-Scale Prestressed Concrete Containment

Item	Test Result [2]	Proposed Simplified Approach	3-D Analysis [2]
Internal Pressure at Rebar Yield MPa (psig)	0.586 (85)	0.683 (99)	0.662 (96)
Internal Pressure at Failure MPa (psig) (Leakage > 100%)	0.772 (112)	0.738 (107)	0.738 (107)

Based on the above discussion, simplified analysis approach provides good agreement with the more detailed finite analysis and test data for the concrete containment performance under internal pressure, and was to determine Surry containment behavior.

2.2 Containment Leakage

The containment performance criteria used for severe accident analysis require prediction of leakage rate as a function of internal pressure and temperature. There is lack of experimental data for containment leakage beyond design pressure. Rizkalla et al. [9], Dameron et al. [4], and others have attempted to quantify leakage through concrete sections. This guidance cannot be used directly to determine leakage thru concrete containments in which steel liner plate is designed to act as a leakage barrier. Detailed 3-dimensional nonlinear analysis of the containments with equipment hatch and other penetrations can determine the local strains in the liner plate and concrete. The results of the 3-dimensional nonlinear analysis can be used to determine airflow through the liner plate and containment concrete. All these complicated analyses will lead to leak rate predictions with large uncertainties due to variation in the properties of the materials, quality and porosity of welds, and concrete placement.

The relationship between containment leakage and internal pressures for reinforced concrete and prestressed concrete containment model tests from References 4 and 5 is shown in Figure A-1 and Figure A-2, respectively. A review of these figures indicates that the concrete containments start to leak appreciably once the liner plate yields. The rate of leakage when the liner plate yields is about 10 times more than normal leakage of 0.10 percent of containment air mass per day at the containment design pressure. The leakage rate increases appreciably with further increase in test pressure. Once the rebars yield, the leakage rate is about 10-15 percent. Thereafter, the leakage rate continues to increase and reaches to about 60-65 percent when the strain in the rebars is about 1-2 percent. Containment pressure does not increase significantly after leakage rate exceeds 60-65 percent of the containment air mass per day. The liner welds and concrete crack after rebars and liner plate yields to create a path for leakage. The leakage occurs in areas such as equipment hatch, personnel airlocks and penetrations where local strains are substantially higher than the global strains.

The results in Figure A-1 and Figure A-2 are for scale model tests of two concrete containments. Rebar and concrete crack spacing, and aggregate size can affect the leakage rates in full size containments. However, based on the results of testing and analyses presented above, it is reasonable to conclude that all concrete containments start to leak once the rebars and liner plate yield. In addition, leakage becomes excessive once the strains in the reinforced and prestressed concrete containments reach about 2 and 1 percent respectively. Based on information of the containment model test results and analyses data presented in Figure A-1 and Figure A-2, it is reasonable to assume that containment leakage is about one percent of the containment mass per day when the liner plate yields, this increases to 13 percent of containment mass per day when rebars yield. Similarly, leakage rate of 62 percent can be used in severe accident analysis when the containment global strains are 1-2 percent. Uncertainty in the leakage rate can be accounted for by conservatively reducing the yield and failure pressure calculated by simplified

analysis to 85 percent of the calculated value.

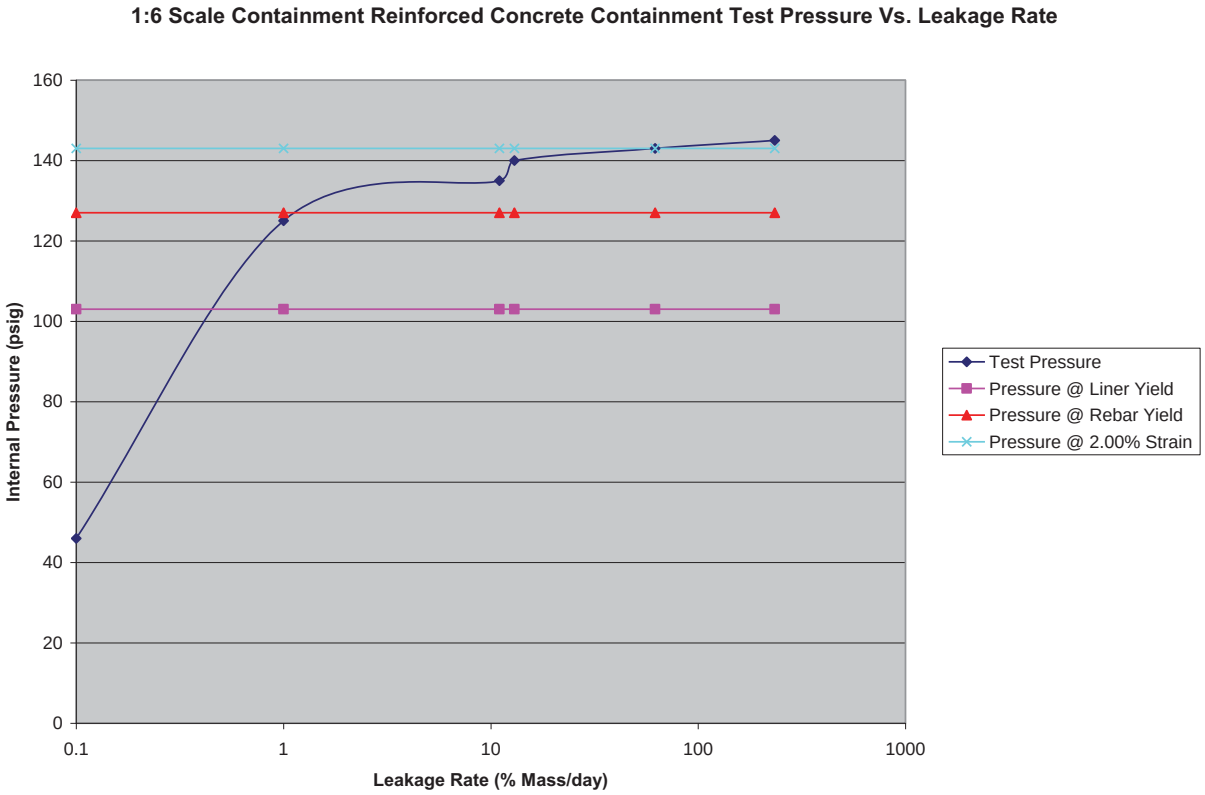

Figure A-1 1:6 Scale Prestressed Concrete Containment Test Pressure versus Leakage Rate

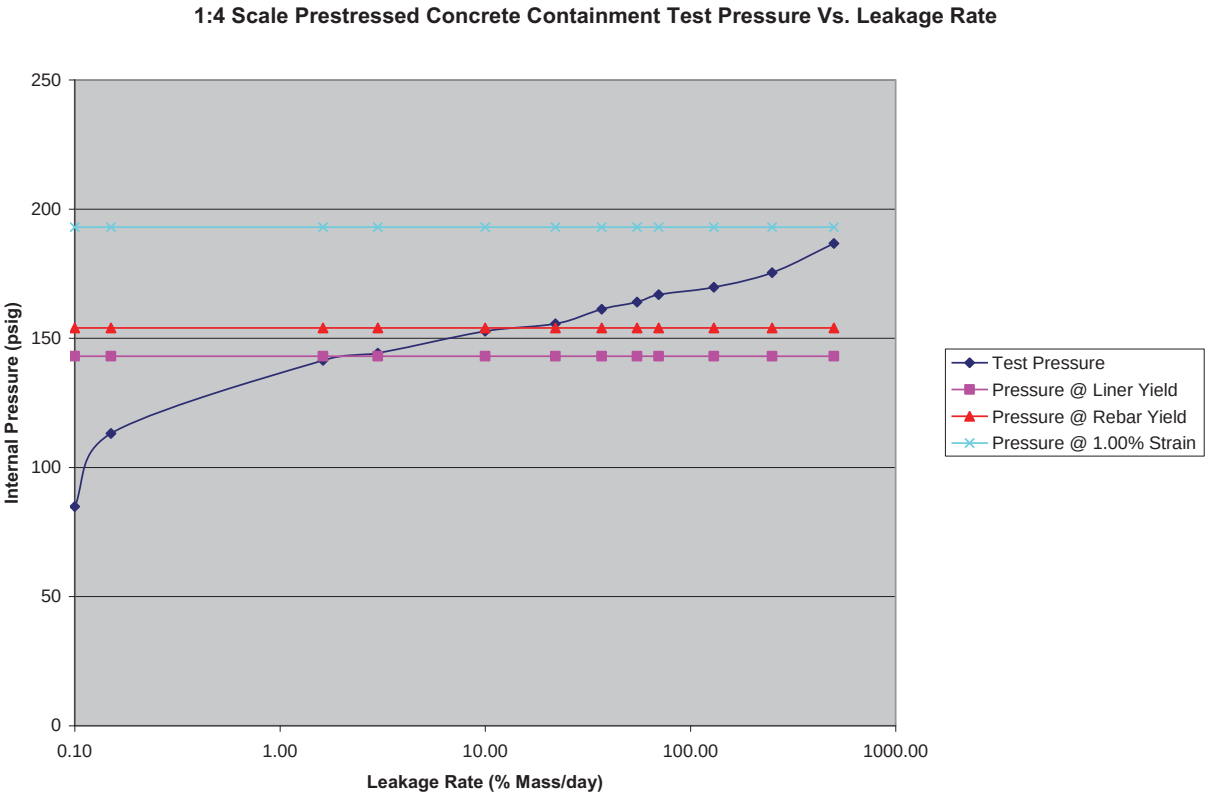

Figure A-2 1:4 Scale Prestressed Concrete Containment Test

The location of the leakage can have a significant effect on the results of the severe accident analysis and dose rates. For instance, if the containment leakage occurs thru penetrations that are located inside adjoining plant buildings, the fission product release into atmosphere would be significantly less as compared to direct leakage to the environment. Previously, some of the severe accident analyses were based on the assumption that the leakage takes place at the top of the containment dome. A more realistic approach is to consider leakage to occur at equipment hatch and other penetrations as demonstrated by tests data, and non-linear analyses.

3.0 ANALYSIS

3.1 Containment Internal Pressure at Liner Plate Yield

The liner plate material yield strength is less than yield strength of rebars. However, modulus of elasticity of carbon steel liner plate and rebars is about the same. Therefore, the liner plate is likely to yield first under internal pressure. When the liner plate yields, the stress in the rebar and liner plate would be the same and equal to yield strength of the liner plate. Using this approach, the internal pressure at which liner plate will yield $P_{lineryield}$ was calculated as follows:

$$P_{lineryield} = (A_{hoop} + A_{liner}) * Y_{liner} / R$$

where:

$P_{lineryield}$ = Containment pressure at which liner plate yield
A_{hoop} = Area of the hoop rebars = 18.777 in^2/ft (Reference 10)
A_{liner} = Area of the 3/8" thick liner plate = 4.5 in^2/ft (Reference 11)
Y_{rebar} = Yield stress of the rebar = 50,000 psi (Reference 12)
Y_{liner} = Yield stress of the liner plate = 32,000 psi (Reference 11)
R = Radius of the containment = 63 feet (Reference 11)

Using the above listed values:

$$P_{lineryield} = 82.10 \text{ psi}$$

To account for uncertainties in material properties and other simplifying assumptions, this pressure at liner plate yield was reduced to 85 percent of the calculated value for the MELCOR analysis.

Therefore:

$$P_{@lineryield} = 69.79 \text{ psi}$$

3.2 Containment Internal Pressure at Rebar Yield

$$P_{yield} = (A_{hoop} * Y_{rebar} + A_{liner} * Y_{liner}) / R$$

Using this equation:

P_{yield} = 119.36 psig

To account for uncertainties in material properties and other simplifying assumptions, this pressure at yield will be reduced to 85 percent of the calculated value for the MELCOR analysis.

Therefore:

$P_{@yield}$ = 101.46 psi

3.3 Containment Internal Pressure at 2% Strain

$$P_{fail} = (A_{hoop} * Y_{rebar@2\%} + A_{liner} * Y_{liner@2\%}) / R$$

where:

P_{fail} = Containment failure pressure at 2% strain
$Y_{rebar@2\%}$ = Stress in the rebar at 2% strain = 53,000 psi
$Y_{liner@2\%}$ = Stress in the liner at 2% strain = 34,300 psi

Using the above listed values:

P_{fail} = 126.71 psi

To account for uncertainties in material properties and other simplifying assumptions, this pressure at failure will be reduced to 85 percent of the calculated value for the MELCOR analysis.

Therefore:

$P_{@fail}$ = 107.70 psi

3.4 Containment Leakage

Surry minimum containment free volume per Table 5.4-24 of Reference 13 = 1, 730,000 ft^3

Density of air at containment pressure of 119.36 psi and 200^{o}F (rebar yield):

$\rho = 0.55$ lb/ft^3, (Page A-10 of Reference 14)

Mass of air inside containment at Pyield

$Mass_{Pyield} = \rho\ V_{containment}$

$Mass_{Pyield} = 9.515 \times 10^5$ lb

Mass leak rate of the containment at Pyield:

$Massleakrate_{Pyield} = 13\%/day$

$Massleak_{perday} = Mass_{Pyield}\ Massleakrate_{Pyield}$

$Massleak_{perday} = 1.237 \times 10^5$ lb/day

Density of air at 70^o F and atmospheric pressure, ρa

$\rho_a = 0.075$ lb/ft^3, (Reference 14)

Leakage flow "Q" calculation

$Q = Massleakperday / \rho_a$

$Q = 1.649 \times 10^6$ lb/day

Therefore, leakage volume

$Volleak_{\%} = Q/V_c$

$Volleak_{\%} = 95.33\%/day$

Table A-5 provides a summary of these results for containment air temperature of 200^o F.

Table A-5 Recommended Leakage Rates and Areas for the Surry Analyses

Containment Pressure (psig)	Containment Temperature (^{o}F)	Containment Leakage (% Mass/day)
45.00	70	0.1
69.79	200	1.0
101.46	200	13
107.70	200	62
123.20	200	352

4.0 CONCLUSION

Simplified analysis of concrete containment provides good agreement with the more detailed finite analysis and test data for the concrete containment performance under internal pressure, and has been used in this report to determine Surry containment.

Extensive research and scale model testing of reinforced and prestressed concrete containments indicate that concrete containments start to leak before a complete rupture or failure. Unless the rate of pressurization is extremely rapid, concrete containments are not likely to have a catastrophic failure. There is some uncertainty about containment leakage rate; however, concrete containments start to leak significantly after the liner plate and rebar yield. Leakage rate becomes excessive after the global strains in the liner plate and rebar reach 2%. Surry containment leakage rates under different internal pressures have been determined using the results of previous tests performed on different scale models of the concrete containments. The leakage rates are presented in Table A-5. Most of the leakage is likely to occur at equipment hatch and other penetrations as demonstrated by tests data, and non-linear analyses.

5.0 REFERENCES

1. U. S. Nuclear Regulatory Commission, NUREG/CR-2239, "Technical Guidance for Siting Criteria Development," Prepared by Sandia National Laboratories, December 1982.

2. Hessheimer, M. F. and Dameron, R. A., "Containment Integrity Research at Sandia National Laboratories," NUREG/CR–6906, 2006.

3. Dameron, R. A., Rashid, Y. R., and Sullaway, M. F., "Pretest Prediction Analysis and Posttest Correlation of the Sizewell-B 1;10 Scale Prestressed Concrete Containment Model Test," NUREG/CR–5671, 1998.

4. Dameron, R. A., Rashid, Y. R., and Tang, H. T., "Leak Area and Leakage Rate Prediction for Probabilistic Risk Assessment of Concrete Containments under Severe Core Conditions," Nuclear Engineering and Design, 1995.

5. Horschell, D. S., "Experimental Results From Pressure Testing a 1:6 – Scale Nuclear Power Plant Containment," NUREG/CR–5121, 1992.

6. Hessheimer, M. F., Klamerus, E. W., Rightly, G. S., Lambert, L. D., and Dameron, R. A., *Overpressurization Test of a 1:4*–Scale Prestressed Concrete Containment Vessel Model, NUREG/CR-6810, 2003.

7. Clauss, D. B., Round Robin Pretest Analyses of a 1:6-Scale Reinforced Concrete Containment Model Subject to Static Internal Overpressurization, NUREG/CR-4913, April 1987.

8. Luk, V. K., "Pretest Round Robin Analysis of a Prestressed Concrete Containment Vessel Model," NUREG/CR-6678, August 2000.

9. Rizkalla, S. H., Lau, B. L., and Simmonds, S. H., "Air leakage Characteristics in Reinforced Concrete, Journal of Structural Engineering, American Society of Civil Engineers, Vol. 110, No. 5, 1984.

10. Surry Power Station, Drawing No. 11448-FC-15C

11. Surry Power Station, Calculation 11448-EA-53

12. Surry Power Station, Drawing No. 11448-FC-15A

13. Surry Power Station Updated Final Safety Analysis Report (UFSAR)

14. Crane Company Technical Paper 410, "Flow of Fluids Through Valves, Fittings, and Pipe."

APPENDIX B
SURRY RADIONUCLIDE INVENTORY

SURRY RADIONUCLIDE INVENTORY

The following tables summarize the radionuclide core inventory for the Surry plant at the time of shutdown. This isotopic inventory was used in each of the accident progression scenarios considered in this report.

Table B-1 Surry radionuclide core inventory and class definition

Radionuclide Class Name	Representative Element	Member Elements	Total Mass (kg)
Noble Gas	Xe	He, Ne, Ar, Kr, Xe, Rn, H, N	448.2
Alkali Metals	Cs	Li, Na, K, Rb, Cs, Fr, Cu	251.7
Alkaline Earths	Ba	Be, Mg, Ca, Sr, Ba, Ra, Es, Fm	187.6
Halogens	I	F, Cl, Br, I, At	17.0
Chalcogens	Te	O, S, Se, Te, Po	40.9
Platinoids	Ru	Ru, Rh, Pd, Re, Os, Ir, Pt, Au, Ni	309.5
Early Transition Elements	Mo	V, Cr, Fe, Co, Mn, Nb, Mo, Tc, Ta, W	323.5
Tetravalent	Ce	Ti, Zr, Hf, Ce, Th, Pa, Np, Pu, C	1226.0
Trivalents	La	Gd, Tb, Dy, Ho, Er, Tm, Yb, Lu, Am, Cm, Bk, Cf	621.2
Uranium	U	U	66770.0
More Volatile Main Group	Cd	Cd, Hg, Zn, As, Sb, Pb, Tl, Bi	7.26
Less Volatile Main Group	Sn	Ga, Ge, In, Sn, Ag	9.19

Table B-2 Surry noble gas radionuclide class specific isotopic activity at the time of reactor shutdown

Isotope	Activity (Bq)
Kr-85	2.94E+16
Kr-85m	8.07E+17
Kr-87	1.60E+18
Kr-88	2.14E+18
Xe-133	6.07E+18
Xe-135	1.80E+18
Xe-135m	1.29E+18

Table B-3 Surry alkali metals radionuclide class specific isotopic activity at the time of reactor shutdown

Isotope	Activity (Bq)
Cs-134	4.32E+17
Cs-136	1.57E+17
Cs-137	3.05E+17
Rb-86	5.36E+15
Rb-88	2.16E+18

Table B-4 Surry alkali earths radionuclide class specific isotopic activity at the time of reactor shutdown

Isotope	Activity (Bq)
Ba-139	5.54E+18
Ba-140	5.37E+18
Sr-89	2.98E+18
Sr-90	2.27E+17
Sr-91	3.75E+18
Sr-92	4.00E+18
Ba-137m	2.92E+17

Table B-5 Surry halogen radionuclide class specific isotopic activity at the time of reactor shutdown

Isotope	Activity (Bq)
I-131	2.78E+18
I-132	4.08E+18
I-133	5.76E+18
I-134	6.48E+18
I-135	5.49E+18

Table B-6 Surry chalcogen radionuclide class specific isotopic activity at the time of reactor shutdown

Isotope	Activity (Bq)
Te-127	2.60E+17
Te-127m	4.22E+16
Te-129	7.79E+17
Te-129m	1.49E+17
Te-131m	5.71E+17
Te-132	4.29E+18
Te-131	2.55E+18

Table B-7 Surry platinoid radionuclide class specific isotopic activity at the time of reactor shutdown

Isotope	Activity (Bq)
Rh-105	2.90E+18
Ru-103	4.61E+18
Ru-105	3.14E+18
Ru-106	1.40E+18
Rh-103m	4.61E+18
Rh-106	1.56E+18

Table B-8 Surry early transition element radionuclide class specific isotopic activity at the time of reactor shutdown

Isotope	Activity (Bq)
Nb-95	5.18E+18
Co-58	4.79E+13
Co-60	2.65E+14
Mo-99	5.68E+18
Tc-99m	5.03E+18
Nb-97	5.24E+18
Nb-97m	4.95E+18

Table B-9 Surry tetravalent radionuclide class specific isotopic activity at the time of reactor shutdown

Isotope	Activity (Bq)
Ce-141	4.87E+18
Ce-143	4.55E+18
Ce-144	3.42E+18
Np-239	5.67E+19
Pu-238	8.31E+15
Pu-239	9.56E+14
Pu-240	1.17E+15
Pu-241	3.39E+17
Zr-95	4.96E+18
Zr-97	5.00E+18

Table B-10 Surry trivalent radionuclide class specific isotopic activity at the time of reactor shutdown

Isotope	Activity (Bq)
Am-241	3.43E+14
Cm-242	1.14E+17
Cm-244	1.13E+16
La-140	5.67E+18
La-141	5.10E+18
La-142	4.92E+18
Nd-147	2.04E+18
Pr-143	4.65E+18
Y-90	2.39E+17
Y-91	3.93E+18
Y-92	4.11E+18
Y-93	4.62E+18
Y-91m	2.20E+18
Pr-144	3.63E+18
Pr-144m	5.06E+16

APPENDIX C
INPUT PARAMETERS
FOR CONSEQUENCE ANALYSIS

INPUT PARAMETERS FOR CONSEQUENCE ANALYSIS

The input parameters used for the LTSBO, STSBO, ISLOCA, TI-SGTR Mitigated and Unmitigated Scenarios are shown in this appendix in tabular form. Table C-1 contains the more general ATMOS input parameters used for these three scenarios. Table C-2 through Table C-4 contains specific inputs related to the source terms that were extracted from MELCOR results via the MELMACCS code. Table C-5 contains general EARLY input parameters. Table C-6 and Table C-7 contain parameters associated with the network evacuation model that was used to treat emergency response. Table C-8 contains the evacuation direction parameters. Table C-9 contains the CHRONC input parameters.

Table C-1 ATMOS Input Parameters Used in the Surry LTSBO, STSBO, ISLOCA, TISGTR Mitigated and Unmitigated scenarios

Variable	Description	LTSBO	STSBO	ISLOCA	TISGTR Mitigated	TISGTR Unmitigated
APLFRC	Method of Applying Release Fraction	PARENT	PARENT	PARENT	PARENT	PARENT
ATNAM1	Title Describing the ATMOS Assumptions	SOARCA Surry Unmitigated LTSBO	SOARCA Surry Unmitigated STSBO	SOARCA Surry Unmitigated STSBO	SOARCA Surry Mitigated TISGTR	SOARCA Surry Unmitigated TISGTR
ATNAM2	Title Describing the Source Term	Surry source term for unmitigated long-term station blackout.	Surry source term for unmitigated short-term station blackout.	Surry source term for unmitigated short-term station blackout.	Surry source term for mitigated, thermally-induced, steam-generator-tube rupture	Surry source term for unmitigated short-term station blackout.
BNDMXH	Boundary Weather Mixing Layer Height	1000	1000	1000	1000	1000
BNDRAN	Boundary Weather Rain Rate	5	5	5	5	5
BNDWND	Boundary Wind Speed	2.2	2.2	2.2	2.2	2.2
BRKPNT	Breakpoint Time for Plume Meander	3600	3600	3600	3600	3600
BUILDH	Building Height for all Plume Segments	50	50	50	50	50
CORINV	Isotopic Inventory at Time of Reactor Shutdown	from MELMACCS (see Appendix B)	from MELMACCS (see Appendix B)	from MELMACCS (see Appendix B)	from MELMACCS (see Appendix B)	from MELMACCS (see Appendix B)
CORSCA	Linear Scaling Factor on Core Inventory	1	1	1	1	1
CWASH1	Linear Coefficient for Washout	1.89E-05	1.89E-05	1.89E-05	1.89E-05	1.89E-05

Variable	Description	LTSBO	STSBO	ISLOCA	TISGTR Mitigated	TISGTR Unmitigated
CWASH2	Exponential Term for Washout	0.664	0.664	0.664	0.664	0.664
CYSIGA	Linear Coefficient for sigma-y					
	Stability Class A	0.7507	0.7507	0.7507	0.7507	0.7507
	Stability Class B	0.7507	0.7507	0.7507	0.7507	0.7507
	Stability Class C	0.4063	0.4063	0.4063	0.4063	0.4063
	Stability Class D	0.2779	0.2779	0.2779	0.2779	0.2779
	Stability Class E	0.2158	0.2158	0.2158	0.2158	0.2158
	Stability Class F	0.2158	0.2158	0.2158	0.2158	0.2158
CYSIGB	Exponential Term for sigma-y					
	Stability Class A	0.866	0.866	0.866	0.866	0.866
	Stability Class B	0.866	0.866	0.866	0.866	0.866
	Stability Class C	0.865	0.865	0.865	0.865	0.865
	Stability Class D	0.881	0.881	0.881	0.881	0.881
	Stability Class E	0.866	0.866	0.866	0.866	0.866
	Stability Class F	0.866	0.866	0.866	0.866	0.866
CZSIGA	Linear Coefficient for sigma-z					
	Stability Class A	0.0361	0.0361	0.0361	0.0361	0.0361
	Stability Class B	0.0361	0.0361	0.0361	0.0361	0.0361
	Stability Class C	0.2036	0.2036	0.2036	0.2036	0.2036
	Stability Class D	0.2636	0.2636	0.2636	0.2636	0.2636
	Stability Class E	0.2463	0.2463	0.2463	0.2463	0.2463
	Stability Class F	0.2463	0.2463	0.2463	0.2463	0.2463
CZSIGB	Exponential Term for sigma-z					
	Stability Class A	1.277	1.277	1.277	1.277	1.277

Variable	Description	LTSBO	STSBO	ISLOCA	TISGTR Mitigated	TISGTR Unmitigated
	Stability Class B	1.277	1.277	1.277	1.277	1.277
CZSIGB	Stability Class C	0.859	0.859	0.859	0.859	0.859
	Stability Class D	0.751	0.751	0.751	0.751	0.751
	Stability Class E	0.619	0.619	0.619	0.619	0.619
	Stability Class F	0.619	0.619	0.619	0.619	0.619
DISPMD	Dispersion Model Flag	LRDIST	LRDIST	LRDIST	LRDIST	LRDIST
DRYDEP	Dry Deposition Flag	Xe = .FALSE. Other Groups = .TRUE.	Xe = .FALSE. Other Groups = .TRUE.	Xe = .FALSE. Other Groups = .TRUE.	Xe = .FALSE. Other Groups = .TRUE.	Xe = .FALSE. Other Groups = .TRUE.
ENDAT1	Control flag indicating only ATMOS is to be run	.FALSE.	.FALSE.	.FALSE.	.FALSE.	.FALSE.
GRPNAM	Names of the Chemical Classes (Used by WinMACCS)					
	Chemical Class 1	Xe	Xe	Xe	Xe	Xe
	Chemical Class 2	Cs	Cs	Cs	Cs	Cs
	Chemical Class 3	Ba	Ba	Ba	Ba	Ba
	Chemical Class 4	I	I	I	I	I
	Chemical Class 5	Te	Te	Te	Te	Te
	Chemical Class 6	Ru	Ru	Ru	Ru	Ru
	Chemical Class 7	Mo	Mo	Mo	Mo	Mo
	Chemical Class 8	Ce	Ce	Ce	Ce	Ce
	Chemical Class 9	La	La	La	La	La
IBDSTB	Boundary Weather Stability Class Index	4	4	4	4	4
IDEBUG	Debug Switch for Extra Debugging Print	0	0	0	0	0
IGROUP	Definition of Radionuclide Group Numbers	1 = Xe	1 = Xe	1 = Xe	1 = Xe	1 = Xe
		2 = Cs	2 = Cs	2 = Cs	2 = Cs	2 = Cs
		3 = Ba	3 = Ba	3 = Ba	3 = Ba	3 = Ba

Variable	Description	LTSBO	STSBO	ISLOCA	TISGTR Mitigated	TISGTR Unmitigated
		4 = I	4 = I	4 = I	4 = I	4 = I
		5 = Te	5 = Te	5 = Te	5 = Te	5 = Te
		6 = Ru	6 = Ru	6 = Ru	6 = Ru	6 = Ru
IGROUP		7 = Mo	7 = Mo	7 = Mo	7 = Mo	7 = Mo
		8 = Ce	8 = Ce	8 = Ce	8 = Ce	8 = Ce
		9 = La	9 = La	9 = La	9 = La	9 = La
INWGHT	Number of Samples for Each Bin Used for Nonuniform Weather Bin Sampling					
	Bin 1	12	12	12	12	12
	Bin 2	14	14	14	14	14
	Bin 3	12	12	12	12	12
	Bin 4	39	39	39	39	39
	Bin 5	85	85	85	85	85
	Bin 6	94	94	94	94	94
	Bin 7	16	16	16	16	16
	Bin 8	12	12	12	12	12
	Bin 9	27	27	27	27	27
	Bin 10	134	134	134	134	134
	Bin 11	119	119	119	119	119
	Bin 12	74	74	74	74	74
	Bin 13	92	92	92	92	92
	Bin 14	43	43	43	43	43
	Bin 15	12	12	12	12	12
	Bin 16	12	12	12	12	12
	Bin 17	37	37	37	37	37
	Bin 18	12	12	12	12	12
	Bin 19	13	13	13	13	13
	Bin 20	17	17	17	17	17
	Bin 21	14	14	14	14	14
	Bin 22	12	12	12	12	12
	Bin 23	6	6	6	6	6
	Bin 24	6	6	6	6	6
	Bin 25	12	12	12	12	12
	Bin 26	12	12	12	12	12
	Bin 27	12	12	12	12	12
	Bin 28	1	1	1	1	1
	Bin 29	5	5	5	5	5
	Bin 30	6	6	6	6	6
	Bin 31	5	5	5	5	5
	Bin 32	12	12	12	12	12
	Bin 33	5	5	5	5	5
	Bin 34	12	12	12	12	12
	Bin 35	12	12	12	12	12
	Bin 36	12	12	12	12	12

Variable	Description	LTSBO	STSBO	ISLOCA	TISGTR Mitigated	TISGTR Unmitigated
IRSEED	Seed for Random Number Generator	79	79	79	79	79
LATITU	Latitude of Power Plant	37° 9' 56"	37° 9' 56"	37° 9' 56"	37° 9' 56"	37° 9' 56"
LIMSPA	Last Interval for Measured Weather	25	25	25	25	25
LONGIT	Longitude of Power Plant	76° 41' 54"	76° 41' 54"	76° 41' 54"	76° 41' 54"	76° 41' 54"
MAXGRP	Number of Radionuclide Groups	9	9	9	9	9
MAXHGT	Flag for Mixing Height	DAY_AND_NIGHT	DAY_AND_NIGHT	DAY_AND_NIGHT	DAY_AND_NIGHT	DAY_AND_NIGHT
MAXRIS	Selection of Risk Dominant Plume	3	3	1	1	1
METCOD	Meteorological Sampling Option Code	2	2	2	2	2
MNDMOD	Plume Meander Model Flag	OFF	OFF	OFF	OFF	OFF
NAMSTB	List of Pseudo stable Nuclides					
	Isotope 1	I-129	I-129	I-129	I-129	I-129
	Isotope 2	Xe-131m	Xe-131m	Xe-131m	Xe-131m	Xe-131m
	Isotope 3	Xe-133m	Xe-133m	Xe-133m	Xe-133m	Xe-133m
	Isotope 4	Cs-135	Cs-135	Cs-135	Cs-135	Cs-135
	Isotope 5	Sm-147	Sm-147	Sm-147	Sm-147	Sm-147
	Isotope 6	U-234	U-234	U-234	U-234	U-234
	Isotope 7	U-235	U-235	U-235	U-235	U-235
	Isotope 8	U-236	U-236	U-236	U-236	U-236
	Isotope 9	U-237	U-237	U-237	U-237	U-237
	Isotope 10	Np-237	Np-237	Np-237	Np-237	Np-237
	Isotope 11	Rb-87	Rb-87	Rb-87	Rb-87	Rb-87
	Isotope 12	Zr-93	Zr-93	Zr-93	Zr-93	Zr-93
	Isotope 13	Nb-93m	Nb-93m	Nb-93m	Nb-93m	Nb-93m
	Isotope 14	Nb-95m	Nb-95m	Nb-95m	Nb-95m	Nb-95m
	Isotope 15	Tc-99	Tc-99	Tc-99	Tc-99	Tc-99
	Isotope 16	Pm-147	Pm-147	Pm-147	Pm-147	Pm-147
NPSGRP	Number of Particle Size Groups	10	10	10	10	10
NRINTN	Number of Rain Intensity Breakpoints	3	3	3	3	3
NRNINT	Number of Rain Distance Intervals	5	5	5	5	5
NSBINS	Number of	36	36	36	36	36

Variable	Description	LTSBO	STSBO	ISLOCA	TISGTR Mitigated	TISGTR Unmitigated
	Weather Bins to Sample					
NUCNAM	Radionuclide Names	See Appendix B	See Appendix B	See Appendix B	See Appendix B	See Appendix B
NUCOUT	Radionuclide Used in Dispersion Print	Cs-137	Cs-137	Cs-137	Cs-137	Cs-137
NUMCOR	Number of Compass Sectors in the Grid	64	64	64	64	64
NUMISO	Number of Radionuclides	69	69	69	69	69
NUMRAD	Number of Radial Spatial Intervals	26	26	26	26	26
NUMREL	Number of Released Plume Segments	28	24	24	49	24
NUMSTB	Number of Defined Pseudo stable Radionuclides	16	16	16	16	16
OALARM	Time to Reach General Emergency Conditions	0	0	0	0	0
PDELAY	Plume Release Times	MELMACCS Data (See Table C-2)	MELMACCS Data (See Table C-2)	MELMACCS Data (See Table C-2)	MELMACCS Data (See Table C-2)	MELMACCS Data (See Table C-2)
PLHEAT	Plume Heat Contents	MELMACCS Data (See Table C-2)	MELMACCS Data (See Table C-2)	MELMACCS Data (See Table C-2)	MELMACCS Data (See Table C-2)	MELMACCS Data (See Table C-2)
PLHITE	Plume Release Heights	MELMACCS Data (See Table C-2)	MELMACCS Data (See Table C-2)	MELMACCS Data (See Table C-2)	MELMACCS Data (See Table C-2)	MELMACCS Data (See Table C-2)
PLMDEN	Plume Mass Density	MELMACCS Data (See Table C-2)	MELMACCS Data (See Table C-2)	MELMACCS Data (See Table C-2)	MELMACCS Data (See Table C-2)	MELMACCS Data (See Table C-2)
PLMFLA	Plume Mass Flow Rate	MELMACCS Data (See Table C-2)	MELMACCS Data (See Table C-2)	MELMACCS Data (See Table C-2)	MELMACCS Data (See Table C-2)	MELMACCS Data (See Table C-2)
PLMMOD	Flag for Plume Rise Input Option	DENSITY	DENSITY	DENSITY	DENSITY	DENSITY
PLUDUR	Plume Segment Durations	MELMACCS Data (See Table C-2)	MELMACCS Data (See Table C-2)	MELMACCS Data (See Table C-2)	MELMACCS Data (See Table C-2)	MELMACCS Data (See Table C-2)
PSDIST	Particle Size Distribution by Group	MELMACCS Data (See Table C-3)	MELMACCS Data (See Table C-3)	MELMACCS Data (See Table C-3)	MELMACCS Data (See Table C-3)	MELMACCS Data (See Table C-3)
REFTIM	Plume Reference Time Point	0. for first 0.5 for	0. for first 0.5 for	0. for first 0.5 for subsequent	0. for first 0.5 for	0. for first 0.5 for

Variable	Description	LTSBO	STSBO	ISLOCA	TISGTR Mitigated	TISGTR Unmitigated
		subsequent	subsequent		subsequent	subsequent
RELFRC	Release Fractions of the Source Term	MELMACCS Data (See Table C-4)	MELMACCS Data (See Table C-4)	MELMACCS Data (See Table C-4)	MELMACCS Data (See Table C-4)	MELMACCS Data (See Table C-4)
RNDSTS	Endpoints of Rain Distance Intervals					
	Interval 1	3.22	3.22	3.22	3.22	3.22
	Interval 2	5.63	5.63	5.63	5.63	5.63
	Interval 3	11.27	11.27	11.27	11.27	11.27
	Interval 4	20.92	20.92	20.92	20.92	20.92
	Interval 5	32.19	32.19	32.19	32.19	32.19
RNRATE	Rain Intensity Breakpoints for Weather Binning					
	Intensity 1	2	2	2	2	2
	Intensity 2	4	4	4	4	4
	Intensity 3	6	6	6	6	6
SCLADP	Scaling Factor for A-D Plume Rise	1.0	1.0	1.0	1.0	1.0
SCLCRW	Scaling Factor for Critical Wind Speed	1.0	1.0	1.0	1.0	1.0
SCLEFP	Scaling Factor for E-F Plume Rise	1.0	1.0	1.0	1.0	1.0
SIGYINIT	Initial Sigma-y for All Plume Segments	9.3	9.3	9.3	9.3	9.3
SIGZINIT	Initial Sigma-z for All Plume Segments	23.3	23.3	23.3	23.3	23.3
SPAEND	Radial distances for grid boundaries					
	Ring 1	0.16	0.16	0.16	0.16	0.16
	Ring 2	0.52	0.52	0.52	0.52	0.52
	Ring 3	1.21	1.21	1.21	1.21	1.21
	Ring 4	1.61	1.61	1.61	1.61	1.61
	Ring 5	2.13	2.13	2.13	2.13	2.13
	Ring 6	3.22	3.22	3.22	3.22	3.22
	Ring 7	4.02	4.02	4.02	4.02	4.02
	Ring 8	4.83	4.83	4.83	4.83	4.83
	Ring 9	5.63	5.63	5.63	5.63	5.63
	Ring 10	8.05	8.05	8.05	8.05	8.05
	Ring 11	11.27	11.27	11.27	11.27	11.27
	Ring 12	16.09	16.09	16.09	16.09	16.09
	Ring 13	20.92	20.92	20.92	20.92	20.92

Variable	Description	LTSBO	STSBO	ISLOCA	TISGTR Mitigated	TISGTR Unmitigated
	Ring 14	25.75	25.75	25.75	25.75	25.75
	Ring 15	32.19	32.19	32.19	32.19	32.19
	Ring 16	40.23	40.23	40.23	40.23	40.23
	Ring 17	48.28	48.28	48.28	48.28	48.28
SPAEND	Ring 18	64.37	64.37	64.37	64.37	64.37
	Ring 19	80.47	80.47	80.47	80.47	80.47
	Ring 20	112.65	112.65	112.65	112.65	112.65
	Ring 21	160.93	160.93	160.93	160.93	160.93
	Ring 22	241.14	241.14	241.14	241.14	241.14
	Ring 23	321.87	321.87	321.87	321.87	321.87
	Ring 24	563.27	563.27	563.27	563.27	563.27
	Ring 25	804.67	804.67	804.67	804.67	804.67
	Ring 26	1609.34	1609.34	1609.34	1609.34	1609.34
TIMBAS	Time Base for Plume Expansion Factor	600	600	600	600	600
VDEPOS	Dry Deposition Velocities					
	Aerosol Bin 1	5.35E-04	5.35E-04	5.35E-04	5.35E-04	5.35E-04
	Aerosol Bin 2	4.91E-04	4.91E-04	4.91E-04	4.91E-04	4.91E-04
	Aerosol Bin 3	6.43E-04	6.43E-04	6.43E-04	6.43E-04	6.43E-04
	Aerosol Bin 4	1.08E-03	1.08E-03	1.08E-03	1.08E-03	1.08E-03
	Aerosol Bin 5	2.12E-03	2.12E-03	2.12E-03	2.12E-03	2.12E-03
	Aerosol Bin 6	4.34E-03	4.34E-03	4.34E-03	4.34E-03	4.34E-03
	Aerosol Bin 7	8.37E-03	8.37E-03	8.37E-03	8.37E-03	8.37E-03
	Aerosol Bin 8	1.37E-02	1.37E-02	1.37E-02	1.37E-02	1.37E-02
	Aerosol Bin 9	1.70E-02	1.70E-02	1.70E-02	1.70E-02	1.70E-02
	Aerosol Bin 10	1.70E-02	1.70E-02	1.70E-02	1.70E-02	1.70E-02
WETDEP	Wet Deposition Flag	Xe = .FALSE. Other groups = .TRUE.	Xe = .FALSE. Other groups = .TRUE.	Xe = .FALSE. Other groups = .TRUE.	Xe = .FALSE. Other groups = .TRUE.	Xe = .FALSE. Other groups = .TRUE.
XPFAC1	Base Time for Meander Expansion Factor	0.2	0.2	0.2	0.2	0.2
XPFAC2	Breakpoint for Expansion Factor Model	0.25	0.25	0.25	0.25	0.25
YSCALE	Scale Factor for Horizontal Dispersion	1	1	1	1	1
ZSCALE	Scale Factor for Vertical Dispersion	1.27	1.27	1.27	1.27	1.27

Table C-2 Plume Parameters Used in the Surry LTSBO, Unmitigated STSBO, TI-SGTR Mitigated and Unmitigated Scenarios

Surry LTSBO						
Plume Segment	**PDELAY**	**PLHEAT**	**PLHITE**	**PLMDEN**	**PLMFLA**	**PLUDUR**
1	1.63E+05	5.11E+04	8.40E+00	1.77E-01	4.85E-01	3.60E+03
2	1.67E+05	1.14E+05	8.40E+00	3.89E-01	4.83E-01	3.60E+03
3	1.70E+05	2.07E+05	8.40E+00	7.01E-01	4.81E-01	3.60E+03
4	1.74E+05	3.05E+05	8.40E+00	1.02E+00	4.79E-01	3.60E+03
5	1.77E+05	3.81E+05	8.40E+00	1.27E+00	4.76E-01	3.72E+03
6	1.81E+05	4.44E+05	8.40E+00	1.46E+00	4.74E-01	3.48E+03
7	1.85E+05	4.82E+05	8.40E+00	1.57E+00	4.72E-01	3.60E+03
8	1.88E+05	5.07E+05	8.40E+00	1.63E+00	4.70E-01	3.60E+03
9	1.92E+05	5.25E+05	8.40E+00	1.67E+00	4.69E-01	3.60E+03
10	1.95E+05	5.38E+05	8.40E+00	1.70E+00	4.67E-01	3.60E+03
11	1.99E+05	5.48E+05	8.40E+00	1.72E+00	4.65E-01	3.60E+03
12	2.03E+05	5.59E+05	8.40E+00	1.73E+00	4.63E-01	3.60E+03
13	2.06E+05	5.71E+05	8.40E+00	1.76E+00	4.62E-01	3.60E+03
14	2.10E+05	5.75E+05	8.40E+00	1.75E+00	4.60E-01	3.60E+03
15	2.13E+05	5.79E+05	8.40E+00	1.75E+00	4.58E-01	3.60E+03
16	2.17E+05	5.85E+05	8.40E+00	1.75E+00	4.57E-01	3.60E+03
17	2.21E+05	5.94E+05	8.40E+00	1.77E+00	4.55E-01	3.60E+03
18	2.24E+05	6.02E+05	8.40E+00	1.78E+00	4.54E-01	3.60E+03
19	2.28E+05	6.11E+05	8.40E+00	1.79E+00	4.52E-01	3.60E+03
20	2.31E+05	6.17E+05	8.40E+00	1.80E+00	4.51E-01	3.60E+03
21	2.35E+05	6.22E+05	8.40E+00	1.80E+00	4.50E-01	3.60E+03
22	2.39E+05	6.33E+05	8.40E+00	1.81E+00	4.48E-01	3.60E+03
23	2.42E+05	6.56E+05	8.40E+00	1.81E+00	4.42E-01	3.60E+03
24	2.46E+05	6.52E+05	8.40E+00	1.76E+00	4.39E-01	3.60E+03
25	2.49E+05	6.46E+05	8.40E+00	1.71E+00	4.36E-01	3.60E+03
26	2.53E+05	6.37E+05	8.40E+00	1.66E+00	4.34E-01	3.72E+03
27	2.57E+05	6.30E+05	8.40E+00	1.62E+00	4.32E-01	2.40E+03
28	2.59E+05	6.27E+05	8.40E+00	1.60E+00	4.31E-01	1.20E+02

Surry Unmitigated STSBO					
Plume Segment	**PDELAY**	**PLHITE**	**PLMDEN**	**PLMFLA**	**PLUDUR**
1	9.19E+04	8.40E+00	4.84E-01	1.97E-01	3.72E+03
2	9.56E+04	8.40E+00	4.81E-01	5.03E-01	3.48E+03
3	9.91E+04	8.40E+00	4.78E-01	9.44E-01	3.72E+03
4	1.03E+05	8.40E+00	4.76E-01	1.35E+00	3.48E+03
5	1.06E+05	8.40E+00	4.73E-01	1.64E+00	3.60E+03
6	1.10E+05	8.40E+00	4.71E-01	1.81E+00	3.60E+03
7	1.14E+05	8.40E+00	4.68E-01	1.90E+00	3.72E+03
8	1.17E+05	8.40E+00	4.66E-01	1.95E+00	3.60E+03
9	1.21E+05	8.40E+00	4.64E-01	1.97E+00	3.60E+03
10	1.24E+05	8.40E+00	4.62E-01	2.00E+00	3.60E+03
11	1.28E+05	8.40E+00	4.60E-01	2.01E+00	3.48E+03
12	1.32E+05	8.40E+00	4.58E-01	2.01E+00	3.60E+03
13	1.35E+05	8.40E+00	4.56E-01	2.01E+00	3.72E+03
14	1.39E+05	8.40E+00	4.54E-01	2.01E+00	3.48E+03
15	1.42E+05	8.40E+00	4.53E-01	2.01E+00	3.60E+03
16	1.46E+05	8.40E+00	4.51E-01	2.01E+00	3.72E+03
17	1.50E+05	8.40E+00	4.49E-01	2.02E+00	3.60E+03
18	1.53E+05	8.40E+00	4.48E-01	2.02E+00	3.48E+03
19	1.57E+05	8.40E+00	4.44E-01	2.01E+00	3.60E+03
20	1.60E+05	8.40E+00	4.38E-01	1.96E+00	3.60E+03
21	1.64E+05	8.40E+00	4.35E-01	1.90E+00	3.72E+03
22	1.68E+05	8.40E+00	4.32E-01	1.84E+00	3.48E+03
23	1.71E+05	8.40E+00	4.30E-01	1.80E+00	1.68E+03
24	1.73E+05	8.40E+00	4.30E-01	1.78E+00	1.20E+02

Surry ISLOCA					
Plume Segment	**PDELAY**	**PLHITE**	**PLMDEN**	**PLMFLA**	**PLUDUR**
1	4.59E+04	2.17E+01	1.07E+00	1.83E+01	4.20E+03
2	4.59E+04	2.17E+01	1.07E+00	1.83E+01	4.20E+03
3	4.83E+04	7.90E+00	8.94E-01	1.05E+00	4.20E+03
4	4.83E+04	5.64E+00	5.77E-01	6.65E-01	4.20E+03
5	4.86E+04	6.39E-01	4.54E-01	1.13E-02	3.90E+03
6	4.86E+04	4.91E+00	5.51E-01	1.75E+00	3.90E+03
7	5.01E+04	4.91E+00	5.10E-01	1.66E+00	3.00E+02
8	5.01E+04	2.17E+01	1.00E+00	1.68E+01	3.30E+03
9	5.01E+04	2.17E+01	1.00E+00	1.68E+01	3.30E+03
10	5.04E+04	4.91E+00	5.09E-01	1.14E+00	3.00E+03
11	5.25E+04	4.91E+00	6.22E-01	2.13E+00	3.60E+03
12	5.25E+04	7.90E+00	9.09E-01	1.23E+00	3.60E+03
13	5.25E+04	5.64E+00	5.99E-01	8.21E-01	3.60E+03
14	5.34E+04	4.91E+00	3.72E-01	1.11E+00	3.60E+03
15	5.34E+04	2.17E+01	1.04E+00	1.76E+01	3.90E+03
16	5.34E+04	2.17E+01	1.04E+00	1.76E+01	3.90E+03
17	5.61E+04	4.91E+00	6.57E-01	2.03E+00	3.60E+03
18	5.61E+04	7.90E+00	9.11E-01	1.21E+00	3.60E+03
19	5.61E+04	5.64E+00	6.86E-01	8.55E-01	3.60E+03
20	5.70E+04	4.91E+00	4.25E-01	1.47E-01	3.60E+03
21	5.73E+04	2.17E+01	1.08E+00	1.75E+01	3.30E+03
22	5.73E+04	2.17E+01	1.08E+00	1.75E+01	3.30E+03
23	5.97E+04	4.91E+00	1.07E+00	8.97E-01	3.60E+03
24	5.97E+04	7.90E+00	1.03E+00	8.08E-01	3.60E+03
25	5.97E+04	5.64E+00	1.06E+00	6.77E-01	3.60E+03
26	6.06E+04	2.17E+01	1.15E+00	1.83E+01	3.90E+03
27	6.06E+04	2.17E+01	1.15E+00	1.83E+01	3.90E+03
28	6.45E+04	2.17E+01	1.16E+00	1.82E+01	3.30E+03
29	6.45E+04	2.17E+01	1.16E+00	1.82E+01	3.30E+03
30	7.02E+04	4.91E+00	1.14E+00	5.20E-02	3.60E+03
31	7.02E+04	7.90E+00	1.12E+00	3.38E-01	3.60E+03
32	7.02E+04	5.64E+00	1.16E+00	2.11E-01	3.60E+03
33	7.17E+04	1.20E+00	8.27E-01	5.62E-05	3.60E+03
34	7.17E+04	3.38E+00	1.12E+00	7.11E+00	3.30E+03
35	7.50E+04	3.38E+00	1.12E+00	7.12E+00	3.90E+03
36	7.53E+04	1.20E+00	8.56E-01	1.19E-04	3.60E+03
37	7.89E+04	1.20E+00	8.51E-01	1.39E-04	3.60E+03
38	7.89E+04	3.38E+00	1.12E+00	7.13E+00	3.60E+03
39	8.10E+04	4.91E+00	1.12E+00	1.80E-01	3.60E+03
40	8.10E+04	5.64E+00	1.14E+00	1.38E-01	3.60E+03
41	8.22E+04	4.91E+00	9.18E-01	1.47E-01	3.60E+03
42	8.25E+04	1.20E+00	8.39E-01	1.50E-04	3.60E+03
43	8.25E+04	3.38E+00	1.12E+00	7.14E+00	3.30E+03

Surry ISLOCA					
Plume Segment	**PDELAY**	**PLHITE**	**PLMDEN**	**PLMFLA**	**PLUDUR**
44	8.46E+04	4.91E+00	1.12E+00	1.60E-01	3.60E+03
45	8.46E+04	5.64E+00	1.15E+00	1.52E-01	3.60E+03
46	8.58E+04	3.38E+00	1.12E+00	7.65E+00	4.20E+03
47	9.00E+04	3.38E+00	1.12E+00	7.15E+00	3.60E+03
48	9.18E+04	4.91E+00	1.14E+00	2.60E-01	4.35E+03
49	9.36E+04	4.91E+00	1.04E+00	6.92E-02	3.60E+03
50	9.36E+04	3.38E+00	1.12E+00	7.16E+00	3.60E+03
51	9.62E+04	4.91E+00	1.12E+00	4.74E-01	3.75E+03
52	9.62E+04	5.64E+00	1.13E+00	1.93E-01	3.75E+03
53	9.72E+04	3.38E+00	1.12E+00	7.17E+00	3.60E+03
54	1.01E+05	3.38E+00	1.13E+00	7.17E+00	3.60E+03
55	1.03E+05	4.91E+00	1.12E+00	3.66E-01	4.50E+03
56	1.04E+05	3.38E+00	1.13E+00	7.18E+00	3.60E+03
57	1.07E+05	4.91E+00	1.10E+00	5.49E-01	2.70E+03
58	1.08E+05	3.38E+00	1.13E+00	7.18E+00	3.60E+03
59	1.10E+05	4.91E+00	1.11E+00	6.23E-01	4.50E+03
60	1.12E+05	3.38E+00	1.13E+00	7.19E+00	3.60E+03
61	1.14E+05	4.91E+00	1.13E+00	6.96E-01	3.60E+03
62	1.15E+05	3.38E+00	1.13E+00	7.20E+00	3.60E+03
63	1.18E+05	4.91E+00	1.12E+00	7.79E-01	3.60E+03
64	1.18E+05	5.64E+00	1.12E+00	2.50E-01	3.60E+03
65	1.19E+05	3.38E+00	1.13E+00	7.21E+00	3.60E+03
66	1.22E+05	4.91E+00	1.07E+00	9.14E-01	3.60E+03
67	1.22E+05	5.64E+00	1.07E+00	3.05E-01	3.60E+03
68	1.22E+05	4.91E+00	9.36E-01	2.44E-01	3.60E+03
69	1.25E+05	4.91E+00	1.04E+00	9.47E-01	2.70E+03
70	1.25E+05	5.64E+00	1.02E+00	3.20E-01	2.70E+03
71	1.26E+05	4.91E+00	8.37E-01	2.63E-01	3.60E+03
72	1.28E+05	4.91E+00	1.08E+00	9.52E-01	4.50E+03
73	1.28E+05	7.90E+00	1.10E+00	3.51E-01	4.50E+03
74	1.28E+05	5.64E+00	1.06E+00	3.22E-01	4.50E+03
75	1.30E+05	4.91E+00	8.29E-01	3.61E-01	3.60E+03
76	1.30E+05	3.38E+00	1.14E+00	7.23E+00	3.60E+03
77	1.32E+05	4.91E+00	1.02E+00	1.06E+00	2.70E+03
78	1.32E+05	7.90E+00	1.09E+00	4.36E-01	2.70E+03
79	1.33E+05	4.91E+00	8.54E-01	6.85E-01	3.60E+03
80	1.35E+05	4.91E+00	1.06E+00	1.10E+00	3.60E+03
81	1.35E+05	7.90E+00	1.08E+00	4.68E-01	3.60E+03
82	1.35E+05	5.64E+00	1.01E+00	3.96E-01	3.60E+03
83	1.37E+05	4.91E+00	8.44E-01	7.07E-01	3.60E+03
84	1.39E+05	4.91E+00	1.09E+00	1.11E+00	3.60E+03
85	1.39E+05	5.64E+00	1.07E+00	4.05E-01	3.60E+03
86	1.40E+05	4.91E+00	8.90E-01	7.59E-01	3.60E+03

Surry ISLOCA					
Plume Segment	**PDELAY**	**PLHITE**	**PLMDEN**	**PLMFLA**	**PLUDUR**
87	1.42E+05	4.91E+00	1.05E+00	1.16E+00	4.50E+03
88	1.42E+05	5.64E+00	1.02E+00	4.22E-01	4.50E+03
89	1.44E+05	4.91E+00	8.54E-01	9.27E-01	3.60E+03
90	1.47E+05	4.91E+00	1.01E+00	1.19E+00	2.70E+03
91	1.48E+05	4.91E+00	8.60E-01	1.09E+00	3.60E+03
92	1.49E+05	4.91E+00	1.06E+00	1.22E+00	3.60E+03
93	1.51E+05	4.91E+00	8.62E-01	1.08E+00	3.60E+03
94	1.53E+05	4.91E+00	1.08E+00	1.21E+00	3.60E+03
95	1.55E+05	4.91E+00	8.62E-01	1.04E+00	3.60E+03
96	1.57E+05	4.91E+00	1.10E+00	1.19E+00	3.60E+03
97	1.58E+05	4.91E+00	8.64E-01	1.02E+00	3.60E+03
98	1.60E+05	4.91E+00	1.05E+00	1.14E+00	4.50E+03
99	1.60E+05	7.90E+00	1.08E+00	5.15E-01	4.50E+03
100	1.60E+05	5.64E+00	1.03E+00	4.25E-01	4.50E+03
101	1.62E+05	4.91E+00	8.64E-01	8.23E-01	3.60E+03
102	1.62E+05	3.38E+00	1.14E+00	7.27E+00	3.60E+03
103	1.65E+05	4.91E+00	1.08E+00	9.95E-01	2.70E+03
104	1.65E+05	7.90E+00	1.08E+00	4.70E-01	2.70E+03
105	1.66E+05	4.91E+00	8.65E-01	6.22E-01	3.60E+03
106	1.67E+05	4.91E+00	1.11E+00	9.62E-01	3.60E+03
107	1.69E+05	4.91E+00	8.69E-01	6.18E-01	3.60E+03

Surry Mitigated TISGTR					
Plume Segment	**PDELAY**	**PLHITE**	**PLMDEN**	**PLMFLA**	**PLUDUR**
1	10600	8.4	0.73919	4.11E-04	3619.6
2	12800	24.643	0.29498	1.0716	3639.9
3	14220	8.4	0.6666	7.40E-04	3600.4
4	16440	24.643	0.3208	0.091864	3600.1
5	17820	8.4	0.64171	8.13E-04	3599.9
6	20040	24.643	0.2937	0.08302	3599.9
7	21420	8.4	0.62148	8.23E-04	3600
8	23640	24.643	0.28461	0.074318	3600
9	25020	8.4	0.60385	8.97E-04	3599.9
10	27240	24.643	0.33478	0.088723	3600.1
11	28620	8.4	0.6199	8.26E-04	3660.1
12	30840	24.643	0.33994	0.069402	3600.1
13	34440	24.643	0.3649	0.039585	3599.9
14	38040	24.643	0.40498	0.01627	3600
15	41640	24.643	0.71955	0.002878	3600
16	52440	24.643	0.71162	0.007903	3600
17	56040	24.643	0.50849	0.036427	3599.9
18	59640	24.643	0.42415	0.045113	3600.2
19	63240	24.643	0.41032	0.05232	3599.9
20	66840	24.643	0.40342	0.058182	3600
21	70440	24.643	0.39798	0.063655	3600.1
22	74040	24.643	0.39336	0.069014	3599.8
23	77640	24.643	0.38949	0.074187	3600
24	81240	24.643	0.38619	0.079248	3600.2
25	84840	24.643	0.38476	0.081656	3599.9
26	88440	24.643	0.3831	0.085028	3600
27	92040	24.643	0.38153	0.088779	3599.9
28	95640	24.643	0.38011	0.09261	3600
29	99240	24.643	0.37894	0.096455	3600.1
30	1.03E+05	24.643	0.37793	0.10035	3600.1
31	1.06E+05	24.643	0.37704	0.10438	3600
32	1.10E+05	24.643	0.3762	0.10847	3599.9
33	1.14E+05	24.643	0.37533	0.11268	3600.1
34	1.17E+05	24.643	0.37489	0.11697	3600.1
35	1.21E+05	24.643	0.37457	0.12131	3599.8
36	1.24E+05	24.643	0.37437	0.12571	3600
37	1.28E+05	24.643	0.37426	0.13016	3600.1
38	1.32E+05	24.643	0.37422	0.13468	3600
39	1.35E+05	24.643	0.37428	0.13924	3600
40	1.39E+05	24.643	0.37442	0.14384	3599.9
41	1.42E+05	24.643	0.37464	0.14848	3600.2
42	1.46E+05	24.643	0.37494	0.15318	3599.9
43	1.50E+05	24.643	0.3753	0.15791	3600.1

Surry Mitigated TISGTR					
Plume Segment	**PDELAY**	**PLHITE**	**PLMDEN**	**PLMFLA**	**PLUDUR**
44	1.53E+05	24.643	0.37573	0.16268	3599.9
45	1.57E+05	24.643	0.37623	0.1675	3599.8
46	1.60E+05	24.643	0.37687	0.17236	3600.3
47	1.64E+05	24.643	0.37757	0.17724	3599.7
48	1.68E+05	24.643	0.37832	0.18216	3600.1
49	1.71E+05	24.643	0.37889	0.1857	1560.1

Surry Unmitigated TISGTR					
Plume Segment	**PDELAY**	**PLHITE**	**PLMDEN**	**PLMFLA**	**PLUDUR**
1	10600	8.4	7.39E-01	4.11E-04	3619.6
2	12800	24.643	2.95E-01	1.07E+00	3639.9
3	14220	8.4	6.67E-01	7.40E-04	3600.4
4	16440	24.643	3.21E-01	9.19E-02	3600.1
5	17820	8.4	6.42E-01	8.13E-04	3599.9
6	20040	24.643	2.94E-01	8.30E-02	3599.9
7	21420	8.4	6.21E-01	8.23E-04	3600
8	23640	24.643	2.85E-01	7.43E-02	3600
9	25020	8.4	6.04E-01	8.97E-04	3599.9
10	27240	24.643	3.45E-01	9.66E-02	3600
11	28620	8.4	5.80E-01	1.08E-03	3660
12	30840	24.643	3.64E-01	1.06E-01	3600
13	32280	8.4	5.66E-01	1.12E-03	3600.2
14	34440	24.643	3.62E-01	1.12E-01	3600.1
15	35880	8.4	5.60E-01	1.18E-03	3600
16	38040	24.643	3.58E-01	1.18E-01	3600.1
17	39480	8.4	5.55E-01	1.24E-03	3600
18	41640	24.643	3.55E-01	1.24E-01	3599.9
19	43080	8.4	5.49E-01	1.31E-03	3600
20	45240	24.643	3.53E-01	1.29E-01	3600.1
21	46680	8.4	5.43E-01	1.37E-03	3600.1
22	48840	24.643	3.55E-01	1.36E-01	3600.1
23	50280	8.4	5.39E-01	1.43E-03	3600
24	52440	24.643	3.52E-01	1.42E-01	3599.8
25	53880	8.4	5.35E-01	1.51E-03	3600
26	56040	24.643	3.48E-01	1.49E-01	3600
27	57480	8.4	5.31E-01	1.60E-03	3599.9
28	59640	24.643	3.45E-01	1.55E-01	3600
29	61080	8.4	5.28E-01	1.66E-03	3600
30	63240	24.643	3.42E-01	1.63E-01	3600.1
31	64680	8.4	5.24E-01	1.74E-03	3599.8
32	66840	24.643	3.39E-01	1.70E-01	3600
33	68280	8.4	5.21E-01	1.83E-03	3600.3
34	70440	24.643	3.36E-01	1.78E-01	3599.9
35	71880	8.4	5.18E-01	1.92E-03	3599.9
36	74040	24.643	3.33E-01	1.86E-01	3600.1
37	75480	8.4	5.14E-01	2.01E-03	3600
38	77640	24.643	3.31E-01	1.95E-01	3600
39	79080	8.4	5.11E-01	2.10E-03	3600
40	81240	24.643	3.29E-01	2.03E-01	3600.1
41	82680	8.4	5.08E-01	2.18E-03	3599.8
42	84840	24.643	3.27E-01	2.12E-01	3599.8
43	86280	8.4	5.05E-01	2.27E-03	3600.3

Surry Unmitigated TISGTR					
Plume Segment	**PDELAY**	**PLHITE**	**PLMDEN**	**PLMFLA**	**PLUDUR**
44	88440	24.643	3.26E-01	2.20E-01	3600.2
45	89880	8.4	5.02E-01	2.36E-03	3600
46	92040	24.643	3.24E-01	2.29E-01	3599.9
47	93480	8.4	4.99E-01	2.45E-03	3599.8
48	95640	24.643	3.23E-01	2.38E-01	3599.8
49	97080	8.4	4.97E-01	2.55E-03	3600
50	99240	24.643	3.22E-01	2.47E-01	3600.3
51	1.00E+05	8.4	4.94E-01	1.72E-01	3720
52	1.01E+05	8.4	4.94E-01	2.63E-03	3600
53	1.03E+05	24.643	3.21E-01	2.55E-01	3600
54	1.04E+05	8.4	4.91E-01	5.45E-01	3480.1
55	1.04E+05	8.4	4.91E-01	2.71E-03	3600.1
56	1.06E+05	24.643	3.20E-01	2.62E-01	3600
57	1.08E+05	8.4	4.89E-01	9.81E-01	3720
58	1.08E+05	8.4	4.89E-01	2.76E-03	3600.1
59	1.10E+05	24.643	3.20E-01	2.67E-01	3600
60	1.11E+05	8.4	4.87E-01	1.36E+00	3599.9
61	1.11E+05	8.4	4.87E-01	2.79E-03	3600
62	1.14E+05	24.643	3.19E-01	2.70E-01	3600
63	1.15E+05	8.4	4.85E-01	1.61E+00	3480.3
64	1.15E+05	8.4	4.85E-01	2.79E-03	3561.3
65	1.17E+05	24.643	3.18E-01	2.71E-01	3600
66	1.18E+05	8.4	4.83E-01	1.77E+00	3719.9
67	1.19E+05	8.4	4.83E-01	2.86E-03	3638.5
68	1.21E+05	24.643	3.18E-01	2.72E-01	3599.8
69	1.22E+05	8.4	4.81E-01	1.86E+00	3599.8
70	1.22E+05	8.4	4.81E-01	2.82E-03	3600.1
71	1.24E+05	24.643	3.17E-01	2.73E-01	3600.2
72	1.26E+05	8.4	4.79E-01	1.91E+00	3600.2
73	1.26E+05	8.4	4.79E-01	2.81E-03	3600.1
74	1.28E+05	24.643	3.17E-01	2.73E-01	3599.9
75	1.29E+05	8.4	4.77E-01	1.94E+00	3480
76	1.29E+05	8.4	4.77E-01	2.81E-03	3600
77	1.32E+05	24.643	3.16E-01	2.74E-01	3600
78	1.33E+05	8.4	4.75E-01	1.95E+00	3600.1
79	1.33E+05	8.4	4.75E-01	2.81E-03	3599.7
80	1.35E+05	24.643	3.16E-01	2.74E-01	3600.1
81	1.36E+05	8.4	4.73E-01	1.97E+00	3599.9
82	1.37E+05	8.4	4.73E-01	2.80E-03	3600.1
83	1.39E+05	24.643	3.16E-01	2.74E-01	3600
84	1.40E+05	8.4	4.72E-01	1.98E+00	3720.1
85	1.40E+05	8.4	4.72E-01	2.80E-03	3600
86	1.42E+05	24.643	3.15E-01	2.74E-01	3599.9

Surry Unmitigated TISGTR					
Plume Segment	**PDELAY**	**PLHITE**	**PLMDEN**	**PLMFLA**	**PLUDUR**
87	1.44E+05	8.4	4.67E-01	2.03E+00	3479.8
88	1.44E+05	8.4	4.67E-01	2.78E-03	3600.1
89	1.46E+05	24.643	3.15E-01	2.71E-01	3599.8
90	1.47E+05	8.4	4.62E-01	2.01E+00	3720.1
91	1.47E+05	8.4	4.62E-01	2.73E-03	3600
92	1.50E+05	24.643	3.15E-01	2.67E-01	3600.3
93	1.51E+05	8.4	4.60E-01	1.97E+00	3479.9
94	1.51E+05	8.4	4.60E-01	2.67E-03	3600
95	1.53E+05	24.643	3.14E-01	2.62E-01	3599.7
96	1.54E+05	8.4	4.57E-01	1.94E+00	3600
97	1.55E+05	8.4	4.57E-01	2.62E-03	3600
98	1.57E+05	24.643	3.14E-01	2.57E-01	3600.4
99	1.58E+05	8.4	4.55E-01	1.90E+00	3600.2
100	1.58E+05	8.4	4.55E-01	2.57E-03	3600.1
101	1.60E+05	24.643	3.14E-01	2.52E-01	3599.6
102	1.62E+05	8.4	4.53E-01	1.86E+00	3719.9
103	1.62E+05	8.4	4.53E-01	2.51E-03	3599.8
104	1.64E+05	24.643	3.14E-01	2.48E-01	3600
105	1.65E+05	8.4	4.51E-01	1.83E+00	3480
106	1.65E+05	8.4	4.51E-01	2.46E-03	3600.3
107	1.68E+05	24.643	3.13E-01	2.43E-01	3600.3
108	1.69E+05	8.4	4.49E-01	1.79E+00	3600
109	1.69E+05	8.4	4.49E-01	2.41E-03	3599.8
110	1.71E+05	24.643	3.13E-01	2.40E-01	1559.9
111	1.72E+05	8.4	4.49E-01	1.77E+00	359.91
112	1.73E+05	8.4	4.48E-01	2.38E-03	120
113	1.73E+05	8.4	4.48E-01	1.77E+00	119.89
114	1.73E+05	8.4	4.48E-01	2.38E-03	119.89
115	1.73E+05	24.643	3.13E-01	2.38E-01	119.89

Table C-3 Plume Parameters Used in the Surry LTSBO, Unmitigated STSBO, TI-SGTR Mitigated and Unmitigated Scenarios

Surry LTSBO										
Class	**Bin 1**	**Bin 2**	**Bin 3**	**Bin 4**	**Bin 5**	**Bin 6**	**Bin 7**	**Bin 8**	**Bin 9**	**Bin 10**
Xe	1.00E-01	1.00E-01	1.00E-01	1.00E-01	1.00E-01	1.00E-01	1.00E-01	1.00E-01	1.00E-01	1.00E-01
Cs	1.73E-03	1.26E-02	6.19E-02	2.00E-01	3.36E-01	2.52E-01	1.09E-01	2.37E-02	2.32E-03	1.05E-03
Ba	6.94E-03	3.56E-02	1.35E-01	3.69E-01	3.45E-01	8.98E-02	1.49E-02	2.50E-03	2.54E-04	3.58E-04
I	6.47E-03	3.22E-02	1.21E-01	3.28E-01	3.57E-01	1.32E-01	1.85E-02	1.95E-03	3.19E-04	1.44E-03
Te	7.53E-03	3.45E-02	1.31E-01	3.49E-01	3.40E-01	1.14E-01	1.86E-02	2.44E-03	2.44E-04	1.34E-03
Ru	8.80E-03	3.73E-02	1.35E-01	3.24E-01	3.13E-01	1.27E-01	2.71E-02	1.02E-02	3.38E-03	1.40E-02
Mo	2.39E-04	3.89E-03	2.78E-02	1.01E-01	2.67E-01	3.30E-01	1.98E-01	6.34E-02	8.46E-03	3.76E-04
Ce	7.52E-03	3.22E-02	1.15E-01	2.85E-01	3.34E-01	1.73E-01	3.59E-02	7.97E-03	1.65E-03	8.02E-03
La	4.89E-03	2.37E-02	9.23E-02	2.54E-01	3.44E-01	2.04E-01	6.15E-02	1.20E-02	1.34E-03	2.86E-03

Surry Unmitigated STSBO										
Class	**Bin 1**	**Bin 2**	**Bin 3**	**Bin 4**	**Bin 5**	**Bin 6**	**Bin 7**	**Bin 8**	**Bin 9**	**Bin 10**
Xe	1.00E-01	1.00E-01	1.00E-01	1.00E-01	1.00E-01	1.00E-01	1.00E-01	1.00E-01	1.00E-01	1.00E-01
Cs	1.22E-03	1.01E-02	5.26E-02	1.73E-01	3.33E-01	2.86E-01	1.21E-01	2.05E-02	1.15E-03	1.19E-03
Ba	7.02E-03	3.61E-02	1.42E-01	3.43E-01	3.18E-01	1.19E-01	2.65E-02	3.58E-03	2.58E-04	4.40E-03
I	6.19E-03	2.94E-02	1.06E-01	2.66E-01	3.44E-01	2.03E-01	3.96E-02	2.54E-03	1.97E-04	2.36E-03
Te	4.03E-03	2.31E-02	9.45E-02	2.70E-01	3.62E-01	1.94E-01	4.57E-02	4.65E-03	2.33E-04	1.50E-03
Ru	5.15E-03	2.69E-02	1.07E-01	2.75E-01	3.43E-01	1.80E-01	4.05E-02	6.86E-03	1.67E-03	1.36E-02
Mo	2.51E-04	4.22E-03	3.10E-02	1.14E-01	2.91E-01	3.42E-01	1.78E-01	3.66E-02	2.37E-03	9.36E-05
Ce	5.06E-03	2.57E-02	9.95E-02	2.57E-01	3.41E-01	2.04E-01	4.92E-02	6.85E-03	1.30E-03	9.52E-03
La	3.14E-03	1.80E-02	7.61E-02	2.18E-01	3.44E-01	2.45E-01	8.08E-02	1.18E-02	7.95E-04	2.68E-03

Surry ISLOCA										
Class	**Bin 1**	**Bin 2**	**Bin 3**	**Bin 4**	**Bin 5**	**Bin 6**	**Bin 7**	**Bin 8**	**Bin 9**	**Bin 10**
Xe	1.00E-01	1.00E-01	1.00E-01	1.00E-01	1.00E-01	1.00E-01	1.00E-01	1.00E-01	1.00E-01	1.00E-01
Cs	9.37E-03	2.56E-02	6.96E-02	2.73E-01	4.01E-01	1.78E-01	4.04E-02	2.62E-03	4.33E-05	5.48E-04
Ba	2.23E-02	4.72E-02	1.38E-01	2.92E-01	3.24E-01	1.41E-01	3.05E-02	2.46E-03	7.74E-05	2.58E-03
I	9.15E-03	2.41E-02	7.56E-02	2.81E-01	3.96E-01	1.72E-01	3.85E-02	2.53E-03	4.28E-05	6.21E-04
Te	1.28E-02	3.01E-02	8.65E-02	2.83E-01	3.82E-01	1.65E-01	3.72E-02	2.50E-03	4.58E-05	5.42E-04
Ru	1.13E-02	3.05E-02	9.69E-02	2.91E-01	3.75E-01	1.59E-01	3.34E-02	2.13E-03	3.54E-05	4.80E-04
Mo	1.02E-02	2.46E-02	6.13E-02	2.34E-01	3.80E-01	2.16E-01	6.41E-02	8.89E-03	7.41E-04	3.93E-04
Ce	7.90E-03	3.31E-02	2.20E-01	4.00E-01	1.92E-01	8.59E-02	4.09E-02	1.27E-02	1.26E-03	6.03E-03
La	2.07E-02	4.49E-02	2.46E-01	3.92E-01	1.74E-01	7.55E-02	3.43E-02	9.34E-03	8.08E-04	2.15E-03

.

Surry Mitigated TISGTR										
Class	**Bin 1**	**Bin 2**	**Bin 3**	**Bin 4**	**Bin 5**	**Bin 6**	**Bin 7**	**Bin 8**	**Bin 9**	**Bin 10**
Xe	1.00E-01	1.00E-01	1.00E-01	1.00E-01	1.00E-01	1.00E-01	1.00E-01	1.00E-01	1.00E-01	1.00E-01
Cs	2.39E-02	3.93E-02	6.33E-02	2.06E-01	3.47E-01	2.16E-01	7.68E-02	2.30E-02	4.35E-03	6.63E-04
Ba	1.29E-02	1.87E-02	5.47E-02	2.44E-01	4.15E-01	1.96E-01	4.50E-02	1.17E-02	2.38E-03	3.65E-04
I	3.45E-02	4.99E-02	6.35E-02	2.09E-01	3.47E-01	2.03E-01	6.82E-02	2.00E-02	3.72E-03	5.92E-04
Te	1.50E-02	2.65E-02	5.69E-02	2.17E-01	3.69E-01	2.16E-01	7.29E-02	2.20E-02	4.16E-03	6.11E-04
Ru	1.60E-03	5.33E-03	3.94E-02	2.20E-01	4.24E-01	2.24E-01	6.31E-02	1.87E-02	3.45E-03	4.43E-04
Mo	1.61E-02	5.22E-02	6.90E-02	2.98E-01	4.12E-01	1.16E-01	2.79E-02	6.85E-03	1.28E-03	1.92E-04
Ce	1.27E-03	8.45E-03	7.31E-02	2.80E-01	4.20E-01	1.79E-01	2.96E-02	7.03E-03	2.00E-03	2.70E-04
La	8.71E-03	2.82E-02	8.14E-02	2.99E-01	4.07E-01	1.45E-01	2.36E-02	5.32E-03	1.43E-03	1.89E-04

Surry Unmitigated TISGTR										
Class	**Bin 1**	**Bin 2**	**Bin 3**	**Bin 4**	**Bin 5**	**Bin 6**	**Bin 7**	**Bin 8**	**Bin 9**	**Bin 10**
Xe	1.00E-01	1.00E-01	1.00E-01	1.00E-01	1.00E-01	1.00E-01	1.00E-01	1.00E-01	1.00E-01	1.00E-01
Cs	4.84E-03	1.55E-02	5.85E-02	1.91E-01	4.04E-01	2.69E-01	5.05E-02	5.54E-03	7.83E-04	1.17E-04
Ba	6.37E-03	2.58E-02	8.09E-02	2.35E-01	3.81E-01	2.25E-01	4.35E-02	2.94E-03	2.34E-04	4.00E-05
I	1.14E-02	2.75E-02	6.76E-02	2.02E-01	3.54E-01	2.49E-01	7.56E-02	1.12E-02	1.36E-03	2.20E-04
Te	8.56E-03	2.61E-02	7.12E-02	2.00E-01	3.56E-01	2.59E-01	7.19E-02	7.63E-03	6.94E-04	1.06E-04
Ru	1.80E-03	6.34E-03	4.20E-02	2.21E-01	4.19E-01	2.23E-01	6.39E-02	1.89E-02	3.48E-03	4.41E-04
Mo	3.95E-03	1.86E-02	6.60E-02	1.76E-01	3.29E-01	2.92E-01	1.04E-01	1.05E-02	3.31E-04	8.27E-05
Ce	4.18E-03	2.17E-02	9.15E-02	2.48E-01	3.59E-01	2.03E-01	5.65E-02	1.35E-02	2.38E-03	2.42E-04
La	2.27E-03	1.47E-02	6.50E-02	2.00E-01	3.99E-01	2.64E-01	5.12E-02	3.73E-03	2.51E-04	2.79E-05

Table C-4 Release Fraction Parameters Used in the Surry LTSBO, Unmitigated STSBO, TI-SGTR Mitigated and Unmitigated Scenarios

Surry LTSBO									
Plume Segment	**Xe**	**Cs**	**Ba**	**I**	**Te**	**Ru**	**Mo**	**Ce**	**La**
1	3.36E-03	3.50E-06	5.31E-07	3.62E-05	5.09E-05	7.77E-08	2.69E-07	1.93E-07	1.21E-08
2	7.20E-03	7.08E-06	1.03E-06	7.43E-05	1.04E-04	1.52E-07	5.22E-07	3.77E-07	2.42E-08
3	1.27E-02	1.17E-05	1.64E-06	1.24E-04	1.75E-04	2.44E-07	8.35E-07	6.06E-07	3.96E-08
4	1.80E-02	1.55E-05	2.17E-06	1.66E-04	2.36E-04	3.18E-07	1.09E-06	7.92E-07	5.28E-08
5	2.24E-02	1.79E-05	2.51E-06	1.94E-04	2.79E-04	3.63E-07	1.23E-06	9.05E-07	6.15E-08
6	2.35E-02	1.76E-05	2.47E-06	1.91E-04	2.78E-04	3.50E-07	1.19E-06	8.74E-07	6.07E-08
7	2.55E-02	1.79E-05	2.52E-06	1.96E-04	2.87E-04	3.50E-07	1.18E-06	8.75E-07	6.20E-08
8	2.59E-02	1.71E-05	2.41E-06	1.88E-04	2.79E-04	3.27E-07	1.10E-06	8.20E-07	5.94E-08
9	2.58E-02	1.60E-05	2.27E-06	1.78E-04	2.66E-04	3.02E-07	1.01E-06	7.57E-07	5.62E-08
10	2.54E-02	1.49E-05	2.12E-06	1.67E-04	2.54E-04	2.76E-07	9.16E-07	6.93E-07	5.27E-08
11	2.50E-02	1.39E-05	1.98E-06	1.57E-04	2.42E-04	2.51E-07	8.29E-07	6.33E-07	4.94E-08
12	2.45E-02	1.29E-05	1.86E-06	1.48E-04	2.32E-04	2.29E-07	7.50E-07	5.79E-07	4.64E-08
13	2.42E-02	1.21E-05	1.75E-06	1.40E-04	2.25E-04	2.10E-07	6.81E-07	5.32E-07	4.38E-08
14	2.34E-02	1.12E-05	1.62E-06	1.30E-04	2.16E-04	1.90E-07	6.09E-07	4.82E-07	4.08E-08
15	2.27E-02	1.04E-05	1.52E-06	1.22E-04	2.09E-04	1.72E-07	5.45E-07	4.37E-07	3.81E-08
16	2.21E-02	9.69E-06	1.42E-06	1.15E-04	2.03E-04	1.56E-07	4.88E-07	3.98E-07	3.59E-08
17	2.16E-02	9.11E-06	1.35E-06	1.09E-04	2.00E-04	1.43E-07	4.40E-07	3.66E-07	3.40E-08
18	2.11E-02	8.57E-06	1.27E-06	1.04E-04	1.98E-04	1.31E-07	3.96E-07	3.36E-07	3.22E-08
19	2.06E-02	8.08E-06	1.21E-06	9.86E-05	1.98E-04	1.20E-07	3.55E-07	3.09E-07	3.07E-08
20	2.00E-02	7.60E-06	1.15E-06	9.37E-05	1.97E-04	1.09E-07	3.17E-07	2.83E-07	2.91E-08
21	1.94E-02	7.17E-06	1.09E-06	8.93E-05	1.97E-04	1.00E-07	2.83E-07	2.60E-07	2.76E-08
22	1.90E-02	6.81E-06	1.04E-06	8.56E-05	1.99E-04	9.19E-08	2.54E-07	2.40E-07	2.64E-08
23	1.87E-02	6.57E-06	9.94E-07	8.34E-05	2.04E-04	8.55E-08	2.31E-07	2.24E-07	2.56E-08
24	1.81E-02	6.23E-06	9.12E-07	7.96E-05	2.08E-04	7.79E-08	2.06E-07	2.05E-07	2.44E-08
25	1.75E-02	5.91E-06	8.37E-07	7.63E-05	2.17E-04	7.08E-08	1.83E-07	1.88E-07	2.32E-08
26	1.75E-02	5.82E-06	7.95E-07	7.57E-05	2.40E-04	6.64E-08	1.68E-07	1.77E-07	2.28E-08
27	1.10E-02	3.62E-06	4.78E-07	4.73E-05	1.67E-04	3.94E-08	9.86E-08	1.06E-07	1.41E-08
28	5.41E-04	1.78E-07	2.32E-08	2.33E-06	8.68E-06	1.90E-09	4.73E-09	5.10E-09	6.93E-10

Surry Unmitigated STSBO									
Plume Segment	**Xe**	**Cs**	**Ba**	**I**	**Te**	**Ru**	**Mo**	**Ce**	**La**
1	0.003864	6.41E-06	1.13E-06	5.54E-05	8.81E-05	1.60E-07	6.91E-07	2.84E-07	1.18E-08
2	0.008938	1.38E-05	2.41E-06	1.24E-04	1.85E-04	3.30E-07	1.41E-06	5.85E-07	2.51E-08
3	0.017434	2.53E-05	4.36E-06	2.35E-04	3.28E-04	5.74E-07	2.42E-06	1.02E-06	4.52E-08
4	0.022579	3.11E-05	5.28E-06	3.00E-04	3.88E-04	6.68E-07	2.79E-06	1.19E-06	5.43E-08
5	0.027673	3.66E-05	6.12E-06	3.64E-04	4.39E-04	7.39E-07	3.05E-06	1.32E-06	6.21E-08
6	0.029568	3.78E-05	6.20E-06	3.89E-04	4.33E-04	7.14E-07	2.91E-06	1.28E-06	6.21E-08
7	0.03103	3.83E-05	6.20E-06	4.05E-04	4.21E-04	6.79E-07	2.73E-06	1.21E-06	6.13E-08
8	0.02978	3.50E-05	5.70E-06	3.78E-04	3.77E-04	5.92E-07	2.35E-06	1.06E-06	5.56E-08
9	0.029251	3.30E-05	5.41E-06	3.64E-04	3.47E-04	5.31E-07	2.08E-06	9.54E-07	5.19E-08
10	0.028631	3.12E-05	5.14E-06	3.51E-04	3.20E-04	4.76E-07	1.83E-06	8.58E-07	4.85E-08
11	0.02691	2.85E-05	4.72E-06	3.27E-04	2.84E-04	4.12E-07	1.55E-06	7.44E-07	4.38E-08
12	0.026992	2.79E-05	4.64E-06	3.27E-04	2.71E-04	3.81E-07	1.40E-06	6.90E-07	4.23E-08
13	0.02698	2.74E-05	4.52E-06	3.27E-04	2.58E-04	3.52E-07	1.27E-06	6.38E-07	4.09E-08
14	0.024411	2.45E-05	4.01E-06	2.97E-04	2.23E-04	2.95E-07	1.04E-06	5.36E-07	3.59E-08
15	0.024422	2.43E-05	3.95E-06	2.99E-04	2.14E-04	2.74E-07	9.45E-07	5.00E-07	3.50E-08
16	0.02437	2.42E-05	3.90E-06	3.02E-04	2.06E-04	2.54E-07	8.57E-07	4.65E-07	3.41E-08
17	0.02283	2.26E-05	3.62E-06	2.86E-04	1.86E-04	2.21E-07	7.32E-07	4.07E-07	3.13E-08
18	0.021296	2.07E-05	3.29E-06	2.64E-04	1.69E-04	1.93E-07	6.25E-07	3.56E-07	2.87E-08
19	0.021444	1.99E-05	3.12E-06	2.55E-04	1.65E-04	1.82E-07	5.78E-07	3.37E-07	2.84E-08
20	0.020818	1.84E-05	2.81E-06	2.37E-04	1.56E-04	1.65E-07	5.15E-07	3.07E-07	2.72E-08
21	0.020733	1.74E-05	2.60E-06	2.25E-04	1.52E-04	1.53E-07	4.70E-07	2.87E-07	2.67E-08
22	0.018699	1.50E-05	2.24E-06	1.95E-04	1.33E-04	1.29E-07	3.90E-07	2.43E-07	2.38E-08
23	0.008789	6.81E-06	1.06E-06	8.87E-05	6.16E-05	5.77E-08	1.73E-07	1.09E-07	1.11E-08
24	6.22E-04	4.76E-07	7.62E-08	6.21E-06	4.33E-06	4.01E-09	1.20E-08	7.59E-09	7.84E-10
25	0.003864	6.41E-06	1.13E-06	5.54E-05	8.81E-05	1.60E-07	6.91E-07	2.84E-07	1.18E-08
26	0.008938	1.38E-05	2.41E-06	1.24E-04	1.85E-04	3.30E-07	1.41E-06	5.85E-07	2.51E-08
27	0.017434	2.53E-05	4.36E-06	2.35E-04	3.28E-04	5.74E-07	2.42E-06	1.02E-06	4.52E-08
28	0.022579	3.11E-05	5.28E-06	3.00E-04	3.88E-04	6.68E-07	2.79E-06	1.19E-06	5.43E-08
29	0.027673	3.66E-05	6.12E-06	3.64E-04	4.39E-04	7.39E-07	3.05E-06	1.32E-06	6.21E-08
30	0.029568	3.78E-05	6.20E-06	3.89E-04	4.33E-04	7.14E-07	2.91E-06	1.28E-06	6.21E-08
31	0.03103	3.83E-05	6.20E-06	4.05E-04	4.21E-04	6.79E-07	2.73E-06	1.21E-06	6.13E-08
32	0.02978	3.50E-05	5.70E-06	3.78E-04	3.77E-04	5.92E-07	2.35E-06	1.06E-06	5.56E-08
33	0.029251	3.30E-05	5.41E-06	3.64E-04	3.47E-04	5.31E-07	2.08E-06	9.54E-07	5.19E-08

Surry ISLOCA									
Plume Segment	Xe	Cs	Ba	I	Te	Ru	Mo	Ce	La
1	1.69E-01	4.06E-05	3.31E-07	2.78E-04	2.62E-04	2.94E-07	5.76E-06	3.45E-11	3.18E-11
2	1.69E-01	4.06E-05	3.31E-07	2.78E-04	2.62E-04	2.94E-07	5.76E-06	3.45E-11	3.18E-11
3	3.74E-02	1.90E-03	7.82E-06	1.38E-02	1.17E-02	1.88E-05	2.58E-04	2.12E-09	1.97E-09
4	6.30E-02	3.39E-03	1.38E-05	2.50E-02	2.12E-02	3.49E-05	4.59E-04	3.94E-09	3.67E-09
5	1.84E-03	9.89E-05	3.27E-07	6.88E-04	5.85E-04	7.40E-07	1.42E-05	8.74E-11	8.20E-11
6	1.67E-01	9.01E-03	3.57E-05	6.62E-02	5.65E-02	9.23E-05	1.22E-03	1.04E-08	9.74E-09
7	1.47E-02	8.96E-04	2.50E-06	6.76E-03	5.66E-03	1.07E-05	1.19E-04	1.15E-09	1.06E-09
8	9.90E-02	2.71E-05	1.22E-07	2.20E-04	2.02E-04	4.19E-07	3.30E-06	4.77E-11	4.49E-11
9	9.90E-02	2.71E-05	1.22E-07	2.20E-04	2.02E-04	4.19E-07	3.30E-06	4.77E-11	4.49E-11
10	3.66E-02	1.88E-03	9.81E-06	1.55E-02	1.40E-02	2.90E-05	2.23E-04	3.34E-09	3.23E-09
11	2.36E-02	8.73E-04	6.97E-06	8.57E-03	5.73E-03	2.66E-05	7.64E-05	4.00E-09	3.78E-09
12	6.07E-03	2.36E-04	1.58E-06	2.13E-03	1.59E-03	5.53E-06	2.43E-05	7.65E-10	7.22E-10
13	8.81E-03	3.27E-04	2.62E-06	3.21E-03	2.14E-03	1.01E-05	2.86E-05	1.51E-09	1.42E-09
14	1.27E-02	3.65E-04	3.51E-06	3.78E-03	2.43E-03	1.45E-05	2.81E-05	2.15E-09	2.03E-09
15	2.21E-02	3.33E-06	3.81E-08	3.55E-05	2.30E-05	1.35E-07	2.38E-07	2.11E-11	1.99E-11
16	2.21E-02	3.33E-06	3.81E-08	3.55E-05	2.30E-05	1.35E-07	2.38E-07	2.11E-11	1.99E-11
17	3.61E-03	1.05E-04	2.45E-06	1.19E-03	6.08E-04	1.11E-06	5.30E-06	3.37E-10	3.19E-10
18	1.09E-03	3.24E-05	5.70E-07	3.58E-04	2.14E-04	7.16E-07	1.91E-06	1.57E-10	1.51E-10
19	1.59E-03	4.62E-05	1.01E-06	5.22E-04	2.64E-04	4.84E-07	2.31E-06	1.47E-10	1.39E-10
20	8.99E-04	2.72E-05	1.12E-06	2.49E-04	1.63E-04	2.26E-07	2.06E-06	3.31E-11	3.18E-11
21	4.73E-03	4.89E-07	1.06E-08	5.62E-06	2.16E-06	2.40E-09	2.06E-08	4.53E-13	4.29E-13
22	4.73E-03	4.89E-07	1.06E-08	5.62E-06	2.16E-06	2.40E-09	2.06E-08	4.53E-13	4.29E-13
23	4.37E-04	3.08E-05	6.50E-07	3.07E-04	1.69E-04	2.27E-07	2.26E-06	8.01E-11	7.47E-11
24	2.90E-04	1.65E-05	3.66E-07	1.67E-04	8.59E-05	1.20E-07	1.16E-06	3.72E-11	3.47E-11
25	2.85E-04	2.04E-05	4.43E-07	2.02E-04	1.12E-04	1.54E-07	1.52E-06	5.24E-11	4.88E-11
26	3.46E-03	1.77E-06	3.53E-08	1.71E-05	1.09E-05	2.35E-08	1.44E-07	8.27E-12	7.63E-12
27	3.46E-03	1.77E-06	3.53E-08	1.71E-05	1.09E-05	2.35E-08	1.44E-07	8.27E-12	7.63E-12
28	2.90E-03	5.23E-07	1.14E-08	5.29E-06	4.57E-06	2.77E-08	4.48E-08	6.73E-12	6.33E-12
29	2.90E-03	5.23E-07	1.14E-08	5.29E-06	4.57E-06	2.77E-08	4.48E-08	6.73E-12	6.33E-12
30	8.94E-07	7.45E-08	9.77E-09	8.72E-07	7.60E-07	7.71E-10	2.91E-09	3.71E-08	1.60E-09
31	2.09E-06	7.89E-08	4.17E-09	8.23E-07	7.30E-07	3.00E-09	5.91E-09	1.06E-08	4.58E-10
32	4.25E-07	3.00E-08	3.70E-09	3.56E-07	3.13E-07	3.82E-10	1.34E-09	1.38E-08	5.95E-10
33	3.73E-08	1.25E-08	2.61E-08	3.42E-08	3.02E-08	2.92E-10	1.20E-09	1.49E-08	6.30E-10
34	8.35E-06	3.37E-07	2.33E-08	4.01E-06	4.02E-06	4.75E-09	1.44E-08	6.59E-08	2.92E-09
35	5.24E-06	9.34E-07	4.54E-08	1.26E-05	1.02E-05	2.62E-09	1.10E-08	1.21E-07	7.04E-09
36	7.76E-08	2.01E-08	4.12E-08	5.86E-08	5.57E-08	4.56E-10	1.92E-09	2.31E-08	1.02E-09
37	8.87E-08	1.69E-08	3.45E-08	5.16E-08	5.16E-08	3.75E-10	1.59E-09	1.90E-08	8.71E-10
38	3.99E-06	1.23E-06	4.35E-08	1.70E-05	1.02E-05	5.72E-10	4.81E-09	1.22E-07	7.92E-09
39	9.39E-07	5.34E-07	9.40E-09	7.47E-06	2.62E-06	8.00E-11	1.16E-09	2.53E-08	1.84E-09
40	3.58E-07	2.00E-07	3.63E-09	2.80E-06	9.87E-07	4.37E-11	3.49E-10	9.88E-09	7.14E-10
41	3.80E-07	2.20E-07	3.55E-09	3.10E-06	8.90E-07	4.37E-11	3.49E-10	1.04E-08	7.33E-10
42	9.27E-08	1.24E-08	2.47E-08	4.36E-08	4.04E-08	2.64E-10	1.13E-09	1.35E-08	6.41E-10
43	2.47E-06	1.26E-06	2.33E-08	1.76E-05	5.90E-06	2.28E-10	2.41E-09	6.36E-08	4.57E-09
44	1.39E-06	8.23E-07	1.15E-08	1.16E-05	2.19E-06	1.31E-10	9.31E-10	3.72E-08	2.54E-09
45	4.47E-07	2.60E-07	3.59E-09	3.65E-06	6.80E-07	4.00E-11	3.49E-10	1.15E-08	7.93E-10
46	3.47E-06	4.51E-06	2.63E-08	6.35E-05	6.90E-06	1.99E-10	3.79E-09	5.78E-08	5.02E-09
47	1.86E-06	7.33E-06	1.40E-08	1.03E-04	4.64E-06	7.55E-11	2.40E-09	2.60E-08	2.93E-09

Surry ISLOCA									
Plume Segment	Xe	Cs	Ba	I	Te	Ru	Mo	Ce	La
48	1.46E-06	1.06E-05	8.87E-09	1.49E-04	4.47E-06	6.55E-11	1.51E-09	1.70E-08	2.13E-09
49	8.05E-07	5.46E-06	5.14E-09	7.72E-05	2.39E-06	2.18E-11	8.73E-10	9.83E-09	1.22E-09
50	1.58E-06	9.65E-06	9.89E-09	1.36E-04	4.27E-06	5.26E-11	1.68E-09	1.81E-08	2.18E-09
51	4.49E-06	1.58E-05	3.21E-08	2.23E-04	7.14E-06	1.38E-10	2.68E-09	4.08E-08	3.39E-09
52	1.42E-06	5.42E-06	9.50E-09	7.66E-05	2.40E-06	4.73E-11	8.15E-10	1.25E-08	1.07E-09
53	3.41E-06	2.10E-05	1.54E-08	2.97E-04	8.60E-06	8.75E-11	2.32E-09	2.37E-08	2.73E-09
54	1.62E-06	2.08E-05	7.31E-09	2.94E-04	1.02E-05	2.64E-11	1.48E-09	9.50E-09	1.65E-09
55	1.74E-06	1.73E-05	9.86E-09	2.44E-04	2.12E-05	2.91E-11	1.51E-09	8.71E-09	1.76E-09
56	1.48E-06	1.69E-05	7.56E-09	2.38E-04	1.55E-05	1.84E-11	1.28E-09	7.19E-09	1.43E-09
57	1.91E-06	1.46E-05	1.53E-08	2.06E-04	3.25E-05	2.18E-11	1.86E-09	8.41E-09	1.82E-09
58	2.08E-06	1.43E-05	1.61E-08	2.03E-04	3.50E-05	2.17E-11	1.83E-09	8.76E-09	1.90E-09
59	3.90E-06	1.14E-05	4.19E-08	1.62E-04	1.05E-04	3.64E-11	3.96E-09	1.48E-08	3.48E-09
60	2.34E-06	6.81E-06	2.39E-08	9.61E-05	5.96E-05	2.07E-11	2.26E-09	8.55E-09	2.01E-09
61	3.84E-06	2.35E-06	6.81E-08	3.29E-05	1.65E-04	2.18E-11	4.89E-09	1.24E-08	3.20E-09
62	2.23E-06	1.70E-06	3.51E-08	2.38E-05	8.65E-05	1.64E-11	2.60E-09	7.05E-09	1.79E-09
63	5.29E-06	7.39E-07	1.45E-07	9.87E-06	3.54E-04	5.09E-11	8.85E-09	1.48E-08	4.12E-09
64	1.60E-06	2.27E-07	4.38E-08	3.02E-06	1.07E-04	1.09E-11	2.79E-09	4.46E-09	1.25E-09
65	1.73E-06	3.55E-07	4.23E-08	4.84E-06	1.02E-04	1.08E-11	2.64E-09	4.78E-09	1.31E-09
66	7.61E-06	8.07E-07	1.97E-07	1.01E-05	7.22E-04	3.64E-11	1.86E-08	1.84E-08	5.55E-09
67	2.27E-06	2.41E-07	5.90E-08	3.02E-06	2.15E-04	7.28E-12	5.47E-09	5.49E-09	1.66E-09
68	2.29E-06	2.46E-07	7.59E-08	3.04E-06	2.40E-04	1.46E-11	6.26E-09	5.34E-09	1.65E-09
69	6.29E-06	6.79E-07	2.28E-06	7.93E-06	7.39E-04	2.18E-11	2.33E-08	1.31E-08	4.25E-09
70	1.91E-06	2.07E-07	6.78E-07	2.41E-06	2.25E-04	1.09E-11	7.16E-09	3.99E-09	1.30E-09
71	3.40E-06	3.77E-07	2.55E-06	4.26E-06	2.86E-04	1.09E-11	1.48E-08	6.70E-09	2.24E-09
72	1.06E-05	1.09E-06	8.55E-06	1.24E-05	4.93E-04	3.64E-11	4.28E-08	1.86E-08	6.51E-09
73	2.33E-06	2.44E-07	1.90E-06	2.73E-06	1.41E-04	9.09E-12	9.78E-09	4.22E-09	1.45E-09
74	3.29E-06	3.39E-07	2.66E-06	3.83E-06	1.54E-04	1.46E-11	1.32E-08	5.77E-09	2.02E-09
75	5.54E-06	4.65E-07	2.61E-06	5.58E-06	1.88E-04	1.82E-11	1.42E-08	8.30E-09	2.98E-09
76	5.90E-07	5.81E-08	4.53E-07	6.57E-07	2.80E-05	1.99E-12	2.28E-09	9.98E-10	3.48E-10
77	8.43E-06	5.09E-07	6.02E-07	6.76E-06	1.37E-04	1.46E-11	7.33E-09	1.00E-08	3.68E-09
78	2.00E-06	1.33E-07	3.32E-07	1.71E-06	4.54E-05	3.64E-12	2.71E-09	2.55E-09	9.28E-10
79	9.52E-06	6.24E-07	6.17E-07	8.24E-06	1.26E-04	1.82E-11	9.72E-09	1.08E-08	4.09E-09
80	1.12E-05	8.62E-07	6.30E-07	1.13E-05	1.43E-04	2.18E-11	1.41E-08	1.19E-08	4.68E-09
81	2.97E-06	2.06E-07	1.84E-07	2.72E-06	3.90E-05	9.09E-12	3.32E-09	3.18E-09	1.23E-09
82	3.60E-06	2.74E-07	2.02E-07	3.62E-06	4.59E-05	3.64E-12	4.42E-09	3.81E-09	1.50E-09
83	9.49E-06	1.10E-06	5.06E-07	1.47E-05	1.19E-04	1.82E-11	1.48E-08	9.45E-09	3.88E-09
84	1.08E-05	2.89E-06	6.09E-07	3.97E-05	1.39E-04	1.46E-11	2.06E-08	1.00E-08	4.28E-09
85	3.49E-06	9.30E-07	1.97E-07	1.28E-05	4.50E-05	0.00E+00	6.64E-09	3.24E-09	1.39E-09
86	9.67E-06	6.08E-06	5.08E-07	8.46E-05	1.38E-04	1.09E-11	2.20E-08	7.74E-09	3.43E-09
87	1.38E-05	1.78E-05	5.18E-07	2.49E-04	1.97E-04	7.28E-12	3.85E-08	9.01E-09	4.16E-09
88	4.51E-06	5.79E-06	1.69E-07	8.11E-05	6.44E-05	1.09E-11	1.26E-08	2.95E-09	1.36E-09
89	1.12E-05	1.43E-05	3.66E-07	2.00E-04	1.69E-04	7.28E-12	3.56E-08	6.76E-09	3.20E-09
90	8.43E-06	1.74E-06	2.92E-07	2.29E-05	1.43E-04	1.46E-11	2.86E-08	4.49E-09	2.22E-09
91	1.27E-05	2.41E-06	4.58E-07	3.15E-05	2.09E-04	1.09E-11	4.58E-08	6.39E-09	3.23E-09
92	1.14E-05	2.90E-06	3.97E-07	3.83E-05	1.90E-04	0.00E+00	4.71E-08	5.45E-09	2.84E-09
93	1.23E-05	4.49E-06	4.21E-07	6.02E-05	2.17E-04	7.28E-12	6.01E-08	5.66E-09	3.05E-09

Surry ISLOCA									
Plume Segment	**Xe**	**Cs**	**Ba**	**I**	**Te**	**Ru**	**Mo**	**Ce**	**La**
94	1.09E-05	5.55E-06	4.05E-07	7.52E-05	1.76E-04	1.46E-11	6.30E-08	4.81E-09	2.68E-09
95	1.16E-05	7.72E-06	4.75E-07	1.05E-04	1.43E-04	3.64E-12	8.27E-08	4.96E-09	2.85E-09
96	1.04E-05	7.01E-06	4.54E-07	9.55E-05	6.92E-05	7.28E-12	9.58E-08	4.26E-09	2.52E-09
97	1.12E-05	5.40E-06	5.25E-07	7.21E-05	2.49E-05	0.00E+00	1.45E-07	4.48E-09	2.72E-09
98	1.21E-05	4.81E-06	5.16E-07	6.34E-05	1.31E-05	3.64E-11	9.60E-05	4.34E-09	2.74E-09
99	3.57E-06	1.41E-06	1.57E-07	1.87E-05	4.95E-06	7.28E-12	1.72E-05	1.30E-09	8.06E-10
100	4.02E-06	1.59E-06	1.72E-07	2.10E-05	4.36E-06	3.64E-12	3.17E-05	1.44E-09	9.10E-10
101	9.43E-06	4.23E-06	3.34E-07	5.63E-05	1.08E-05	4.37E-11	1.02E-04	3.11E-09	2.03E-09
102	1.29E-06	4.87E-07	5.19E-08	6.43E-06	1.39E-06	2.10E-12	7.90E-06	4.29E-10	2.70E-10
103	6.71E-06	3.05E-06	1.26E-07	4.09E-05	8.04E-06	5.09E-11	7.34E-06	1.95E-09	1.37E-09
104	1.90E-06	8.34E-07	3.97E-08	1.12E-05	2.07E-06	7.28E-12	9.25E-06	5.33E-10	3.65E-10
105	7.76E-06	2.48E-06	1.35E-07	3.25E-05	9.91E-06	7.28E-11	6.71E-06	2.16E-09	1.55E-09
106	8.48E-06	1.70E-06	1.43E-07	2.11E-05	1.16E-05	5.82E-11	5.76E-06	2.26E-09	1.67E-09
107	7.34E-06	1.64E-06	1.28E-07	2.05E-05	1.09E-05	5.82E-11	4.12E-06	1.95E-09	1.47E-09

Surry Mitigated TISGTR									
Plume Segment	**Xe**	**Cs**	**Ba**	**I**	**Te**	**Ru**	**Mo**	**Ce**	**La**
1	2.59E-06	1.08E-06	9.51E-09	9.49E-07	9.10E-07	4.72E-09	2.76E-07	9.80E-14	9.80E-14
2	0.055065	0.00187	1.69E-05	0.00218	0.00138	7.61E-06	4.68E-04	1.91E-10	1.90E-10
3	1.89E-05	4.81E-06	2.49E-08	4.65E-06	4.80E-06	1.09E-07	1.28E-06	1.85E-12	1.85E-12
4	0.002275	2.77E-04	2.55E-06	2.81E-04	2.88E-04	9.07E-06	7.27E-05	2.37E-10	2.37E-10
5	2.62E-05	7.31E-06	5.41E-08	7.33E-06	7.52E-06	1.97E-07	1.93E-06	4.79E-12	4.79E-12
6	0.013924	7.47E-04	2.18E-05	0.00103	0.00105	6.80E-05	1.96E-04	1.81E-09	1.81E-09
7	3.05E-05	6.87E-06	8.66E-08	7.48E-06	7.63E-06	2.82E-07	1.81E-06	7.39E-12	7.44E-12
8	0.011313	8.78E-04	4.59E-05	0.00132	0.00149	1.29E-04	2.25E-04	6.95E-08	4.28E-09
9	3.40E-05	5.25E-06	8.35E-07	6.06E-06	6.27E-06	3.27E-07	1.38E-06	1.53E-07	2.77E-09
10	0.001501	1.26E-04	5.64E-05	8.95E-05	9.78E-05	1.47E-05	3.38E-05	9.75E-06	2.06E-07
11	3.17E-05	8.52E-07	4.11E-07	9.50E-07	9.84E-07	5.43E-08	2.24E-07	8.03E-08	1.64E-09
12	4.35E-04	5.64E-06	5.95E-07	5.57E-05	2.36E-06	3.33E-08	4.74E-07	6.44E-08	4.02E-09
13	2.18E-04	3.60E-06	3.96E-08	4.98E-05	8.47E-07	1.02E-09	1.96E-08	2.16E-09	7.28E-10
14	1.29E-04	1.75E-06	6.61E-09	2.47E-05	3.21E-07	1.31E-10	2.21E-09	3.47E-10	1.66E-10
15	1.83E-06	1.58E-08	4.37E-11	2.23E-07	2.79E-09	0	0	3.64E-12	1.39E-12
16	1.85E-06	1.30E-08	1.75E-10	1.81E-07	7.45E-09	0	9.71E-08	4.55E-12	4.41E-12
17	6.48E-06	1.12E-07	6.32E-09	1.58E-06	2.22E-07	0	4.21E-06	1.47E-10	1.46E-10
18	8.20E-07	1.03E-07	1.36E-08	1.46E-06	2.74E-07	0	8.92E-06	2.76E-10	2.81E-10
19	5.22E-08	1.03E-07	1.59E-08	1.46E-06	1.98E-07	0	1.01E-05	3.06E-10	3.09E-10
20	7.45E-09	9.31E-08	1.59E-08	1.32E-06	1.29E-07	0	9.80E-06	2.97E-10	3.00E-10
21	0	8.66E-08	1.58E-08	1.23E-06	8.66E-08	0	9.43E-06	2.88E-10	2.92E-10
22	0	7.92E-08	1.55E-08	1.12E-06	6.01E-08	0	9.02E-06	2.79E-10	2.83E-10
23	0	7.08E-08	1.53E-08	1.00E-06	4.05E-08	0	8.70E-06	2.73E-10	2.76E-10
24	0	6.29E-08	1.49E-08	8.83E-07	2.93E-08	0	8.27E-06	2.62E-10	2.66E-10
25	0	5.40E-08	1.43E-08	7.66E-07	2.10E-08	0	7.75E-06	2.48E-10	2.51E-10
26	0	4.80E-08	1.37E-08	6.77E-07	1.54E-08	0	7.30E-06	2.35E-10	2.38E-10
27	0	4.38E-08	1.32E-08	6.17E-07	1.21E-08	0	6.94E-06	2.22E-10	2.25E-10
28	0	3.91E-08	1.31E-08	5.54E-07	8.85E-09	0	6.78E-06	2.16E-10	2.19E-10
29	0	3.73E-08	1.28E-08	5.23E-07	8.38E-09	0	6.56E-06	2.08E-10	2.10E-10
30	0	3.40E-08	1.26E-08	4.84E-07	7.45E-09	0	6.38E-06	1.98E-10	2.02E-10
31	0	3.03E-08	1.25E-08	4.27E-07	6.52E-09	0	6.25E-06	1.95E-10	1.96E-10
32	0	2.56E-08	1.19E-08	3.66E-07	4.66E-09	0	5.92E-06	1.81E-10	1.84E-10
33	0	2.33E-08	1.13E-08	3.24E-07	3.26E-09	0	5.54E-06	1.67E-10	1.69E-10
34	7.45E-09	2.00E-08	1.13E-08	2.83E-07	3.26E-09	0	5.52E-06	1.63E-10	1.66E-10
35	3.73E-08	1.72E-08	1.13E-08	2.46E-07	1.86E-09	0	5.48E-06	1.60E-10	1.62E-10
36	1.42E-07	1.49E-08	1.13E-08	2.14E-07	1.40E-09	0	5.41E-06	1.56E-10	1.58E-10
37	1.71E-07	1.35E-08	1.13E-08	1.88E-07	1.86E-09	0	5.35E-06	1.52E-10	1.54E-10
38	8.20E-08	1.16E-08	1.12E-08	1.64E-07	9.31E-10	0	5.25E-06	1.47E-10	1.50E-10
39	3.73E-08	1.02E-08	1.14E-08	1.44E-07	9.31E-10	0	5.28E-06	1.47E-10	1.49E-10
40	7.45E-09	8.85E-09	1.05E-08	1.24E-07	9.31E-10	0	4.82E-06	1.33E-10	1.34E-10
41	7.45E-09	7.45E-09	1.07E-08	1.09E-07	9.31E-10	0	4.89E-06	1.32E-10	1.34E-10
42	0	6.98E-09	1.17E-08	9.59E-08	4.66E-10	0	5.26E-06	1.41E-10	1.43E-10
43	0	6.05E-09	1.19E-08	8.52E-08	9.31E-10	0	5.31E-06	1.42E-10	1.43E-10
44	0	5.12E-09	1.20E-08	7.45E-08	0	0	5.30E-06	1.38E-10	1.41E-10
45	0	4.66E-09	1.17E-08	6.47E-08	9.31E-10	0	5.13E-06	1.33E-10	1.35E-10
46	0	4.19E-09	1.11E-08	5.68E-08	4.66E-10	0	4.84E-06	1.25E-10	1.26E-10
47	0	3.26E-09	1.10E-08	4.94E-08	0	0	4.74E-06	1.21E-10	1.22E-10

Surry Mitigated TISGTR									
Plume Segment	**Xe**	**Cs**	**Ba**	**I**	**Te**	**Ru**	**Mo**	**Ce**	**La**
48	0	2.79E-09	1.04E-08	4.28E-08	0	0	4.43E-06	1.11E-10	1.13E-10
49	0	1.40E-09	4.38E-09	1.68E-08	0	0	1.85E-06	4.64E-11	4.69E-11

Surry Unmitigated TISGTR									
Plume Segment	**Xe**	**Cs**	**Ba**	**I**	**Te**	**Ru**	**Mo**	**Ce**	**La**
1	2.59E-06	1.08E-06	9.51E-09	9.49E-07	9.10E-07	4.72E-09	2.76E-07	9.80E-14	9.80E-14
2	0.055065	0.00187	1.69E-05	0.002182	0.001379	7.61E-06	4.68E-04	1.91E-10	1.90E-10
3	1.89E-05	4.81E-06	2.49E-08	4.65E-06	4.80E-06	1.09E-07	1.28E-06	1.85E-12	1.85E-12
4	0.0022745	2.77E-04	2.55E-06	2.81E-04	2.88E-04	9.07E-06	7.27E-05	2.37E-10	2.37E-10
5	2.62E-05	7.31E-06	5.41E-08	7.33E-06	7.52E-06	1.97E-07	1.93E-06	4.79E-12	4.79E-12
6	0.013924	7.47E-04	2.18E-05	0.001034	0.001054	6.80E-05	1.96E-04	1.81E-09	1.81E-09
7	3.05E-05	6.87E-06	8.66E-08	7.48E-06	7.63E-06	2.82E-07	1.81E-06	7.39E-12	7.44E-12
8	0.011313	8.78E-04	4.59E-05	0.001322	0.001489	1.29E-04	2.25E-04	6.95E-08	4.28E-09
9	3.40E-05	5.25E-06	8.35E-07	6.06E-06	6.27E-06	3.27E-07	1.38E-06	1.53E-07	2.77E-09
10	0.0024109	1.36E-04	6.16E-05	1.07E-04	1.10E-04	1.53E-05	3.62E-05	1.07E-05	2.30E-07
11	3.79E-05	3.39E-06	1.63E-06	3.74E-06	3.87E-06	2.17E-07	8.92E-07	3.21E-07	6.45E-09
12	0.0032437	2.29E-05	1.02E-05	5.99E-05	3.03E-05	1.24E-06	5.31E-06	1.93E-06	5.04E-08
13	3.79E-05	1.72E-06	8.32E-07	2.00E-06	2.00E-06	1.10E-07	4.51E-07	1.63E-07	3.38E-09
14	0.0034168	1.21E-05	4.71E-06	4.71E-05	2.04E-05	6.96E-07	2.52E-06	1.04E-06	2.50E-08
15	3.83E-05	8.91E-07	4.25E-07	1.18E-06	1.08E-06	5.69E-08	2.30E-07	8.46E-08	1.78E-09
16	0.0035156	9.70E-06	2.59E-06	6.63E-05	1.50E-05	4.16E-07	1.44E-06	6.22E-07	1.56E-08
17	3.87E-05	5.65E-07	2.56E-07	1.13E-06	7.06E-07	3.48E-08	1.39E-07	5.17E-08	1.11E-09
18	0.0035655	1.17E-05	1.73E-06	1.18E-04	1.35E-05	2.82E-07	9.46E-07	4.21E-07	1.11E-08
19	3.91E-05	4.54E-07	1.74E-07	1.76E-06	5.49E-07	2.41E-08	9.42E-08	3.58E-08	7.89E-10
20	0.0036008	1.74E-05	1.40E-06	2.12E-04	1.55E-05	2.06E-07	8.74E-05	3.08E-07	8.68E-09
21	3.94E-05	4.56E-07	1.30E-07	3.02E-06	5.05E-07	1.80E-08	1.33E-06	2.68E-08	6.09E-10
22	0.0036017	6.49E-06	1.52E-06	6.58E-05	1.81E-05	1.63E-07	0	2.46E-07	7.91E-09
23	3.97E-05	3.95E-07	1.06E-07	2.90E-06	5.28E-07	1.44E-08	0	2.15E-08	5.11E-10
24	0.003629	5.13E-06	1.29E-06	5.19E-05	1.97E-05	1.32E-07	0	1.98E-07	6.77E-09
25	3.99E-05	3.18E-07	8.60E-08	2.42E-06	5.49E-07	1.13E-08	0	1.69E-08	4.22E-10
26	0.0036535	4.56E-06	1.05E-06	4.91E-05	2.30E-05	9.99E-08	0	1.51E-07	5.56E-09
27	4.02E-05	2.38E-07	6.51E-08	1.89E-06	5.63E-07	8.25E-09	0	1.23E-08	3.25E-10
28	0.0036759	3.98E-06	8.17E-07	4.55E-05	2.68E-05	7.08E-08	0	1.08E-07	4.40E-09
29	4.04E-05	1.72E-07	4.75E-08	1.42E-06	5.90E-07	5.75E-09	0	8.62E-09	2.42E-10
30	0.0036984	3.46E-06	6.34E-07	4.15E-05	2.88E-05	5.00E-08	0	7.63E-08	3.54E-09
31	4.06E-05	1.27E-07	3.54E-08	1.10E-06	6.34E-07	4.06E-09	0	6.09E-09	1.84E-10
32	0.0037173	2.96E-06	5.20E-07	3.66E-05	2.78E-05	3.61E-08	0	5.56E-08	2.94E-09
33	4.08E-05	9.77E-08	2.77E-08	8.82E-07	6.72E-07	2.96E-09	0	4.45E-09	1.47E-10
34	0.0037368	2.10E-06	4.41E-07	2.59E-05	2.41E-05	2.71E-08	0	4.20E-08	2.52E-09
35	4.09E-05	7.75E-08	2.26E-08	7.27E-07	6.80E-07	2.23E-09	0	3.36E-09	1.22E-10
36	0.0037562	1.30E-06	4.02E-07	1.55E-05	2.15E-05	2.09E-08	0	3.27E-08	2.22E-09
37	4.10E-05	6.28E-08	1.93E-08	6.11E-07	6.74E-07	1.72E-09	0	2.61E-09	1.05E-10
38	0.0037724	9.50E-07	3.74E-07	1.13E-05	1.90E-05	1.64E-08	0	2.59E-08	1.97E-09
39	4.11E-05	5.15E-08	1.70E-08	5.16E-07	6.56E-07	1.35E-09	0	2.06E-09	9.24E-11
40	0.003791	7.33E-07	3.50E-07	8.66E-06	1.66E-05	1.32E-08	0	2.09E-08	1.78E-09
41	4.12E-05	4.26E-08	1.54E-08	4.37E-07	6.29E-07	1.08E-09	0	1.65E-09	8.26E-11
42	0.0038074	7.72E-07	3.26E-07	9.60E-06	1.44E-05	1.06E-08	0	1.71E-08	1.63E-09
43	4.13E-05	3.62E-08	1.42E-08	3.82E-07	5.92E-07	8.73E-10	0	1.35E-09	7.50E-11
44	0.0038235	8.27E-07	3.04E-07	1.07E-05	1.27E-05	8.67E-09	0	1.41E-08	1.50E-09
45	4.14E-05	3.19E-08	1.32E-08	3.48E-07	5.51E-07	7.13E-10	0	1.11E-09	6.89E-11
46	0.0038394	8.64E-07	2.85E-07	1.14E-05	1.13E-05	7.17E-09	0	1.18E-08	1.38E-09
47	4.14E-05	2.89E-08	1.24E-08	3.26E-07	5.09E-07	5.88E-10	0	9.20E-10	6.38E-11

Surry Unmitigated TISGTR									
Plume Segment	Xe	Cs	Ba	I	Te	Ru	Mo	Ce	La
48	0.0038542	9.01E-07	2.60E-07	1.21E-05	9.93E-06	5.97E-09	0	9.97E-09	1.29E-09
49	4.14E-05	2.68E-08	1.17E-08	3.13E-07	4.67E-07	4.90E-10	0	7.72E-10	5.97E-11
50	0.0038672	9.73E-07	2.41E-07	1.32E-05	8.72E-06	5.04E-09	0	8.50E-09	1.21E-09
51	0.0027853	1.70E-06	7.38E-07	2.05E-05	2.83E-05	2.71E-08	0	4.32E-08	3.75E-09
52	4.14E-05	2.54E-08	1.10E-08	3.05E-07	4.25E-07	4.10E-10	0	6.53E-10	5.61E-11
53	0.0038613	1.06E-06	2.32E-07	1.45E-05	7.72E-06	4.21E-09	0	7.25E-09	1.13E-09
54	0.0079969	4.70E-06	2.04E-06	5.80E-05	7.49E-05	6.69E-08	0	1.08E-07	1.03E-08
55	4.11E-05	2.42E-08	1.05E-08	2.98E-07	3.85E-07	3.44E-10	0	5.54E-10	5.27E-11
56	0.0038298	1.21E-06	2.37E-07	1.68E-05	6.85E-06	3.54E-09	0	6.20E-09	1.06E-09
57	0.014864	8.52E-06	3.71E-06	1.07E-04	1.27E-04	1.06E-07	0	1.73E-07	1.82E-08
58	4.04E-05	2.32E-08	1.01E-08	2.92E-07	3.46E-07	2.89E-10	0	4.70E-10	4.95E-11
59	0.0037684	1.42E-06	2.26E-07	1.98E-05	6.07E-06	2.97E-09	0	5.29E-09	1.00E-09
60	0.019254	1.09E-05	4.74E-06	1.40E-04	1.51E-04	1.18E-07	0	1.95E-07	2.27E-08
61	3.95E-05	2.23E-08	9.71E-09	2.86E-07	3.09E-07	2.42E-10	0	3.99E-10	4.66E-11
62	0.0036753	1.40E-06	2.17E-07	1.95E-05	5.40E-06	2.47E-09	0	4.56E-09	9.52E-10
63	0.021255	1.19E-05	5.18E-06	1.56E-04	1.53E-04	1.13E-07	0	1.89E-07	2.44E-08
64	3.80E-05	2.13E-08	9.25E-09	2.78E-07	2.73E-07	2.01E-10	0	3.36E-10	4.34E-11
65	0.0035692	1.41E-06	2.08E-07	1.97E-05	4.86E-06	2.10E-09	0	3.94E-09	9.06E-10
66	0.024223	1.35E-05	5.88E-06	1.79E-04	1.61E-04	1.12E-07	0	1.90E-07	2.71E-08
67	3.75E-05	2.09E-08	9.11E-09	2.77E-07	2.49E-07	1.73E-10	0	2.93E-10	4.20E-11
68	0.0034562	1.38E-06	1.99E-07	1.94E-05	4.46E-06	1.76E-09	0	3.43E-09	8.66E-10
69	0.023745	1.32E-05	5.76E-06	1.77E-04	1.48E-04	9.61E-08	0	1.66E-07	2.62E-08
70	3.58E-05	2.00E-08	8.69E-09	2.68E-07	2.22E-07	1.45E-10	0	2.49E-10	3.96E-11
71	0.0033394	1.34E-06	1.92E-07	1.88E-05	4.10E-06	1.54E-09	0	3.02E-09	8.35E-10
72	0.023485	1.32E-05	5.72E-06	1.78E-04	1.38E-04	8.37E-08	0	1.47E-07	2.58E-08
73	3.45E-05	1.94E-08	8.41E-09	2.62E-07	2.02E-07	1.23E-10	0	2.16E-10	3.79E-11
74	0.0032239	1.32E-06	1.86E-07	1.86E-05	3.80E-06	1.27E-09	0	2.67E-09	8.07E-10
75	0.0222	1.26E-05	5.45E-06	1.71E-04	1.24E-04	7.02E-08	0	1.26E-07	2.43E-08
76	3.33E-05	1.88E-08	8.16E-09	2.57E-07	1.85E-07	1.04E-10	0	1.88E-10	3.64E-11
77	0.0031118	1.25E-06	1.80E-07	1.76E-05	3.54E-06	1.09E-09	0	2.37E-09	7.81E-10
78	0.022319	1.26E-05	5.53E-06	1.73E-04	1.19E-04	6.29E-08	0	1.16E-07	2.46E-08
79	3.20E-05	1.80E-08	7.94E-09	2.48E-07	1.70E-07	8.97E-11	0	1.65E-10	3.52E-11
80	0.0030011	1.16E-06	1.74E-07	1.63E-05	3.33E-06	9.60E-10	0	2.12E-09	7.58E-10
81	0.021661	1.19E-05	5.44E-06	1.64E-04	1.12E-04	5.46E-08	0	1.03E-07	2.41E-08
82	3.08E-05	1.68E-08	7.75E-09	2.33E-07	1.58E-07	7.70E-11	0	1.46E-10	3.42E-11
83	0.0028905	1.11E-06	1.68E-07	1.57E-05	3.18E-06	8.44E-10	0	1.91E-09	7.35E-10
84	0.021648	1.16E-05	5.52E-06	1.61E-04	1.09E-04	4.88E-08	0	9.50E-08	2.43E-08
85	2.96E-05	1.59E-08	7.56E-09	2.20E-07	1.49E-07	6.65E-11	0	1.30E-10	3.33E-11
86	0.0027884	1.05E-06	1.64E-07	1.49E-05	3.06E-06	6.69E-10	0	1.74E-09	7.19E-10
87	0.020122	1.07E-05	5.24E-06	1.49E-04	1.00E-04	4.10E-08	0	8.24E-08	2.31E-08
88	2.86E-05	1.52E-08	7.44E-09	2.12E-07	1.42E-07	5.80E-11	0	1.17E-10	3.28E-11
89	0.0026983	8.68E-07	1.62E-07	1.23E-05	3.03E-06	6.26E-10	0	1.62E-09	7.16E-10
90	0.020926	1.13E-05	5.58E-06	1.59E-04	1.05E-04	3.89E-08	0	8.09E-08	2.46E-08
91	2.75E-05	1.49E-08	7.34E-09	2.09E-07	1.38E-07	5.09E-11	0	1.06E-10	3.24E-11
92	0.0025999	8.47E-07	1.58E-07	1.20E-05	3.11E-06	5.82E-10	0	1.51E-09	7.08E-10
93	0.018819	1.05E-05	5.14E-06	1.48E-04	9.61E-05	3.20E-08	0	6.88E-08	2.27E-08

Surry Unmitigated TISGTR									
Plume Segment	**Xe**	**Cs**	**Ba**	**I**	**Te**	**Ru**	**Mo**	**Ce**	**La**
94	2.64E-05	1.48E-08	7.21E-09	2.08E-07	1.35E-07	4.46E-11	0	9.64E-11	3.19E-11
95	0.002504	8.43E-07	1.54E-07	1.20E-05	3.28E-06	4.80E-10	0	1.40E-09	6.99E-10
96	0.018722	1.09E-05	5.22E-06	1.53E-04	9.93E-05	2.91E-08	0	6.51E-08	2.32E-08
97	2.53E-05	1.47E-08	7.07E-09	2.08E-07	1.35E-07	3.90E-11	0	8.77E-11	3.14E-11
98	0.0024121	7.11E-07	1.49E-07	1.01E-05	3.52E-06	4.51E-10	0	1.31E-09	6.95E-10
99	0.017989	1.10E-05	5.10E-06	1.55E-04	1.01E-04	2.55E-08	0	5.97E-08	2.29E-08
100	2.43E-05	1.48E-08	6.88E-09	2.10E-07	1.37E-07	3.42E-11	0	8.03E-11	3.10E-11
101	0.0023166	6.38E-07	1.17E-07	9.05E-06	3.94E-06	3.64E-10	0	1.23E-09	6.87E-10
102	0.017843	1.15E-05	4.96E-06	1.63E-04	1.09E-04	2.31E-08	0	5.66E-08	2.34E-08
103	2.33E-05	1.50E-08	6.47E-09	2.13E-07	1.43E-07	3.00E-11	0	7.37E-11	3.06E-11
104	0.0022242	6.10E-07	1.11E-07	8.66E-06	4.47E-06	3.35E-10	0	1.15E-09	6.80E-10
105	0.016027	1.09E-05	4.35E-06	1.55E-04	1.10E-04	1.90E-08	0	4.89E-08	2.16E-08
106	2.23E-05	1.53E-08	6.05E-09	2.17E-07	1.53E-07	2.63E-11	0	6.80E-11	3.02E-11
107	0.0021344	6.16E-07	1.05E-07	8.75E-06	5.07E-06	2.91E-10	0	1.09E-09	6.72E-10
108	0.015927	1.15E-05	4.24E-06	1.63E-04	1.24E-04	1.73E-08	0	4.70E-08	2.22E-08
109	2.14E-05	1.55E-08	5.69E-09	2.20E-07	1.67E-07	2.32E-11	0	6.29E-11	2.98E-11
110	8.98E-04	2.63E-07	4.40E-08	3.73E-06	2.41E-06	1.31E-10	0	4.51E-10	2.89E-10
111	0.0015566	1.16E-06	4.11E-07	1.65E-05	1.30E-05	1.61E-09	0	4.51E-09	2.20E-09
112	6.97E-07	5.20E-10	1.84E-10	7.39E-09	5.86E-09	6.82E-13	0	1.88E-12	9.88E-13
113	5.17E-04	3.86E-07	1.36E-07	5.49E-06	4.38E-06	5.33E-10	0	1.50E-09	7.34E-10
114	6.96E-07	5.20E-10	1.83E-10	7.39E-09	5.89E-09	6.82E-13	0	1.99E-12	9.88E-13
115	6.84E-05	2.00E-08	3.33E-09	2.86E-07	1.91E-07	0	0	3.27E-11	2.23E-11

Table C-5 EARLY Parameters Used in the Surry LTSBO, Unmitigated STSBO, TI-SGTR Mitigated and Unmitigated Scenarios

Variable	Description	LTSBO	Unmitigated STSBO	ISLOCA	TISGTR Mitigated	TISGTR Unmitigated
ACNAME	Latent Cancer Effect					
	Cancer Type 1	LEUKEMIA	LEUKEMIA	LEUKEMIA	LEUKEMIA	LEUKEMIA
	Cancer Type 2	BONE	BONE	BONE	BONE	BONE
	Cancer Type 3	BREAST	BREAST	BREAST	BREAST	BREAST
	Cancer Type 4	LUNG	LUNG	LUNG	LUNG	LUNG
	Cancer Type 5	THYROID	THYROID	THYROID	THYROID	THYROID
	Cancer Type 6	LIVER	LIVER	LIVER	LIVER	LIVER
	Cancer Type 7	COLON	COLON	COLON	COLON	COLON
	Cancer Type 8	RESIDUAL	RESIDUAL	RESIDUAL	RESIDUAL	RESIDUAL
ACSUSC	Population Susceptible to Cancer	1.0 for all cancers	1.0 for all cancers	1.0 for all cancers	1.0 for all cancers	1.0 for all cancers
ACTHRE	Linear Dose-Response Threshold	0	0	0	0	0
BRRATE	Breathing Rate (for all activity types)	0.000266	0.000266	0.000266	0.000266	0.000266
CFRISK	Lifetime Cancer Fatality Risk Factors					
	Cancer Type 1	0.0111	0.0111	0.0111	0.0111	0.0111
	Cancer Type 2	0.00019	0.00019	0.00019	0.00019	0.00019
	Cancer Type 3	0.00506	0.00506	0.00506	0.00506	0.00506
	Cancer Type 4	0.0198	0.0198	0.0198	0.0198	0.0198
	Cancer Type 5	0.000648	0.000648	0.000648	0.000648	0.000648
	Cancer Type 6	0.003	0.003	0.003	0.003	0.003
	Cancer Type 7	0.0208	0.0208	0.0208	0.0208	0.0208
	Cancer Type 8	0.0493	0.0493	0.0493	0.0493	0.0493

Variable	Description	LTSBO	Unmitigated STSBO	ISLOCA	TISGTR Mitigated	TISGTR Unmitigated
CIRISK	Lifetime Cancer Injury Risk Factors					
	Cancer Type 1	0.0113	0.0113	0.0113	0.0113	0.0113
	Cancer Type 2	0.000271	2.71E-04	2.71E-04	2.71E-04	2.71E-04
	Cancer Type 3	0.0101	0.0101	0.0101	0.0101	0.0101
	Cancer Type 4	0.0208	0.0208	0.0208	0.0208	0.0208
	Cancer Type 5	0.00648	0.00648	0.00648	0.00648	0.00648
	Cancer Type 6	0.00316	0.00316	0.00316	0.00316	0.00316
	Cancer Type 7	0.0378	0.0378	0.0378	0.0378	0.0378
	Cancer Type 8	0.169	0.169	0.169	0.169	0.169
CRIORG	Critical Organ for EARLY Phase	L-ICRP60ED	L-ICRP60ED	L-ICRP60ED	L-ICRP60ED	L-ICRP60ED
CSFACT	Cloudshine Shielding Factors					
	Evacuation Shielding Factor for All but Cohort 4	1	1	1	1	1
	Normal Activity Shielding Factor for All but Cohort 4	0.68	0.68	0.68	0.68	0.68
	Sheltering Shielding Factor for All but Cohort 4	0.6	0.6	0.6	0.6	0.6
	Evacuation Shielding Factor for Cohort 4	1	1	1	1	1
	Normal Activity Shielding Factor for Cohort 4	0.31	0.31	0.31	0.31	0.31
	Sheltering Shielding Factor for Cohort 4	0.31	0.31	0.31	0.31	0.31

Variable	Description	LTSBO	Unmitigated STSBO	ISLOCA	TISGTR Mitigated	TISGTR Unmitigated
DCF_FILE	Name of Dose Conversion Factor File	FGR13GyEquivDCF.INP	FGR13GyEquivDCF.INP	FGR13GyEquivDCF.INP	FGR13GyEquivDCF.INP	FGR13GyEquivDCF.INP
DDREFA	Dose-Dependent Reduction Factor					
	Cancer Type 1	2	2	2	2	2
	Cancer Type 2	2	2	2	2	2
	Cancer Type 3	1	1	1	1	1
	Cancer Type 4	2	2	2	2	2
	Cancer Type 5	2	2	2	2	2
	Cancer Type 6	2	2	2	2	2
	Cancer Type 7	2	2	2	2	2
	Cancer Type 8	2	2	2	2	2
DDTHRE	Threshold for Applying Dose-Dependent Reduction Factor	0.2	0.2	0.2	0.2	0.2
DLTSHL	Delay from Alarm Time to Shelter					
	Cohort 1	9900	9900	9900	9900	9900
	Cohort 2	9900	9900	9900	9900	9900
	Cohort 3	900	900	900	900	900
	Cohort 4	9900	9900	9900	9900	9900
	Cohort 5	9900	9900	9900	9900	9900
	Cohort 6					
DLTEVA	Delay from Beginning of Shelter to Evacuation					
	Cohort 1	3600	3600	3600	3600	3600
	Cohort 2	3600	3600	3600	3600	3600
	Cohort 3	3600	3600	6300	3600	3600
	Cohort 4	39600	39600	39600	39600	39600
	Cohort 5	39600	39600	39600	39600	39600
	Cohort 6					
DOSEFA	Cancer Dose-Response Linear Factors	1 for all organs	1 for all organs	1 for all organs	1 for all organs	1 for all organs

Variable	Description	LTSBO	Unmitigated STSBO	ISLOCA	TISGTR Mitigated	TISGTR Unmitigated
DOSEFB	Cancer Dose-Response Quadratic Factors	0 for all organs	0 for all organs	0 for all organs	0 for all organs	0 for all organs
DOSHOT	Hot-Spot Relocation Dose Threshold	0.05	0.05	0.05	0.05	0.05
DOSMOD	Dose-Response Model Flag	AT	AT	AT	AT	AT
DOSNRM	Normal Relocation Dose Threshold	0.01	0.01	0.01	0.01	0.01
DURBEG	Duration of Beginning of Evacuation Phase					
	Cohort 1	900	900	900	900	900
	Cohort 2	900	900	900	900	900
	Cohort 3	900	900	900	900	900
	Cohort 4	3600	3600	3600	3600	3600
	Cohort 5	3600	3600	3600	3600	3600
	Cohort 6	N/A	N/A	N/A	N/A	N/A
DURMID	Duration of Middle of Evacuation Phase					
	Cohort 1	35100	35100	35100	35100	35100
	Cohort 2	35100	35100	35100	35100	35100
	Cohort 3	1800	1800	1800	1800	1800
	Cohort 4	3600	3600	3600	3600	3600
	Cohort 5	3600	3600	3600	3600	3600
	Cohort 6	N/A	N/A	N/A	N/A	N/A
EANAM1	Text Describing the EARLY Assumptions	SOARCA Surry Long-term SBO Calculation	SOARCA Surry Short-term SBO Calculation	SOARCA Surry Short-term SBO Calculation	SOARCA Surry Short-term SBO TI-SGTR Calculation	SOARCA Surry Short-term SBO Calculation
EANAM2	Text Describing the Emergency Response					
	Cohort 1	Group 1	Group 1	Group 1	Group 1	Group 1
	Cohort 2	Group 2	Group 2	Group 2	Group 2	Group 2
	Cohort 3	Group 3	Group 3	Group 3	Group 3	Group 3
	Cohort 4	Group 4	Group 4	Group 4	Group 4	Group 4
	Cohort 5	Group 5	Group 5	Group 5	Group 5	Group 5
	Cohort 6	Group 6	Group 6	Group 6	Group 6	Group 6
EFFACA	LD50 for Early Fatality Types					
	A-RED MARR	5.6	5.6	5.6	5.6	5.6
	A-LUNGS	23.5	23.5	23.5	23.5	23.5

Variable	Description	LTSBO	Unmitigated STSBO	ISLOCA	TISGTR Mitigated	TISGTR Unmitigated
EFFACA	A-STOMACH	12.1	12.1	12.1	12.1	12.1
EFFACB	Shape Factor for Early Fatality Types					
	A-RED MARR	6.1	6.1	6.1	6.1	6.1
	A-LUNGS	9.6	9.6	9.6	9.6	9.6
	A-STOMACH	9.3	9.3	9.3	9.3	9.3
EFFACY	Efficacy of the KI Ingestion	0.7	0.7	0.7	0.7	0.7
EFFTHR	Threshold Dose to Target Organ					
	A-RED MARR	2.32	2.32	2.32	2.32	2.32
	A-LUNGS	13.6	13.6	13.6	13.6	13.6
	A-STOMACH	6.5	6.5	6.5	6.5	6.5
EIFACA	D50 For Early Injuries					
	PRODROMAL VOMIT	2	2	2	2	2
	DIARRHEA	3	3	3	3	3
	PNEUMONITIS	16.6	16.6	16.6	16.6	16.6
	SKIN ERYTHRMA	6	6	6	6	6
	TRANSEPIDERMAL	20	20	20	20	20
	THYROIDITIS	240	240	240	240	240
	HYPOTHYROIDISM	60	60	60	60	60
EIFACB	Shape Factor for Early Injuries					
	PRODROMAL VOMIT	3	3	3	3	3
	DIARRHEA	2.5	2.5	2.5	2.5	2.5
	PNEUMONITIS	7.3	7.3	7.3	7.3	7.3
	SKIN ERYTHRMA	5	5	5	5	5
	TRANSEPIDERMAL	5	5	5	5	5
	THYROIDITIS	2	2	2	2	2
	HYPOTHYROIDISM	1.3	1.3	1.3	1.3	1.3

Variable	Description	LTSBO	Unmitigated STSBO	ISLOCA	TISGTR Mitigated	TISGTR Unmitigated
EINAME	Early Injury Effect Names and Corresponding Organ					
	PRODROMAL VOMIT	A-STOMACH	A-STOMACH	A-STOMACH	A-STOMACH	A-STOMACH
	DIARRHEA	A-STOMACH	A-STOMACH	A-STOMACH	A-STOMACH	A-STOMACH
	PNEUMONITIS	A-LUNGS	A-LUNGS	A-LUNGS	A-LUNGS	A-LUNGS
	SKIN ERYTHRMA	A-SKIN	A-SKIN	A-SKIN	A-SKIN	A-SKIN
	TRANSEPIDERMAL	A-SKIN	A-SKIN	A-SKIN	A-SKIN	A-SKIN
	THYROIDITIS	A-THYROID	A-THYROID	A-THYROID	A-THYROID	A-THYROID
	HYPOTHYROIDISM	A-THYROID	A-THYROID	A-THYROID	A-THYROID	A-THYROID
EISUSC	Susceptible Population Fraction	1. for all health effects	1. for all health effects	1. for all health effects	1. for all health effects	1. for all health effects
EITHRE	Early Injury Dose Threshold					
	PRODROMAL VOMIT	0.5	0.5	0.5	0.5	0.5
	DIARRHEA	1	1	1	1	1
	PNEUMONITIS	9.2	9.2	9.2	9.2	9.2
	SKIN ERYTHRMA	3	3	3	3	3
	TRANSEPIDERMAL	10	10	10	10	10
	THYROIDITIS	40	40	40	40	40
	HYPOTHYROIDISM	2	2	2	2	2
ENDAT2	Control flag indicating only ATMOS and EARLY are to be run	.FALSE.	.FALSE.	.FALSE.	.FALSE.	.FALSE.
ENDEMP	Time Duration for the Emergency Phase	604800	604800	604800	604800	604800
ESPEED	Evaluation Speed					
	Initial Evacuation Phase, Cohort 1	2.235	2.235	2.235	2.235	2.235

Variable	Description	LTSBO	Unmitigated STSBO	ISLOCA	TISGTR Mitigated	TISGTR Unmitigated
ESPEED	Middle Evacuation Phase, Cohort 1	0.447	0.447	0.447	0.447	0.447
	Late Evacuation Phase, Cohort 1	8.941	8.941	8.941	8.941	8.941
	Initial Evacuation Phase, Cohort 2	2.235	2.235	2.235	2.235	2.235
	Middle Evacuation Phase, Cohort 2	0.447	0.447	0.447	0.447	0.447
	Late Evacuation Phase, Cohort 2	8.941	8.941	8.941	8.941	8.941
	Initial Evacuation Phase, Cohort 3	4.47	4.47	4.47	4.47	4.47
	Middle Evacuation Phase, Cohort 3	4.47	4.47	4.47	4.47	4.47
	Late Evacuation Phase, Cohort 3	8.941	8.941	8.941	8.941	8.941
	Initial Evacuation Phase, Cohort 4	0.447	0.447	0.447	0.447	0.447
	Middle Evacuation Phase, Cohort 4	4.47	4.47	4.47	4.47	4.47
	Late Evacuation Phase, Cohort 4	8.941	8.941	8.941	8.941	8.941
	Initial Evacuation Phase, Cohort 5	0.447	0.447	0.447	0.447	0.447
	Middle Evacuation Phase, Cohort 5	4.47	4.47	4.47	4.47	4.47

Variable	Description	LTSBO	Unmitigated STSBO	ISLOCA	TISGTR Mitigated	TISGTR Unmitigated
ESPEED	Late Evacuation Phase, Cohort 5	8.941	8.941	8.941	8.941	8.941
	Cohort 6	N/A	N/A	N/A	N/A	N/A
ESPGRD	Speed Multiplier to Account for Grid-Level Variations in Road Network	Table A.2-5	Table A.2-5	Table A.2-5	Table A.2-5	Table A.2-5
ESPMUL	Speed Multiplier Employed During Precipitation	0.7	0.7	0.7	0.7	0.7
EVATYP	Evacuation Type	NETWORK	NETWORK	NETWORK	NETWORK	NETWORK
GSHFAC	Groundshine Shielding Factors					
	Evacuation Shielding Factor for All but Cohort 4	0.5	0.5	0.5	0.5	0.5
	Normal Activity Shielding Factor for All but Cohort 4	0.26	0.26	0.26	0.26	0.26
	Sheltering Shielding Factor for All but Cohort 4	0.2	0.2	0.2	0.2	0.2
	Evacuation Shielding Factor for Cohort 4	0.5	0.5	0.5	0.5	0.5
	Normal Activity Shielding Factor for Cohort 4	0.05	0.05	0.05	0.05	0.05
	Sheltering Shielding Factor for Cohort 4	0.05	0.05	0.05	0.05	0.05
IDIREC	Direction in Network Evacuation Model	Table C-6 Table C-7	Table C-6 Table C-7	Table C-6 Table C-7	Table C-6 Table C-7	Table C-6 Table C-7

Variable	Description	LTSBO	Unmitigated STSBO	ISLOCA	TISGTR Mitigated	TISGTR Unmitigated
IPLUME	Plume Model Dispersion Code	3	3	3	3	3
KIMODL	Model Flag for KI Ingestion	KI	KI	KI	KI	KI
LASMOV	Last Ring in Movement Zone	17	17	17	17	17
NUMACA	Number of Latent Cancer Health Effects	8	8	8	8	8
NUMEFA	Number of Early Fatality Effects	3	3	3	3	3
NUMEIN	Number of Early Injury Effects	7	7	7	7	7
NUMEVA	Outer Boundary of Evacuation/Shelter Region	Cohort 1 - 15 Cohorts 2 to 6 - 12	Cohort 1 - 15 Cohorts 2 to 6 - 12	Cohort 1 - 15 Cohorts 2 to 6 - 12	Cohort 1 - 15 Cohorts 2 to 6 - 12	Cohort 1 - 15 Cohorts 2 to 6 - 12
NUMFIN	Number of Fine Grid Subdivisions	7	7	7	7	7
ORGFLG	Doses to be Calculated for Specified Organ	All TRUE for FGR-13 All TRUE for DOSFAC2 except for A-Lower LI and L-Liver, which are FALSE	All TRUE for FGR-13 All TRUE for DOSFAC2 except for A-Lower LI and L-Liver, which are FALSE	All TRUE for FGR-13 All TRUE for DOSFAC2 except for A-Lower LI and L-Liver, which are FALSE	All TRUE for FGR-13 All TRUE for DOSFAC2 except for A-Lower LI and L-Liver, which are FALSE	All TRUE for FGR-13 All TRUE for DOSFAC2 except for A-Lower LI and L-Liver, which are FALSE
OVRRID	Wind Rose Probability Override	.FALSE.	.FALSE.	.FALSE.	.FALSE.	.FALSE.
POPFLG	Population Distribution Flag	FILE	FILE	FILE	FILE	FILE
POPFRAC	Population Fraction Ingesting KI	Cohort 2 - 1.0 Cohort 1, 3-6 - 0.0	Cohort 2 - 1.0 Cohort 1, 3-6 - 0.0	Cohort 2 - 1.0 Cohort 1, 3-6 - 0.0	Cohort 2 - 1.0 Cohort 1, 3-6 - 0.0	Cohort 2 - 1.0 Cohort 1, 3-6 - 0.0
PROTIN [E]	Inhalation Protection Factor – evacuation for all but Cohort 4	0.98	0.98	0.98	0.98	0.98
PROTIN [N]	Inhalation Protection Factor - normal activity for all but Cohort 4	0.46	0.46	0.46	0.46	0.46

Variable	Description	LTSBO	Unmitigated STSBO	ISLOCA	TISGTR Mitigated	TISGTR Unmitigated
PROTIN [S]	Inhalation Protection Factor – sheltering for all but Cohort 4	0.33	0.33	0.33	0.33	0.33
PROTIN [E]	Inhalation Protection Factor – evacuation for Cohort 4	0.98	0.98	0.98	0.98	0.98
PROTIN [N]	Inhalation Protection Factor - normal activity for Cohort 4	0.33	0.33	0.33	0.33	0.33
PROTIN [S]	Inhalation Protection Factor – sheltering for Cohort 4	0.33	0.33	0.33	0.33	0.33
REFPNT	Reference Time Point (ARRIVAL or SCRAM)	ALARM	ALARM	ALARM	ALARM	ALARM
RESCON	Emergency phase resuspension coefficient	0.0001	0.0001	0.0001	0.0001	0.0001
RESHAF	Resuspension Concentration Half-Life	182000	182000	182000	182000	182000
RISCAT	Risk by Weather-Category Flag	.FALSE.	.FALSE.	.FALSE.	.FALSE.	.FALSE.
RISTHR	Risk Threshold for Fatality Radius	0	0	0	0	0
SKPFAC [E]	Skin Protection Factors – evacuation for all but Cohort 4	0.98	0.98	0.98	0.98	0.98
SKPFAC [N]	Skin Protection Factors - normal activity for all but Cohort 4	0.46	0.46	0.46	0.46	0.46
SKPFAC [S]	Skin Protection Factors – sheltering for all but Cohort 4	0.33	0.33	0.33	0.33	0.33

Variable	Description	LTSBO	Unmitigated STSBO	ISLOCA	TISGTR Mitigated	TISGTR Unmitigated
SKPFAC [E]	Skin Protection Factors – evacuation for Cohort 4	0.98	0.98	0.98	0.98	0.98
SKPFAC [N]	Skin Protection Factors - normal activity Cohort 4	0.33	0.33	0.33	0.33	0.33
SKPFAC [S]	Skin Protection Factors – sheltering for Cohort 4	0.33	0.33	0.33	0.33	0.33
TIMHOT	Hot Spot Relocation Time	86400	86400	86400	86400	86400
TIMNRM	Normal Relocation Time	129600	129600	129600	129600	129600
TRAVEL POINT	Evacuee Movement Option	CENTER POINT	CENTER POINT	CENTER POINT	CENTER POINT	CENTER POINT
WTFRAC	Weighting Fraction Applicable to this Scenario					
	Cohort 1	0.2	0.2	0.2	0.2	0.2
	Cohort 2	0.535	0.535	0.535	0.535	0.535
	Cohort 3	0.193	0.193	0.193	0.193	0.193
	Cohort 4	0.007	0.007	0.007	0.007	0.007
	Cohort 5	0.062	0.06	0.06	0.06	0.06
	Cohort 6	0.005	0.005	0.005	0.005	0.005
WTNAME	Type of Weighting for Cohorts	PEOPLE	PEOPLE	PEOPLE	PEOPLE	PEOPLE

Table C-6 Grid-Level Evacuation Speed Multipliers Used in the Surry LTSBO, Unmitigated STSBO, TI-SGTR Mitigated and Unmitigated Scenarios for Cohorts 1-2

Compass Sector																
Radial Ring	**1**	**2**	**3**	**4**	**5**	**6**	**7**	**8**	**9**	**10**	**11**	**12**	**13**	**14**	**15**	**16**
1	3	3	3	3	3	3	3	3	3	3	3	3	3	3	3	3
2	3	3	3	3	3	3	3	3	3	3	3	3	3	3	3	3
3	3	3	3	3	3	3	3	3	3	3	3	3	3	3	3	3
4	3	3	3	3	3	3	3	3	3	3	3	3	3	3	3	3
5	3	3	3	3	3	3	3	3	3	3	3	3	3	3	3	3
6	3	3	3	3	3	3	3	3	3	3	3	3	3	3	3	3
7	3	3	3	3	3	3	3	3	3	3	3	3	3	3	3	3
8	3	3	3	3	3	3	3	3	3	3	3	3	3	3	3	3
9	3	3	3	3	3	3	3	3	3	3	3	3	3	3	3	3
10	1	1	1	1	1	1	3	3	3	3	3	3	3	3	3	3
11	1	1	1	1	1	1	1	1	1	1	1	1	1	1	1	1
12	1	1	1	1	1	1	1	1	1	1	1	1	1	1	1	1
13	1	1	1	1	1	1	1	1	1	1	1	1	1	1	1	1
14	1	1	1	1	1	1	1	1	1	1	1	1	1	1	1	1
15	1	1	1	1	1	1	1	1	1	1	1	1	1	1	1	1
16	1	1	1	1	1	1	1	1	1	1	1	1	1	1	1	1
17	1	1	1	1	1	1	1	1	1	1	1	1	1	1	1	1

Compass Sector																
Radial Ring	**17**	**18**	**19**	**20**	**21**	**22**	**23**	**24**	**25**	**26**	**27**	**28**	**29**	**30**	**31**	**32**
1	3	3	3	3	3	3	3	3	3	3	3	3	3	3	3	3
2	3	3	3	3	3	3	3	3	3	3	3	3	3	3	3	3
3	3	3	3	3	3	3	3	3	3	3	3	3	3	3	3	3
4	3	3	3	3	3	3	3	3	3	3	3	3	3	3	3	3
5	3	3	3	3	3	3	3	3	3	3	3	3	3	3	3	3
6	3	3	3	3	3	3	3	3	3	3	3	3	3	3	3	3
7	3	3	3	3	3	3	3	3	3	3	3	3	3	3	3	3
8	3	3	3	3	3	3	3	3	3	3	3	3	3	3	3	3
9	3	3	3	3	3	3	3	3	3	3	3	3	3	3	3	3
10	3	3	3	3	3	3	3	3	3	3	3	3	3	3	3	3
11	1	1	1	1	1	1	3	3	3	3	3	3	3	3	3	3
12	1	1	1	1	1	1	1	3	3	3	3	3	3	3	3	3
13	1	1	1	1	1	1	1	3	3	3	3	3	3	3	3	3
14	1	1	1	1	1	1	1	3	3	3	3	3	3	3	3	3
15	1	1	1	1	1	1	1	1	3	3	3	3	3	3	3	3
16	1	1	1	1	1	1	1	1	1	3	3	3	3	3	3	3
17	1	1	1	1	1	1	3	3	3	3	3	3	3	3	3	3

Compass Sector																
Radial Ring	**33**	**34**	**35**	**36**	**37**	**38**	**39**	**40**	**41**	**42**	**43**	**44**	**45**	**46**	**47**	**48**
1	3	3	3	3	3	3	3	3	3	3	3	3	3	3	3	3
2	3	3	3	3	3	3	3	3	3	3	3	3	3	3	3	3
3	3	3	3	3	3	3	3	3	3	3	3	3	3	3	3	3
4	3	3	3	3	3	3	3	3	3	3	3	3	3	3	3	3
5	3	3	3	3	3	3	3	3	3	3	3	3	3	3	3	3
6	3	3	3	3	3	3	3	3	3	3	3	3	3	3	3	3
7	3	3	3	3	3	3	3	3	3	3	3	3	3	3	3	3
8	3	3	3	3	3	3	3	3	3	3	3	3	3	3	3	3
9	3	3	3	3	3	3	3	3	3	3	3	3	3	3	3	3
10	3	3	3	3	3	3	3	3	3	3	3	3	3	3	3	3
11	3	3	3	3	3	3	3	3	3	3	3	3	3	3	3	3
12	3	3	3	3	3	3	3	3	3	3	3	3	3	3	3	3
13	3	3	3	3	3	3	3	3	3	3	3	3	3	3	3	3
14	3	3	3	3	3	3	3	3	3	3	3	3	3	3	3	3
15	3	3	3	3	3	3	3	3	3	3	3	3	3	3	3	3
16	3	3	3	3	3	3	3	3	3	3	3	3	3	3	3	3
17	3	3	3	3	3	3	3	3	3	3	3	3	3	3	3	3

Compass Sector																
Radial Ring	**49**	**50**	**51**	**52**	**53**	**54**	**55**	**56**	**57**	**58**	**59**	**60**	**61**	**62**	**63**	**64**
1	3	3	3	3	3	3	3	3	3	3	3	3	3	3	3	3
2	3	3	3	3	3	3	3	3	3	3	3	3	3	3	3	3
3	3	3	3	3	3	3	3	3	3	3	3	3	3	3	3	3
4	3	3	3	3	3	3	3	3	3	3	3	3	3	3	3	3
5	3	3	3	3	3	3	3	3	3	3	3	3	3	3	3	3
6	3	3	3	3	3	3	3	3	3	3	3	3	3	3	3	3
7	3	3	3	3	3	3	3	3	3	3	3	3	3	3	3	3
8	3	3	3	3	3	3	3	3	3	3	3	3	3	3	3	3
9	3	3	3	3	3	3	3	1	1	1	1	3	3	3	3	3
10	3	3	3	3	3	3	3	1	1	1	1	1	1	1	1	1
11	3	3	3	3	3	3	3	1	1	1	1	1	1	1	1	1
12	3	3	3	3	3	3	3	1	1	1	1	1	1	1	1	1
13	3	3	3	3	3	1	1	1	1	1	1	1	1	1	1	1
14	3	3	3	3	3	1	1	1	1	1	1	1	1	1	1	1
15	3	3	3	3	3	1	1	1	1	1	1	1	1	1	1	1
16	3	3	3	3	1	1	1	1	1	1	1	1	1	1	1	1
17	3	3	3	3	1	1	1	1	1	1	1	1	1	1	1	1

Table C-7 Grid-Level Evacuation Speed Multipliers Used in the Surry LTSBO, Unmitigated STSBO, TI-SGTR Mitigated and Unmitigated Scenarios for Cohorts 3-5

	Compass Sector															
Radial Ring	**1**	**2**	**3**	**4**	**5**	**6**	**7**	**8**	**9**	**10**	**11**	**12**	**13**	**14**	**15**	**16**
1	2	2	2	2	2	2	2	2	2	2	2	2	2	2	2	2
2	2	2	2	2	2	2	2	2	2	2	2	2	2	2	2	2
3	2	2	2	2	2	2	2	2	2	2	2	2	2	2	2	2
4	2	2	2	2	2	2	2	2	2	2	2	2	2	2	2	2
5	2	2	2	2	2	2	2	2	2	2	2	2	2	2	2	2
6	2	2	2	2	2	2	2	2	2	2	2	2	2	2	2	2
7	2	2	2	2	2	2	2	2	2	2	2	2	2	2	2	2
8	2	2	2	2	2	2	2	2	2	2	2	2	2	2	2	2
9	2	2	2	2	2	2	2	2	2	2	2	2	2	2	2	2
10	1	1	1	1	1	1	2	2	2	2	2	2	2	2	2	2
11	1	1	1	1	1	1	1	1	1	1	1	1	1	1	1	1
12	1	1	1	1	1	1	1	1	1	1	1	1	1	1	1	1
13	1	1	1	1	1	1	1	1	1	1	1	1	1	1	1	1
14	1	1	1	1	1	1	1	1	1	1	1	1	1	1	1	1
15	1	1	1	1	1	1	1	1	1	1	1	1	1	1	1	1
16	1	1	1	1	1	1	1	1	1	1	1	1	1	1	1	1
17	1	1	1	1	1	1	1	1	1	1	1	1	1	1	1	1

Compass Sector																
Radial Ring	**17**	**18**	**19**	**20**	**21**	**22**	**23**	**24**	**25**	**26**	**27**	**28**	**29**	**30**	**31**	**32**
1	2	2	2	2	2	2	2	2	2	2	2	2	2	2	2	2
2	2	2	2	2	2	2	2	2	2	2	2	2	2	2	2	2
3	2	2	2	2	2	2	2	2	2	2	2	2	2	2	2	2
4	2	2	2	2	2	2	2	2	2	2	2	2	2	2	2	2
5	2	2	2	2	2	2	2	2	2	2	2	2	2	2	2	2
6	2	2	2	2	2	2	2	2	2	2	2	2	2	2	2	2
7	2	2	2	2	2	2	2	2	2	2	2	2	2	2	2	2
8	2	2	2	2	2	2	2	2	2	2	2	2	2	2	2	2
9	2	2	2	2	2	2	2	2	2	2	2	2	2	2	2	2
10	2	2	2	2	2	2	2	2	2	2	2	2	2	2	2	2
11	1	1	1	1	1	1	2	2	2	2	2	2	2	2	2	2
12	1	1	1	1	1	1	1	2	2	2	2	2	2	2	2	2
13	1	1	1	1	1	1	1	2	2	2	2	2	2	2	2	2
14	1	1	1	1	1	1	1	2	2	2	2	2	2	2	2	2
15	1	1	1	1	1	1	1	1	2	2	2	2	2	2	2	2
16	1	1	1	1	1	1	1	1	1	2	2	2	2	2	2	2
17	1	1	1	1	1	1	2	2	2	2	2	2	2	2	2	2

Compass Sector																
Radial Ring	**33**	**34**	**35**	**36**	**37**	**38**	**39**	**40**	**41**	**42**	**43**	**44**	**45**	**46**	**47**	**48**
1	2	2	2	2	2	2	2	2	2	2	2	2	2	2	2	2
2	2	2	2	2	2	2	2	2	2	2	2	2	2	2	2	2
3	2	2	2	2	2	2	2	2	2	2	2	2	2	2	2	2
4	2	2	2	2	2	2	2	2	2	2	2	2	2	2	2	2
5	2	2	2	2	2	2	2	2	2	2	2	2	2	2	2	2
6	2	2	2	2	2	2	2	2	2	2	2	2	2	2	2	2
7	2	2	2	2	2	2	2	2	2	2	2	2	2	2	2	2
8	2	2	2	2	2	2	2	2	2	2	2	2	2	2	2	2
9	2	2	2	2	2	2	2	2	2	2	2	2	2	2	2	2
10	2	2	2	2	2	2	2	2	2	2	2	2	2	2	2	2
11	2	2	2	2	2	2	2	2	2	2	2	2	2	2	2	2
12	2	2	2	2	2	2	2	2	2	2	2	2	2	2	2	2
13	2	2	2	2	2	2	2	2	2	2	2	2	2	2	2	2
14	2	2	2	2	2	2	2	2	2	2	2	2	2	2	2	2
15	2	2	2	2	2	2	2	2	2	2	2	2	2	2	2	2
16	2	2	2	2	2	2	2	2	2	2	2	2	2	2	2	2
17	2	2	2	2	2	2	2	2	2	2	2	2	2	2	2	2

Compass Sector																
Radial Ring	**49**	**50**	**51**	**52**	**53**	**54**	**55**	**56**	**57**	**58**	**59**	**60**	**61**	**62**	**63**	**64**
1	2	2	2	2	2	2	2	2	2	2	2	2	2	2	2	2
2	2	2	2	2	2	2	2	2	2	2	2	2	2	2	2	2
3	2	2	2	2	2	2	2	2	2	2	2	2	2	2	2	2
4	2	2	2	2	2	2	2	2	2	2	2	2	2	2	2	2
5	2	2	2	2	2	2	2	2	2	2	2	2	2	2	2	2
6	2	2	2	2	2	2	2	2	2	2	2	2	2	2	2	2
7	2	2	2	2	2	2	2	2	2	2	2	2	2	2	2	2
8	2	2	2	2	2	2	2	2	2	2	2	2	2	2	2	2
9	2	2	2	2	2	2	2	1	1	1	1	2	2	2	2	2
10	2	2	2	2	2	2	2	1	1	1	1	1	1	1	1	1
11	2	2	2	2	2	2	2	1	1	1	1	1	1	1	1	1
12	2	2	2	2	2	2	2	1	1	1	1	1	1	1	1	1
13	2	2	2	2	2	1	1	1	1	1	1	1	1	1	1	1
14	2	2	2	2	2	1	1	1	1	1	1	1	1	1	1	1
15	2	2	2	2	2	1	1	1	1	1	1	1	1	1	1	1
16	2	2	2	2	1	1	1	1	1	1	1	1	1	1	1	1
17	2	2	2	2	1	1	1	1	1	1	1	1	1	1	1	1

Table C-8 Evacuation Direction Parameters Used in the Surry LTSBO, Unmitigated STSBO, TI-SGTR Mitigated and Unmitigated Scenarios

Compass Sector																
Radial Ring	**1**	**2**	**3**	**4**	**5**	**6**	**7**	**8**	**9**	**10**	**11**	**12**	**13**	**14**	**15**	**16**
1	1	1	1	1	1	1	1	1	1	1	1	1	1	1	1	1
2	1	1	1	1	1	1	1	1	1	1	1	1	1	1	1	1
3	1	1	1	1	1	1	1	1	1	1	1	1	1	1	1	1
4	1	1	1	2	2	2	2	2	2	2	2	2	2	2	2	2
5	1	1	1	2	2	2	2	2	2	2	2	2	2	2	2	2
6	1	1	1	2	2	2	2	2	2	2	2	2	2	2	2	2
7	1	1	1	1	1	1	1	1	1	1	1	1	1	1	1	1
8	1	1	1	1	1	2	1	1	1	1	1	1	1	1	1	1
9	1	1	1	1	1	1	1	1	1	1	1	1	1	1	1	1
10	1	1	1	1	1	1	1	1	1	1	1	1	1	1	1	1
11	1	1	1	1	1	1	1	1	1	1	1	1	1	1	4	4
12	1	1	1	1	4	4	4	4	2	2	2	2	2	1	1	1
13	1	4	1	1	1	1	1	1	1	1	1	1	1	1	1	1
14	4	4	2	2	2	2	2	1	4	4	4	4	1	2	2	2
15	1	2	2	2	1	1	4	4	4	4	4	4	4	1	1	1
16	2	2	1	4	4	4	4	1	1	1	1	1	1	1	1	1
17	1	1	1	1	1	1	1	1	1	1	1	1	1	1	1	1

Compass Sector																
Radial Ring	**17**	**18**	**19**	**20**	**21**	**22**	**23**	**24**	**25**	**26**	**27**	**28**	**29**	**30**	**31**	**32**
1	1	1	1	1	1	1	1	1	1	1	1	1	1	1	1	1
2	1	1	1	1	1	1	1	1	1	1	1	1	1	1	1	1
3	1	1	1	1	1	4	4	4	4	2	2	2	1	1	1	1
4	2	2	2	2	2	2	2	2	2	2	2	2	2	1	1	1
5	2	2	2	2	2	2	2	2	2	2	2	2	2	2	2	1
6	2	2	2	2	2	2	2	2	2	2	2	2	2	1	1	1
7	1	1	1	1	1	1	1	1	1	1	1	1	1	1	1	1
8	1	1	1	1	1	1	1	1	2	2	2	1	1	2	2	2
9	1	1	1	1	1	1	1	1	1	1	2	2	2	1	1	1
10	1	1	1	1	1	1	1	1	1	1	1	2	2	2	2	1
11	4	4	4	4	4	4	1	1	1	1	1	1	1	2	2	2
12	1	1	1	1	4	4	1	1	1	1	1	1	1	1	1	1
13	1	1	1	1	1	4	1	1	1	1	2	2	1	1	1	1
14	2	2	2	2	1	4	4	1	1	2	2	2	1	1	1	1
15	1	2	2	2	2	1	1	4	1	2	2	2	1	4	4	4
16	1	1	2	2	1	1	4	2	1	1	1	1	1	1	1	1
17	1	1	1	1	1	1	1	1	1	1	1	1	1	1	1	1

Compass Sector																
Radial Ring	**33**	**34**	**35**	**36**	**37**	**38**	**39**	**40**	**41**	**42**	**43**	**44**	**45**	**46**	**47**	**48**
1	1	1	1	1	1	1	1	1	1	1	1	1	1	1	1	1
2	1	1	1	1	1	1	1	1	1	1	1	1	1	1	1	1
3	4	4	4	4	4	4	4	4	4	1	1	1	1	1	1	1
4	1	1	1	1	1	1	1	1	1	1	1	1	1	1	1	1
5	1	1	1	1	1	1	1	1	1	1	1	1	1	1	1	1
6	1	1	1	1	1	1	1	1	1	1	1	1	1	1	1	1
7	1	1	1	1	1	1	1	1	1	1	1	1	1	1	1	1
8	1	1	4	4	4	4	1	1	1	1	1	1	1	1	1	1
9	1	1	1	1	1	1	1	1	1	1	1	1	1	1	1	1
10	1	1	1	2	2	2	1	1	1	4	4	4	4	4	4	4
11	2	2	2	2	2	1	1	4	4	2	2	1	1	1	1	1
12	1	1	1	1	1	1	1	4	4	2	2	1	1	1	1	4
13	1	1	1	1	1	1	2	2	1	2	1	4	4	2	2	1
14	1	4	4	4	4	2	2	2	1	2	1	2	2	2	2	2
15	1	1	4	1	1	1	1	1	1	1	1	1	1	1	1	4
16	1	1	1	2	2	2	2	2	2	2	2	2	1	1	1	1
17	4	4	4	4	4	4	2	2	2	1	1	1	2	2	2	1

Compass Sector																
Radial Ring	**49**	**50**	**51**	**52**	**53**	**54**	**55**	**56**	**57**	**58**	**59**	**60**	**61**	**62**	**63**	**64**
1	1	1	1	1	1	1	1	1	1	1	1	1	1	1	1	1
2	1	1	1	1	1	1	1	1	1	1	1	1	1	1	1	1
3	1	1	1	1	1	1	1	1	1	1	1	1	1	1	1	1
4	1	1	1	1	1	1	1	1	1	1	1	1	1	1	1	1
5	1	1	1	1	1	1	1	1	1	1	1	1	1	1	1	1
6	1	1	1	1	1	1	1	1	1	1	1	1	1	1	1	1
7	1	1	1	1	1	1	1	1	1	1	1	1	1	1	1	1
8	1	1	1	1	1	1	1	1	1	1	1	1	1	1	1	1
9	1	1	1	1	1	1	1	1	1	1	1	1	1	1	1	1
10	1	2	1	1	1	1	1	1	1	1	1	1	1	1	1	1
11	1	4	4	4	4	1	1	1	1	1	1	1	1	1	1	1
12	4	4	4	4	1	1	1	1	1	1	1	1	1	1	1	1
13	4	4	4	1	1	2	1	1	2	2	1	1	1	1	1	1
14	1	1	4	4	2	2	2	2	2	2	2	2	2	1	1	4
15	4	1	1	1	1	1	1	1	1	1	1	1	1	1	1	1
16	1	1	1	1	1	1	2	2	2	2	2	1	4	4	4	2
17	1	1	1	1	1	1	1	1	1	1	1	1	1	1	1	1

Table C-9 CHRONC Input Parameters Used in the Surry LTSBO, Unmitigated STSBO, TISGTR Mitigated and Unmitigated Scenarios

Variable	Description	LTSBO	Unmitigated STSBO	ISLOCA	TISGTR Mitigated	TISGTR Unmitigated
CHNAME	CHRONC Problem Identification	Surry with no Food-Chain Modeling	Surry with no Food-Chain Modeling	Surry with no Food-Chain Modeling	Surry with no Food-Chain Modeling	Surry with no Food-Chain Modeling
CDFRM	Farmland Decontamination Cost					
	Level 1	1330	1330	1330	1330	1330
	Level 2	2960	2960	2960	2960	2960
CDNFRM	Non farmland Decontamination Cost					
	Level 1	7110	7110	7110	7110	7110
	Level 2	19000	19000	19000	19000	19000
CRTOCR	Critical Organ for CHRONC Phase	L-ICRP60ED	L-ICRP60ED	L-ICRP60ED	L-ICRP60ED	L-ICRP60ED
DPRATE	Property Depreciation Rate	0.2	0.2	0.2	0.2	0.2
DLBCST	Hourly Labor Cost for Decontamination Worker	84000	84000	84000	84000	84000
DPFRCT	Farm Production Dairy Fraction	0	0	0	0	0
DSCRLT	Long-Term Phase Dose Criterion	0.04	0.04	0.04	0.04	0.04
DSCRTI	Intermediate-Phase Dose Criterion	100000	100000	100000	100000	100000
DSRATE	Societal Discount Rate for Property	0.12	0.12	0.12	0.12	0.12
DSRFCT	Decontamination Factors					
	Level 1	3	3	3	3	3
	Level 2	15	15	15	15	15
DUR_INTPHAS	Duration of the Intermediate Phase	0	0	0	0	0
EVACST	Emergency Phase Cost of Evacuation/Relocation	172	172	172	172	172
EXPTIM	Maximum Exposure Time	1580000000	1580000000	1580000000	1580000000	1580000000
FDPATH	COMIDA2 vs. MACCS Food Model Switch	OFF	OFF	OFF	OFF	OFF
FRACLD	Fraction of Area that is Land					
FRCFRM	Fraction of Area Used for Farming					
FRFDL	Fraction of Decontamination Cost for Labor					
	Level 1	0.3	0.3	0.3	0.3	0.3
	Level 2	0.35	0.35	0.35	0.35	0.35
FRFIM	Farm Wealth Improvements Fraction	0.25	0.25	0.25	0.25	0.25
FRMPRD	Average Annual Farm Production					
FRNFIM	Nonfarm Wealth Improvements Fraction	0.8	0.8	0.8	0.8	0.8
FRNFDL	Nonfarm Labor Cost Fraction					
	Level 1	0.7	0.7	0.7	0.7	0.7
	Level 2	0.5	0.5	0.5	0.5	0.5

Variable	Description	LTSBO	Unmitigated STSBO	ISLOCA	TISGTR Mitigated	TISGTR Unmitigated
GWCOEF	Long-Term Groundshine Coefficients					
	Term 1	0.5	0.5	0.5	0.5	0.5
	Term 2	0.5	0.5	0.5	0.5	0.5
KSWTCH	Diagnostic Output Option Switch	0	0	0	0	0
LBRRATE	Long-Term Breathing Rate	0.000266	0.000266	0.000266	0.000266	0.000266
LGSHFAC	Long-Term Groundshine Protection Factor	0.26	0.26	0.26	0.26	0.26
LPROTIN	Long-Term Inhalation Protection Factor	0.46	0.46	0.46	0.46	0.46
LVLDEC	Number of Decontamination Levels	2	2	2	2	2
NGWTRM	Number of Terms in Groundshine Weathering Equation	2	2	2	2	2
NRWTRM	Number of Terms in Resuspension Weathering Equation	3	3	3	3	3
POPCST	Per Capita Cost of Long-Term Relocation	12000	12000	12000	12000	12000
RELCST	Relocation Cost per Person-Day	172	172	172	172	172
RWCOEF	Long-Term Resuspension Factor Coefficients					
	Term 1	0.00001	0.00001	0.00001	0.00001	0.00001
	Term 2	0.0000001	0.0000001	0.0000001	0.0000001	0.0000001
	Term 3	0.000000001	0.000000001	0.000000001	0.000000001	0.000000001
TFWKF	Fraction Farmland Worker Time in Contaminated Zone					
	Level 1	0.1	0.1	0.1	0.1	0.1
	Level 2	0.33	0.33	0.33	0.33	0.33
TFWKNF	Fraction Non farmland Worker Time in Contaminated Zone					
	Level 1	0.33	0.33	0.33	0.33	0.33
	Level 2	0.33	0.33	0.33	0.33	0.33
TGWHLF	Groundshine Weathering Half-Lives					
	Term 1	16000000	16000000	16000000	16000000	16000000
	Term 2	2800000000	2800000000	2800000000	2800000000	2800000000
TIMDEC	Decontamination Times					
	Level 1	5184000	5184000	5184000	5184000	5184000
	Level 2	10368000	10368000	10368000	10368000	10368000
TMPACT	Time Action Period Ends	158000000	158000000	158000000	158000000	158000000
TRWHLF	Resuspension Weathering Half-Lives					
	Term 1	16000000	16000000	16000000	16000000	16000000
	Term 2	160000000	160000000	160000000	160000000	160000000
	Term 3	1600000000	1600000000	1600000000	1600000000	1600000000

Variable	Description	LTSBO	Unmitigated STSBO	ISLOCA	TISGTR Mitigated	TISGTR Unmitigated
VALWF	Value of Farm Wealth	6900	6900	6900	6900	6900
VALWNF	Value of Nonfarm Wealth	220000	220000	220000	220000	220000

APPENDIX D

ISLOCA MODELING DETAILS

1 INTRODUCTION

This appendix expands on the subjects only mentioned or described briefly regarding the Interfacing System Loss of Coolant Accident (ISLOCA) in the main body of the report.

2 SAFEGUARD BUILDING MODELING DETAIL

Table D-1 delineates the flow paths defined in the Surry MELCOR model to represent doors, penetrations, etc., interconnecting the Safeguards Area, Containment Spray Pump Area, and Main Steam Valve House (MSVH). These flow paths are shown in Figure D-1.

Table D-1 Description of Flow Paths in MELCOR Representation of Surry Safeguards Area, Containment Spray Pump Area, and Main Steam Valve House

Flow Path I.D.	From Control Volume	To Control Volume	Size	Description of Modeled Door, Penetration, etc.
600	850	855	4” radius half circle through 1’ thick wall	Wall drain at base of Outside Recirculation Spray Pump 2A cubicle
601	850	855	1’ diameter hole through 1’ thick wall with 10” diameter pipe passing through it	Pipe penetration in Outside Recirculation Spray Pump 2A cubicle wall, centered 3’-8” off floor
602	851	855	4” radius half circle through 1’ thick wall	Wall drain at base of Low Head Safety Injection Pump 1A cubicle
603	851	855	1’ diameter hole through 1’ thick wall with 10” diameter pipe passing through it	Pipe penetration in Low Head Safety Injection Pump 1A cubicle wall, centered 3’-8” off floor
604	852	856	4” radius half circle through 1’ thick wall	Wall drain at base of Low Head Safety Injection Pump 1B cubicle
605	852	856	1’ diameter hole through 1’ thick wall with 10” diameter pipe passing through it	Pipe penetration in Low Head Safety Injection Pump 1B cubicle wall, centered 3’-8” off floor
606	853	856	4” radius half circle through 1’ thick wall	Wall drain at base of Outside Recirculation Spray Pump 2B cubicle
607	853	856	1’ diameter hole through 1’ thick wall with 10” diameter pipe passing through it	Pipe penetration in Outside Recirculation Spray Pump 2B cubicle wall, centered 3’-8” off floor
608	854	855	6’-6” tall, 6’ wide	Intra-volume connection, sill at floor
609	854	856	6’-6” tall, 6’ wide	Intra-volume connection, sill at floor

Flow Path I.D.	From Control Volume	To Control Volume	Size	Description of Modeled Door, Penetration, etc.
610	857	851	2' wide, 1.5' tall, through 1' thick wall	Electrical opening in Low Head Safety Injection Pump 1A cubicle wall, sill 13’ off floor
611	860	866	3'-5" wide, 7' tall, through 1' thick wall	Unlatched personnel door at grade for entry to Safeguards Area
612	860	819	3" wide, 60'-4" long	Shaker space between Safeguards Area roof and Containment (covered with flashing), opens at 37.5 psf differential pressure
613	860	819	10 m^2	Safeguards Area gross roof failure, opens at 75 psf differential pressure
614	850	860	2’-6” x 2’-6”	Open manway to Outside Recirculation Spray Pump 2A cubicle, at grade
615	851	860	2’-6” x 2’-6”	Open manway to Low Pressure Injection Pump 1A cubicle, at grade
616	857	860	2’-6” x 4’	Open manway to 19'-6" level, at grade
617	852	860	2’-6” x 2’-6”	Open manway to Low Pressure Injection Pump 1B cubicle, at grade
618	853	860	2’-6” x 2’-6”	Open manway to Low Pressure Injection Pump 2B cubicle, at grade
619	854	857	2’-6” x 4’	Open manway in 19’-6” elevation floor to 12' level outside of pump cubicles
620	854	857	5 total openings each 2'-6" square, assume 3/16" steel plate ==> each plate weighs 47.9 lb and requires 0.0532 psi differential pressure to move	Openings in 19'-6" elevation floor covered with unsecured steel plate, plates assumed to be wholly displaced from the openings by 0.0532 psi differential pressure
621	854	865	2'-6" x 4'	Opening at 12' elevation to Valve Pit
622	862	819	3'-4" x 7'-2", through 1’ thick wall	Personnel door at grade for entry to Containment Spray Pump Area and MSVH

Flow Path I.D.	From Control Volume	To Control Volume	Size	Description of Modeled Door, Penetration, etc.
623	861	862	30” x 30”	Open manway to lower level of Containment Spray Pump Area building
624	856	861	2'-6" tall, 2' wide, through 1’ thick wall, estimated to be 50% full, sill 12’ off floor	Electrical opening between Safeguards Area and Containment Spray Pump Area
625	856	861	21" tall, 5' long, sill 4’-9” off floor, estimated to be 50% full of piping	Pipe opening between Safeguards Area and Containment Spray Pump Area
626	862	819	2’ x 2’	4,000 cfm exhaust fan in the roof of the Containment Spray Pump Area
627	862	864	4'-4 1/2" wide, 8' high, through 1’ thick wall, opens to MSVH, 1/16” wide x 24’-10” tall shaker space between buildings included as fixed open fraction	Closed door between upper levels of Containment Spray Pump Area and MSVH assumed always closed
628	861	863	Doorway is 4' wide x 7' high, opening is 6'-6" wide x 11’-6” high, thresholds at floor	Open doorway & taller opening between lower levels of Containment Spray Pump Area and MSVH
629	862	819	2 holes of 1' diameter through 2’ thick wall, estimated to be 12’ off floor	Abandoned pipe penetrations in the wall of the upper level of the Containment Spray Pump Area leading to the environment
630	864	819	8' wide x 4'-6" high but area reduced to 1.195 m^2 to give zero flow (pre transient) from upper floor to lower floor of MSVH through chained-open manway, sill 2’ off floor	Fixed louvers in the wall of the upper level of MSVH
631	864	819	4’ x 4’ through 2’ thick wall, sill 10’ off floor	13,500 cfm exhaust ventilation fan in the wall of the upper level of MSVH
632	863	864	3' x 3'-7", assume 25 lbf is required to open the cover	Covered manway to lower level of MSVH

Flow Path I.D.	From Control Volume	To Control Volume	Size	Description of Modeled Door, Penetration, etc.
633	863	810	Assume 4” std piping, 103’ long, minor loss coefficient for elbows, branches, etc., of 7.9	4" drain from MSVH pit to Auxiliary Building, inlet at 11’-0” elevation, attaches to complex drain network terminating at 2’ elevation
634	863	810	7'-7" wide, 18" tall, through 2’ thick wall, sill at 8’-3” elevation	Pipe tunnel between MSVH pit and Auxiliary Building, filled with sprayed penetration sealant, assumed to dislodge when water fills the pit
636	853	861	1/32" equivalent width,** 14'-6" tall, extends up from floor, assume angle iron overlaps concrete by 3"	Shaker space between Safeguards Area and Containment Spray Pump Area, 3" shaker space with angle iron on each side
642	863	814	1/16" wide x 16' tall, extending up from floor, assume angle iron overlaps concrete by 3"	Shaker space between MSVH and Aux Bldg, 3" shaker space with angle iron on each side
643	862	819	3" wide x 22'-9" long	Shaker space between Containment Spray Pump Area roof and Containment (covered with flashing), opens at 37.5 psf differential pressure
645	857	855	2’-6” tall, 2’ wide, through 1’ thick wall, estimated to be 50% blocked	Penetration high in the wall
646	857	856	2’-6” tall, 2’ wide, through 1’ thick wall, estimated to be 50% blocked	Penetration high in the wall
647	862	819	10 m^2	Containment Spray Pump Area gross roof failure, opens at 75 psf differential pressure
648	863	864	2’-6” x 2’-6”	Other covered (but chained open) manway to lower level (11'-6" elevation) of MSVH, the cover to this manway was chained open the day of NRC/SNL site visit (1/18/2011). Modeling assumes manway is uncovered

Flow Path I.D.	From Control Volume	To Control Volume	Size	Description of Modeled Door, Penetration, etc.
649	860	862	5'-7" tall x 2'-10" wide (with half circle top), through 1' thick wall, estimated to be 80% blocked	Ventilation ducting penetration between top levels of Safeguards Area and Containment Spray Pump Area
812	240	855	132' of 6" Sch. 160 pipe, 17' of 10" Sch. 160 pipe, 26' of 10" Sch. 40 pipe, stainless steel, uninsulated, 2.57" diameter cavitating venturi, piping connects to top of cold leg, break centerline 1'-9" off Safeguards Area floor, 7.7" elevation drop from top of cold leg to break centerline	LHSI piping, Loop A Cold Leg backwards to Safeguards Area, failed check valves, ISLOCA pipe break, active pool scrubbing, DFs to manage aerosol turbulent deposition and impaction

** For flow path I.D. 636 the width was determined based on review of site construction drawing details.

3 LOW HEAD SAFETY INJECTION PIPE MODELING DETAIL

The low head safety injection (LHSI) piping that would be subjected to reactor coolant system (RCS) pressure, should the two serial check valves in any one of the three cold leg injection lines fail, extends backwards from the check valves into the Safeguards Area and then through the Containment Spray Pump Area and Main Steam Valve House well into the Auxiliary Building. Two MELCOR representations of LHSI piping were utilized in the ISLOCA analysis – a simple representation where the fluid volume and metal mass of the piping was unaccounted for and a detailed representation where these parameters were accounted for. In the simple representation, frictional losses, form losses, and critical flow areas were represented in a single flow path. No control volumes or heat structures were included in the simple representation. In the detailed representation, flow losses and critical flow areas were portioned among several flow paths, and several control volumes and heat structures were included to account for the fluid volume and metal mass of the piping. Figure D-1 illustrates the detailed MELCOR model of the LHSI piping and roughly identifies the attributes of the physical piping. The specific piping modeled is the safety injection piping serving Cold Leg #2.

From the check valves to the isolation motor operated valve (MOV) 1890C, the 6” and 10” piping is Schedule 160 with 0.718” and 1.125” wall thicknesses, respectively, and a pressure rating higher than RCS operating pressure. From MOV 1890C back, none of the piping is rated strong enough to withstand RCS operating pressure. Between MOV 1890C and Flow Element (FE) 1945 for LHSI Train A and FE 1946 for LHSI Train B, the piping (10”) is Schedule 40 having a 0.365” wall thickness. The 8” piping in the Safeguards buildings and all of the way back to isolation points within the Auxiliary Building is Schedule 40 having a wall thickness of 0.322”. Between FEs 1945 and 1946 and the LHSI pump discharge check valves, the piping (10”) is Schedule 10 with a 0.165” wall thickness. It is these relatively short sections of thin-walled 10” piping that are judged as most susceptible to rupture given the dual check valve failure of the postulated ISLOCA. This piping ranges in centerline elevation from 13’-9” to 15’-8” (1’-9” to 3’-8” off the floor). Significantly more of this piping exists outside the pump cubicles than inside them and slightly more of the piping is at the 13’-9” elevation than at the 15’8” elevation. Figure D-2 shows the location of the different LHSI pipe sections in the Safeguards Area.

The ISLOCA break is assumed to occur centered 1’-9” above the floor with an area equivalent to the orifice area of FE 1945 or FE 1946 (each of which are of diameter 7.1469”). Only one of the thin-walled 10” piping sections is assumed to rupture (not both). The break is assumed to happen outside of a LHSI pump cubicle.

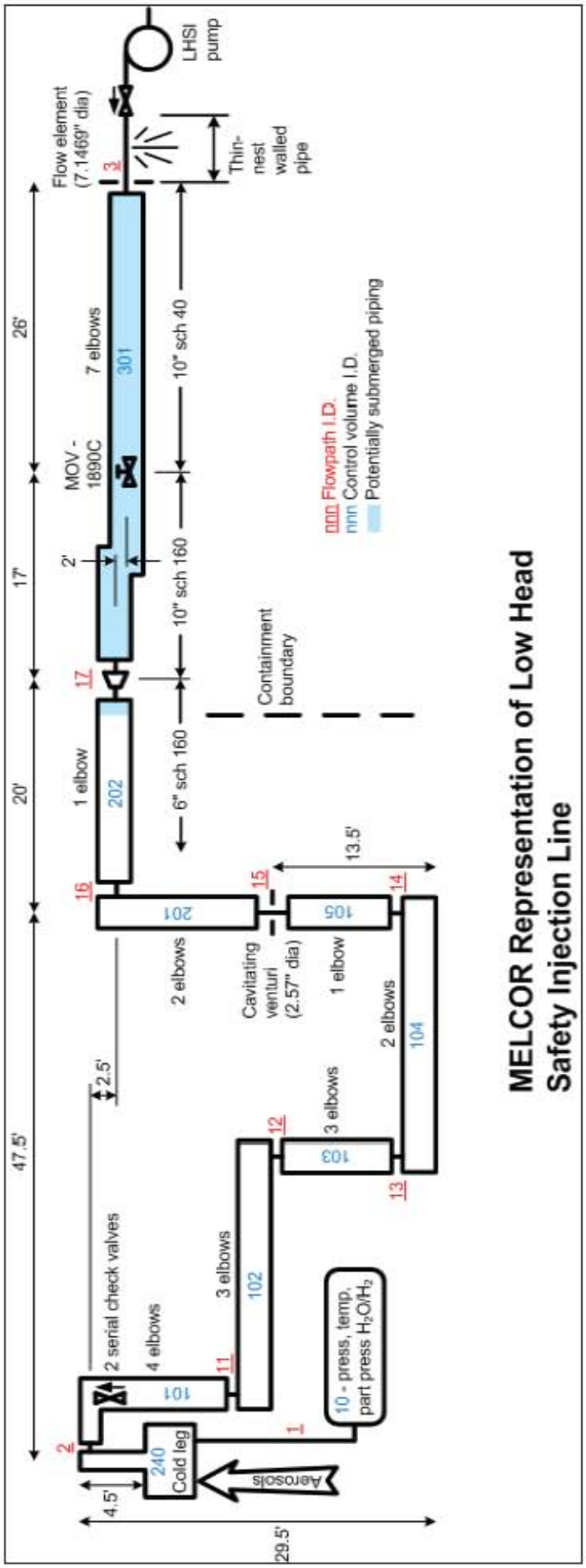

Figure D-1 Low Head Safety Injection Piping MELCOR Nodalization

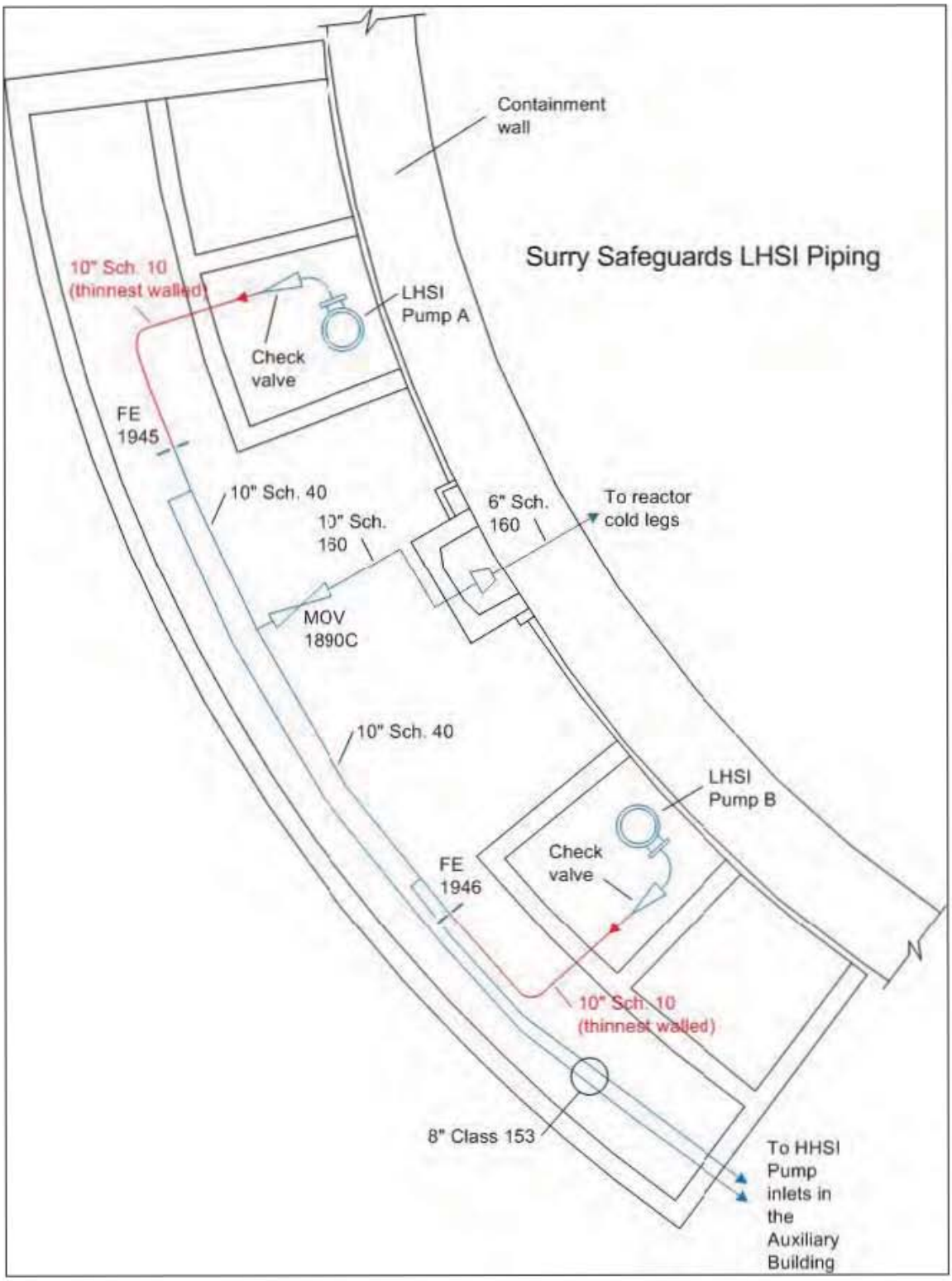

Figure D-2 Low Head Safety Injection Pipe Sections in Safeguard Building

Noteworthy specifics of this piping and the modeling of it follow.

Size, length, schedule, etc. of the different sections:
All of the piping is either 6" or 10". Most of the piping is 6". All of the piping inside Containment is 6" while all of the piping in the Safeguards Area is 10". All of the 6" pipe is Schedule 160. The schedule of the 10" piping varies as identified above. All of the pipe is stainless steel. Only the 3' of pipe closest to the cold leg is insulated. This short length of insulation was disregarded in the MELCOR modeling because it was of negligible length and would not affect the deposition. Potentially, the piping in the Safeguards Area (and hence the break location) would be submerged for some time given the postulated ISLOCA.

Number of elbows, fittings, etc. in the different sections:
The following elbows, fittings, etc. exist in the different sections:

- 6" piping from the cold leg to the venturi - 1 entrance, 13 elbows, 2 swing-type check valves
- 6" pipe from venturi to 6"-to-10" transition - 3 elbows, 1 flow-branched tee, 1 expansion
- 10" piping from transition to MOV 1890C - 3 elbows, 1 gate valve (1890C)
- 10" piping from MOV 1890C to FE1946 - 3 elbows, 1 flow-branched tee, 1 gate valve (MOV 1864B)

Flow elements:
Flow elements (FE 1945/1946) between the LHSI pumps and MOV 1890C are characterized by sharp-edged orifices of diameter 7.1469". The pipe rupture is assumed to be larger than the orifice such that the orifice is the more limiting flow area.

Isolation valve MOV 1890C:
Main LHSI isolation valve MOV 1890C, beyond which only Schedule 160 piping exists (reaching all the way to the cold leg), is not of submersible design. Consequently, this valve is susceptible to failure in an ISLOCA. This is because water issuing from the ISLOCA pipe break will flood the valve's motor before the valve can be closed against the RCS blowdown proceeding through it. The assumption has been made in the ISLOCA analysis that this valve fails to close, i.e., remains in its normal open position.

Venturi:
Each LHSI piping run to an RCS cold leg has a flow venturi incorporated. The venturi is a cavitating venturi with a gradual contraction and a gradual expansion. Its minimum flow diameter is 2.57". The smallest flow area in an LHSI piping run is the minimum flow area in the venturi.

Check valves:
Each LHSI piping run to an RCS cold leg has two check valves in series. The check valves are swing type. It is the failure of both of these valves in one of the LHSI piping runs that results in the ruptured pipe outside of containment in the ISLOCA scenario. The first check valve (in the normal flow direction) is 12'-9" from the cold leg. The second check valve is 2'-3" from the cold leg.

Safety injection piping approach to the cold leg:
The safety injection piping to Cold Leg #2 drops 4'-6" from its high point to where it adjoins the top of the cold leg. Between the two check valves in the 6" piping, 2" high head safety injection (HHSI) piping adjoins such that LHSI and HHSI share the last 3'-7" length of 6" piping leading to the cold leg. This commonality of piping between LHSI and HHSI proves important in the ISLOCA scenario as the HHSI delivered to the broken injection piping can't reach the cold leg. Instead, it is driven out the pipe break by the strength of the blowdown. This phenomena is modeled in the MELCOR calculation by simply delivering the portion of HHSI destined to Cold Leg #2 directly to the Safeguards Area (to Control Volume 855).

Noteworthy in relation to this commonality of piping between LHSI and HHSI is that accumulator injection is through separate dedicated 12" piping to each cold leg. All accumulator injection, therefore, reaches the cold legs.

Pool scrubbing at potentially underwater break location:
Optional MELCOR pool scrubbing logic (SPARC) was enabled in the flow path representing the LHSI piping (Flow Path 812) in the simple representation. This logic removes radionuclide aerosols and vapors from a gas as it flows through a pool of water. The flow area of Flow Elements 1945/1946 (7.1469" diameter) was specified. A single vent hole with horizontal orientation was called out.

The LHSI piping at Surry is not insulated. As the reactor core overheated in an ISLOCA, flow backwards through this piping would heat it. Fission product aerosols deposited in the piping would heat it further raising its temperature above that of the vapor flowing through it. The piping would lose heat from its outer surface via convection and radiation. Both of these heat transfer modes are enabled in the MELCOR modeling. For the LHSI piping internal to containment, convection heat transfer is to an isolated control volume filled with atmospheric air at 20℃ and radiation is to an encompassing environment at 20°C with an emissivity of 0.4 defined for the piping. For the piping internal to the Safeguards Area, heat transfer is to an isolated control volume containing a water pool and air. Convection heat transfer is to the pool and or the air dependent upon whether the piping is submerged, partially submerged, or above the level of the pool. The level and temperature of the pool are time dependent and set equal to the level and temperature of the pool in the Safeguards Area in the initial overall ISLOCA calculation. Radiation is to an encompassing environment at the temperature of the pool with an emissivity of 0.4 defined for the piping. Note that radiation heat loss from the piping would be disabled by MELCOR given submergence of the piping in the pool.

4 SAFETY-RELATED FILTERED VENTILTION SYSTEM MODELING DETAIL

The ventilation system enlists both an exhaust train and a supply train, depicted in Figure D-3. There are two operational configurations for the exhaust train, normal and safety-related operations. Common to each operational state, the exhaust ventilation has seven inlets from the Safeguards Area and one inlet from the Containment Spray Pump Area with a combined rated volumetric flow rate of 11,000 cfm. A length of 205 ft is estimated for ducting connecting the Safeguards Area and the Containment Spray Pump Area (referred to jointly in this Section as Safeguards) with fans and filters located in the Auxiliary Building.

During normal operations, the 11,000 cfm is drawn by dual 6,000 cfm exhaust fans. Once an injection signal has occurred, the exhaust from Safeguards is instead provided by dual 36,000 cfm fans drawing though HEPA and charcoal filters. In addition to the 11,000 cfm from Safeguards, 61,000 cfm is drawn through Central Flow ducting serving the Auxiliary Building and other potentially contaminated areas. This 61,000 cfm is simply drawn from the environment in the MELCOR model. The safety-related fans and filters are housed in the Auxiliary Building. Two parallel filter banks are employed. The filter banks are unique to the safety-related filtration fans, unlike the normal exhaust fans. The safety-related fan ducting exhausts to the environment through a common stack located on the roof of the Auxiliary Building. Figure D-4 presents the safety-related filtration fan curve.

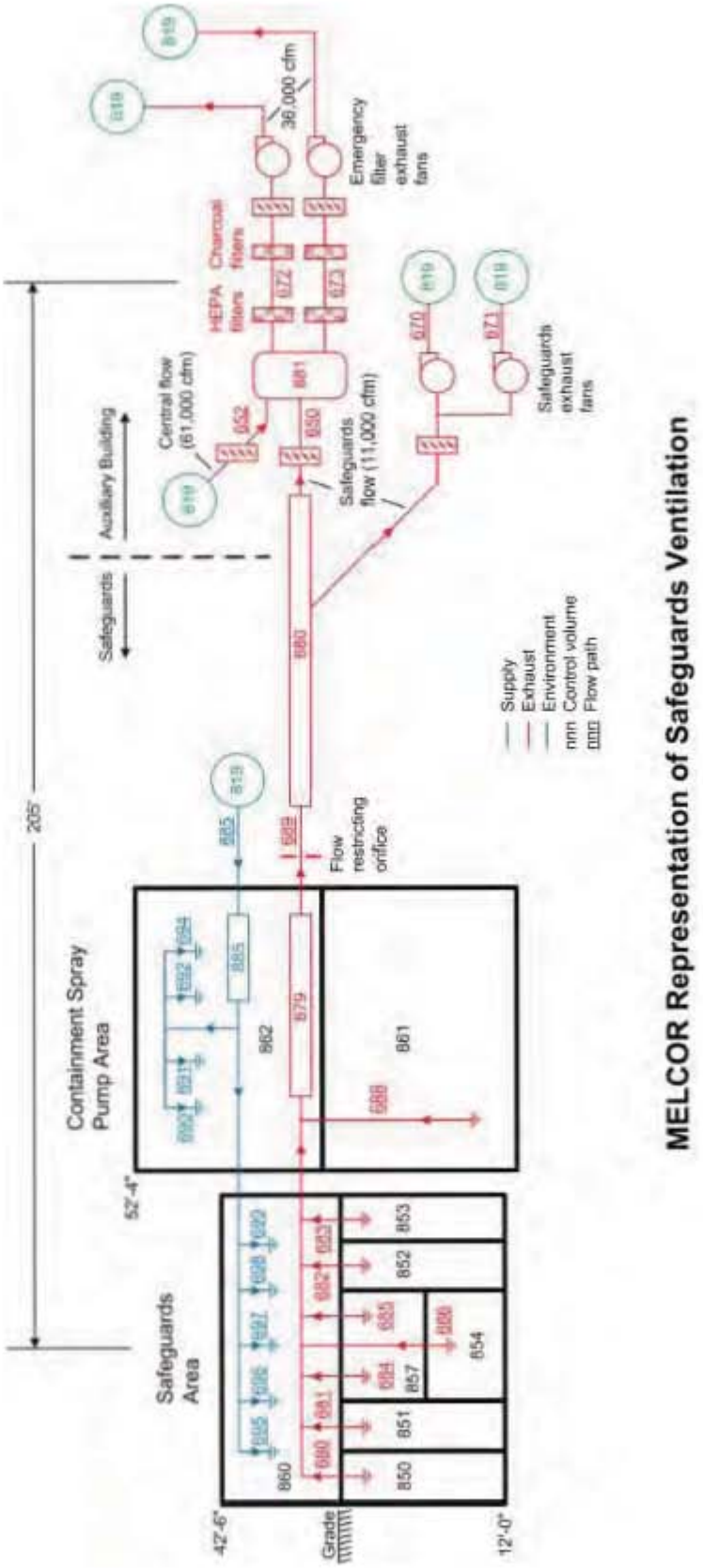

Figure D-3 Safeguards Building Ventilation MELCOR Nodalization

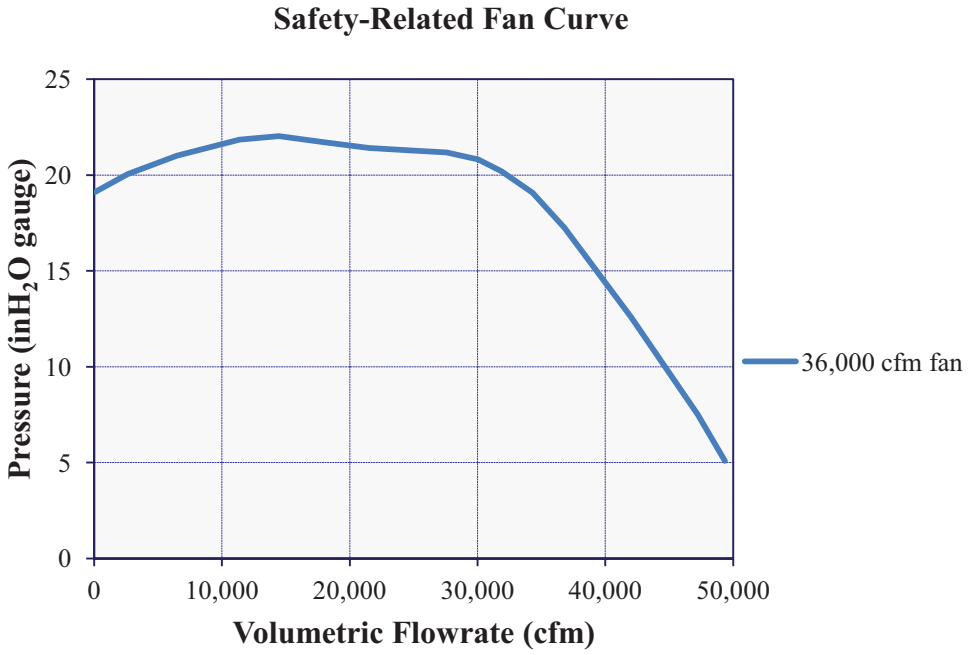

Figure D-4 Auxiliary Ventilation System Safety-Related Fan Curve

The common ducting nodalization is divided into two control volumes, CV879 and CV880. CV879 represents the section of the ductwork where each exhaust line, flow paths FL680, FL686, and FL688, connect to the ducting. CV880 represents the estimated remaining physical volume of the ducting connecting Safeguards to the filters and fans in the Auxiliary Building. The ducting is represented by a ½-cm thick, cylindrical, stainless-steel heat structure and a flow area of 4.54 ft^2. Original calculations provided by the utility demonstrated a 6 in. H_2O gauge pressure drop due to an orifice in the ducting. FL689 captures this pressure drop as well as the remaining frictional losses and flow characteristics throughout the ducting.

The exhaust ventilation ducts in CV850-CV853 are sized to withdraw 21% of the total flow, 11,000 cfm, from each of the 4 pump cubicles during normal operations. Similarly FL684, FL685, FL686, and FL688 flow areas are defined to withdraw 2%, 3%, 1%, and 11%, respectively (see Table D-2).

Table D-2 Ventilation Flow Path Flow Rates

Flow Path	Vent Area (ft^2)	Fraction of Total Flow Rate
FL680	1.36	21%
FL681	1.36	21%
FL682	1.36	21%
FL683	1.36	21%
FL684	0.13	2%
FL685	0.18	3%
FL686	0.11	1%
FL688	0.68	11%

Whether a safety injection signal has occurred will determine which fan/filtration system is employed during the calculation. During the steady state analysis, prior to an injection signal, the normal exhaust system is functional and the system exhausts to the environment through FL670 and FL671. A constant fan head was applied for the normal exhaust fans to produce the necessary steady state condition, given the 11,000 cfm reportedly drawn from Safeguards. After injection initiates, the normal-operation exhaust fans are isolated and the safety-related filtration and fans are utilized. Flow from the common ducting is passed to CV881, which acts as a homogeneous mixing volume between the Central Flow ventilation system and Safeguards ventilation prior to the atmosphere constituents passing through the filtration system.

The filtration system is comprised of pre-filters, particulate filters (HEPA filters) and charcoal filters. Filter cells are constructed, from inlet to outlet, with one pre-filter, one HEPA filter, and two parallel charcoal filters. The filter cells are assembled into filter banks. Each bank is 10 filter cells wide and 3 filter cells high. There are two filter banks in parallel corresponding with the two parallel fans. Each bank was designed for a flow rate of 36,000 cfm.

Due to limited information, the pre-filter is not represented in the model. The HEPA filter dimensions are 24” x 24” x 12”. Manufactured clean filter resistance, per Surry technical specification, are not to exceed 1 in. H_2O gauge for the HEPA filters and 2 in. H_2O gauge for the charcoal filters at 300 ft/min. A hydraulic diameter of 0.00105 m was specified for the HEPA filter to produce the reported upper bound resistance given laminar flow. The charcoal filter is modeled with identical laminar flow loss characteristics, but with twice the depth to produce the reported 2 in. H_2O gauge clear filter resistance, twice the clean filter resistance as the HEPA filter. Decontamination factors of 200 and 100 are defined for the aerosol captured by HEPA filters and inorganic and elemental iodine vapor species capture by charcoal filters, respectively.

As aerosols are captured, the flow resistance through the HEPA filters increases. The pressure drop due to mass loading is modeled by adjusting the laminar flow coefficient. A 2^{nd} -order polynomial least squares fit of the data presented in “The Effects of Media Area on the Dust Holding Capacity of Deep Pleat HEPA Filters” [1] was applied to capture the increase in flow resistance (see equation below). FL672 and FL673 incorporate the delta pressure contributions

from the fans, the particulate filters (clean loss), and the charcoal filters as well as from the aerosol loading on the particulate filters.

$$SLAM \approx 0.0019\ W^2 + 0.1943W$$

where:
SLAM is the laminar flow coefficient and
W is the aerosol mass captured by a HEPA filter within the filter bank (kg)

Per vendor description, due to the standard use of neoprene in the construction of nuclear installation HEPA filter gaskets, the specified maximum continuous service temperature is identified as 250 °F. Temperatures in the MELCOR calculation upstream of the filtration system, in CV881, were observed relative to this maximum service temperature, but the failure criterion is not included in the modeling. Note that any heating of the filters by the decay heat of captured fission products is not accounted for in the MELCOR model. Effectively, the assumption has been made that as long as the fans are running decay heat in the filters would be carried away by the flow through them.

Pressure switches located just upstream of the safety related fans of the Auxiliary Ventilation System will trip the fans should pressure drop below -21 in. H_2O gauge at the switches. This design feature is included in the MELCOR fan control logic.

The supply air to Safeguards, depicted in Figure D-3, is drawn from the environment. Fans originally installed in the supply ducting are no longer energized to ensure a sub-atmospheric pressure in Safeguards - negative pressure being maintained by exhaust ventilation operation. The supply ducting provides five inlets to the Safeguards Area and four inlets to the Containment Spray Pump Area.

5 BUILDING BOUNDARY FAILURE CRITERIA DETAIL

An ISLOCA at Surry and consequential RCS blowdown into the Safeguards Area would pressurize the Safeguards buildings potentially failing building boundaries. Further insults to building boundaries could potentially result from subsequent hydrogen burns. A scrutinizing of the construct of the Safeguard buildings identified weak points as described here.

Opening of the Safeguards Area personnel door:
The lone personnel door for accessing the Safeguards Area is centrally located in the top floor of the building at ground level. The door opens outward and is equipped with a closer. The door is 36" x 80" and opens to a modest push by hand. It has no latch. Flow Path 611 shown in Figure D-5 represents this door in the MELCOR model. Given a meaningful elevation of Safeguards Area pressure (i.e., 1 in. H_2O gauge or 5.19 psfg), this flow path is opened to the environment. The flow path is reclosed upon loss of the elevated pressure. (1" of water would put a force of over 100 lb on this door.)

Tearing of the flashing covering Safeguards Area and/or Containment Spray Pump Area roof shaker spaces:
Per the Surry UFSAR, certain buildings at Surry are designed to withstand a tornado with winds up to 360 mph, which equates to a pressure differential of 2.30 psi (the dynamic pressure of a 360 mph wind). The Safeguards buildings are not such buildings, i.e., the Safeguards buildings are not designated as designed to withstand a tornado. The Safeguards buildings are however, reinforced concrete buildings and the UFSAR points out that no structural damage is known to have resulted to a reinforced concrete building in a tornado. Buildings that are not designed to withstand a tornado, also per the UFSAR, are designed to withstand wind loads (on their walls) based on their elevation. Roofs are designed for uplift load using 1.25 times the wind load. For the Safeguards Area, the design load is 30 psf (0.208 psi) for the walls and the roof uplift load is 1.25 x 30 psf or 37.5 psf (0.260 psi).

The construction of the Safeguards buildings is reinforced concrete with steel roofing. The walls and floors of the buildings are largely below grade. Given the stout construct of the walls, the assumption has been made in the ISLOCA analysis that the weak points in the pressure boundaries of the buildings are their roofs. This assumption is exclusive of the latch-less personnel door to the Safeguards Area described above.

The Safeguards buildings do not have integral back walls. The buildings back up to Containment and the Containment cylinder serves as a back wall to the buildings. The steel roofing on the buildings extends to within a few inches of the Containment wall leaving a gap (i.e., shaker space) that is closed with flashing. This roof flashing has been judged as the weak point in the Safeguards building roofs and hence the weakest point in the pressure boundaries of the buildings notwithstanding the Safeguards Area personnel door. The flashing has been specified in the MELCOR model to tear given a pressure differential across it of 37.5 psf (i.e., the design uplift load for the Safeguards Area roof). The flashing is represented with Flow Paths 612 and 643 for the Safeguards Area and the Containment Spray Pump Area, respectively. Flow Path 612 reflects a gap 3" wide by 60'-4" long while Flow Path 643 reflects a gap 3" wide by 22'-9" long.

Gross failure of the Safeguards Area and/or Containment Spray Pump Area roof as a consequence of a hydrogen burn:
The tearing of roof flashing described above would significantly vent the Safeguards buildings given an ISLOCA and consequential RCS blowdown into them. The venting, however, might not be sufficient to curtail further damage to the boundaries of the buildings from the blowdown or from subsequent hydrogen burns occurring within the buildings.

To address the potential for further damage to the Safeguards buildings due to overpressure, additional flow paths have been included in the MELCOR model between the buildings and the environment. These flow paths manage a gross roof failure. The flow paths open given a pressure greater than twice the design uplift load for the roofs (2 x 37.5 psf or 0.520 psi). The factor of two here reflects a reasonable assumption of safety margin in the building's design and the observation that the roofs consist of heavy-gauge corrugated steel topped by waterproof fabric, foam board, and concrete pavers. The particular flow paths are 613 and 647 for the Safeguards Area and the Containment Spray Pump Area, respectively. The flow paths have an area of 10 m^2 (each).

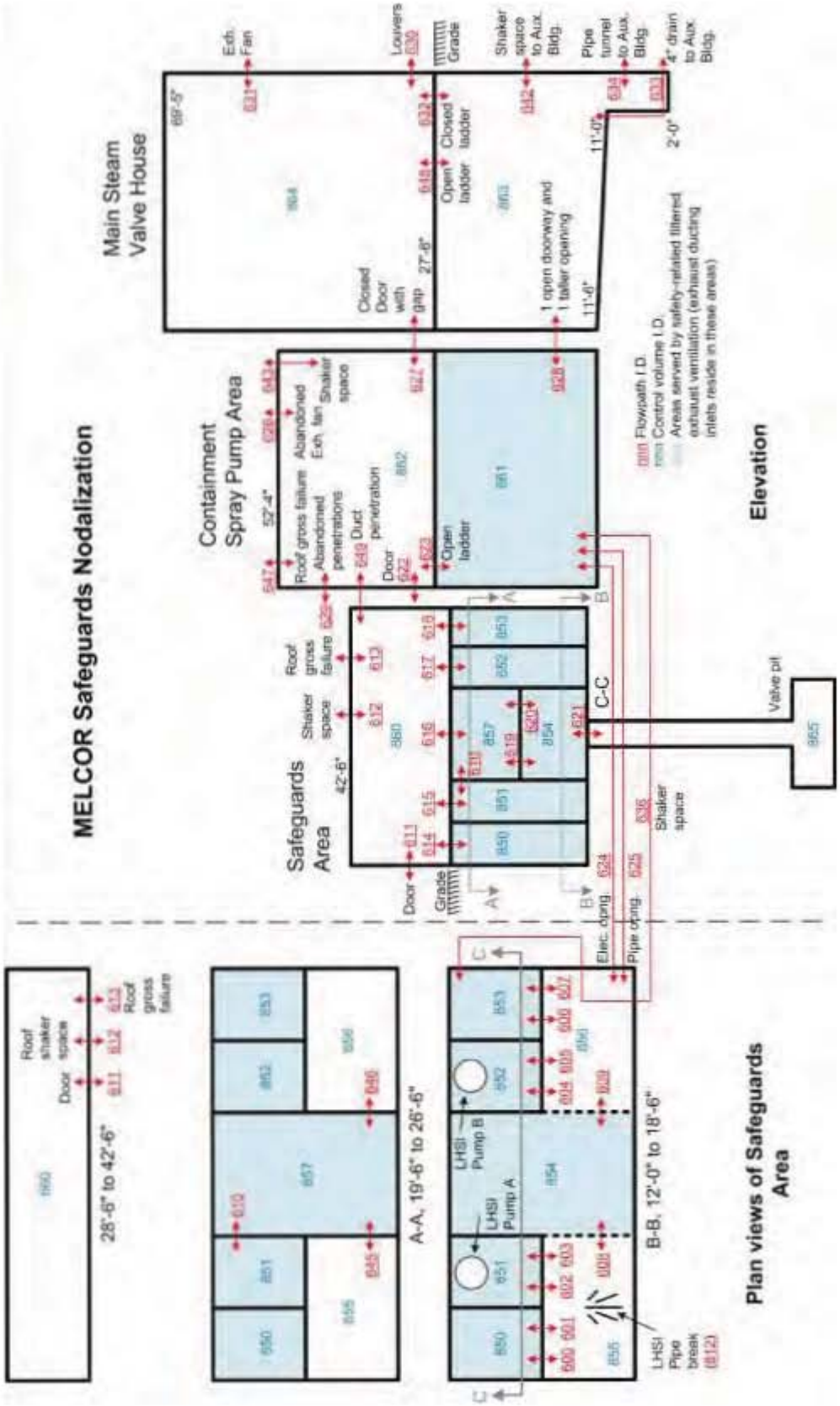

Figure D-5 Safeguards Building MELCOR Nodalization

6 IMPACTION MODELING AND TURBULENT DEPOSITION

The new MELCOR models for turbulent deposition in straight pipes and deposition in elbows were validated against the results of the LWR Aerosol Containment Experiments (LACE) Project. The LACE project, organized by Electric Power Research Institute, performed large-scale experiments to investigate aerosol behavior under simulated LWR accident conditions to provide a database for testing containment-aerosol and related thermal-hydraulic computer codes. The tests studied aerosol behavior under postulated severe accidents conditions not adequately addressed by previous test programs. The studied conditions included total containment bypass (i.e., ISLOCA). Individual LACE tests that studied ISLOCA conditions were CB-1, CB-2, CB-3, LA1, LA3A, LA3B, and LA3C. LACE reports for these tests are the following:

- "Aerosol Behavior Under LWR Containment Bypass Conditions—Results of Tests CB-1, CB-2 and CB-3," LACE TR-001, November 1986

- "Aerosol Behavior in LWR Containment Bypass Piping—Results of LACE Test LA3," LACE TR-011, July 1987

- "Summary of Posttest Aerosol Code Comparisons for LWR Aerosol Containment Experiment (LACE) LA1," LACE TR-022, ORNL/M-365, October 1987

- "Summary of Posttest Aerosol Code-Comparisons Results for LWR Aerosol Containment Experiment (LACE) LA3," LACE TR-024, ORNL/M-492, June 1988

A summary of the LACE project is given in "The LWR Aerosol Containment Experiments (LACE) Project, Summary Report" [3].

The new MELCOR models were applied in a separate-effects calculation that used boundary conditions from the integral full-plant calculation to estimate aerosol retention in the LHSI piping. The estimated aerosol retention for each fission product class was in turn used to specify a decontamination factor (DF) for each MELCOR radionuclide class as input to the integral full-plant calculation which represented the LHSI piping as a single junction.

Assessment Against LACE Experiments

The LACE tests experimentally examined the transport and retention of aerosols typical of LWRs through pipes with high speed flow and in containment volumes during rapid depressurization. In particular, the LA1 and LA3 tests examined deposition in pipe flow under conditions of containment bypass to provide a database for validation of aerosol computer simulation. Accident scenarios represented by the LACE tests include potentially high consequence accidents for which containment may be bypassed altogether, the containment function is impaired early in the accident, or a large fission product release occurs simultaneously with containment failure.

Specific objectives of these tests were to provide validation data that would expose important dependencies in modeling deposition. In particular the following test conditions were examined:

- Effect of gas velocity through the pipe
- Effect of aerosol composition
- Effect of aerosol size distribution

Overall test conditions and results are summarized in Table D-4 below. It is important to note that the range of gas velocities ranges from 23 m/s to 100 m/s, which comprises a range of Reynolds numbers between 30,000 to 300,000. The Wood models [22] implemented into MELCOR were validated against the data of Liu and Agarwal [12], which was performed at Reynolds numbers of 10,000 – 50,000. The VICTORIA models are based on Friedlander & Johnstone's data [7] with Reynolds numbers of 2800 – 44,000 as well as some of Sehmel's [17] experiments with Reynolds numbers of 4200 - 61,000. The conditions of the LA1 and LA3A tests were beyond the range of Reynolds numbers in the database used to develop these deposition models though it has been observed that the dependence on Reynolds number may be small. However, some accident conditions may extend to even higher flow velocities, approaching sonic velocities, well beyond the database for these models. As discussed later in this section, higher velocities can lead to other effects, such as resuspension and/or entrainment of deposited material. There does not appear to be any data that can be used to validate flow approaching sonic velocities.

Table D-3 Aerosol and Thermal-Hydraulic Conditions at Inlet to Test Pipe

Test	Aerosol	CsOH Mass Fraction	Carrier Gas	Gas Velocity (m/s)	Temp. (^{o}C)	Aerosol Source Rate (g/s)	Aerosol Size AMMD (μm)	Mass Retention Fraction
LA1	CsOH/ MnO	0.42	Air-steam	96	247	1.1	1.6	> 0.98
LA3 A	CsOH/ MnO	0.18	N_2-steam	75	298	0.6	1.4	> 0.7
LA3B	CsOH/ MnO	0.12	N2-steam	24	303	0.9	2.4	> 0.4
LA3C	CsOH/ MnO	0.38	N2-steam	23	300	0.9	1.9	> 0.7

Figure D-6 and Figure D-7 are photographs from LACE TR-011 that show pipe deposits observed in test LA3C.

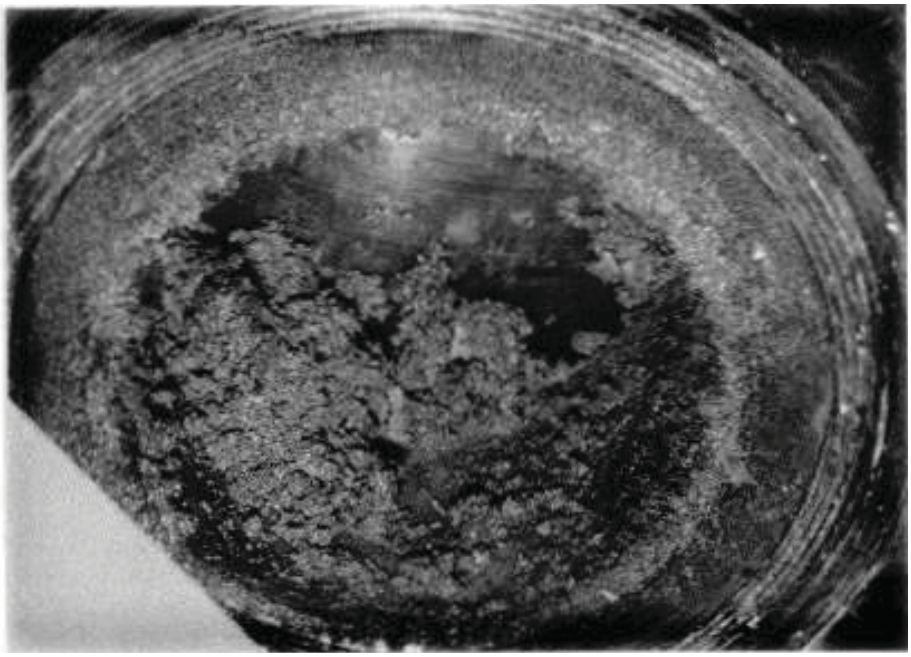

Figure D-6 Test LA3C, Downstream end of pipe 6 showing large deposit

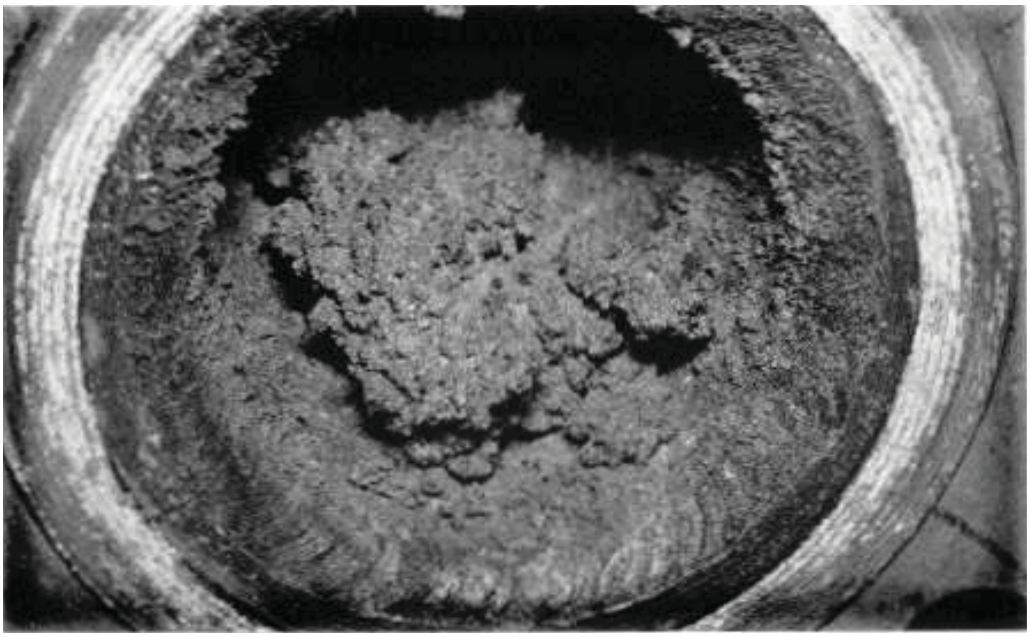

Figure D-7 Test LA3C, downstream end of pipe section 5 showing large bend deposit

MELCOR Turbulent Deposition Models

MELCOR has long had models for predicting aerosol deposition from gravitational settling, diffusion to surfaces, thermophoresis, diffusion to surfaces, and diffusiophoresis [8]. Recently, however, several models for turbulent deposition in pipes have been implemented into MELCOR 1.8.6. In particular, Wood's models for turbulent deposition in pipes with smooth and rough surfaces, as well as the models used by the VICTORIA code were added to MELCOR's deposition modeling capabilities. These models are based on a few fundamental assumptions. For example, it is assumed that the concentration of aerosol in the gas is small enough that the effect of particle-particle interactions is small. In addition, it is assumed that the influence of the aerosol particles on the flow stream is negligible. Not only does this mean that the micro effects on turbulent eddies are negligible, but the macro effects from deposition on surfaces with the subsequent modification of surface roughness and reduction in flow area is not modeled.

Particle deposition is modeled in terms of a deposition velocity V_d, defined as the ratio of the time-averaged particle flux to the surface to the time-averaged airborne particle concentration in the duct. This is then implemented into MELCOR in calculating the rate of deposition on a surface:

$$\frac{1}{A}\frac{dM_C}{dt} = V_d C \qquad (1)$$

Where:

V_d	-	deposition velocity
C	-	particle mass concentration
M_C	-	Mass deposition rate
A	-	Surface area of deposition surface

It is common to correlate the deposition velocity with the particle relaxation time, τ. This is the characteristic time for a particle velocity to respond to a change in air velocity. For spherical particles of diameter d_p and density ρ_p in the Stokes flow regime, it is calculated as:

$$\tau = \frac{\rho_m D_p^2 C_{slip}}{18\mu_g} \qquad (2)$$

Where:

C_{slip}	-	slip correction factor (-)

Non-dimensional forms for the deposition velocity and relaxation time are used in the MELCOR models :

$$V_d^* = \frac{V_d}{u^*} \qquad (3)$$

$$\tau^* = \frac{\tau \rho_g \left(u^*\right)^2}{\mu_g} \qquad (4)$$

Where:

u^* - friction velocity

For flow through smooth cylindrical channels, the friction velocity is found from:

$$u^* = V\sqrt{\frac{f}{2}} \qquad (5)$$

$$f = \frac{0.0791}{\mathrm{Re}^{1/4}} \qquad (6)$$

$$\mathrm{Re} = \frac{D_H \rho_g V}{\mu_g} \qquad (7)$$

Where:

D_H -hydraulic diameter of conduit

Three models, Wood's model for turbulent deposition in rough pipes, Wood's model for turbulent deposition in smooth pipes, and Sehmel's correlation for perfect particle sinks (i.e., the VICTORIA model) for turbulent deposition in smooth pipes were implemented in MELCOR and assessed against LACE data in this study. In addition, we have plotted the non-dimensional deposition velocity as a function of the non-dimensional relaxation time in Figure D-8 and Figure D-9 along with non-dimensionalized data from numerous studies on turbulent deposition. There is significant scatter in the data depicted in Figure D-8 and Figure D-9. Friedlander & Johnstone [7] provided some of the earliest experimental data from particle deposition in turbulent flows. Their investigations qualitatively demonstrated that deposition velocity increased with flow velocity and particle diameter. The data of Liu & Agarwal [12] shows much less scatter with a definite trend for increased deposition at higher relaxation times. These experiments are frequently referenced because of their credibility due the reproducibility of the data and the quality of their methods in obtaining the data. This data set is typically used to benchmark correlations for turbulent deposition. The data from Sehmel [17] is the most extensive in range of relaxation times, Reynolds number, and the effect of pipe size. However, this data shows a significant degree of scatter possibly due to less rigorous experimental techniques.

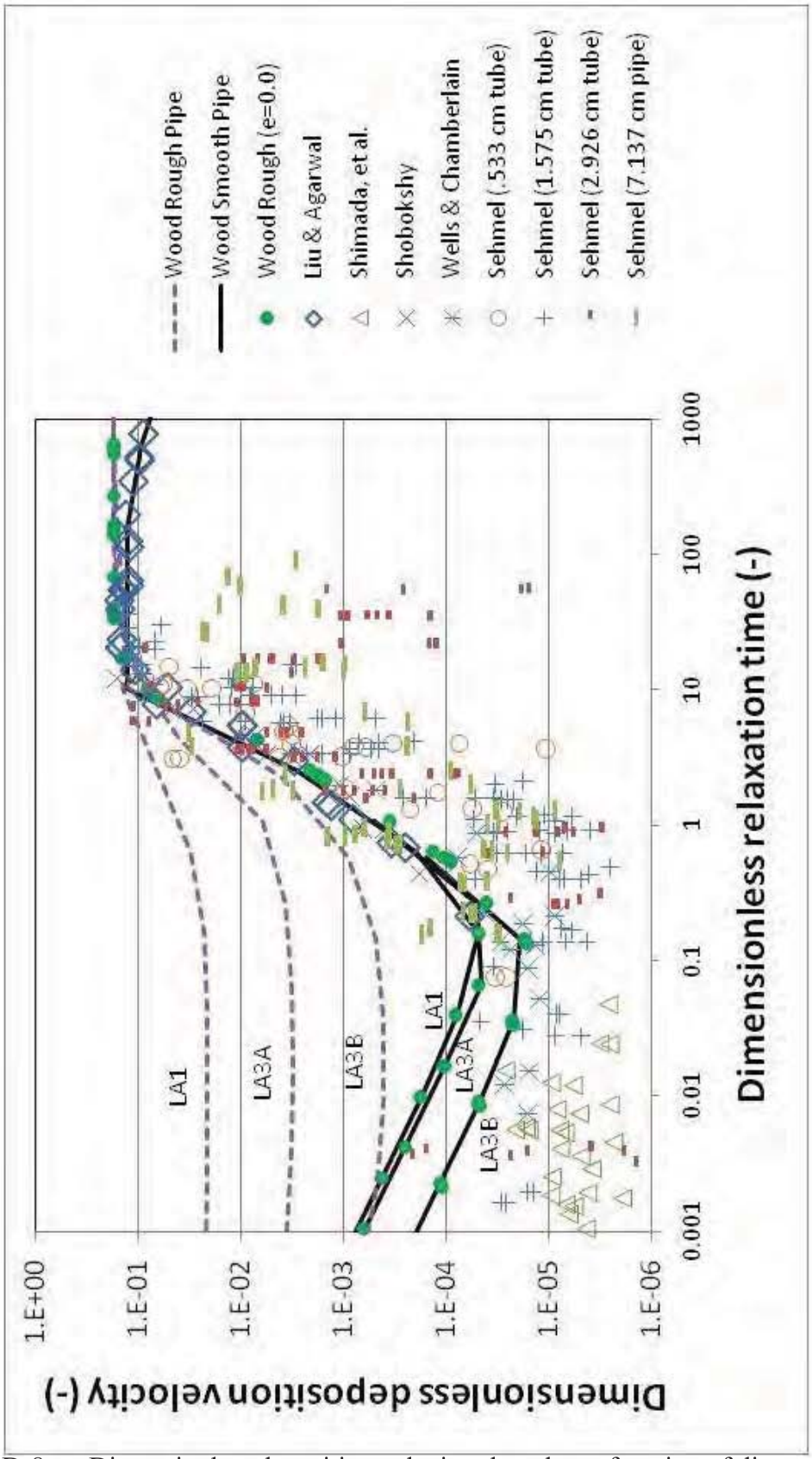

Figure D-8 Dimensionless deposition velocity plotted as a function of dimensionless relaxation time for MELCOR turbulent deposition models

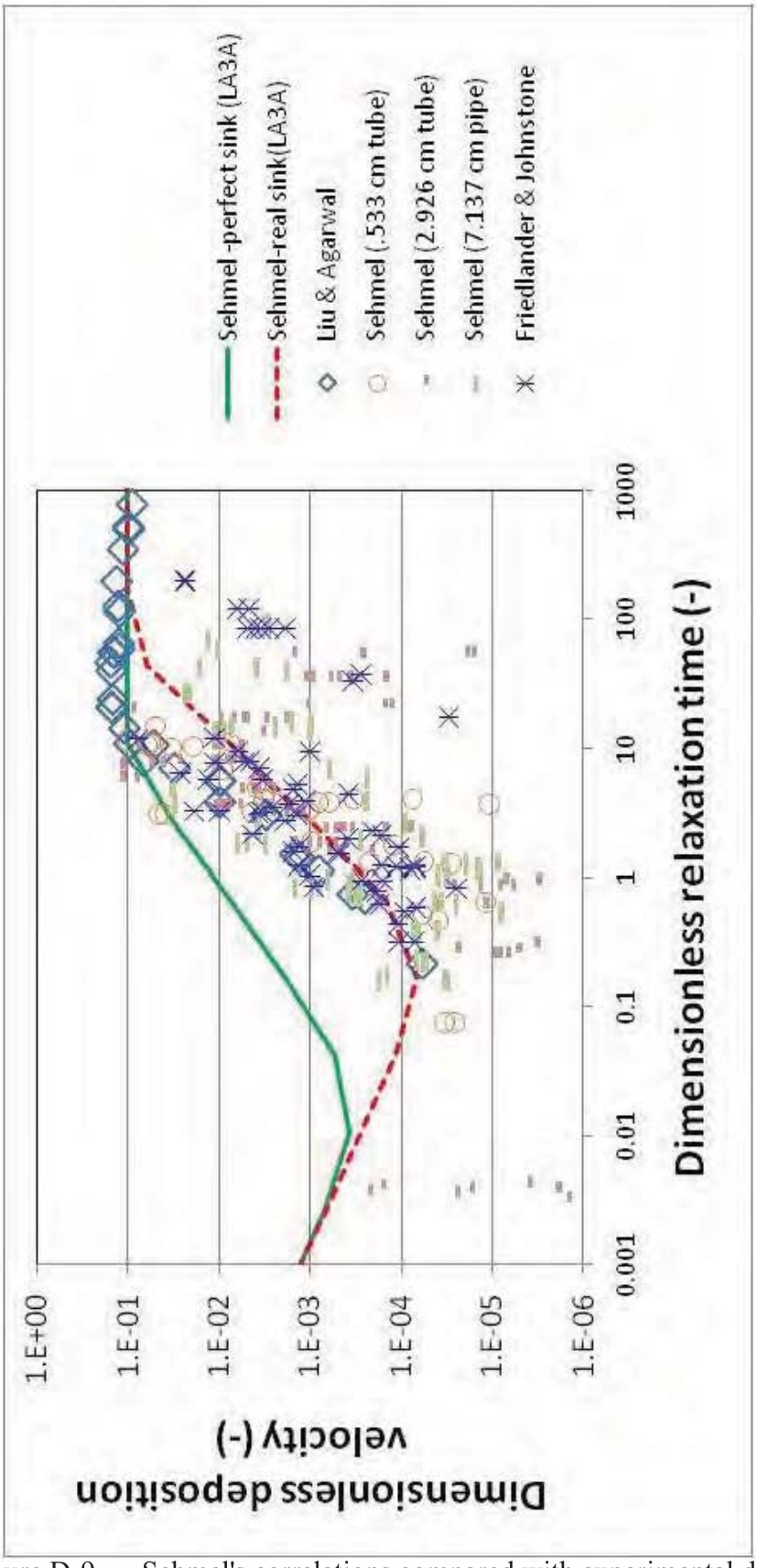

Figure D-9 Sehmel's correlations compared with experimental data

Note that Wood's models are based on the data from Liu and Agarwal whereas the Sehmel's model (VICTORIA) are based on data from Sehmel [17] and Friedlander and Johnstone [7]. For $\tau^* > 1.0$, the Wood model for smooth pipes closely reproduces the data from Liu and Agarwal. For $\tau^* < 1.0$, the curve depends on the particular test since the model now depends on the Sc number and not just the non-dimensional relaxation time. Also, note that the Wood model for rough surfaces collapses to the same curves as predicted for the Wood model for smooth surfaces when the roughness is zero. When the pipes are rough, the Wood model predicts larger deposition velocities for small particles, dependent on the flow conditions of the test being modeled. It has been noted that even micro scale roughness can significantly enhance particle deposition, particularly for small particles, for which Brownian diffusion is an important mechanism for transporting the particle to the wall. These models are discussed in more detail in Section G of this appendix.

In the section describing the details of the Sehmel model incorporated into MELCOR, it was pointed out that Sehmel obtained two curve fits to correlate data from his tests as well as data from Friedlander and Johnstone. The first curve in Figure D-9 shows the correlation that was implemented into MELCOR based on the VICTORIA code. Note that this equation was fit to a limited data set corresponding to those experiments alone where surfaces were treated, often with petroleum jelly or viscous oils, to minimize particle bounce. The second curve, also published by Sehmel, represents a curve fit to a more complete set of experimental data for real surfaces with non-perfect particle sinks. The Sehmel – perfect sink (VICTORIA) model therefore predicts higher deposition velocities than was observed for many of the tests on turbulent deposition.

MELCOR Bend Impaction Models

In addition, three models for simulation of inertial deposition in bends were added to MELCOR, the Pui model (VICTORIA), the INL bend model (Merrill), and McFarland's bend model. The Pui model and McFarland's model are purely empirical fits to either experimental data (Pui) or Lagrangian simulations [13]. The INL model is more theoretical in nature and is based on the terminal velocity of a particle due to the centrifugal force acting on a particle traversing a bend. Pui's experiments were for 90^o bends in 0.503-0.851 cm diameter tubes and his correlation does not correlate any dependency on bend angle or radius of curvature whereas the other models do.

The dependence of these three bend models on the particle Stokes number is shown in Figure D-10 for the case of a 90^o bend. Note that McFarland's model depends on the radius of curvature of the bend. For the LA3 tests, this radius of curvature is 2.86, and the penetration of particles for bends with this radius of curvature is shown in this plot. Note that there is good agreement between the INL model and that of McFarland's. The Pui model appears to predict more deposition in the bend in comparison to the other models.

Validation calculations for the LA1 and LA3 tests were made for both the Pui and INL model and are reported in the following sections. Deposition from McFarland's model is similar enough to the INL model to give insignificant differences in the MELCOR simulations. Sensitivity calculations were also conducted to assess the importance of nodalization of control volumes as well as the number of discrete aerosol particle size bins.

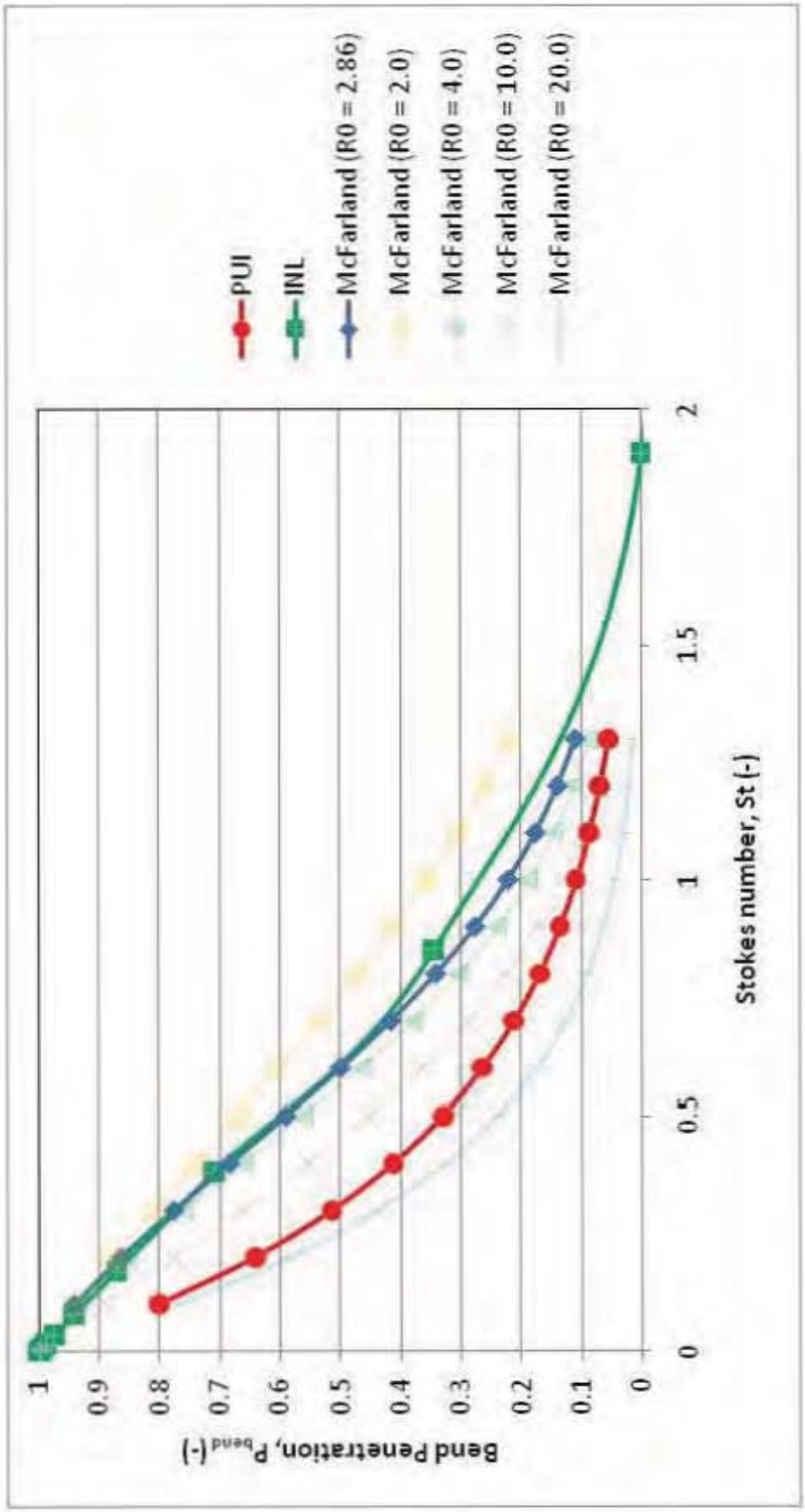

Figure D-10 Bend penetration calculated as function of Stokes # for various bend models

LACE LA1

6.1.1 Test Conditions and Modeling

The LA1 test was designed to simulate the LWR containment bypass accident (i.e., ISLOCA) sequence conditions. CsOH and MnO aerosols were injected into a 0.063-m diameter, approximately 30-m-long test pipe. The pipe had six 90^{o} bends. The pipe inlet flow velocity was roughly 100 m/s, and the outlet flow velocity was roughly 200 m/s due to the pressure drop through the pipe. Aerosols that transported out of the pipe were then allowed to become airborne in the 852-m^3 CSTP vessel, where their subsequent aerosol behavior was then studied. During part of the experiment, (i.e., the aerosol generation period), steam, non-condensable gas, and aerosols were vented or "leaked" to a scrubber.

A description of the LA1 test sections is provided in Table D-4 below. For validation of the models, a detailed nodalization was performed in which bends were isolated in control volumes or combined with adjacent valves, which had small deposition surface areas. However, a sensitivity calculation was also performed in which several test sections were lumped into a single control volume and deposition was calculated on a single heat structure associated with that control volume. Using this nodalization, all surfaces associated with that control volume compete equally for aerosol deposition. In reality, those surfaces upstream would remove aerosols from the flow that would reduce the source for those surfaces that are downstream. This lumped nodalization was used to assess the accuracy of the calculations when multiple heat surfaces are lumped into a single volume, as might be performed in a calculation for a commercial reactor. Figure D-11 and Figure D-12 show a schematic of the test section where pipe section numbers corresponding to MELCOR control volumes are shown in the drawing and in the accompanying table.

Source aerosol diameters are nodalized into 10 sections in MELCOR starting with a lower limit of $5x10^{-8}$ m to an upper bound of $1x10^{-4}$ m. The source distribution assumed in MELCOR was a lognormal distribution characterized by an aerodynamic mass median diameter (AMMD) and a geometric standard deviation (GSD). The LACE data includes both an AMMD and a GSD for an assumed lognormal particle size distribution where samples were taken four times during the test and analyzed by a cascade impactor with a reported accuracy of 25%. The assumed source distributions the LA1 test are shown in Figure D-13 and the AMMD used is the average of the four measurements. Notice that 92% of the aerosol source particles have diameters in the three size bins between 0.489 μm and 2.24 μm. In addition, a calculation is performed where the number of sections is doubled to 20 to assess the sensitivity of the calculations to the section nodalization. The 20-section source distribution is also shown in this figure.

Deposition velocities calculated by size bin for various deposition models are also shown in Figure D-14. These velocities were calculated at representative conditions in pipe section 4. For the Wood models depicted, all models clearly display three regimes of deposition. Though the Brownian and eddy diffusion regime is not visible for the Victoria model, it is because it predicts an earlier onset of the eddy diffusion impaction zone at extremely small aerosol diameters beyond the range of the plot. Consequently, deposition velocities predicted by the Victoria model for submicron particles are generally greater than predicted by the Wood models. For supermicron sized particles, all models predict a relatively constant or slightly decreasing

deposition velocity as particle size increases. As would be expected, the Wood model for rough pipes shows greater deposition (compared to his model for smooth pipes) for submicron particles when the roughness is about $5x10^{-5}$ m, but when the roughness is small, the deposition velocity for Wood's model for rough pipes and his model for smooth pipes give approximately the same curve. In the MELCOR implementation, the initial surface roughness is specified by the user, however, as particles accumulate on the surface, the roughness calculated internally is reduced by the mass that accumulates, with a minimum roughness being the particle size. This would mean that for significant accumulation on the surface, Wood's model for rough surfaces would give similar results as for his model for smooth pipes.

Deposition efficiencies are used to characterize deposition in the pipe bends and have been plotted in Figure D-14. These velocities were calculated at conditions in pipe section 3. Both the Pui and INL bend model are used in these assessment calculations. Both predict a rapidly increasing deposition efficiency for supermicron particles where the Pui model predicts larger deposition efficiencies than the INL bend model for all particle diameters.

Table D-4 LA1 Experiment – Test Section Dimension

Section No.	LA1 - Detailed HS Number	LA1- Coarse HS Number	Pipe Description	Flow Direction	Diameter (cm)	Length (m)
1a	1011	1011	Straight	East	30	1.52
1b	1011	1011	90' Bend	---	30	0.72
1c	1011	1011	Reducer	UP	30 - 10	0.28
2	1010	1010	Ball Valve	UP	10	0.23
3	1010	1010	Reducer	UP	10 - 6.3	0.28
4	1110	1100	Straight	UP	6.3	2.26
5	1120	1100	90' Bend	UP	6.3	0.36
6V	1120	1200	Ball Valve	Horizontal	6.3	0.19
6	1130	1200	Straight	Horizontal	6.3	4.2
7	1140	1200	90' Bend	Horizontal	6.3	0.36
8	1150	1300	Straight	Horizontal	6.3	3.74
9	1160	1400	Straight	Horizontal	6.3	4.32
10	1170	1500	90' Bend	Horizontal	6.3	0.36
11	1180	1500	Straight	Horizontal	6.3	0.62
11V	1190	1500	Ball Valve	Horizontal	6.3	0.19
12	1190	1600	90' Bend	Vertical	6.3	0.36
13	1200	1600	Straight	Vertical	6.3	4.32
14	1210	1700	Straight	Vertical	6.3	4.34
15	1220	1800	90' Bend	Vertical	6.3	0.35
16	1230	1800	Straight	Horizontal	6.3	1.74
17	1240	1900	90' Bend	Horizontal	6.3	0.33
18	1240	1900	Ball Valve	Horizontal	6.3	0.19
19	1240	1900	Straight	Horizontal	6.3	0.71
22	1250	2250	Transition	Horizontal	6.3 - 30	1.17
23a	2250	2250	Straight	Horizontal	30	1.95
23b	2250	2250	90' Bend	UP	30	0.58
					Total	**35.67**

MELCOR Model Nodalization:

Control Volume	*HS*	*Pipe Sections*
CV011	*1011*	*1*
CV012	*1010*	*2,3*
CV011	*1110*	*4*
CV012	*1120*	*5,6V*
CV013	*1130*	*6*
CV014	*1140*	*7*
CV015	*1150*	*8*
CV016	*1160*	*9*
CV017	*1170*	*10*
CV018	*1180*	*11*
CV019	*1190*	*11V,12*
CV020	*1200*	*13*
CV021	*1210*	*14*
CV022	*1220*	*15*
CV023	*1230*	*16*
CV024	*1240*	*17,18,19*
CV025	*1250*	*20*

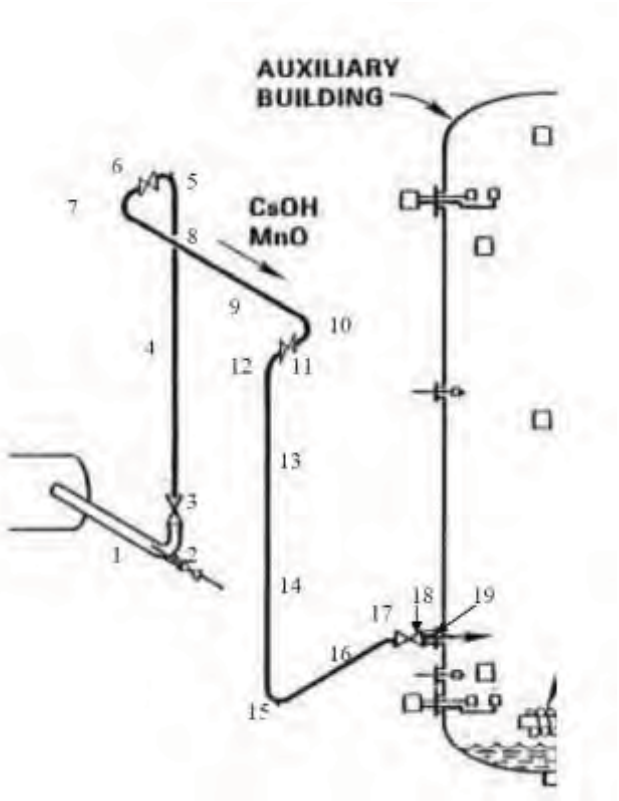

Figure D-11 Detailed LA1 MELCOR Nodalization

MELCOR Model Nodalization:

Control Volume	*HS*	*Pipe Sections*
CV011	*1011*	*1a,1b,1c*
CV012	*1010*	*2,3,*
CV013	*1100*	*4,5*
CV014	*1200*	*6,7*
CV015	*1300*	*8*
CV016	*1400*	*9*
CV017	*1500*	*10,11*
CV018	*1600*	*12,13*
CV019	*1700*	*14*
CV020	*1800*	*15,16*
CV021	*1900*	*17,18,19*

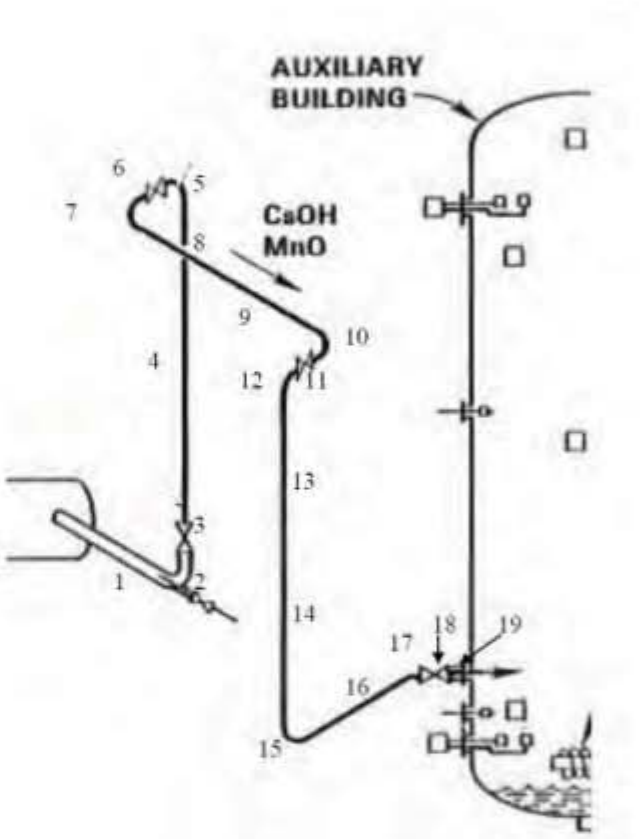

Figure D-12 Coarse LA1 MELCOR Nodalization

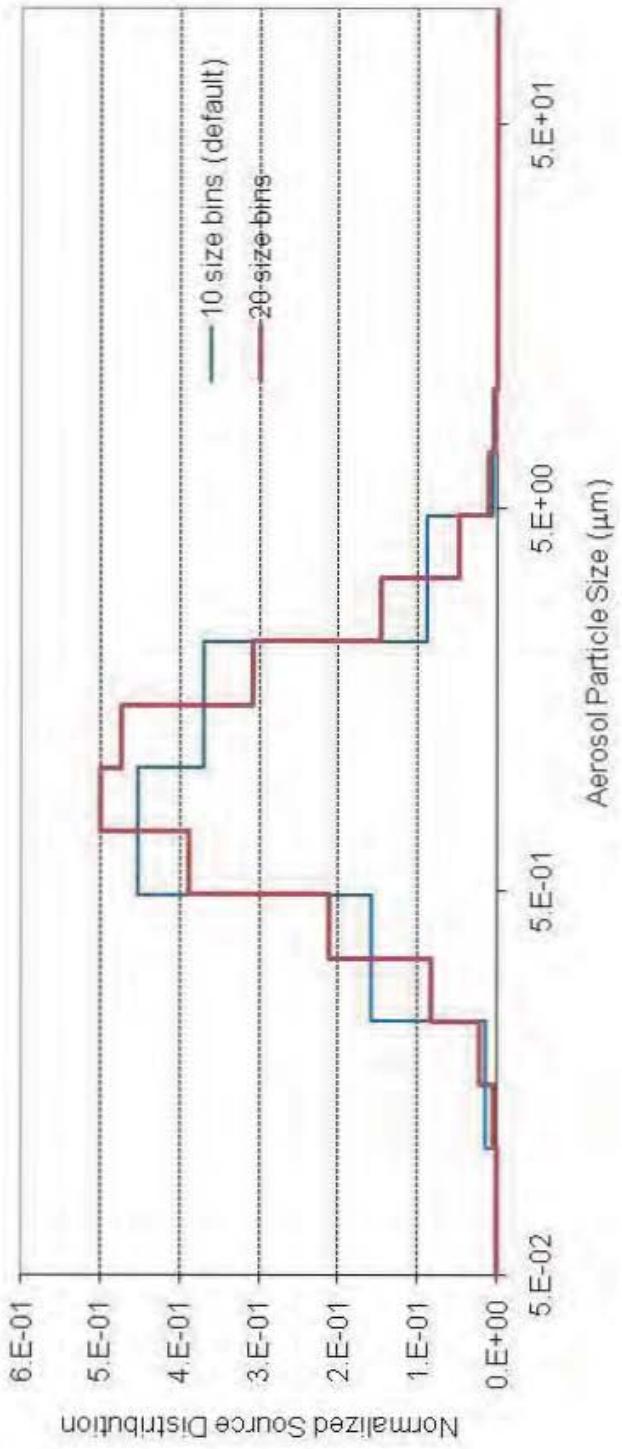

Figure D-13 MELCOR CsOH log-normal source distribution using AMMD = 2.1 µm and GSD =1.80**.** (10 particle sizes for base case and 20 particle sizes for sensitivity calculation)

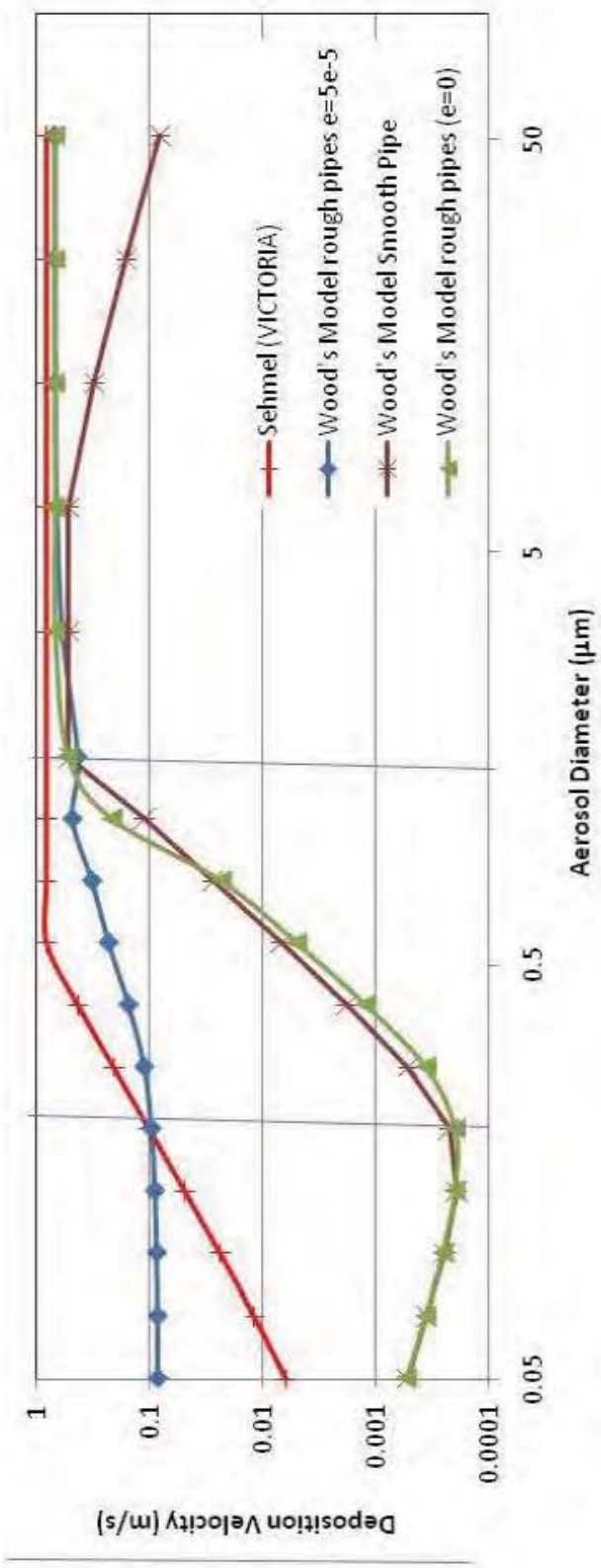

Figure D-14 Calculated deposition velocity for LA1 test using MELCOR models. In Figure D-14, the green curve (triangles) shows Wood's model for rough pipes evaluated for a surface roughness of approximately zero.

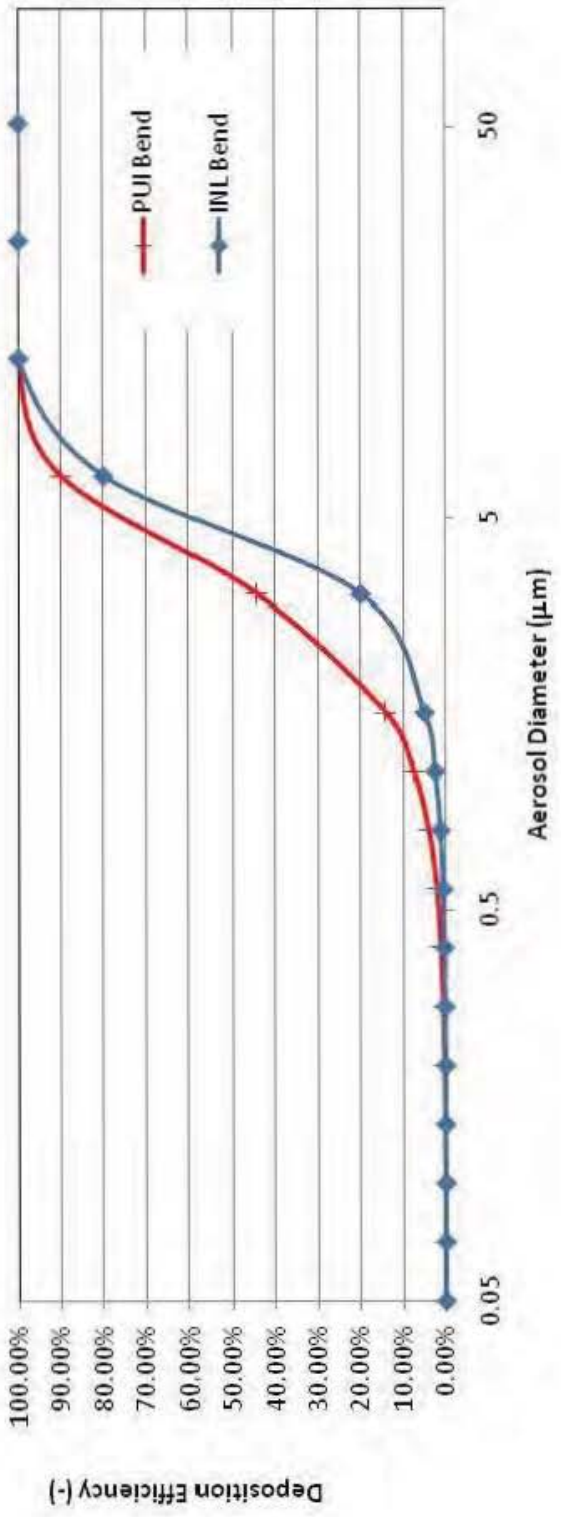

Figure D-15 Deposition efficiency calculated for LA1 bends using new MELCOR models

6.1.2 Results

Table D-5 shows that MELCOR predicts a retention factor of 94 -97% which is in good agreement with the LA1 test data (>98%). MELCOR also predicts retention in the bends that are reasonably accurate, particularly when the bend deposition model is used.

Table D-5 MELCOR and LA1 Experiment Retention Factors

	Experimental Results	Calculated[a]			
		INL[d]	VIC[e]	Wood[f]	I-V**[g]
Retention in 6.3 cm pipe[b] (%)	>98%	94%	97%	94%	95%
Bend Deposition[c] (%)	37%	29%	35%	42%	37%

** I-V indicates indicate the INL model for the straight sections (I) and the Victoria model for the bends (V).

[a] Values reported are for fine nodalization model.

[b] Values reported are the deposited mass divided by the total source mass less the mass deposited upstream of the 6.3 cm pipe (i.e., mass deposited on torches, aerosol mixing vessel (AMV), and bypass).

[c] Values reported are the fraction of the deposition in the 6.3 cm pipe that was found in the pipe bends.

[d] Uses Wood model for rough pipes and INL bend model.

[e] Uses Sehmel model for perfect particle sinks in straight pipes and Pui bend model.

[f] Uses Wood's model for smooth pipes and Pui bend model.

[g] Uses Wood's model for rough pipes and Pui bend model.

The following sections graphically present calculation results along the test piping. Where available, data is presented alongside the calculated results. In addition, results are presented from the code comparison study that was performed as part of the LACE project.

Several sensitivity calculations were also performed. Because the deposition velocity is dependent on particle size, a sensitivity calculation was performed where the particle size distribution was modeled with 20 nodes, compared to the default value of 10. A calculation was also performed in which several volumes (i.e., bends and straight pipe sections) were lumped together for a coarser nodalization. This is important to know because it may influence the nodalization choices in building a nodalization for a commercial reactor where volume size constraints can affect calculation performance. For this calculation, if more than one straight pipe section is lumped together, the deposition plotted for each surface is estimated by partitioning the total deposition for the combined heat structure by the surface area of each pipe section. Similarly, if two bends are lumped together and associated with a single heat structure with combined surface area, the total bend deposition calculated is split between the two bends when generating the plots.

Finally, a calculation was performed to investigate the importance of the sticking factor. Uncertainty may be associated with this sticking factor so it is important to know how sensitive the calculation is to the calculated value. A calculation was performed for

which the sticking factor was assumed to be 1.0 and compared to the results generated from the calculated sticking factor.

6.1.2.1 Thermal Hydraulic Results

Pressures and velocities along the pipe train are plotted below (i.e., Figure D-16 and Figure D-17). Note that the calculated velocities agree well with the values reported (100 m/s at inlet and 200 m/s at outlet) in the code comparison report.

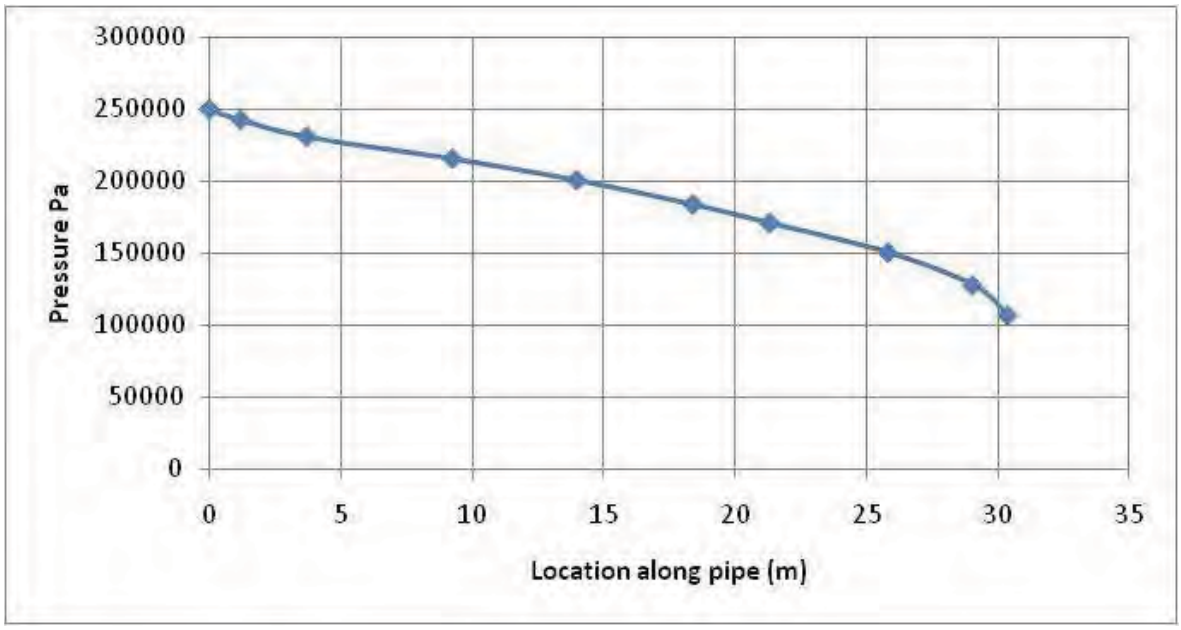

Figure D-16 Pressure profile along test pipe

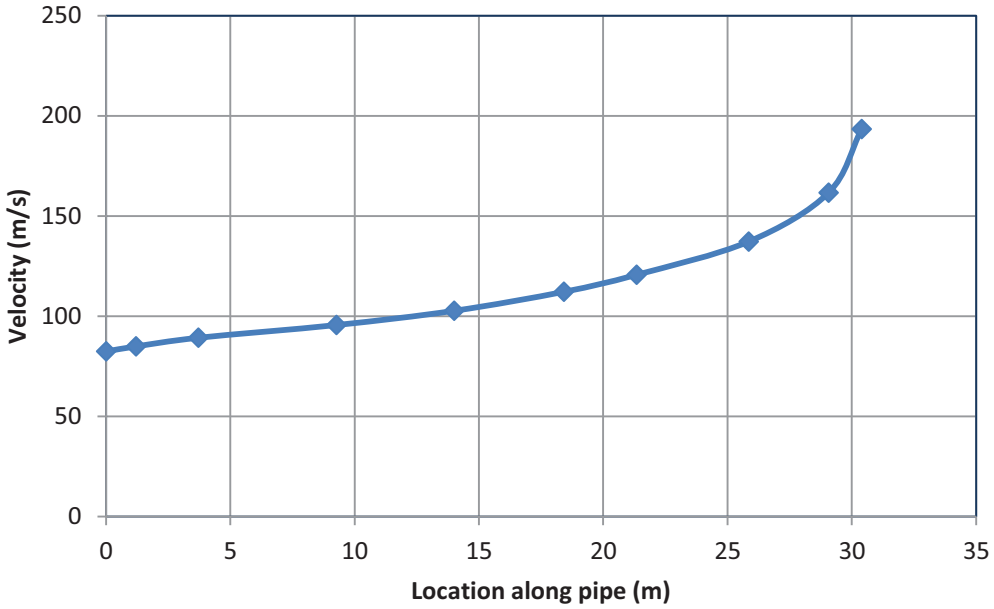

Figure D-17 Velocity profile along test pipe

6.1.2.2 Deposition Profiles

Deposition profiles along the pipe train are plotted below in Figure D-18 through Figure D-23.

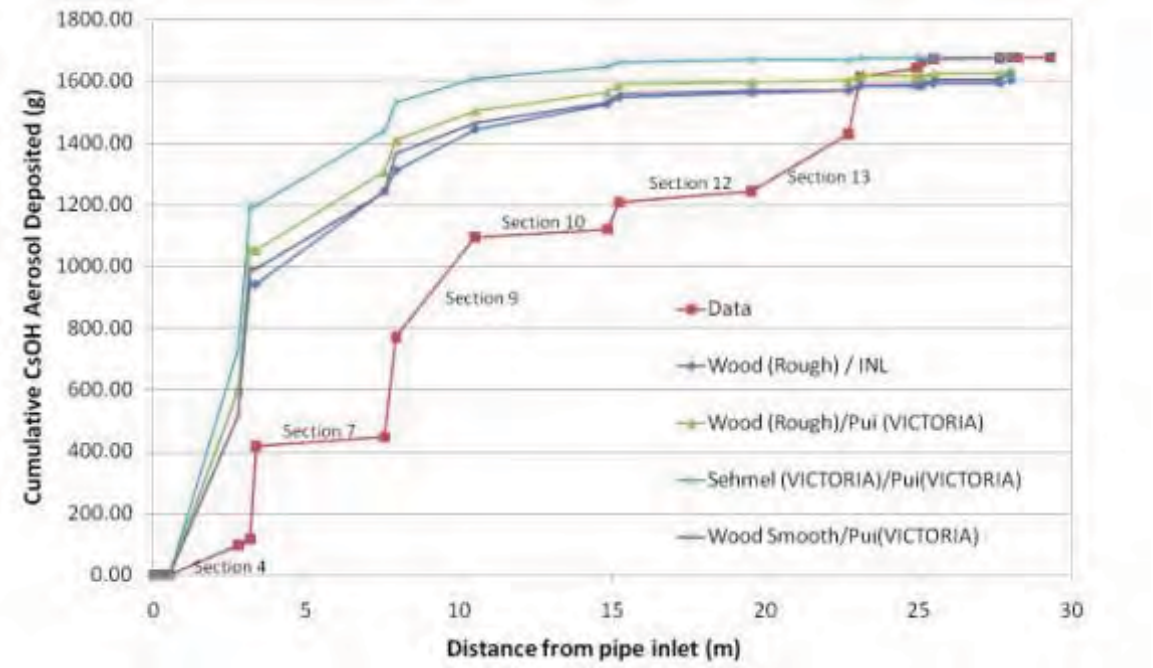

Figure D-18 Deposition profile for CsOH along LA1 test section (Calculated sticking factor)

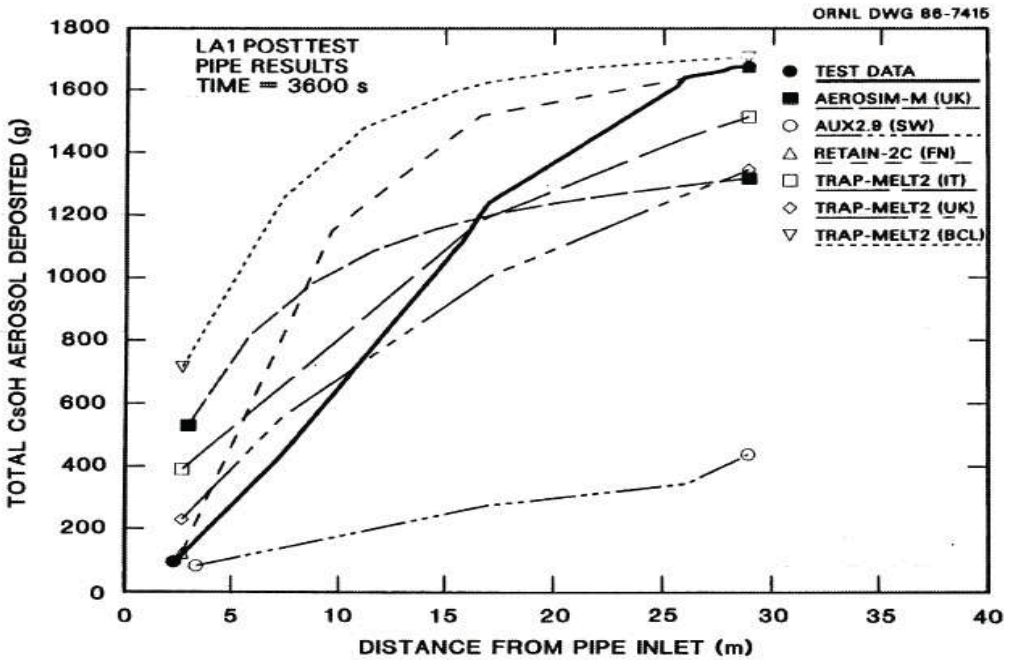

Figure D-19 LA1 post test calculation of CsOH aerosol deposition for codes in code comparison report including bend deposition models (LACE TR-022)

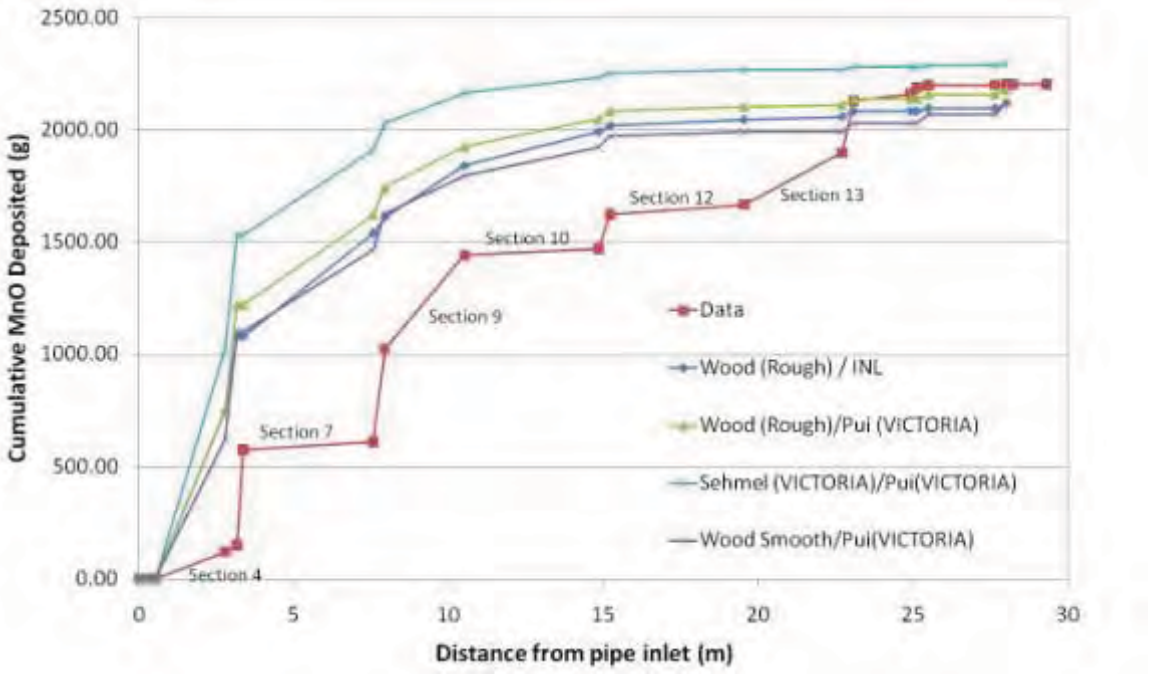

Figure D-20 Deposition profile for MnO along LA1 test section (Calculated sticking factor)

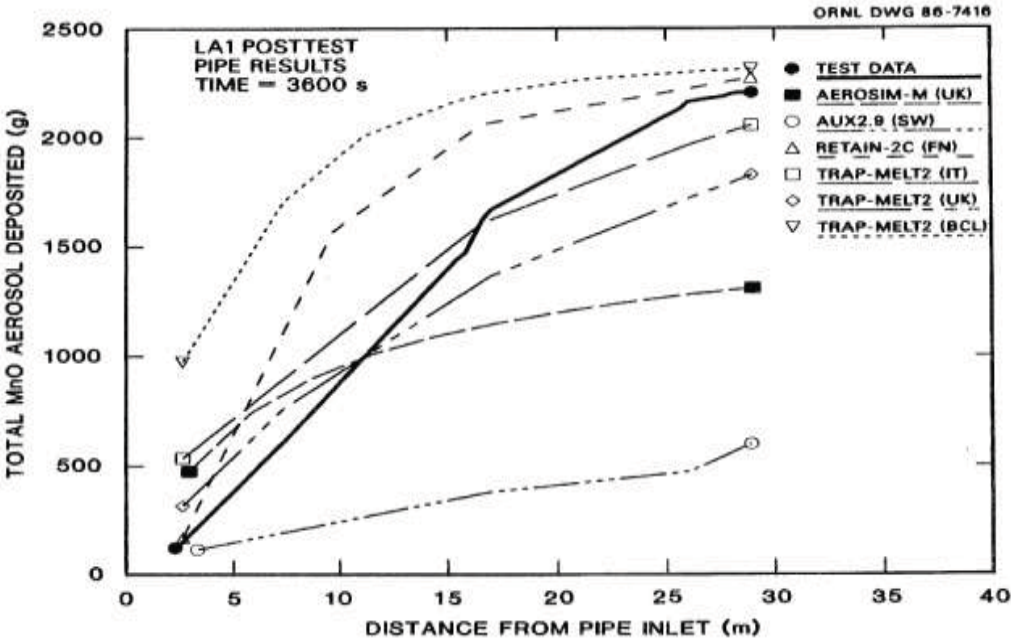

Figure D-21 LA1 post test calculation of MnO aerosol deposition for codes in code comparison report including bend deposition models (LACE TR-022)

Figure D-22 shows the integrated deposition at a few points along the piping and therefore shows the cumulative deposition for multiple sections.

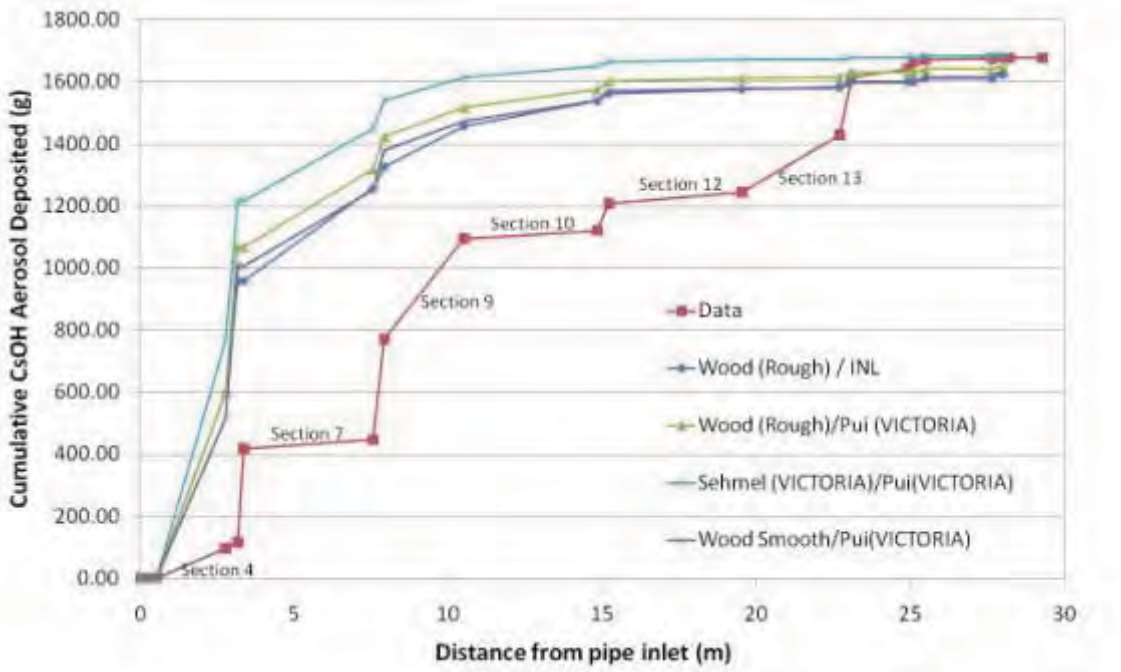

Figure D-22 Deposition profile for CsOH along LA1 test section (Sticking factor = 1)

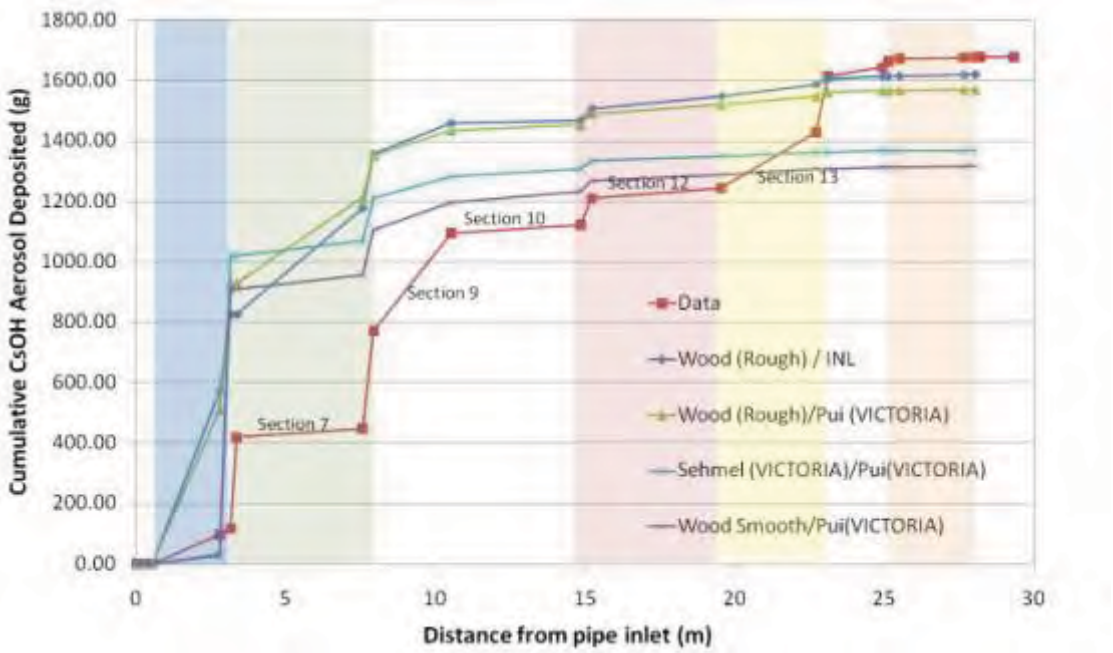

Figure D-23 Deposition profile for CsOH along LA1 test section - colored (Colored regions indicate lumped nodalization)

6.1.2.3 Observations

1. The MELCOR calculations over predict deposition early in the test train even though overall retention for the test section is well predicted. This is true for all models tested. In contrast, the test data shows that the linear deposition density in the straight pipe sections is nearly uniform along most of the test train, though it does taper off at the end. To explain this behavior, it may be possible that the high flow velocities (100 – 200 m/s) lead to resuspension and deposition further down the pipe or flow of deposited mass along the pipe. MELCOR does not calculate resuspension of aerosol particles or entrainment of deposited material. This is consistent with recommendations by the VICTORIA peer review committee [24].

2. When compared with the code comparison calculation (TR-022), the MELCOR models estimate the total pipe retention as well as any of the other codes participating in that activity. MELCOR tends to overestimate the deposition, particularly in upstream test sections where many of the other codes underestimate total deposition.

3. All MELCOR models greatly over predict deposition in test section 4 (< 2.5 m). This pipe section happens to be a vertical pipe section and it is possible that the orientation of the pipe may be an important role. However, note also that sections 13 and 14 are also vertical pipe sections. For these pipe sections, MELCOR

predicts very little deposition though they occur much further downstream after airborne aerosol source has been greatly depleted by deposition upstream.

4. Deposition in bends is important, since about 37% of the deposited mass is found in the bends. Both the Pui and the INL model do a reasonable job of predicting the bend deposition.

5. The MELCOR calculation of MnO deposition along the piping is similar in characteristics to that of CsOH deposition. About 94% of the MnO aerosol was deposited in the test section while the MELCOR models predict between 91% (Wood's smooth/Pui) and 98% (Sehmel/Pui).

6. Calculating the sticking factor with Merrill's model does not significantly affect results for these calculations. The calculated sticking factor varies with time. As mass is accumulated the sticking factor approaches 1.0 very quickly.

7. Lumping the bends with straight pipe sections leads to a modest reduction in the overall retention in the test section and increases the spread between the various models. The approximation appears to be less significant for the Wood (rough) models. Overall, this approximation was quite reasonable for all models.

LACE LA3

6.1.3 Test Conditions and Modeling

The intent of LA3 experiments was to characterize the aerosol transport and deposition in a pipe with the two parameters: gas velocity, and ratio of insoluble to soluble aerosol. LA3 was designed to explore the intermediate and low gas velocities (i.e., ~20 to 100 m/s at the test section inlet). The ratio of the insoluble to soluble (hygroscopic) aerosol determines the absorption of water and therefore the liquid content and stickiness of the aerosol. Both LA3A and LA3B were intended to have a higher ratio of 8:1, in comparison to LA3C of roughly 2:1. Test conditions are summarized in Table D-3.

A description of the LA3 test sections is provided in Table D-6. Note that for the purpose of these calculations, several test sections were combined into a single control volume and deposition was calculated on a single heat structure associated with that control volume. However, both a detailed and a coarser lumped calculation (Figure D-24 and Figure D-25) were performed to assess the impact of nodalization.

Source aerosol diameters are nodalized into 10 sections in MELCOR starting with a lower limit of $1x10^{-7}$ m to an upper bound of $5x10^{-5}$ m. The source distribution is assumed to be a lognormal distribution with average and geometric standard deviation reported for the experiment and the total source is assumed to be released at a constant average rate. The assumed source distribution for each LA3 test is shown in Figure D-26. Note that the AMMD and GSD reported for each test are based on the average of four samples taken during the test and analyzed by a cascade impactor with a reported

accuracy of 25%. The measured source distribution at each of the four sample times is presented in Figure D-27 to Figure D-29. This distribution does not vary much for LA3B or LA3C but the variation for LA3A is large enough to affect results. Because of this, a more detailed calculation was performed using these four source distributions and the time dependent source generation rate, which is shown in Figure D-30.

Deposition velocities calculated by size bin for various deposition models are shown in Figure D-31 through Figure D-33. These velocities were calculated at conditions in pipe section 3. All models are consistent in their trends and three regions of deposition are seen though there are differences in magnitudes. The VICTORIA models show an earlier onset of the eddy diffusion-impaction zone and consequently, deposition velocities for submicron particles are greater than predicted by the Wood models. For supermicron sized particles, all models predict a relatively constant or slightly decreasing deposition velocity as particle size increases. As would be expected, the Wood model for rough pipes shows greater deposition (compared to his model for smooth pipes) for submicron particles when the roughness is about $5x10^{-5}$ m, but when the roughness is smaller, the deposition velocity for Wood's model for rough pipes and his model for smooth pipes give approximately the same curve. In the MELCOR implementation, the initial surface roughness is specified by the user, however, as particles accumulate on the surface, the roughness calculated internally is reduced by the mass that accumulates, with a minimum roughness being the particle size. This would mean that for significant accumulation on the surface, Wood's model for rough surfaces would give similar results as for his model for smooth pipes.

Figure D-34 shows the deposition efficiency calculated for LA3 bends using the MELCOR Pui, INL and McFarland bend penetration models. The INL and McFarland models are in good agreement for all LA3 experiments. The MELCOR Pui model consistently is lower than the INL and McFarland models for all LA3 experiments.

Table D-6 LA3 Experiment – Test Section Dimension

Section No.	LA3 - Detailed HS Number	LA3 - Coarse HS Number	Pipe Description	Flow Direction	Diameter (cm)	Length (m)
1a	1110	1110	Straight	East	30	1.52
1b	1110	1110	90' Bend	---	30	0.72
1c	1110	1110	Reducer	UP	30 - 10	0.28
2	1120	1120	Ball Valve	UP	10	0.23
3	1120	1120	Reducer	UP	10 - 6.3	0.28
4	1130	1120	Straight	UP	6.3	2.26
5	1140	1120	90' Bend	---	6.3	0.38
6	1140	1120	Ball Valve	West	6.3	0.19
7	1150	1130	Straight	West	6.3	4.2
8	1160	1130	90' Bend	---	6.3	0.38
9	1170	1130	Straight	South	6.3	2.58
10	1180	1130	Straight	South	6.3	4.32
11	1190	1130	90' Bend	---	6.3	0.38
12	1200	1140	Straight	East	6.3	4.32
13	1210	1140	Straight	East	6.3	3.17
14	1220	1140	90' Bend	---	6.3	0.38
15	1230	1140	Straight	North	6.3	1.84
16	1230	1140	Ball Valve	North	6.3	0.19
17	1240	1150	90' Bend	---	6.3	0.38
18	1240	1150	Straight	Down	6.3	2.15
19	1240	1150	90' Bend	---	6.3	0.38
20	1240	1150	Ball Valve	West	6.3	0.19
21	1240	1150	Straight	West	6.3	1.09
22	1250		Transition	West	6.3 - 30	1.17
23a			Straight	West	30	1.95
23b			90' Bend	UP	30	0.58
					Total	**35.51**

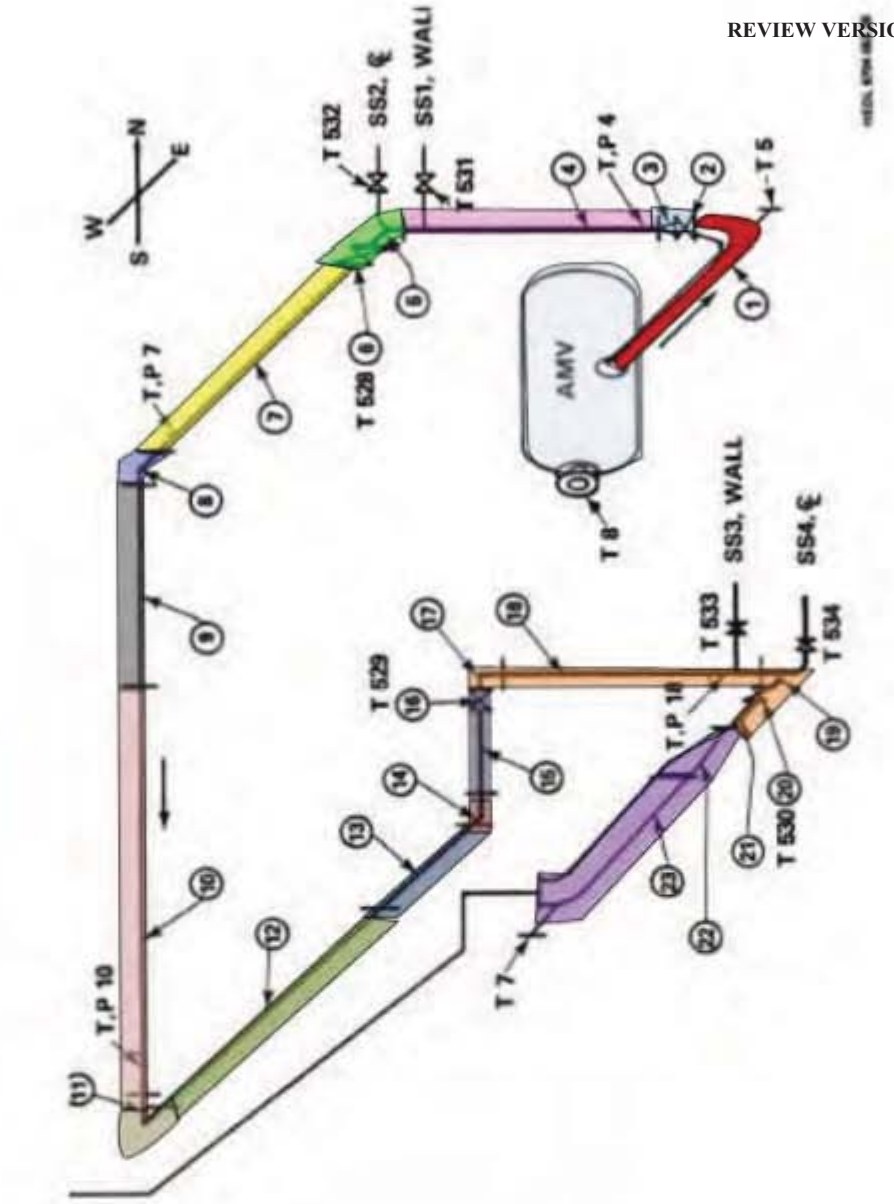

MELCOR Model Nodalization:

Control Volume	HS	Pipe Sections
CV011	1110	1a,1b,1c
CV012	1120	2,3
CV013	1130	4
CV014	1140	5,6
CV016	1160	8
CV017	1170	9
CV019	1190	11
CV020	1200	12
CV031	1210	13
CV032	1220	14
CV033	1230	15,16
CV034	1240	17,18,19,20,21,22
CV		23

Figure D-24 Detailed LA3 MELCOR Nodalization

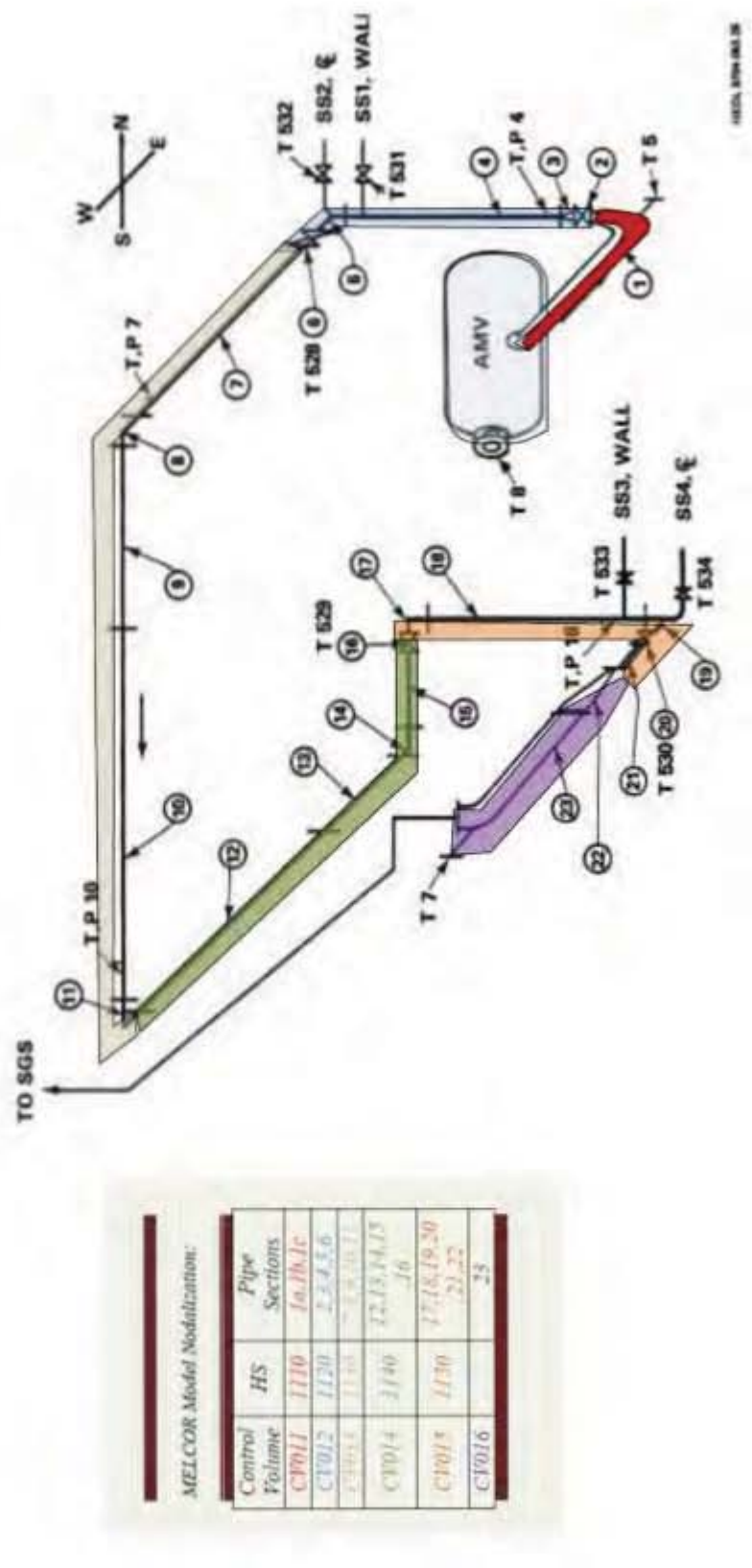

Figure D-25 Coarse LA3 MELCOR Nodalization

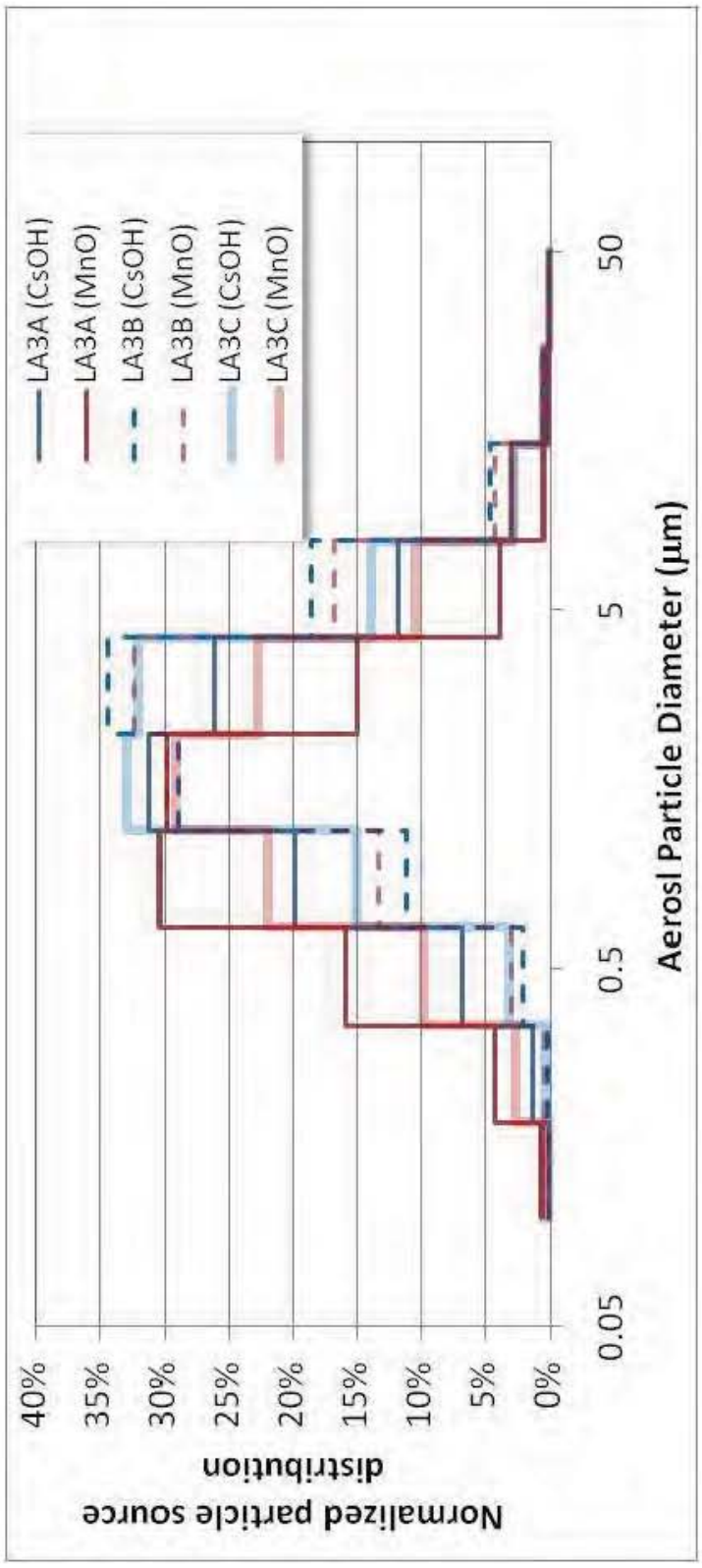

Figure D-26 Source distribution for MELCOR simulation of LA3 tests using average AMMD and GSD

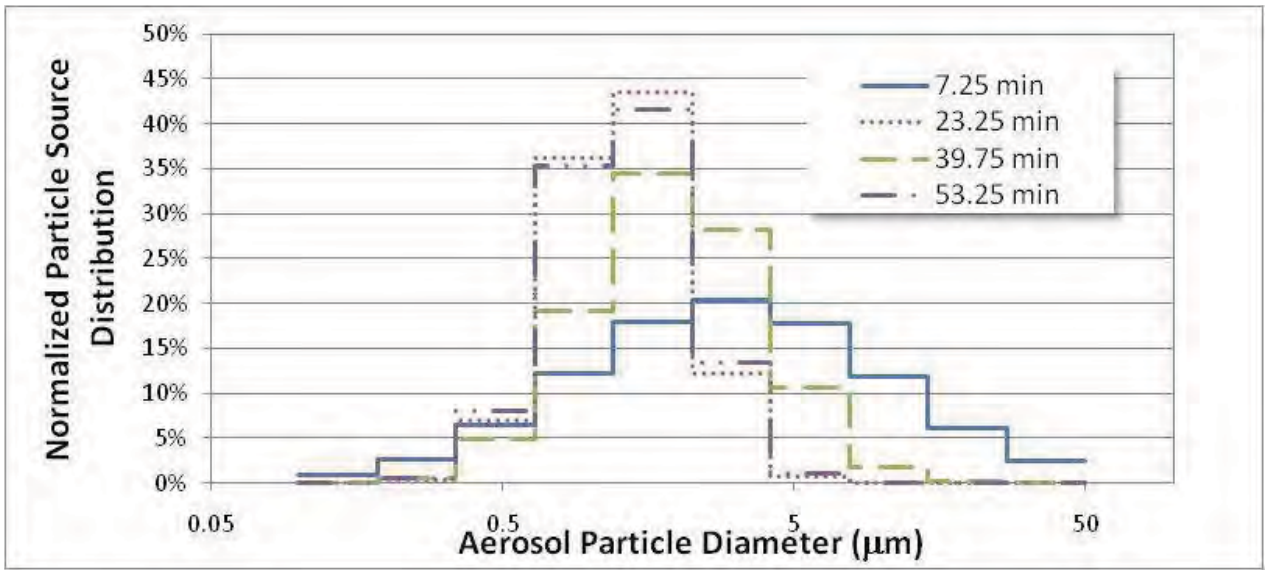

Figure D-27 Source distribution for LA3A tests at four times of measurement

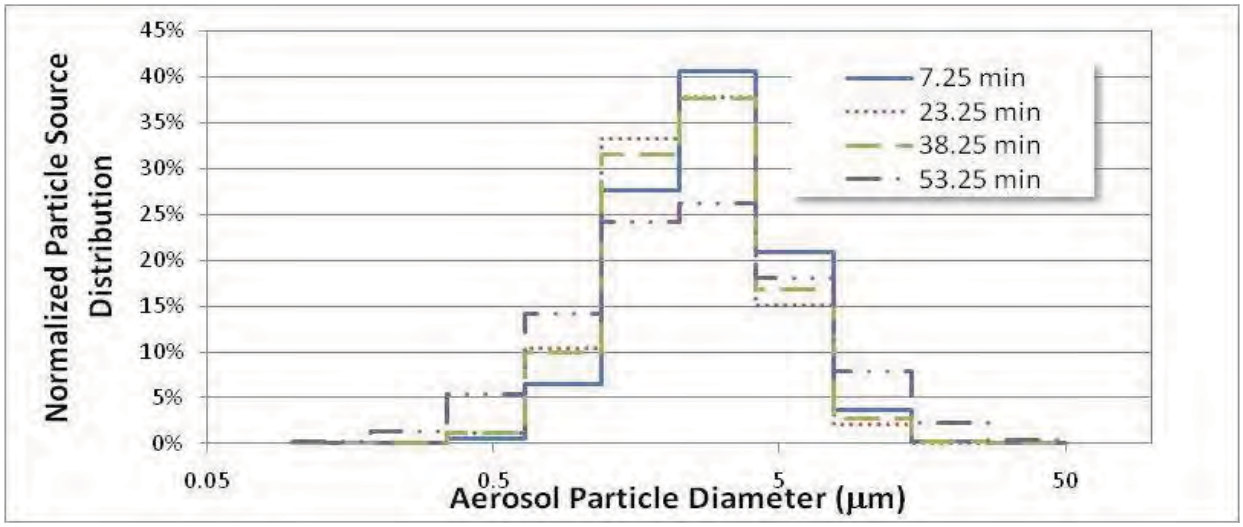

Figure D-28 Source distribution for LA3B tests at four times of measurement

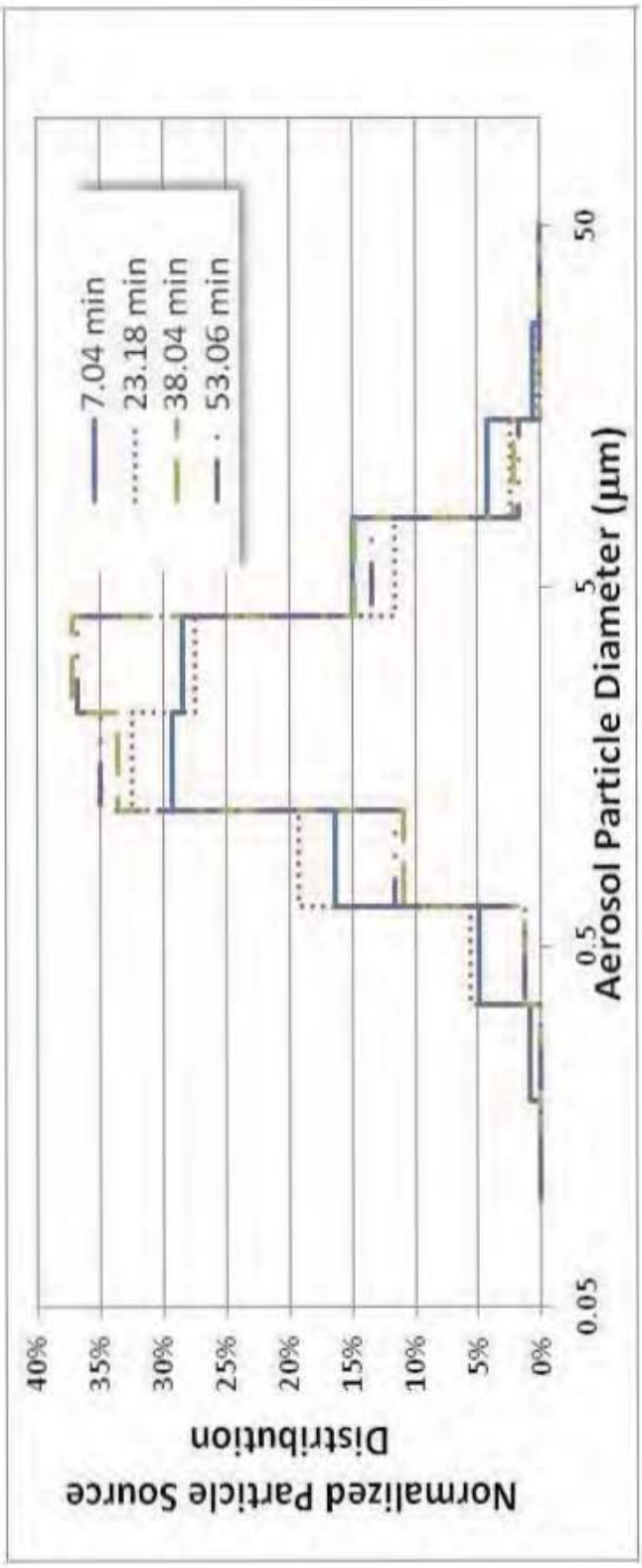

Figure D-29 Source distribution for LA3C tests at four times of measurement

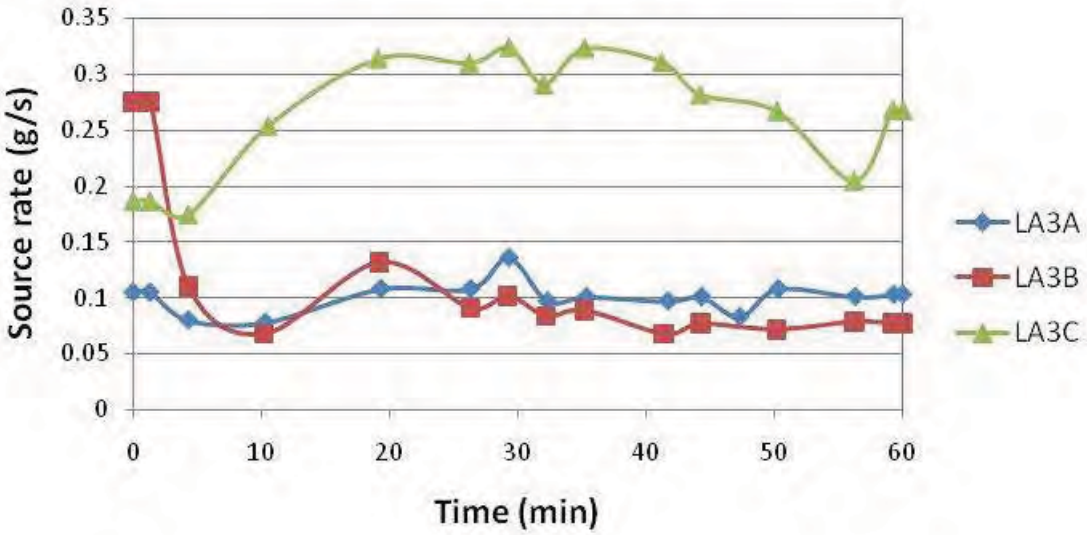

Figure D-30 Source rate reported for each LA3 test

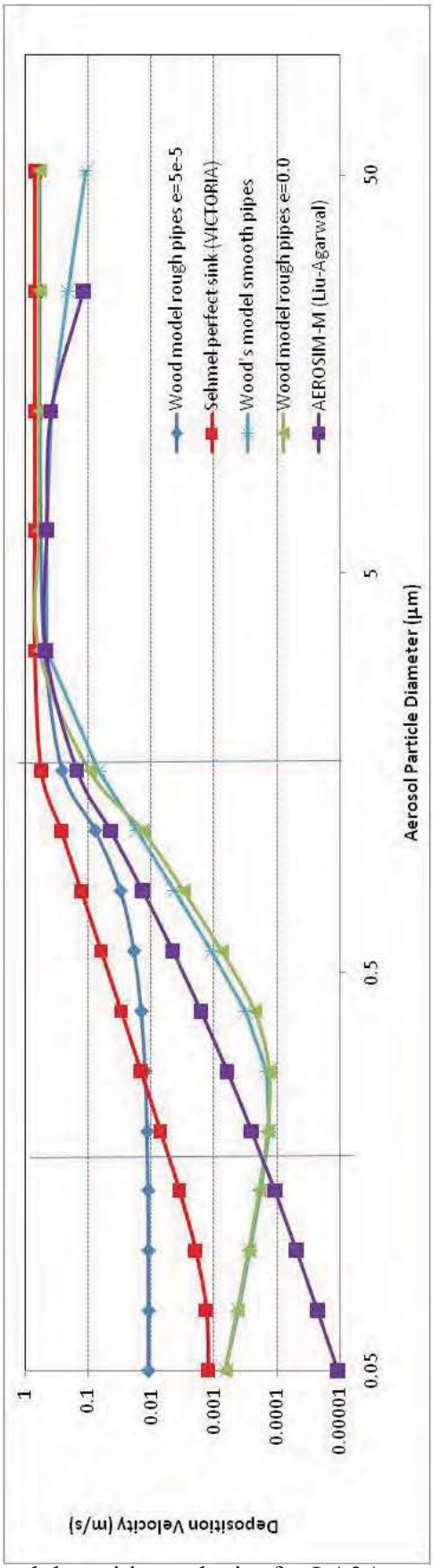

Figure D-31 Calculated deposition velocity for LA3A test using various models

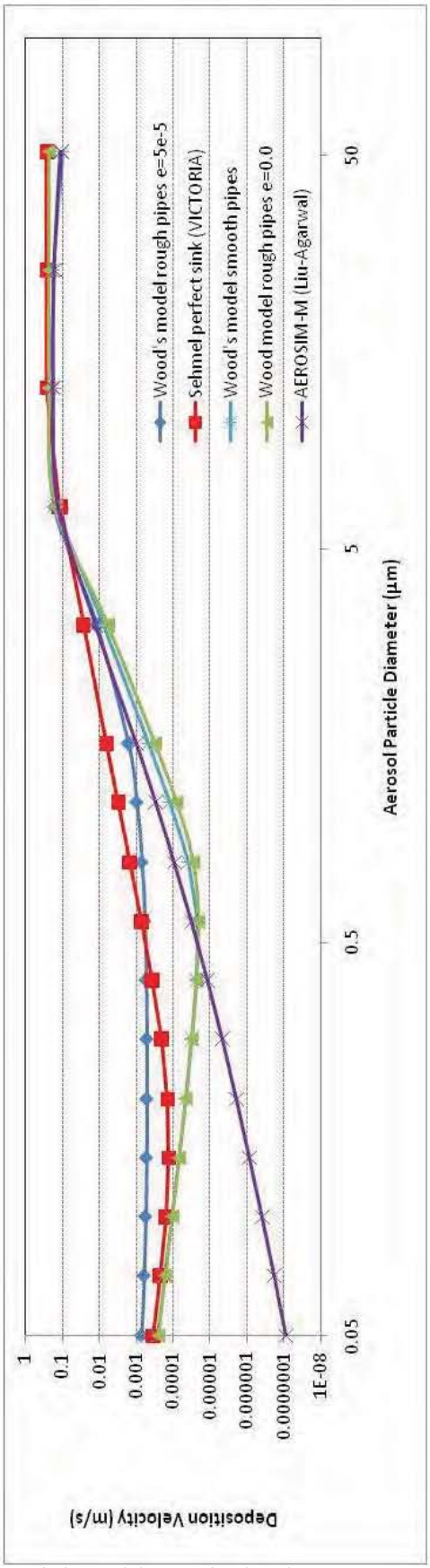

Figure D-32 Calculated deposition velocity for LA3B test using various models

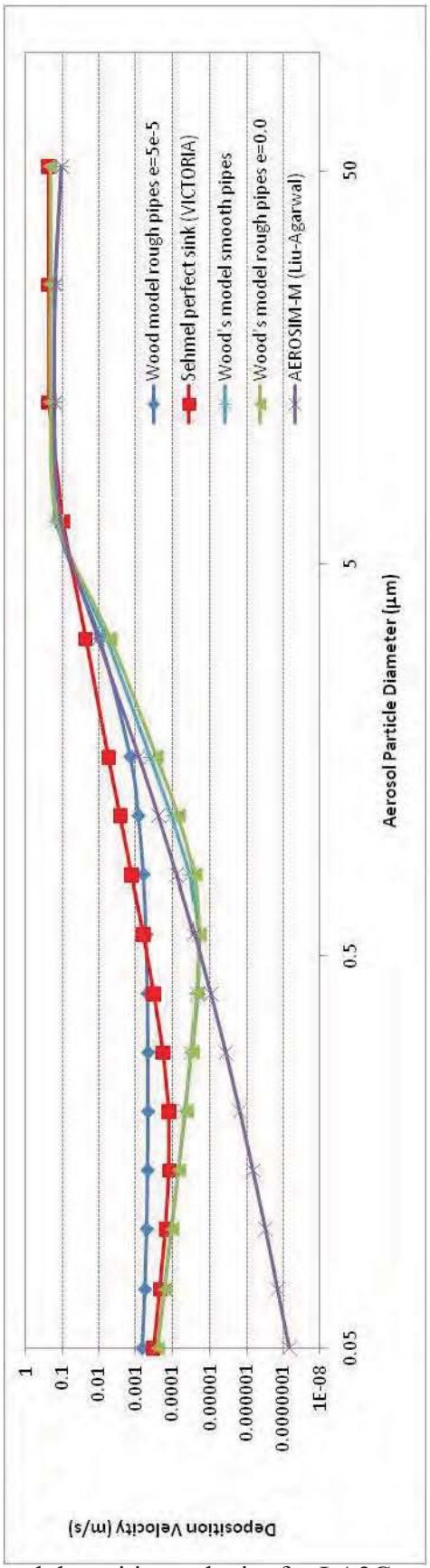

Figure D-33 Calculated deposition velocity for LA3C test using various models

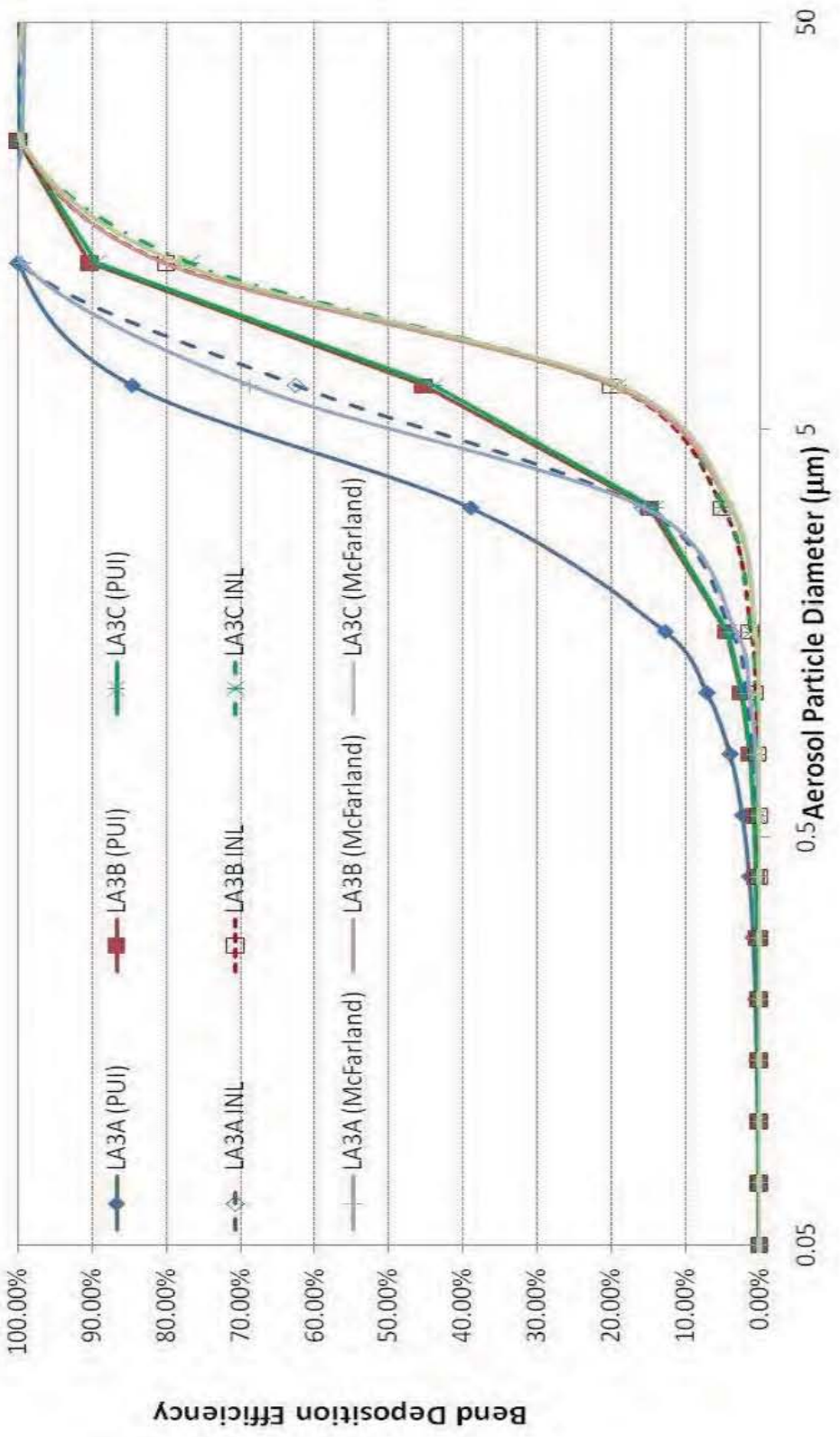

Figure D-34 Deposition efficiency calculated for LA3 bends using MELCOR Pui, INL and McFarland bend penetration model

6.1.4 Results

Overall retention factors measured for the tests are compared with the MELCOR calculated values in Table D-7. The retention factors reported are the fraction of the aerosol mass entering pipe section 1 that is deposited in the 6.3 cm pipe sections and components. Also shown is the fraction of the CsOH aerosol mass deposited in the 6.3 cm pipe that is found in the bend sections.

It can be helpful to look at detailed deposition patterns as well as overall deposition factors. For example, the overall bend deposition calculated with the INL model is closest to the experimental value for LA3B. However, when each pipe section is examined closely, it is found that this model over predicts deposition in the first bend and under predicts in subsequent bends.

Table D-7 Summary of Deposition Calculated for LA3 tests

Test	Experimental Data		Calculated[b]							
	Retention in 6.3 cm pipe[a] (%)	Bend Deposition[c] (%)	Retention in 6.3 cm pipe[a] (%)				Bend Deposition[c] (%)			
			INL[d]	VIC[e]	Wood[f]	I-V[g**]	INL[d]	VIC[e]	Wood[f]	I-V[g**]
CsOH										
LA3A	63	46	67	78	57	79	7	10	43	14
LA3B	43	76	50	70	62	63	35	27	65	58
LA3C	47	35	61	76	68	55	95	38	94	92
MnO										
LA3A	68	44	94	78	90	95	20	25	42	31

[**] I-V indicates indicate the INL model for the straight sections (I) and the Victoria model for the bends (V).

[a] Values reported are the deposited mass, including mass deposited in bends, divided by the total source mass less the mass deposited upstream of the 6.3 cm pipe (mass deposited on torches, Aerosol Mixing Vessel (AMV), and bypass).

[b] Values reported are for fine nodalization model.

[c] Values reported is the fraction of the deposition in the 6.3 cm pipe that was found in the pipe bends.

[d] Uses Wood model for rough pipes in straight pipes and INL bend model.

[e] Uses Sehmel model for perfect particle sinks in straight pipes and Pui bend model.

[f] Uses Wood's model for smooth pipes and Pui bend model.

[g] Uses Wood's model for rough pipes and Pui bend model.

LA3A

Thermal Hydraulic Results

Pressures and velocities along the pipe train are plotted in Figure D-35 and Figure D-36.

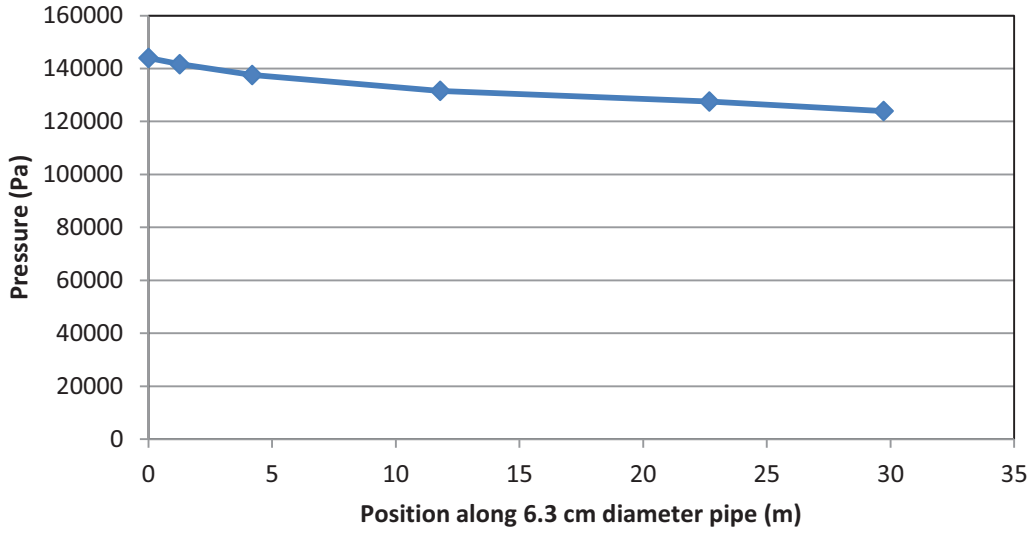

Figure D-35 Pressure profile along test pipe

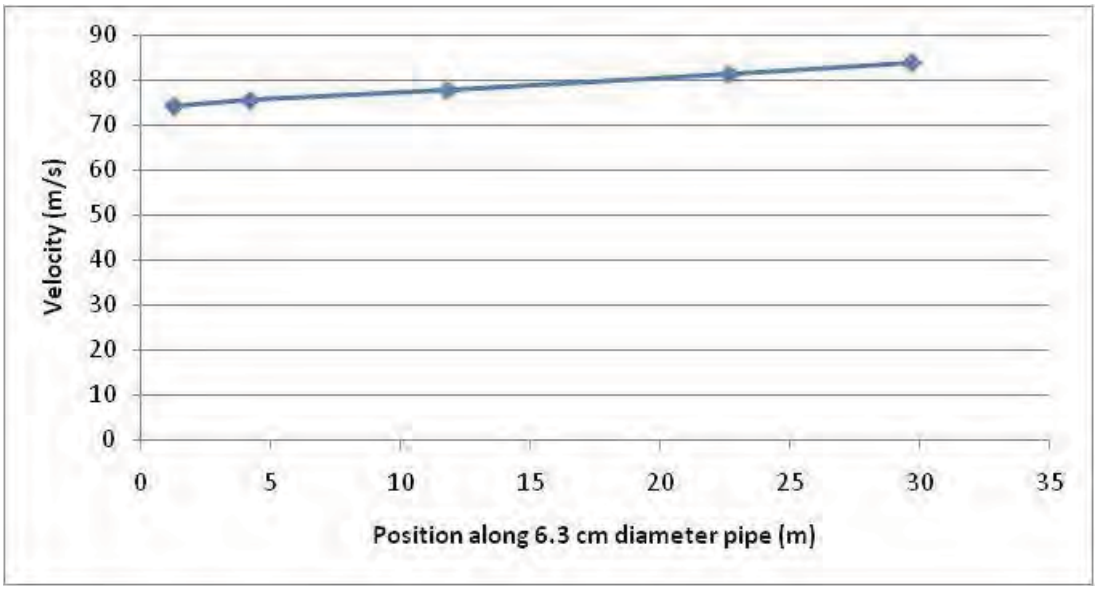

Figure D-36 Velocity profile along test pipe

Deposition Profiles

Deposition profiles along the pipe train are plotted in Figure D-37 through Figure D-44.

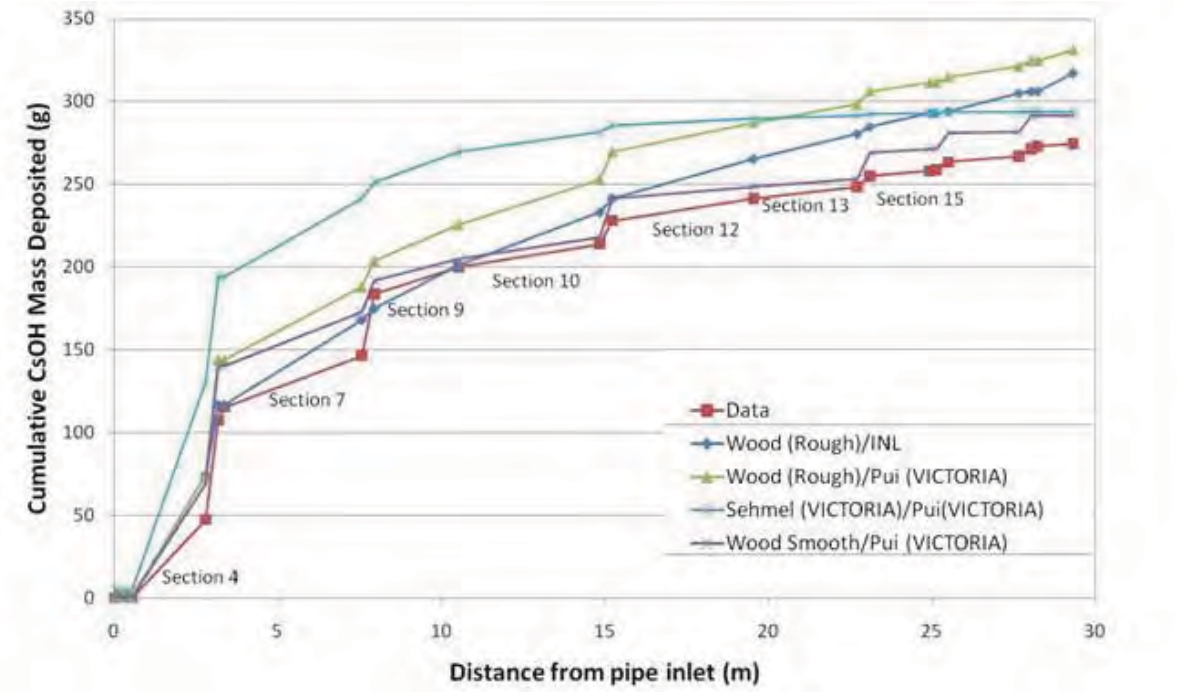

Figure D-37 Deposition profile for CsOH along LA3A test section (Calculated sticking factor)

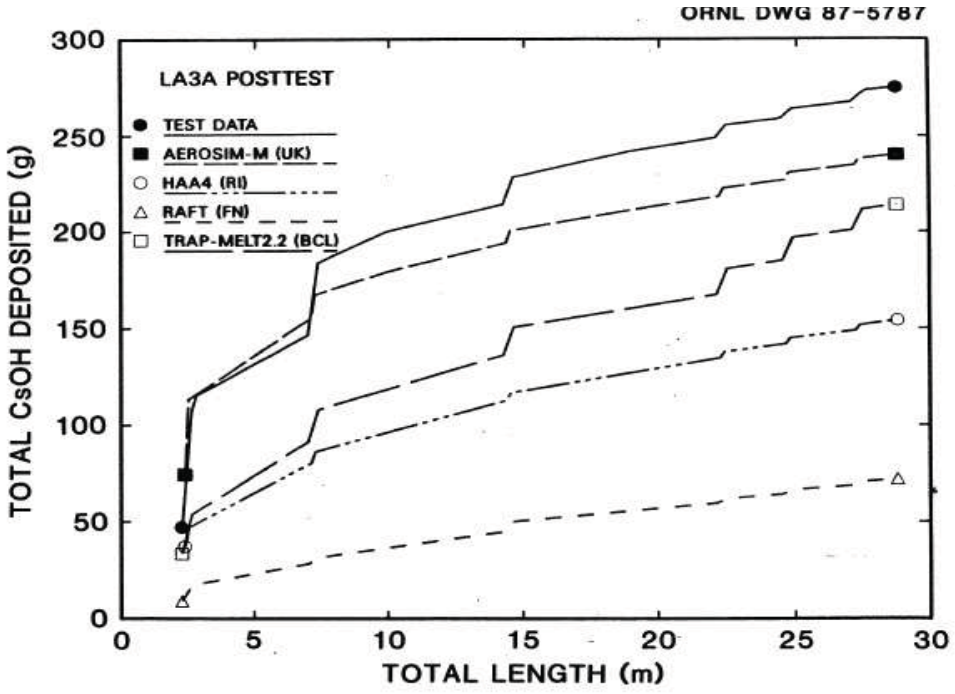

Figure D-38 LA3A post test calculation of CsOH aerosol deposition for codes including bend deposition models
(LACE TR-024)

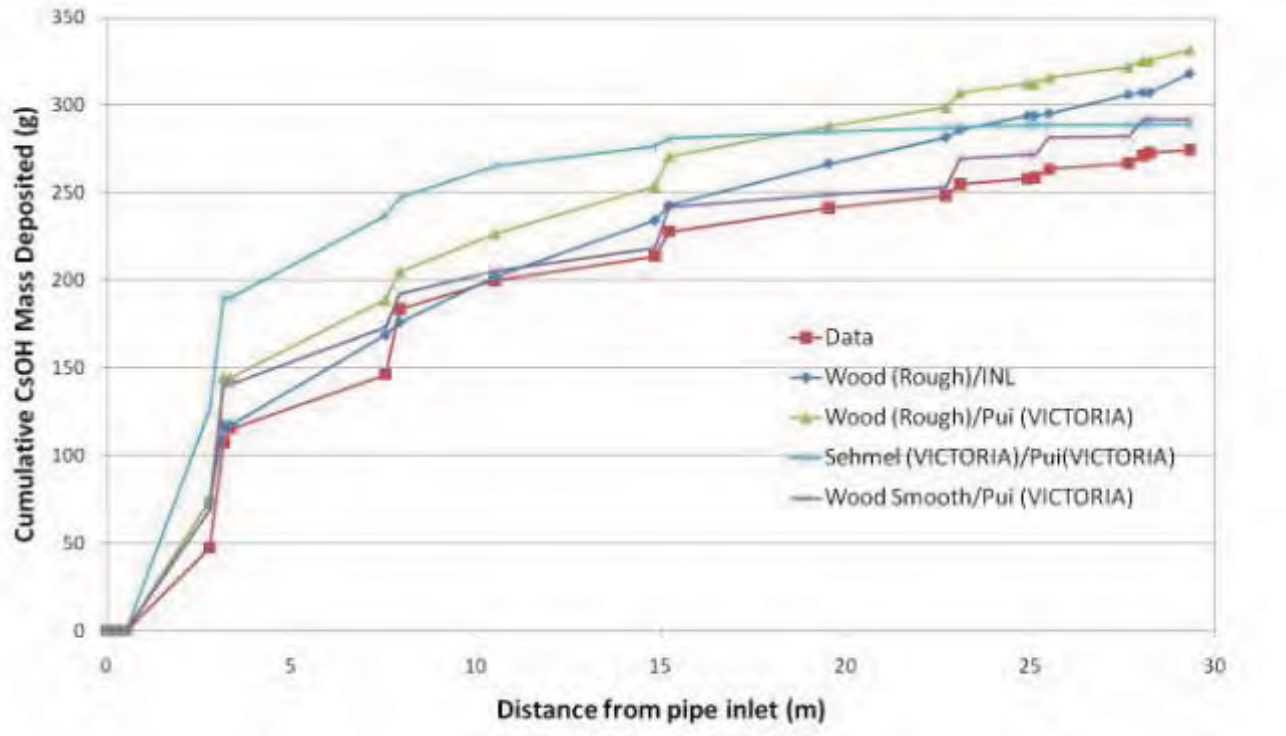

Figure D-39 Deposition profile for CsOH aerosols along LA3A test section
(Sticking factor = 1)

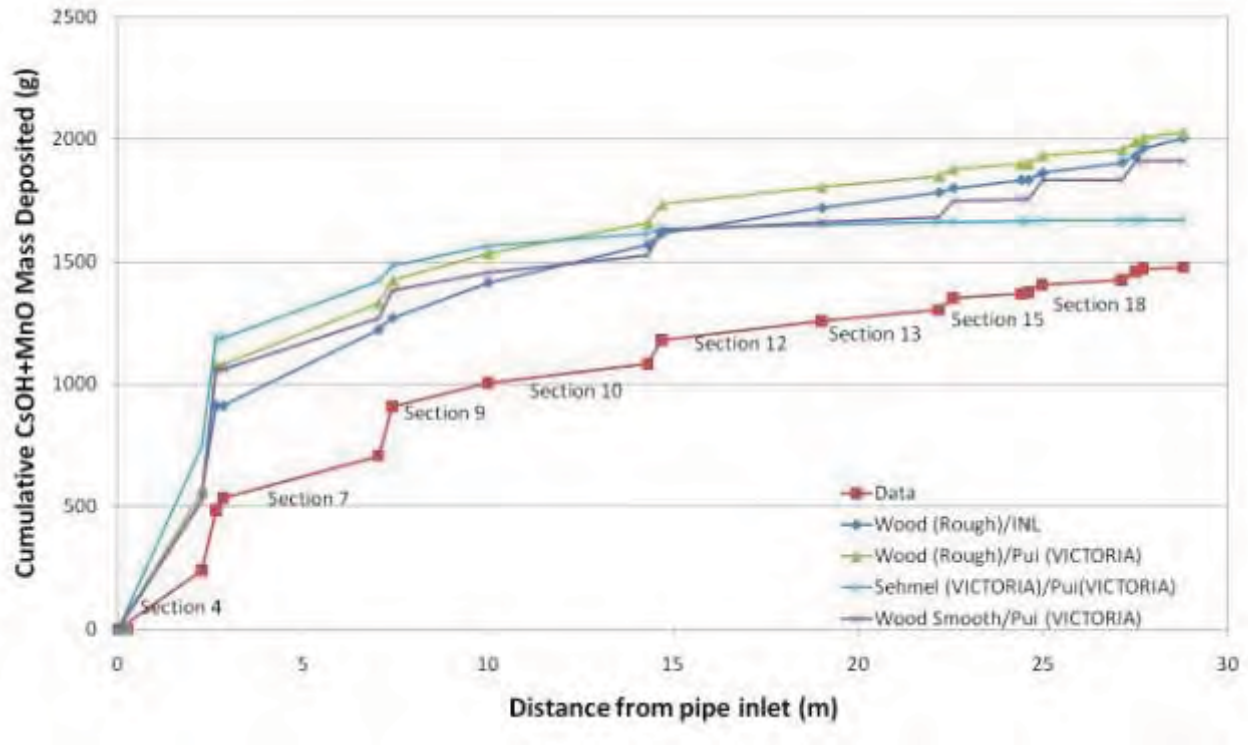

Figure D-40 Deposition profile for CsOH + MnO aerosols along LA3A test section (Calculated sticking factor)

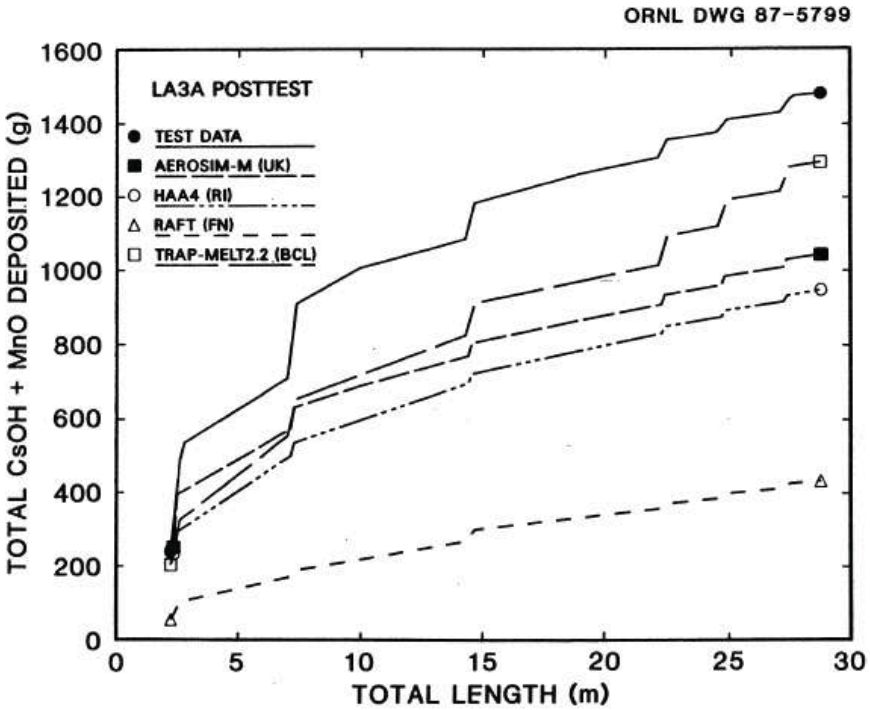

Figure D-41 LA3A post test calculation of CsOH + MnO aerosol deposition for codes in code comparison report including bend deposition models (LACE TR-024)

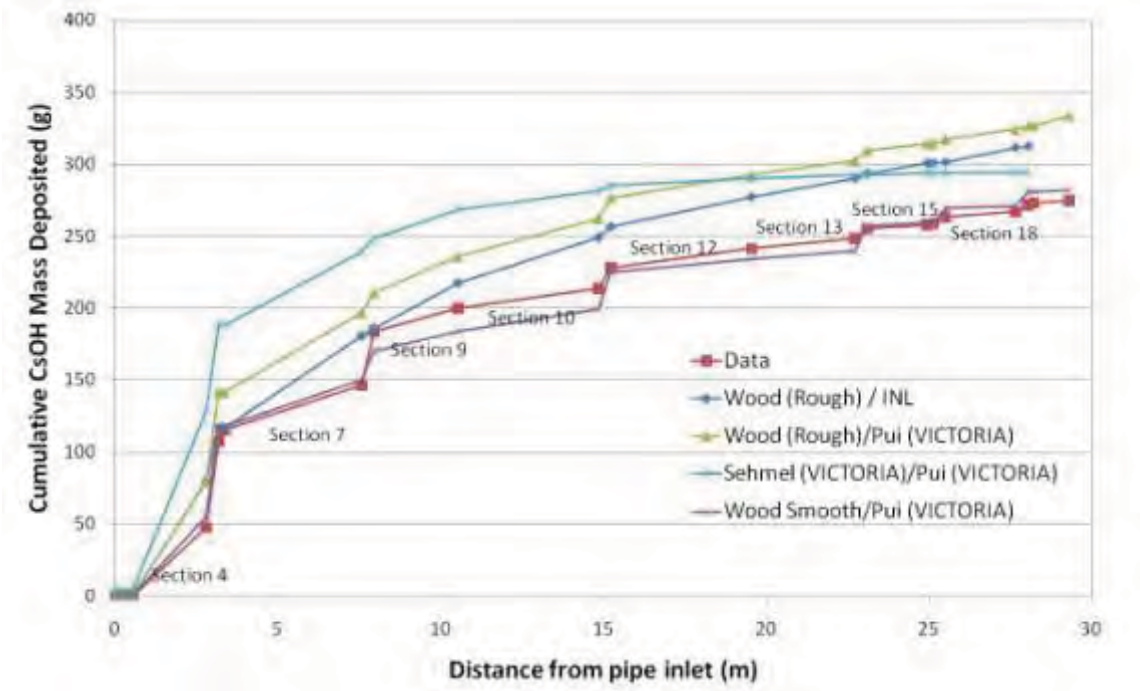

Figure D-42 Deposition profile along LA3A test section
(20 aerosol size bins)

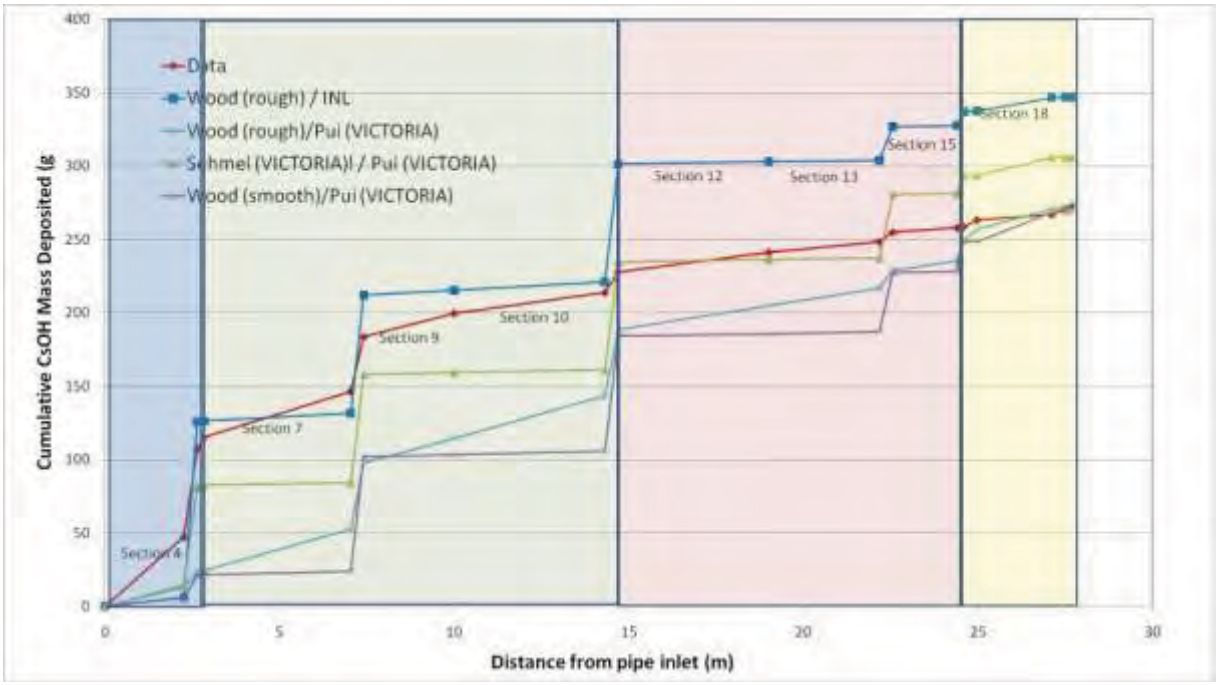

Figure D-43 Deposition profile for CsOH along LA3A test section
(Colored regions indicate lumped nodalization)

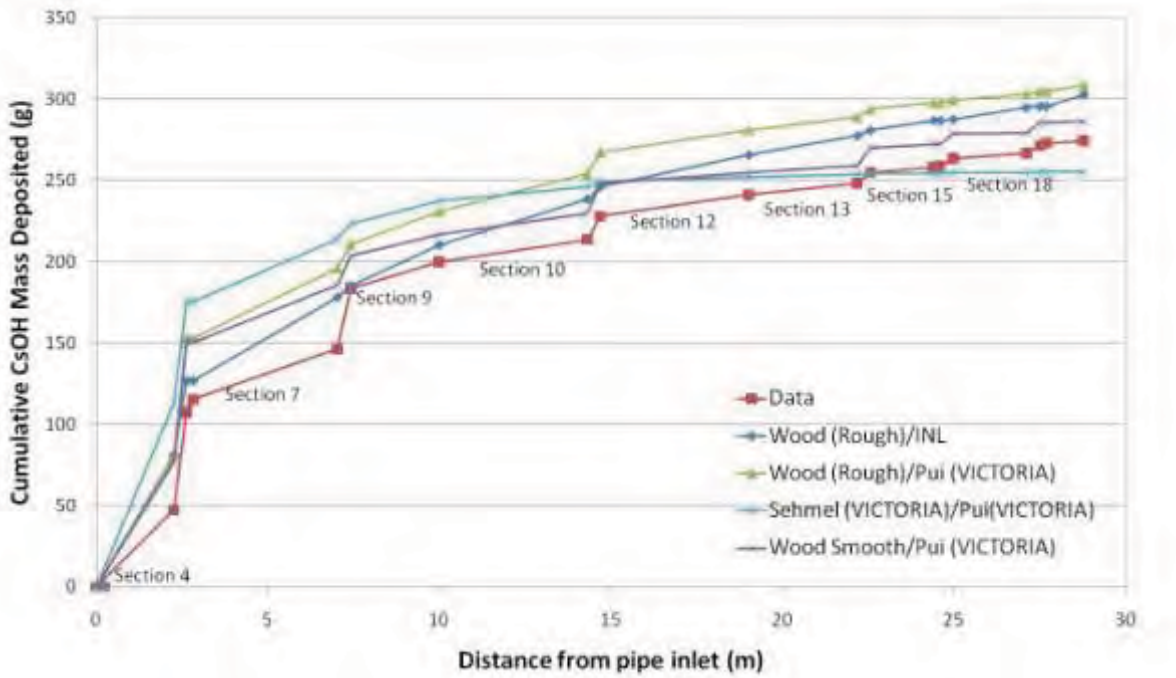

Figure D-44 Deposition profile for CsOH along LA3A test section using the time dependent source rate and the four aerosol source distributions measured during the test

Observations

1. Overall, the MELCOR models do an excellent job of predicting deposition in the test train. The results for all models are generally consistent, though the Sehmel model tends to predict more deposition upstream than the other models with little or no deposition near the end of the test train.

2. All MELCOR calculations slightly over predict deposition upstream in the test train, though not to the extent observed for LA1. As noted for LA1, this may be an indication of resuspension or flow of deposited material along the wall.

3. When compared with the code comparison calculation (TR-022), the MELCOR models estimate the total pipe retention better than most of the codes participating in that activity. MELCOR tends to overestimate the deposition, particularly in upstream test sections where many of the other codes underestimate total deposition.

4. All MELCOR models over predict deposition in test Section 4 (< 2.5 m). This pipe section happens to be a vertical pipe section and it is possible that the orientation of the pipe may have an important role not accounted for in these models.

5. Deposition in bends is important, since about 46% of the deposited mass is found in the bends. The Wood (smooth)/Pui model does a reasonable job of predicting the bend deposition (54%) while other models predict closer to 30%.

6. The MELCOR calculation of MnO deposition along the piping is similar in characteristic to that of CsOH deposition. About 94% of the MnO aerosol was deposited in the test section while the MELCOR models predict between 91% (Wood's smooth/Pui) and 98% (Sehmel/Pui).

7. Calculating the sticking factor with Merrill's model does not significantly affect results for these calculations.

8. Lumping the bends with straight pipe sections reduces the overall retention in the test section.

9. Using the four measured aerosol source distributions and the time dependent source rate provided for this test shows a small (5-10%) but noticeable improvement in the calculated deposition profile. This demonstrates the sensitivity of the calculation to the assumed source profile.

LA3B

Thermal Hydraulic Results

Pressures and velocities along the pipe train are plotted in Figure D-45 and Figure D-46.

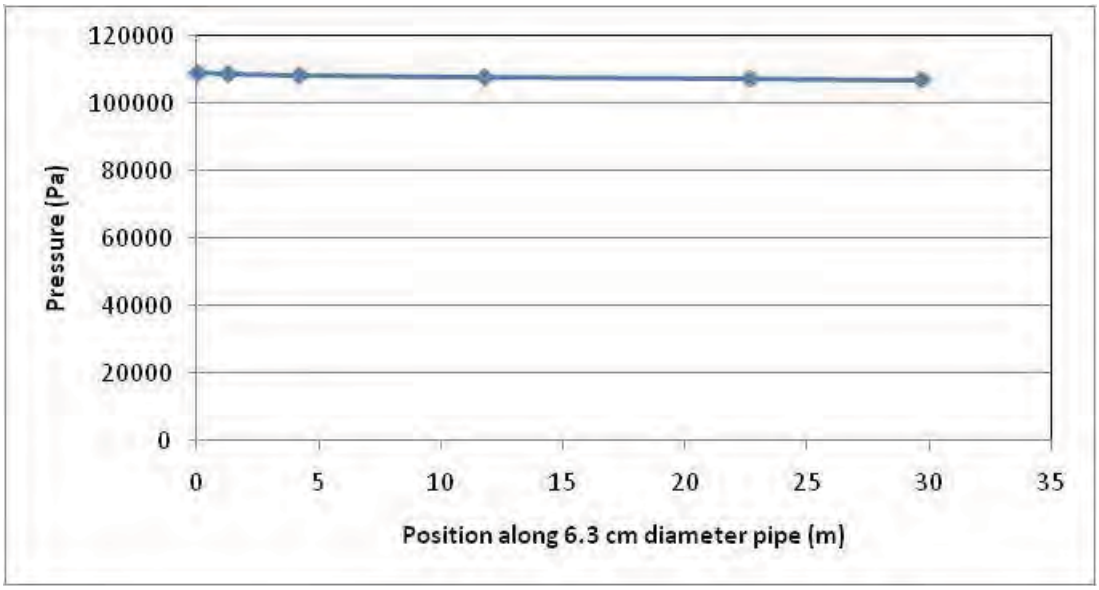

Figure D-45 Pressure profile along test pipe

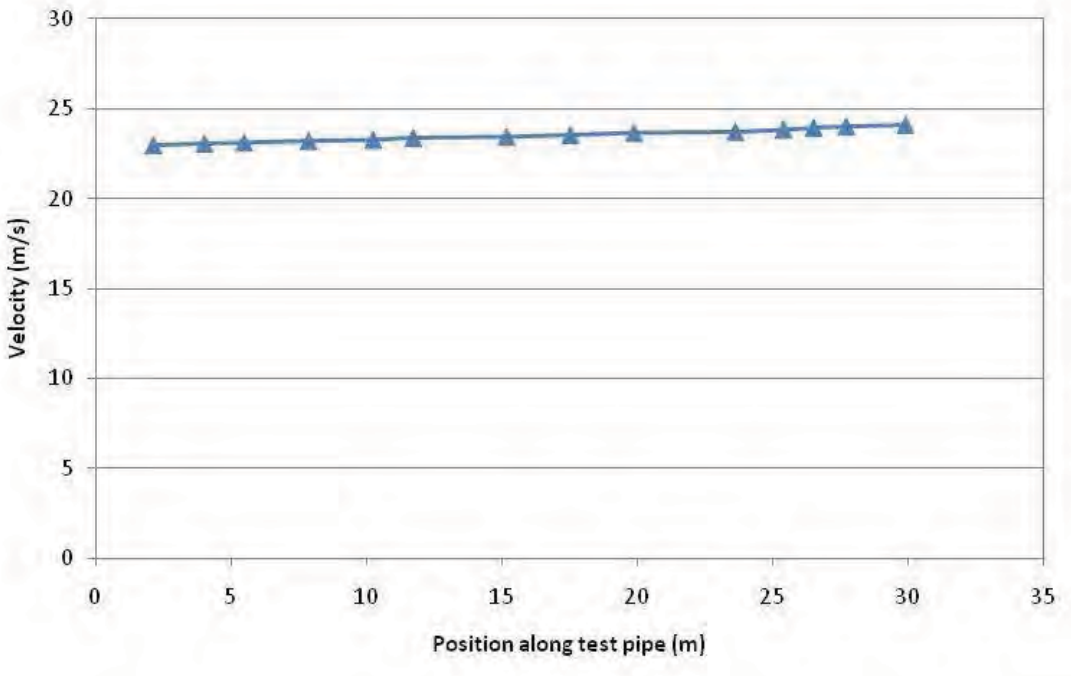

Figure D-46 Velocity profile along test pipe

Deposition Profiles

Deposition profiles along the pipe train are plotted below in Figure D-47 through D-52.

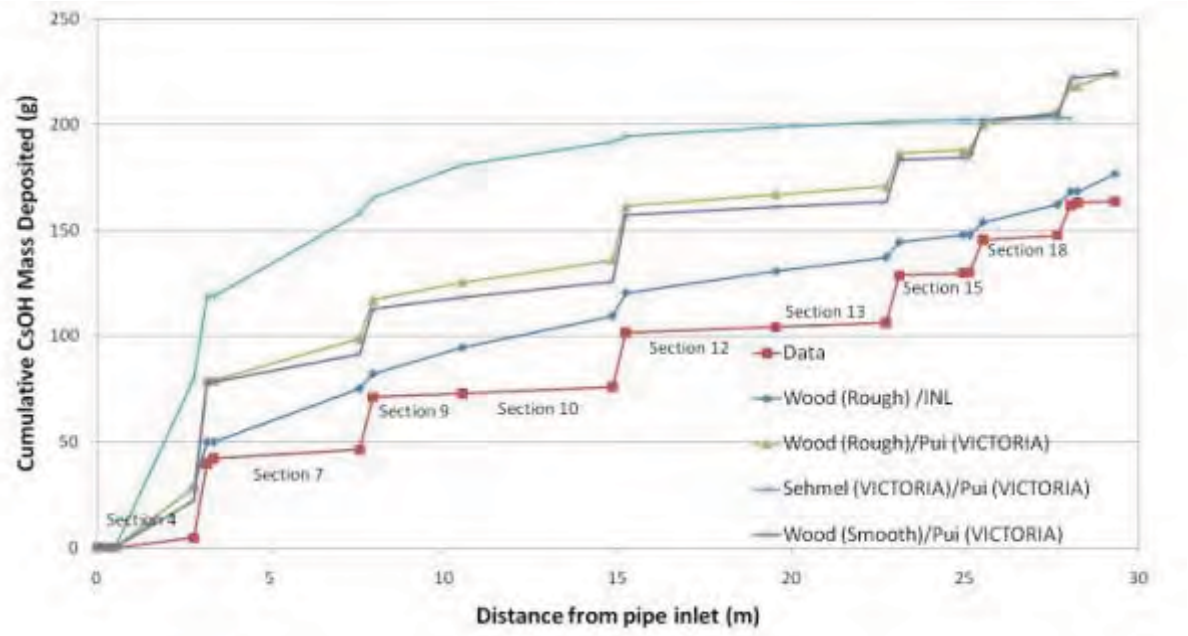

Figure D-47 Deposition profile for CsOH along LA3B test section

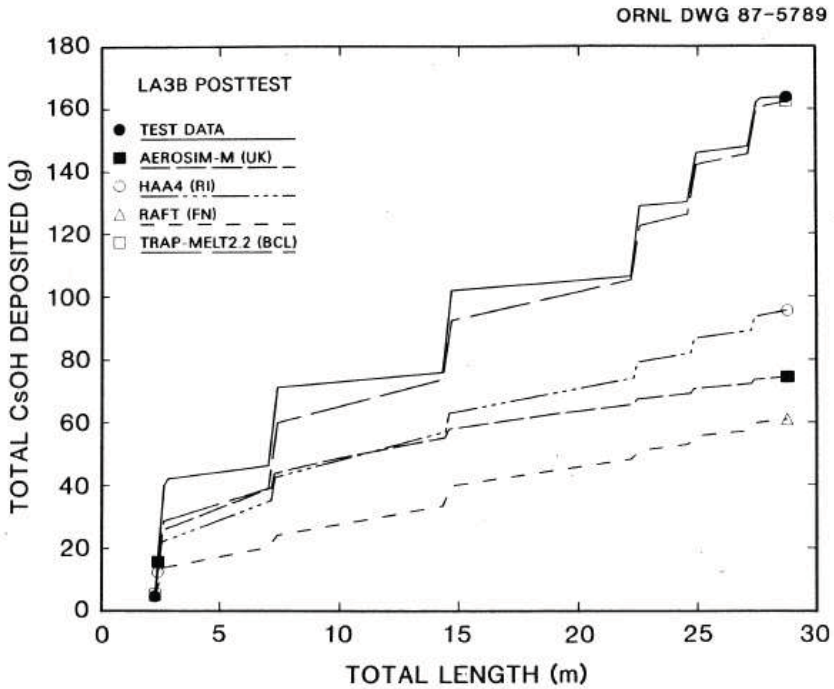

Figure D-48 LA3B post test calculation of CsOH aerosol deposition for codes including bend deposition models

(LACE TR-024)

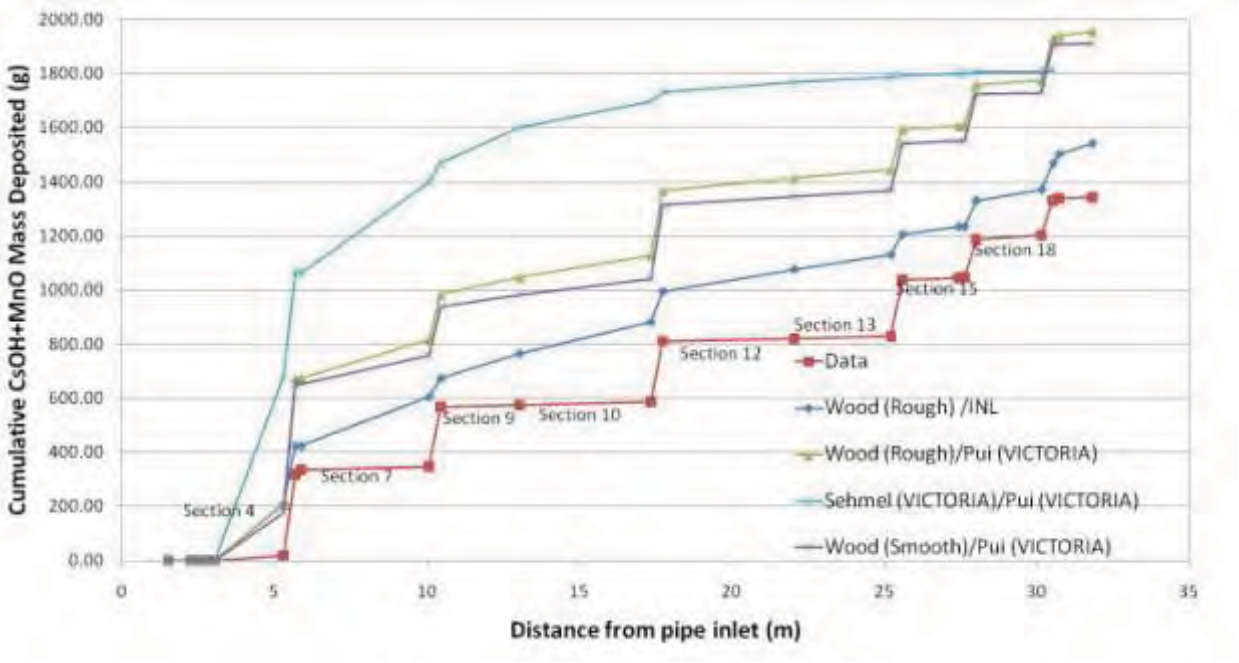

Figure D-49 Deposition profile for CsOH + MnO aerosols along LA3B test section (Sticking factor = 1)

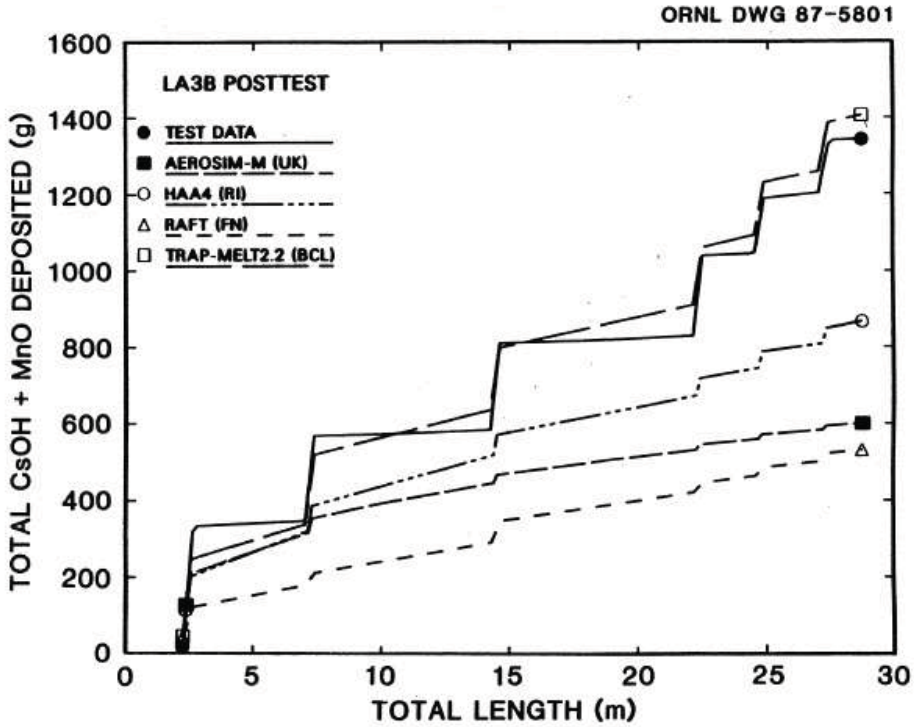

Figure D-50 LA3B post test calculation of CsOH + MnO aerosol deposition for codes including bend deposition models
(LACE TR-024)

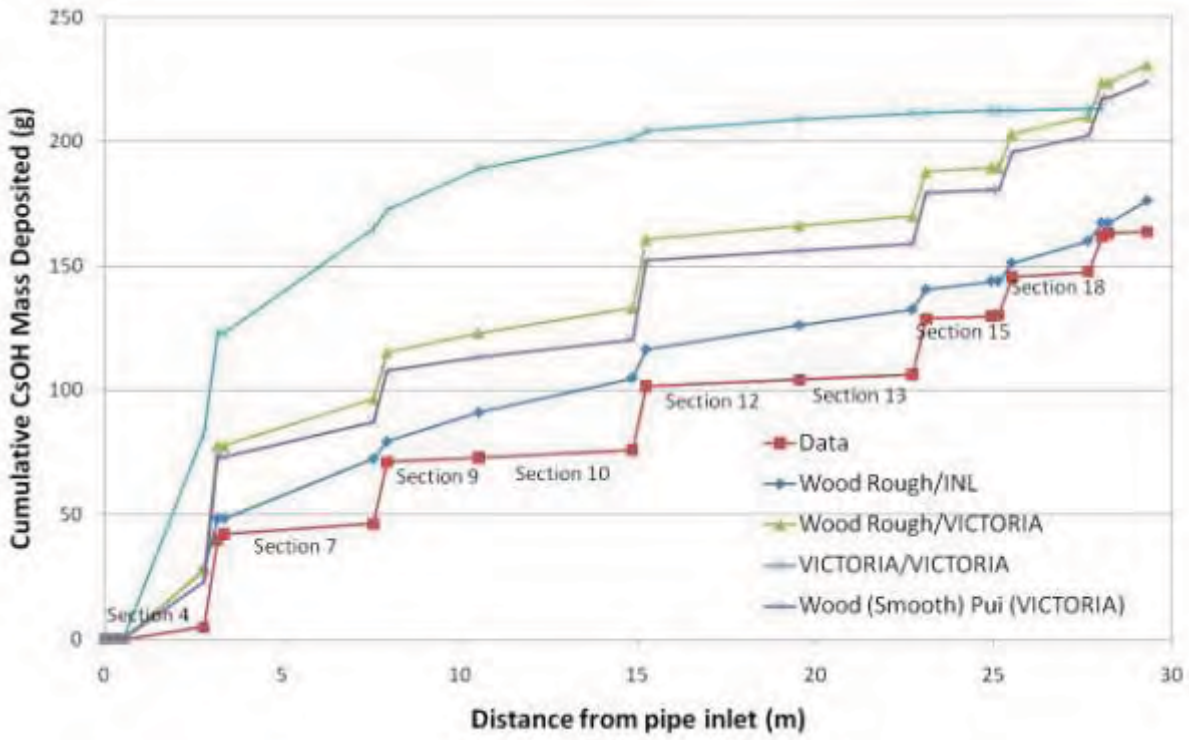

Figure D-51 Deposition profile along LA3B test section
(20 aerosol size bins)

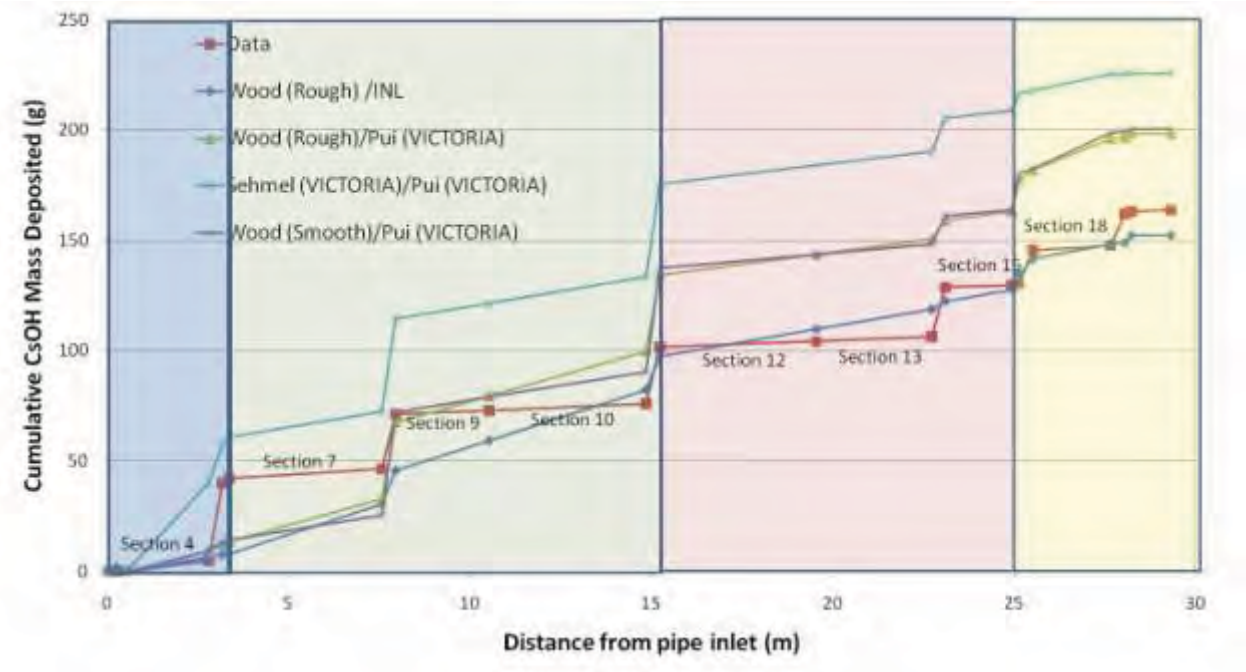

Figure D-52 Deposition profile along LA3B test section - colored
(Colored regions indicate lumped nodalization)

Observations

1. The deposition calculated by the VICTORIA model for the straight pipe early in the test train is larger than was measured in the experiment and exceeds the deposition predicted by the Wood model for rough pipes. Investigation showed that most of this deposition was from supermicron sized particles. The VICTORIA model uses a separate correlation by Sehmel for supermicron sized particles. In addition, for the fine nodalization, the VICTORIA model predicts more deposition in the straight section of HS 1120, which is the smaller diameter pipe.

2. For the coarse nodalization (see Figure D-25), deposition in the reducer region (i.e., pipe section 3) is over predicted by all models. It was reasoned that this could be a result of the nodalization for HS 1120. Deposition in the reducer for the fine nodalization cases is well calculated.

3. Deposition in the bends is under predicted by the INL model for the coarse model but is over predicted for the fine nodalization.

4. For this test, the Wood model for smooth pipes gives the best results. The INL model, which is the Wood model for rough pipes, gives better results for the straight pipe sections 2, 4, and 6.

LA3C

Thermal Hydraulic Results

Pressures and velocities along the pipe train are plotted below (i.e., Figure D-53 and Figure D-54).

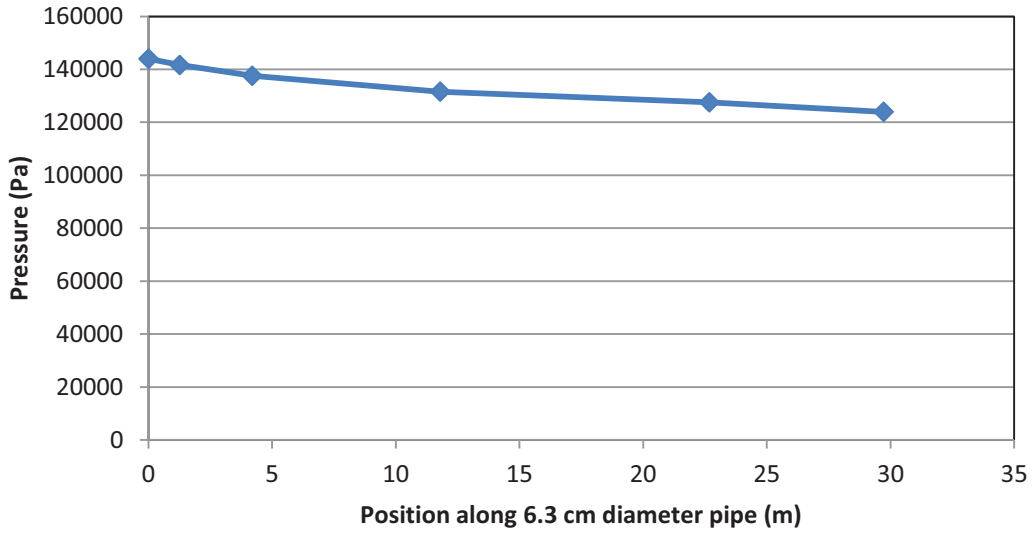

Figure D-53 Pressure profile along test pipe

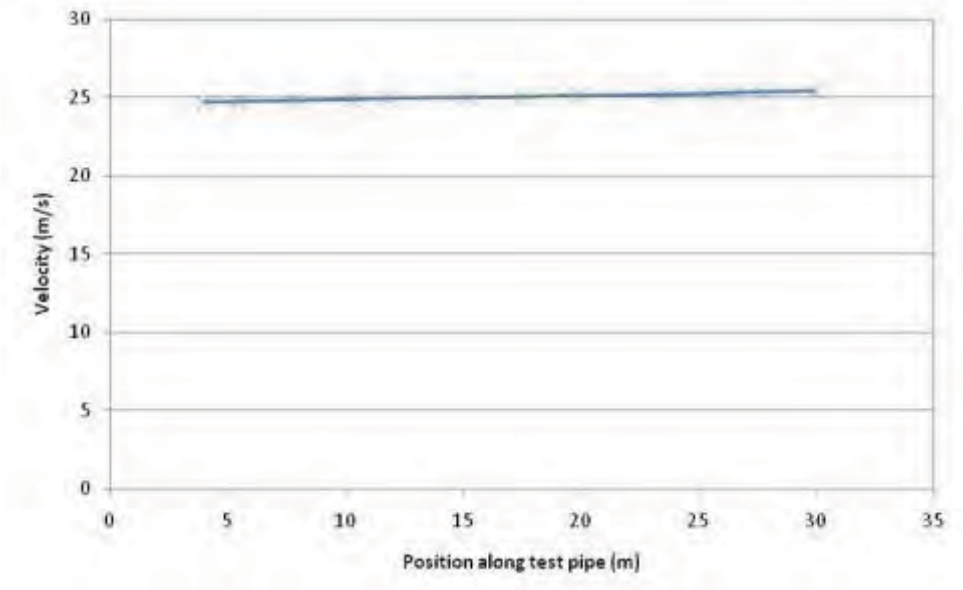

Figure D-54 Velocity profile along test pipe

Deposition Profiles

Deposition profiles for CsOH along the pipe train are plotted in Figure D-55 and Figure D-56.

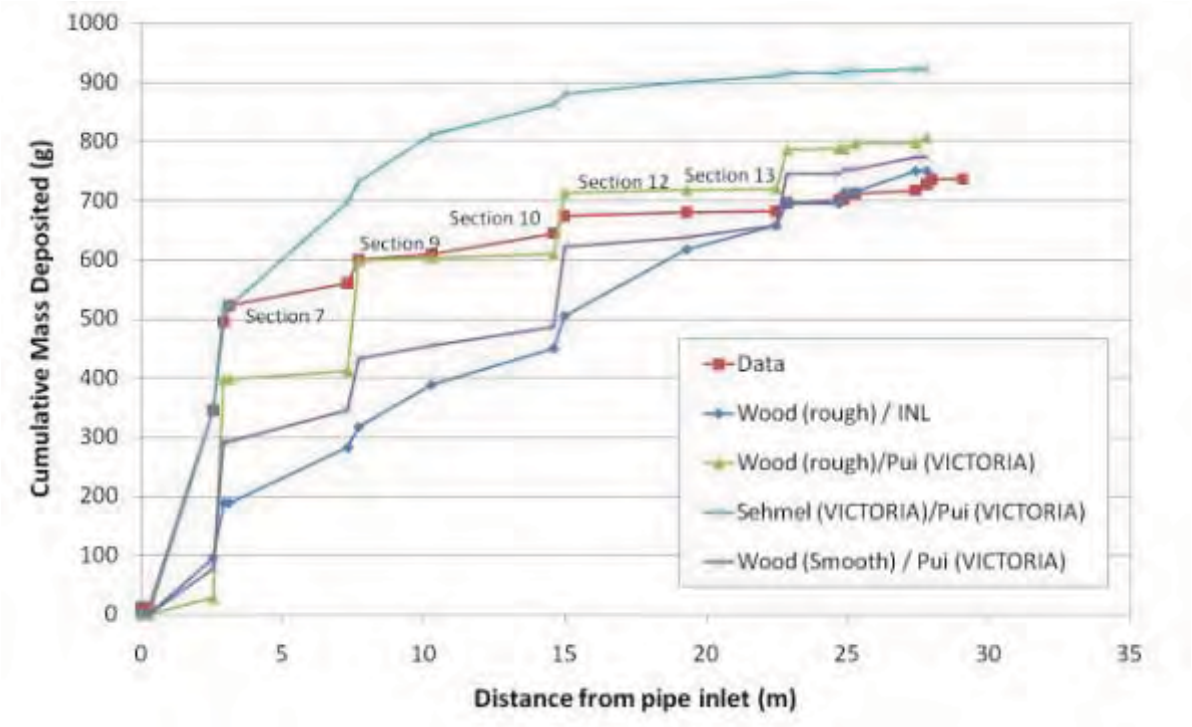

Figure D-55 Deposition profile of CsOH along LA3C test section

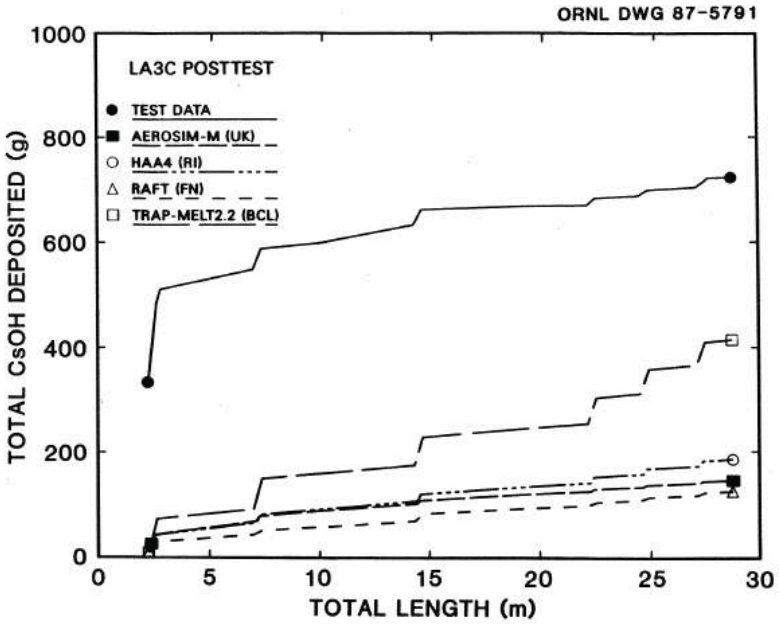

Figure D-56 LA3C post test calculation of CsOH aerosol deposition for codes including bend deposition models
(LACE TR-024)

Observations

1. Figure D-55 shows the VICTORIA model was the same as measured in the experiment for the first 3 meters (Sehmel/Pui), and exceeds the deposition predicted by the INL model. Investigation showed that most of this deposition was from supermicron sized particles. The VICTORIA model uses a separate correlation by Sehmel for supermicron sized particles. However, for the fine nodalization (see Figure D-24), the VICTORIA model does the best job of predicting deposition in the straight section of HS 1120 which is the smaller diameter pipe. This is contrary to the observations for the previous two tests.

2. For this test, deposition in the reducer (i.e., pipe section 3 in Figure D-25) is well predicted by the VICTORIA model for the coarse nodalization. However, for the finer nodalization (see Figure D-24), which would be expected to give better results, deposition in the reducer is roughly five times greater than is predicted.

3. Deposition in the bends is under predicted by the INL model for the coarse model but is over predicted for the fine nodalization.

4. For this test, the VICTORIA model gives the best results.

Turbulent Deposition Models

6.1.5 Wood's Model for Turbulent Deposition on Surfaces

Wood developed a semi-empirical model for predicting turbulent deposition in pipes. His model characterizes deposition over three deposition regimes, which are characteristic of particle size:

1. Turbulent particle diffusion for very small particles where Brownian motion is important to transport particles across the viscous sub layer.

2. Eddy Diffusion – Impaction regime for larger particles dominated by eddy diffusion where particles are accelerated to the wall due to turbulent eddies in the core and buffer layer and coast across the viscous sub layer.

3. Inertia-Moderated Regime – Very large particles, which are subject to reduced acceleration by the turbulent core and little or no acceleration to small eddies in the buffer near the wall.

In the turbulent particle diffusion regime, Brownian diffusion is important and deposition occurs by a combination of Brownian and eddy diffusion. Davies [26] proposed the following equation for the deposition velocity in this regime:

$$u_{t,s} = \frac{Sc^{-2/3}\tilde{v}}{14.5\left\{\frac{1}{6}1n\left[\frac{(1+\varphi)2}{1-\varphi+\varphi^2}\right]+\frac{1}{\sqrt{3}}atan\left[\frac{2\varphi-1}{\sqrt{3}}\right]+\frac{\pi}{\sqrt{3}}\right\}} \qquad (8)$$

where:

$u_{t,s}$ – Turbulent deposition velocity for submicron particles (m/s)

$\tilde{v}$ – Friction velocity (m/s), defined by the following expression:

$$\tilde{v} = U\sqrt{\frac{f}{2}} \qquad (9)$$

f – Fanning friction factor (dimensionless)

φ – $SC^{1/3}/2.9$

Wood found that for particles that are order of the mean free path or greater, this equation could be approximated by:

$$V_d^* = \frac{u_{t,s}}{\tilde{v}} = \frac{3\sqrt{3}}{29\pi}Sc^{-2/3} \qquad (10)$$

where the deposition velocity is non-dimensionalized by the friction velocity.

In terms of the dimensionless relaxation time, τ_*, this can be written:

$$V_d^* = \frac{3\sqrt{3}}{29\pi\tau_*^{1/3}} Sc^{-2/3} \ \tau_*^{1/3} \qquad (11)$$

As particle size increases, impaction increases and a second term is added to this equation:

$$V_d^* = \frac{3\sqrt{3}}{29\pi\tau_*^{1/3}} Sc^{-2/3} \ \tau_*^{1/3} + K\tau_*^2 \qquad (12)$$

The coefficient, K, is derived by solving a diffusion equation written in the form of a turbulent version of Fick's law, i.e.,

$$N = \left(D_p + \ \varepsilon\right)\frac{dc}{dy} \quad (13)$$

where:

N – particle flux ($\#/m^2$-s)
D_p – particle diffusion coefficient (m^2/s)
ϵ – particle turbulent eddy-diffusivity (m^2/s)
c – particle concentration ($\#/m^3$)
y – distance from surface (m)

For smooth pipes, Wood [22] proposed the following approximation for the deposition velocity:

$$V_d^* = \frac{3\sqrt{3}}{29\pi\tau_*^{1/3}} Sc^{-2/3} \ \tau_*^{1/3} + 0.00045\tau_*^2 \qquad (14)$$

For large particles, $\tau_* > 10$, particle inertia becomes important in the inertia-moderated regime and the deposition velocity becomes constant, though dependent on the Reynolds number through the friction factor:

$$\begin{aligned} V_d^* &= \sqrt{\frac{f}{2}} && 10 \le \tau_* < 270 \\ V_d^* &= \frac{2.6}{\sqrt{\tau_*}}\left(1 - \frac{50}{\tau_*}\right) && \tau_* \ge 270 \end{aligned} \qquad (15)$$

For rough pipes, this equation is a little more complicated but was formulated for MELCOR by Merrill:

$$V_d^* = \frac{1}{(I_s + I_B)} \qquad for\ \tau_* \leq 10$$
$$V_d^* = 0.69\sqrt{\frac{2}{\pi}}erfc\left(\frac{1}{\sqrt{2}}\left[1 + \frac{b_+}{s_+}\right]\right) \qquad for\ \tau_* > 20 \tag{16}$$

Where I_S and I_B result from integration of the non-dimensional diffusion equation over the buffer layer and sub-layer respectively, b_+ is the non-dimensional roughness, and s_+ is the non-dimensional perpendicular stopping distance. This model was originally implemented into MELCOR 1.8.0 by Merrill [14] for a branch version of the code for safety analysis of the International Thermonuclear Experimental Reactor (ITER).

6.1.6 VICTORIA Deposition Model

The VICTORIA model also predicts three regimes for turbulent deposition as was observed for the Wood models. Similar to the Wood model, deposition in the turbulent particle diffusion regime, follows that of Davies [26] (i.e., Equation 8). Though the approximation in Equation 9 is not used for the VICTORIA model, this does not lead to significant differences in results. This term is then added to a term derived by Sehmel [17] for the particle impaction regime:

$$u_{t,s} = 1.47 * 10^{-16} \left(\frac{\rho_a}{1000}\right)^{1.01} \left(\frac{2 * 10^4 r_a}{D_H}\right)^{2.1} Re^{3.02} \tilde{v} \qquad (17)$$

To obtain the following equation for the non-dimensional deposition velocity:

$$V_d^* = \frac{Sc^{-\frac{2}{3}}}{14.5\left\{\frac{1}{6}ln\left[\frac{(1+\varphi)2}{1-\varphi+\varphi^2}\right] + \frac{1}{\sqrt{3}}atan\left[\frac{2\varphi-1}{\sqrt{3}}\right] + \frac{\pi}{\sqrt{3}}\right\}} + 1.47 * 10^{-16} \left(\frac{\rho_a}{1000}\right)^{1.01} \left(\frac{2 * 10^4 r_a}{D_H}\right)^{2.1} Re^{3.02} \qquad (18)$$

Note that the correlation reported in Equation 17 was based on a least squares curve fit to a restricted data set based on experiments for which surfaces were treated, often with petroleum jelly, to simulate a perfect particle sink, by eliminating or drastically reducing particle bounce. Sehmel recommended use of another correlation, fit over a more general data set, for untreated surfaces:

$$u_{t,s} = 1.0 * 10^{-16} \left(\frac{\rho_a}{1000}\right)^{1.83} \left(\frac{2 * 10^4 r_a}{D_H}\right)^{2.99} Re^{3.08} \tilde{v} \qquad (19)$$

This equation was not used by the VICTORIA code and not implemented into MELCOR, but is reported here for completeness.

It should also be pointed out that the VICTORIA user manual indicates Sehmel's equation is used for supermicron particles and Davies model is used for submicron particles. However, this is an issue with VICTORIA users manual. Doing so leads to a discontinuity in the deposition velocity. Examination of the source code indicates that the sum of these two terms is actually used.

A maximum is placed on the non-dimensional deposition velocity so that it does not exceed a value of 0.1. This leads to the constant deposition velocity characteristic of the inertia-moderated regime. This is also undocumented in the VICTORIA manual.

6.1.7 INL Bend Model

For the INL Bend Model [14], to calculate the inertial deposition of aerosols in pipe bends, we start with the centrifugal force acting on the particle as the fluid turns a pipe bend. This force is given by:

$$F_C = \frac{\pi}{6}\left(\rho_p - \rho_f\right) d_p^3 \frac{u_f^2}{r_b} \approx m_p \frac{u_f^2}{r_b} \tag{20}$$

Where:

d_p – particle diameter (m)
u_f – fluid velocity (m/s)
r_b – bend radius of pipe (m)
ρ_p – particle density (kg/m^3)
ρ_f – fluid density (kg/m^3)
m_p – particle mass (kg)
Θ_b – bend turning angle (radians)
S – the particle radial drift (m)
B – the particle mobility

The terminal velocity in the radial direction that a particle will obtain because of this force is given by:

$$u_p = BF_c \tag{21}$$

where "B" is the particle mobility defined as:

$$B = \frac{1}{(3\pi\mu_g d_p)} \tag{22}$$

where μ_g, is the carrier gas viscosity.

The time that it will take for a particle to travel around a bend is given by:

$$t_b = \frac{r_b \Theta_b}{u_f} \tag{23}$$

where Θ_b is the pipe turning angle in radians.

Consequently, the radial distance a particle will drift in this turn is the product of bend travel time and the particle radial velocity, which becomes:

$$S = \Theta_b B m_p u_f \quad (24)$$

Equation 24 is used to express the centrifugal force. By assuming a well mixed particle concentration in the pipe (c_o), the fraction of particles that will collide with the wall in the bend is approximately the radial drift distance divided by the pipe diameter (i.e. s/D). The particle flux (#/m^2-s) for inertial deposition based on this collided fraction, when averaged over the pipe surface area, can be expressed as:

$$\Gamma_i = \frac{s}{D} \frac{c_o u_f A_c}{A_s} \quad (25)$$

where:

D – pipe diameter (m)
A_C – pipe cross-sectional area (m^2)
A_s – pipe surface area (m^2)

The deposition velocity associated with this particle flux is as follows:

$$V_i = \frac{r_i}{c_o} \quad (26)$$

6.1.8 Pui Bend Model

The model used in VICTORIA for deposition in 90° pipe bends under turbulent conditions (i.e., Re ≥ 2300) is based on the experimental and theoretical work of Pui et al., [25]. Their experiments covered a range of Reynolds numbers from 10^2 to 10^4. They found that an exponential relationship between Stokes number and deposition efficiency correlated well with their data. This relationship is:

$$\eta_b = 1 - 10^{-0.963St} \tag{27}$$

where:

η_b – deposition efficiency due to flow irregularity (dimensionless)

And the particle Stokes number is given by:

$$St = \frac{C_c \rho_p d_p^2 U_{ave}}{9 \mu D_h} \tag{28}$$

Deposition efficiency is defined as the fraction of aerosol particles of a specific size that deposit. More specifically for Equation 27, the deposition efficiency represents the fraction of aerosol particles that deposit near the pipe bend because of inertial effects induced by curvature of the fluid streamlines. Deposition efficiency is converted to deposition velocity in VICTORIA by the following definition:

$$u_b = \eta_b \frac{U}{L} \frac{V_B}{A} \tag{29}$$

where:

u_b – deposition velocity for flow through a bend
V_B – volume of bulk gas subregion (m^3), as defined in chapter 3
A – surface area for aerosol deposition (m^2)

6.1.9 McFarland Bend Model

McFarland's model is purely empirical and is based on fitting an equation to data obtained from physical experiments and Lagrangian simulations [13]:

$$\eta_b = 1 - 0.01\exp\left(\frac{4.61 + a\theta St}{1 + b\theta St + c\theta St^2 + d\theta^2 St}\right) \quad (30)$$

Where: Θ = the angle of the bend;

$$a = -0.9526 - 0.0568\delta \quad (31)$$

$$b = \frac{-0.297 - 0.0174\delta}{1 - 0.07\delta + 0.0171\delta^2} \quad (32)$$

$$c = -0.306 + \frac{1.895}{\sqrt{\delta}} - \frac{2.0}{\delta} \quad (33)$$

$$d = \frac{0.131 - 0.0132\delta + 0.000383\delta^2}{1 - 0.129\delta + 0.0136\delta^2} \quad (34)$$

$$\delta = \frac{2R_{bend}}{h} \quad (35)$$

and where:

R_{bend} – radius of the bend in the flow path

6.1.10 Sticking Factor

Particles that strike a surface may either stick to the surface or bounce and are possibly re-entrained if adhesive forces are not sufficient to overcome the incident momentum of the particle. An optional factor can be used to calculate the probability of sticking to the surface. This factor is calculated [14] by considering both capillary forces and Van der Waals forces:

$$F_a = 4\pi r_p \sigma + \tfrac{3}{2}\pi r_p \gamma f_r \qquad (36)$$

Where:

σ – surface tension of possible film on surface (J/m^2)
γ – surface energy per unit area for Van der Waals interaction (J/m^2)
f_r – surface energy reduction factor due to surface roughness

The minimum required momentum necessary for a particle to overcome adhesion is then given by the following:

$$m_p u_c = \int_0^t F_S dt = \int_0^t F_a dt + \int_0^t F_d dt \approx F_a t_a + F_d t_d \qquad (37)$$

Where:

u_c – critical escape velocity (m/s)
m_p – particle mass (kg)
t_a – surface adhesion time (s)
t_d – film residence time (s)
F_d – drag force = $\tfrac{3}{2}\pi r_p \mu_f u$

Several assumptions are made regarding the surface adhesion time and the film residence time. For example, it is assumed that the distance over which these forces act are on the order of the magnitude of the particle radius and that this distance divided by the critical escape velocity gives the film residence time. It is also assumed that the viscous drag force acts over approximately twice the film thickness. With these assumptions, the critical velocity can be calculated:

$$u_c = \frac{3\pi r_p \mu_f \delta_f}{2m_p} + \sqrt{\left(\frac{3\pi r_p \mu_f \delta_f}{2m_p}\right)^2 + \frac{\pi r_p}{m_p}\left(r\sigma + \tfrac{3}{2}\gamma f_r\right)} \qquad (38)$$

Finally, it is assumed that this critical velocity is the vector sum of the perpendicular velocity component and the parallel stream velocity component and equations for standard turbulent velocity profiles are then used to determine the fractional area of the pipe for which particle velocities would be insufficient to overcome the adhesion forces. The perpendicular velocity component is approximated by $u = 0.69\tilde{v}$ where $\tilde{v}$ is the friction velocity defined in Equation 5.

New MELCOR RN Package Input Records

RNTURB Record – Deposition Modeling Record

Optional

(1) IMODEL - Deposition Modeling flag for gravitational, thermophoresis, and diffusiophoresis components
= 0, Gravitational, thermophoresis, and diffusiophoresis velocities are calculated once at the beginning of the calculation.
= 2, Gravitational, thermophoresis, and diffusiophoresis velocities are recalculated at each time step.

(type = integer, default=0, units = none)

(2) ITURB - Deposition Modeling flag for turbulent component
= 0, MELCOR 1.8.6 deposition modeling
= 1, VICTORIA modeling of deposition in straight pipe sections. If negative, the sticking factor is assumed to be 1.0
= 2, INL modeling of deposition in straight pipe sections. This is essentially Wood's model for rough pipes and approaches Wood's model for smooth pipes when the roughness is small. If negative, the sticking factor is assumed to be 1.0
= 3, INL model for submicron particles, VICTORIA for larger particles. If negative, the sticking factor is assumed to be 1.0
= 4, VICTORIA model for submicron particles, INL for larger particles If negative, the sticking factor is assumed to be 1.0
= 5, Wood's model for smooth pipes.

(type = integer, default=0, units = none)

(3) ITRANS - Deposition Modeling flag for impact deposition in transitions
= 0, MELCOR 1.8.6 deposition modeling
= 1, VICTORIA modeling of deposition in bends and other transitions. If negative, the sticking factor is assumed to be 1.0
= 2, INL modeling of deposition in bends and other transitions. If negative, the sticking factor is assumed to be 1.0

(type = integer, default=0, units = none)

RNMGnnn Record – RN Turbulent Deposition Record

nnn is a sequence number
Optional

(1) VOL_ID - The volume in which to apply the bend and/or turbulent deposition model
(type = integer, default=none, units = none)

(2) CHARL - characteristic dimension (i.e., pipe diameter)
(type = real, default=none, units = m)

(3) No_Bnd - Number of bends associated with the volume
(type = integer, default=none, units = none)

(7) ANGLE - Turning angle of the bends
(type = real, default=none, units = radians)

(5) RAD_BND - Radius of curvature for bend
(type = real, default=none, units = m)

(6) ROUGH - Surface roughness for the turbulent deposition model (not used in VICTORIA model)
(type = real, default=none, units = none)

RNTRSnnn Record – Transition Deposition Record

nnn is a sequence number
Optional

(1) VOL_ID - The volume in which to apply the bend and/or turbulent deposition model
(type = integer, default=none, units = none)

(2) CHARL - characteristic dimension (i.e., pipe diameter)
(type = real, default=none, units = m)

(3) DODI - Diameter at exit divided by diameter at entrance (<=1)
(type = real, default=none, units = none)

(4) NCONTR - Number of contraction transition
(type = integer, default=none, units = none)

(5) NVENTUR - Number of venturi transitions
(type = integer, default=none, units = none)

(6) FACONT - Multiplier on deposition velocity for contraction
(type = integer, default=none, units = none)

(7) FAVENT - Mulitiplier on deposition velocity for venturi transition
(type = integer, default=none, units = none)

RNSTnnn Record – Sticking Factor Options

nnn is a sequence number
Optional

(1) iCOMP - RN Component
(type = integer, default=none, units = none)

(2) SIGMAW - Surface Tension
(type = real, default=none, units = N/m)

(3) ETAF - Surface Viscosity (mu/rho)
(type = real, default=none, units =kg/m-sec)

6.1.11 New Control Function

RN1-DEPHS-x-s-II.HS /c/ Total radionuclide mass of class x deposited on side s of heat structure HS from deposition model II. The deposition models that are tracked are as follows:
II = 1, Diffusion deposition
II = 2, Thermophoresis
II = 3, Gravitational settling
II = 4, Turbulent deposition in straight sections
II = 5, Deposition in pipe bends
II = 6, Deposition in Venturi transitions
II = 7, Deposition in Contraction transitions
(units = kg)

Summary and Conclusions for LACE Experiments

The LACE tests provide an experimental database for validation of turbulent deposition modeling over a wide range of conditions. Entrance flow velocities in these tests ranged from 23 m/s (LA3C) to 96 m/s (LA1) while the exit flow velocity for LA1 was as high as 200 m/s.

The Wood's model for both rough and smooth pipes as well as the VICTORIA model were tested. In addition, the Pui model for bends as well as Merrill's model were examined. Deposition profiles along the test section were used to compare the relative importance of these deposition mechanisms. The results were also compared against the code comparison study that was part of the LACE experimental program (LACE TR-022 and LACE TR-024).

Furthermore, several sensitivity analyses were performed. A calculation utilizing a coarse nodalization, where straight pipe sections were lumped with bends by sharing the same control volume and heat structure, were tested against experimental results and compared with results from the detailed nodalization. In addition, the dependency of results on the number of section bins used in the calculation was examined. Finally, the dependency of the results on the assumed sticking factor was considered.

In general, the overall deposition in the experiment is captured by the all models. LA1, which has the greatest flow velocities, shows approximately 97 % retained in the pipes compared to 98% in the experiment. For the LA3 tests, the trends in total retention are captured by the MELCOR models, though they all slightly over predict deposition. Also, the fraction that is deposited in bends does not appear to be consistent between tests. The VICTORIA models appear to predict larger depositions than the other modeling approaches. This is consistent with the velocity profiles plotted for these models and shown in Figure D-31 through Figure D-33.

Some of this difference in the predicted deposition profiles may be an indication of resuspension or flow of deposited material along the wall. This could explain why this effect is more pronounced for LA1 where velocities are greater where it would be expected that resuspension or flow of deposited material would be greater for the higher Reynolds numbers.

7 REFERENCES

1. 24th DOE/NRC Nuclear Air Cleaning and Treatment Conference, "The Effect of Media Area on the Dust Holding Capacity of Deep Pleat HEPA Filters." J Dyment AWE plc Aldermaston RG7 4PR United Kingdom D Loughborough AEAT Harwell Oxford OX11 ORA United Kingdom Proceedings of the 24th DOE/NRC Nuclear Air Cleaning and Treatment Conference: Held in Portland, Oregon, July 15–18, 1996 (NUREG/CP-0153, CONF-960715), Figure 1, 21.0 sq.m 72pl HV curve from 600g-840g of captured dust

2. J.K. Agarwal and B.Y.H. Liu, "A criterion for accurate sampling in calm air", American Industrial Hygiene Association Journal, *41* (1980) 191-197.

3. N.E. Bixler, "VICTORIA 2.0: A Mechanistic Model for Radionuclide Behavior in a Nuclear Reactor Coolant System Under Sever Accident Conditions", SAND93-2301, 1998.

4. D.R. Dickinson, et al, "Aerosol Behavior in LWR Containment Bypass Piping – Results of LACE Test LA3", LACE TR-011, July 1987.

5. M.S. El-Shobokshy, "Experimental Measurements of Aerosol Deposition to Smooth and Rough Surfaces", Atmospheric Environment, *17* (1983) 639-644.

6. L.J. Forney and L.A. Spielman, "Deposition of Course Aerosols from Turbulent Flows", J. Aerosol Science, *5* (1974) 257-271.

7. S.K. Friedlander and H.F. Johnstone, "Deposition of Suspended Particles from Turbulent Gas Streams", Ind. Eng. Chem., *49* (1957) 1151-1156.

8. R. 0. Gauntt et al, "MELCOR Computer Code Manuals, Reference Manual, Version 1.8.5, Vol. 2, Rev. 2", Sandia National Laboratories, NUREG/CR-6119, SAND2000-2417/1.

9. K.H. Im and R.K. Ahluwalia, "Turbulent Eddy Deposition of Particles on Smooth and Rough Surfaces", J. Aerosol Science, *20* (1989) 431-436.

10. D.B. Ingham, "Diffusion of aerosols from a stream flowing through a cylindrical tube," J. Aerosol Science, *6* (1975) 125-132.

11. K.E. Lee and J.A. Gieseke, "Deposition of Particles in Turbulent Pipe Flows", J. Aerosol Science, *25* (1994) 699.

12. B.Y. H. Liu and J.K. Agarwal, "Experimental Observation of Aerosol Deposition in Turbulent Flow", J. Aerosol Science, *5* (1974) 145-155.

13. A.R. McFarland, H. Gong, A. Muyshondt, W.B Wente, and N.K. Anand, "Aerosol Deposition in Bends with turbulent Flow", Environmental Science and Technology, *31* (1997) 3371-3377.

14. B.J. Merrill and D.L. Hagrman, "MELCOR Aerosol Transport Module Modification for NSSR-1", INEL-96/0081, ITER/US96i/TE/SA-03, 1996.

15. T.L. Montgomery and M. Corn, "Aerosol Deposition in a Pipe with Turbulent Air Flow", J. Aerosol Science, *1* (1970) 185-213.

16. P.G. Papavergos and A.B. Hedley, "Particle deposition behaviour from turbulent flows", Chemical engineering Research and Design, *62* (1984) 275-295.

17. G.A. Sehmel, "Particle Deposition from Turbulent Air Flow", J. Geophysical Research, *75* (1970) 1766-1781.

18. M. Shimada, K. Okuyama, and M. Asai, "Deposition of Submicron Aerosol Particles in Turbulent and Transition Flow", AIChE J., *39* (1993) 17-26.

19. D. Sinclair, R.J. Countess, B.Y.H. Liu, and D.H.H. Pui, Experimental Verification of Diffusion Battery Theory", Air Pollution Control Association Journal, *26* (1976) 661-663.

20. M.R. Sippola and W.W. Nazaroff, Particle Deposition from Turublent Flow: Review of Published Research and Its Applicability to Ventilation Ducts in Commercial Buildings, LBNL-51432, Lawrence Berkeley National Laboratory Report, June 2002.

21. A.C. Wells and A.C. Chamberlain, "Transport of small particles to vertical surfaces", British J. Appl. Physics, *18* (1967) 1793-1799.

22. N.B. Wood, "A Simple Method for the Calculation of Turbulent Deposition to Smooth and Rough Surfaces", J. Aerosol Sci. Vol 12. No 3 (1981), 275-290.

23. A.L. Wright and P. C. Arwood, "Summary of posttest aerosol code-comparison results for LWR Aerosol Containment Experiment (LACE) LA3", LACE TR-024, ORNL/M-492, June 1988.

24. VICTORIA Independent Peer Review, Technical Report W-6436 4-17-97, Brookhaven National Laboratory, April 1997.

25. Pui, Romay-Novas F, Liu. Experimental study of particle deposition in bends of circular cross section. Aerosol Sci Technol; 7: 301–15. (1987).

26. Davies, C.N., "Deposition of Aerosols from Turbulent Flow through Pipes," *Proc. Roy. Soc.,* London, A-289, pages 235-46, 1966.

NRC FORM 335 (12-2010) NRCMD 3.7

U.S. NUCLEAR REGULATORY COMMISSION

BIBLIOGRAPHIC DATA SHEET

(See instructions on the reverse)

1. REPORT NUMBER (Assigned by NRC, Add Vol., Supp., Rev., and Addendum Numbers, if any.)

NUREG/CR-7110, Volume 2

2. TITLE AND SUBTITLE

State-of-the-Art Reactor Consequence Analyses Project, Volume 2, Surry Integrat ed Analysis

3. DATE REPORT PUBLISHED

MONTH	YEAR
01	2012

4. FIN OR GRANT NUMBER

5. AUTHOR(S)

Nathan Bixler, Randall Gauntt, Larry Humphries, Joseph Jones, Kyle Ross, Kenne th Wagner (dycoda LLC)

6. TYPE OF REPORT

NUREG

7. PERIOD COVERED *(Inclusive Dates)*

8. PERFORMING ORGANIZATION - NAME AND ADDRESS *(If NRC, provide Division, Office or Region, U S. Nuclear Regulatory Commission, and mailing address; if contractor, provide name and mailing address.)*

Sandia National Laboratories
Albuquerque, New Mexico 87185
Operated for the U.S. Department of Energy

9. SPONSORING ORGANIZATION - NAME AND ADDRESS *(If NRC, type "Same as above"; if contractor, provide NRC Division, Office or Region, U.S. Nuclear Regulatory Commission, and mailing address.)*

Division of Systems Analysis
Office of Nuclear Regulatory Research
U.S. Nuclear Regulatory Commission
Washington DC 20555-0001

10. SUPPLEMENTARY NOTES

11. ABSTRACT *(200 words or less)*

The evaluation of accident phenomena and the offsite consequences of severe rea ctor accidents has been the subject of considerable research by the U.S. Nuclear Regulatory Commission (NRC) over the last several decades. As a consequence of this research focus, analyses of severe accidents at nuclear power reactors are more detailed, integrated, and realistic than at any time in the past. A desire to leverage this capability to address conserva tive aspects of previous reactor accident analysis efforts was a major motivating factor in the genesis of the State of the Art Re actor Consequence Analysis (SOARCA) project. By applying modern analysis tools and techniques, the SOARCA project developed a body of knowledge regarding the realistic outcomes of severe nuclear reactor accidents. To accomplish this objective, th e SOARCA project used integrated modeling of accident progression and offsite consequences using both state-of-the-art compu tational analysis tools and best modeling practices drawn from the collective wisdom of the severe accident analysis comm unity. This study has focused on providing a realistic evaluation of accident progression, source term, and offsite conseque nces for the Surry Nuclear Power Station. By using the most current emergency preparedness practices, plant capabilities, an d best available modeling, these analyses are more detailed, integrated, and realistic than past analyses. These analyses al so consider all mitigative measures, contributing to a more realistic evaluation.

12. KEY WORDS/DESCRIPTORS *(List words or phrases that will assist researchers in locating the report.)*

State-of-the-Art Reactor Consequence Analyses
SOARCA
Severe Reactor Accidents
Peach Bottom Analysis

13. AVAILABILITY STATEMENT

unlimited

14. SECURITY CLASSIFICATION

(This Page)

unclassified

(This Report)

unclassified

15. NUMBER OF PAGES

16. PRICE

Federal Recycling Program

UNITED STATES
NUCLEAR REGULATORY COMMISSION
WASHINGTON, DC 20555-0001

OFFICIAL BUSINESS